INFORMATION TO USERS

This manuscript has been reproduced from the microfilm master. UMI films the text directly from the original or copy submitted. Thus, some thesis and dissertation copies are in typewriter face, while others may be from any type of computer printer.

The quality of this reproduction is dependent upon the quality of the copy submitted. Broken or indistinct print, colored or poor quality illustrations and photographs, print bleedthrough, substandard margins, and improper alignment can adversely affect reproduction.

In the unlikely event that the author did not send UMI a complete manuscript and there are missing pages, these will be noted. Also, if unauthorized copyright material had to be removed, a note will indicate the deletion.

Oversize materials (e.g., maps, drawings, charts) are reproduced by sectioning the original, beginning at the upper left-hand corner and continuing from left to right in equal sections with small overlaps.

Photographs included in the original manuscript have been reproduced xerographically in this copy. Higher quality 6" x 9" black and white photographic prints are available for any photographs or illustrations appearing in this copy for an additional charge. Contact UMI directly to order.

Bell & Howell Information and Learning
300 North Zeeb Road, Ann Arbor, MI 48106-1346 USA
800-521-0600

Université d'Ottawa · University of Ottawa

Geochemical Investigation Of The Lower Crustal Rocks In Bamble Shear Belt, Southern Norway: Implications For The Source Of Gold In Lode Gold Deposits.

By :

Saeed Alirezaei

Ottawa-Carleton Geoscience Center and

Department of Geology,

University of Ottawa.

Ottawa, Canada, 1999

A thesis submitted to the School of Graduate Studies and Research

in partial fulfillment of the requirements for the degree of Doctor of Philosophy at the

University of Ottawa

Abstract

The source of gold in lode gold deposits in metamorphic terrains is debatable. The occurrence of the deposits in major shear zones and under a variety of crustal regimes suggests that gold and fluids were derived from the deep and wider portions of the shears. As a test of the "deep source model", the Bamble Shear Belt of southern Norway was studied. A transition from amphibolite to granulite facies takes place over the 30 km width of the Shear Belt. Some 400 samples from various rock units across the Belt were analyzed for a wide range of elements. The results, combined with petrographic studies and data from elemental and isotopic composition of sulfides, are interpreted with emphasis on the processes that have affected the distribution of gold.

The oldest exposed rocks in Bamble are a sequence of sedimentary and volcanic materials of early- to mid-Proterozoic age. During the Kongsbergian, or Gothian, orogeny (1600-1450 Ma), all the supracrustal rocks were intruded by a suite of acid-intermediate magmas, and a series of basic dykes and sills known as metabasites. All rocks were metamorphosed under upper amphibolite and granulite facies conditions.

During a second orogenic phase, known as Sveconorwegian (1250-1000 Ma), numerous mafic stocks and dykes, known as hyperites, intruded the older rocks. Intrusion occurred under amphibolite to locally granulite-facies conditions. The orogeny culminated with the intrusion of post-orogenic alkali granites at 1000-900 Ma.

The highest grade portion of Bamble is dominated by tonalitic-trondhjemitic charnockites and subordinate metabasites and metasediments. All rocks in this zone are strongly depleted in LILE, LREE, and HFSE relative to their equivalent rocks from amphibolite and transition zones. Depletion of the elements can be explained by the presence of a CO_2-rich fluid during magmatic crystallization, or metamorphic recrystallization. The involvement of carbonic fluids in granulite metamorphism at Bamble is supported by fluid inclusion studies (e.g. Touret, 1971, 1986; Hoefs and Touret, 1975; Van Den Kerkhof et al., 1994).

Metabasites have totally metamorphic minerals and textures, implying that they have equilibrated to the conditions of metamorphism. Hyperites vary from troctolitic gabbro to olivine ferrogabbro and norite. Fe-Cu-Ni sulfide ores are locally associated with the hyperites.

After emplacement, most hyperite bodies underwent retrograde reactions, with the development of coronitic cores and amphibolitized margins. Both metabasites and hyperites are of low-Mg tholeiitic nature (MgO <10%), and bear features typical of destructive margin settings. On MORB-normalized plots, they exhibit marked enrichments in LILE and LREE. The absence of Mg-rich cumulates argues against a fractional crystallization model. Both series are the products of low degrees of partial melting.

Hyperites equilibrated near the QFM buffer in the stability field of pyrrhotite. Metabasites and the amphibolitized hyperites display varying degrees of replacement of pyrrhotite by pyrite and magnetite. Sulfides have locally been replaced by silicates (particularly Fe-rich chlorite) and carbonates. Mass balance calculations indicate that amphibolitization of hyperites was associated with introduction of LILE and Cl. Chalcophile elements remained constant, or locally remobilized and reprecipitated. This is supported by analysis of sulfide concentrates.

The metasedimentary rocks show a large variation in $\delta^{34}S$ (-1 to +12‰) consistent with data from sedimentary rocks of early- to mid-Proterozoic age. No distinction can be made between various metamorphic zones. Charnockites show a wide spread in $\delta^{34}S$ values and relatively high S/Se ratios, in the same range as in the metasediments, implying that the country rocks had an important role in the formation of the charnockites.

Mafic rocks from various metamorphic zones display a clustering of $\delta^{34}S$ values around 0‰, consistent with a mantle source for S. Pyrrhotite and pyrite exhibit similar isotopic composition implying that no fractionation of S isotopes occurred upon oxidation of pyrrhotite. There is evidence that ^{34}S-rich S from country rocks was involved in the formation of the Ni-Cu ores.

Supracrustal rocks of varied type and origin in Bamble are strongly depleted in Au, As, Sb, and Se relative to the crustal abundance of these elements. The average Au in the Bamble rocks, 0.35 ppb, is only 25% of the crustal abundance of this element. Charnockites are also depleted in Au, As, Sb, and Se. The mean value of Au in these rocks (0.2 ppb) is 20% of the general abundance of this element in felsic rocks elsewhere.

The mean contents of Au in the Bamble hyperites and metabasites (0.4 and 0.25 ppb, respectively) are considerably lower than the general abundance of Au in tholeiitic mafic rocks elsewhere (~ 2 ppb). The Bamble mafic rocks are also depleted in Ir, but not in As, Se, Bi, or

S. A model consistent with all geochemical data favors an initial magmatic origin for the low concentration of Au. Metamorphism and oxidation of sulfides might have led to further depletion of Au in the metabasites, but not in the hyperites.

The post-orogenic granites contain 0.18 ppb Au that is 20% of that in the mean granites elsewhere. Assuming a crustal source for the granites, the low content of Au is likely a reflection of the low Au content of the source rocks.

Gold could have been remobilized at different stages during evolution of Bamble:

1) During progressive metamorphism. Depletion of Au in supracrustal rocks of varied type and origin indicates that loss of Au, together with As, Sb, and Se, may have occurred during prograde devolatilization of these rocks and any magmatic rocks that had been intruded prior to the high grade metamorphism.

2) Oxidation of sulfides during post-solidus reactions in mafic rocks. This is evident from replacement of pyrrhotite by pyrite and magnetite. The lower contents of Au in the metabasites, compared to the hyperites, might be attributed to this process. However, for an efficient remobilization of chalcophile elements to occur, the f_{O2} should be above the pyrrhotite-pyrite-magnetite buffer. The boundary was hardly crossed at Bamble; oxidation of sulfides occurred commonly in systems closed to significant removal of chalcophile elements.

3) Replacement of sulfides by alteration minerals (Fe-rich chlorite, quartz, and carbonates). This is a low temperature retrograde reaction, occurring during uplift. When pervasive, the enclosing rock is strongly depleted in Au.

Lode gold deposits are commonly associated with alkaline and light REE metasomatism, and a significant enrichment in As, Sb, and Se. The same elements are considerably depleted in the Bamble lower crustal rocks. However, while depletion of LILE and REE is restricted to the granulite zone, all pre-Kongsbergian rocks from various metamorphic zones are depleted in Au. Granulite metamorphism is a continuation of deformation at upper crustal levels. Neither special Au-enriched rocks, nor unreasonably large volumes of source rocks are required to produce a giant gold deposit. Shear zones serve as major source areas and principal conduits for extraction and transportation of Au.

Acknowledgements

I wish to thank Dr. Eion Cameron for suggesting this thesis and for his academic support throughout this study. Dr. Cameron's editorial background forced me to improve my writing style. I would like to acknowledge Gilles St-Jean from the Stable Isotope Laboratory, University of Ottawa, for helpful discussions concerning the analysis of sulfur isotopes. I am grateful to John Stirling from the Geological Survey of Canada and Peter Jones from the Department of Geology, Carleton University, for electron microprobe analyses, and Ron Hartree from the University of Ottawa for XRF analyses. George Mrazek taught me how to make polished and polished-thin sections. Edward Hearn helped me with the graphical objects. My wife, Sepideh, patiently tolerated me in the past few years. Her support and understanding is a real treasure.

List of Figures

List of Plates

List of Tables

Table of Contents

1. Introduction

1-1. Preview

Gold ores associated with quartz-carbonate veins in metamorphic terrains have been a major source of gold. The deposits, also known as "mesothermal gold" or "lode gold" occurred in metamorphic belts of all ages, from Archean to Cenozoic, and in a wide range of host rocks. They characteristically occur along shear zones, with the majority of the deposits located near the brittle-ductile transition (e.g. Phillips et al., 1987; Bohlke, 1989; Goldfarb et al., 1991; De Ronde et al., 1992; Kerrich and Cassidy, 1994; Witt and Vanderhor, 1998).

The great majority of the deposits are hosted by greenschist to lower amphibolite facies rocks. Examples include: Yellowknife Gold Camps, Canada (Colvine et al., 1988); Kolar, India (Siddaiah and Rajamani, 1989); Golden Mile, Australia (Phillips et al., 1987); Mother Lode, California (Weir and Kerrick, 1987); and Juneau Gold Belt, Alaska (Goldfarb et al., 1991). Comparable deposits, however, have been discovered in host rocks of sub-greenschist facies (Hagemann et al., 1994; Gebre-Mariam et al., 1993; Troop, 1986; Colvine, 1989), as well as middle amphibolite-granulite facies (Barnicot et al., 1991; Shengfei et al., 1992; Groves et al., 1992; McCuaig et al., 1993; Neumayr et al., 1993; Pan and Fleet, 1995; Van Reenen et al., 1994).

Considering the broad depth range of formation, the term "mesothermal" no longer seems to be appropriate for these deposits. Regarding the unique temporal and spatial association with orogeny, the term "orogenic gold deposits" has recently been proposed for the deposits (Groves et al., 1998; Goldfarb et al., 1998; Witt and Vanderhor, 1998).

The deposits share many characteristics, such as structural hosting, ore fluid chemistry, carbonate alteration, alkali metasomatism, and metal inventory (e.g. Colvine et al., 1988; Roberts, 1986; Kerrich, 1989 a, 1993; Groves et al., 1992, 1998; Witt and Vanderhor, 1998). They are typified by quartz-dominant vein systems with $\leq$3-5% sulfide minerals, and $\leq$5-15%

carbonate minerals (Groves, 1998). The deposits are characteristically enriched in Au with variable enrichments in As, Ag, Sb, Se, Bi, W, and Te, but rarely base metals, and the ore fluids were CO_2-rich and of low to moderate salinity (e.g. Boyle, 1979; Kerrich and Fryer, 1981; Colvine et al., 1988; Roberts, 1987; Kerrich, 1989 a, 1990, 1993; Groves et al., 1992, 1998; Groves, 1993; Witt and Vanderhor, 1998).

The deposits have been studied extensively by numerous authors, and there is a voluminous literature on the different aspects of mineralization. However, the origin of gold and fluids is still debatable. The hypothesized sources include:

- Felsic magmatic. Derivation of gold and ore fluids from granitoid magmas (Emmons, 1937; Mason and Melnik, 1986; Burrows and Spooner, 1987; Mueller et al., 1991), or oxidized felsic magmas (Hattori, 1987; Cameron and Hattori, 1987).
- Alkaline magmatic. Derivation of metals and fluids from mantle together with alkaline igneous rocks (Rock and Groves, 1988; McNeil and Kerrich, 1986; Rock et al., 1988, 1989; Cameron, 1990).
- Structurally focused metamorphic outgassing. Extraction of ore elements from various rock units by metamorphic fluids (Kerrich and Fryer, 1979; Kerrich, 1987; Groves and Phillips, 1987; Boulter et al., 1987; McKeag and Carw, 1989; Kerrich and Wyman, 1990; Goldfarb et al., 1991, 1998; Phillips and Powell, 1993; Groves et al., 1995).
- Lateral secretion. Derivation of solutes from immediate country rocks (Boyle, 1979).
- Exhalative. Initial formation from submarine volcanic exhalations, with later metamorphic remobilization (Fripp, 1976; Ridler, 1976; Hutchinson and Burlington, 1984).
- Meteoric water circulation. Fluids supplied by circulation of meteoric water (Nesbitt et al., 1986, Shelton et al., 1988; Shaw et al., 1991).
- Granulitization-mantle degassing. Derivation of fluids and ore metals from lower crust and mantle (Colvine et al., 1984, 1988; Fyon et al., 1983, 1988; Cameron, 1988, 1989a, b, 1993a; Hodgson et al., 1989; Groves et al., 1992).

The felsic magmatic model, also known as the tonalite-trondhjemite-granodiorite model, or TTG model, has been criticized based on the inconsistent geochronological data, the paucity of gold deposits in ≥3 Ga greenstone belts where TTGs are abundant, and stable and radiogenic isotope data (Kerrich, 1988, 1989 b, 1990; Witt and Vanderhor, 1998).

An alkaline magmatic-mantle affiliation has been criticized based on the geochemistry, stable isotope data, and tectonic setting (Wyman and Kerrich, 1989; Kerrich, 1989a, 1990) as well as radiogenic isotope data (Hattori, 1993). It has been indicated that alkaline magmas are not particularly Au-enriched (Wymann and Kerrich, 1989; Barron, 1990; Rowins et al., 1993). However, the spatial and temporal relationship between lode gold and alkaline rocks in some gold camps suggests that gold-bearing structures communicated with the mantle (McNeil and Kerrich, 1986; Wymann and Kerrich, 1988).

Available stable isotope data are non-definitive (c.f. Golding et al., 1989; Wyman and Kerrich, 1989; Kerrich, 1989a, 1990), but are consistent with derivation of ore metals from a variety of crustal reservoirs intersected by fluids advecting along vertically extensive conduits (Phillips et al., 1987; Groves et al., 1995).

Radiogenic isotope data provide more definitive evidence on the source of ore metals. The data suggest a heterogeneous source for Au, rather than a single specialized reservoir (Kerrich, 1989a; Powell et al., 1991; Hattori, 1993; Mc Naughton et al., 1993; Groves et al., 1995). Even in a single deposit, Au might have been derived from different sources (Kerrich, 1989a; Hattori, 1993; Qui and McNaughton, 1999).

The relation between metamorphism and ore genesis has been a long-standing debate. A variable timing of mineralization with respect to peak-metamorphism has been documented, with the majority of the deposits being syn- to post-peak metamorphism (e.g. Kerrich, 1983, 1986; Colvine et al., 1984, Groves et al., 1992; Groves, 1993; Kerrich and Cassidy, 1994; Witt et al., 1997). In most deposits and ore districts, wallrock alteration assemblages and ore mineral paragenesis vary according to metamorphic grade of host rocks (e.g. Witt, 1991;

Meuller and Groves, 1991; McCuaig et al., 1993; Witt et al., 1997), implying mineral stabilities under ambient P-T of regional metamorphism.

The occurrence of lode gold deposits under amphibolite and granulite facies conditions cogenetic with the common greenschist facies mineralization discredits the models based on the high level sources such as exsolution of fluids from high level felsic magmas, meteoric water circulation, or greenschist-amphibolite devolatilisation of greenstones, as the major contributors to the mineralizing fluids. Metamorphic processes explain the structural siting of gold deposits at regional and local scales, as well as the provinciality of stable and radiogenic isotope systematics (Kerrich, 1990, Hattori, 1993). However, the ultimate source of gold and its extraction and transportation is an enigma.

As an alternative to high level sources, granulitization of lower crustal rocks has been proposed as the main process driving the ore-forming system of lode gold deposits (Colvine et al., 1984, 1988; Cameron, 1988, 1989a, b, 1993a; Fyon et al, 1988; Hodgson et al., 1989; Zweng et al., 1993; Santosh et al., 1995). This is also implicit in the continuum model of Groves et al. (1992) and Groves (1993). This genetic model is based on the hypothesis of granulite formation by influx of a mantle-derived carbonic fluid, as proposed by Touret (1971, 1985) and Newton (1980).

To explain the general features of lode gold deposits (i.e. occurrence under variable P-T, yet comparable ore fluid chemistry, alteration and mineralization during peak to post-peak metamorphism, association with felsic bodies, and extensive carbonatization), Colvine et al. (1988) depicted a model based on the granulitization and partial melting of the lower crust coupled with mantle magmatism and degassing. A similar "terminal-stage tectonic" model was suggested by Fyon et al. (1989) and Hodgson et al. (1989) to explain the formation of lode gold deposits in Abitibi, Canada. Zweng et al. (1993) proposed a model involving mantle-derived basalts underplating the lower crust during peak granulite metamorphism. According to the model, magmatic CO_2-rich fluids interacted with other fluids, magmas, and rocks at

their source or during migration in shear zones, where they promoted extensive carbonatization and deposited gold ores.

Santosh et al. (1995) reported a narrow spread in $\delta^{13}C$ (-4.1 to -5.9‰), $\delta^{18}O$ (+7.6 to +7.8‰), and $\delta^{34}S$ (+1.4 to +4.8‰) of the CO_2-rich fluid inclusions, quartz-calcite, and sulfide minerals from Wynad Gold Field, southern India. The occurrence of the gold deposits in granulite-facies host rocks, and the correspondence of the C-O isotopic data with juvenile CO_2 of mantle origin was interpreted as an evidence for a genetic link between CO_2 influx, granulite formation, carbonate alteration, and gold mineralization.

Glassley (1983) reported a pervasive oxidation of sulfides and significant loss of S from the granulite facies rocks in Nodre Stromfjord shear zone, West Greenland. The author noticed that relicts of pyrrhotite and pyrite were mantled by magnetite if graphite was present; in the absence of graphite, no oxidation was observed. The author suggested that the genesis of graphite was accompanied by the oxidation of sulfides and that graphite was derived from the reduction of CO_2. The author related the source of carbon to metasomatic reactions between marble and various gneisses in the area.

Cameron (1988, 1989a, b, 1993a) suggested the "oxidative metamorphism of deep ductile shear zones" as an efficient mechanism for dissolution of sulfides and mobilization of sulfur and chalcophile elements from lower crustal rocks. According to the model, the dehydration of lower crustal rocks in shear zones under CO_2 streaming produces a relatively oxidized CO_2-H_2O fluid that dissolves sulfides and liberates chalcophile elements from large volumes of country rocks. Gold, in the form of S-complexes is focused and precipitated at or above the brittle-ductile transition. This model would explain the common carbonate alteration with $\delta^{13}C$ values close to that of the juvenile CO_2 (e.g. Colvine et al., 1988; Santosh et al., 1995), high oxidation state of the ore fluids in some of the large Archean deposits (Cameron and Hattori, 1987b), and the common occurrence of the lode gold deposits in major shear zones.

Cameron (1989a, b) showed that granulite facies rocks at Bamble Shear Belt, southern Norway, equilibrated under a relatively high f_{O2} at peak metamorphic conditions. The f_{O2} calculated for charnockites and metabasites is ~2.7 log units above the normal f_{O2} for igneous rocks that commonly equilibrate at or near the FMQ buffer at log f_{O2} = -14.5. Cameron (1989a, b) further argued that the uniformity in f_{O2} within the charnockites and metabasites is consistent with their equilibration in the presence of a high fluid flux.

Cameron (1989a, b, 1993a) reported a strong depletion of chalcophile elements in the granulite and amphibolite facies rocks from Bamble. Mafic rocks from the granulite zone contain, on average, 0.17 ppb Au which is 4% of the general abundance of this element in similar mafic rocks elsewhere. Charnockites and metasedimentary rocks are depleted in Au by one order of magnitude relative to the crustal abundance of this element. Cameron (1994) also documented a strong depletion of Au in granulite facies rocks from Lewisian Complex, Scotland. Depletion of chalcophile elements in Bamble was related to oxidation of sulfides under high f_{O2}.

More recently, Harlov et al. (1997) documented an oxidative metamorphism and replacement of pyrrhotite by pyrite and magnetite in granulites from Shevaroy Hills Massif, South India. With regard to the consistency of f_{O2} calculated from pyrrhotite-pyrite-magnetite assemblage with that from other oxygen barometers, the authors suggested a high temperature equilibrium control on the oxidation of pyrrhotite. The occurrence of extensive vein networks of magnetite and pyrite was proposed as an evidence for the involvement of an oxidizing fluid. The source of the fluids were related to exhalations from deep-seated alkali basalts. However, the authors did not rule out the possibility that the high oxidation states were set by initially oxidized protoliths.

1-2. Objectives

Shear zones serve as principal conduits for transportation of fluids and metals, and many types of deposits, including "lode gold" are spatially associated with these structures. The

occurrence of lode gold deposits in major shear zones and under a variety of crustal regimes from sub-greenschist to amphibolite and granulite facies conditions, suggests that gold was derived from the deep and wider portions of the shears (e.g. Cameron, 1988; Wymann and Kerrich, 1988; Robert, 1989; Witt and Vanderhor, 1998). As a test of the "deep source model" Bamble Sector of southern Norway is studied.

1-3. Study Area

Bamble Sector is part of the South-West Scandinavian Domain (SWSD) of the Baltic Shield (Gaal and Gorbatschev, 1987) which comprises southern Norway and southwest of Sweden (Figure 1-1). It is also known as Bamble Shear Belt, or Bamble Linear Belt (Falkum and Petersen, 1980). The term "Sector" refers to an area of rocks with a similar geological history, comparable to North American term "Province".

Major north-south trending structural zones separate the SWSD into several crustal blocks, or "Sectors" (Figure 1-1). The structural zones have had complex histories from the Gothian orogeny until after the formation of Permian Oslo Graben (Padget, 1990; Starmer, 1990, 1991). Variable movements along the zones presently expose different levels of the crust.

1-3-1. South-West Scandinavian Domain

The geological history of the SWSD has been discussed by several authors (e.g. Verschure, 1985; Falkum, 1985; Gaal and Gorbatschev, 1987; Padget, 1990; Gower et al., 1990; Starmer, 1985a, b, 1990, 1991, 1993). Most of the SWSD was created by accretionary tectonics in the period 2.1 to 1.6 Ga. The period from 1.65 to 1.55 Ga marks the last major phase of crustal accretion that is accompanied by subduction of oceanic crust along the margins of the SWSD and high grade metamorphism. This phase of deformation and metamorphism is coincident with the "Gothian", or, "Kongsbergian" orogeny. While the term "Gothian orogeny" initially referred to the orogeny in Sweden, it is often used to describe the orogeny across the SWSD. The term Kongsbergian has been used to refer to the same orogeny in southern Norway (e.g. Oftedhal, 1980; Starmer, 1990).

From ~1.55 to ~1.25 Ga there was a period of relative crustal stability, characterized by anorogenic magmatism, rift-related tectonism and deposition of supracrustal rocks in most parts of the Baltic Shield. The Sveconorwegian orogeny (~1.25-0.9 Ga) was a period of magmatism and metamorphic reworking in SWSD. During the early part of the orogeny, there are evidence for granitoid emplacement and an initial extensional phase associated with rifting and mafic magmatism. In the Bamble and Kongsberg Sectors, the mafic intrusions have a subduction affinity (Smalley and Field, 1991; present study). Post-Sveconorwegian events include intrusions and faulting. Large "Post-Tectonic" granites intruded southern Norway and Sweden between 0.95 and 0.88 Ga.

1-3-2. Bamble Shear Belt

Bamble Shear Belt comprises an area 20-30 km wide and about 150 km long of variably deformed high grade metamorphic rocks along the east coast of southern Norway, south of Oslo Graben (Figure 1-1). The area is polymetamorphic with maximum metamorphism under upper amphibolite and granulite facies conditions. A simplified geological map of Bamble is shown in Figure 1-2.

Bamble Shear Belt is bounded by two major fault complexes with significant strike-slip movements (Padget, 1990). The Kristiansand-Porsgrunn, or, Nelaug, Fault Complex defines the northwest border of the shear Belt, and Tromoy Fault, possibly part of the Nidelv Fault Complex, defines the southeast border (Figure 1-2). The fault systems played an important role in providing conduits for mantle-derived magmas and fluids (Padget, 1990). Structural models suggest that the dominant northeast-southwest foliation and shearing at Bamble is the result of large scale dextral transcurrent movements older than ~1150 Ma (Falkum and Petersen, 1980; Starmer, 1981, 1985b, 1993; Padget, 1990).

Variations in mineralogy and chemical composition have been used to divide the coastal area of the Bamble into four zones labeled A through D, which run roughly parallel to the coast (Field et al., 1980; Clough and Field, 1980; Smalley et al., 1983). Zone A is entirely within

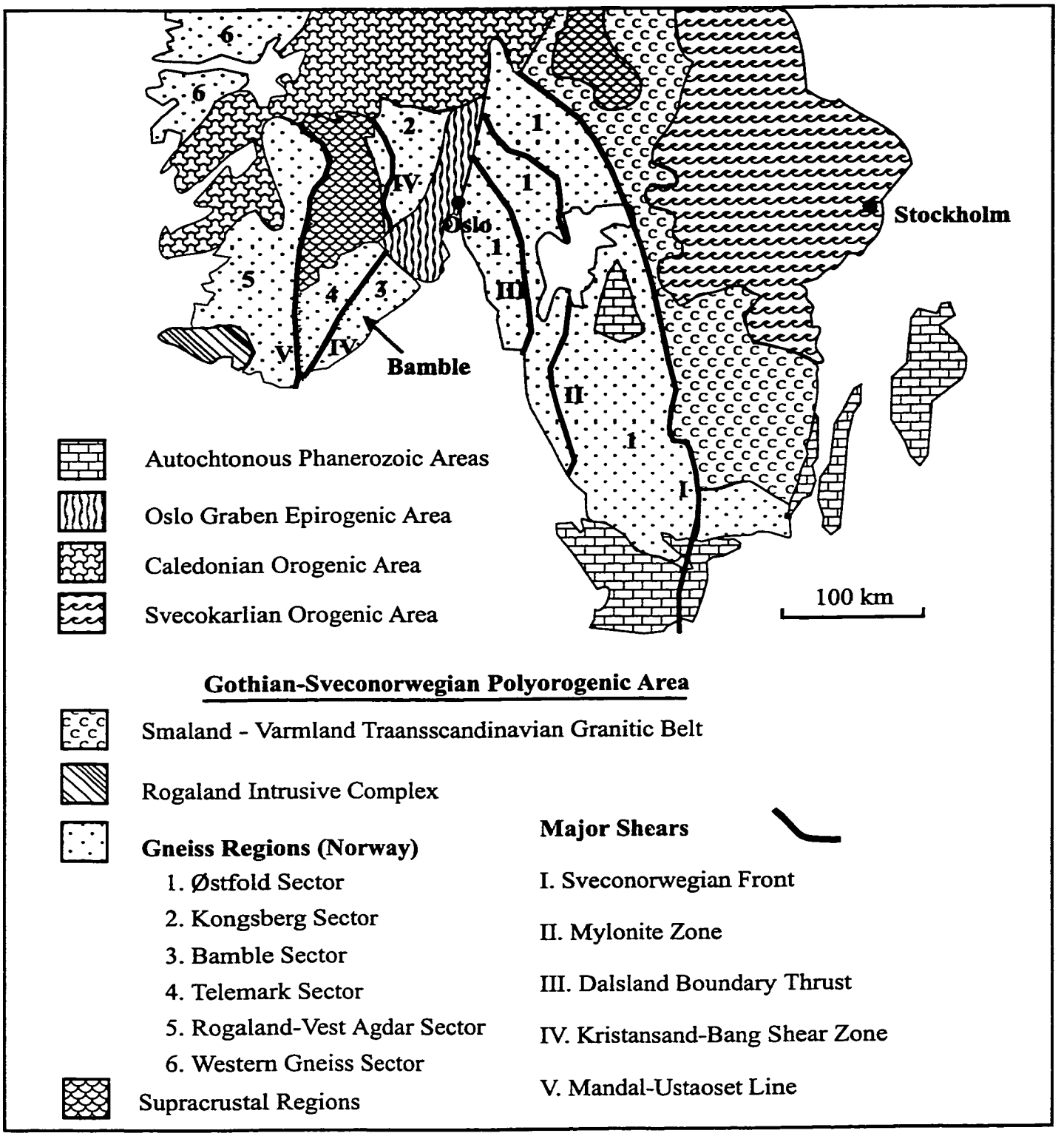

Figure 1-1. Major Geologic and Structural Ddivisions in Southern Scandinavia (after Verschure, 1985).

the amphibolite facies, and is separated from zone B (transition zone) by an orthopyroxene (Opx) isograd in metabasites. The location of the Opx-in isograd is shown in Figure 1-2. Zone C is granulite grade, with Opx in most metabasites and in metasediments of suitable composition. Zone D, also known as Tromoy Complex, is dominated by charnockitic gneisses that are very poor in K-feldspar, hornblende and biotite. All rocks in this zone are strongly deficient in large ion lithophile elements (Cooper and Field, 1977; Field and Cooper, 1980; Field et al., 1980; Smalley et al., 1983; Field et al., 1985; Lamb et al., 1986; Cameron, 1989b).

1-3-3. Geological Evolution of Bamble

The geologic history of Bamble has been studied by several authors (e.g. Starmer, 1969, 1979, 1985a, b, 1990, 1991, 1993; Verschure, 1985; Falkum, 1985; Padget, 1990). There seems to be an agreement that the present geology of Bamble is the result of two separate, relatively high grade, metamorphic events. The first took place during the Kongsbergian orogeny (1600-1450 Ma) under upper amphibolite and granulite grades (O'Nions and Baadsgard, 1971, Starmer, 1977, 1990, 1991; Starmer and Milne, 1982; Field et al., 1985; Nijland and Senior, 1991). The second occurred during the Sveconorwegian orogeny (1250-950 Ma) under amphibolite and locally granulite grades (O'Nions and Baadsgaard, 1971; Jacobsen and Heier, 1978; Starmer, 1972, 1990, 1991; Nijland and Senior, 1991).

The occurrence of a high grade metamorphic event during Sveconorwegian times has been challenged by some workers (Field and Råheim, 1979, 1981; Smalley et al., 1983; Field et al., 1985; Smalley and Field, 1985; Brickwood, 1984, 1986). The authors argue that Bamble underwent a major metamorphism during Kongsbergian orogeny, and that the Sveco-norwegian event was essentially a thermal metamorphism with limited structural deformation, and only locally reached upper amphibolite facies. More recent data, however, support the occurrence of a major metamorphic event in 1200-1100 Ma, corresponding to the Sveconorwegian orogeny (Munz, 1990; Munz and Morvick, 1991; Kullerud and Machado, 1991; Kullerud and Dahlgren, 1993; Hagelia, 1995; Knudsen and Andersen, 1999). The occurrence of a separate Kongsbergian high grade metamorphism has recently been criticized by Knudsen and Andersen (1999). Starmer (1985b, 1991, 1993) discussed the evolution of

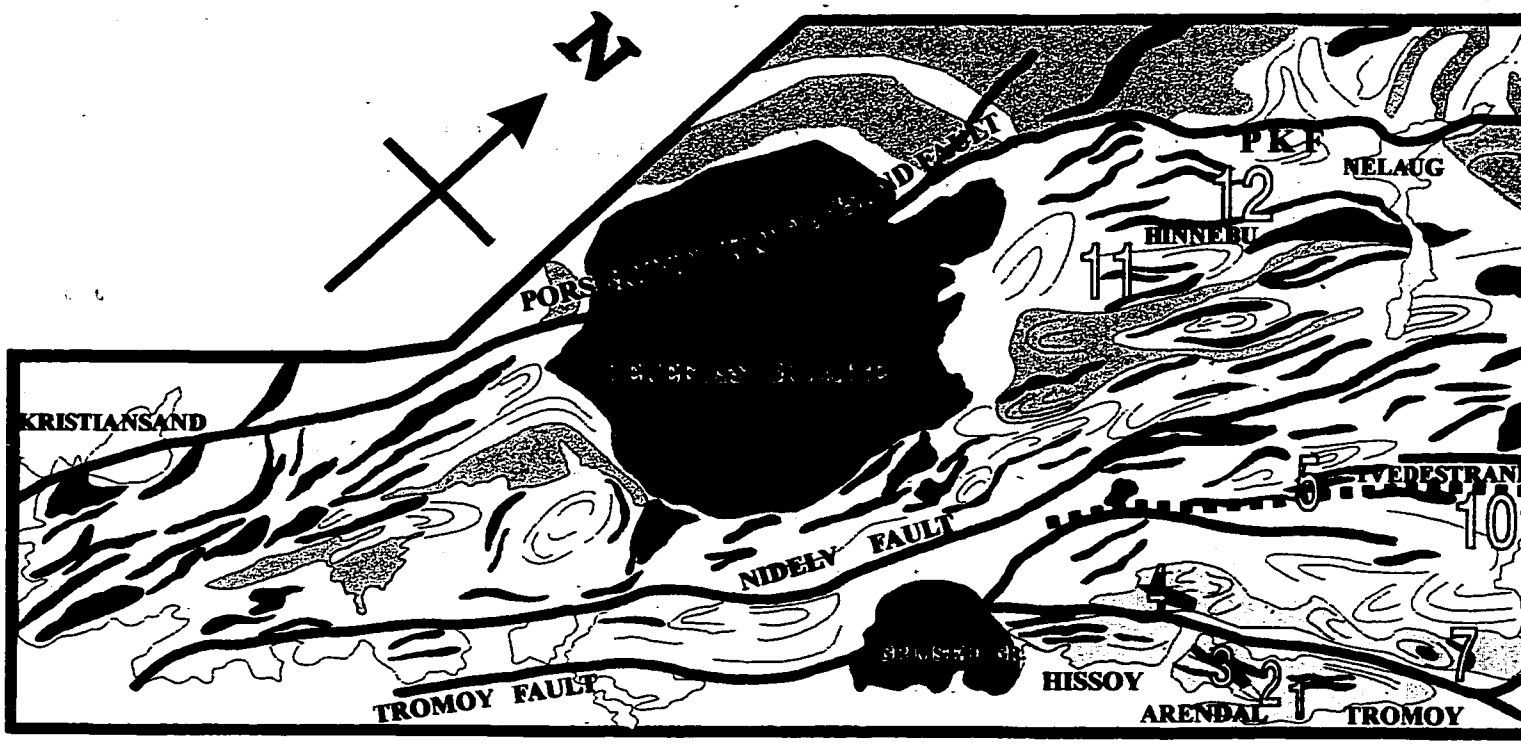

Metasupracrustal rocks: Variable Qtz-Bt-Pl ± Hbl ± Grt gneisses; Bt-schists; graphitic ± sul

Migmatites and granitic gneisses (variable gneisses with partial to intensive migmatisation

Charnockitic-enderbitic orthogneisses, locally mixed with metasupracrustal rocks (Kongsb

Granitic-charnockitic augen gneisses; granodioritic gneisses; metagabbro and anorthositic g

Metamorphosed basic intrusives: Gabbroid coronite of main phase hyperite intrusions; amp

Protomylonites and mylonites, formed from variable gneisses of various ages.

Coarse grained granite (post-Sveconorwegian).

0

Figure 1-2. Geological Map of Bamble Sector; South Norway. Simplified after

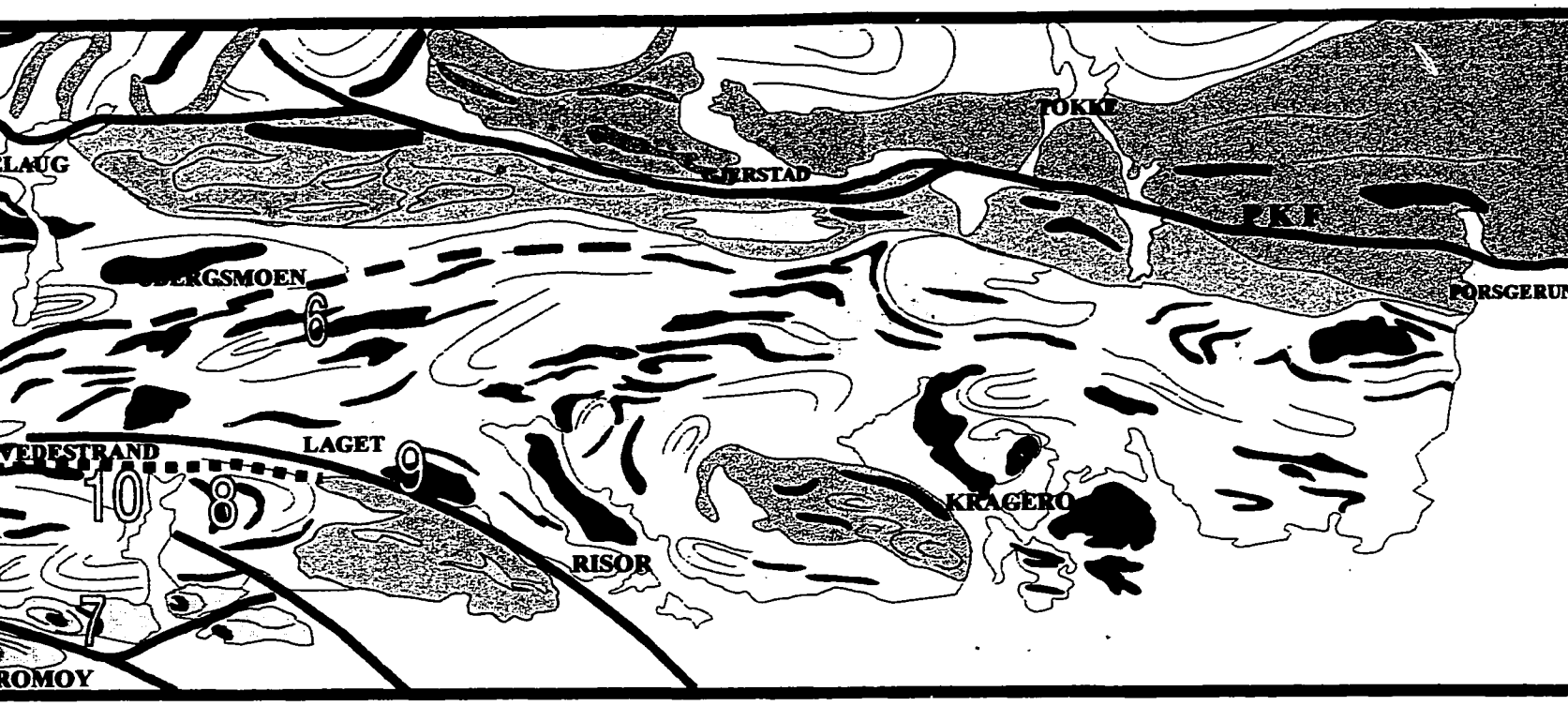

aphitic ± sulfidic Bt-schists; Qtz-Bt-Sil-Pl gneisses; quartzite; amphibolites; marbles and calc-silicates (Pre-Kongsbergian

gmatisation and/or granitisation; granitic and granodioritic gneisses) (Kongsbergian to mid-Sveconorwegian).

ks (Kongsbergian).

northositic gabbro (pre-Sveconorwegian).

usions; amphibolite of main and late phase hyperite intrusions (early and mid-Sveconorwegian).

Structural Line

Orthopyroxene Isograd (approximate)

10 20 km

1, 2, ... Traverse Location (approximate)

ied after Starmer (1985).

Table 1-1. Evolution of the Bamble Shear Zone (Data mainly from Starmer, 1985, 1991, 1993)		
Major Stage	Event	Approximate date (Ma)
Post-tectonic phase	Uplift and faulting continues to post-Permian times	
	Uplift and faulting (sub-Cambrian peneplain)	725
	Gabbro dykes (Gjerstad)	800
	Post-tectonic granites (e.g. Herefoss and Grimstad)	915 ± 35
	Medium grained "Post-Sveconorwegian" granites	945
Main Sveconorwegian orogenic phase	Folding and shearing	
	Medium grained "Late Sveconorwegian" granites	1000-990
	Dolerite sheets	
	Medium grained granites	
	Static metamorphism	1060-1050
	Coarse grained granites	
	Upper amphibolite, locally granulite facies metamorphism	1100
	Folding and thrusting	
Inter-Sveconorwegian extensional period	"Late phase" hyperites (basic sheets and sills)	1150-1140
	Medium grained granites, migmatites and mobilized gneisses	1200-1140
	"Main phase" hyperites (gabbroids)	1250-1220
Early Sveconorwegian compressional phase	Thrusting and shear folding	1250
	"Early phase" hyperites	
	Coarse grained granites	
	Thrusting	1270
Post - Kongsbergian anorogenic period	Anorogenic alkaline augen gneiss bodies	<1300
	Alkaline (basic-intermediate-acid) complexes	1500
Kongsbergian (Gothian) orogeny	Upper amphibolite-granulite facies metamorphism	1540
	Folding and thrusting	
	Intrusion of granites and charnockites	1600-1580
	Folding and thrusting	
	Deposition of supracrustal rocks	< 1700

Bamble by relating the deformation events to intrusive and metamorphic phases dated by whole-rock Rb-Sr, and zircon U-Pb data. A summary of the geological evolution of Bamble is shown in Table 1-1.

The oldest rock units in Bamble include a suite of supracrustal rocks consisting of quartzites, variable gneisses, graphitic and sulfidic schists, calc-silicates, and intercalated volcanic materials (e.g. Bugge, 1939; Bugge, 1943; Touret, 1968; Morton et. al., 1970; Starmer, 1972, 1985b). The initial sediments deposited during early- to mid-Proterozoic times (Knudsen et al., 1997) and were metamorphosed and intruded by basic and acidic magmas during Kongsbergian (Gothian) and Sveconorwegian (Grenvillian) orogenic episodes (Verschure, 1985; Starmer, 1985b, 1990, 1991).

The northeast-southwest trending structures in Bamble were established during a first deformation phase (D1 of Starmer, 1991, 1993) during Kongsbergian orogeny. This phase of deformation was associated with the intrusion of acid-intermediate rocks (now charnockites) along the coast near Arendal and Gjerstad, and of basic dykes and sills, known as metabasites, near Arendal (Figure 1-2). The intrusion age of the charnockites has been determined to be ~ 1.59 Ga (O'Nions and Baadsgaard, 1971; Lamb et al., 1986). Kongsbergian orogeny was associated with a high grade metamorphism. Peak metamorphic conditions have been estimated by different methods to be in the range of 7 to 8 kbar and 750 to 850°C (Lamb et al., 1986; Visser and Senior, 1990; Kihle and Bucher-Nurminen, 1992; Cameron, 1989b; Harlov, 1992; Nijland and Meijer, 1993; Visser, 1993).

After Kongsbergian, there was a period of transtension and attenuated rifting under upper amphibolite, and locally granulite, facies conditions (Starmer, 1990b). Numerous alkaline complexes intruded the older rocks. The timing of the intrusions is not well established. The proposed ages are in the range 1240-1450 Ma (Smalley et al., 1988; Starmer, 1990b; Nijland and Senior, 1991). A thick sequence of volcanic and sedimentary materials accumulated in the neighboring Telemark Sector. The post-Kongsbergian anorogenic period and its extensional

conditions were probably coeval with the rifting and separation of Fennoscandia from Laurentia (Starmer, 1993).

The post-Kongsbergian anorogenic period was followed by Sveconorwegian orogeny, which included three main phases: 1) Early Sveconorwegian Compressional Phase; 2) Inter-Sveconorwegian Extension; and 3) Main Sveconorwegian Orogenic Phase.

The Early-Sveconorwegian compressional phase is distinguished by emplacement of voluminous granite sheets under mid- to upper-amphibolite facies conditions. The Inter-Sveconorwegian Phase was associated with the intrusion of mafic bodies, known as hyperites. Hyperites are present throughout the SWSD and can be correlated with the broadly contemporaneous mafic magmatism in eastern Canada and southern Greenland (Patchett et al., 1978). Magmatic Ni-Cu deposits are locally associated with the hyperites. The Inter-Sveconorwegian Phase culminated with the intrusion of granite bodies, followed by the intrusion of "Late Hyperite" sheets.

The Main Sveconorwegian Phase was associated with further deformation under mid- to upper-amphibolite facies conditions, and intrusion of granite sheets. The margins of the Main Phase hyperite bodies were altered to amphibolite and garnet-amphibolite, and smaller stocks and sheets, including the late hyperite sheets, were generally completely amphibolitized. In the final stages of Sveconorwegian orogeny, thin (<1m wide) dolerite sheets intruded, which were subsequently amphibolitized, folded and weakly foliated. The Main Sveconorwegian Phase was coeval with the "Grenvillian Orogenic Cycle" in North America (Rivers et al., 1989).

Post-Sveconorwegian events comprised faulting and intrusion. Large, post-tectonic felsic intrusions, exemplified by the Herefoss Granite dated at 960 ± 60 Ma (whole rock Rb-Sr; Brueckner, 1972), and the Grimstad Granite dated at 990 ± 100 Ma (zircon and titanite U-Pb; Kullerud and Machado, 1991), are the last representatives of Sveconorwegian magmatic activity in Bamble.

Fahlbands, concordant rusty zones in gneisses containing sulfide impregnations, are widespread in Bamble and Kongsberg Sectors (Gammon, 1966; Starmer, 1985b). Major occurrences are restricted to local zones in quartz-plagioclase-biotite gneisses. They rarely form workable deposits; most are a few meters wide, and discontinuous (Gammon, 1966). The sulfides are dominantly pyrite, pyrrhotite, and marcasite with subordinate chalcopyrite and sphalerite. Fahlbands are syngenetic mineralizations which resulted from biological action in sapropelic muds (Gammon, 1966) or exhalative activities (Starmer, 1985b). Apatite and skarn iron, are other ores reported from Bamble (e.g. Barth, 1925; Morton et al., 1970).

Transition from amphibolite- to granulite-facies rocks at Bamble has been a controversial issue. Touret (1971, 1985) showed that the transition is correlated with a change from water- to CO_2-dominated fluid regime. Lamb et al. (1986) showed that neither pressure, nor temperature, vary significantly across the entire transition zone from amphibolite to granulite. According to the authors, the change in metamorphic grade parallels the increasing dominance of CO_2 over H_2O in the fluid phase. This was further supported by Visser and Senior (1990), and Bucher-Nurminen (1994). In contrast, Neijland and Maijer (1993) showed that transition from amphibolite to granulite was accompanied by an increase in pressure from 7.1 $\pm$ 0.4 to 7.7 $\pm$ 0.3 kbar, and a rise in temperature from 752 $\pm$ 34°C to 836 $\pm$ 49°C. Similarly, Knudsen (1996) found an increase in temperature, of approximately 80°C, from amphibolite to granulite zone.

1-4. Methodology and Contributions

Some 400 samples of supracrustal rocks, charnockites, metabasites, hyperites, Ni-Cu sulfide ores, and post-tectonic granites from various metamorphic zones were subjected to petrographic and geochemical studies. Results from the studies appeared partly in Cameron (1989a, b, 1993a, b) and Cameron et al. (1993).

1-4-1. Sampling

Samples were collected along several traverses using a randomized design. A description of the sampling method appeared in Cameron (1989b). Charnockites were sampled along two road cuttings in Tromoy (traverses 1 and 2) in successive intervalls of 200 m; four samples were taken from each interval. Locations of the traverses are shown in Figure 1-2.

Metabasites were sampled from the largest body of metabasite on Tromoy (traverse 3), from Hissoy (traverse 4), from several dykes near Tvedestrand (traverse 5) and several dykes in Ubergsmoen (traverse 6). The metabasite dykes were sampled at intervals of 2-5 m across the strike of the bodies. Hyperites were sampled from several dykes and stocks at Tromoy, Tvedestrand, and Laget (traverses 7-9) in the same manner as for metabasites.

Supracrustal rocks were collected along traverse 10 in Tvedestrand and traverses 11 and 12 in Hinnebu. Scattered metasediments were sampled from granulite zone in Tromoy and Hissoy.

1-4-2. Geochemical Analysis

All samples were analyzed for a wide range of elements. To achieve optimum accuracy and detection limits, various analytical techniques were employed (Table 1-2). Precision and accuracy were evaluated using reference materials and triplicate analysis of selected samples. Analytical accuracy is better than ± 2% for oxides at concentrations above 1%, and ± 5% for trace elements in amounts of greater than 10 ppm. Precision is better than 2% and 5% for major and trace elements, respectively.

Table 1-2. Techniques and detection limits for whole-rock geochemical analyses		
Element (Oxide)	Analytical Technique	Detection Limit
Major oxides	Fused Disc XRF	0.01%
Rb	Pressed Pellet XRF	1 ppm
Fe^{+2}, Fe^{+3}	Pratt	0.01%
H_2O, total C	Leco Furnace	0.05%
Transition metals, Ba, Sr, Y, Zr	Ind. Coup. Plas. At. Emis. Spec. (ICPAES)	5 ppm
Rare Earth Elements, Cs, U, Th	Instrumental Neutron Activation	2 (Ce); 1 (La, Sm, Yb); 0.5 (Eu, Tb); 0.1 ppm (Cs, U, Th, Lu)
S	Ion Chromatography	20 ppm
Sb, As, Se	Hydride Atomic Absorption Spectrometry	20, 20, 10 ppb
Au	Graphite Furnace	0.1 ppb

For Au, Sb, and As, all samples were initially analyzed by Instrumental Neutron Activation (INA) technique on 10-15 g of sample (Bondar-Clegg and Company). These data showed that most samples contained less than the detection limits of 2 ppb Au, 0.1 ppm Sb, and 0.5 ppm As. Test of a commercial radiochemical-NAA technique to measure Au to lower levels failed to yield acceptable reproducibility.

To achieve a high reproducibility for Au, a method was developed involving the decomposition of ~15 g samples in HF-aqua regia; extraction with small amounts of MIBK; and multiple injection of the MIBK into a graphite furnace-atomic absorption spectrometer (GFAAS) (Cameron, 1989a). The precision, expressed as relative standard deviation, is better than 10% for a range of concentrations from 0.02 to 3 ppb. Most samples were analyzed in duplicate and the two results averaged. Accuracy was evaluated by analyses of reference materials to be in the range ±10% (Table 1-3).

Most international reference materials contain much higher levels of Au than samples from the Bamble Belt. Accordingly, check analyses on a number of samples were carried out by Dr. Esko Kontas of the Geological Survey of Finland. The data given in Table 1-4 were obtained by the method of Kontas et al. (1986), which also is by GFAAS using 1.0 g samples of rocks.

Table 1-3. Analyses of standard reference materials for Au. Values in ppb;
figures in brackets indicate the number of analyses and sample weight (Hall G. E. M. et al., unpublished work).

Sample	GFAAS (This work)	Kontas (1986)	Schwarz and Barker (1976)	Benedetti et al. (1987)	Bornhorst et al. (1984)	Meier (1984)	Elson and Chatt (1983)	Anoshin and Perezhogin (1976)	Tarashima (1988)
BHVO-1 (basalt)	1.10 ± 0.04 (2, 10 g)	0.7 (2, 1 g)	1.57 ± 0.10 (6, 1 g)		1.3 (1, 1 g)	1.34 (1, 10 g)	2.3 ± 0.3 (1, 0.3-1.3 g)	1.82 ± 0.4 (6, 0.2-0.4 g)	1.78 ± 0.19 (5, 1 g)
MAG-1 (marine mud)	2.84 ± 0.81 (2, 1 g)	1.5 (2, 1 g)	2.58 ± 0.33 (6, 1 g)		2.8 (1, 1 g)	2.44 (1, 10 g)	3.1 (1, 0.3-1.3 g)	2.43 ± 0.11 (6, 0.2-0.4 g)	2.70 ± 0.56 (5, 1 g)
SGR-1 (shale)	9.33 ± 0.21 (3, 1 g)	0.6 (2, 1 g)	8.9 ± 0.30		6.0 (1, 1 g)	6.0 (1, 10 g)	9.8 (1, 0.3-1.3 g)	10.8 ± 1.8 (6, 0.2-0.4 g)	7.90 ± 0.67 (5, 0.1-2 g)
MA-N (granite)	2.83 ± 0.22 (4, 1 g)	2.3 (2, 1 g)		3.74 ± 0.3 (2, 5 g)	2.7 (1, 1 g)				3.96 ± 2.7 (5, 0.1-2 g)
GXR-3 (Fe-Mn deposit)	3.21 ± 0.24 (3, 1g)	2.4 ± 1.7 (3-5, 1g)		3.2 ± 0.2 (2, 5 g)		3 ± 0.6 (5, 10 g)			0.66 ± 0.24 (5, 0.1-2 g)
GXR-5 (soil)	6.13 ± 0.45 (6, 1 g)	7.o ± 0.9 (3-5, 1g)		8.9 ± 0.9 (2, 5 g)		7 ± 1.2 (5, 10 g)			7.3 ± 0.75 (5, 0.1-2 g)
GXR-2 (soil)	24.4 ± 0.1 (2, 5 g)	1.0 ± 0.3 (3-5, 1g)		33.5 ± 2 (2, 5 g)		22 ± 2 (5, 10 g)			24.4 ± 1.1 (5, 0.1-2 g)

Antimony, As, and Se were analyzed by a modified hydride-AAS method to obtain detection limits of 20, 20, and 10 ppb.

Table 1-4. Comparative analysis for Au (ppb) in metabasites by instrumental neutron activation analysis (INAA) and by graphite furnace-atomic absorption spectrometer (GFAAS).

Method	INAA	GFAAS		GFAAS		
Analyst	Bondar-Clegg	(this work)		Kontas		
Sample Weight	15 g	15 g		1 g		
Experiments	1	1	2	1	2	3
Sample No.						
1711	< 2	0.06	0.05	0.1	0.1	< 0.1
1712	< 2	0.04	0.05	0.1	0.1	0.2
3805	< 2	0.16	0.17	0.1	0.2	0.2
3903	< 2	0.07	0.27	0.1	0.2	0.2
3906	< 2	0.15	0.22	0.2	0.1	0.1
3907	< 2	0.11	0.18	0.2	0.2	0.2
4103	< 2	0.1	0.14	0.1	0.2	< 0.1
4506	< 2	0.06	0.1	0.1	< 0.1	< 0.1
4507	< 2	0.06	0.19	0.1	0.1	0.1

1-4-3. Contribution from the Present Study

Works carried out during the present study include:

1) Preparation and analysis of some 50 additional samples of metabasites from the amphibolite zone for major, minor and trace elements by fused disc XRF method. Sulfur was measured by ion chromatography. Gold, Sb, and As were determined by the same methods described above.

2) Petrographic study of polished-thin sections of all samples for both silicate and non-silicate minerals.

3) Investigation of the whole-rock geochemical data to characterize the nature of the initial, pre-metamorphic materials, and to evaluate the role of high grade metamorphism on the whole rock geochemistry, with emphasis on the behavior of chalcophile elements.

4) Analysis of various parageneses of sulfides, by a combination of electron- and proton-probe, instrumental neutron activation (INA), and hydride-inductively coupled plasma mass spectrometry (ICPMS) techniques.

5) Determination of sulfur isotope ratios in various rock units using laser vaporization and conventional techniques.

Sample preparation for petrographic studies, and for electron-probe, proton-probe, stable isotope, XRF and INA analyses were carried out by the writer. Sulfur isotope and XRF analyses were carried out by the writer at the Department of Earth Sciences, University of Ottawa; electron probe analysis at the Geological Survey of Canada and the Department of Geology, Carleton University; and proton probe analyses at the Department of Physics, University of Guelph. Hydride ICPMS and INA analyses were performed by Actlabs Inc., Ancaster, Ontario.

Petrographic studies allowed different parageneses of silicates, sulfides, and oxides, and their inter-relations to be identified. Sulfides are of special concern, as they are known to be the main host to Au in most rock types (c.f. Gottfried et al., 1972; Crocket, 1974; Boyle, 1979; Keays et al., 1981; Saager et al., 1982; Korobeynikov, 1989). Studies on natural assemblages have shown that Au in sulfides is more easily accessible to fluids than that locked in the lattices of rock-forming silicates and oxides (Keays and Scott, 1976; Saager et al., 1983). Cameron (1989a, b, 1993a) suggested that breakdown of sulfides in oxidized rocks at Bamble led to depletion of Au.

An initial test, by proton-induced x-ray emission technique (PIXE), to determine the variations of chalcophile elements in sulfides failed to yield satisfactory results, as concentrations of most elements were below the detection limits of PIXE. In the absence of other techniques of in-situ analysis of sulfides with high spatial resolution and low detection limits, concentrates of sulfides, of various paragenesis, were analyzed by a combination of INAA and hydride-ICPMS methods. The sulfide concentrates were prepared using magnetic separation, HF digestion, and heavy liquid methods.

To trace the behavior of sulfides during metamorphism and oxidation, sulfur isotope ratios were studied employing laser vaporization and conventional techniques. The very low sulfur

contents (commonly < 0.1%), and the fact that most samples contained more than one generation of sulfide phases, rendered the bulk analysis an inappropriate way of isotopic determinations. Laser vaporization technique allowed in-situ isotopic determination of selected sulfide grains. Isotopically homogeneous materials were characterized and calibration curves were constructed to standardize the laser raw data. In cases where the sulfide grains were too small for the laser combustion method, sulfide concentrates were prepared for conventional analysis using an HF-digestion method.

Data from the experiments are connected to the available theoretical and experimental data to inspect possible genetic links between high grade metamorphism in deep shear zones and formation of lode gold deposits.

2. Supracrustal Rocks

2-1. Introduction

The oldest exposed rocks in Bamble include a suite of supracrustal rocks, consisting of quartzite, variable gneisses and schists, marbles, and intercalated volcanic materials (Bugge, 1939; Bugge, 1943; Touret, 1968; Morton, 1971; Beeson, 1975; Starmer, 1972, 1976, 1985a; Knudsen et al., 1997). The individual rock units form broad bands but with some gradations along and across the strike (e.g. Field, 1969; Starmer, 1976). All types of supracrustal rocks may grade into granitic gneisses and may show varying degrees of granitization and microcline porphyroblastesis (e.g. Field, 1966; Starmer, 1976).

The metasedimentary rocks have a maximum detrital zircon age of 1939 ± 10 Ma (SIMS U-Pb age; Knudsen et al., 1997). A minimum detrital zircon age of 1370 Ma from the metasedimentary rocks (SIMS U-Pb age; Knudsen et al., 1997) gives the youngest age of the sedimentation. Field and Råheim (1981) determined a metamorphic age of 1536 ± 26 Ma (Rb-Sr method) for metasedimentary rocks in Arendal area, corresponding to Kongsbergian, or Gothian, Orogeny.

Supracrustal rocks were sampled from Hinnebu (amphibolite zone), Tvedestrand (transition zone), and Hissoy (granulite zone). Sample locations are shown in Figure 1-2. Considering the mineralogy and the whole-rock geochemistry, the supracrustal rocks can be grouped into several rock units (Table 2-1). Summary statistics for various rock units is shown in Table 2-2; average composition of post-Archean shales and greywackes, and mean composition of continental crust are also shown for comparison. A complete list of geochemical data is included in the Appendix 2-1. Following, the geochemistry of individual rock units are discussed.

Table 2-1. Modal composition of various supracrustal rock units; Bamble.

Metamorphic Facies	Amphibolite					Transition	Granulite
Lithology	Bt-Schist	Bt-Gneiss	Hbl-Gneisses	Calc-Silicates	Amphibolite	Grt-Bt Gneiss	Opx-Grt-Bt Granulite
Number of Samples	7	14	12	5	19	12	16
Quartz	5 - 20	20 - 70	20 - 50	x	2-15	20 - 60	20 - 60
Plagioclase	15 - 50	15 - 50	15 - 40	0 - 10	25-50	10 - 50	10 - 50
K-feldspar	0 - 4	0 - 10	o	o	o	2 - 15	0 - 5
Biotite	20 - 50	5 - 25%	0 - 5	x	1-10	5 - 20	0 - 15
Garnet	0 - 5	x	o	o	0-10	5 - 35	3 - 15
Hornblende	2 - 15	0 - 3	10 - 40	x	30 - 70	o	o
Orthopyroxene	o*	o	o	o	o	o	3 - 20
Clinopyroxene	o	o	x	35 - 65	x	o	0 - 2
Forsterite	o	o	o	0 - 10	o	o	o
Calcite	o	o	o	20 - 45	o	o	o
Titanite	x**	x	0 - 2	0 - 2	x	x	o
Graphite	o	o	o	o	o	0 - 2	x
Zircon	x	x	o	o	x	x	x
Apatite	x	x	x	o	x	x	x
Fe-Ti Oxides	x	0.5 - 2	< 0.5 - 2	x	0.5 - 3	< 0.5 - 2	0.5 - 2
Sulfides	x	x	x	1	x	x	1
Epidote	o	0 - 2	o	x	x	x	o
Chlorite	o	x	x	o	x	o	o
Muscovite	x	x	o	o	o	o	o

* Not found ** Trace (< 1%)

Table 2-2. Summary statistics for Bamble supracrustal rocks. Mean greywacke, post-Archean shale, and continental crust shown for comparison

Oxides	Bt-Schist		Amphibolite		Bt-Gneiss		Hbl-Gneiss		Calc-Silicate		Quartzite	Grt-Bt Gneiss		Opx-Grt-Bt Gneiss		Mean	Post-Archean	Continental
(Elements)	X	1 σ	X	1 σ	X	1 σ	X	1 σ	X	1 σ	X	X	1 σ	X	1 σ	Greywacke*	Shale**	Crust*
SiO_2+	50.5	3.5	50.3	2.7	69.5	3.8	61.8	3.9	42.6	5.0	87.1	68.2	3.8	65.4	6.1	69.1	62.8	61.5
TiO_2	2.0	0.7	1.8	0.9	0.6	0.18	0.97	0.32	0.7	0.5	0.75	0.9	0.4	0.75	0.23	0.72	1.0	0.68
Al_2O_3	14.8	1.8	14.7	1.4	14.5	1.28	14.5	1.7	10.8	3.6	5.7	13.9	1.4	13.4	1.6	13.5	18.9	15.1
Fe_2O_3	3.8	0.9	3.45	1.0	1.05	0.56	2.7	1.6	nd++		0.2	1.07	0.4	2.5	1.4			
FeO	10.2	3.0	9.7	2.0	3.4	1.22	3.3	1.1	nd		2.0	4.6	2.2	4.6	1.5			
Fe_2O_3+FeO	14.2	2.2	13.15	2.4	4.5	1.6	5.8	1.2	12	5.5	2.2	5.7	1.7	7.1	2.8	5.9	6.5	6.28
MnO	0.22	0.04	0.21	0.05	0.07	0.03	0.02	0.01	0.2	0.15	0.01	0.09	0.04	0.12	0.08	0.1	0.11	0.1
MgO	5.3	1.5	5.6	1.2	1.60	0.7	5.56	1.80	5.5	2.5	0.56	1.9	0.7	2.9	1.0	2.3	2.2	3.7
CaO	5.0	2.0	8.2	1.3	3.0	1.2	8.28	2.28	22	7.5	0.12	2.0	0.8	3.2	1.2	2.6	1.3	5.5
Na_2O	2.7	1.0	2.85	1.0	4.02	0.98	0.5	0.2	0.8	0.5	0.5	2.48	0.6	3.8	1.0	3.0	1.2	3.2
K_2O	3.4	1.25	1.3	0.5	2.10	0.52	0.55	0.25	0.9	0.5	1.66	3.38	1.3	1.0	0.5	2.0	3.7	2.4
P_2O_5	0.27	0.12	0.27	0.15	0.09	0.04	0.23	0.13	0.1	0.05	0.05	0.11	0.06	0.11	0.07	0.13	0.16	0.18
H_2O	2.0	0.8	1.8	0.07	0.83	0.25	1.5	0.9	1.4	0.5	0.5	0.9	0.4	0.8	0.25			
CO_2	0.15	0.15	<0.1		<0.1		<0.1		20	12	<0.1	<0.1		0.3	0.3			
Cr	80	40	82	50	24	15	55	25	650	630	35	42	12	43	20	88	110	126
Ni	45	15	50	22	15	9.0	60	25	270	170	8.0	19	10	24	8.0	24	55	56
Co	45	5.0	48	9.0	23	6.0	24	4.0	46	15	17	18	9.0	44	10	15	20	24
Sc	38	10	37	7.0	12	5.0	13.0	4.0	41	12	6.5	17.5	5.5	23	8.0	16	16	16
V	250	50	210	45	55	30	100	40	265	120	53	86	40	115	55	98	150	98
Zn	230	60	127	37	52	25	12	5.0	120	50	5.0	86	30	130	70	76		65
Mo	1.4	0.6	1.8	0.75	1.80	1.0	1.0	1.0	1.0	0.5	nd	2.0	0.6	2.6	1.0		1.0	1.1
Be	2.6	1.4	1.5	0.75	1.4	0.65	1.7	1.1	1.1	0.37	nd	1.2	0.6	0.74	0.55			2.4
S	950	650	1050	650	230	170	180	150	2250	1150	nd	630	650	3200	2400			697
Cu	60	30	63	26	26	14	15	6.0	155	95	nd	19	12	135	65	24	45	25
Se	0.08	0.05	0.11	0.06	0.02	0.01	0.3	0.14	0.2	0.1	nd	0.05	0.03	0.56	0.3			0.12
As	1.0	0.65	0.52	0.35	0.45	0.3	0.01	0.007	7.5	0.5	nd	0.07	0.04	0.3	0.2			1.7
Sb	0.07	0.05	0.055	0.03	0.034	0.015	0.02	0.01	0.17	0.08	nd	0.045	0.026	0.07	0.04			0.3
Au (ppb)	1.3	1.1	0.16	0.1	0.32	0.2	0.22	0.20	1.9	0.6	nd	0.4	0.2	0.37	0.3	4.8		2.5
Rb	145	35	42	20	77	27	25	8.0	47	29	51	114	31	42	17	72	160	78
Cs	5.5	2.5	3.3	1.7	3.10	2.2	4.00	2.00	3.0	2.0	0.7	1.3	0.7	0.6	0.4	2.2	15	3.4
Ba	450	110	310	140	520	250	75	25	340	175	348	615	215	175	67	426	650	584
Sr	100	30	185	105	242	90	570	120	170	100	62	150	27	78	28	201	200	333
Hf	6.2	1.5	5.3	2.5	8	3.0	11.0	3.0	3	1.2	30	11.2	2.0	4.0	1.5	3.5	5.0	4.9
Zr	190	100	185	105	195	52	340	70	72	36	1113	293	55	170	70	302	210	203
Y	48	15	45	22	26	8.0	48	6.0	32	15	38	41	8.0	42	20	26	27	24
Th	3.2	1.2	1.45	1.0	8.0	6.0	12.0	4.0	1.1	0.6	35.8	17	6.0	2.7	2.0	9.0	14.6	8.5
U	2.0	0.5	0.8	0.5	2.50	1.7	4.3	1.75	0.8	0.8	6.2	2.3	0.5	0.7	0.3	2.0	3.1	1.7
La	27	12	21	9.0	30	12	84	21	8.0	2.2	72	56	15	15	7.0	34	38	30
Ce	55	20	39	19	54	22	145	30	20	7.0	140	102	25	28	12	58	80	60
Sm	7.0	2.0	5.5	2.6	4.5	1.8	11	3.0	3.7	1.4	11.5	8.7	1.5	4.8	2.0	4.6	5.6	5.3
Eu	1.6	0.5	1.8	1.0	1.1	0.65	2.75	1.0	0.5	0.5	2.0	1.1	0.6	0.85	0.45	1.2	1.1	1.3
Tb	1.9	0.6	1.7	1.0	1.0	0.35	1.9	0.25	0.8	0.25	1.5	1.9	0.3	1.3	0.6	0.63	0.77	0.65
Yb	5.5	1.7	4.6	2.0	2.5	1.5	4.75	0.70	1.9	0.9	3.0	5.4	1.2	3.3	1.9	2.1	2.8	2.0
Lu	1.0	0.5	0.7	0.3	0.5	0.25	0.78	0.15	0.2	0.1	0.25	0.9	0.2	0.55	0.27	0.37	0.43	0.35
Cl	450	200	300	170	96	45	58	22	520	280	nd	105	67	135	65			472
F	1600	550	980	500	430	184	1100	350	300	110	nd	570	275	400	150			525

X = arithmetic mean σ = standard deviation + oxides in %; elements in ppm ++ not detected * Wedepohl (1995) ** Taylor and McLennan (1985)

2-2. Biotite Schist

Biotite schists were sampled from traverse 11 in Hinnebu area (Figure 1-2). These are medium grained rocks with schistosity defined by the alignment of biotite grains. Modal composition and summary statistics for biotite-schists are shown in Tables 2-1 and 2-2, respectively.

Biotite, plagioclase, and quartz are the major minerals, being accompanied by minor hornblende, garnet, K-feldspar, titanite, apatite, Fe-Ti oxides, and sulfides. Pyrite is the principal sulfide phase occurring commonly as interstitial to silicates; it is also present as secondary fracture filling and replacement bodies. Pyrrhotite was found in one sample (2012) as the main sulfide; it is rare in other samples. Chalcopyrite may occur associated with both pyrite and pyrrhotite in composite grains, or less commonly, as discrete grains.

2-2-1. Geochemistry

The biotite schists are characterized by low SiO_2, but relatively high $FeO_{(total\ Fe)}$, MgO, CaO, TiO_2, and P_2O_5, and in this respect are comparable to concordant amphibolites from the same area that originated from mafic volcanic materials (Table 2-2). However, the relatively high concentrations of large ion lithophile elements (LILE) distinguishes the biotite schists from mafic rocks. Considering the whole rock geochemistry, the biotite schists may be compared to low-silica metapelites and micaschists (c.f. McLennan et al., 1984; Taylor and McLennan, 1985). For the sake of discussion, the distribution of elements in the biotite schists is compared against the mean composition of Post-Archean Australian Shale (Figure 2-1). Mean composition of low-silica metapelites from West Greenland, and of concordant amphibolites from Hinnebu, are also shown for comparison.

The biotite schists display a marked depletion in LILE and light rare earth elements (LREE) but a considerable enrichment in heavy rare earth elements (HREE) and most transition metals compared to PAAS. The pattern of variations closely follow that of the low-silica metapelites or concordant amphibolites.

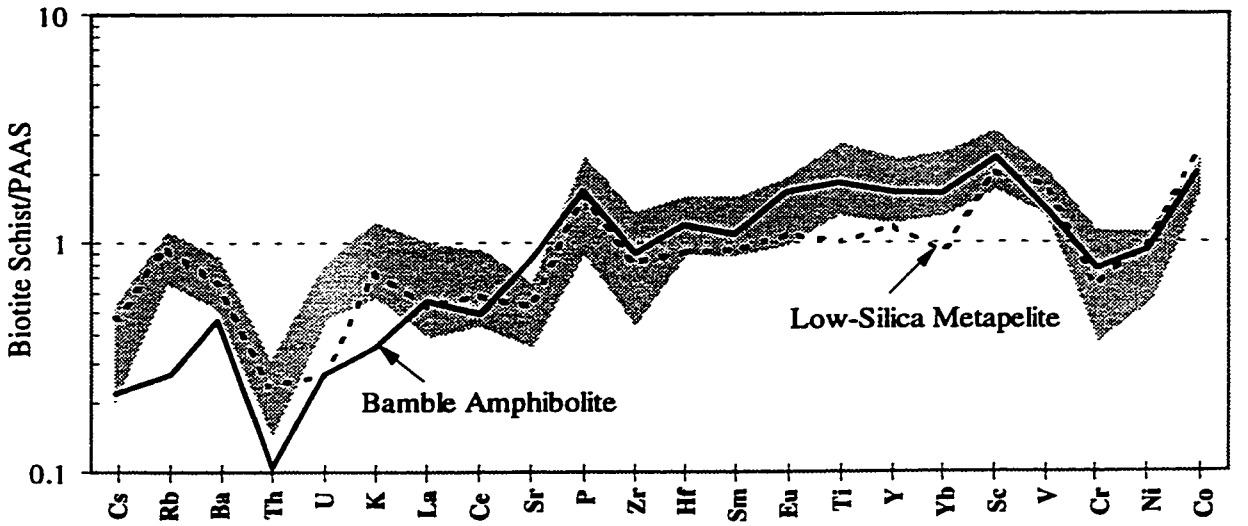

Figure 2-1. Spidergram plot for elements in the Bamble biotite schists, normalized to the mean composition of post-Archean Australian Shale (PAAS). The shaded area represents $\bar{x} \pm \frac{1}{2}\sigma$. Mean composition of the Bamble concordant amphibolites and West Greenland low-silica metapelites, both normalized to PAAS, are shown for comparison. Normalization data from Taylor and McLennan (1985).

Rare earth elements (REE) have frequently been shown to preserve a record of the source rock composition, even in strongly metamorphosed sediments (e.g. McLennan et al., 1979; Taylor and McLennan, 1985, Taylor et al., 1986). A chondrite-normalized REE plot for the biotite schists is shown in Figure 2-2. Mean composition of Archean and Post-Archean sedimentary rocks are also shown for comparison.

The biotite-schists are distinguished from Archean sediments by considerably higher Σ REE and negative Eu anomaly. A negative Eu anomaly is a characteristic feature of most post-Archean sediments, as the main source of materials for Proterozoic and Phanerozoic sediments are Eu-depleted granitoids (e.g. Condie, 1976, Taylor and McLennan, 1985).

The REE pattern of the biotite schists is comparable to that of the post-Archean shales, or early Proterozoic metapelites (Figure 2-2). However, the biotite schists are relatively depleted in LREE, but enriched in HREE, and display a less fractionated REE pattern. The La_N/Yb_N

ratio in the biotite schists is considerably lower than that for PAAS, or early Proterozoic shales (2 to 3.6 vs. 9.2 and 10.2, respectively).

The REE pattern of the biotite-schists, with relatively low La_N/Yb_N ratios, compares favorably with that of the concordant amphibolites from the same area (Figure 2-2), suggesting a basaltic source region for the biotite-schists. Contribution from a basaltic source rocks is also supported by Al/Ti ratios, as the Al_2O_3/TiO_2 ratios in the biotite schists (4–12) are very close to that in mafic rocks (3-8). Al/Ti ratios in sedimentary rocks generally retain their source rock values (e.g. Holland, 1984; Hayashi et al., 1997). However, the relatively high contents of LILE suggest that alkaline igneous or metamorphic rocks had important influence.

Alternatively, the biotite schists could be the product of alkaline metasomatism of basic rocks. The major element geochemistry of the biotite schists is comparable to that of the concordant

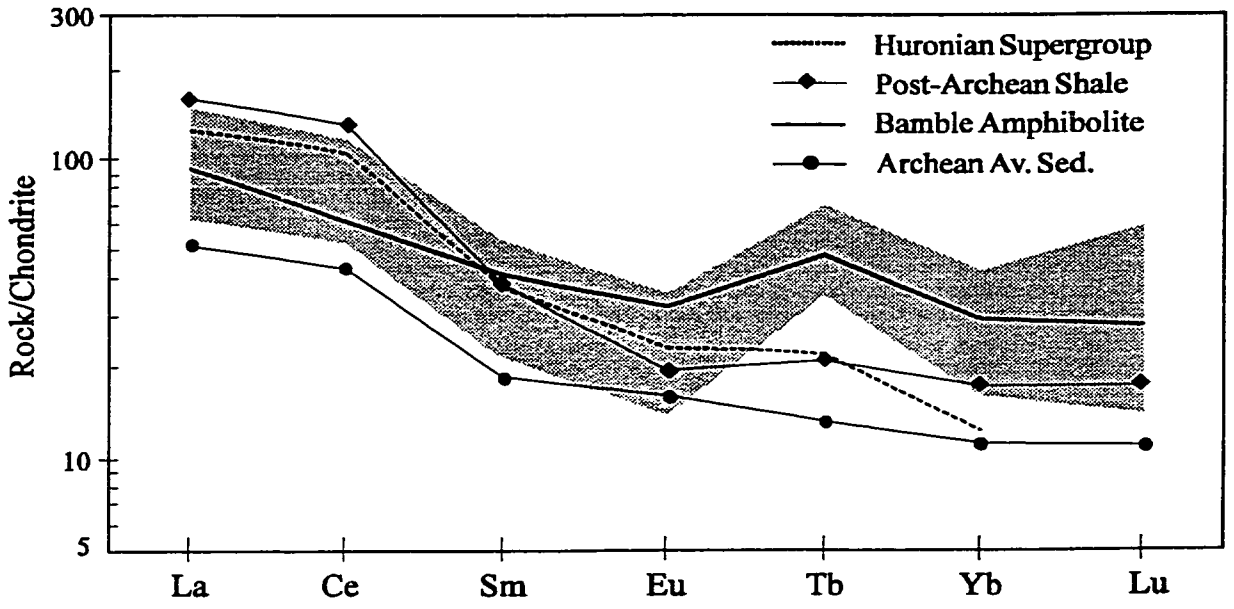

Figure 2-2. Chondrite-normalized REE plot for Bamble biotite schists. Shaded area represents $\bar{x}$ $\pm$½σ.). Distribution of REE for Archean average sedimentary rocks (Taylor and McLennan, 1980), Early Proterozoic shales from Huronian Supergroup (McLennan, 1979), Post Archean Australian Shale (Taylor and McLennan, 1985), and Bamble concordant amphibolites (present study) are shown for comparison. Chondrite values after McDonough and Sun (1995).

amphibolites (Table 2-2). The spidergrams in Figure 2-1 indicate that most minor elements are similarly distributed in the two rock types, the major differences being higher contents of LILE, particularly K and Rb, and lower content of Sr.

Potassium and Rb were probably introduced into the amphibolites (now biotite schists) at the expense of Ca and Sr. A metasomatic origin is also supported by the higher Ba/Sr and Rb/Sr ratios in the biotite schists compared to the mean post-Archean shale or low-silica metapelites. LILE may have been carried in halide solutions, as the biotite schists are also considerably enriched in halogens, Cl and F (Table 2-2). One sample is strongly enriched in both Cl (9500 ppm) and F (6700 ppm).

2-2-2. Distribution of Chalcophile Elements

Assuming a sedimentary origin, distribution of chalcophile elements in the biotite schists may be compared to that in shales or slates (Figure 2-3). The biotite schists display large variations

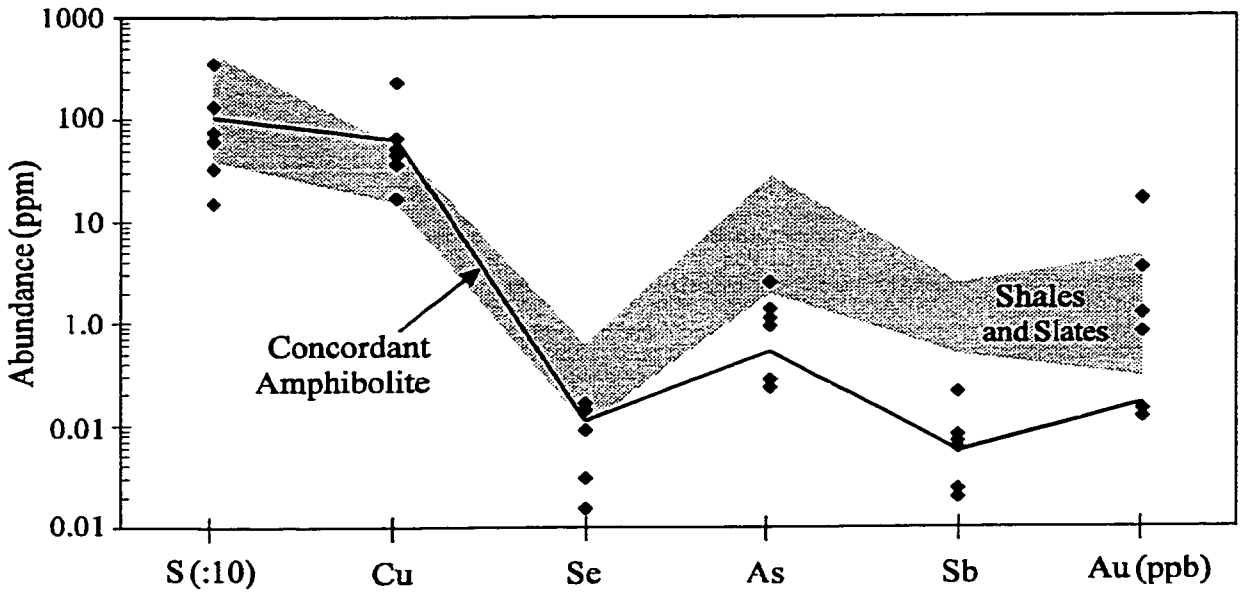

Figure 2-3. Distribution of chalcophile elements in the Bamble biotite schists. The common range of the abundances of chalcophile elements in shales and slates shown for comparison. Also shown is the mean composition of the Bamble concordant amphibolites. See Appendix 2-2 for the average composition of shales and slates.

in chalcophile elements. Sulfur is in the same range as in the average shales, or slightly depleted. Cu is enriched; Se, As, and Sb are considerably depleted. Gold varies from 0.05 ppb to 16 ppb. Compared to the concordant amphibolites, the biotite schists are enriched in Au and As. Other elements are almost equally distributed in the two rock types. Presuming a secondary metasomatic origin for the biotite schists, the alkaline-rich fluids have also introduced some Au and As into the rocks. One sample (3621) is remarkably enriched in Au (16.5 ppb).

2-3. Biotite Gneiss

This is a medium to coarse grained rock with a well developed gneissosity. All samples are from traverses 11 and 12 in Hinnebu area in the amphibolite zone (Figure 1-2). Modal composition of the biotite gneisses is shown in Tables 2-1. Summary statistics is given in Table 2-2.

Quartz, plagioclase, and biotite are the main constituents. Accessory minerals include K-feldspar, hornblende, titanite, epidote, apatite, Fe-Ti oxides, and sulfides. Minor chlorite, muscovite, and carbonates are present as secondary alteration products after biotite and feldspars. Trace pyrite and chalcopyrite, the only sulfides present, appear as interstitial to silicates.

2-3-1. Geochemistry

Considering the whole rock geochemistry, the Bamble biotite gneisses are comparable to average post-Archean greywacke (Figure 2-4). Similarly, they may be compared to the well known Proterozoic paragneisses from Adirondack Mountains, New York, where Engel and Engel (1958, 1960) postulated a greywacke or a monotonous tuff as the initial lithology. The relatively low contents of Cr, Ni, Sc, V, and P in the biotite gneisses suggest that the initial sediments originated mainly from felsic rocks. This is supported by Al_2O_3/TiO_2 ratios, as the values for the biotite gneisses (20-45) correspond to those in felsic igneous rocks (>20, Hayashi et al., 1997).

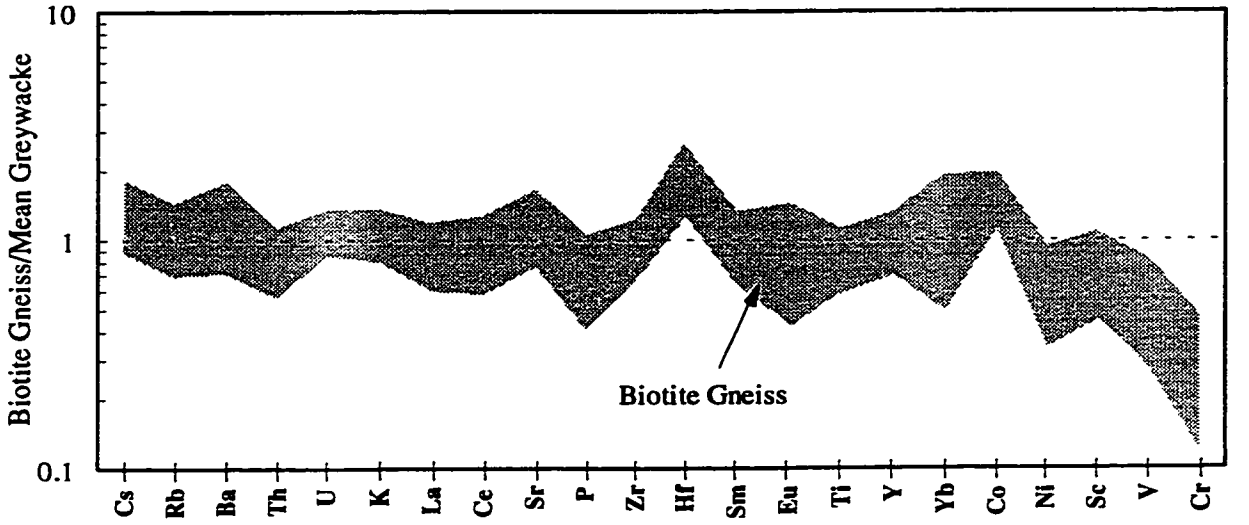

Figure 2-4. Spidergram plot for elements in the Bamble biotite gneisses, normalized to the mean composition of greywackes. The shaded area represents $\bar{x} \pm \frac{1}{2}\sigma$. Normalization data after Wedepohl (1995).

Rare earth elements provide further information on the origin of the biotite gneisses. A chondrite-normalized REE plot is shown in Figure 2-5. Mean Archean and Phanerozoic quartz-intermediate greywacke, and mean post-Archean shale are also shown for comparison.

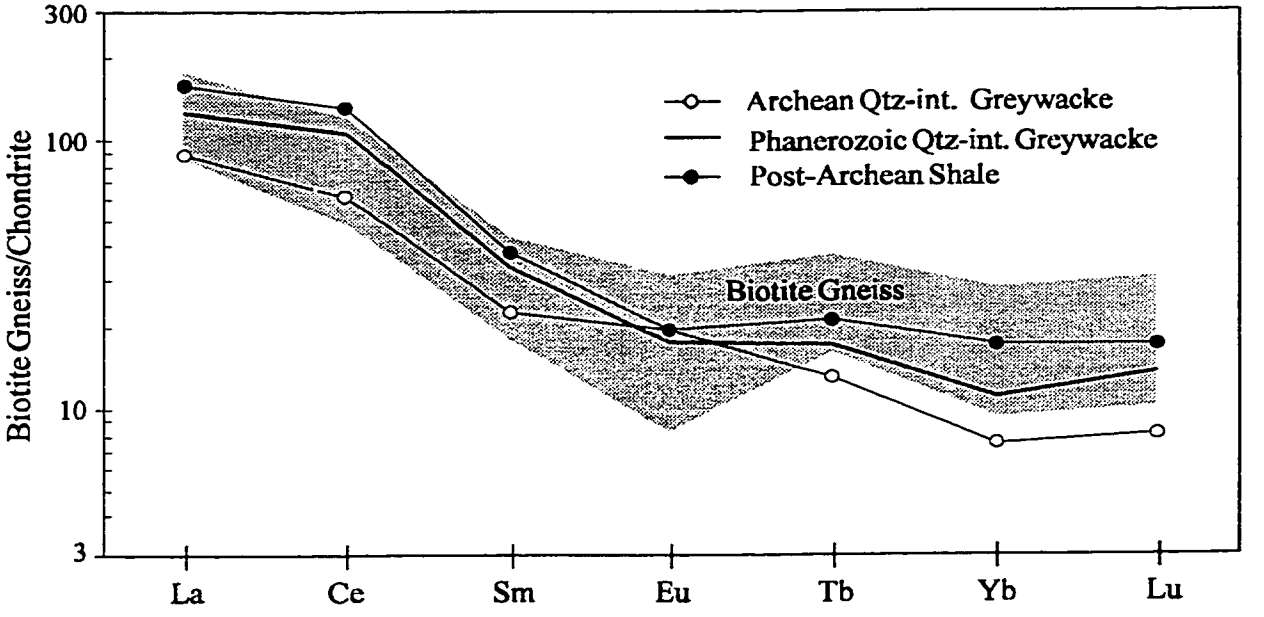

Figure 2-5. Chondrite normalized REE plot for Bamble biotite gneisses. The shaded area represents $\bar{x} \pm \frac{1}{2}\sigma$. Distribution of REE for Archean and post-Archean greywackes and post-Archean shales (Taylor and McLennan, 1985) are shown for comparison. Chondrite values from McDonough and Sun (1995).

The biotite gneisses are distinguished from Archean greywackes by higher ΣREE and negative Eu anomaly. This is in agreement with data from other studies of post-Archean greywackes and meta-greywackes (c.f. Taylor and McLennan, 1985). The chondrite-normalized REE pattern of the biotite gneisses conforms well with that of the mean Phanerozoic quartz-intermediate greywacke. A comparison may be made to Post-Archean Shale; however, the biotite gneisses are relatively depleted in LREE.

2-3-2. Distribution of Chalcophile Elements

Assuming a greywacke protolith, distribution of chalcophile elements in the biotite gneisses is compared against the common range of the abundances of the elements in greywackes (Figure 2-6). The biotite gneisses display large variations in chalcophile elements. Compared to the greywackes, all elements, except Cu, are considerably depleted.

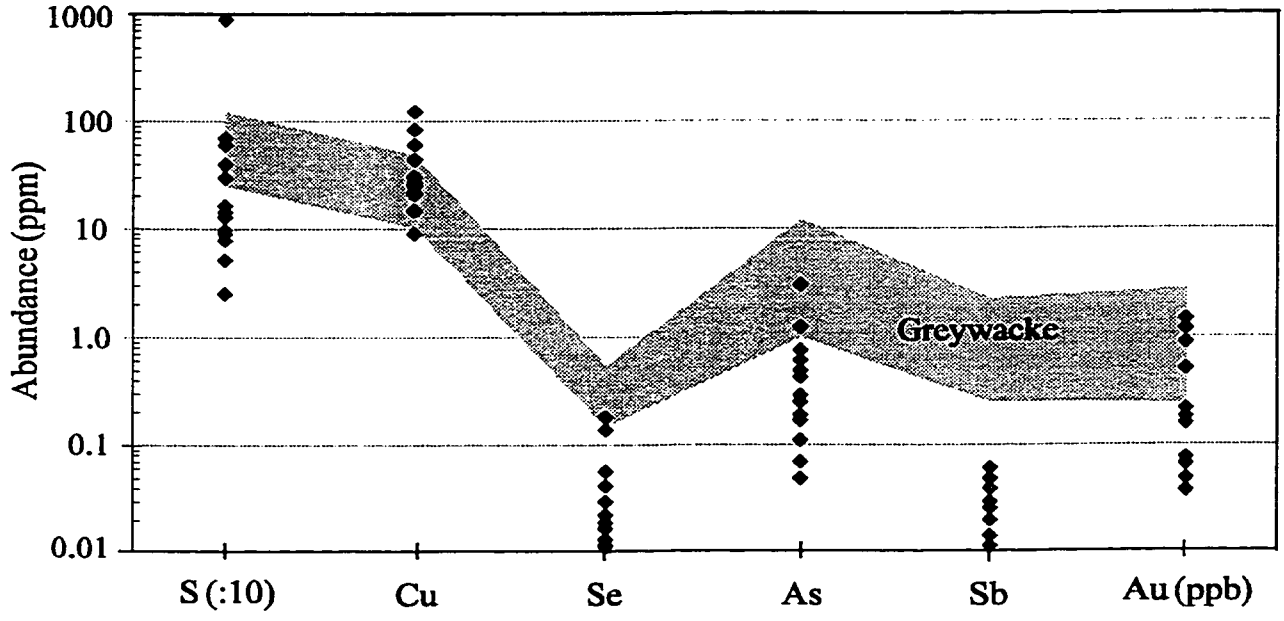

Figure 2-6. Distribution of chalcophile elements in the Bamble biotite gneisses. The common range of the abundances of chalcophile elements in greywackes is shown for comparison. See Appendix 2-2 for greywacke composition.

2-4. Quartzite and Impure Quartzite

Quartzites and impure quartzites are widespread in Bamble, particularly in the amphibolite zone (Field, 1966; Beeson, 1975; Starmer, 1969, 1976; Nijland, 1990; Knudsen et al., 1997). Primary sedimentary structures, like cross-bedding and ripple marks, are locally preserved (Nijland 1990). The thin persistent nature of the quartzites is interpreted as a littoral sandstone deposit (Starmer, 1969). Our data is limited to two samples of impure quartzites from Transition zone in Tvedestrand.

Quartz, occurring as granoblastic polyhedral grains, is accompanied by minor feldspars (both plagioclase and K-feldspar), biotite, and garnet. Detrital zircon is abundant in one sample, giving rise to Zr content in excess of 1000 ppm, and high values of REE. Geochemical data on the two quartzite samples is shown in the Appendix 2-1. No data is available on the distribution of chalcophile elements. They will not be further discussed.

2-5. Hornblende Gneiss

This is a medium-grained rock with hornblende as the dominant ferromagnesian mineral defining the foliation. Hornblende gneisses were collected along traverse 11 in Hinnebu. Hornblende, plagioclase and quartz are the main minerals being accompanied by accessory (<1%) biotite, titanite, and Fe-Ti oxides (ilmenite, magnetite, and hematite). Trace sulfides (Pyrite>> chalcopyrite) as interstitial to silicates were found in half of the samples. Modal composition and summary statistics for hornblende gneisses are shown in Tables 2-1 and 2-2, respectively.

2-5-1. Geochemistry

The hornblende gneisses are characterized by relatively low contents of K and Na (Na_2O + K_2O <1.5% in most samples). The chemistry of the gneisses can not be matched with any known classical sedimentary or igneous protoliths. The initial lithology is probably a modified sediment or an intermediate, low Na-K, igneous rock. Considering the SiO_2 content (mean 61.8%), the parent lithology could be an intermediate igneous rock; however, the very low

K_2O and Na_2O contents (mean 0.55% and 0.5%, respectively) are inconsistent with a direct igneous origin. For the sake of discussion, a comparison is made to the mean composition of the continental crust (Figure 2-7). Mean composition of Andean-type andesite, a common intermediate igneous rock, is also shown for comparison.

The gneisses are strongly depleted in some LILE (K, Rb, and Ba), while enriched in others (U, Th). They are also enriched in REE. The normal abundance of Cs is in contrast to the strong depletion of K, Rb, and Ba. This dual character of the hornblende gneisses can not be easily explained by either of magmatic or sedimentary processes.

The hornblende gneisses are comparable to andesites with respect to the concentration of the relatively compatible and less mobile elements (i.e. Ni, Cr, V, Sc, P, and Ti). However, the gneisses are considerably enriched in REE and HFSE. This is difficult to be attributed to secondary introduction of these elements, as they are generally known to be immobile during alteration and metamorphic processes (c.f. Drury, 1978; Weaver and Tarney, 1980, 1981; Hajash, 1984; Jahn and Zhang, 1984; Condie and Allen, 1984).

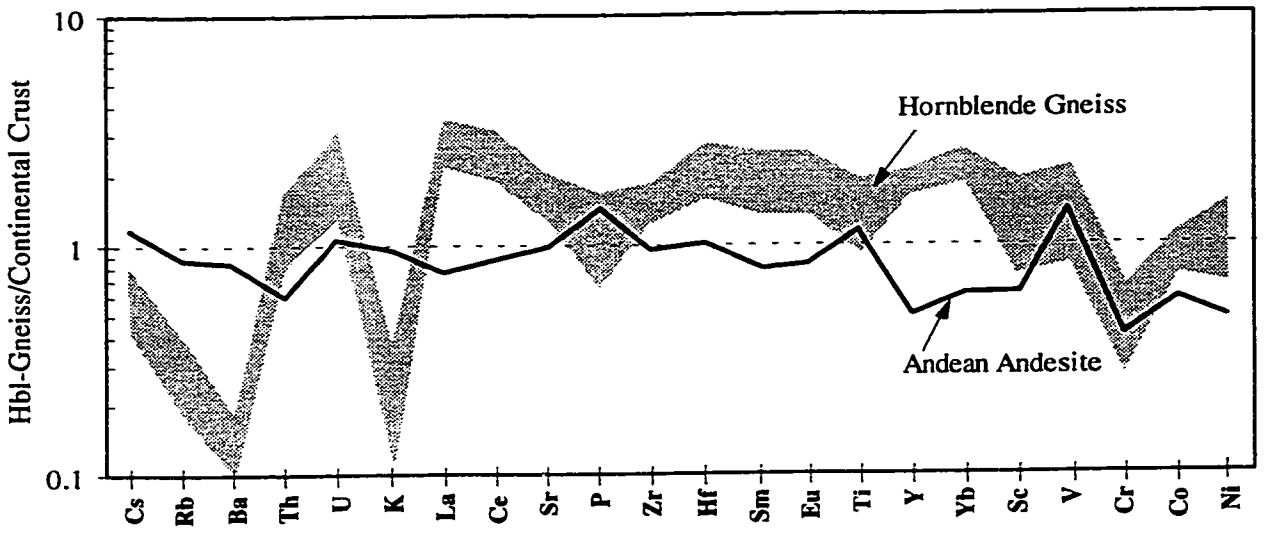

Figure 2-7. Spidergram plot for elements in the Bamble hornblende gneisses, normalized to the mean continental crust. Shaded area represents $\bar{x} \pm \frac{1}{2}\sigma$. Average composition of Andean andesites (Lopez-Escobar et al., 1977), also normalized to the mean continental crust, is shown for comparison. Normalization data from Wedepohl (1995).

The hornblende gneisses are distinguished from the biotite schists and biotite gneisses by a more fractionated REE pattern. In this regard, the gneisses may be compared to Andean andesites (Figure 2-8). The hornblende gneisses further display relatively high contents of REE. High Σ REE is typical of fractionated, alkaline igneous rocks (c.f. Ewart, 1982, Wilson, 1989). A comparison to continental trachyandesites is shown in Figure 2-8.

The high Σ REE in the gneisses may be attributed to the common presence of hornblende, as REE partition strongly into this mineral during magmatic crystallization (c.f. Grouch, 1989). Considering the high concentration of REE, the parent rock should have formed from a differentiated magma. This is supported by the similarly high concentrations of incompatible elements, Th, U, Y, Zr, and Hf. Assuming a magmatic origin, the initial rock was severely depleted in K, Rb, and Ba during metamorphism. Cesium might have been reintroduced into the gneisses.

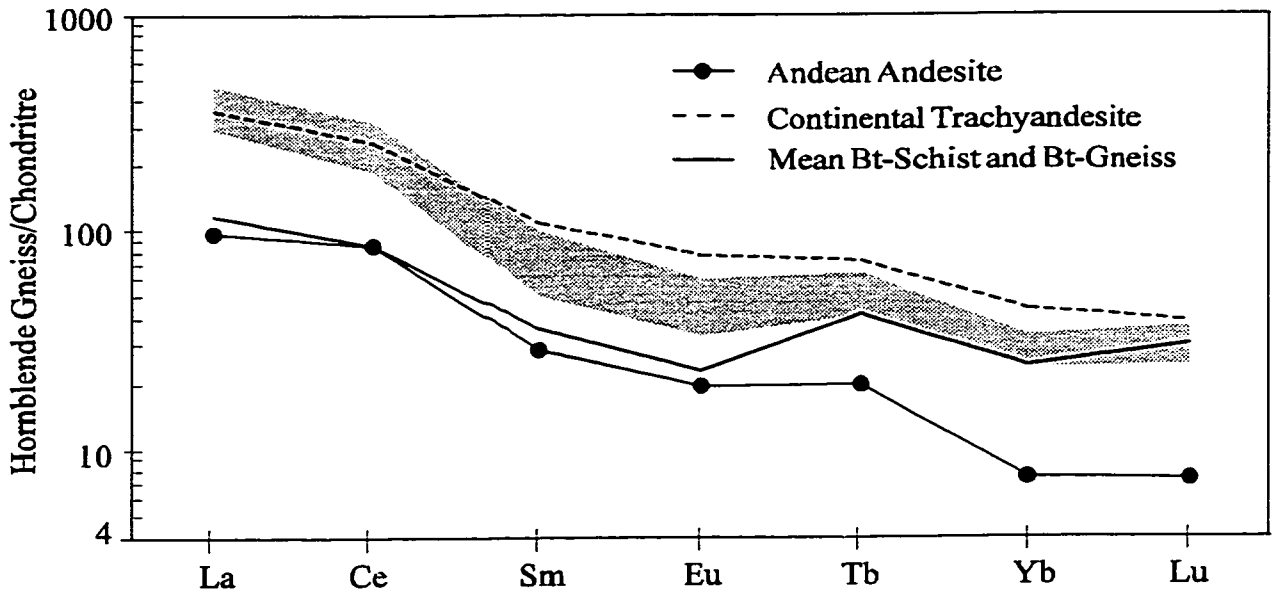

Figure 2-8. Chondrite-normalized REE plot of the Bamble hornblende gneisses. The shaded area represents $\bar{x} \pm \frac{1}{2}\sigma$. Distribution of REE for Andean andesites (Lopez-Escobar et al., 1979), continental trachyandesites (Wilson, 1989) and mean Bamble biotite-schist and biotite gneiss is shown for comparison.

2-5-2. Distribution of Chalcophile Elements

Assuming an igneous origin, the distribution of chalcophile elements in the hornblende gneisses may be compared to that in felsic igneous rocks (Figure 2-9). The hornblende gneisses are strongly depleted in Au, Sb, Se, and As. They are also depleted in S. The mean concentration of Au in the gneisses (0.22 ppb) is 20% of that in felsic igneous rocks elsewhere.

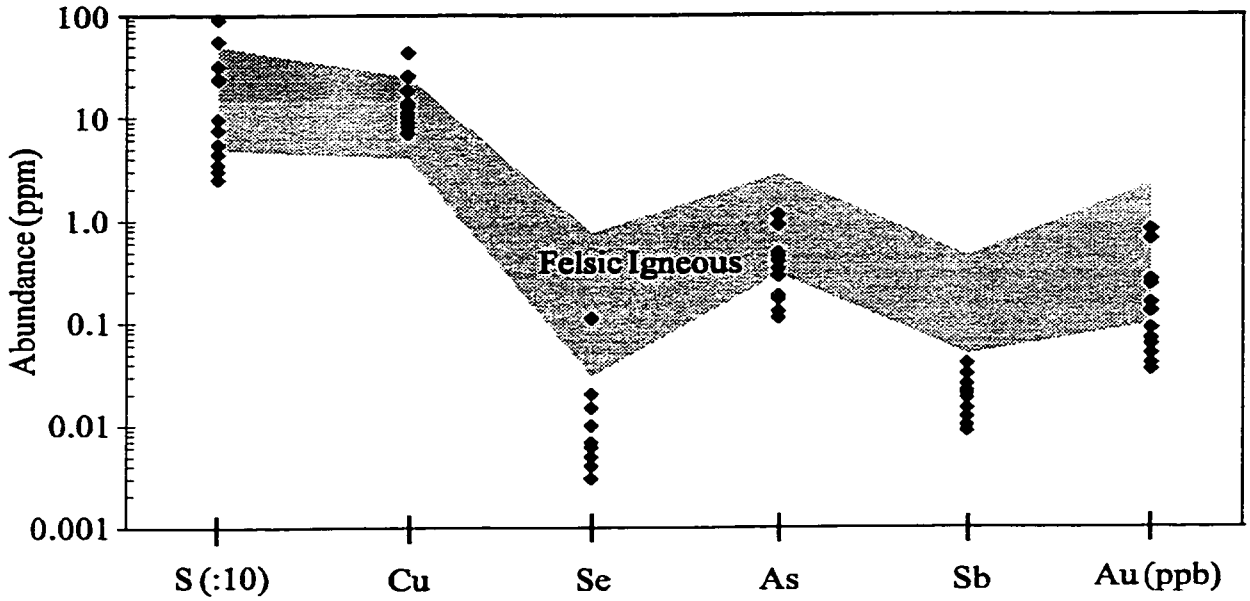

Figure 2-9. Distribution of chalcophile elements in the Bamble hornblende gneisses. The common range of the abundances of chalcophile elements in felsic igneous rocks is shown for comparison. See Appendix 2-2 for composition of felsic igneous rocks.

2-6. Calc-Silicates

Metamorphosed carbonates and impure carbonates occur sporadically in Bamble (Field, 1966; Beeson, 1975; Starmer, 1976). Calc-silicates were sampled along traverse 10 in Tvedestrand. Calcite, diopside, forsterite, plagioclase, and quartz are the main constituents, being accompanied by accessory titanite, Fe-Ti oxides, and sulfides. Pyrrhotite, commonly occurring as interstitial to silicates and carbonates, is the dominant sulfide. Minor pyrite and chalcopyrite accompany pyrrhotite in composite sulfide grains, or as discrete interstitial grains. Modal

composition and summary statistics for the calc-silicates are shown in Tables 2-1 and 2-2, respectively.

2-6-1. Geochemistry

Calc-silicates display relatively wide variations in the distribution of major and minor elements, implying a heterogeneous initial composition. Considering the mineralogy and the whole rock geochemistry, the initial sediments were possibly argillaceous carbonates, or calcareous shales. Relatively high content of S (Table 2-2) suggests a euxinic environment of deposition.

2-6-2. Distribution of Chalcophile Elements

From data in the literature, carbonates and impure carbonates exhibit a large variation in the abundance of chalcophile elements. Concentration of Au in carbonates varies in a wide range from 0.2 to 20 ppb, with an estimated average of 1.5 ppb (Allemann and Crocket, 1974; Boyle, 1979; Korobeynikov, 1985). A comparison to the mean continental crust, or mean carbonates, indicates that Bamble calc-silicates carry considerably higher contents of S, Cu, and As (Figure 2-10). They are also enriched in Au and Se; Sb is depleted. One sample (5502) containing 18 ppb Au is not considered in the average.

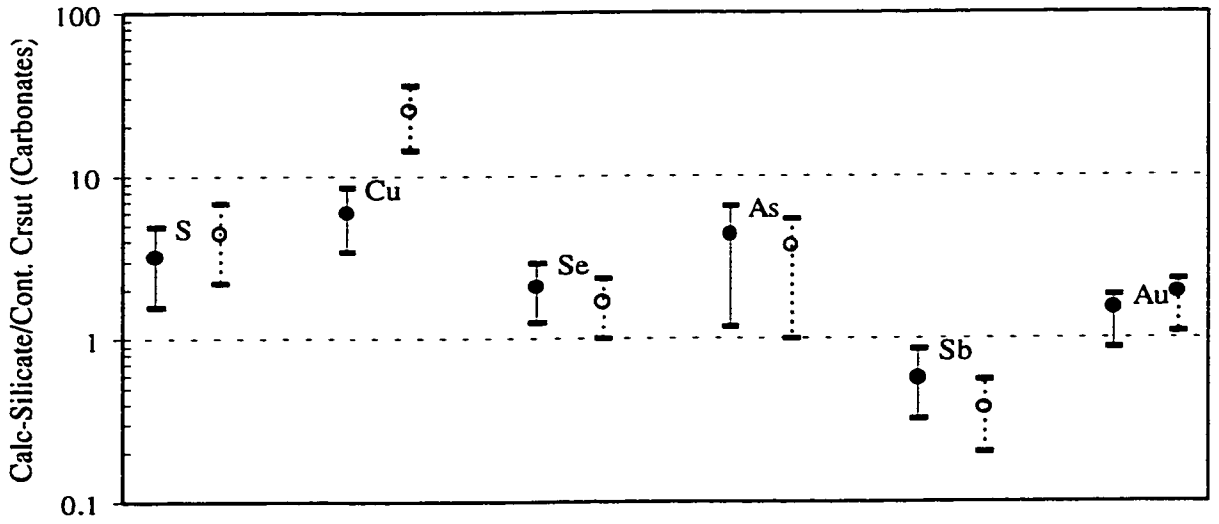

Figure 2-10. Distribution of chalcophile elements in the Bamble calc-silicates, normalized to the mean continental crust (solid bars) and mean carbonates (broken bars). Circles represent the mean values, and bars represent 1σ standard deviation. See Appendix 2-2 for normalization data.

2-7. Amphibolites

Thin concordant amphibolite bands are common in Bamble. The modal composition of the amphibolites is rather consistent (Table 2-1). Hornblende and plagioclase are the main constituents, accompanied by minor quartz, biotite, clinopyroxene, garnet and Fe-Ti oxides. Accessory minerals include K-feldspar, apatite, zircon, titanite, and sulfides. Chlorite, epidote, and sericite may occur as secondary alteration products after hornblende, plagioclase, and biotite. Pyrite and subordinate chalcopyrite are the main sulfide minerals, commonly occurring as interstitial to silicates and oxides. Pyrrhotite is rare. Pyrite also occurs as fracture filling and replacement bodies. The amphibolites were sampled along traverses 11 and 12 in Hinnebu area (Figure 2-2).

2-7-1. Geochemistry

The whole rock geochemistry of the concordant amphibolites may be compared to that of the basaltic rocks, or Fe-Mg rich sediments. Similar amphibolite intercalations have been reported from Risor area (Field, 1966; Starmer, 1976). According to the authors, some of the thicker bands, show minor intrusive features. Summary statistics for concordant amphibolites is shown in Table 2-2.

Distribution of the elements commonly known as immobile, or least mobile, in alteration and metamorphic processes (i.e. Ti, Ni, P, Zr, and Y) may be used to reveal the origin of the metamorphosed rocks. Plot of the amphibolites on a TiO_2-Ni discriminant diagram (Figure 2-11-A) exhibit a negative correlation, consistent with an igneous origin (c.f. Van de Kemp, 1969). A basic igneous origin is also supported by plot of the amphibolites on the Ni-Zr/TiO_2 discriminant diagram of Winchester et al. (1980), as all data points fall in the igneous field (Figure 2-11-B).

To investigate the role of alteration and metamorphism on the initial geochemistry, Harker diagrams have been constructed with Niggli Mg# as differentiation index (Figure 2-12). Distribution of the relatively immobile elements follow typical magmatic trends (Figure 2-12-

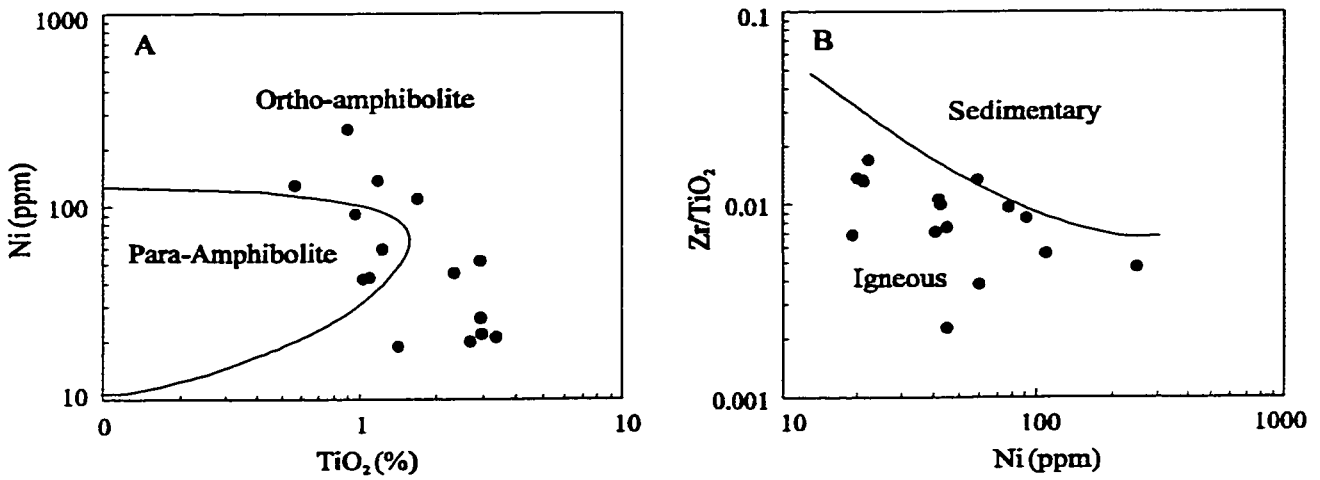

Figure 2-11. Discrimination diagrams used to denote the origin of the concordant amphibolites. (A) Ni-TiO_2 (Van de Kemp, 1969) and (B) Ni-Zr/TiO_2 (Winchester et al., 1980) plots to distinguish between sedimentary and igneous protoliths.

C-H). Large ion lithophile elements (LILE) display large scatters, implying that the elements were variably mobile during alteration and metamorphism. Variations of K_2O and Rb are shown in Figure 2-12-A-B.

On a chondrite-normalized plot, the amphibolites display a marked enrichment in the incompatible elements (Figure 2-13), and in this respect are comparable to calc-alkaline basalts (c.f. Pearce, 1982; Kay, 1984). A comparison to basalts of known tectonic settings suggest a destructive plate margin for the amphibolites (c.f. Pearce, 1982). As a reference, the mean composition of Andean calc-alkaline basalts is shown in Figure 2-13.

2-7-2. Distribution of Chalcophile Elements

The Bamble concordant amphibolites are considerably depleted in Au and Sb compared to the general abundance of these elements in mafic igneous rocks elsewhere (Figure 2-14). They are also depleted in As and Se. Sulfur and Cu, however, show normal abundances. The relatively low contents of the chalcophile elements might be of primary magmatic origin, or, a consequence of alteration and/or metamorphism.

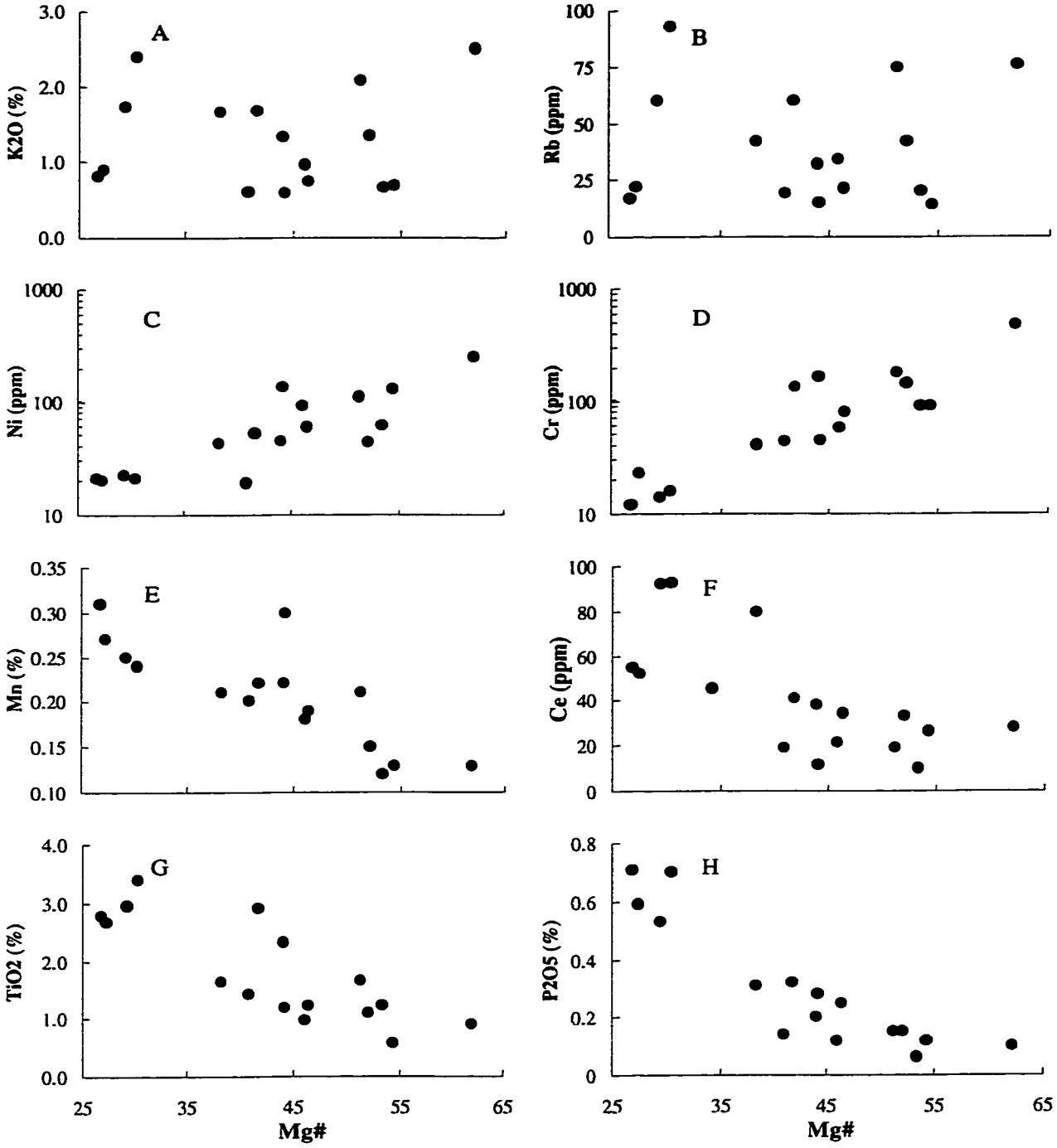

Figure 2-12. Variations of elements (oxides) with Niggli Mg# in concordant amphibolites; Bamble.

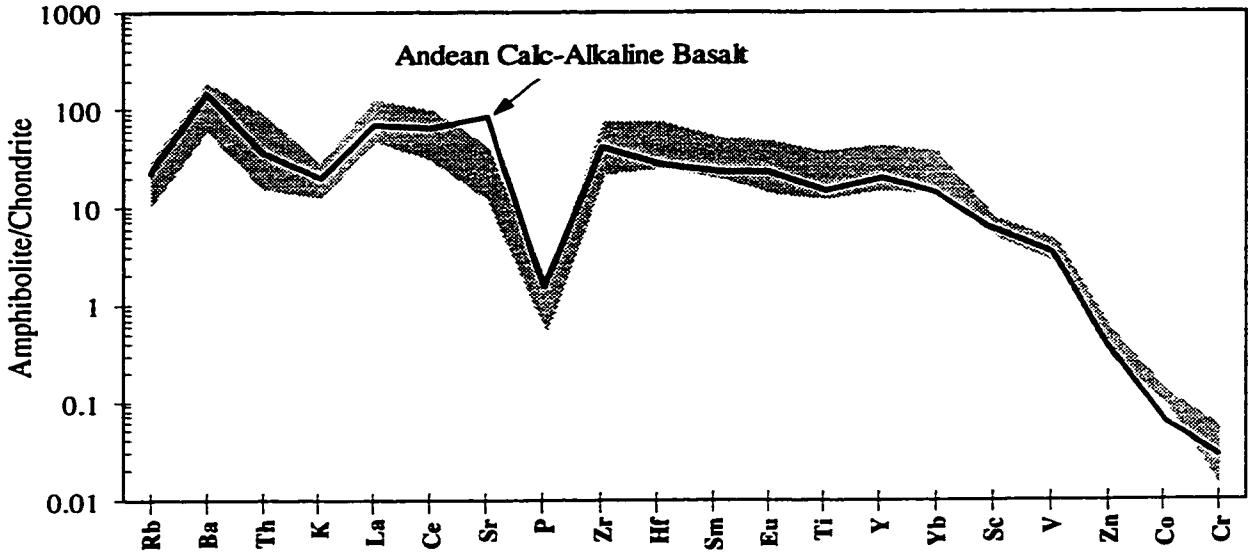

Figure 2-13. Chondrite-normalized plot for concordant amphibolites. Shaded area represents $\bar{x} \pm \frac{1}{2}\sigma$. Mean composition of Andean calc-alkaline basalts (solid line) (Ewart, 1982) shown for comparison. Chondrite values from McDonough and Sun (1995).

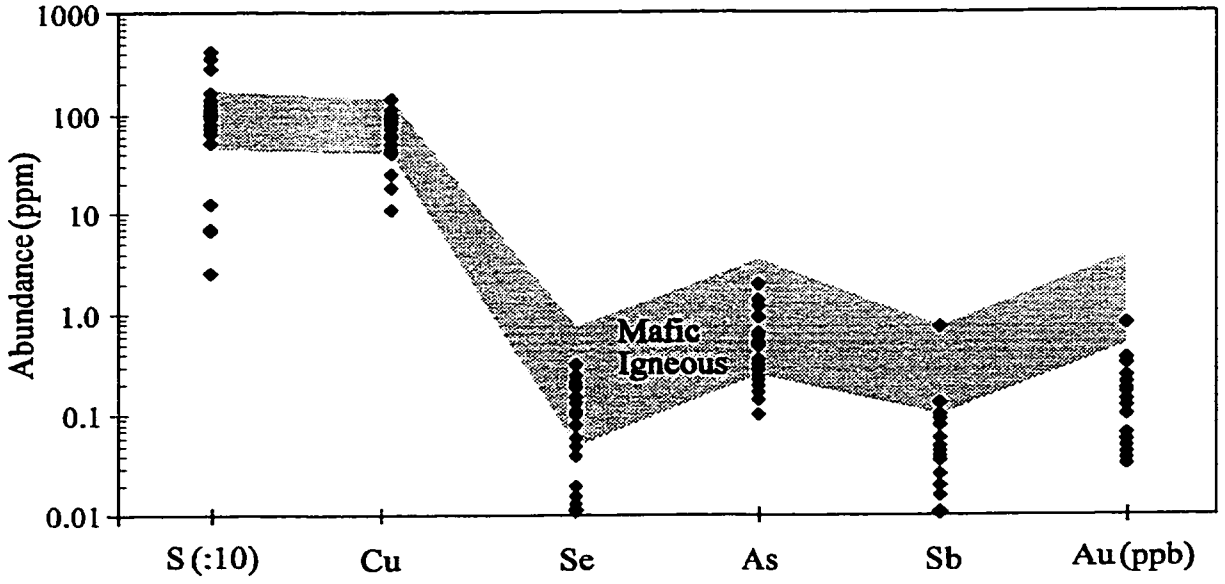

Figure 2-14. Distribution of chalcophile elements in the Bamble concordant amphibolites. The common range ($\bar{x} \pm 1\sigma$) of the abundances of chalcophile elements in mafic igneous rocks is shown for comparison. See Appendix 2-2 for composition of mafic igneous rocks.

2-7-2-A. Effects of Magmatic Differentiation

Chalcophile elements behave incompatibly during differentiation of mafic magmas, being increasingly concentrated in the late Fe-rich fractions (e.g. Hamlyn et al., 1985; Brügmann et al., 1987). Distribution of chalcophile elements against Niggli Mg# in the concordant amphibolites indicates that the primary magmatic patterns are preserved, in spite of the high-grade metamorphism (Figure 2-15). The similar patterns of distribution, exhibited by trendlines in Figure 2-15, suggest that all elements behaved similarly during initial emplacement and subsequent alteration and metamorphism.

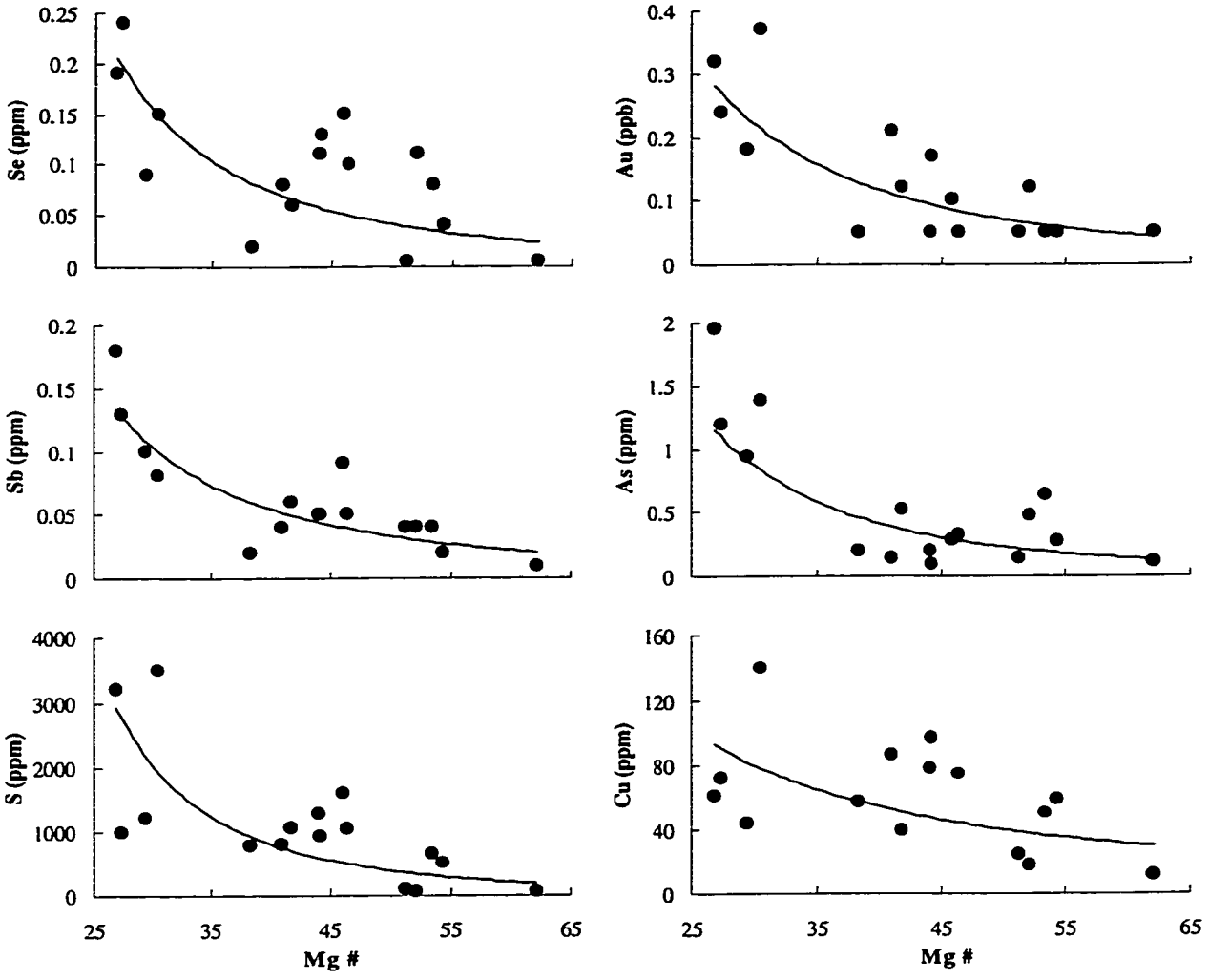

Figure 2-15. Distribution of the chalcophile elements with respect to Niggli Mg# as differentiation index. Trendlines correspond to the least squares fit through points according to the power equation $y = cx^b$.

2-7-2-B. Effects of Alteration and Metamorphism

The concordant amphibolites originated from submarine basaltic lavas. Interaction of submarine lavas with seawater may lead to mobilization of chalcophile elements. Variable loss of S has been reported by several authors (e.g. Keays and Scott, 1976; Hamlyn et al., 1985; Gitlin, 1985). However, S in the amphibolites occurs in the same range as in the mean mafic rocks elsewhere, implying that no significant gain or loss in the element occurred during alteration and metamorphism. The common occurrence of secondary pyrite as fracture filling and replacement suggests that S has been variably remobilized and reprecipitated. The timing of this event, however, is difficult to establish.

Selenium and Cu also occur in the same range as in the mean mafic rocks (Figure 2-14). Selenium has been reported to be inert during seawater alteration of submarine lavas (Hamlyn et al., 1985). Studies on the mobility of Se under a wide range of Eh and pH suggests that it is considerably more stable than S during low temperature alteration (Yamomoto, 1976; Howard, 1977). A sporadic loss of Cu was indicated by Keays and Scott (1976) and Hamlyn et al. (1985) for submarine basalts.

Gold has been indicated to be mobile during submarine alteration of mafic and ultramafic rocks (Keays and Davison, 1976; Ross and Keays, 1979; Hertogen et al., 1980; Oshin and Crocket, 1982). Precious metal depletion is a widespread and primary characteristic of mid-ocean ridge basalts (Hertogen et al., 1980). Keays and Scott (1976) showed that the interior, crystalline parts of pillow lavas are depleted in Au and S, by a factor of 7 and 2.5 respectively, relative to their glassy rims. The depletion was attributed to the loss of the more easily accessible Au in sulfides from the crystalline pillow interiors during seawater-basalt interaction.

Whether the relatively low contents of Au, As, and Sb in the amphibolites is a primary feature inherited from the parent magma, or a secondary, submarine alteration, or metamorphic effect, is difficult to substantiate. That the initial magmatic trends are still preserved, implies that magmatic processes had important effects. This is further discussed in Chapter 6.

2-8. Garnet-Biotite Gneiss

This class is characterized by the common occurrence of pink garnet that constitutes up to 30% of the modal composition of the rocks (Table 2-1). Associated minerals include quartz, plagioclase, biotite, and K-feldspar. Minor graphite, apatite, epidote, Fe-Ti oxides, and sulfides occur as accessory phases. Pyrite and pyrrhotite are the dominant sulfides. Pyrrhotite occurs exclusively in graphitic samples. Minor chalcopyrite is associated with both pyrite and pyrrhotite in composite grains, or as discrete grains. All samples in this class belong to the transition zone B in Tvedestrand area (Figure 1-2).

The occurrence of garnet-biotite gneisses in Tvedestrand area was first reported by Field (1966). Similar rocks have been reported from Risor-Sondeled (Starmer, 1967), Arendal (Andreae, 1972), and Songe-Ubergsmoen (Beeson, 1975). A sedimentary origin for the gneisses is postulated from the presence of graphite and the intergradational nature of the rocks with quartzite and impure quartzite horizons (Field, 1966; Beeson, 1975). Summary statistics for the garnet-biotite gneisses is shown in Table 2-2.

2-8-1. Geochemistry

Considering the major element geochemistry, the garnet-biotite gneisses are comparable to the biotite gneisses (Table 2-2) and might be the higher grade equivalent of these rocks. However, higher contents of LILE, particularly K, Rb, and Ba, and of REE, distinguishes the garnet-biotite gneisses from biotite gneisses. The similarity in major oxide geochemistry between garnet-biotite gneisses and biotite gneisses in Bamble was also noted by Field (1966) who attributed the higher contents of K and Rb in the former to K-metasomatism and K-feldspathization.

A consistent enrichment in REE in the garnet-biotite gneisses is difficult to be explained by secondary metasomatic processes, as REE have frequently been shown to be immobile during alteration and metamorphism (c.f. Weaver and Tarney, 1980, 1981; Hajash, 1984; Jahn and Zhang, 1984; Condie and Allen, 1984). The garnet-biotite gneisses formed from a different

initial sediment. Compared to the biotite gneisses, they represent a less oxidized depositional environment. This is supported by lower ratios of $Fe^{+3}/Fe^{+2} + Fe^{+3}$ (0.18 vs. 0.24), and by the occurrence of graphite. They are also relatively enriched in S.

A comparison of the geochemistry of the garnet-biotite gneisses to the known sedimentary rocks suggests the shales as the most likely parent lithology. A spidergram for elements in the gneisses, normalized to post-Archean shale, is shown in Figure 2-16; a contrast is also made to the mean greywacke composition.

The garnet-biotite gneisses are characterized by a strong depletion in Cs (Figure 2-16). They are also depleted in Rb and U. Cesium, Rb, and U are amongst the elements frequently reported to have been depleted in high grade metamorphic rocks (e.g. Heier, 1973; Weaver and Tarney, 1981; Rudnick et al., 1985). The garnet-biotite gneisses possess considerably higher ratios of K/Cs and Th/U relative the biotite schists and biotite gneisses, or the mean continental crust, implying a metamorphic fractionation of Cs and U with progressive metamorphism.

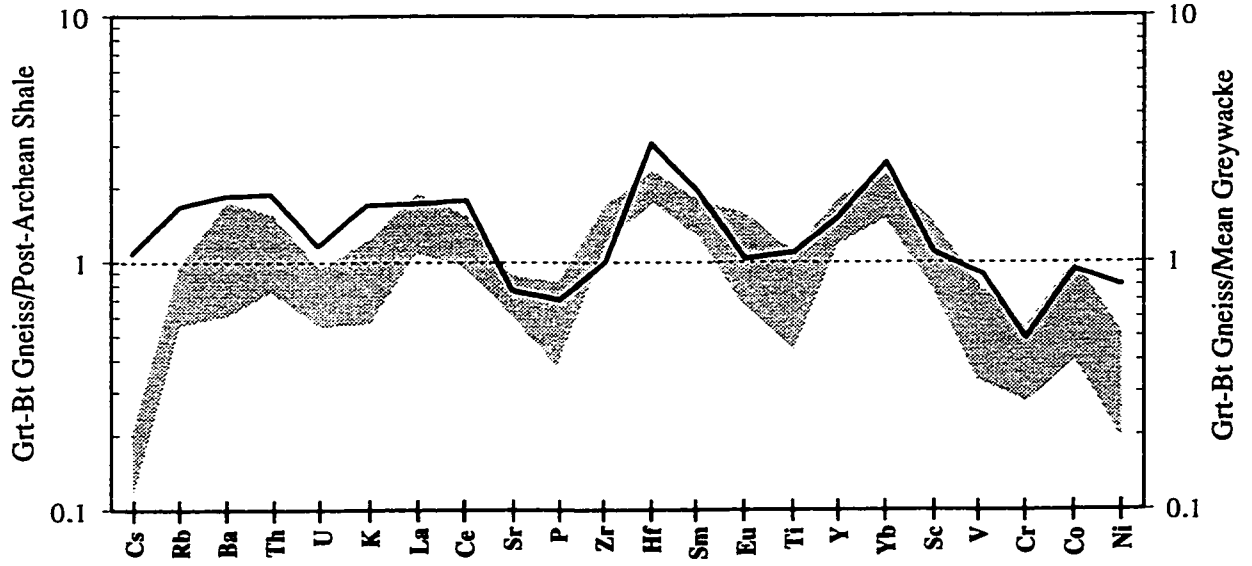

Figure 2-16. Spidergram plot for elements in the Bamble garnet-biotite gneisses, normalized to Post-Archean Shale (shaded area) and mean greywacke (solid line). The shaded area represents $\bar{x} \pm \frac{1}{2}\sigma$. Normalization data as in Table 2-2.

The garnet-biotite gneisses display a marked enrichment in REE, particularly HREE, relative to the post-Archean shale (Figure 2-17). The gneisses further show a marked negative Eu anomaly. The chondrite-normalized REE pattern of the garnet-biotite gneisses is comparable to those of the biotite schists and biotite gneisses. Enrichment in HREE may be attributed to the common presence of garnet that makes up to 30% modal composition of the gneisses.

The initial sediments probably originated from alkaline felsic rocks. This is supported by the relatively high Σ REE and the marked negative Eu anomaly. The REE pattern of the gneisses may be compared to that of the fine grained sediments from the early Proterozoic Wyloo Group, Western Australia (Figure 2-17), where McLennan (1980) proposed the late Archean alkali granites as the most likely source rocks.

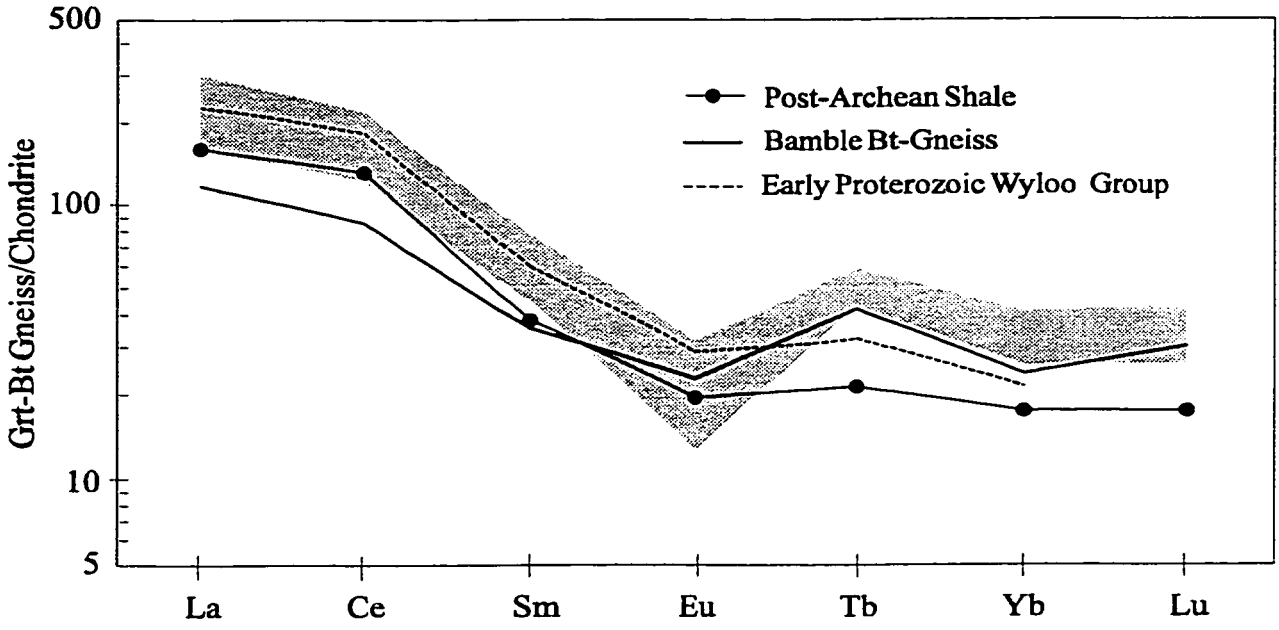

Figure 2-17. Chondrite normalized plot for REE in garnet-biotite gneisses. Mean Bamble biotite gneisses, mean post-Archean shale (Taylor and McLennan, 1985), and mean composition of the shale-greywacke sequence from Early Proterozoic Wyloo Group, Western Australia (McLennan, 1980) is shown for comparison.

2-8-2. Distribution of Chalcophile Elements

Assuming an initial argillaceous protolith, the abundance of chalcophile elements in the garnet-biotite gneisses is compared to that in shales or slates (Figure 2-18). The mean composition of the continental crust is also shown for further reference. Chalcophile elements display large scatters in the garnet-biotite gneisses. Sulfur and Cu are in the same range as in the mean continental crust, or slightly depleted relative to shales. Other elements, however, are significantly depleted.

It is noteworthy that peaks in Au correspond to graphitic samples. This is in agreement with the data in the literature, where graphitic schists and gneisses have frequently been reported to carry higher contents of Au relative to their non-graphitic equivalents (e.g. Boyle, 1979; Korobeynikov, 1985).

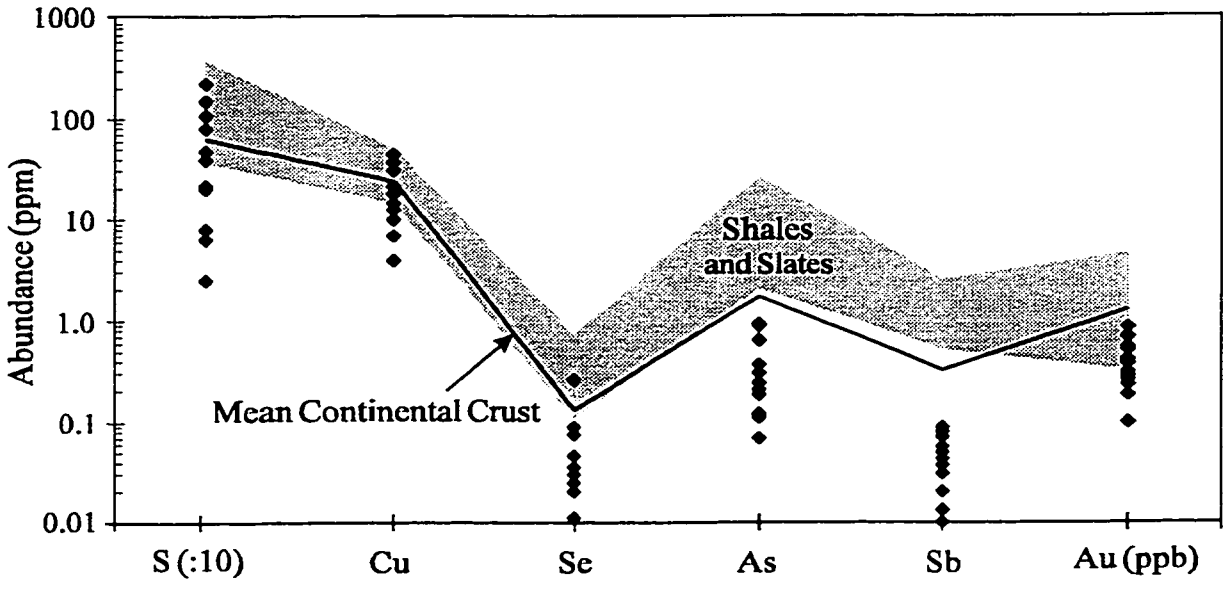

Figure 2-18. Distribution of chalcophile elements in the Bamble garnet-biotite gneisses. The common range of the abundances of chalcophile elements in shales and slates, and the mean composition of the continental crust, are shown for comparison. See Appendix 2-2 for the average shale (slate) and continental crust composition.

2-9. Orthopyroxene-Garnet-Biotite Gneiss

Metasedimentary rocks also occur in the granulite zone. Occurrences of metapelites, semi-metapelites, and impure quartzites have been reported from Hissoy, Tromoy, and Grimstad areas (Andreae, 1974; Kihle and Bucher-Nurminen, 1992; Nijland, 1990; Knudsen, 1996; Knudsen et al., 1997). The granulite facies metasediments are characterized by the presence of high pressure minerals such as orthopyroxene, sillimanite, cordierite, and sapphirine. Samples of granulite facies gneisses were collected from Tromoy and Hissoy.

The granulite facies metasediments are medium to coarse grained with a well developed granoblastic texture. Orthopyroxene (Opx) is a characteristic mineral and constitutes 3 to 20% of the modal composition of the rocks. Garnet (Grt) appears in most samples forming up to 15% of the modal composition. Quartz and plagioclase are variably present in all samples. Biotite (Bt) and perthitic orthoclase are minor constituents. Accessory minerals include clinopyroxene, apatite, Fe-Ti oxides, and sulfides. Trace graphite (~1%) was observed in one sample (812).

Orthopyroxene is strongly pleochroic in shades of pink and green. It contains up to 5% Al_2O_3 (Table 2-3). Al_2O_3-rich pyroxenes are typical of high grade metamorphism, as the solubility of Al_2O_3 increases with increasing pressure (Deer et al., 1992). Garnet is a brownish to pinkish almandine, fairly rich in pyrope molecules (Table 2-3), in accordance with the increasing solubility of MgO in almandine with increasing metamorphic grade (c.f. Deer et al., 1992).

The Opx-Grt-Bt gneisses are further characterized by dominance of magnetite over ilmenite, and the presence of ilmenite-hematite exsolution lamellae, implying a relatively high oxidation state for the gneisses. Sulfide minerals include pyrrhotite, pyrite, and chalcopyrite occurring as discrete or composite grains interstitial to silicates. Mantling of pyrite by magnetite was observed in few samples. Modal composition and summary statistics for the Opx-Grt-Bt gneisses are shown in Tables 2-1 and 2-2, respectively.

Table 2-3. Composition of orthopyroxene and garnet in the Opx-Grt-Bt gneisses;

	Orthopyroxene			Garnet			
SiO_2	49.59	49.57	49.85	38.29	37.77	38.05	38.43
Al_2O_3	4.86	4.94	4.65	21.87	21.39	21.49	21.94
TiO2	0.08	0.06	0.08	0	0	0.02	0
FeO	25.2	25.73	25.03	28.74	28.73	28.05	27.54
MnO	0.25	0.32	0.24	1.89	2.01	2	1.89
MgO	19.47	19.18	19.47	7.75	7.47	8.15	8.5
CaO	0	0	0	1.41	1.42	1.49	1.41
Na_2O	0.02	0	0.01				
Total	99.47	99.8	99.33	99.95	98.79	99.25	99.71

2-9-1. Geochemistry

A comparison of the major element geochemistry of the Opx-Grt-Bt gneisses with those of the other supracrustal rocks (Table 2-2) suggests the biotite gneisses or garnet-biotite gneisses as likely protoliths. Slightly higher contents of Fe, Mg, and Ca, and lower contents of Si and K might be attributed to the metamorphic fractionation processes. However, the possibility that the granulite-facies rocks originated from different sediments can not be ruled out.

The Opx-Grt-Bt gneisses are strongly depleted in large ion lithophile elements (LILE) and light rare earth elements (LREE) compared to metasedimentary rocks from amphibolite and transition zones, or the mean comosition of the continental crust (Figure 2-19). In this respect, the geochemistry of the granulite-facies metasediments may be compared to that of the Tromoy acid-intermediate gneisses, or charnockites. Charnockites are discussed in Chapter 3.

Depletion of LILE in granulite facies rocks is well established (e.g. Sighinolfi, 1971; Heier, 1973; Sheraton et al., 1973; Tarney, 1976; Weaver and Tarney, 1981; Lamb and Valley, 1985; Rudnick et al., 1985). The Opx-Grt-Bt gneisses are further characterized by a considerable depletion in LREE.

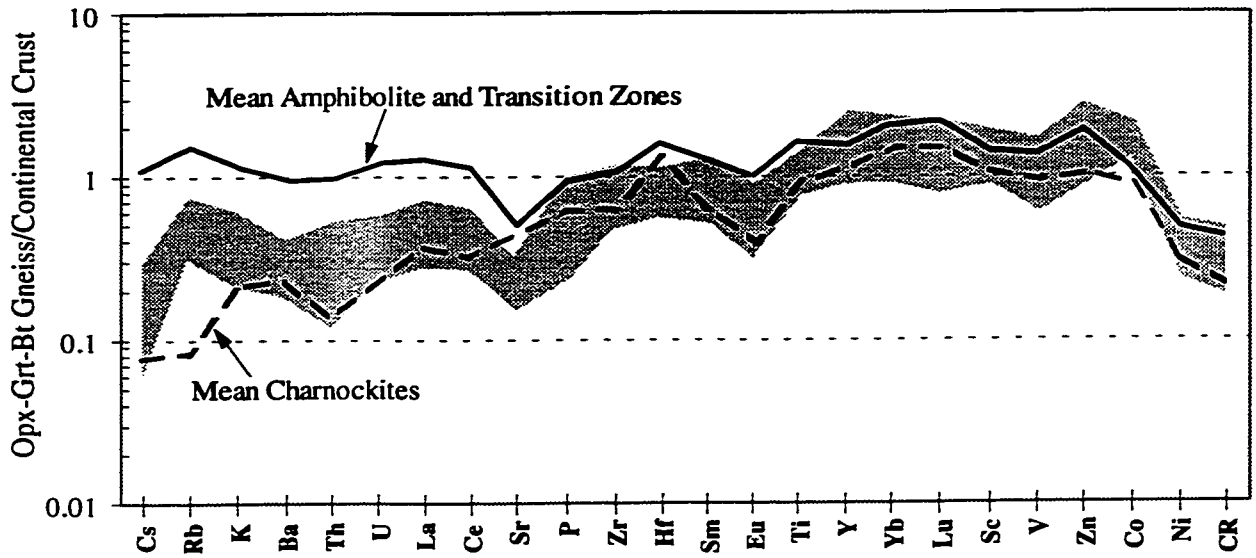

Figure 2-19. Spidergram plot for elements in the Bamble Opx-Grt-Bt gneisses normalized to the mean continental crust. The shaded area represents $\bar{x} \pm \frac{1}{2}\sigma$. The mean composition of metasediments from amphibolite and transition zones (solid line) and the mean composition of acid-intermediate gneisses, or charnockites, from granulite zone (broken line), are shown for comparison. Normalization data from Wedepohl (1995).

Compared to metasedimentary rocks from amphibolite and transition zones, the Opx-Grt-Bt gneisses display a less fractionated chondrite-normalized REE pattern (Figure 2-20). In this respect, the gneisses are comparable to Tromoy charnockites. As in the other metasediments, the Opx-Grt-Bt gneisses display a marked negative Eu anomaly.

2-9-2. Distribution of Chalcophile Elements

The Opx-Grt-Bt gneisses carry considerably higher concentrations of S, Cu, and Se relative to the metasediments from amphibolite and transition zones, or the mean continental crust (Figure 2-21). Selenium is notably enriched in two samples, 9506 and 9507. Electron probe analysis of pyrite from these samples revealed high Se in the range 700 to 1000 ppm. Although strongly enriched in S, Cu, and Se, the granulite facies gneisses are considerably depleted in Au, As, and Sb relative to the mean continental crust. A comparison to shales or greywackes as possible protoliths would imply a much stronger depletion in Au, As, and Sb.

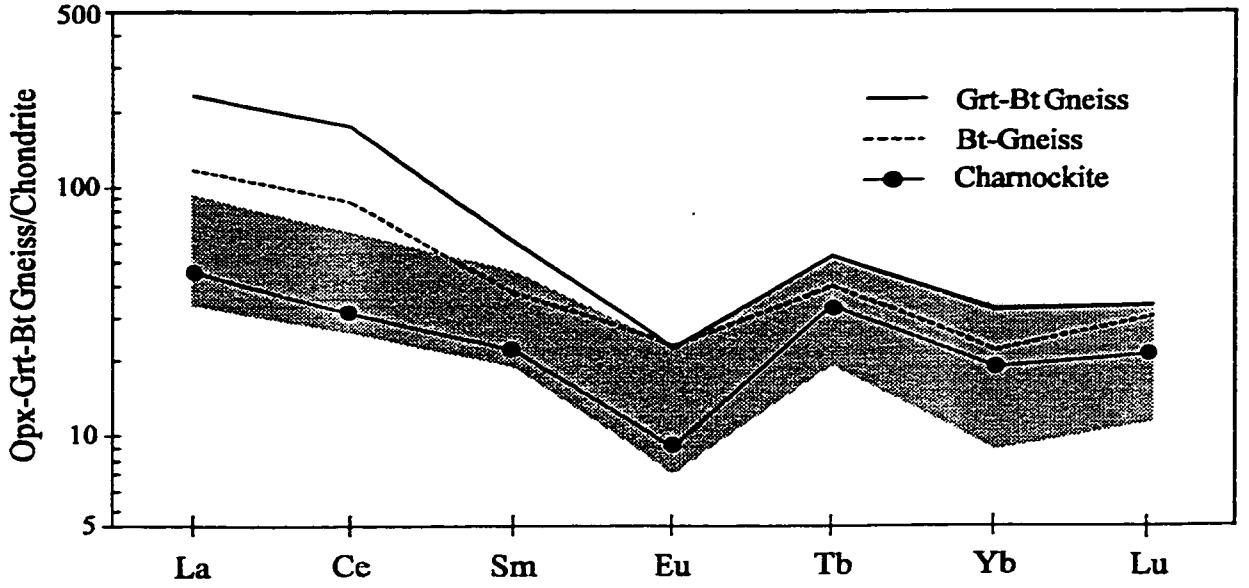

Figure 2-20. Chondrite-normalized REE plot for the orthopyroxene-garnet-biotite gneisses. The shaded area represents $\bar{x} \pm \frac{1}{2}\sigma$. The mean composition of the biotite schists and biotite gneisses from amphibolite zone and of the garnet-biotite gneisses from transition zone, and the mean composition of Tromoy charnockites, are shown for comparison. Normalization data from McDonough and Sun (1995).

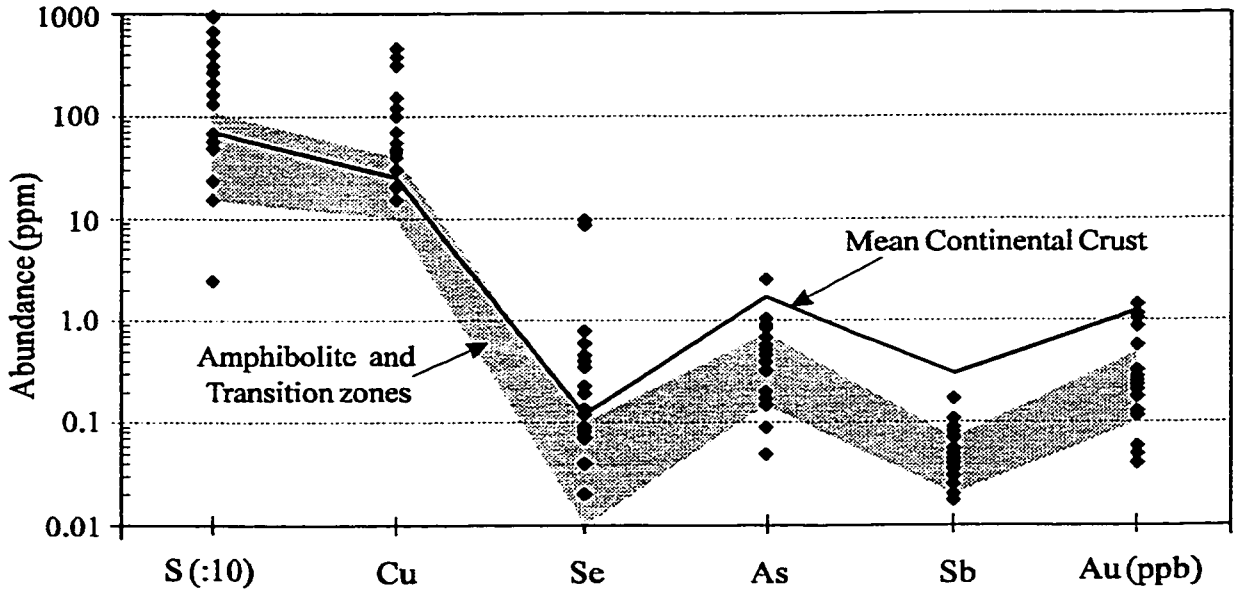

Figure 2-21. Distribution of chalcophile elements in the Bamble orthopyroxene-garnet-biotite gneisses. The abundance of chalcophile elements in the biotite gneisses and garnet-biotite gneisses from amphibolite and transition zones, respectively, and the mean composition of the continental crust, are shown for comparison. See Appendix 2-2 for the mean continental crust.

2-10. Discussion

Bamble metasupracrustal rocks include a variety of protoliths and depositional environments, from shallow littoral sandstones to deeper greywackes and pelites, with local euxinic conditions to produce graphitic and sulfidic sediments. The common presence of volcanic materials intercalated with sediments suggest that deposition occurred in a mobile basin. Starmer (1985a) suggested a marginal basin environment for the Bamble supracrustal rocks.

Amphibolite bands are of igneous origin and bear features typical of calc-alkaline basalts produced at destructive plate margins. Plagioclase-quartz-hornblende gneisses, severely depleted in alkaline ions, appear to be modified volcanic materials. There is evidence that biotite schists are, at least partly, the products of alkaline metasomatism of basaltic materials.

Graphite occurs as a minor constituent in garnet-biotite gneisses from Tvedestrand in transition zone. Occurrence of graphite has also been reported from amphibolite and granulite zones (e.g. Field, 1966; Starmer, 1967; Andrea, 1974; Beeson, 1975; Broekmans et al., 1994). A biogenic origin was indicated for the graphite based on the carbon isotopic composition (Andrea, 1974; Field and Starmer, 1982; Broekmans et al., 1994). The local nature of the graphite-bearing horizons has been interpreted to denote formation in small, isolated areas within lagoonal, deltaic, or lacustrine conditions (Field, 1966; Beeson, 1975).

Sulfides occur as accessory phases in all rock units. Sulfide mineralogy is rather simple. Pyrite, the dominant sulfide in supracrustal rocks from amphibolite zone, is variably replaced by pyrrhotite in transition and granulite zones. Chalcopyrite may accompany both pyrite and pyrrhotite in composite grains, or, less commonly, as discrete grains.

2-10-1. Comparative Geochemistry

While sedimentary units from amphibolite and transition zones carry normal concentrations of elements compared to their possible non-metamorphosed equivalents, or mean continental crust, the granulite facies rocks are strongly depleted in LILE, REE, and HFSE. The causes of

depletion of certain elements in granulite facies rocks has been a controversial issue. Models for the genesis of the depleted rocks typically fall into two general categories:

1) Partial melting with partitioning of granithophile elements into the melts (Fyfe, 1973; Pride and Muecke, 1980; Nesbitt, 1980).

2) Metasomatic fluid processes, involving either dehydration with increasing pressure and temperature (e.g. Heier, 1973; Thompson, 1984) or CO_2 streaming (e.g. Sheraton et al. 1973; Tarney 1976; Newton, 1980; Stahle et al., 1985).

The marked depletion of incompatible elements is consistent with the granulite facies gneisses as being the refractory residuum of crustal anatexis. Alternatively, it might be attributed to metasomatic fluid processes. The ratios of certain element pairs may be used to investigate the evolution of rocks during high grade metamorphism (Table 2-4).

Although containing lower contents of K and Rb, metasediments from granulite zone are comparable to those from amphibolite and transition zones in K/Rb ratios (Figure 2-22). This is in agreement with an earlier study by Knudsen et al. (1997) on pelitic to semi-pelitic rocks from Hissoy (granulite zone) and Froland (amphibolite zone). The consistent K/Rb ratios imply that no significant fractionation of Rb from K occurred during granulite metamorphism.

Table 2-4. Ratios of elements in Bamble Supracrustal Rocks.

	Metamorphic Zone	K/Rb	Rb/Sr	Ba/Sr	La/Th	La_N/Yb_N	Eu/Eu*
Biotite Schist	A	183	1.50	4.70	13	3.0	0.5
Semi-Metapelite*	A	280	3				
Biotite Gneiss	A	240	0.32	2.50	4.0	7.5	0.73
Impure Quartzite	A	220	0.87	7.0	2.9	21	
Hornblende Gneiss	A	190	0.05	0.14	8.0	14	0.50
Amphibolite	A	290	0.27	2.00	21	4.5	0.73
Garnet-Biotite Gneiss	B	240	0.77	4.50	3.0	7.2	0.42
Opx-Grt-Bt Gneiss	D	225	0.45	2.30	16	3.5	0.54
Semi-Metapelite*	D	300	1.5				
Continental Crust**		255	0.23	1.75	3.5	10.2	0.9
Mean Greywacke**		230	0.36	2.1	3.7	11	0.7
Post-Archean Shale***		192	0.8	3.25	2.6	9.2	0.9

* Knudsen et al. (1997) ** Wedepohl (1995) *** Taylor and McLennan (1985)

An average K/Rb ratio of 250 for Bamble metasediments is typical of undepleted crustal rocks (c.f. Taylor and McLennan, 1985).

Ba/Sr ratio is a sensitive indicator of partial melting, as the dominant residual phase in all gneiss compositions will be plagioclase feldspar with considerably higher partition coefficient for Sr (Arth, 1976; Weaver and Tarney, 1981). Ba/Sr ratios in Bamble metasediments are comparable to that for the mean continental crust, or post-Archean sediments (Figure 2-23). The slightly higher ratios for the Bamble metasediments may be attributed to the relatively lower contents of Sr in these rocks (see Table 2-2 for a comparison). The low concentrations of Sr in Bamble metasediments was also noted by Knudsen et al. (1997) who attributed it to the composition of the source rocks.

The Ba/Sr ratios suggest that high grade metamorphism was not accompanied by removal of a significant melt fraction. This supports earlier studies by Knudsen (1996) and Knudsen et al. (1997) who showed that the granulite facies metapelites experienced only local partial melting. The authors proposed the reaction "biotite + sillimanite + quartz → garnet + melt" associated with the infiltration of brine- and CO_2-bearing fluids from local metasediments.

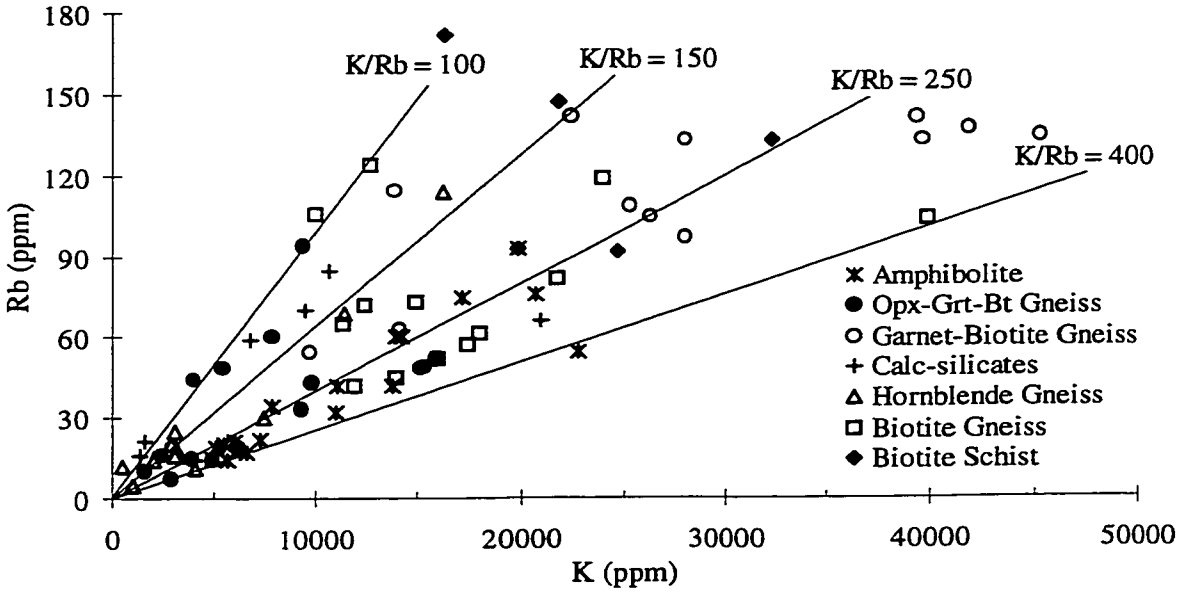

Figure 2-22. Variations of K and Rb in various supracrustal rocks, Bamble.

Hornblende gneisses are distinguished from other supracrustal rocks by considerably lower Ba and Ba/Sr ratios. They are also depleted in Rb and K. The gneisses appear to be highly modified intermediate igneous rocks. The relatively high Ba/Sr ratio in the biotite schists may be interpreted as an evidence in favor of a metasomatic origin for the schists.

Rb/Sr ratios for most rock units are comparable to that for the mean continental crust, or post-Archean sediments (Table 2-4), further suggesting that Rb was not fractionated during metamorphism, and that no significant partial melting occurred. The considerably higher Rb/Sr ratios for the biotite schists provides further evidence in favor of a metasomatic origin for the schists. In contrast, the very low Rb/Sr ratio in hornblende gneisses may be taken as an evidence for depletion of LILE in the gneisses.

Lanthanum and Th behave coherently during most sedimentary processes (Nance, 1975; McLennan et al., 1980). The Bamble supracrustal rocks display large variations in La/Th ratios (Figure 2-24). The La/Th ratios for quartzites, biotite gneisses and garnet-biotite gneisses are comparable to those in the average crustal rocks. Other rock units, however,

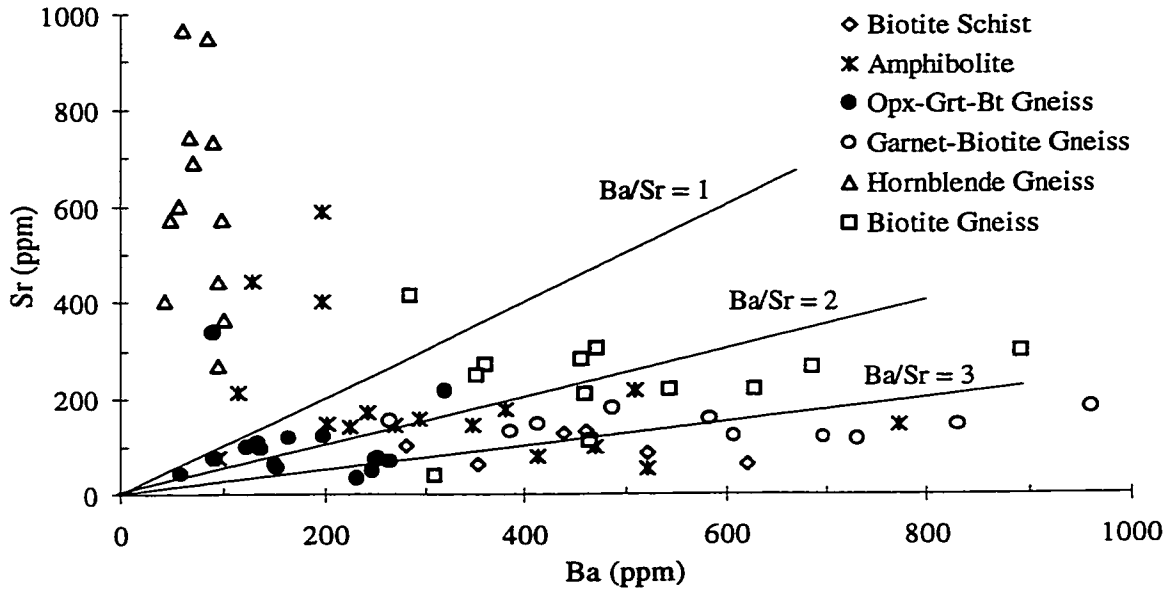

Figure 2-23. Distribution of Ba and Sr in Bamble supracrustal rocks.

show considerably higher values. The high La/Th ratio in Opx-Grt-Bt gneisses may be attributed to depletion of Th during granulite metamorphism. Similarly, the high La/Th ratios in hornblende gneisses might be a consequence of Th depletion.

La/Th ratios for concordant amphibolites (21 ± 6) are in the same range as in the non-metamorphosed calc-alkaline basalts (20 ± 5, Pearce, 1982), implying that no metamorphic fractionation of Th or La ccurred. A relatively high La/Th ratio for biotite schists may be interpreted as a further evidence for derivation of the rocks from mafic protoliths.

The Bamble metasediments display relatively less fractionated REE patterns compared to the post-Archean sediments, or the mean continental crust. This is evident from lower ratios of La_N/Yb_N in the Bamble rocks (Table 2-4). Hornblende gneiss is an exception, as it appears to have been formed from a fractionated magma. The REE patterns of the quartzites are determined by minor feldspars that are commonly enriched in LREE relative to HREE.

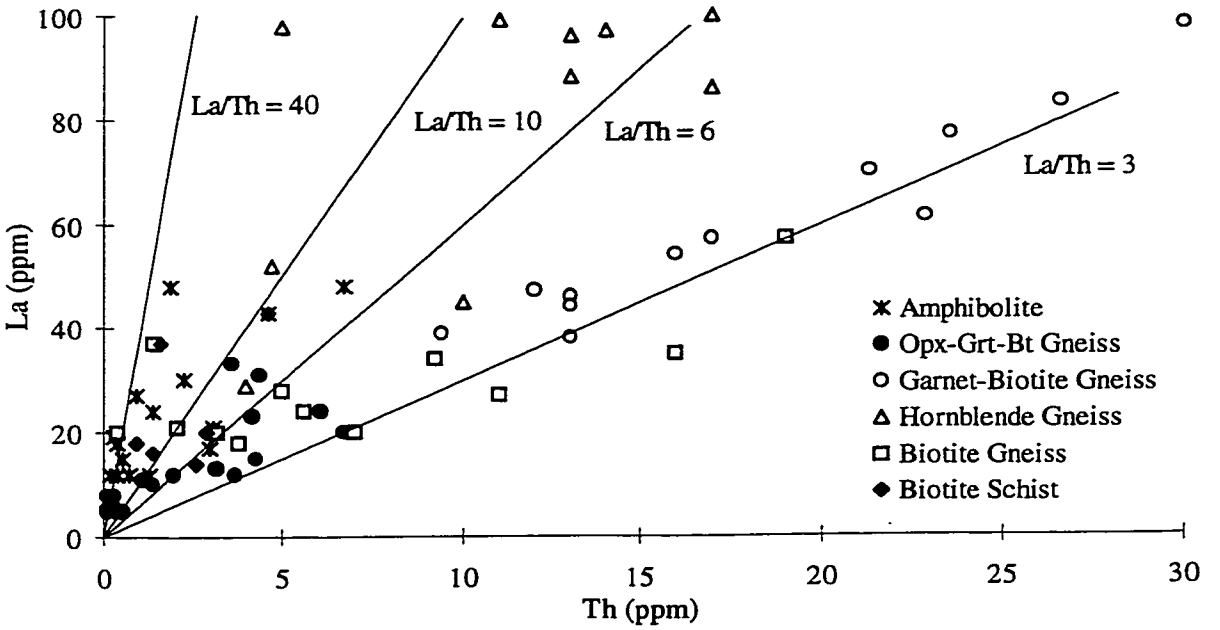

Figure 2-24. Distribution of Th and La in Bamble supracrustal rocks.

The low La_N/Yb_N ratios in the Bamble supracrustal rocks might be attributed to:

1) Removal of LREE during high grade metamorphism;

2) Enrichment of HREE;

3) Derivation of the initial sediments from poorly fractionated source rocks;

4) A combination of the above processes.

The Bamble metasediments are relatively enriched in HREE. The concentration of Y, a close associate of HREE, in the Bamble rocks is almost twice that of the mean post-Archean sediments. Accordingly, the low La_N/Yb_N ratios in the metasediments may be attributed to the relatively high concentrations of HREE rather than a removal of LREE. Except for the granulite facies rocks, other rock units contain normal abundances of LREE relative to mean continental crust, or post-Archean sediments.

The granulite facies gneisses are depleted in LREE, and display a relatively less fractionated REE pattern. The mean La_N/Yb_N ratio in metasediments from granulite zone is considerably lower than that in those from amphibolite and transition zones (3.5 vs. ~7.5 and 7.2, respectively). The low La_N/Yb_N ratios in the granulite facies gneisses may be attributed to the removal of LREE during high grade metamorphism.

As in other metasediments, the Opx-Grt-Bt gneisses display a marked negative Eu anomaly. This might be interpreted as a further evidence against partial melting and removal of an anatectic melt, as this process would be expected to leave Eu-enriched rocks behind (c.f. McLennan et al., 1980; Taylor and McLennan, 1985; Taylor et al., 1986).

Fluids during granulite facies metamorphism are known to be CO_2-rich (e.g. Touret, 1974; Newton et al., 1980), and could be the agent responsible for complexing and removal of LILE (Weaver and Tarney, 1981; Newton et al., 1980; 1985; Janardhan et al, 1982; Condie et al., 1982; Condie and Allen, 1984; Hanson et al., 1984; Stahle et al., 1987; Taylor and McLennan, 1988). K^+, $(KCl)^0$ and other aqueous complexes can also be important

components in syn-metamorphic fluid phase in metasediments (Henley, 1984; Touret, 1985; Knudsen and Andersen, 1997).

CO_2 fluids also account for depletion of REE. Experimental studies have indicated that REE form stable carbonate complexes and strongly partition into carbonic fluids over a wide range of temperatures (Kosterin, 1959; Wendladth and Harrison, 1979; Cantrell and Byrne, 1987). Wendladth and Harrison (1979) showed that LREE are more soluble than HREE in CO_2 fluids. Cantrell and Byrne (1987) indicated that $(CO_3)^+$ is important for LREE and $(CO_3)_2^-$ for HREE. A strong depletion of REE is reported from Kabbaldurga charnockites, India, where granulite metamorphism is believed to have been induced by infiltration of carbonic fluids along a system of ductile shears and foliation planes (Stahle et al., 1987). The authors showed that partial transformation of biotite-hornblende gneisses to massive charnockites was associated with dissolution of REE-bearing minerals, zircon, apatite, and monazite.

2-10-2. Implications for Source Rocks

Bamble metasediments are depleted in Sr compared to the mean continental crust, or Post-Archean sediments. This is supported by the relatively higher Ba/Sr ratios and Rb/Sr ratios (Table 2-4). The metasediments are also depleted in P_2O_5, compared to average post-Archean sediments (0.1% vs 0.16%). Low concentrations of Sr and P was also reported by Knudsen et al. (1997) for metapelites and semi-metapelites from Hissoy and Froland areas. The Bamble metasediments are further characterized by relatively high concentrations of Y and HREE, and low concentrations of Cr, Ni, and V.

Geochemical characteristics of the Bamble metasediments (i.e. low Sr, P, and transition metals, and high Y and HREE) suggest that they derived mostly from granitic rocks (c.f. Collins et al., 1982; Taylor, 1986; Kerr et al., 1993; Whalen et al., 1987, 1996). Such origin is further supported by strongly negative Eu anomalies. The mean Eu/Eu* values for various supracrustal rocks in Bamble are considerably lower than those for the mean post-Archean sedimentary rocks (Table 2-4). Depletion of Eu in upper crustal rocks is related to intracrustal

processes whereby felsic igneous rocks, depleted in Eu, are produced (Taylor and McLennan, 1985; Taylor et al., 1986). Derivation from felsic igneous or metamorphic rocks is also supported by the common occurrence of quartzites and impure quartzites.

2-10-3. Abundance of Chalcophile Elements

The Bamble supracrustal rocks are strongly depleted in Au, As, Sb, and Se relative to their likely protoliths, shales, greywackes, and volcanic materials, or the mean composition of the continental crust (Figure 2-25). The mean abundance of Au in the Bamble rocks (0.35 ppb) is 25% of the crustal abundance of this element. Only in calc-silicates does Au come close to the abundance of equivalent rocks; however, these rocks are considerably enriched in other chalcophile elements, but not Au or Sb.

In the absence of equivalent rocks from lower metamorphic grades in Bamble, it is difficult to evaluate whether the low concentrations of chalcophile elements are of primary sedimentary origin, or the elements were depleted during metamorphic processes. The initial sediments originated principally from older granitoids. The low contents of certain chalcophile elements in the Bamble supracrustal rocks may partly be attributed to their provenance. Felsic rocks are commonly depleted in chalcophile elements compared to other rock types (Appendix 2-2).

Concordant amphibolites are of igneous origin and display features characteristic of calc-alkaline basalts emplaced at destructive plate margins. As in the metasediments, the amphibolites are also strongly depleted in Au, as well as As and Sb, relative to non-metamorphosed mafic rocks elsewhere. That all supracrustal units, of varied type and origin, are depleted in certain elements, suggest that factors other than source rocks or depositional environments were involved. It is difficult to model a series of independent processes that can account for the scarcity of Au in all individual rock types. The possible mechanisms of Au depletion are discussed in Chapter 6.

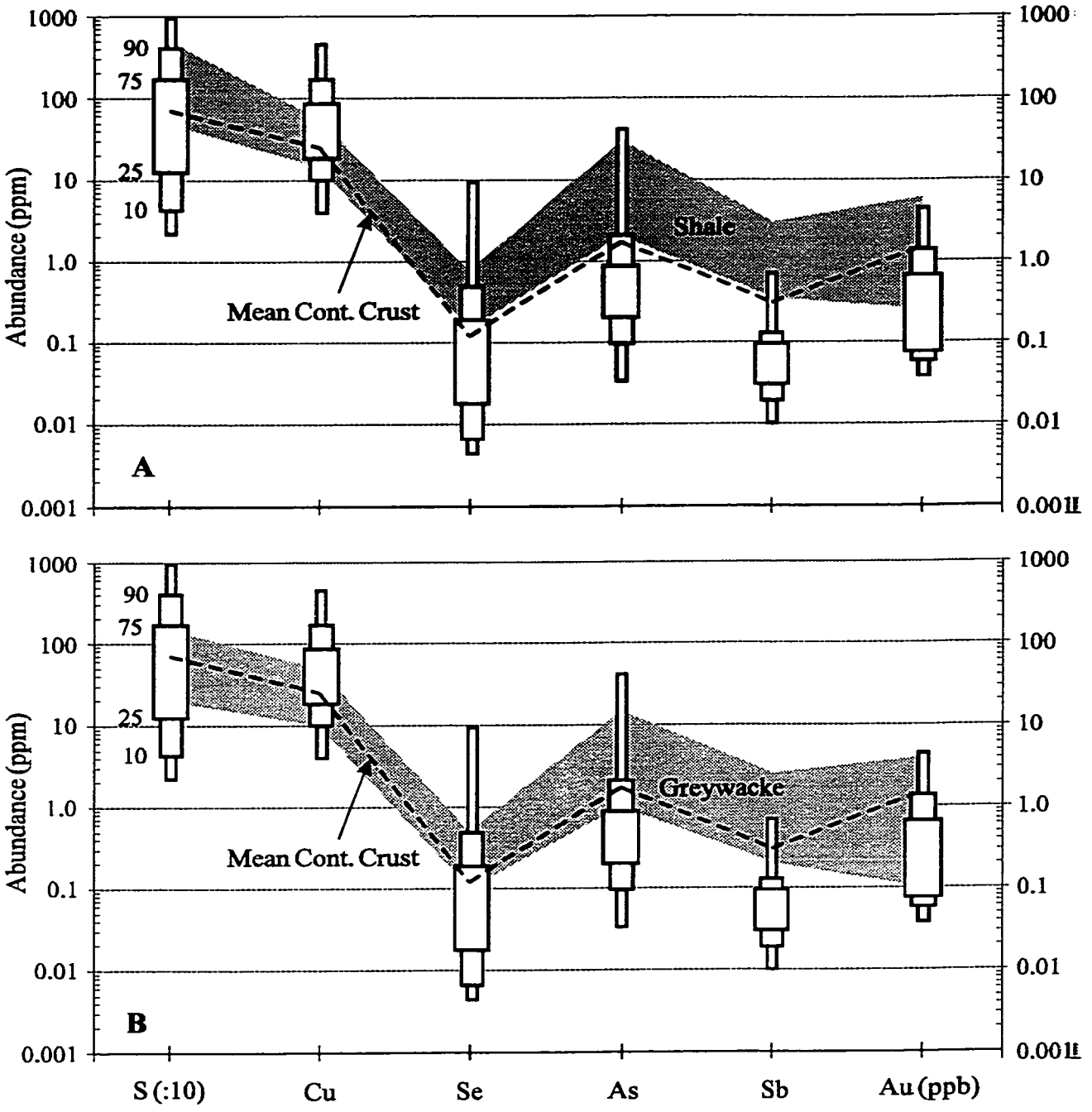

Figure 2-25. Abundances of chalcophile elements in the Bamble supracrustal rocks. Cumulative frequencies for 10, 25, 75, and 90% are indicated. The common ranges of the abundances of chalcophile elements in shales (A) and greywackes (B) are shown for comparison. Also shown is the mean composition of the continental crust (broken line). See Appendix 2-2 for the composition of shales, greywackes, and the mean continental crust.

3. Felsic Igneous Rocks

Several igneous suites are intrusive to the supracrustal rocks in Bamble. Some of the major suites include acid-intermediate gneisses, basic dykes and sills known as metabasites, mafic bodies known as hyperites, and post-orogenic granites. Acid-intermediate gneisses are widespread in the granulite zone. Metabasites and hyperites are common in all metamorphic zones; they are discussed in Chapter 4. Post-orogenic granites occur as small stocks to large batholiths. They are discussed in Section 3-2.

3-1. Acid-Intermediate Gneisses

The highest grade portion of the Bamble Shear Belt (zone D), makes up the islands of Tromoy and Hissoy. This zone contains outcrops of dark green, poorly foliated, acid-intermediate gneisses, also known as charnockites. These are the oldest observable intrusive rocks in Bamble, except for some of the metabasites (e.g. Starmer, 1976; Smalley and Field, 1985). The charnockitic nature of the rocks was first recognized by Bugge (1940) who originally termed them "Arendalite", but later renamed them "Arendal charnockite".

The acid-intermediate rocks intruded the older supracrustal rocks at 1587 ± 6 Ma (U-Pb zircon age, Lamb et al., 1986), and were metamorphosed at 1540 ± 20 Ma during Kongsbergian, or Gothian, Orogeny (Rb-Sr whole rock age, Field and Råheim, 1979, 1981; Field et al, 1980, 1985; Machado, 1991). In some places, the gneisses have yielded much younger Rb-Sr and K-Ar dates of ~1100 Ma (Field and Råheim, 1979). The isotopic resetting has alternatively been attributed to a regional Sveconorwegian high grade metamorphism (Verschure, 1985) or a low-grade hydrous alteration episode (Brickwood, 1984; Field et al., 1985). The pressure and temperature at peak metamorphic conditions have been estimated to be in the range 7 ± 2 kbar and 750 ± 50°C, respectively (Lamb et al., 1986; Cameron, 1989b; Harlov, 1992; Visser, 1993; Nijland and Maijer, 1993).

Acid-intermediate gneisses, comparable in composition to those from the granulite zone, also occur in the amphibolite and transition zones. Some 50 samples of the granulite facies rocks were collected along traverses 1 and 2 in Tromoy Island (Figure 1-2). Equivalent rocks from amphibolite zone were sampled along traverse 6 in Ubergsmoen area. On a ternary albite-anorthite-orthoclase diagram, the acid-intermediate gneisses from both granulite and amphibolite zones fall in the compositional range tonalite-trondhjemite (Figure 3-1).

3-1-1. Mineralogy

Orthopyroxene (X_{Fs} = 0.27-0.68), plagioclase (X_{An} = 0.05-0.48), and quartz are the dominant minerals. Hornblende, garnet, clinopyroxene, Fe-Ti oxides, and K-feldspar are minor phases, making up to 10% of the modal composition of the rocks. The composition of garnet has been determined to be in the range X_{Alm} = 0.55-0.70, X_{pyr} = 0.09-0.40, X_{Gr} = 0.01-0.24, X_{Spess} = 0.01-0.15, and of clinopyroxene in the range X_{HD} = 0.36-0.48 (Harlov, 1992). Biotite (X_{Annite} = 0.40-0.60), cordierite, apatite, monazite, titanite, rutile, zircon, hercynite, and sulfides are usually present as accessory phases, rarely exceeding 1% by mode. Minor sericite, muscovite, chlorite, and biotite may occur as secondary retrograde minerals. The mineralogy of the

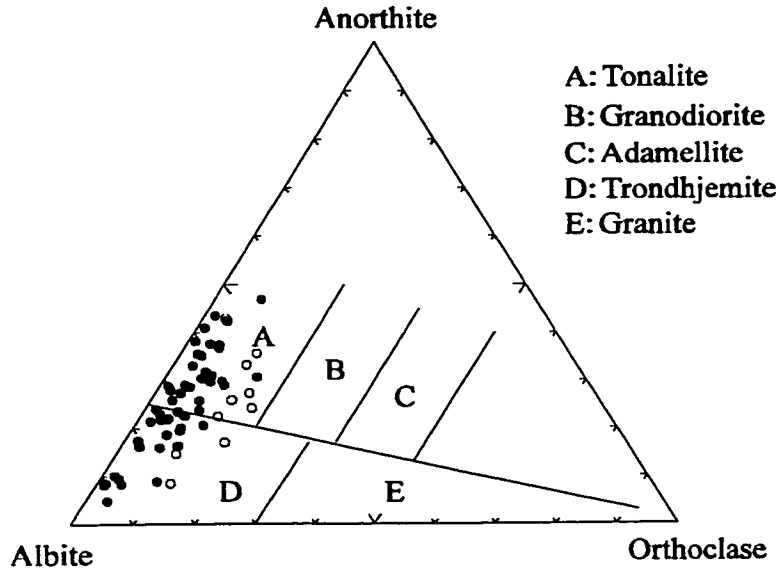

Figure 3-1. Plot of acid-intermediate gneisses from granulite zone (solid circles) and amphibolite zone (open circles) on normative feldspar diagram. Boundary lines from O'Connor (1965).

Bamble charnockites has been explained in some detail by several authors (Lamb et al., 1986; Peterson, 1988; Harlov, 1992; Cameron, 1989a, b). An estimate of the modal composition of the charnockites is given in Table 3-1.

Oxides include magnetite, titaniferous magnetite, ilmenite, and hematite. The titaniferous magnetite contains ilmenite in varying degrees of exsolution, while ilmenite commonly contains hematite, also in varying degrees of exsolution. The mineralogy, textures, and conditions of formation of oxides in the Bamble charnockites have been discussed by Cameron (1989b) and Harlov (1992) who showed that the charnockites equilibrated under relatively oxidized conditions, ~2.5 log units above QFM buffer, at peak metamorphism.

Sulfides occur as accessory minerals, rarely exceeding 0.2% by mode. Pyrite and pyrrhotite are the main sulfides, generally occurring as fine grains (20-250 μm in diameter) interstitial to silicates and oxides; minor chalcopyrite may occur as discrete grains, or, more commonly, as lamellae and patches associated with both pyrrhotite and pyrite. Interstitial pyrite is commonly

Table 3-1. Modal composition of acid-intermediate gneisses, Bamble.

	Granulite Zone (n* = 50)	Amphibolite Zone (n = 10)
Quartz	30 - 50	30 - 60
Plagioclase	25 - 50	25 - 50
K-feldspar	x **	x
Orthopyroxene	2 - 20	o ***
Clinopyroxene	0 - 3	o
Hornblende	2 - 15	5 - 30
Biotite	0 - 4	5 - 20
Garnet	0 - 5	o
Chlorite	x	x
Apatite	x	x
Zircon	x	x
Monazite	x	x
Hercynite	x	o
Ilmenite	<1	x - 2
Magnetite	1 - 2	1
Hematite	x	o
Sulfides	x	x

* Number of samples ** Less than 1% *** Not found

associated with magnetite in composite pyrite + magnetite ± chalcopyrite grains. In few samples, pyrite was found as fracture filling and replacement bodies.

The mineralogy of the amphibolite facies gneisses is rather different. Quartz, plagioclase, biotite, and hornblende are the major constituents; orthopyroxene is absent. Titanite, Fe-Ti oxides, zircon, apatite, and sulfides are the accessory phases. Minor chlorite occurs as a secondary product replacing hornblende and biotite.

Oxides include ilmenite and magnetite; hematite is absent. Ilmenite is partially replaced by titanite and rutile. Trace pyrite and chalcopyrite occur as fine, discrete or composite grains (<200 μm in diameter), interstitial to silicates; pyrrhotite is rare. An estimate of the modal composition of the amphibolite facies gneisses is shown in Table 3-1. Summary statistics for both granulite and amphibolite facies rocks is shown in Table 3-2. A complete list of the geochemical data is available in the Appendix 3-1

3-1-2. Geochemistry

The origin of the Tromoy charnockites is controversial. The long and complex metamorphic and tectonic history has obscured original charnockite-metasediment contacts (Starmer, 1972; Cooper and Field, 1977). Cooper and Field (1977) reported the presence of intercalations of both undoubted metasediments (e.g. marble, quartzite, graphitic gneisses) and former intrusives (metabasites) within the Tromoy gneiss complex.

Bugge (1940) first proposed an igneous origin for the charnockites. In contrast, Moine et al. (1972) suggested that the charnockites and associated basic rocks represent a metamorphosed spilite-keratophyre-greywacke series. Alberti and Comin-Chiaramonti (1976) interpreted the charnockites as metamorphosed sedimentary or mixed sedimentary-volcanic materials. A sedimentary origin was also considered as an alternative by Andreae (1974) and Field and Clough (1976). More recent works, however, support an igneous origin, based on evidences such as the preservation of igneous textures (Touret, 1985; Smalley and Field, 1985) and

Table 3-2. Summary statistics for Bamble acid-intermediate gneisses.

	Granulite Facies			Amphibolite Facies		
	X	1σ	C. V.	X	1σ	C. V.
SiO_2*	66.9	6.2	9.0	67	7.2	11
TiO_2	0.62	0.3	48	0.57	0.3	53
Al_2O_3	14.25	1.5	11	14.1	2.0	16
Fe_2O_3	2.18	1.1	50	1.6	0.8	50
FeO	3.9	2.1	54	3.8	1.2	32
$FeO + Fe_2O_3$	6.08	1.9	31	5.4	2.0	37
MnO	0.11	0.07	64	0.1	0.05	50
MgO	2.1	1.3	62	2.2	0.8	36
CaO	3.9	1.7	44	4.0	2.0	51
Na_2O	4.6	0.88	19	4.1	0.33	8.0
K_2O	0.5	0.3	60	1.22	0.3	29
P_2O_5	0.11	0.07	64	0.07	0.05	60
H_2O	0.74	0.45	61	0.9	0.3	33
CO_2	0.23	0.2	87	0.1	0.06	60
Cr	25	15	77	33	15	45
Ni	17	11	65	24	11	46
Co	22	12	55	31	7.0	23
Sc	17	8.0	47	18	9.0	50
V	88	70	80	82	60	73
Cu	20	12	60	33	18	50
Zn	63	38	60	60	28	47
Mo	2.7	0.7	26	2.4	1.2	50
Be	0.61	0.22	36	3.8	2.2	58
S	235	185	79	390	145	37
As	0.21	0.25	119	0.45	0.35	73
Se	0.026	0.03	115	0.04	0.02	50
Sb	0.027	0.022	81	0.05	0.03	50
Au (ppb)	0.22	0.27	108	0.15	0.1	59
Rb	6.3	6.0	95	45	25	44
Cs	0.25	0.2	67	4.5	3.0	66
Ba	132	60	45	250	60	24
Sr	144	65	45	240	75	30
Hf	7.2	2.6	36	11	5.0	45
Zr	126	60	48	225	100	44
Y	28	14	50	57	27	47
Th	1.1	1.0	91	4.5	2.5	56
U	0.38	0.3	74	1.7	1.0	59
La	11	4.0	36	30	15	50
Ce	19	8.0	42	55	25	45
Sm	3.3	1.2	36	8.0	4.0	50
Eu	0.5	0.4	57	1.85	0.7	36
Tb	1.2	0.4	33	2.4	1.5	60
Yb	3.06	1.56	51	7.0	4.0	57
Lu	0.52	0.24	46	1.1	0.6	55
F	307	253	82	460	220	48
Cl	90	80	89	170	90	53
Br	1.5	0.8	53	1.0	1.0	0.0

X = arithmetic mean σ = standard deviation C.V. = coefficient of variation

* oxides in %; elements in ppm.

modeling of minor and trace elements (Cooper and Field, 1977; Field et al., 1980; Clough and Field, 1980; Knudsen and Andersen, 1999). Radiogenic isotope data suggest a mantle source for the parent magmas (Field and Råheim, 1979; Knudsen and Andersen, 1999). However, the mantle-derived magmas are contaminated with crustal rocks (Knudsen and Andersen, 1999).

Great majority of the samples display positive scores for discriminant function (DF) proposed by Shaw (1971) to distinguish between igneous and sedimentary origin. The discriminant function is written as:

$$DF = 10.44 - 0.21SiO_2 - 0.32Fe_2O_3 \text{ (total Fe)} - 0.98MgO + 0.55CaO + 1.46Na_2O + 0.54K_2O$$

Generally, positive values suggest an igneous origin, while negative values point to a sedimentary parent rock. The equation is only applicable to quartzofeldspathic rocks with MgO <6% and SiO_2 <90%.

The major element geochemistry of the acid-intermediate gneisses from the amphibolite zone is comparable to that of the granulite zone, significant differences being lower K_2O and higher Na_2O in the granulite facies rocks. Difference in Na_2O is reflected in the anorthite content of plagioclase, as plagioclase from the granulite facies rocks is more sodic (Cooper and Field, 1977). However, marked differences exist for most minor and trace elements. The granulite facies rocks are considerably depleted in LILE and LREE (Table 3-2).

Distribution of major oxides in the acid-intermediate gneisses from both amphibolite and granulite zones define continuous trends from intermediate to felsic compositions. On chemical variation diagrams, most oxides display igneous-type differentiation trends (Figure 3-2-B-H). An exception is K_2O, which, regardless of silica content, varies between 0.15 and 1% (Figure 3-2-A). The wide scatter of K_2O may be attributed to variable mobilization of potassium during high grade metamorphism (c.f. Sheraton et al., 1973; Tarney, 1976; Condie, 1984; Finn, 1991). Like potassium, other large ion lithophile elements also show wide scatters against SiO_2, further indicating variable mobilization of these elements. Variations of Rb and U against SiO_2 is shown in Figure 3-3-A-B.

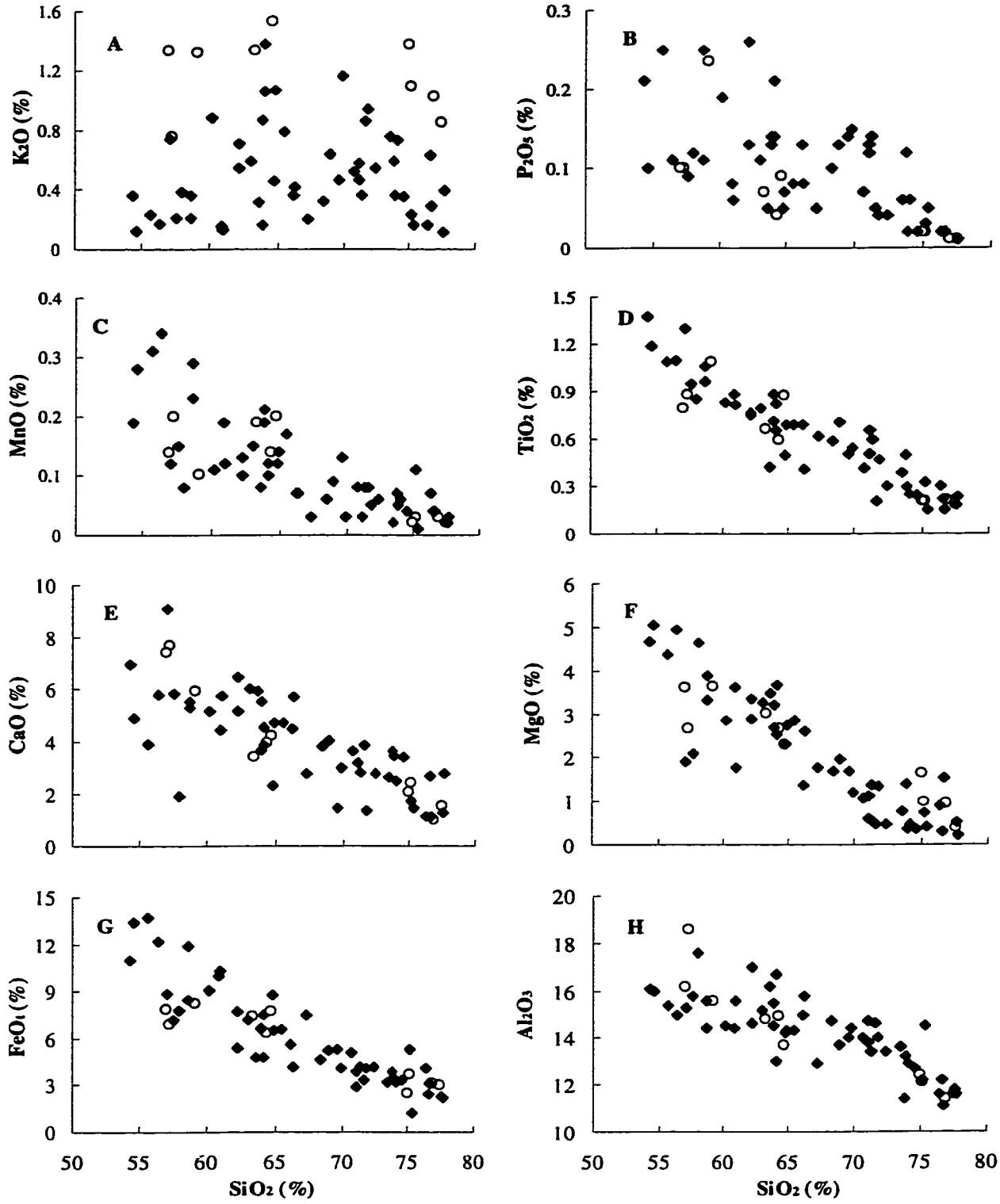

Figure 3-2. Variations of major oxides with SiO_2 in the Bamble acid-intermediate gneisses from granulite zone (squares) and amphibolite zone (circles). See text for discussion.

Transition metals and high field strength elements are amongst the least mobile elements in metamorphic and alteration processes (e.g. Pearce and Cann, 1973; Floyd and Winchester, 1975; Pearce et al., 1984). It has been suggested that these elements remain immobile at the highest grades of metamorphism (Winchester and Floyd, 1976). Variations of Ni and Hf as examples of these elements follow typical magmatic fractionation trends (Figure 3-3-C-D) further supporting an igneous origin for the charnockites. Hafnium is known to become increasingly enriched in the late, SiO_2-rich fractionates, during differentiation of felsic magmas (e.g. Correia Neves et al., 1974; Deer et al., 1992). The smooth continuous trends on chemical variation diagrams suggest that the petrologic evolution of the acid-intermediate gneisses was dominated by fractional crystallization.

Considering the geochemical classification of tonalite-trondhjemite series (Barker et al., 1976; Barker, 1979; Condie, 1981), the Tromoy gneisses, containing on average 14.2% Al_2O_3 at

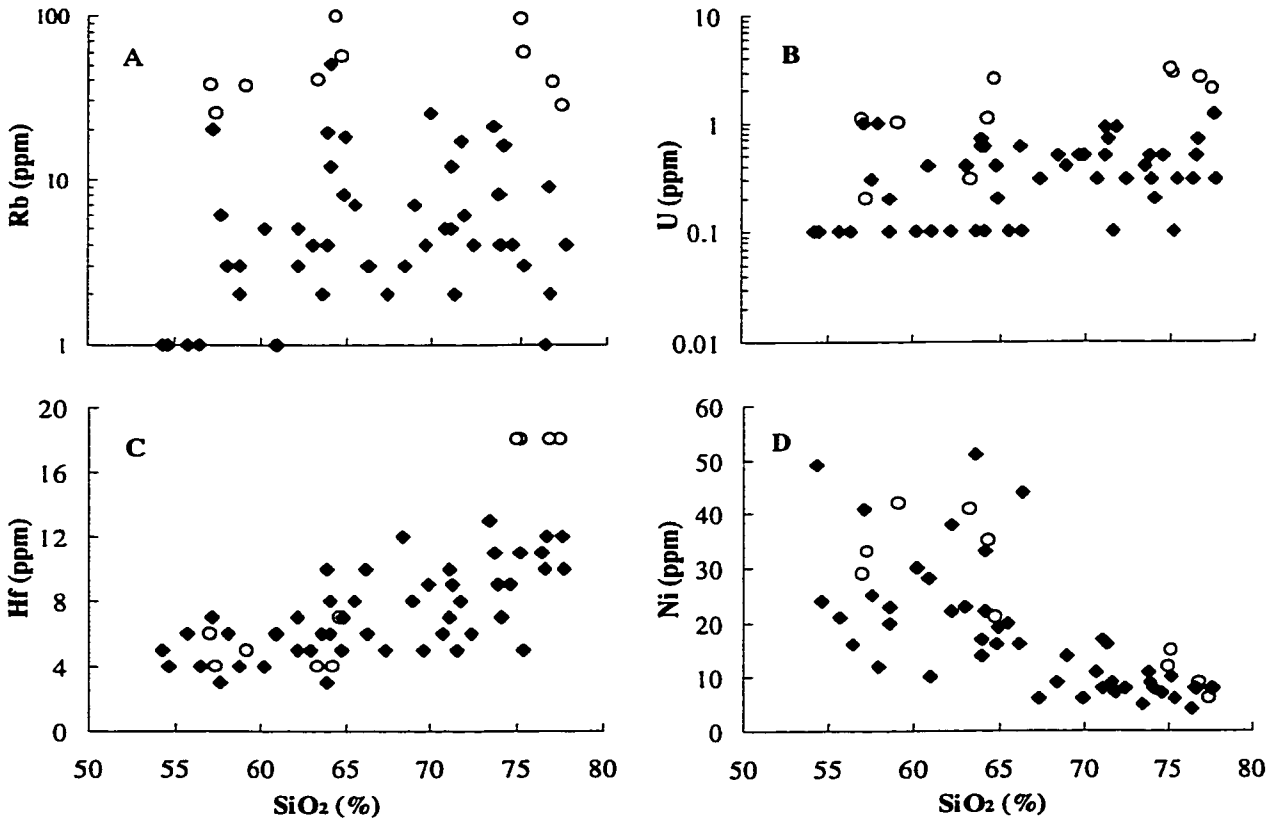

Figure 3-3. Variations of elements with SiO_2 in the Bamble acid-intermediate gneisses from granulite zone (squares) and amphibolite zone (circles). See text for discussion.

67% SiO_2, fall in the low-Al type. The low-Al series are characterized by relatively low Sr (commonly <200 ppm) but enriched Y and HREE (Barker and Arth, 1976; Drummond and Defant, 1990).

Tonalite-trondhjemite suites are important constituents of the Archean crust. They have been described from throughout the world by many workers (e.g. Glikson, 1979; Weaver and Tarney, 1981; John et al., 1983; Condie and Allen, 1984; Jahn and Zhang, 1984; Rudnick and Taylor, 1986; Martin, 1987; Wit and Armstrong, 1987; Drummond and Defant, 1990). Great majority of the Archean suites are of high-Al type. Low-Al type has been reported from Abitibi, Canada (Feng et al., 1993).

Proterozoic tonalite-trondhjemite suites are less widely distributed. Those reported in the literature are mostly of high-Al type (Arth et al., 1978; Jackson et al., 1984; Thomas, 1989; Anderson and Cullers, 1987; Puffer and Volker, 1990; Wolde and Team, 1995). Low-Al examples have been reported from Western United States (Barker et al., 1978; Condie, 1978).

The Bamble charnockites are strongly depleted in LILE relative to their amphibolite grade equivalents. This is clearly evident from chondrite-normalized plots for elements in these rocks (Figure 3-4). Mean composition of Archean and Proterozoic high-Al and low-Al tonalite-trondhjemite suites are also shown for comparison.

Depletion of K, Rb, Cs, U, and Th during granulite metamorphism is well established (e.g. Sighinolfi, 1971; Heier, 1973; Rollinson and Windley, 1980; Newton et al., 1980; Weaver and Tarney, 1981; Condie and Allen, 1984; Lamb and Valley, 1985). The Bamble charnockites are also strongly depleted in Ba and LREE, the elements commonly reported as being inert during high grade metamorphism (c.f. Tarney, 1976; Drury, 1978; Weaver and Tarney, 1980, 1981; Pride and Muecke, 1982; Jahn and Zhang, 1984; Condie and Allen, 1984).

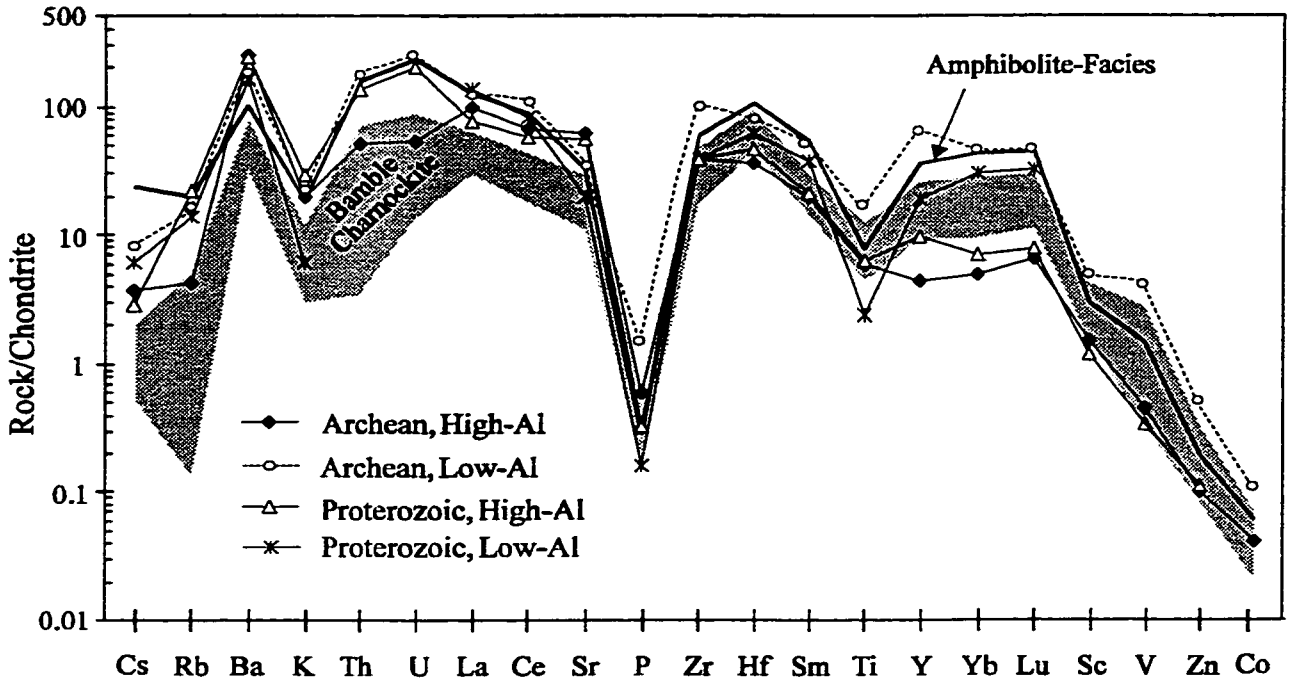

Figure 3-4. Chondrite-normalized plot for Bamble charnockites. Mean composition of equivalent rocks from amphibolite zone, and mean composition of Archean and Proterozoic high-Al and low-Al tonalite-trondhjemite suites are shown for comparison. Archean high-Al rocks are from granulite terrains. Shaded area represents $X \pm \frac{1}{2}\sigma$. Chondrite values from McDonough and Sun (1995). See Appendix 3-2 for Archean and post-Archean data.

Most granulites exhibit high K/Rb ratios, typically >300, as compared to ratios of about 250 for average continental crust, or Shaw's (1968) main trend for igneous rocks (e.g. Sheraton et al., 1973; Tarney and Windley, 1977; Condie and Allen, 1984). Bamble charnockites exhibit a range of K/Rb ratios from 300 to 2000 (Figure 3-5) that is one of the highest K/Rb ratios reported in the literature (c.f. Sighinolfi, 1971; Tarney and Windley, 1977; Cooper and Field, 1977; Condie and Allen, 1984; Cameron, 1994). In this respect, the Bamble charnockites are comparable to the Hebei granulite gneisses, China, where Jahn and Zhang (1984) reported K/Rb ratios in excess of 1000. Mean values of 0.5% K_2O and 6 ppm Rb for Bamble rocks are considerably lower than those of other granulite-facies tonalite-trondhjemite suites reported in the literature. High values of K/Rb ratios have been attributed to the loss of Rb relative to K during high grade metamorphism (e.g. Newton et al., 1980; Sheraton and Black, 1983; Jahn and Zhang, 1984).

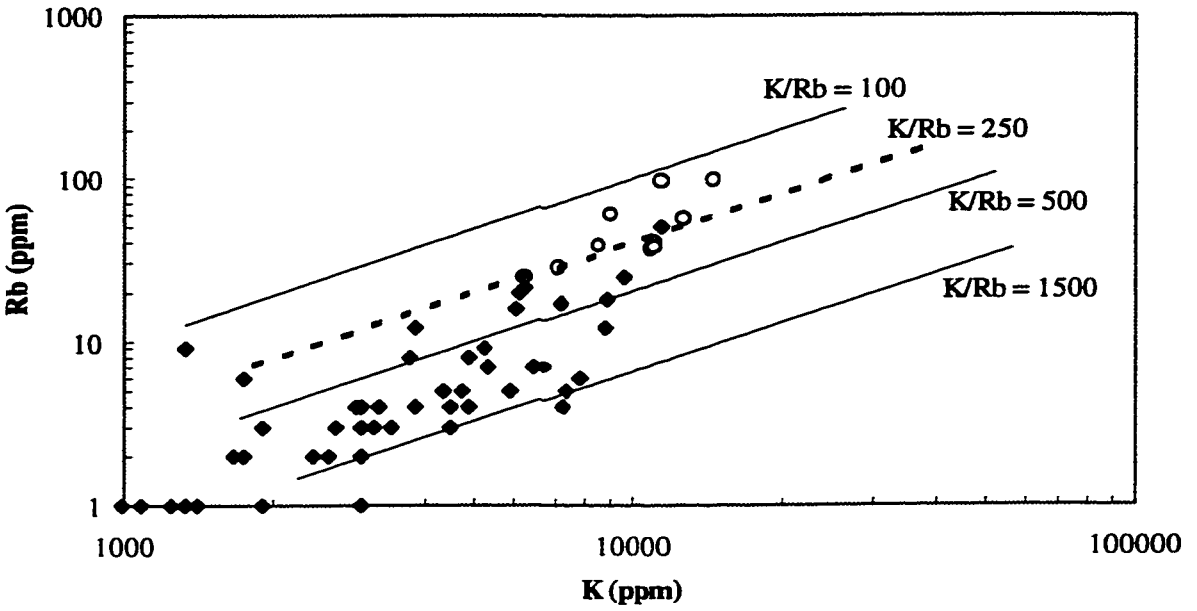

Figure 3-5. Distribution of K and Rb in Bamble tonalite-trondhjemite gneisses from granulite zone (squares) and amphibolite zone (circles). The broken line at K/Rb = 250 represents Shaw's (1968) main trend for igneous rocks.

The Bamble charnockites are strongly depleted in Th and U. However, Th/U ratios are similar in both amphibolite and granulite facies rocks (2.7 and 2.8, respectively) and close to that in the mean felsic igneous rocks (~3, Wedepohl, 1995). Uranium and Th display strong positive correlations and similar patterns of distribution in both amphibolite and granulite facies rocks (Figure 3-6-A).

Ba is positively correlated with K (Figure 3-6B). The mean K/Ba ratio in the charnockites is similar to that in the mean felsic rocks or the mean continental crust at ~30 (c.f. Wedepohl, 1995). Similar patterns of distribution for Th-U and K-Ba in the granulite and amphibolite facies rocks might be interpreted as an evidence in favor of a magmatic origin for variations of the elements. Alternatively, the similar patterns might simply be attributed to similar behavior of the elements during granulite facies metamorphism. The average Rb/Sr ratio in the Bamble charnockites (0.035) is significantly lower than that in the mean lower continental crust (0.12, Wedepohl, 1995), or the mean composition of Archean and Proterozoic tonalite-trondhjemite series (Appendix 3-2). Considering the stability of Sr during high-grade metamorphism (c.f.

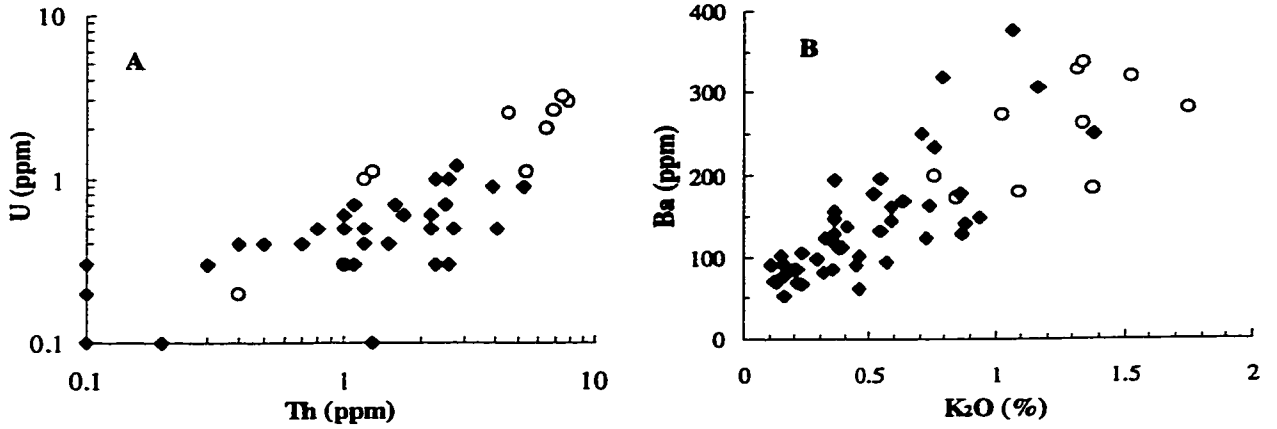

Figure 3-6. Distribution of U vs Th (A) and K_2O vs Ba (B) in Bamble tonalite-trondhjemite gneisses from granulite zone (squares) and amphibolite zone (circles).

Rollinson and Windley, 1980; Condie and Allen, 1984), a low Rb/Sr ratio further supports the metamorphic fractionation of Rb.

As in other low-Al series, the Bamble rocks are enriched in HREE and display flat chondrite-normalized REE patterns (Figure 3-7). The amphibolite facies rocks exhibit a slightly more fractionated REE pattern relative to charnockites (mean La_N/Yb_N = 4.2 and 3.2, respectively). The Bamble charnockites are significantly depleted in LREE compared to their amphibolite facies equivalents or other tonalite-trondhjemite series (Figure 3-7).

The Bamble tonalite-trondhjemite series show distinct negative Eu anomalies, regardless of the total REE contents (Figure 3-7). Negative Eu anomaly seems to be a characteristic feature of low-Al series. This is in contrast to an earlier study by Field et al. (1980) who, based on a small number of samples, concluded that most granulite facies rocks (charnockites) are relatively enriched in Eu, particularly at high Σ REE. The Bamble charnockites further display a flat to negative Ce anomaly, unlike other tonalite-trondhjemite suites with commonly positive Ce anomaly (Figure 3-7).

Enrichment of HREE in Bamble charnockites might be attributed to contamination of the parent magma with sedimentary country rocks (c.f. Field et al., 1980). Earlier in Chapter 2 it was shown that Bamble metasedimentary rocks are relatively enriched in HREE and display poorly fractionated chondrite-normalized REE patterns. A countryrock effect is also supported by sulfur isotope data, as the charnockites display $\delta^{34}S$ values in the same range as in their metasedimentary host rocks. Similarly, Hubbard and Whitley (1979) showed that the high HREE contents and low La/Yb ratios in the quartzofeldspathic granulites from southwest Sweden were inherited from their sedimentary parent rocks.

The Bamble charnockites display no distinct correlation between SiO_2 and ΣREE (Figure 3-8). An inverse correlation between REE and SiO_2 has been reported from many tonalite-trondhjemite series, consistent with a magmatic fractionation model (e.g. Arth et al., 1978; Arth, 1979; Rollinson and Windley, 1980; Condie and Allen, 1984; Anderson and Cullers, 1987).

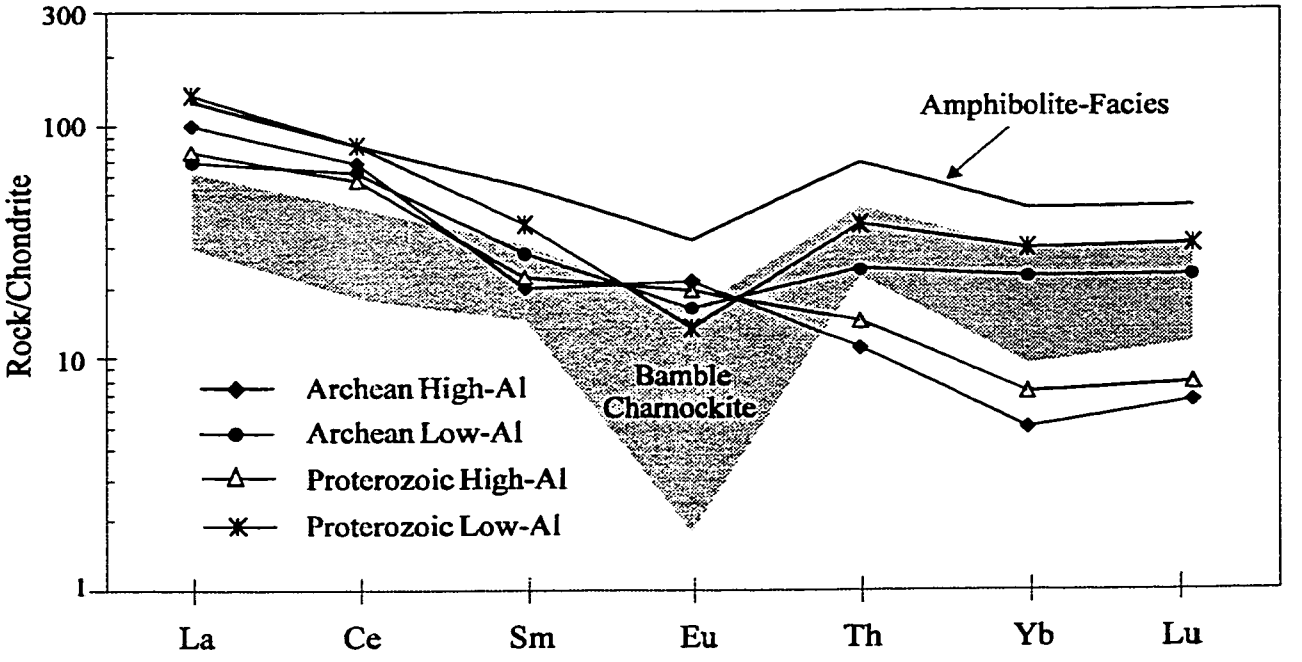

Figure 3-7. Chondrite-normalized REE pattern for Bamble charnockites. Shaded area represents X ± ½ σ. The mean composition of equivalent rocks from amphibolite zone, and the mean composition of Archean and Proterozoic high-Al and low-Al tonalite-trondhjemite suites are shown for comparison. Chondrite values from McDonough and Sun (1995). See Appendix 3-2 for Archean and post-Archean data.

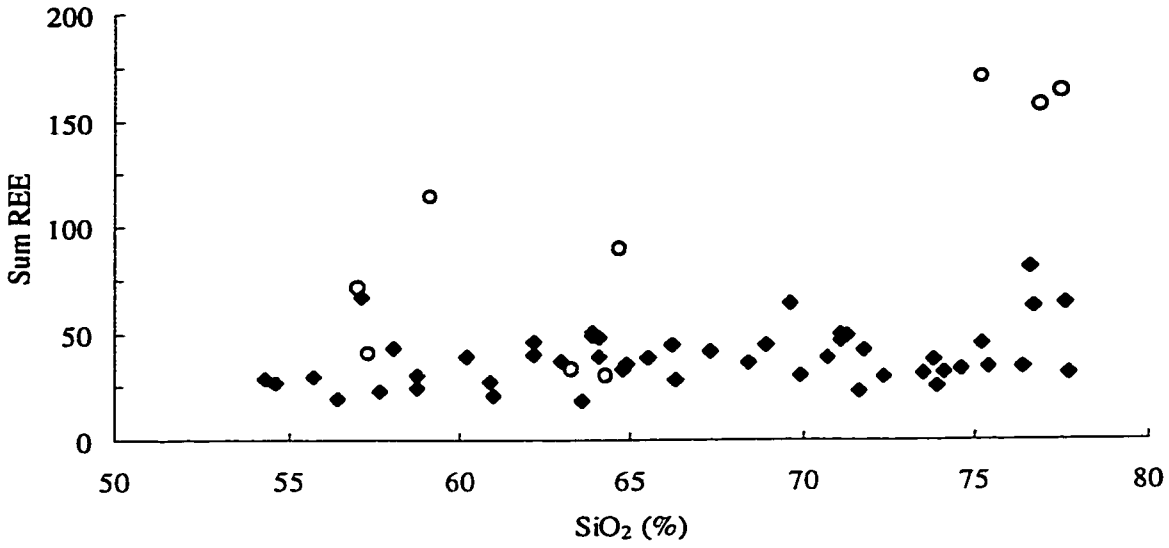

Figure 3-8. Variations of rare earth elements (REE) with SiO_2 in Bamble tonalite-trondhjemite gneisses from granulite (squares) and amphibolite (circles) zones.

3-1-3. Petrogenesis

Tonalite-trondhjemite suites are common constituents of the Precambrian terrains, and their petrogenesis has been studied by many authors (e.g. Barker and Arth, 1976; Hunter et al., 1978; Arth et al., 1978; Tarney et al., 1979; Rollinson and Windley, 1980; Rudnick and Taylor, 1986; Martin et al., 1987; Anderson and Kullers, 1987). The great majority of the Precambrian tonalite-trondhjemite suites are of high-Al type.

The genesis of tonalite-trondhjemite suites have alternatively been attributed to:

1) Partial melting of basalts or amphibolites ± garnet (e.g. Barker and Arth, 1976; Tarney et al., 1979; Rollinson and Windley, 1980; Martin, 1987), or of eclogite or garnet-granulite (e.g. Arth and Hanson, 1975; Compton, 1978; Rudnick and Taylor, 1986; Anderson and Kullers, 1987).

2) Fractional crystallization of basaltic magmas (Arth et al., 1978; Rollinson and Windley, 1980).

The low-Al suites are distinguished by low Sr, enriched Y and HREE, negative Eu anomaly, and flat or mildly fractionated REE patterns. The low Al and Sr contents and negative Eu anomalies suggest that feldspar fractionation, either in the source region (residual phase), or during fractional crystallization (cumulate phase), had a significant influence (c.f. Barker et al., 1976; Hanson, 1978; Mc Kay, 1989). Removal of feldspar would also deplete the magma in LREE (c.f. Darke and Weill, 1975).

The enriched HREE is attributable to the extraction of phases which do not efficiently remove HREE, such as plagioclase and pyroxene. The relatively low La_N/Yb_N ratios and flat REE patterns suggest that garnet was not residual. Partial melting of basalt with a plagioclase-rich (40-60%) residue, has been suggested for the genesis of Proterozoic low-Al trondhjemite and dacite of northern New Mexico and southwest Colorado (Barker et al., 1976; Condie, 1978).

Field et al. (1980) showed that tonalite-trondhjemite gneisses from both granulite and transition zones in Bamble are part of the same Sr isotopic system, and that their low initial $^{87}Sr/^{86}Sr$ ratio (0.70345 ± 0.00014) is consistent with a low Rb/Sr source region in the upper mantle. The authors interpreted the gneisses as new additions to the continental crust, and not as reworked older gneisses or anatexis of high Rb/Sr metasediments. A similar source region was proposed for mid-Proterozoic, low-Al tonalite-trondhjemite suites from New Mexico and Colorado with low initial Sr^{87}/Sr^{86} values (Barker et al., 1976; Condie, 1978). In a recent radioisotope study, however, Knudsen and Andersen (1999) proposed the involvement of both mantle- and crustal-derived source materials in the petrogenesis of the Bamble gneisses.

Generation of tonalite-trondhjemite magmas with low initial $^{87}Sr/^{86}Sr$ ratios has alternatively been attributed to:

1. A low degree of partial melting of mantle (Holland and Lambert, 1975; Rollinson and Windley, 1980).
2. Partial melting of basalt or quartz-eclogite (Arth and Hanson, 1975; Barker et al., 1976; Rollinson and Windley, 1980).
3. Fractional crystallization of a wet basaltic magma (Arth et al., 1978).

The absence of basic and intermediate rocks temporally and genetically associated with the tonalitic-trondhjemitic rocks at Bamble, and the relatively high contents of transition metals, favors an origin of the rocks by partial melting rather than fractional crystallization. A direct mantle source is rejected because of the low degree of partial melting required, and the difficulty in extracting small amount of melt (c.f. O'Nion and Pankhurst, 1978; Tarney et al., 1979; Rollinson and Windley, 1980; Drummond and Defant, 1990). The low contents of Sr, K, Rb, and Ba, and negative Eu anomaly suggest that the Bamble charnockites probably derived from a basaltic source with plagioclase and phlogopite in the residue.

Although sharing many features with low-Al tonalite-trondhjemite series, the Bamble rocks are further characterized by high iron content. They contain, on average, 6% FeO_t at 67% SiO_2, while comparable rocks commonly contain <3% FeO_t. In this respect, the Bamble rocks may be compared to the intrusive rapakivi granite suites of Scandinavia and North America (c.f. Silver et al., 1977; Anderson and Cullers, 1978). However, the Bamble rocks are distinguished from rapakivi granites by considerably lower contents of LILE. The rapakivi suites were emplaced under anorogenic conditions within a broad crustal belt extending from the Urals to the Western United States during the period 1800-1000 Ma (Bridgwater and Collerson, 1976, Silver et al., 1977; Anderson and Cullers, 1978).

3-1-4. Tectonic Setting

The Bamble tonalite-trondhjemite gneisses plot mostly in the calc-alkaline field on Jensen's oxide diagram (Figure 3-9). The Fe-rich nature of the gneisses shifts the plots towards the tholeiitic field. Plot of the samples on the tectonic discrimination diagrams of Maniar and Piccoli (1989) suggest a continental arc or island arc setting (Figure 3-10-A-B).

Considering the distribution of the major oxides, SiO_2, FeO, and MgO (Figure 3-10-A), the Bamble tonalite-trondhjemite gneisses share features with continental collision granitoids (CCG) and post-orogenic granitoids (POG). However, both CCG and POG are characterized by relatively higher K and Na, and plot away from continental and island arc granitoids on Shand's alumina index diagram (Figure 3-10-B).

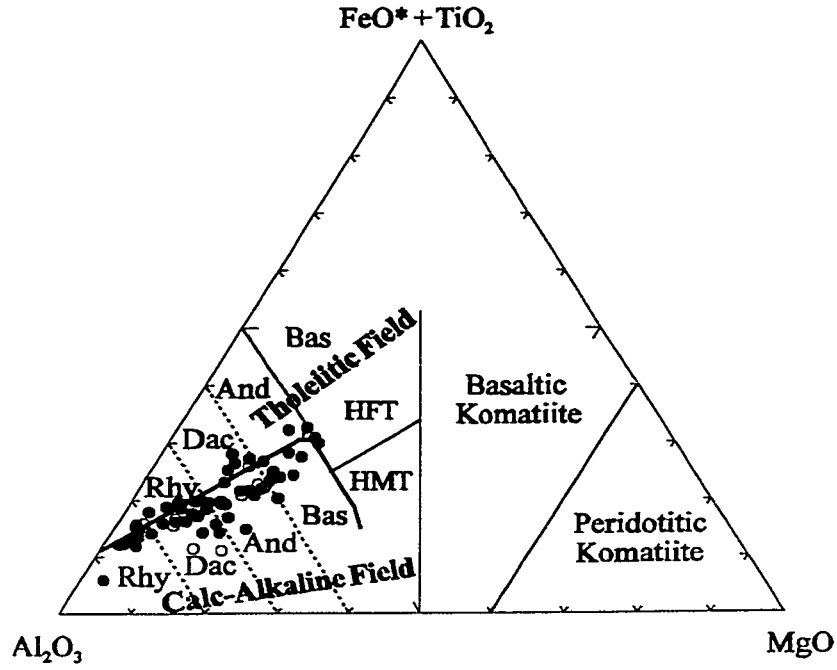

Figure 3-9. Plot of the tonalite-trondhjemite gneisses from granulite zone (solid circles) and amphibolite zone (open circle) on Jensen's oxide diagram (Jensen, 1976). Note that most samples fall in the calc-alkaline field.

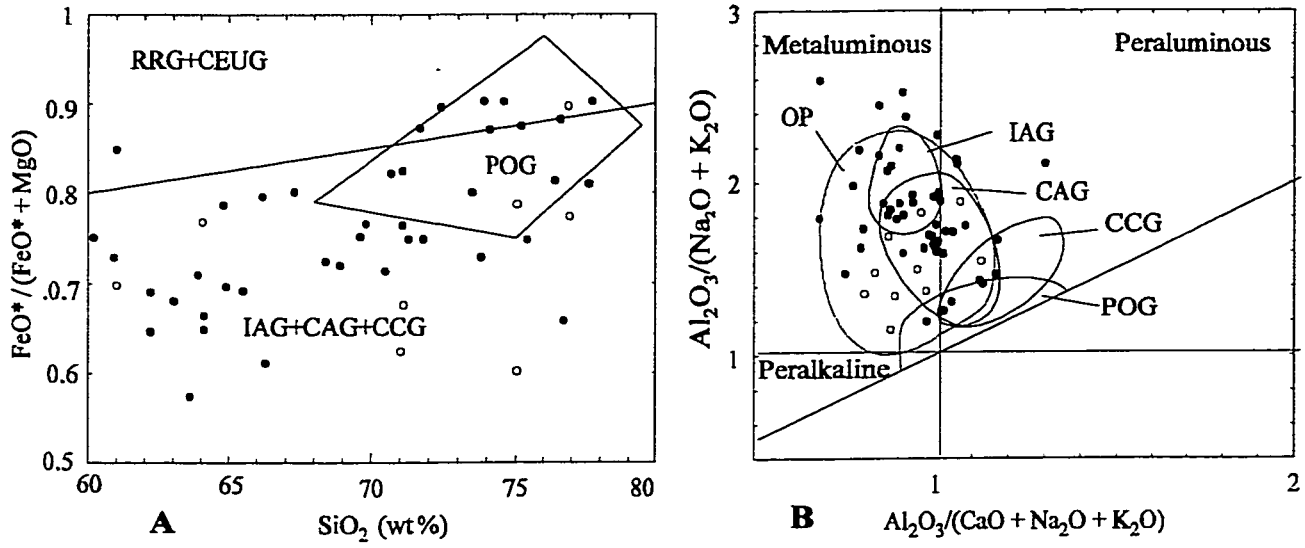

Figure 3-10. Plot of the tonalite-trondhjemite gneisses from granulite zone (solid circles) and amphibolite zone (open circle) on Shand's alumina index (A) and SiO_2 vs. FeO*/FeO* + MgO (B). Tectonic discrimination boundary lines from Maniar and Piccoli (1989). CAG = continental arc granitoids; IAG = island arc granitoids; OP = oceanic plagiogranite; CCG = continental collision granitoids; POG = post-orogenic granitoids; RRG = rift-related granitoids; CEUG = continental epirogenic uplift granitoids.

Tonalite-trondhjemite series occur largely in continental margins related to subduction or to subsidiary back-arc spreading (Barker et al., 1976; Barker, 1979; Grabezhev et al., 1986; Puffer and Volkert, 1991; Smith et al., 1997). A destructive margin setting has been proposed for many Proterozoic and Phanerozoic tonalite-trondhjemite series (Barker, 1979). Smalley and Field (1985) proposed an Andean (Cordilleran) type magmatic arc setting for the Bamble charnockites.

3-1-5. Distribution of Chalcophile Elements

The Bamble tonalite-trondhjemite gneisses are depleted in Au, Sb, As, and Se compared to the general abundances of the elements in felsic igneous rocks elsewhere (Figure 3-11). Sulfur is in the same common range as in the felsic rocks; Cu is slightly enriched. No significant differences exist between the granulite and the amphibolite zones with respect to the abundances of chalcophile elements (Table 3-2).

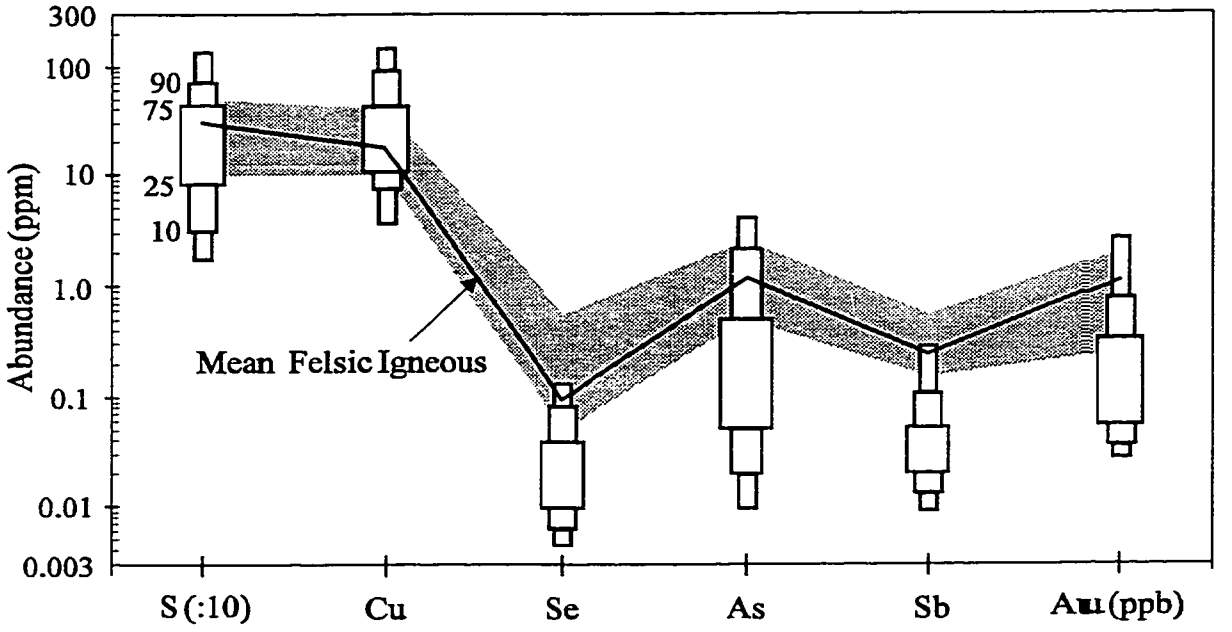

Figure 3-11. Abundance of chalcophile elements in the Bamble tonalitic-trondhjemitic gneisses, with cumulative frequencies indicated for 10, 25, 75, and 90%. The common range (shaded area) and the mean abundance (solid line) of chalcophile elements in felsic igneous rocks worldwide are shown for comparison. See Appendix 2-2 for the composition of felsic igneous rocks.

The abundance of Au in felsic igneous rocks has been determined to fall in a wide range from 0.1 ppb to 10 ppb, with most values in the range 0.2-2.5 ppb (e.g. Gottfried et al., 1972; Saager and Meyer, 1983; Grabezhev et al., 1986; Korobeynikov, 1986; Yoon, 1991; Feng et al., 1993). A comparison of data from Bamble with those in the literature is shown Figure 3-12. The median Au value in the Bamble tonalite-trondhjemite gneisses is significantly lower than that in felsic igneous rocks elsewhere. Gold in 30% of the Bamble rocks is below the detection limit of 0.1 ppb. The abundance of gold in these samples is arbitrarily taken as half the detection limit.

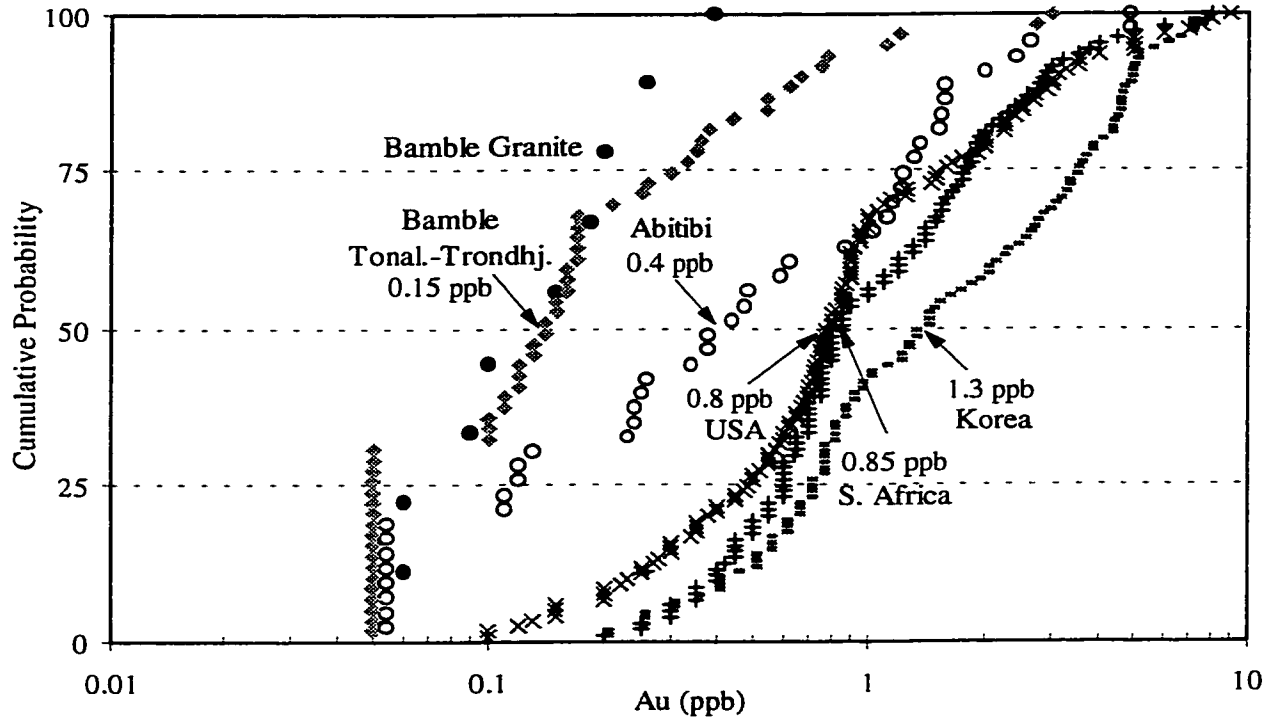

Figure 3-12. Probability distribution of Au in the Bamble tonalite-trondhjemite gneisses. Distribution of Au in granitoids from Abitibi, Canada (Feng et al., 1993), USA (Gottfried et al., 1972), South Africa (Saager and Meyer, 1983), and Korea (Yoon, 1991) shown for comparison. Also plotted are post-orogenic granites from Bamble (solid spheres). Arrows indicate the median values.

3-1-6. Discussion

3-1-6-A. Depletion of LILE and REE

The causes of depletion in certain elements, particularly LILE, in charnockites has been a controversial issue. Models for the genesis of LILE-depleted charnockites fall into 4 general categories:

1) Partial melting with partitioning of granithophile elements into the melts (Fyfe, 1973; Pride and Muecke, 1980; Nesbitt, 1980).

2) Crystallization from a depleted parent magma (Holland and Lambert, 1975; Tarney et al., 1979).

3) Intrusion of water-undersaturated magma into dry crust during, or subsequent to, granulite-facies metamorphism (Holland and Lambert 1975; Drury 1978; Martignole, 1979; Field et al., 1980; Tarney and Weaver, 1987; Frost et al., 1989).

4) Metasomatic fluid processes, involving either dehydration with increasing pressure and temperature (e.g. Heier 1973; Thompson, 1982) or CO_2 streaming (e.g. Sheraton et al. 1973; Tarney 1976; Newton, 1980, 1992; Stahle et al., 1987; Frost et al., 1989).

A partial melting model is not supported by the existing evidence. The Tromoy granulite complex as a whole, and especially the Tromoy charnockites, are SiO_2-rich. The Tromoy granulite complex is one of the most silicic Precambrian granulite terrains reported in the literature (c.f. Glikson, 1979; Clough and Field, 1980; Weaver and Tarney, 1980; Rao and Rao, 1980; Jahn and Zhang, 1984; Martin, 1987).

A partial melting is also rejected by Ba/Sr ratios. This process is expected to lead to a plagioclase-rich residual phase with considerably higher partition coefficient for Sr (c.f. Arth, 1976; Weaver and Tarney, 1981). Ba/Sr ratios for both granulite and amphibolite facies gneisses are similar (0.92 and 1.0, respectively) implying that granulites have not lost a significant melt fraction. This is in agreement with earlier works by Knudsen (1996) and Knudsen et al. (1997) who showed that granulite facies rocks at Bamble experienced only

local anatexis. A marked negative Eu anomaly in the charnockites argues against their origin as residuum of crustal anatexis.

Field et al. (1980) suggested that the Bamble tonalite-trondhjemite series formed as synmetamorphic intrusives from a parent dacitic magma, the LILE-depleted and K-feldspar deficient orthogneisses from the granulite zone representing plagioclase-rich cumulates, and the equivalent, normal-LILE rocks from transition and amphibolite zones representing the relatively LILE-rich residual liquids. A similar model was proposed by Rollinson and Windley (1980) to explain the geochemical differences between granulite and amphibolite facies tonalite-trondhjemite suites at Scourie, Scotland.

A cumulate origin, as proposed by Field et al. (1980) is based on the assumption of positive Eu anomaly in the granulite-facies rocks, and negative Eu anomaly in the equivalent rocks from transition and amphibolite zones. However, our data based on a larger number of samples clearly indicate that both granulite and amphibolite facies rocks are similarly depleted in Eu. A cumulate origin is also rejected by the lower concentration of Sr in the granulite facies rocks.

Intrusion of water-undersaturated magma into dry crust during high grade metamorphism has been proposed as a possible origin for LILE depletion (Holland and Lambert 1975; Drury 1978; Martignole, 1979; Field et al., 1980; Smalley et al., 1983; Tarney and Weaver, 1987; Frost et al., 1989). It has been indicated that the distribution of elements in deep-seated intrusive rocks is controlled by the pressure and temperature conditions during synmetamorphic intrusion (Smalley et al., 1983; Holland and Lambert, 1975).

Tarney et al. (1979) proposed that depletion of LILE in tonalitic rocks might be a feature inherited from the parent magma, and not necessarily a metamorphic overprint. The authors argued that if the source material was the subducting oceanic crust, LILE may have been removed by hydrothermal activities during subduction, prior to the generation of the tonalitic magmas. Tarney and Weaver (1987) suggested that depleted tonalitic granulites are formed in

a two-stage process, in which LILE are first extracted from oceanic crust, followed by partial melting of the depleted residue to generate primary depleted tonalitic magmas.

LILE-deficiency in the charnockites might be attributed to crystallization of the parent magma under high CO_2/H_2O fluid conditions (c.f. Weaver and Tarney, 1981; Lamb et al., 1986). A high CO_2/H_2O would reduce the stability fields of hydrous phases, and initiate their replacement by anhydrous mineral assemblages (Wyllie, 1977).

Alternatively, depletion of certain elements in charnockites might be attributed to granulite metamorphism. Fluids during granulite-facies metamorphism are known to be CO_2-rich (e.g. Touret, 1974; Newton et al., 1980), and could be the agent responsible for complexing and removal of radioactive heat-producing elements, K, Rb, U, and Th, as well as Cs (Weaver and Tarney, 1981; Newton et al., 1980; 1985; Janardhan et al., 1982; Condie et al., 1982; Condie and Allen, 1984; Hanson et al., 1984; Stahle et al., 1987; Taylor and McLennan, 1988).

Fluid inclusion studies have indicated that Bamble charnockites crystallized, or recrystallized, in a high P_{CO2} environment (Touret, 1971, Hoefs and Touret, 1975; Van Den Kerkhof et al., 1994). The large volumes of CO_2 required were probably derived from the mantle (Hoefs and Touret, 1975; Newton et al., 1980; Anderson et al., 1984), but most likely via an intermediate stage of basic magmas (Newton et al., 1980; Lamb et al, 1986;).

Depletion of REE might be related to the presence of fluids that form soluble complexes with these elements. The low Y and HREE, and the relatively high La_N/Yb_N of Archean high grade gneisses have been attributed to removal of HREE by CO_2 fluids (Collerson and Fryer, 1979; Collerson and Bridgwater, 1979). According to the authors, CO_2- and halogen-rich fluids that invade gneissic rocks may deplete the gneisses in HREE, modifying the initial distribution patterns of REE. Depletion of REE in charnockites from Kabbaldurga, India, was attributed to the dissolution of REE-bearing minerals, zircon, apatite, and monazite, as a consequence of

infiltration of carbonic fluids along a system of ductile shears and foliation planes (Stahle et al., 1987).

Transportation of REE by carbonate complexes is supported by experimental works (Kosterin, 1959; Wendlandt and Harrison, 1979; Cantrell and Byrne, 1987). REE form stable carbonate complexes and strongly partition into CO_2-rich fluids over a wide range of temperatures (Kosterin, 1959). Cantrell and Byrne (1987) indicated that $(CO_3)^+$ is important for LREE and $(CO_3)_2^-$ for HREE. Wendlandt and Harrison (1979) showed that LREE are more soluble than HREE in CO_2 fluids. Partitioning of REE into carbonic fluids is supported by high concentrations of REE in carbonate veins reported from some high-grade metamorphic terrains (Lausch et al., 1974; Bogoch et al., 1986; Dahlgren et al., 1993). The relatively low contents of LREE and low La_N/Yb_N ratios in the Bamble granulite-facies rocks may be attributed to preferential removal of LREE.

The marked negative Eu anomaly in the Bamble charnockites is explicable in terms of the presence of an oxidizing CO_2 fluid during magmatic crystallization, or metamorphic recrystallization. Experimental works have indicated that Eu behaves differently from other REE in that its partitioning is strongly dependent on oxygen fugacity (Darke, 1975; Darke and Weill, 1975; Mysen et al., 1978). Europium occurs in two oxidation states, Eu^{+2} and Eu^{+3}. Eu^{+2} preferentially occurs in feldspars, for which rather low oxygen fugacity is required (Puchelt and Emmermann, 1976). Apatite structure favors Eu^{+3} with a lower ionic radii. A high f_{O2}, as indicated for Bamble charnockites (Cameron, 1989b; Harlov, 1992), could have prevented Eu from being incorporated into feldspars during magmatic crystallization, retaining this element in the residual melt. The low abundance of Eu in Ameralik anorthosites, west Greenland, was explained by crystallization under a high f_{O2} (O'Nions and Pankhurst, 1974).

Under oxidizing conditions, Eu, presumably in its trivalent state, is taken up by apatite. A positive Eu anomaly in apatite suggests a high f_{O2} (Puchelt and Emmermann, 1976). Analysis of apatite would probably show whether the magma crystallized under oxidizing conditions, or the high oxidation state recorded for the charnockites, is a secondary metamorphic overprint.

A marked negative correlation between P_2O_5 and SiO_2 (Figure 3-2-B) indicates that apatite crystallized early in the crystallization of the acid-intermediate gneisses.

Bamble charnockites are further distinguished by a flat to negative Ce anomaly, unlike other tonalite-trondhjemite suites with commonly positive Ce anomaly (Figure 3-7). Cerium is a divalent element, occurring both as Ce^{+3} and Ce^{+4}. A negative Ce anomaly may be taken as a further evidence for crystallization of magma under a high f_{O2}, or, alternatively, recrystallization of the charnockites under an oxidizing condition during metamorphism.

It has been indicated that Bamble charnockites equilibrated, at peak metamorphic conditions, under a high f_{O2}, ~2.7 log units above the QFM buffer (Cameron, 1991a; Harlov, 1992). Whether the high oxidation state is inherited from the parent magma (crystallization under oxidizing conditions) or is a secondary metamorphic overprint, is not precisely known. Fluid inclusion studies have indicated the presence of abundant CO_2 during crystallization, or recrystallization, of the charnockites (Touret, 1974; Newton et al., 1980).

Field et al. (1986) proposed a different timing for intrusion and metamorphism of the Bamble charnockites, based on the marked difference between the age of the closure of the whole rock Rb/Sr system (1540 ± 20 Ma) and the age of the intrusion (1578 ± 6 Ma, zircon U-Pb). However, the authors do not rule out the possibility that the Rb and/or Sr fractionation could have been complete before the late, post-metamorphic closure of the Rb-Sr whole rock systems, and that the different dates reflect differential closure of the zircon U-Pb and whole-rock Rb-Sr systems.

Whether depletion in certain elements occurred during magmatic crystallization, or subsequent metamorphic recrystallization, can not be resolved from the chemical data alone. In either case, CO_2 appears to have played a critical role, either by suppressing the formation of hydrous phases during magmatic crystallization, or by complexing and removal of LILE and REE during granulite metamorphism. The same chemical changes generated by crystallization under high P_{CO2} could be produced by post-solidus infiltration of carbonic fluids.

3-1-6-B. Depletion of Gold

The Bamble tonalite-trondhjemite gneisses are strongly depleted in Au, compared to the general abundance of this element in felsic igneous rocks elsewhere. They are also depleted in As, Sb, and Se, but not in S or Cu. The median value of Au in the gneisses (0.15 ppb) is less than 20% of that in most granitoids. The relatively low concentration of Au in the Bamble gneisses might be of primary magmatic origin, or a consequence of metamorphism. The gneisses bear features typical of continental arc settings. Tonalites and trondhjemites are common constituents of orogenic magmatic suites, occurring generally during the early tectonic stages (e.g. Barker et al., 1976; Saager and Meyer, 1983; Grabezhev et al., 1986; Feng et al., 1993). A compilation of data on the abundance of Au in felsic igneous rocks of various ages and tectonic cycles is shown in Table 3-3.

No systematic relationship exists between the abundance of Au and the tectonic cycle of the intrusive activities. Whereas data from Eastern Transvaal (Saager and Meyer, 1982) show an increase in Au towards the post-orogenic granitoids, data from Abitibi (Feng et al. 1993) suggest a decrease in this direction; and yet data from Urals (Grabezhev et al., 1986) show no significant difference in the abundance of Au from the early orogenic towards the late orogenic granitoids.

Sulfides are known to be the main host to Au in igneous rocks (Keays et al., 1981; Saager et al., 1982; Korobeynikov, 1989). An effective removal of Au requires a modification of the initial magmatic sulfides (Cameron, 1989a, b, 1994). Sulfides occur as accessory minerals in the Bamble charnockites, rarely exceeding 0.2% by mode. Pyrite is the main sulfide, followed by pyrrhotite and chalcopyrite. The sulfide minerals occur as discrete, as well as composite, grains interstitial to silicates.

Pyrrhotite was the stable Fe-sulfide phase at peak metamorphism, at ~ 800 °C, given that pyrite is not stable above ~740 °C (Kullerud and Yoder, 1959). Interstitial pyrite is commonly associated with magnetite in composite pyrite + magnetite ± chalcopyrite grains, and appears

Table 3-3. Distribution of Au (ppb) in felsic intrusive rocks of various ages and tectonic settings

Lithology	Tectonic setting	Age	Locality	Mean	Range	Ref.*
Tonalite-trondhjemite	Early orogenic	Archean	E. Transvaal	1.2	0.4 - 7.8	1
alkali granite	Syn- orogenic	"	"	1	0.4 - 5.2	"
granodiorite-syenodiorite	Post-orogenic	"	"	1.7	0.4 - 5.5	"
Tonal.-trondhjem.-granodior.	Synvolcanic	Archean	Abitibi	1.5	1.1 - 2.6	2
Tonal.-granod.-qtz-monzonite	syn-tectonic	"	Abitibi	0.4	0.05-0.6	"
Syenite-monzonite-granite	Late- to post-tectonic	"	Abitibi	0.05		"
Syenite-qtz-syenite	Post-tectonic	"	Abitibi	0.7	0.2 - 2	"
Monz.- monzodio.-granod.-syen.	Syn- to late tectonic	Archean	Pontiac	0.7	0.1 - 1.6	
Tonalite-granodiorite	Early orogenic	Paleozoic	Urals	2.5	1 - 7	3
granite	Late orogenic	"	"	2	1 - 6	"
leucogranite-adamellite	Post-orogenic	"	"	2.7	1 - 8	"
Granitoid association	Various	Paleozoic	Central Asia	2		4
Granitoid association	Various	Mesozoic	Central Asia	2.2		"
Tonal., Qtz-monzonite, granod.	Calc-alkalic provinces	Mesoz.- Cenoz.	United states	1.2	0.1 - 5	5
Syenite, monzonite, granite	Alkalic provinces	"	"	0.7	0.1 - 2	"
Tonal., Qtz-monzonite, granod.	Various	Mesozoic	Sierra Nevada	1	0.2 - 5	6
Tonalite - trondhjemite	Early orogenic	Mid- Proteroz.	Bamble	0.25	0.05 - 1	7
Alkali-granite	Post-orogenic	Late-Proterozoic	Bamble	0.18	0.05-0.39	7

* References: 1. Saager and Meyer (1982); 2. Feng et al. (1993); 3. Grabezhev et al. (1986); 4. Korobeynikov (1986); 5. Gottfried et al. (1972); 6. Tilling et al. (1973); 7. Present study

to be pseudomorphic after pyrrhotite. Magnetite may occur as rims of varying thickness (10-50 μm), or as euhedral to anhedral grains and patches in the composite sulfide-oxide grains.

Phase relations in Fe-O-S system (e.g. Kullerud and Yoder, 1959; Kullerud, 1957, 1967) show that below ~750°C, the addition of oxygen to pyrrhotite saturated with S would lead to the oxidation of Fe in the pyrrhotite to magnetite and the formation of pyrite:

$$6FeS + 2O_2 \leftrightarrow 3FeS_2 + Fe_3O_4$$

A similar reaction is proposed to explain the common association of magnetite with pyrite in Bamble charnockites and metabasites (Cameron, 1989b, Cameron et al., 1993), in Lewisian granulites, Scotland (Cameron, 1994), and in Shevaroy Hills charnockites, India (Harlov et al.,

1997). Further oxidation would lead to the replacement of pyrite by magnetite. Cameron (1989b) and Harlov (1992) indicated that the granulite grade rocks at Bamble equilibrated, at peak metamorphism, under a high f_{O2}, ~2.5 log unit above the QFM buffer. Cameron (1989 a, b) suggested that serial changes from pyrrhotite to pyrite and magnetite led to the mobilization of chalcophile elements.

3-2. Granites

Post-Sveconorwegian events comprised intrusion and faulting (e.g. Falkum, 1985; Padget, 1990; Starmer, 1985, 1991, 1993). Large, post-tectonic felsic intrusions, exemplified by Herefoss Granite (Figure 1-2) dated at 0.96 ± 0.06 Ga (whole rock Rb-Sr; Brueckner, 1972) and Grimstad Granite dated at 0.99 ± 0.01 Ga (zircon and titanite U-Pb; Kullerud and Machado, 1991) are the last representatives of Sveconorwegian magmatic activity in Bamble. The intrusions were emplaced diapirically, commonly forming subcircular bodies (Starmer, 1991, 1993). Some 10 samples of the post-tectonic granites were collected from a small stock in Arendal area.

3-2-1. Mineralogy

The granites are characterized by abundant coarse K-feldspar phenocrysts and scant ferromagnesian minerals. Biotite and hornblende are minor phases rarely exceeding 10% by mode. Accessory phases include zircon, apatite, Fe-Ti oxides, and sulfides. Minor sericite, chlorite, and epidote occur as alteration products after feldspars, biotite and hornblende.

Trace pyrite is present in most samples as fine (<200μ in diameter) euhedral to subhedral grains typically associated with biotite, but also interstitial to quartz and feldspars. No pyrrhotite was observed on reflected light microscope. Based on textural evidence, interstitial pyrite appears to be primary, although some pyrite may be of secondary origin.

3-2-2. Geochemistry and Tectonic Setting

The granites contain relatively high SiO_2 and K_2O in their norms. On a mesonormative quartz-alkali feldspar-plagioclase diagram, the samples plot in monzogranite and syeno-granite fields (Figure 3-13). For the sake of simplicity, the samples are collectively referred to as granites. Summary statistics for Bamble granites is shown in Table 3-4. A complete list of the wholerock geochemical data is included in the Appendix 3-3.

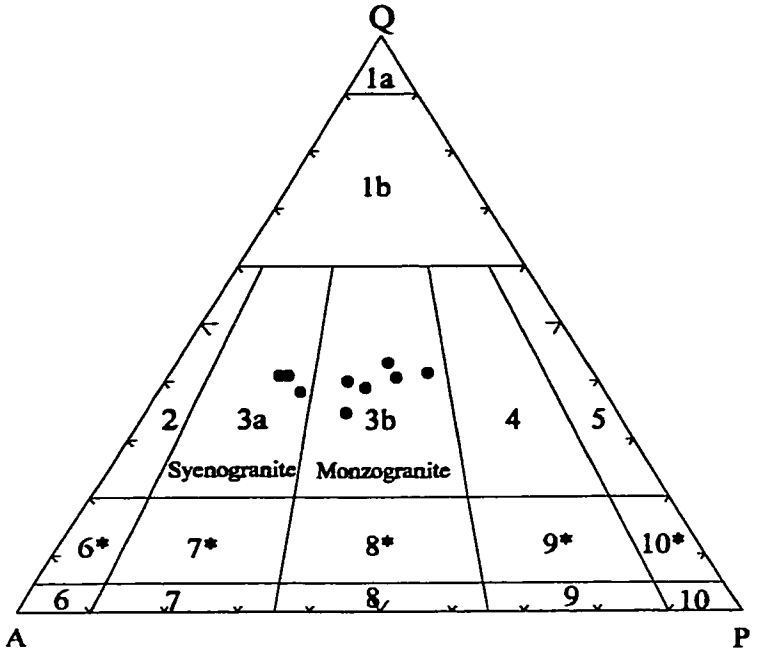

Figure 3-13. Plot of the Bamble granites on mezonormative quartz-alkali feldspar-plagioclase diagram. Fields for various rocks adapted from Le Maitre (1989). See the reference for nomenclature.

The Bamble granites bear the distinctive geochemical signatures of A-type granites, such as enrichment in K, REE (except Eu), Zr, and Y, and depletion in Sr, Ba, and transition metals (c.f. Loiselle and Wones, 1979; White and Chappel, 1983; Hermes and Zartman, 1985; Whalen et al., 1987; 1996). A chondrite-normalized extended element plot for the Bamble granites is shown in Figure 3-14. Mean composition of A-type granites from Australia (Collins et al., 1982) and Topsails granites from Newfoundland Appalachians (Whalen et al., 1996) are shown for comparison.

An A-type character for the Bamble granites is supported by the distribution of the relatively immobile elements, Zr-Nb-Ce-Y, vs. major oxides, on discriminant diagrams proposed by Whalen et al. (1987) (Figure 3-15-A, B). The granites further display features in common with "post-orogenic granitoids" and "continental epirogenic uplift granitoids" (Figure 3-16-A-B). A post-orogenic timing for the late Proterozoic granitic intrusions in Bamble is in agreement with the tectonic scenario of the southern Norway as depicted by Starmer (1985; 1991, 1993), Verschure (1985), and Padget (1990).

Table 3-4. Summary statistics for Bamble post-orogenic granites.

	X	1σ	C. V.
SiO_2 *	76.5	0.8	1.0
TiO_2	0.19	0.02	11
Al_2O_3	11.8	0.4	3
Fe_2O_3	0.7	0.5	71
FeO	0.9	0.2	22
MnO	0.02	0.01	50
MgO	0.44	0.15	34
CaO	0.8	0.2	25
Na_2O	2.7	0.6	22
K_2O	5.70	1.10	19
P_2O_5	0.02	0.01	50
H_2O	0.3	0.2	53
CO_2	0.19	0.16	84
Cr	7.0	3.0	43
Ni	1.0	1.0	100
Co	38	10	26
Sc	5.6	0.9	16
V	1.0	0.5	50
Zn	8.0	2.0	25
Mo	0.50	0.0	0.0
Be	1.8	1.0	56
S	90	40	44
Cu	9.0	3.0	33
As	0.25	0.12	48
Sb	0.05	0.025	50
Au (ppb)	0.18	0.12	67
Rb	127	25	20
Cs	0.30	0.10	33
Ba	560	150	27
Sr	50	18	36
Nb	39	15	38
Hf	6.3	1.2	19
Zr	260	32	12
Y	80	18	23
Th	26.0	8.0	31
U	4.3	1.2	28
La	54	15	36
Ce	112	40	40
Sm	13	3.5	31
Eu	1.2	0.5	54
Tb	2.5	0.9	37
Yb	6.4	2.5	36
Lu	0.5	0.2	45
F	160	60	38
Cl	50	0.0	0.0
Br	0.4	0.1	25

X= arithmetic mean σ = standard deviation C.V.= coefficient of variation
* oxides in %; elements in ppm.

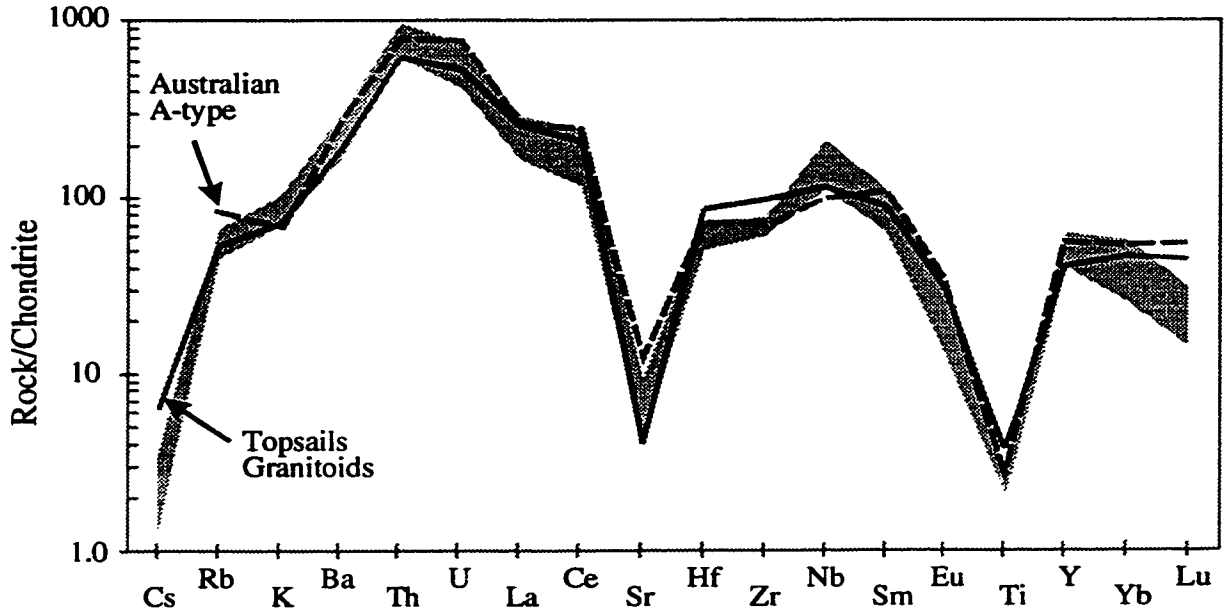

Figure 3-14. Chondrite-normalized plot for Bamble granites. The shaded area represents $\bar{x} \pm \frac{1}{2}\sigma$. Mean composition of A-type granites from Australia (Collins et al., 1982) and Topsails granites from Newfoundland Appalachians (Whalen et al., 1996) are shown for comparison.

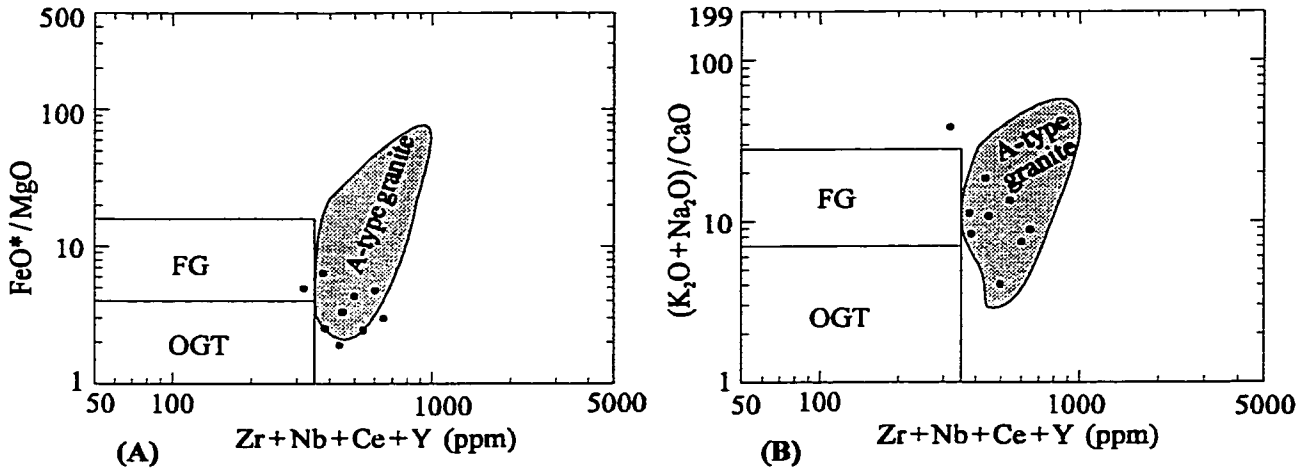

Figure 3-15. Plot of Bamble granites on (A): Zr + Nb + Ce + Y vs. FeO*/MgO and (B): (K_2O + Na_2O)/CaO discrimination diagram of Whalen et al. (1987). Almost all samples plot in the A-type granite field. Fields for fractionated felsic granites (FG) and unfractionated M-, I, and S-type granites (OGT) shown for reference.

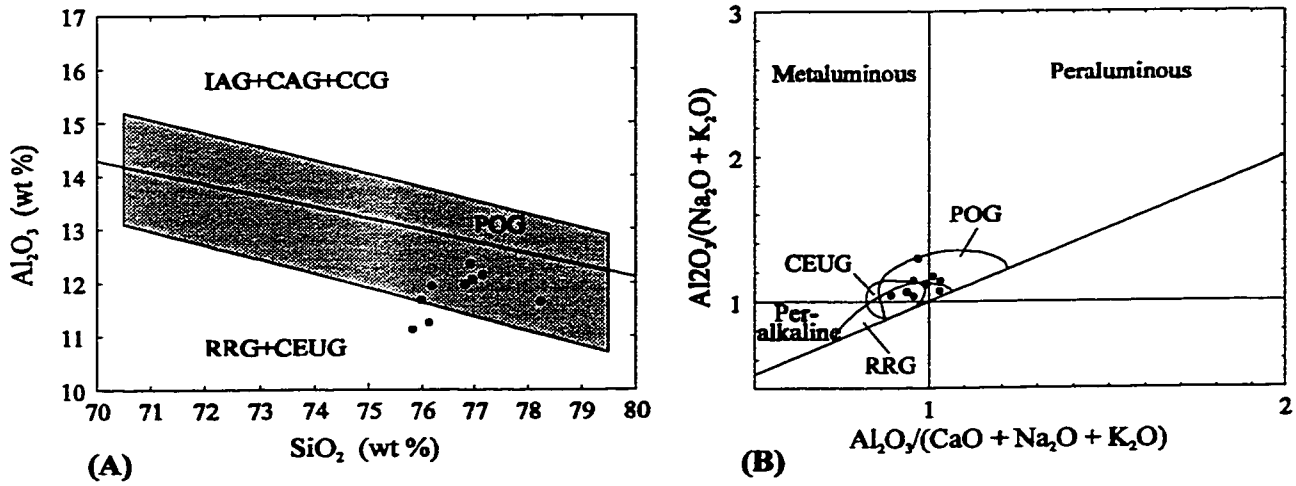

Figure 3-16. Plot of Bamble granites on Shand's alumina index. IAG = island arc granitoids; CAG = continental arc granitoids; CCG = continental collision granitoids. POG = post-orogenic granitoids; CEUG = continental epirogenic uplift granitoids; RRG = rift related granitoids. Boundary lines and fields for different types of granitoids from Maniar and Piccoli (1989).

3-2-3. Distribution of Chalcophile Elements

The Bamble granites are considerably depleted in chalcophile elements compared to the mean composition of granitoids elsewhere (Figure 3-17). The granites contain, on average, 0.18 ppb Au that is 20% of the general abundance of this element in granitic rocks. A comparison of the distribution of Au in the Bamble granites and felsic rocks worldwide in shown in Figure 3-12.

The abundance of chalcophile elements in granitic rocks is mainly controlled by their source region and the degree of partial melting. Experimental studies have indicated that solubility of S in magmas depends strongly on FeO content (e.g. Haughton et al., 1974; Wendlandt, 1982). A relation between the abundance of Fe, S, and Au has been reported from several granitoid complexes (e.g. Davletov, 1970; Zvereva and Gavrilenko, 1971; Gottfried et al., 1972; Grabezhev et al., 1986). Grabezhev et al. (1986) reported a positive correlation between the abundances of Au and Fe in granitoids from different tectonic settings. Saager and Meyer (1982) showed that Au in granitoids is preferentially hosted in sulfide minerals and that precipitation of Au from a crystallizing magma is essentially determined by its sulfur fugacity.

The Bamble post-orogenic granites are characterized by low Fe_t, compared to similar granites elsewhere (c.f. Collins et al., 1982; Whalen et al., 1987; Whalen et al., 1997). The relatively low contents of S and chalcophile elements in the Bamble granites is, at least partly, explicable in terms of the low initial Fe_t content. However, regarding the small number of samples, and the restriction of the samples to a small body, the data presented here can not be representative of the Bamble post-orogenic granites at large.

Alternatively, the depletion of chalcophile elements might be attributed to the source rocks. Post-orogenic, alkaline granites are the products of partial melting of older metamorphic rocks (e.g. Longstaffe et al., 1980; Chappell et al., 1987; Kerr et al., 1993; Whalen et al., 1997). Earlier in Chapter 2, it was shown that the Bamble supracrustal rocks are considerably depleted in chalcophile elements, particularly in Au. Accordingly, the granitoids generated by partial melting of these rocks would be relatively depleted in chalcophile elements. Removal of chalcophile elements by late-magmatic fluids of pegmatitic or hydrothermal nature can not be ruled out.

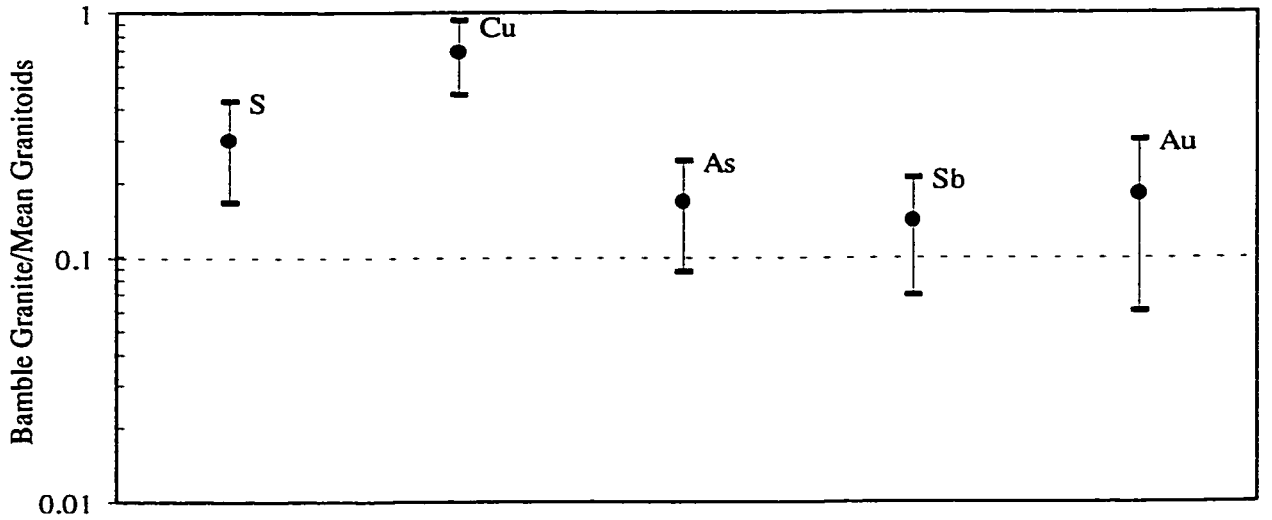

Figure 3-17. Distribution of chalcophile elements in the Bamble granites, normalized to the mean composition of granitoids. See Appendix 2-2 for normalization data.

4. Mafic Igneous Rocks and Associated Fe-Ni-Cu Ores

Two major intrusive mafic series occur in the Bamble Shear Belt:

1. Entirely metamorphosed, concordant to discordant intrusions, known as metabasite, emplaced during the Kongsbergian Orogeny.
2. Composite bodies with cores of coronitic gabbro and amphibolitized margins, known as hyperite, emplaced during the Sveconorwegian Orogeny. The hyperites are locally associated with Cu-Ni sulfide deposits.

4-1. Metabasites

Basic igneous rocks metamorphosed under amphibolite and granulite grades are widespread in the Bamble and the adjacent Telemark and Kongsberg Sectors (e.g. Field, 1966; Clough and Field, 1980; Smalley et al., 1983; Atkin and Brewer, 1989; Cameron, 1989a, b; Starmer, 1990). The basic rocks, known as metabasites, form subconcordant to concordant minor dykes and sheets, parallel to the northeast-southwest regional foliation (Smalley et al., 1983). The metabasites intruded older supracrustal rocks during the early stages of the Kongsbergian (Gothian) Orogeny (Smalley and Field, 1985; Starmer, 1991, 1993). Some 110 samples of metabasites are collected from Ubergsmoen in the amphibolite zone A, Tvedestrand in the transition zone B, Hissoy in the transition zone C, and Tromoy in the granulite zone D. The locations of the sampling sites are shown in Figure 1-2.

4-1-1. Mineralogy

4-1-1-A. Silicates

The metabasites have totally metamorphic textures and mineral assemblages, implying that they have equilibrated to the conditions of metamorphism. Hornblende, the principal ferro-magnesian silicate in the amphibolite zone is increasingly replaced by pyroxenes toward the granulite zone. Hornblende and plagioclase are the major minerals in the metamorphic zones A, B, and C, usually accompanied by variable amounts of pyroxenes, garnet, biotite, and

quartz. Apatite may occur as an accessory phase. Pyroxenes appear in zone B, increase in modal ratio in zone C, and may dominate hornblende in zone D.

Biotite is, at least partly, of secondary origin. It commonly occurs as elongated laths cutting across, and replacing, other minerals, particularly hornblende. Minor chlorite, epidote, sericite, and carbonates may occur as secondary alteration products after ferromagnesian minerals and plagioclase. A visual estimate of the modal composition of metabasites from various metamorphic zones is shown in Table 4-1.

4-1-1-B. Oxides

Fe-Ti oxides are present as minor phases in all zones. Ilmenite is the dominant oxide in metabasites from zones A, B, and C. The granulite facies metabasites, however, are characterized by predominance of magnetite over ilmenite. Exsolution lamellae of magnetite in ilmenite, and vice versa, are common. Hematite, when present, usually occurs as exsolution lamellae within ilmenite. It is rare in zone A, but common in other zones. It is most common in zone B, forming up to 50% of the ilmenite body. Minor rutile was found as an alteration product after ilmenite in the amphibolite grade metabasites.

Table 4-1. Modal composition of metabasites from various metamorphic zones, Bamble.

Metamorphic Zone	Zone A (41*)	Zone B (16)	Zone C (22)	Zone D (29)
Plagioclase	25 - 50	35 - 50	40 - 55	30 - 60
Quartz	0 - 8	0 - 3	0 - 5	0 - 15
Hornblende	35 - 75	35 - 75	40 - 60	35 - 55
Orthopyroxene	o**	0 - 4	0 - 15	5 - 40
Clinopyroxene	0 - 5	0 - 5	0 - 5	0 - 10
Biotite	0 - 10	0 - 10	0 - 10	0 - 2
Garnet	0 - 10	o	0 - 5	0 - 2
Chlorite	x***	x	x	x
Titanite	x	x	x	x
Apatite	x	x	x	x
Zircon	x	x	x	x
Fe-Ti Oxides	1 - 4	1 - 3	1 - 3	1 - 4
Sulfides	x	x	x	x

* Number of samples ** Not found *** Trace (< 1%)

Magnetite may occur as discrete entirely magnetite grains, or, less commonly, associated with lamellae of ilmenite. Exsolution of ilmenite in magnetite is a common feature in igneous rocks (e.g. Buddington and Lindsley, 1964; Lindsley, 1991; Haggerty, 1991). At temperatures above ~550°C, ulvospinel and magnetite form a continuous solid solution (Lindsley, 1981). Slow cooling from 700 to 400°C and subsequent oxidation of ulvospinel to ilmenite results in rapid unmixing and formation of ilmenite exsolution lamellae along the 111 directions of the magnetite host crystal, according to the reaction:

$$6Fe_2TiO_4 + O_2 = 2Fe_3O_4 + 6FeTiO_3 \qquad \text{(Buddington and Lindsley, 1964)}$$

Ilmenite takes different forms, the most common of which include: a) ilmenite-only type, b) ilmenite-magnetite type, and c) ilmenite-hematite-magnetite type (c.f. Cameron et al., 1993). The ilmenite-only type includes entirely ilmenite grains that may contain sparse, thin lamellae of hematite along the 0001 planes. The ilmenite-magnetite type is rather similar to the ilmenite-only type, but contains thin, straight lamellae of magnetite along the 0001 planes (Plate 4-1-A). Subordinate lamellae of hematite may be present.

The ilmenite-hematite-magnetite type includes ilmenite and exsolution lamellae of magnetite and hematite along the 0001 planes. This type is interpreted to have formed at high temperature as homogeneous grains of hemoilmenite (Buddington et al., 1963; Cameron, 1989b, Cameron et al., 1993). Cameron (1989b, 1993a) showed that hemoilmenite was the stable oxide phase at peak metamorphism around 800°C. During cooling from peak metamorphism, the ilmenite-hematite solvus was intersected at approximately 740°C (Figure 4-1) leading to exsolution of broad lamellae of ilmohematite along the 0001 planes. With further cooling and expansion of the two phase region, there was exsolution of further generations of hematite in ilmenite, and vice versa, as fine lamellae (Plate 4-1-B). Further cooling was associated with the formation of magnetite lamellae in ilmenite grains, also along the 0001 plane.

From the composition of the magnetite lamellae and the adjoining ilmenite, Cameron et al. (1993) calculated a f_{O2} of ~2.5 log unit above QFM buffer and a temperature of 450-500°C

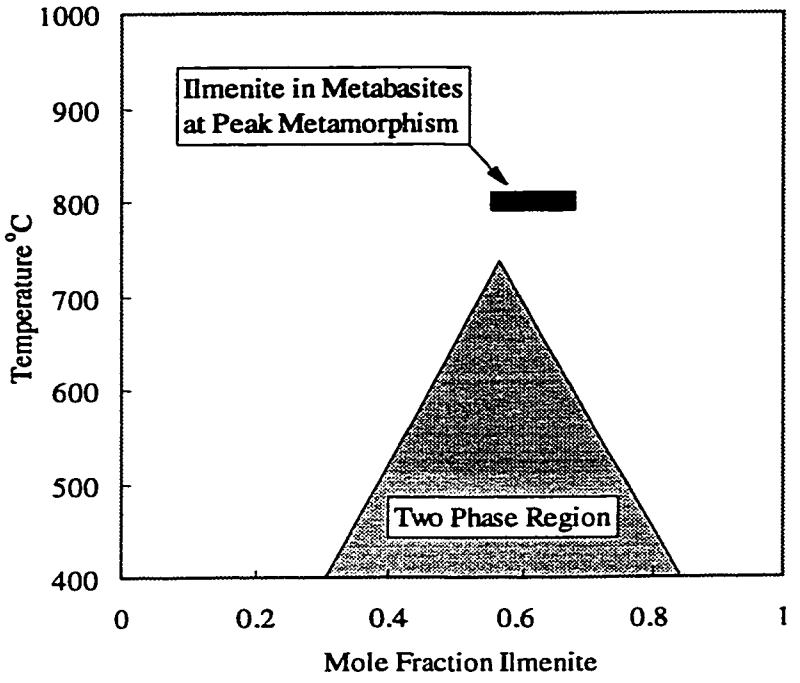

Figure 4-1. Two phase region for ilmenite-hematite mixtures. Solid bar represents the composition of hemoilmenite in Bamble metabasites at metamorphic peak. Adapted from Cameron et al. (1993a).

for the ilmenite-hematite-magnetite equilibrium. The magnetite lamellae have been interpreted to be late, since they occur mainly within broad lamellae of ilmohematite, implying that magnetite formed after phase separation of hematite (Cameron et al., 1993a). Magnetite exsolution results from the subsolidus reduction of hematite component of ilmenite (Buddington et al., 1963):

$$6Fe_2O_3 \leftrightarrow 4Fe_3O_4 + O_2$$

The ilmenite-hematite-magnetite type is the main form of ilmenite in the metabasites. Some grains show late replacement by titanite particularly on fractures along 0001 planes.

4-1-1-C. Sulfides

Sulfides occur as accessory phases in the metabasites, rarely exceeding 0.5% by mode. However, sulfides are known to be the main host to Au in igneous rocks (e.g. Gottfried et al., 1972; Tilling et al., 1973; Boyle, 1979; Keays et al., 1981; Saager et al., 1982; Korobeynikov,

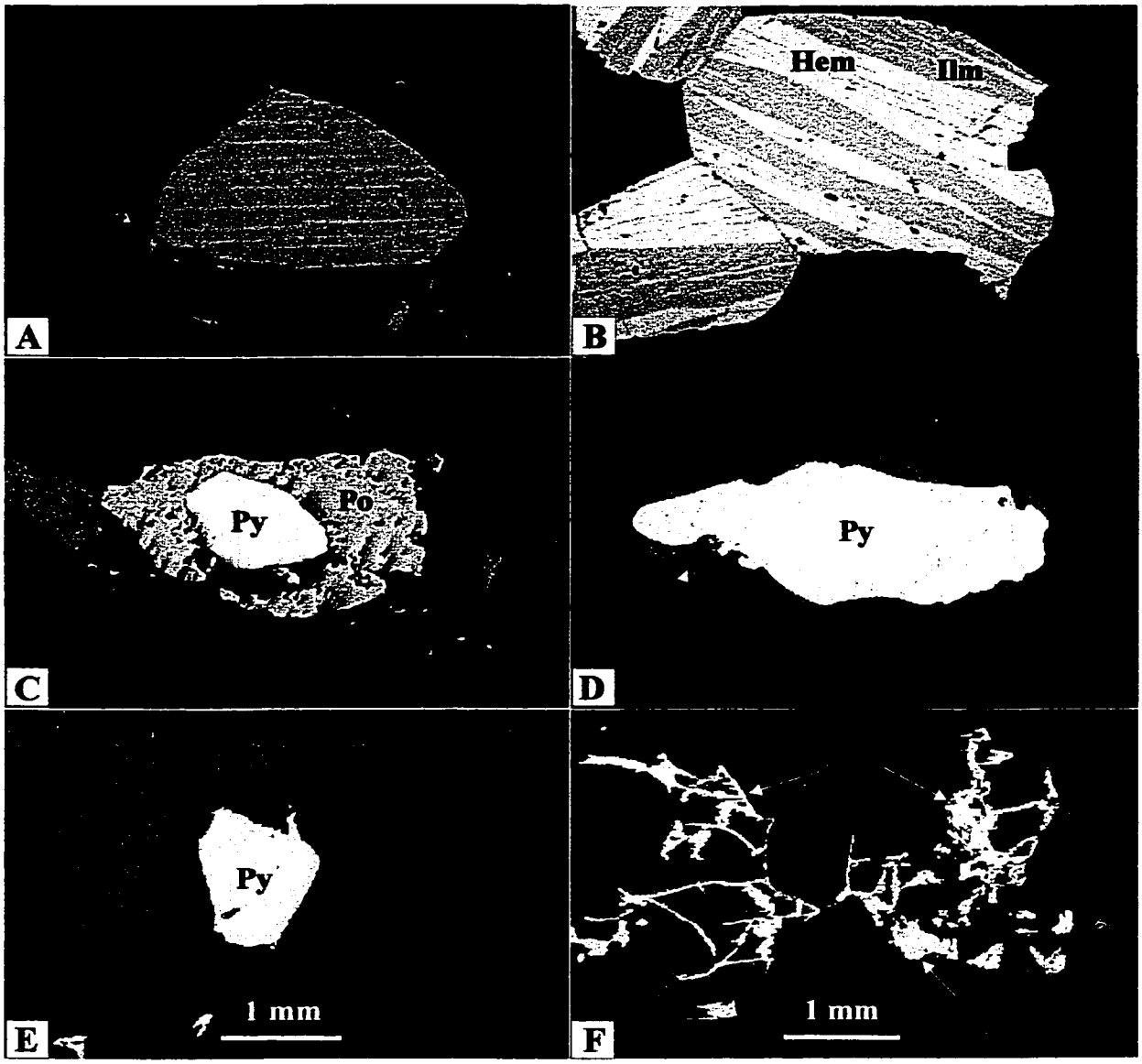

Plate 4-1. Various textural and compositional types of oxides and sulfides in the Bamble meta-basites. (A) Ilmenite containing exsolution lamellae of magnetite; sample 6804. (B) Exsolution lamellae of hematite in ilmenite, and vice versa; sample 3907. (C) Ni-rich pyrite (Py_{Ni}) as an euhedral grain within interstitial pyrrhotite; sample 6801. (D) Co-rich pyrite (Py_{Co}) mantled by magnetite; sample 3901. (E) Interstitial pyrite partially replaced by chlorite; sample 4101. (G) Secondary sulfides (pyrite and chalcopyrite) occurring as fracture filling and replacement in hornblende; sample 6504.

1989). During magmatic crystallization, Au strongly partitions into the sulfide phase. The partitioning of Au between sulfide and silicate liquids has been determined to be in the range 10^3 to 10^5 (Peach and Mathez, 1987; Peach et al., 1990; Stone et al., 1990; Crocket et al., 1991, 1997; Barnes, 1993; Fleet et al., 1996).

Depletion of Au in the Bamble and Lewisian lower crustal rocks has been attributed to the oxidation of the country rocks and the breakdown of sulfides (Cameron, 1989b, 1991, 1993, 1994). Accordingly, the mineralogy of sulfides and their behavior during metamorphic and post-metamorphic processes are of particular concern in the present study.

Considering the mineralogy, composition, and mode of occurrence, several parageneses of sulfides can be identified in the metabasites. Data from electron probe analyses indicated that various textural and compositional types of sulfides may be distinguished according to Ni and Co contents (Figure 4-2):

Interstitial pyrrhotite (Po_i) occurs as euhedral to anhedral grains, 20 to 400 μm in diameter, interstitial to silicates and oxides (Plate 4-1-C). Po_i is commonly associated with exsolution lamellae and/or patches of chalcopyrite and pentlandite. Pyrrhotite-chalcopyrite-pentlandite is a common sulfide paragenesis in mafic rocks, forming from a monosulfide solid solution with decreasing temperature (e.g. Vaughan et al., 1971; Naldrett, 1989). With increasing f_{O2}, pyrrhotite may be replaced by pyrite + magnetite (e.g. Kullerud, 1967; Glassley, 1983; Cameron, 1989b; Harlov et al., 1997).

The metal/sulfur percentages (100[Fe + Ni + Co + Cu]/[Fe + Ni + Co + Cu + S]) suggest the presence of two types of pyrrhotites, in accordance with the variations described by Arnold (1966) for hexagonal (>47.2%) and monoclinic (<47.2%) polymorphs. Monoclinic pyrrhotite is commonly associated with pyrite. The large variation of Ni in Po_i is related to the local variations of Ni in the parent magmas and the presence or absence of pentlandite in the sulfide paragenesis.

Bleb pyrrhotite (Po_b) occurs as small rounded blebs, <20 μm in diameter, enclosed in silicates. As in Po_i, the Po_b may contain exsolution lamellae of chalcopyrite and pentlandite.

Interstitial pyrite (Py_i) exists as euhedral to anhedral grains, 20 to 400 μm in diameter, interstitial to silicates and oxides. Py_i may occur as discrete entirely pyrite grains, or in composite pyrite ± magnetite ± chalcopyrite ± pentlandite grains. Pyrite ± magnetite appears to be an oxidation product after initial magmatic pyrrhotite. Three major types of Py_i are identified (Figure 4-2):

1. Ni-rich pyrite (Py_{Ni}). This type is characterized by relatively high Ni in the range 1-4%. Py_{Ni} commonly occurs as euhedral to subhedral grains or grain aggregates associated with chalcopyrite, pentlandite and/or magnetite. It may also occur as euhedral to subhedral grains enclosed in pyrrhotite (Plate 4-1-C).
2. Co-rich pyrite (Py_{Co}). This type commonly occurs as polygonal grains associated with little or no chalcopyrite or pentlandite. Mantling by magnetite is common (Plate 4-1-D).
3. Ni-Co pyrite (Py_{Ni-Co}). This pyrite is known by variable Ni and Co contents. It commonly occurs in composite grains of pyrite ± chalcopyrite ± pentlandite ± magnetite (Plate 4-1-E). Pyrites of various textural types show little deviation from stoichiometric composition.

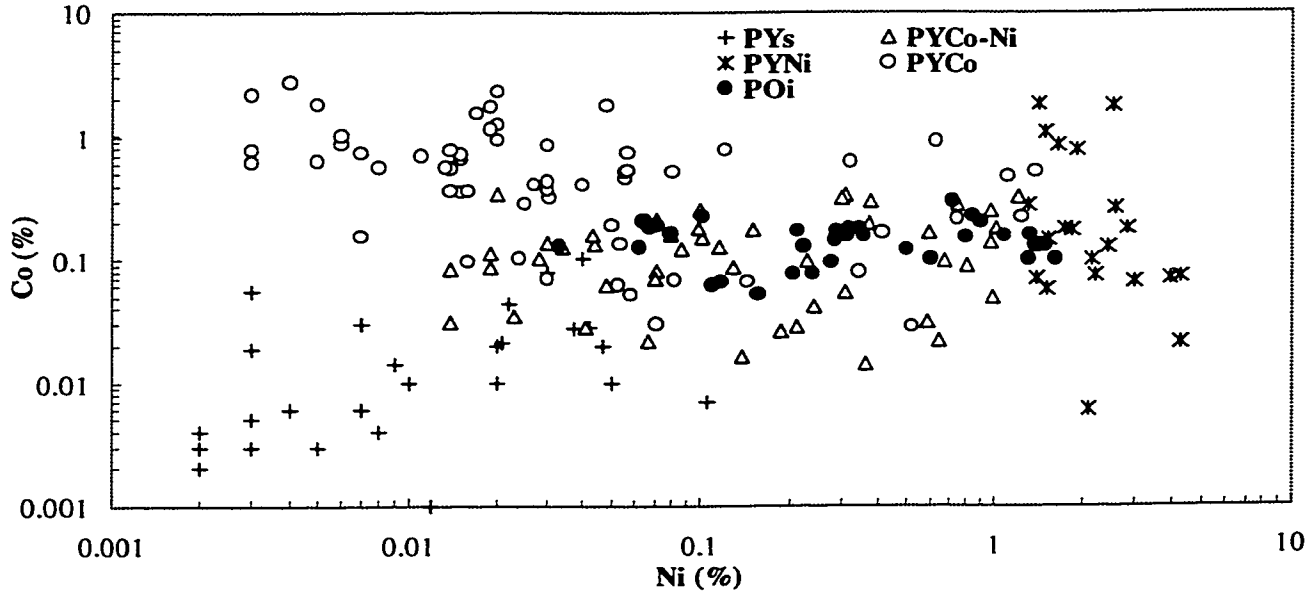

Figure 4-2. Various compositional types of pyrite and pyrrhotite in Bamble metabasites.

The composition of the magnetite associated with pyrite is different from the primary interstitial magnetite. The primary magnetite is enriched in Ti and V, containing up to 2% TiO_2 and 1% V_2O_3. Secondary magnetite is characterized by low TiO_2 and V_2O_3, commonly below 0.1%, but relatively high Ni, up to 0.5%. Possible mechanisms responsible for oxidation of the initial pyrrhotite and formation of various types of pyrite are discussed in Section 4-3.

Interstitial pyrite was found, in some samples, to have been partially to completely replaced by secondary silicates and carbonates. In the advanced stages of alteration, islands of pyrite and/or chalcopyrite are left embedded in a matrix of alteration minerals (Plate 4-1-F). Electron probe analysis of the alteration materials indicated the presence of Fe-rich chlorite as the most common mineral. The results are shown in the Appendix 4-1. Calcite, dolomite, and quartz may accompany chlorite or occur as independent minerals.

Secondary pyrite (Py_s) is common in the Bamble metabasites. The Py_s occurs along fractures and as overgrowths on hornblende and plagioclase (Plate 4-1-G). Minor chalcopyrite may accompany the pyrite. The Py_s is poor in both Ni and Co, but may be rich in As. Electron probe analysis of the secondary pyrite indicated the presence of up to 0.3% As.

4-1-2. Geochemistry

On Jensen oxide diagram (Jensen, 1976), almost all samples plot in the tholeiitic field (Figure 4-3). Fe/Mg ratio is relatively high, and there is a broad trend towards iron enrichment, analogous to differentiated basic suites. No systematic trend of variation can be inferred from the plots on the oxide diagram. Summary statistics for metabasites from all zones is shown in Table 4-2. A complete list of geochemical data is included in the Appendix 4-2.

Metabasites from amphibolite and transition zones are comparable in their major and minor element geochemistry (Table 4-2). The granulite grade metabasites, however, are

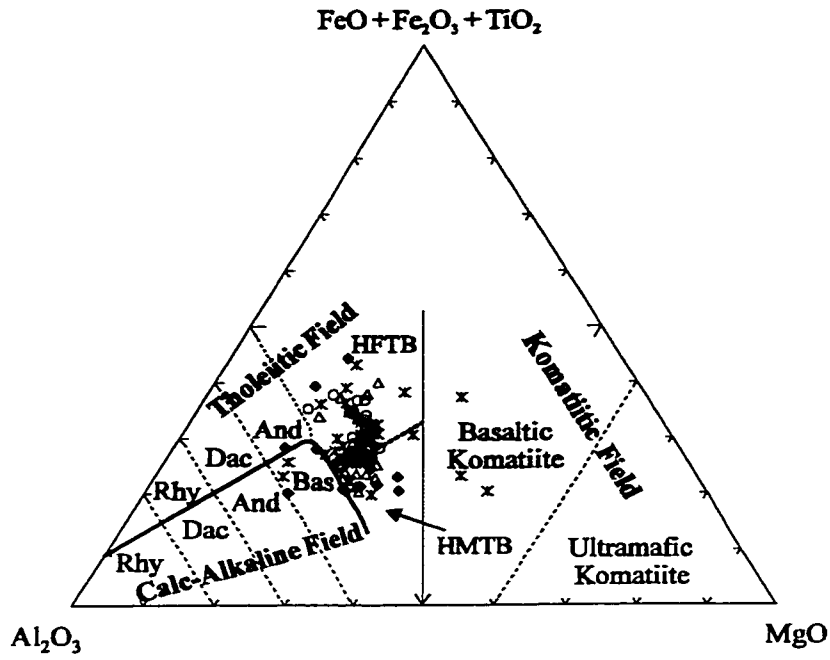

Figure 4-3. Plot of metabasites from various metamorphic zones on Jensen's oxide diagram. HFTB: High-Fe Tholeiitic Basalt; HMTB: High-Mg Tholeiitic Basalt. Symbols represent:
* Zone A; ○ Zone B; △ Zone C; ◆: Zone D

characterized by higher SiO_2 and Na_2O. They are also consistently depleted in LILE, REE, and HFSE. This is best shown on chondrite-normalized plots for elements in metabasites from various metamorphic zones (Figure 4-4). Difference in Na_2O is reflected in the anorthite content of plagioclases. The composition of plagioclase from granulite grade metabasites, An_{15-44}, is considerably more sodic than that from amphibolite and transition zones, An_{30-65} (Clough and Field, 1980).

4-1-2-A. Magmatic or Metamorphic Fractionation

To evaluate the role of magmatic fractionation, Harker diagrams have been constructed using Niggli Mg# ((1000*molar MgO/(MgO + Fe_2O_3 + FeO + MnO)) as differentiation index (Figures 4-5 and 4-6). Phosphorus, Ti, Ni, Cr, V, and Zr are considered amongst the least mobile elements in metamorphic and alteration processes (e.g. Pearce and Cann, 1973; Floyd and Winchester, 1975, 1983; Winchester and Floyd, 1976; Pearce et al., 1984). Variations of the elements with Mg# are consistent with igneous fractionation trends, both within individual zones and in a regional scale (Figure 4-5).

Table 4-2. Summary statistics for metabasites from various metamorphic zones, Bamble.

	Zone A (n = 42)		Zone B (n = 16)		Zone C (n = 22)		Zone D (n = 29)	
	X	1 σ	X	1 σ	X	1 σ	X	1 σ
SiO_2	46.5	2.2	46.4	0.9	47.3	1.9	49.3	2.3
TiO_2	1.9	0.6	2.3	0.5	1.8	0.6	1.1	0.5
Al_2O_3	15.5	2	15.7	8.0	16.2	1.6	15.6	1.54
Fe_2O_3	5.0	1.3	5.5	1.2	3.8	1.1	4.6	1.9
FeO	8.9	1.7	8.8	1.2	8.9	1.4	7.8	1.1
$Fe_2O_3/FeO + Fe_2O_3$	0.36	0.17	0.4	0.1	0.3	0.1	0.37	0.12
MnO	0.18	0.06	0.21	0.03	0.2	0.05	0.22	0.08
MgO	7.3	2.0	7.0	1.1	7.6	1.3	7.2	1.6
CaO	9.2	1.4	8.7	0.82	8.6	1.1	8.7	1.6
Na_2O	2.8	0.7	2.7	0.5	2.6	1.0	3.6	0.7
K_2O	0.9	0.36	0.84	0.4	0.82	0.45	0.41	0.22
P_2O_5	0.2	0.07	0.19	0.05	0.22	0.11	0.15	0.1
H_2O	1.4	0.68	1.5	0.35	1.6	0.6	0.98	0.24
CO_2	0.3	0.18	0.1	0.1	0.1	0.1	0.1	0.1
Cr*	114	70	90	40	135	60	127	86
Ni	105	45	94	30	127	45	80	35
Co	54	16	60	4.0	76	9.0	49	8.0
Sc	42	10	34	9.0	31	8.0	36	6.4
V	245	65	240	70	250	70	235	50
Zn	102	40	100	25	135	50	125	40
Rb	27	15	25	15	38	20	4.1	2.6
Cs	0.75	0.5	0.6	0.4	0.6	0.5	0.25	0.15
Ba	232	180	234	120	210	105	95	27
Sr	245	90	206	64	202	44	170	55
Nb	5.6	2.5	ND	ND	7.0	5.0	ND**	ND
Hf	3.6	1.5	4.4	1.3	2.2	1.5	1.8	1.0
Zr	120	50	132	35	140	53.0	55	25
Y	31	12	35	10	48	8.0	25	10
Th	0.62	0.4	0.76	0.26	0.7	0.6	0.2	0.12
U	0.39	0.3	0.38	0.2	0.3	0.2	0.12	0.08
La	12.5	10	12	5.0	11.5	6.0	6.5	2.7
Ce	26	15	22	7.0	26	12	12	7.0
Sm	5.6	2.8	4.6	1.1	5.7	2.5	2.95	1.5
Eu	1.55	1.1	1.5	0.5	1.5	0.7	0.65	0.3
Tb	1.22	0.6	1.3	0.3	1.2	0.6	0.78	0.4
Yb	3.3	1.7	3.5	1.0	3.2	1.5	2.1	1.2
Lu	0.4	0.2	0.52	0.15	0.45	0.2	0.33	0.15
F	ND		540	200	490	220	510	240
Cl	ND		740	290	400	230	200	140
K/Rb	350		279		179		830	
Rb/Sr	0.11		0.12		0.19		0.02	
Ba/Sr	0.95		1.14		1.04		0.56	
Th/Hf	0.17		0.17		0.32		0.11	

X = arithm. mean; σ = standard deviation * all elements in ppm; Au in ppb ** ND = not determined

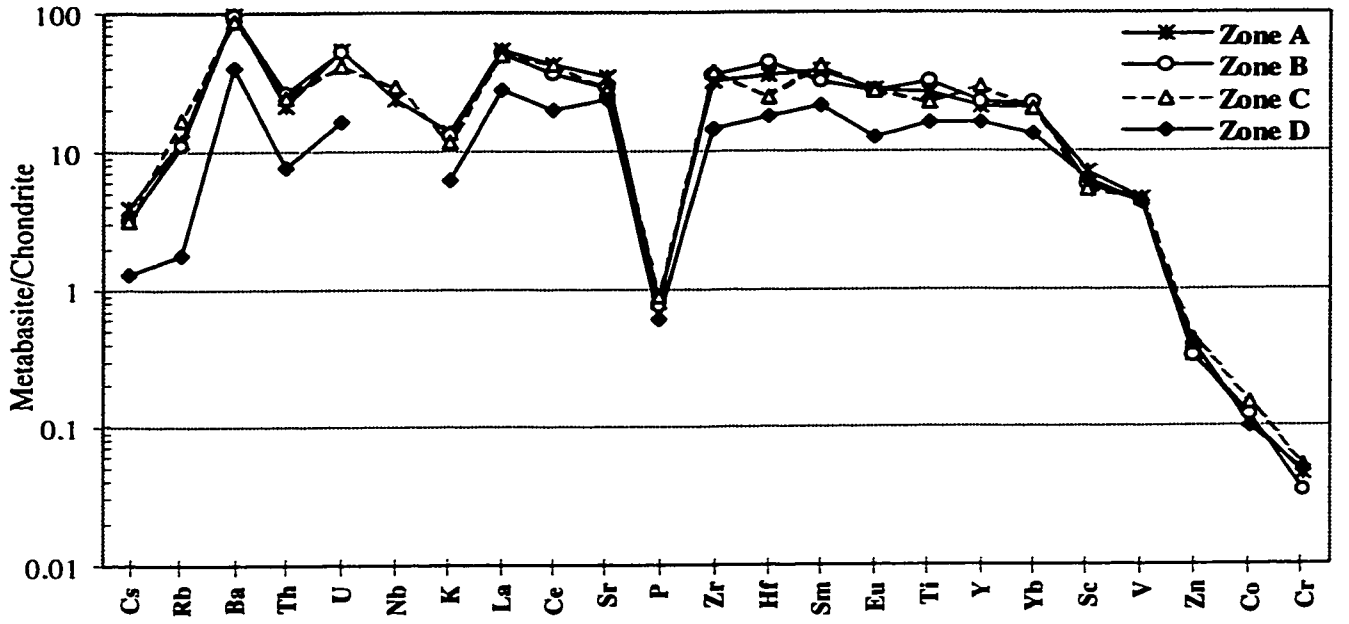

Figure 4-4. Chondrite-normalized plots for elements in metabasites from various metamorphic zones; Bamble. Normalization data from McDonough and Sun (1995). Symbols as in Figure 4-3.

The relatively higher values of Mg# for metabasites from zone D suggest that the least fractionated metabasites occurred in this zone. This is supported by the distribution of the compatible element, Cr, as metabasites from zones A and B are relatively depleted in this element. However, distribution of Ni does not follow this trend; the granulite grade metabasites are relatively depleted in Ni. They are also depleted in the incompatible elements Ti, P, and Zr, at equal Mg# scores. Zirconium further displays a different pattern in the granulite grade rocks.

LILE display relatively large scatters against Niggli Mg# (Figure 4-6), implying variable mobilization of the elements during metamorphic processes. Metabasites from granulite zone are considerably depleted in LILE. This could partly be attributed to the relative absence of Fe-rich differentiates in the granulite zone. However, comparisons at equal Mg# scores indicate that the fields of variations for granulite zone fall below those of the other zones, suggesting that the deficiencies in LILE can not be related entirely to magmatic differentiation.

K/Rb relations in Bamble metabasites have been documented by several authors (Field and Clough, 1976; Clough and Field, 1980; Cameron, 1989a, b). The granulite grade rocks are distinguished by considerably higher K/Rb ratios relative to similar rocks from transition and amphibolite zones (Figure 4-7). This is in agreement with data from other studies on

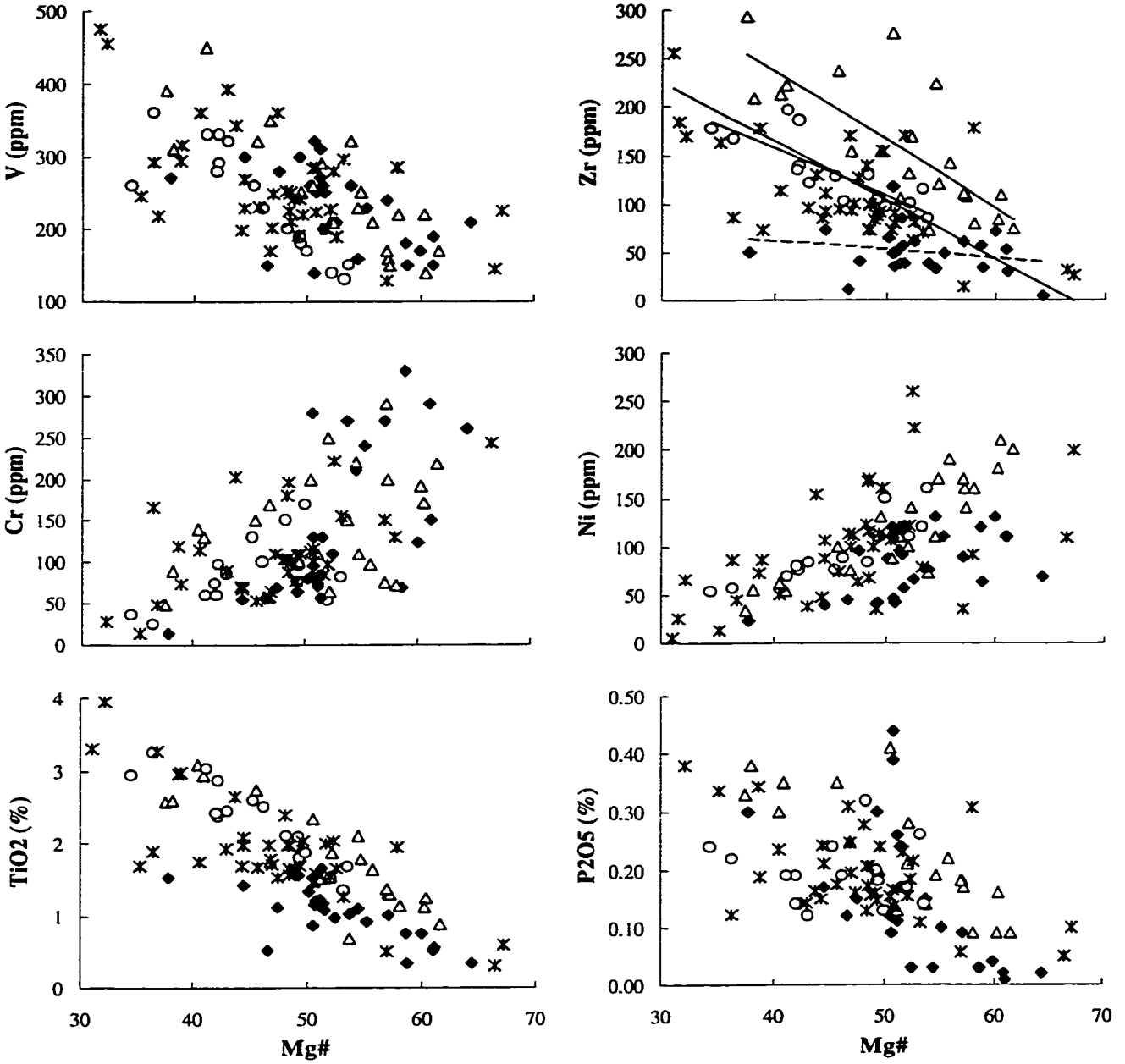

Figure 4-5. Variations of Ti, P, Cr, Ni, Zr, and V with Niggli Mg# as differentiation index in Bamble metabasites. Symbols as in Figure 4-3. Trends of variations are shown for Zr, where metabasites from zone D (broken line) display a different pattern compared to those from other zones (continuous lines).

amphibolite-granulite transition (c.f. Sheraton, 1973; Lewis and Spooner, 1973; Tarney and Windley, 1977; Condie and Allen, 1984). The granulite zone further displays the lowest Rb/Sr and Ba/Sr ratios of all zones (Table 4-2).

Rare earth elements (REE) behave incompatibly during crystallization of mafic magmas (e.g. McKay, 1989; Wilson, 1989). Distribution of La and Sm as representatives of light REE and heavy REE, respectively, follow typical magmatic fractionation trends in metabasites from amphibolite and transition zones (Figure 4-8). The granulite grade metabasites are considerably depleted in REE, and display different patterns. They are further distinguished by a less fractionated chondrite-normalized REE pattern and a more pronounced negative Eu anomaly (Figure 4-9). The mean Eu/Eu* for metabasites from granulite zone is lower than that for amphibolite and transition zones (0.16 vs ~ 0.24).

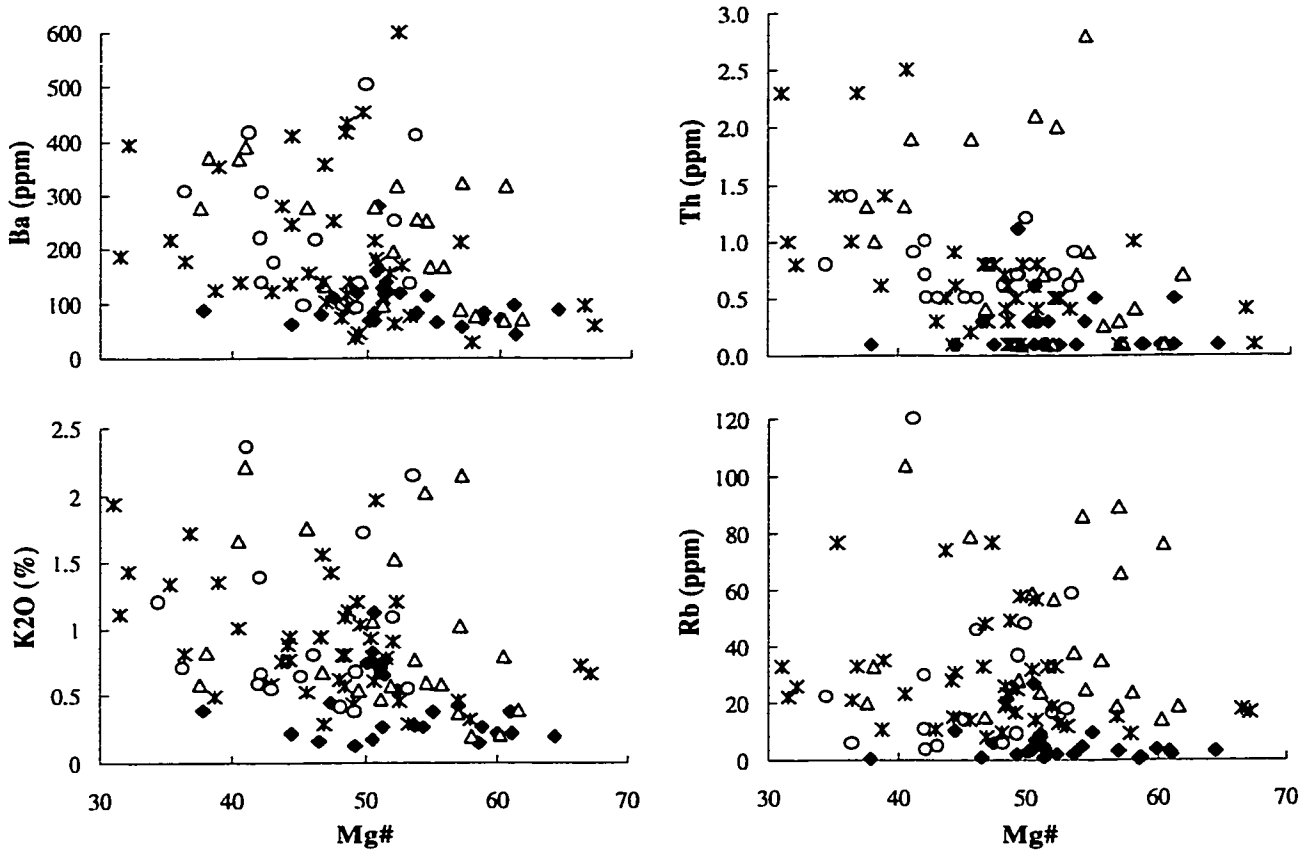

Figure 4-6. Variations of large ion lithophile elements with Niggli Mg# in Bamble metabasites. Symbols as in Figure 4-3.

Our data on the distribution of REE in metabasites do not support an earlier study by Smalley et al. (1983) who, based on a small number of samples, reported higher concentrations of REE in the granulite grade metabasites. The authors further concluded that the granulite zone contains the most fractionated of all metabasites.

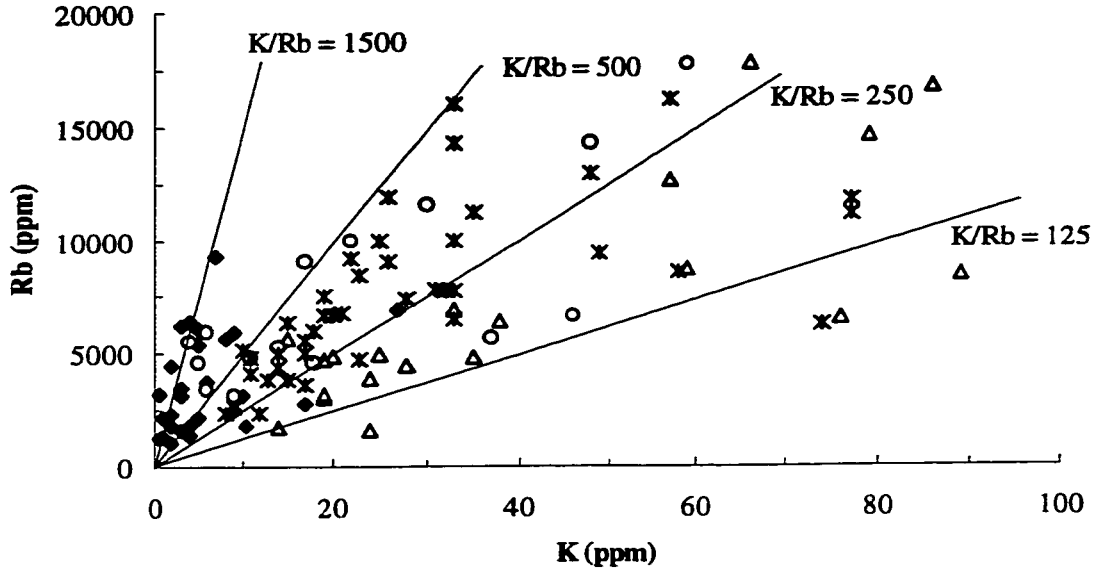

Figure 4-7. Variations of K and Rb in metabasites from various metamorphic zones, Bamble. Symbols as in Figure 4-3.

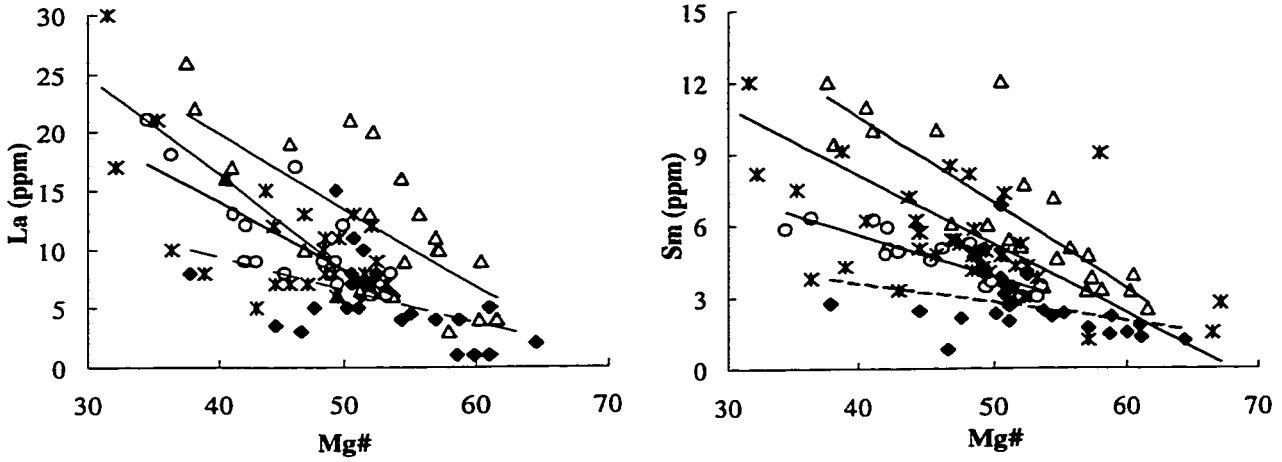

Figure 4-8. Variations of La and Sm as representatives of LREE and HREE, respectively, against Niggli Mg# in metabasites from various metamorphic zones, Bamble. Trends of variations are similar for metabasites from zones A, B, and C (solid lines). The granulite grade metabasites display a different trend (broken line). Symbols as in Figure 4-3.

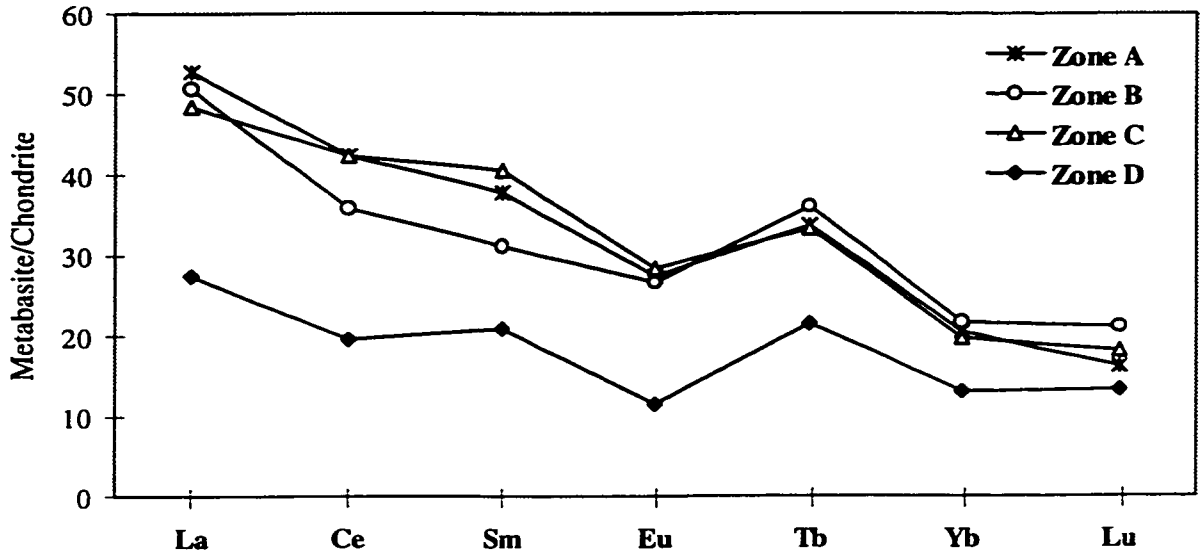

Figure 4-9. Chondrite-normalized REE pattern for metabasites from various metamorphic zones; Bamble. Chondrite values from McDonough and Sun (1995). Symbols as in Figure 4-2.

4-1-3. Tectonic Setting

Metabasites from all zones display a tholeiitic character (Figure 4-2). A comparison to mid-ocean ridge basalts (MORB) provides further information on the origin and tectonic setting of the metabasites (Figure 4-10). The main features of the Bamble metabasites with respect to MORB include:

- Large ion lithophile elements (LILE) and light rare earth elements (LREE) are variably enriched relative to MORB. Enrichment in LREE is a common feature among continental tholeiites (Norrey and Fitton, 1982; Pearce, 1982, 1983; Dupuy and Dostal, 1984). A continental setting for the metabasites was also proposed by Smalley et al. (1983) and Smalley and Field (1985).
- Large ion lithophile elements (LILE) are variable, but generally enriched relative to high field strength elements (HFSE) and rare earth elements (REE).
- Metabasites from all metamorphic zones show low Th abundance relative to other LILE, and distinct Nb troughs.

The above features are characteristics of tholeiitic basalts produced in volcanic arc settings at destructive plate margins (c.f. Wood et al., 1979, 1981; Pearce, 1982; Kay, 1984). This is in

agreement with earlier studies by Thorske (1977), Smalley et al. (1983) and Smalley and Field (1985) who proposed a destructive margin setting for Bamble metabasites.

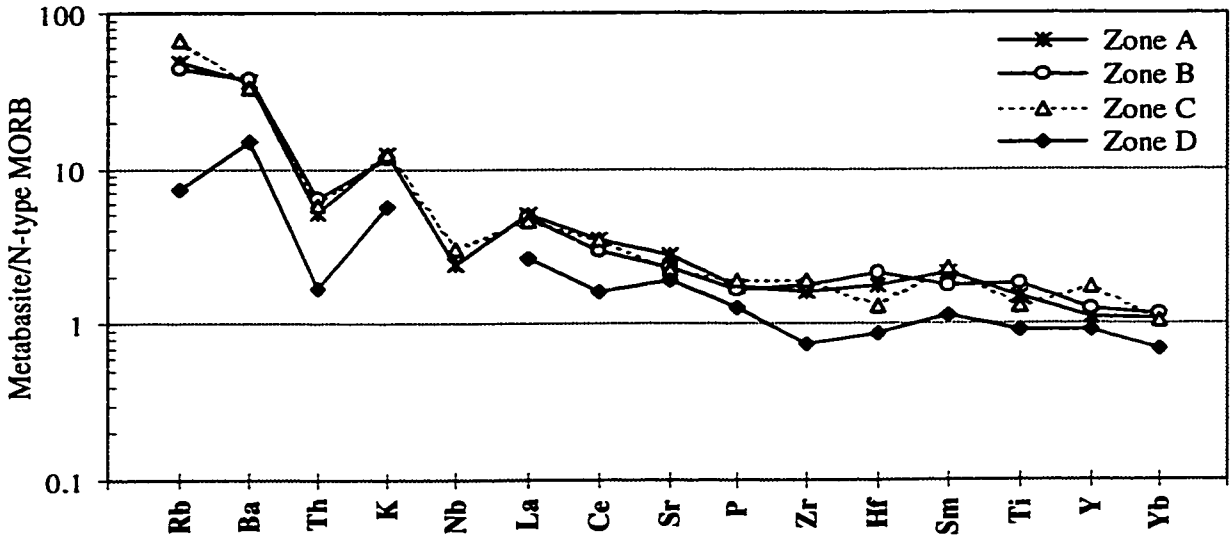

Figure 4-10. MORB-normalized plots for elements in metabasites. Normalization data from Sun and McDonough (1989).

4-1-4. Distribution of Chalcophile Elements

Summary statistics for chalcophile elements in metabasites from various metamorphic zones is shown in Table 4-3. Chalcophile elements display large scatters in the metabasites, with coefficients of variations up to 100%. They tend to have a log-normal rather than a Gaussian distribution; therefore, the geometric means are also shown for reference.

Interstitial pyrite (Py_i) is the dominant type of sulfide in all zones, commonly associated with lamellae and patches of chalcopyrite and pentlandite. Magnetite may occur in the paragenesis as fine grains or grain aggregates within, or mantles about, pyrite. Pyrite also occurs as secondary fracture filling and replacement bodies. Secondary pyrite is common in zone A, forming up to 20% of the total sulfides. It is less common in other zones. Marcasite may be found as an alteration product of pyrite.

Table 4-3. Summary statistics for chalcophile elements in Bamble metabasites.

Metamorphic Zone	S (ppm)	Cu (ppm)	Se (ppm)	As (ppm)	Sb (ppm)	Au (ppb)
Zone A (N = 42)						
X	1100	105	0.15	2.5	0.2	0.36
1σ	700	25	0.05	2.1	0.15	0.22
GM	700	100	0.15	2	0.15	0.32
CV	63	36	33	75	83	60
Zone B (N = 16)						
X	1350	90	0.16	0.34	0.06	0.16
1σ	520	50	0.07	0.15	0.02	0.07
GM	1150	72	0.14	0.28	0.06	0.14
CV	38	55	43	44	33	44
Zone C (N = 22)						
X	975	68	0.13	0.36	0.07	0.19
1σ	550	25	0.07	0.27	0.05	0.13
GM	870	62	0.11	0.2	0.05	0.12
CV	58	37	54	80	71	70
Zone D (N = 29)						
X	300	42	0.05	0.28	0.03	0.27
1σ	275	30	0.04	0.25	0.023	0.22
GM	120	32	0.03	0.22	0.024	0.19
CV	92	71	79	84	77	81

X = arithmetic mean GM = geometric mean σ = standard deviation CV = coefficient of variation

Pyrrhotite is common in metabasites from zone A, occurring in almost half of the samples. It is less common in zones C and D, and rare in zone B. Pyrrhotite occurs exclusively as interstitial grains, generally associated with exsolution lamellae and patches of chalcopyrite and pentlandite.

Interstitial pyrite was found partially replaced by silicates (mainly Fe-rich chlorite and quartz) and carbonates in some samples. The alteration is generally of local nature, rarely affecting more than 10% of the total sulfides. Sample 4403 from zone B with the highest silicate replacement is considerably depleted in Au.

It is noteworthy that peaks in As and Sb correspond to samples containing secondary pyrite. Electron probe analysis of secondary pyrite from three samples 6401, 6408 and 7501, all from zone A, indicated relatively high contents of As in the range 1000 to 2000 ppm. The same samples are relatively enriched in Au.

Chalcophile elements display no consistent trends of variations among various metamorphic zones. This is clearly evident from cumulative probability diagrams for S, As, Sb, and Au (Figure 4–11-A-D). Metabasites from granulite zone carry the lowest concentrations of S. They are similarly depleted in Cu and Se (Table 4-3). However, they are not so depleted in As and Au. Metabasites from amphibolite zone are significantly enriched in As and Sb, but not in Au. A comparison is made to the post-Kongsbergian mafic bodies known as hyperites (hypersthene gabbros). Hyperites are discussed in Section 4-2. They display typical magmatic textures and mineral assemblages. The primary sulfide parageneses are preserved in the least altered rocks. Compared to the hyperites, the metabasites are slightly depleted in Au. No significant differences exist for other elements (Figure 4-11-A-D).

Metabasites from various metamorphic zones are considerably depleted in Au relative to the general abundance of this element in mafic rocks elsewhere (Figure 4-12). They are also depleted in As, and Sb. The abundances of S, Cu, and Se are in the same common range for mafic rocks. The Bamble metabasites contain, on average, 0.23 ppb Au that is one order of magnitude below the mean concentration of Au in tholeiitic basalts (c.f. Gottfried and Greenland, 1972; Krocket and Truta, 1977; Kwong and Crocket, 1978; Korobeynikov, 1986, 1990).

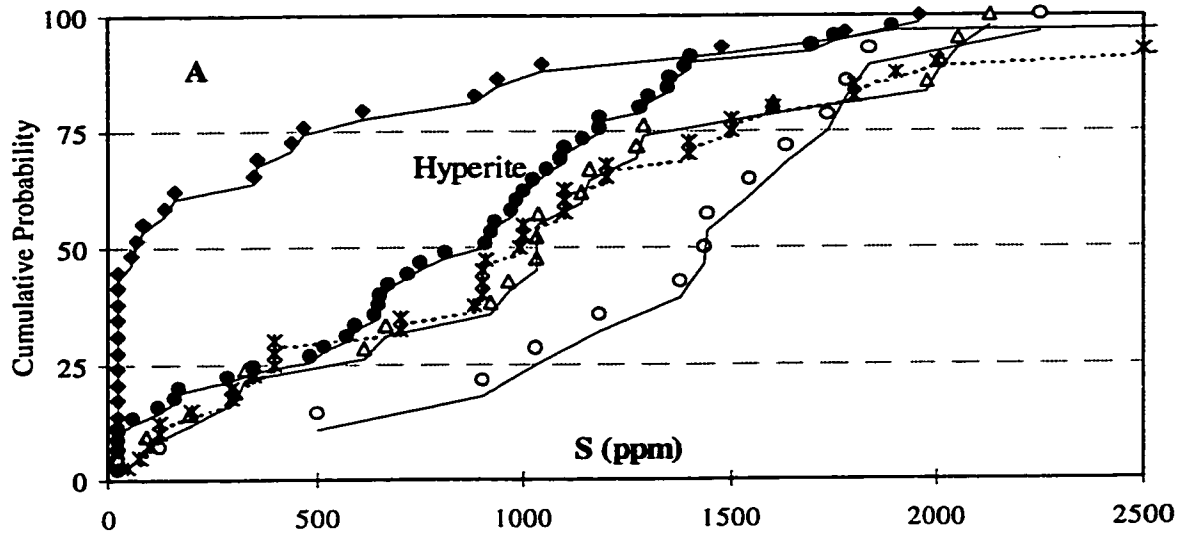
A
Hyperite
Cumulative Probability
S (ppm)
100
75
50
25
0
0
500
1000
1500
2000
2500

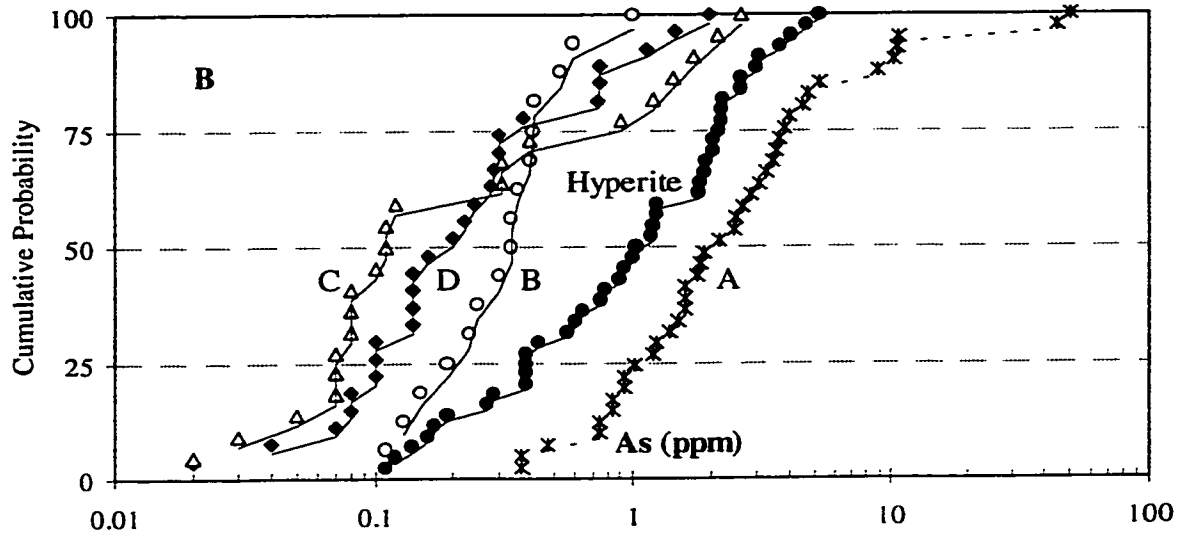
B
Hyperite
C
D
B
A
As (ppm)
Cumulative Probability
100
75
50
25
0
0.01
0.1
1
10
100

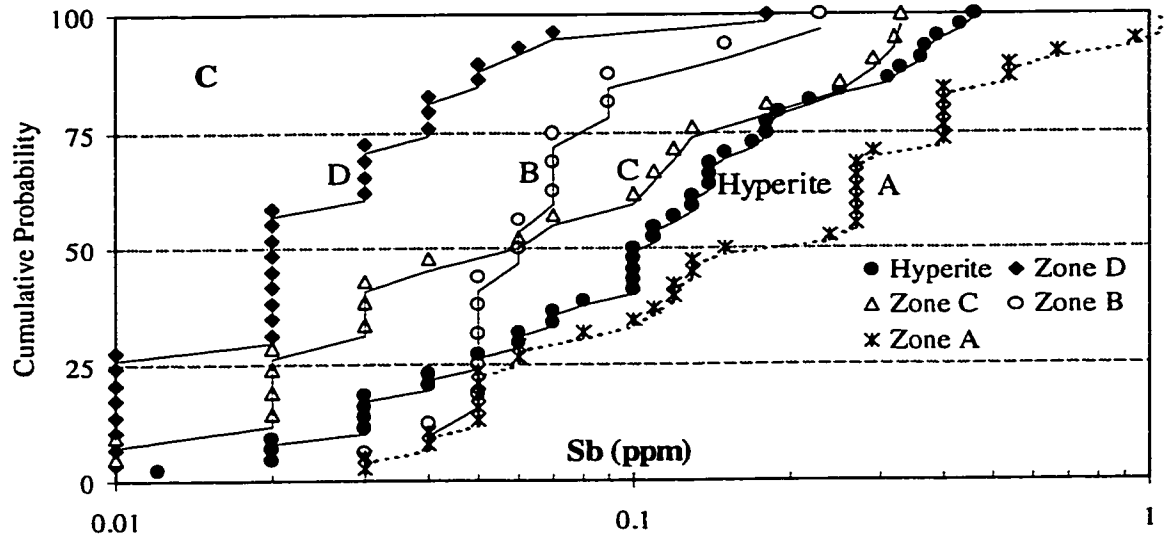
C
D
B
C
Hyperite
A
Hyperite
Zone D
Zone C
Zone B
Zone A
Sb (ppm)
Cumulative Probability
100
75
50
25
0
0.01
0.1
1

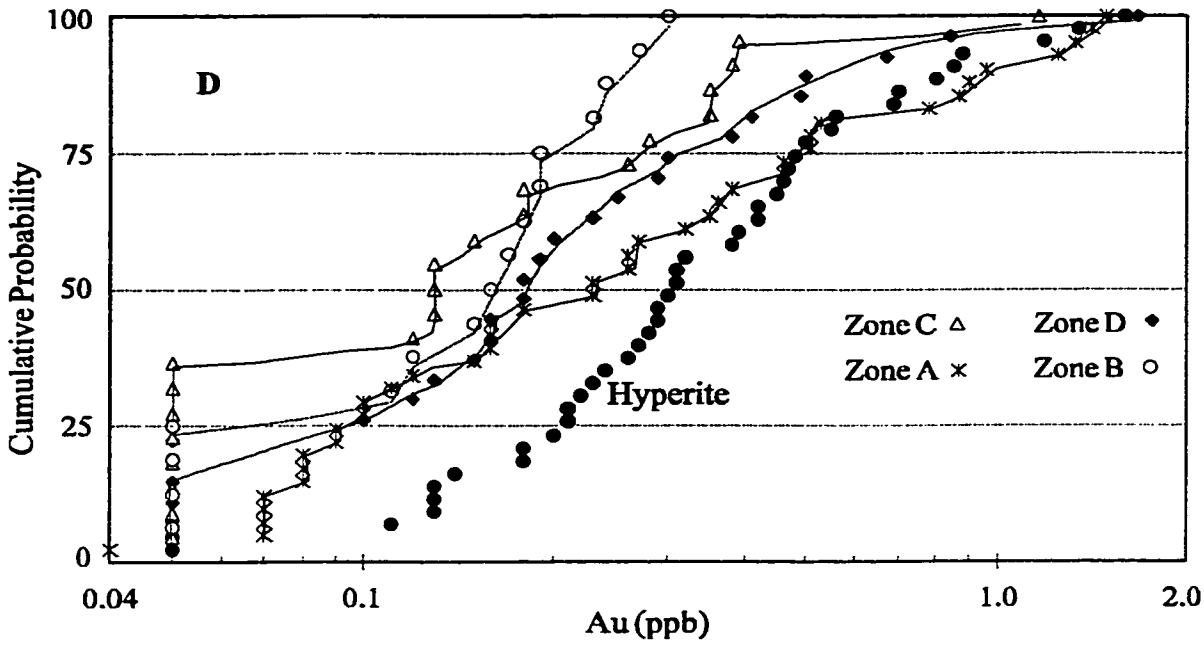

Figure 4-11 (A-D). Cumulative frequency distribution of S, As, Sb, and Au in metabasites from various metamorphic zones, Bamble. Distribution of the same elements in the post-Kongsbergian hyperites (hypersthene gabbros) are shown for comparison. Hyperites are discussed in Section 4-2.

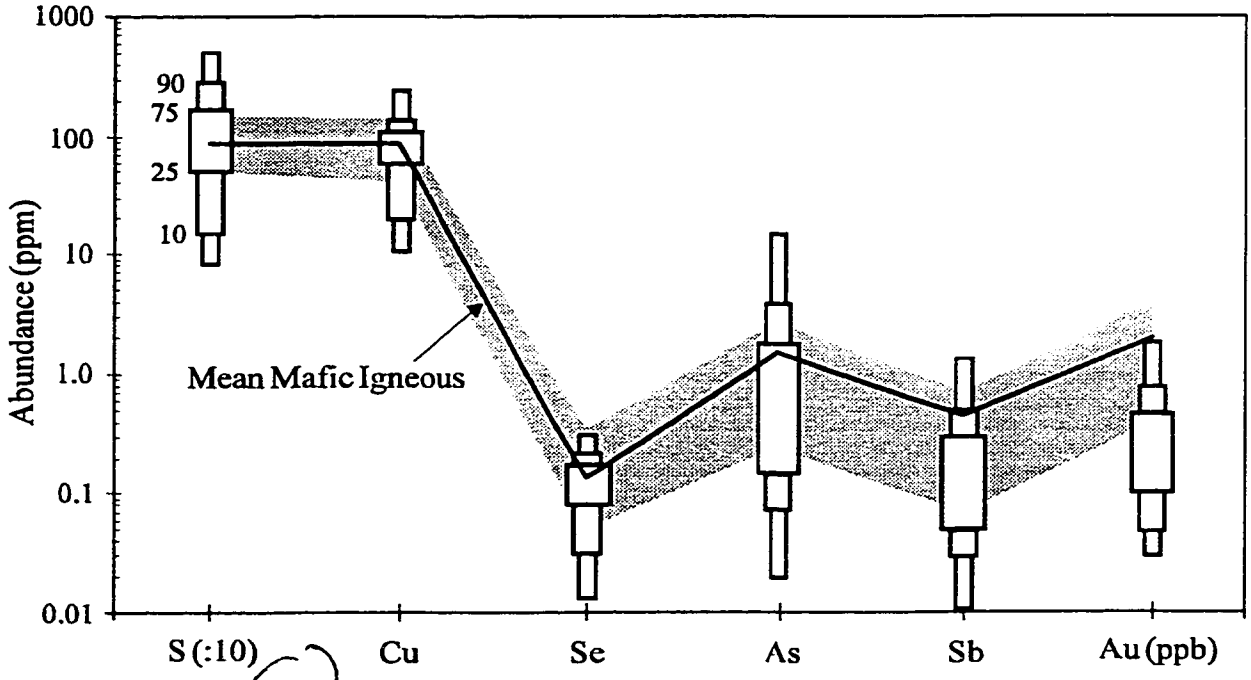

Figure 4-12. Abundacne of chalcophile elements in the Bamble metabasites, with cumulative frequencies indicated for 10, 25, 75, and 90%. The common range (shaded area) and the mean abundance (solid line) of chalcophile elements in mafic igneous rocks are shown for comparison. See Appendix 2-2 for composition of mafic rocks.

4-1-5. Discussion

Metamorphosed basic intrusive rocks, known as metabasites, occur in various metamorphic zones in the Bamble Shear Belt. The metabasites form subconcordant to concordant minor dykes and sheets parallel to the regional foliation. They intruded older supracrustal rocks during the early stages of the Kongsbergian (Gothian) Orogeny. Metabasites from various metamorphic zones bear features characteristic of tholeiitic basalts emplaced at active continental margins.

Metabasites from amphibolite and transition zones are comparable in their major and minor element geochemistry and belong to a regional differentiation trend. The granulite facies rocks, however, are distinguished by considerably lower concentrations of LILE, REE, and HFSE. Depletion of LILE during granulite metamorphism is well established (e.g. Heier, 1973; Rollinson and Windley, 1980; Newton et al., 1980; Weaver and Tarney, 1981; Condie and Allen, 1984; Lamb and Valley, 1985). Depletion of REE and HFSE is not common. REE and HFSE are amongst the least mobile elements in alteration and metamorphism (e.g. Floyd and Winchester, 1975; Winchester and Floyd, 1976; Pearce et al., 1984).

The lower contents of the incompatible lithophile elements in the metabasites from metamorphic zone D may partly be attributed to the absence of more fractionated rocks in this zone. However, that fields of variations for the elements in zone D fall below those of the other zones at equal Mg# values, implies that processes other than magmatic differentiation were involved. Recently, depletion of the incompatible elements in zone D have been attributed to the parent magma, rather than metamorphism (Knudsen and Andersen, 1999). The authors proposed that Tromoy gneiss complex (metabasites and charnockites) is the remnant of an oceanic island arc accreted onto the Baltic Shield continental margin at high grade metamorphic conditions.

The granulite grade metabasites are characterized by lower ΣREE and a less fractionated chondrite-normalized REE pattern. This is in contrast to an earlier study by Smalley et al.

(1983) who, based on a small number of samples, reported higher ΣREE in the granulite grade rocks. The authors further proposed that the granulite zone contains the most fractionated of all metabasites.

Chemical patterns for metabasites closely parallel those in the surrounding acid-intermediate gneisses, or charnockites. Both rock types are distinguished by strong depletion in LILE, REE, and HFSE compared to their equivalents rocks from amphibolite and transition zones.

As in the charnockites, depletion of elements can not be attributed to anatexis and partial melting, as these processes are expected to leave a SiO_2-depleted, less-alkaline fraction behind. The granulite grade metabasites contain considerably higher SiO_2 and Na_2O compared to their lower grade equivalents.

Intrusion under lower P-T conditions, with subsequent dehydration and recrystallization to granulite facies rocks is not supported by the existing evidence. A metasomatic model of this type would be able to account for depletion of LILE (c.f. Clough and Field, 1980). However, it can not be matched with the considerably higher contents of Na_2O and SiO_2, and lower contents of REE and HFSE in the granulite grade metabasites.

It has been suggested that the Bamble metabasites are syn-metamorphic intrusions (Field and Clough, 1976; Clough and Field, 1980), the main evidences being:

- Absence of fine grained chilled margins, implying that the host rocks were still hot at the time of intrusion.
- Absence of evidence of progressive replacement of hornblende by pyroxene (arrested hornblende-pyroxene reaction textures), as is expected in a progressive metamorphism.
- The emplacement of the basic dykes along the same single regional foliation as their gneissic host rocks.

Depletion of LILE and REE in the granulite grade metabasites has been attributed to crystallization under granulite facies metamorphism (Clough and Field, 1980; Smalley et al.,

1983). According to the authors, the lower contents of REE in the metabasites reflect the low partitioning of these elements into minerals under granulite P-T conditions.

CO_2 is interpreted to have played an important role by suppressing the formation of hydrous minerals (Smalley et al., 1983). A CO_2-dominated regime would inhibit the early formation of LILE-bearing minerals such as biotite and hornblende (Lamb et al., 1986). Basic magmas intruding into a CO_2-dominated regime would inevitably crystallize to an anhydrous mineralogy, and LILE would strongly partition into the residual fluid phase (Lamb et al., 1986).

Alternatively, depletion in the incompatible lithophile elements might be the consequence of granulite metamorphism. Fluids during granulite metamorphism are known to be CO_2-rich (e.g. Touret, 1974; Newton et al., 1980), and could be the agent responsible for complexing and removal of radioactive heat-producing elements, K, Rb, U, and Th, as well as Cs (Weaver and Tarney, 1981; Newton et al., 1980; 1985; Janardhan, 1982; Condie et al., 1982; Condie and Allen, 1984; Hanson et al., 1984; Stahle et al., 1987).

The involvement of carbonic fluids in granulite metamorphism at Bamble is supported by the presence of abundant CO_2-rich fluid inclusions in granulite facies rocks (Touret, 1971, 1974; Hoefs and Touret, 1975; Touret and Dietworst, 1983; Van den Kerkhof et al., 1994; Knudsen and Lidwin, 1996). There is a consensus that transition from amphibolite to granulite metamorphism at Bamble occurred in response to progressive change in fluid composition from H_2O-rich to CO_2-rich. The pressure and temperature at peak metamorphism has been calculated to be in the range 7.3 $\pm$ 0.5 kbar and 800 $\pm$ 60°C, respectively (Touret and Dietworst, 1983; Visser and Senior, 1985; Lamb et al., 1986; Cameron, 1989b; Harlov, 1992; Visser, 1993).

The lower La_N/Yb_N ratio for granulite grade rocks relative to other zones (2.1 vs ~2.5) may be attributed to preferential depletion of LREE during magmatic crystallization, or metamorphic recrystallization, under CO_2 streaming. It has been indicated that CO_2- and halogen-rich fluids

that invade gneissic rocks may deplete the gneisses in REE, modifying the initial distribution patterns of REE (Collerson and Fryer, 1978).

Our data on the distribution of REE in metabasites do not support an earlier study by Smalley et al. (1983) who, based on a small number of samples, reported higher concentrations of REE in the granulite grade metabasites. The authors further concluded that the granulite zone contains the most fractionated of all metabasites.

Chalcophile elements display no consistent trends of variations among various metamorphic zones. Metabasites from granulite zone carry the lowest concentrations of S. They are similarly depleted in Cu and Se. However, they are not so depleted in As and Au. Compared to the post-Kongsbergian mfaic bodies, the metabasites are slightly depleted in Au. No significant differences exist for other elements.

Metabasites from various metamorphic zones are depleted in Au, As, and Sb compared to the general abundances of the elements in mafic rocks elsewhere. The low concentrations of chalcophile elements might be of primary magmatic origin, or, alternatively, a metamorphic overprint.

Sulfide mineralogy is simple and fairly consistent. Pyrite is the dominant sulfide, commonly associated with patches and lamellae of chalcopyrite and pentlandite. Magnetite may occur as fine grains or grain aggregates within, or as mantles about, pyrite. The assemblage pyrite ± magnetite ± chalcopyrite ± pentlandite occurs as interstitial to silicates and oxides, and appears to be an oxidation product after initial pyrrhotite, or pyrrhotite monosulfide solid solution.

Replacement of sulfides by silicates and carbonates was observed in some samples. Fe-rich chlorite is the main mineral. The alteration is generally of local nature. When pervasive, however, the enclosing rock is strongly depleted in Au. Secondary pyrite as fracture filling and overgrowth is common, and may be enriched in As, Sb, and Au.

Fe-Ti oxides are present as minor phases in all metabasites. Ilmenite is the dominant oxide in metabasites from zones A, B, and C, but subordinate to magnetite in the granulite grade metabasites. Hematite, where present, commonly occurs as exsolution lamellae within ilmenite. It is common in zone B, less common in zones C and D, and rare in zone A.

Cameron (1989b) showed that metabasites from zones B and D equilibrated at $\log f_{O2} \cong -11.8$ that is considerably more oxidized than the common redox states for mafic igneous rocks. A relatively high f_{O2} is supported by the predominance of magnetite over ilmenite (zone D), and the common presence of hematite in ilmenite (zone B). Both zones are characterized by replacement of the initial pyrrhotite by pyrite + magnetite. No estimation of the f_{O2} is available for metabasites from zones A and C.

The oxidizing capacity of the infiltrating fluids was mostly buffered by silicate/fluid reactions (c.f. Keays, 1987; Cameron, 1989b). Sulfide minerals initially present in the rocks resisted the oxidation. The most important change appears to be the replacement of pyrrhotite by pyrite + magnetite. Continued oxidation locally led to the mantling of pyrite by magnetite. Keays (1987) showed that during regional metamorphism of mafic rocks, sulfide/fluid reaction might be buffered through oxidation of Fe in the reaction:

$$\text{FeO (in Fe-Mg silicates)} \rightarrow Fe_3O_4 \text{ (magnetite)}$$

The ratio $Fe_2O_3/(FeO + Fe_2O_3)$ may be used as a rough index of oxidation. In this respect, metabasites from zone B are the most oxidized of all zones, followed by zones D, C, and A. Plots of Au against $Fe_2O_3/(FeO + Fe_2O_3)$ for metabasites indicate no consistent trends of variation (Figure 4-13), suggesting that Fe-Mg silicates buffered the oxidizing fluids and protected the sulfides from decomposition and remobilization of chalcophile elements.

A fractionation of Rb from K has been reported from many granulite terrains. The granulite grade metabasites at Bamble are distinguished by relatively high K/Rb ratios, in excess of 1000. Plots of K/Rb against Au for metabasites from various metamorphic zones show no

consistent trend of variations (Figure 4-14). This is in accordance with an earlier study by Cameron (1994) who showed that loss of Au in the Lewisian and Bamble granulites was essentially independent of LILE depletion.

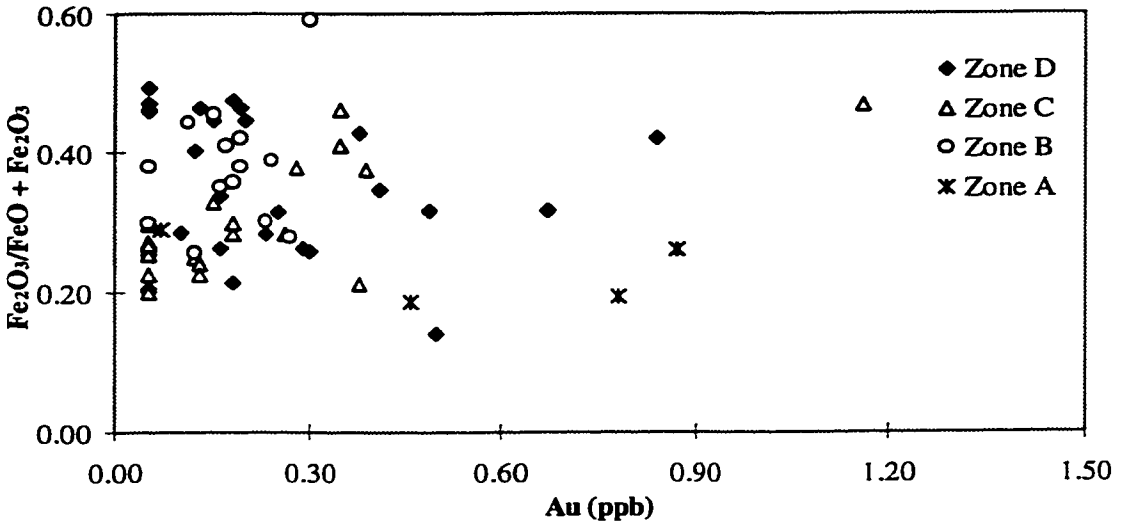

Figure 4-13. Plots of Au vs $Fe_2O_3/(FeO + Fe_2O_3)$ as an index of oxidation in metabasites from various metamorphic zones, Bamble.

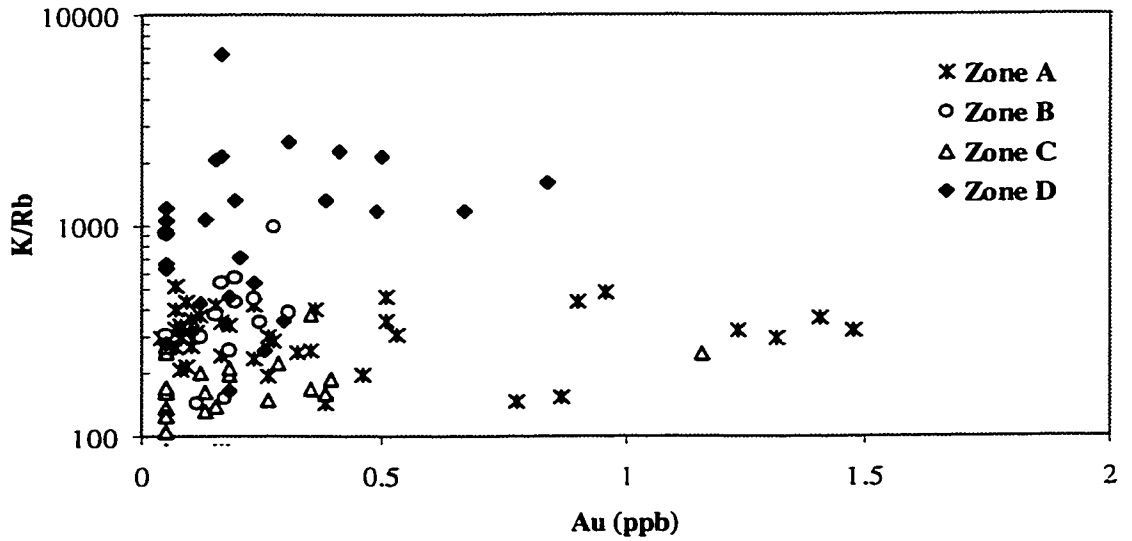

Figure 4-14. Variations of Au vs K/Rb in metabasites from various metamorphic zones, Bamble.

Arsenic and Sb behave incompatibly during crystallization of mafic magmas, and show a strong correlation with the light rare earth element, Ce (Sims et al., 1990; Noll et al., 1996). The As/Ce and Sb/Ce ratios in the Bamble metabasites (Figure 4-15) are in the same range as in the average mafic igneous rocks (c.f. Noll et al., 1996). The mean As/Ce and Sb/Ce ratios (0.08 and 0.008, respectively) are very close to those in the mean continental crust (0.08 ± 0.03 and 0.007 ± 0.002, respectively; Sims et al., 1990).

Considering the immobility of Ce at Bamble, at least in metabasites from amphibolite and transition zones (Clough and Field, 1983; Smalley et al., 1983, 1985; Smalley and Field, 1991; present study), normal ratios of As/Ce and Sb/Ce argue against a post-solidus origin for depletion of As and Sb. Such process would be expected to lead to a significant drop in the As/Ce and Sb/Ce ratios. The similar patterns of plots in Figure 4-15 implies that no fractionation of As and Sb from Ce occurred during metamorphism.

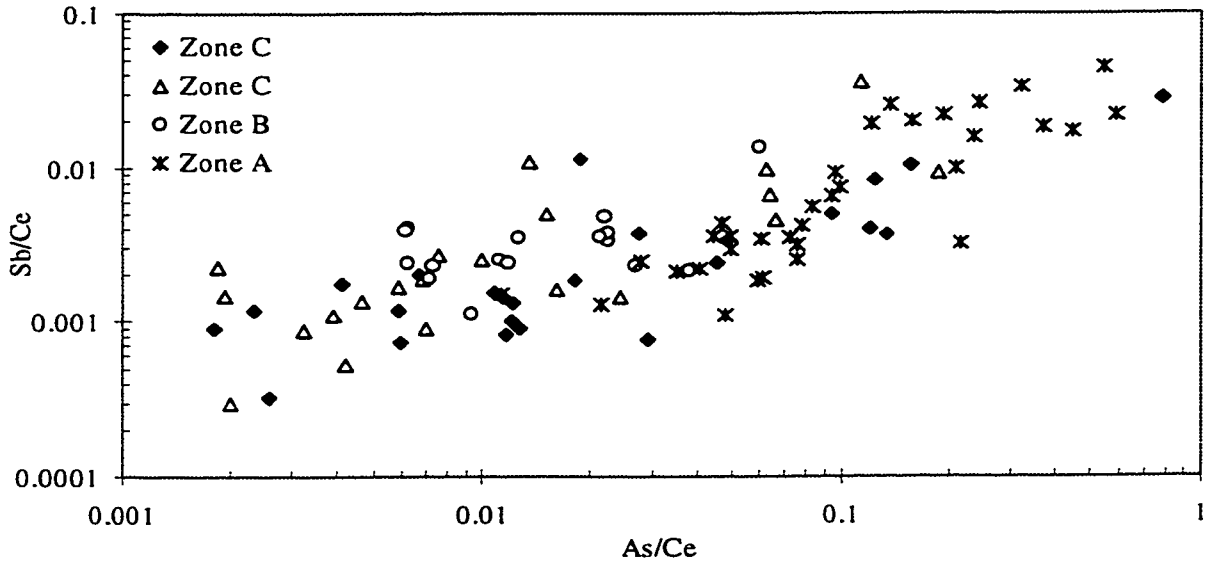

Figure 4-15. Variations of As/Ce vs. Sb/Ce in metabasites from various metamorphic zones, Bamble.

4-2. Hyperites (Gabbros) and Amphibolites

4-2-1. Introduction

Numerous mafic intrusions as small stocks, lopolithic and dyke-like bodies, traditionally termed "hyperites" (Brøgger, 1934) intruded all supracrustal units in Bamble at the initial stages of the Sveconorwegian Orogeny (e.g. Touret et al., 1968; Starmer, 1969, 1985; Brickwood and Craig, 1987). Hyperites are widespread throughout the Scandinavian Shield (e.g. Starmer, 1981; Morthorst et al., 1983; Zeck and Willadsen, 1990; Munz and Morvik, 1991; Waque, 1996).

"Hyperite" is a common term among Scandinavian geologists, and may apply to all kinds of gabbroic rocks. The term "hyperite" is Swedish and was introduced by A. Erdmann and J. H. Forselles (1855) as a general petrographic name for a granular rock composed mainly of labradorite and hypersthene occurring as voluminous intrusives of black doleritic gabbro in the Värmland gneiss basement, Sweden (Morthorst et al., 1983). Brøgger (1934) applied the term "hyperite" only to coronitic gabbros. Amphibolitization of the gabbros is common, and Bugge (1943) did even include under the name hyperite practically all kinds of massive amphibolites occurring in southern Norway.

The intrusion age has been determined, by various methods, to be in the range 1.23-1.11 Ga, corresponding to Sveconorwegian Orogeny (Jacobsen and Heier, 1978; Dahlgren et al., 1990; Munz and Morvik, 1991; de Haas, 1992; de Haas et al., 1993). Bugge (1943) noted that the Bamble hyperites were not all of the same age. The presence of more than one generation of hyperites was also noticed by Touret (1969) and de Haas (1992). De Haas (1992) reported whole rock Sm-Nd isochron ages of 1.77 ± 0.19 Ga and 1.64 ± 0.23 Ga for two hyperite bodies in Arendal and Nelaug areas, corresponding to Kongsbergian Orogeny. A Kongsbergian age for hyperites has been questioned by Andersen and Sundvoll (1995).

The intrusions vary in size from stocks less than 1 km^2 to sheet-like bodies more than 20 km in length (e.g. Starmer, 1969; Brickwood and Craig, 1987). They vary in composition from subordinate ultramafic rocks (pyroxenite, picrite and peridotite) through troctolitic varieties to olivine ferrogabbro and olivine-free gabbros and norites. Based on a nomenclature using the olivine/(olivine + pyroxene) ratios, Starmer (1969) recognized 3 trends in the hyperites: 1) troctolite-troctolitic norite; 2) troctolite-olivine gabbro; 3) olivine-free gabbros. All the mafic intrusions are plagioclase-rich and display sub-ophitic to ophitic, mesocumulate to orthocumulate type textures (c.f. Starmer, 1969; Brickwood and Craig, 1987).

After differentiation and intrusion, some of the mafic bodies underwent retrograde reactions under prolonged high P-T conditions. Corona growth around ferromagnesian minerals and metamorphism converted the rocks into coronitic gabbro and amphibolite. Amphibolization is most profound at the margins, but locally also in the cores. Considered in three dimensions, most bodies have a dominantly coronitic core which passes outwards into an amphibolitized margin. Patches of coronitic gabbros in amphibolites, and vice versa, are common, and seem to be the result of differential permeation of water during metamorphism (Starmer, 1969).

Hyperites occur in a metamorphic gradient from amphibolite- to granulite-facies conditions. Hydration and recrystallization is more extensive in the intrusions emplaced into the amphibolite-facies country rocks. Greenschist-facies assemblages are locally developed along minor fissures, shears, and around the margins of some of the intrusions (e.g. Verdonk et al., 1986; Brickwood and Craig, 1987; Munz et al., 1994; Waque, 1996).

The relict igneous mineralogy of the hyperites indicates that crystallization took place at temperatures of 1100-1000°C and at a pressure less than 5-8 kbar (Brickwood and Craig, 1987; Munz and Morvick, 1991). Metamorphism and partial recrystallization to amphibolite occurred at 800-600°C and 7-10 kbar (Munz, 1990; Munz and Morvick, 1991).

From literature, the term "hyperite" has variously been applied to normal gabbros, olivine-gabbros, coronitic gabbros, gabbros transitional into norite (hypersthene-gabbro) and into

amphibolite. All kinds of transitions from normal gabbro to coronitic gabbro and to wholly amphibolitized gabbro exist in Bamble. In this study, the term "hyperite" has been limited to hypersthene-gabbros. Olivine-gabbros, where displaying coronitic textures, are referred to as "coronitic gabbro", or simply "coronite". Amphibolitized gabbros and hyperites are referred to as "amphibolitized gabbro", "amphibolitized hyperite", or simply "amphibolite".

Some 50 samples of coronitic gabbros and hyperites, and their amphibolitized equivalents, have been collected from several bodies in Laget (amphibolite zone), Tvedestrand (transition zone), and Tromoy (granulite zone). Approximate locations of the samples are shown in Figure 1-2.

4-2-2. Sulfides in Hyperites (Gabbros) and Their Amphibolitized Equivalents

Sulfides are minor constituents of the Bamble gabbros and amphibolites, rarely exceeding 0.5% by mode; however, as the main host to Au, they are of particular concern in this study. The sulfide mineralogy is simple and comparable to that from metabasites. Pyrrhotite and pyrite are the main sulfides commonly associated with lamellae and patches of chalcopyrite and pentlandite. Minor magnetite may occur associated with pyrite. As in the metabasites, several textural types of pyrite and pyrrhotite are recognized including: interstitial pyrrhotite (Po_i), bleb pyrrhotite (Po_b), interstitial pyrite (Py_i), and secondary pyrite (Py_s). Various textural types of sulfides are distinguished by their Ni and Co contents (Figure 4-16).

Considering the metal/S ratio (e.g. Arnold, 1962, 1966), interstitial pyrrhotite (Po_i) from the central, least altered, parts of the gabbros and hyperites is principally of hexagonal (Fe_9S_{10}) and that from the marginal amphibolites of monoclinic (Fe_7S_8) type. Monoclinic pyrrhotite is commonly associated with pyrite. No distinction can be made between the hexagonal and monoclinic pyrrhotites with regard to the abundances of Ni and Co. Both types contain high Ni (0.5 to 1%) and low Co (0.05 to 0.3%). Copper was found to be below 0.01% in both types. Po_b is exclusively of hexagonal type. It constitute a very small fraction of the total sulfides, rarely exceeding 1%. The composition of the Po_b is similar to that of the Po_i.

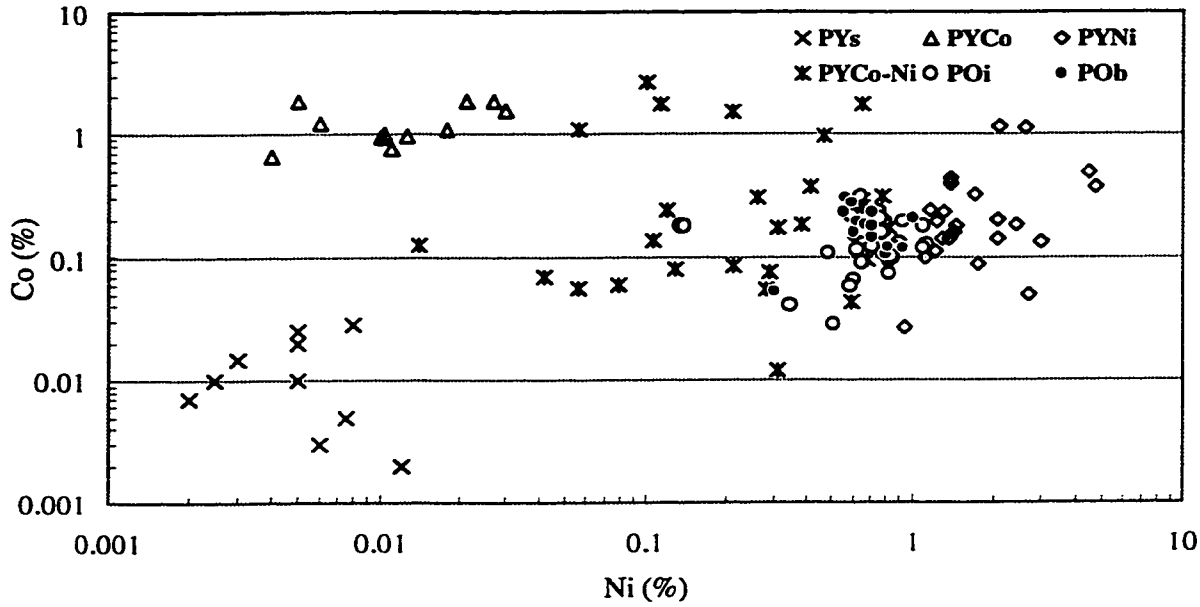

Figure 4-16. Various textural types of pyrite and pyrrhotite in Bamble gabbros, hyperites, and amphibolites.

Po_i, the dominant sulfide in the least altered gabbros and hyperites, has partially to totally been replaced by pyrite ± magnetite in the marginal amphibolites (Plates 4-2-A-B). The pyrite is commonly associated with minor chalcopyrite and pentlandite. Considering the textures and Ni and Co contents, three major types of interstitial pyrite may be distinguished (Figure 4-15):

1. Nickeloan pyrite (Py_{Ni}), occurring in composite grains associated with chalcopyrite and/or magnetite, or as euhedral to subhedral grains enclosed in pyrrhotite.
2. Co-rich pyrite (Py_{Co}), occurring as neat discrete grains, or as composite grains associated with chalcopyrite. Mantling by magnetite is common (Plate 4-2-C).
3. Ni-Co pyrite (Py_{Ni-Co}), commonly occurring in composite grains of pyrite ± chalcopyrite ± pentlandite ± magnetite.

As in metabasites, the composition of the magnetite associated with pyrite is different from the primary interstitial magnetite. The primary magnetite is invariably enriched in Ti and V, containing up to 5% TiO_2 and 1% V_2O_5. Secondary magnetite is characterized by very low Ti and V, commonly below 0.1%, but relatively high Ni, up to 0.5%.

Secondary pyrite (Py_s) may occur in the marginal amphibolites along microfractures, grain boundaries, and cleavages in mafic silicates. The Py_s rarely constitute more than 10% of the total sulfides in the enclosing rock. Minor chalcopyrite may occur associated with the secondary pyrite. The Py_s is poor in both Ni and Co, but may be rich in As.

Fe-Ni-Cu sulfide ores are locally associated with the gabbros and amphibolites. The ores experienced the same retrograde reactions and sulfide phase changes as in the minor disseminated sulfides in their host rocks, thus providing a larger window to investigate the retrograde reactions. The Fe-Ni-Cu ores and possible mechanisms responsible for oxidation of sulfides are discussed in Section 4-3.

Following, the mineralogy and geochemistry of the individual mafic bodies are discussed, with emphasis on the processes that controlled the distribution of chalcophile elements. A complete list of the geochemical data is given in the Appendix 4-3.

4-2-3. Laget Coronitic Gabbros and Amphibolites

Laget intrusive, Tvedestrand, is an elliptical body 1 km long and 0.5 km wide at the surface. Hydration and metamorphism under amphibolite grade has turned the margins of the Laget body into a foliated amphibolite. Samples have been collected from the central, least altered part (9 samples, 8501-9) as well as the amphibolitized margin (11 samples, 8401-11).

4-2-3-A. Laget Coronitic Gabbro

A striking feature in the Bamble gabbros is the development of coronitic microstructures on the former interface between olivine and plagioclase, and between Fe-Ti oxides and plagioclase. Gabbros with coronitic microstructures, also known as coronitic gabbro or coronite, are widespread throughout Bamble and elsewhere in SWSD.

In spite of the corona formation, the original textures have not been obliterated. The igneous fabrics is ophitic to sub-ophitic (Plate 4-3-A). The olivine-plagioclase coronas have a variable mineralogy, but they generally consist of an inner shell of orthopyroxene and/or clinopyroxene, rimmed by amphibole, and/or an amphibole-spinel symplectite. An outer rim of garnet is present in most samples.

The composition of the primary olivine in Laget and other gabbros in Risor area varies with original rock type from chrysolite to hyalosiderite (Fo_{74-62}) (Starmer, 1969). Brickwood and Craig (1987) determined olivine compositions of Fo_{75-36} for Bamble and Fo_{60-14} for Kongsberg gabbros. Olivines in Bamble and Kongsberg gabbros are generally more fayalitic than typical olivine compositions from tholeiitic mafic plutons (e.g. Fo_{60-80}, Deer et al., 1982).

Plagioclase laths are usually crowded with dust and inclusions of magnetite, hematite, and spinel in their cores. The formation of the Fe-oxide cloudings has been attributed to the liberation of some Fe during the formation of secondary orthopyroxene and hornblende (Starmer, 1969). The plagioclase crystals in Bamble gabbros are commonly more sodic towards the edges (Starmer, 1969; Field, 1969; Brickwood, 1984).

Like plagioclase, the primary pyroxenes are also clouded with dusts and inclusions of Fe-oxides. Clinopyroxene is of augite composition, and orthopyroxene of bronzite and hypersthene (Starmer, 1969; Cameron and Cogulu, unpublished data). Both orthopyroxene and clinopyroxene have developed coronas of hornblende, and are locally replaced by hornblende along cracks and cleavages.

Where developed, the outer corona of garnet occurs as granoblastic crystals or as a continuous growth rim. The garnet, which is a brownish almandine (Starmer, 1969; Cameron and Cogulu, unpublished data), grows inwards replacing hornblende coronas, or develops around cores of both secondary orthopyroxene and remnant olivine. Chlorine metasomatism has locally affected the coronitic gabbros, with the development of scapolite at the expense of the plagioclase.

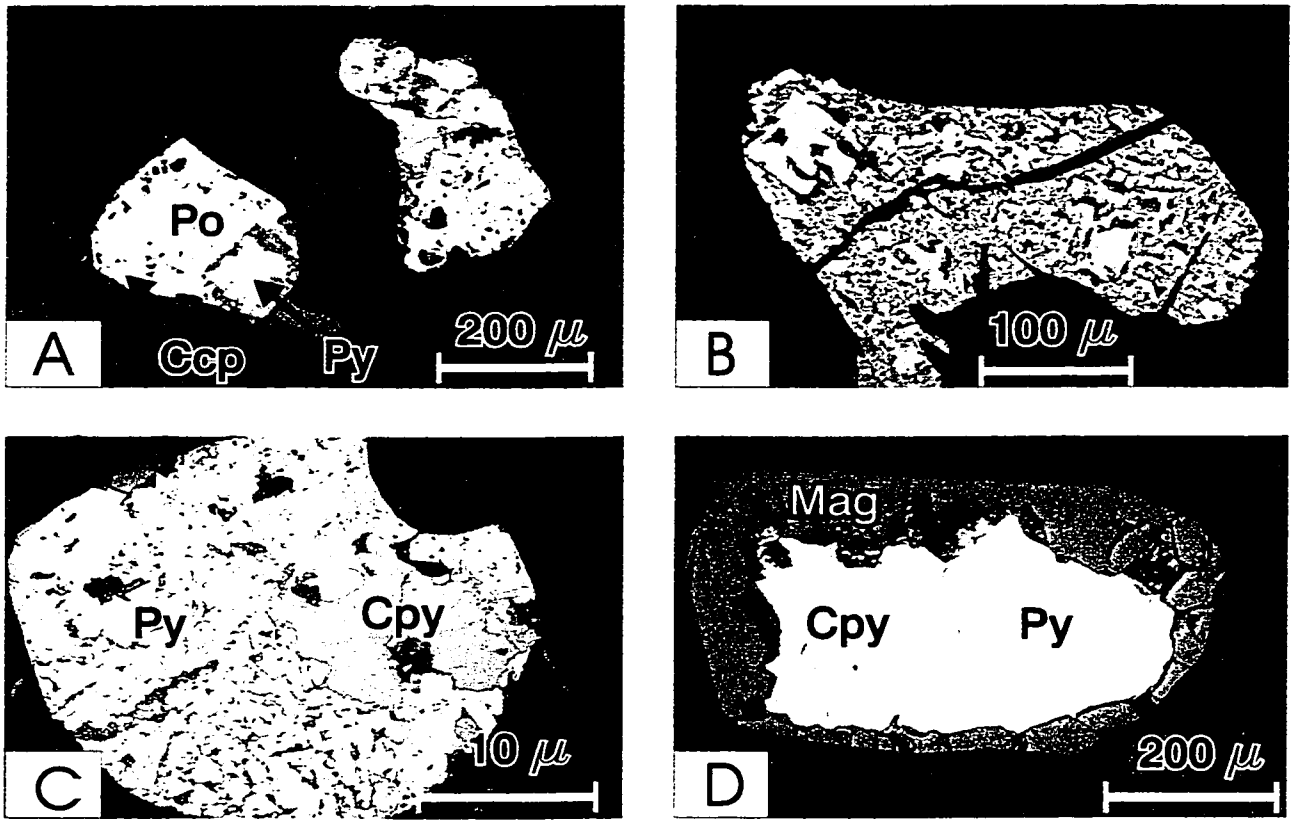

Plate 4-2. Typical textures displayed by sulfides in Bamble gabbros (hyperites) and amphibolites. (A) Initial and (B) advanced stages of replacement of pyrrhotite by pyrite and magnetite; samples 4001 and 4007 from the interior and the amphibolitized margin of a hyperite dyke from Tvedestrand. (C) Replacement of bleb pyrrhotite by pyrite; sample 8403 from Laget amphibolite. (D) Mantling of pyrite and chalcopyrite by magnetite; sample 4009 from Tvedestrand.

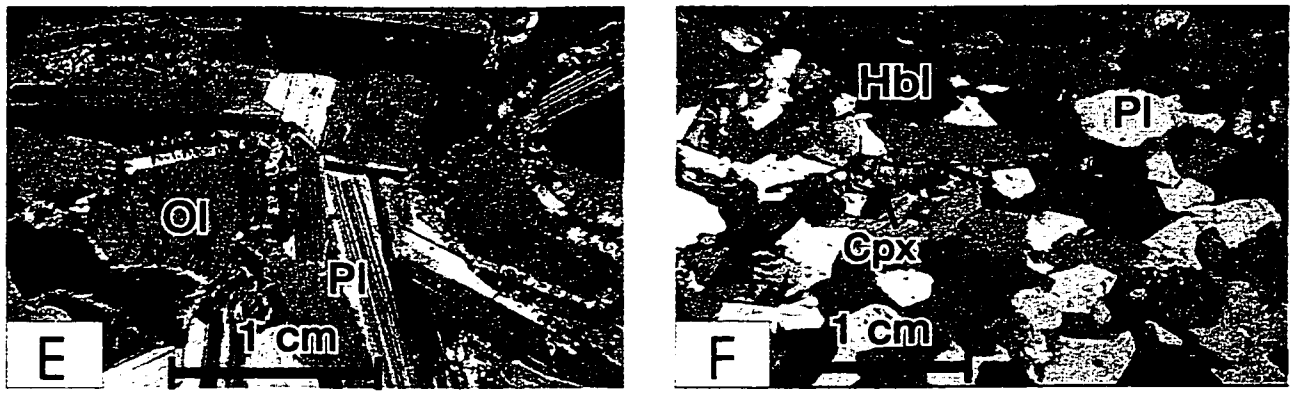

Plate 4-3. Typical textures displayed by coronitic gabbros and their amphibolitized equivalents from Laget. (A) Sub-ophitic texture in gabbro, with the development of coronas at olivine-plagioclase boundary. (B) Amphibolite consisting basically of hornblende and plagioclase.

Fe-Ti oxides, apatite, and sulfides occur as accessory minerals. Fe-Ti oxides consist of Ilmenite and subordinate titanomagnetite occurring in composite or discrete crystals. Pyrrhotite is the main sulfide, commonly accompanied by subordinate chalcopyrite and pentlandite. In two samples, pyrrhotite was found partially (<10%) replaced by pyrite. Both Fe-Ti oxides and sulfides may display an inner corona of brown or red brown biotite and an outer growth of hornblende or hornblende-spinel symplectite. A visual estimate of the modal composition, and the reconstructed mode, of the coronitic gabbros and their amphibolitized equivalents is shown in Table 4-4.

In recalculating the initial modal composition, coronitic orthopyroxene and bordering spinel-bearing symplectites were considered as olivine and plagioclase, respectively. Scapolite was considered as plagioclase, and hornblende as clinopyroxene. Garnet, replacing hornblende coronas inward or developing around olivine or secondary orthopyroxene, was counted partly as olivine and partly clinopyroxene. Considering the nomenclature of the gabbros (Starmer, 1969), Laget coronitic gabbros fall into the troctolitic gabbro class (Figure 4-16).

Table 4-4. Modal composition of the Laget coronitic gabbro and amphibolite, and recalculated mode for coronitic gabbro.

	Coronitic Gabbro (n = 9)	Recalculated Mode	Amphibolite (n = 11)
Plagioclase	38	42	36
Olivine	20	21	trace*
Orthopyroxene	1	0	trace
Clinopyroxene	10	37	4
Hornblende (± Spinel)	25	0	50
Garnet	3	0	trace
Biotite	trace*	0	1
Quartz	o **	0	trace
Fe-Ti oxides	1	1	1
Sulfides	trace	trace	trace
Apatite	trace	trace	trace
Scapolite	2	o	7

* less than 1% ** not found

Mineral reactions during corona formation have been discussed by several authors (e.g. Reynolds and Frederickson, 1962; Starmer, 1969; Brickwood, 1984; Brickwood and Craig, 1987). The growths around olivine involve the mobility of Fe, Mg, and to a lesser extent Al, Ca, and Si. The olivine-bronzite transformation causes the exit of Fe and Mg and an increase in Si. The replacement by amphibole (± spinel) requires the accession of Mg, Fe, and H_2O and the relative reduction of Ca, Al, and Si (Starmer, 1969). Iron and Mg released during olivine-bronzite transformation is consumed for the formation of biotite and hornblende coronas around iron ores. The replacement of labradorite by actinolite or actinolitic hornblende releases some Al which probably causes the formation of spinel as a symplectic intergrowth.

The formation of coronas has been attributed to late-magmatic or metamorphic processes (e.g. Reynolds and Frederickson, 1962; Ashworth, 1986; Joeston, 1986; Brickwood and Craig, 1987). Reynolds and Frederickson (1962) stressed the role of water in the formation of coronas. The authors regarded the corona growth as a metamorphic process caused by introduction of silica-bearing solutions. A metamorphic origin was supported by Morton et al. (1970).

The formation of the coronas has been attributed to isochemical recrystallization in a solid-state, promoted by inter-granular diffusion (Starmer, 1969). This model was supported by Ashworth (1986) and Brickwood and Craig (1987), who proposed that the coronas grow early in the cooling history, and continue to develop in response to isobaric cooling at elevated pressure. A metamorphic origin is also supported by chronology of corona minerals (Davidson and Van Breemen, 1988). Munz and Morvick (1991) determined a P-T range of 7-10 kbar and 800-600°C for the formation of coronas in Modum Complex, Kongsberg.

Figure 4-17. Classification of Laget and Tromoy Gabbros*

Noritic Trend ◄						► **Gabbroic Trend**			
Lithology	Troctolitic Norite	Noritic Troctolite	Opx Troctolite	Troctolite	Cpx Troctolite	Gabbroic Troctolite	Troctolitic Gabbro	Olivine Gabbro	Gabbro
Oliv/Oliv+Pyrox %	40 50	70	90	100	90	70	50	L 30	T 10 0

* Classification scheme after Starmer (1969) L Laget Coronite T Tromoy Coronite

4-2-3-B. Laget Amphibolite

The Laget coronitic gabbro grades into a foliated amphibolite at its margins. Primary mineralogy is obscured by intense amphibolitization and recrystallization. Green and green-brown hornblende has replaced the primary and secondary pyroxenes, and the stubby labradorite-andesine laths were transformed into granoblastic andesine, leading to the occurrence of a fine- to medium-grained rock consisting essentially of hornblende and plagioclase in subequal proportions (Plate 4-2-B).

Plagioclase and hornblende appear as granoblastic or xenoblastic equant crystals; hornblende also occurs as lepidoblastic or poikiloblastic crystals enclosing Fe-Ti oxides, plagioclase, and accessory quartz blebs. Biotite, almandine garnet, apatite, and quartz are present in most samples as accessory phases. Biotite displays a cross-cutting habit and appears to be, at least partly, of secondary origin, forming from hornblende, or less commonly, from garnet (Plate 4-2-C). An estimate of the modal composition of the amphibolites is shown in Table 4-4.

Laget amphibolites, and locally the interior coronitic gabbros, have been affected by chlorine metasomatism and formation of scapolite at the expense of plagioclase. The alteration is partial in most samples, with some plagioclase completely replaced, some marginally affected and some unaltered. The scapolite is a Cl-rich, CO_2-poor, marialite variety, as the whole-rock geochemistry suggest. Scapolite in similar rocks from Modum Complex, Kongsberg Sector, contains, on average, 3.1 wt % Cl, but minor CO_2 and SO_2 (Waque, 1996). Chlorine metasomatism has been reported from other areas in Bamble (e.g. Frodesen, 1973; Elliot, 1973; Starmer, 1969, 1973; Brickwood, 1984). The Cl-metasomatism and formation of scapolite was synchronous to the formation of amphibolites.

4-2-3-C. Mass Balance in Gabbro-Amphibolite Transition

Transition of gabbros to amphibolites in Bamble and elsewhere in SWSD was not isochemical (e.g. Frodesen, 1968, 1973; Starmer, 1969; Elliot, 1973; Field and Elliot, 1974; Zeck and Toft, 1989; Cameron, 1989a, 1993; Waque, 1996). Cameron (1989a, b) suggested that the

amphibolitization of the gabbros led to remobilization and removal of chalcophile elements, including Au. Summary statistics for Laget coronitic gabbros and amphibolites is shown in Table 4-5.

To assess the magnitude of introduction and removal of ions during gabbro-amphibolite transition, and to identify the nature of the fluids involved in the process, the whole-rock geochemistry of the central (least altered) and the marginal (most altered) parts of the Laget intrusive are compared using the equation of Gresens (Gresens, 1967). The equation has widely been used in the study of metamorphic and alteration processes (e.g. Appleyard, 1980; Kerrich et al., 1980; Grant, 1982; Gibson et al., 1983; Zeck and Toft, 1989; Kretz, 1994). Gresens equation can be expressed as:

$$f_V\,(g_B/g_A)\,C^Bn - C^An = Xn, \quad \text{where}$$

g_A = specific gravity of rock A (parent rock, or initial rock)

g_B = specific gravity of rock B (daughter or altered rock)

C^An = weight fraction of component n in rock A

C^Bn = weight fraction of component n in rock B

f_V = volume factor: volume of product divided by volume of parent rock.

Xn = weight fraction of component n lost or gained

In most cases, a certain f_V value is assumed or inferred on the basis of the assumption that an oxide or element has been immobile (e.g. $X_{Al_2O_3} = 0$, or $X_{TiO_2} = 0$).

Concentrations of individual elements and oxides are already known. To solve the Gresens equation, specific gravities and volume effect should be calculated. Specific gravities of the least altered and altered rocks were calculated from the proportions and specific gravities of individual minerals. Proportions of the minerals are visually estimated; specific gravities are taken from Deer et al. (1992). Specific gravities calculated in this way are:

Table 4-5. Summary statistics for Laget coronitic gabbros and amphibolites

	Coronitic Gabbro (n = 9)			Amphibolite (n = 11)			Gresens Xn Score	Gain and Loss %
	X	1 σ	C. V.	X	1 σ	C. V.		
SiO_2	46.6	1.1	2.0	46.7	1.2	3.0	0.40	0.8
TiO_2	1.0	0.30	30	1.6	0.75	45	0.61	61
Al_2O_3	17.8	1.6	9.0	17.5	2.3	13	0.01	0.1
Fe_2O_3	1.6	0.5	28	1.9	0.4	24	0.03	2.0
FeO	9.6	1.3	14	8.7	1.9	22	-0.85	-9.0
MnO	0.21	0.10	48	0.2	0.5	250	-0.01	-4.0
MgO	9.60	1.70	18	7.8	0.9	12	-1.87	-20
CaO	8.95	0.90	10	8.6	1.0	12	-0.15	-1.6
Na_2O	2.7	0.4	15	3.2	0.5	15	0.52	19
K_2O	0.27	0.09	33	0.68	0.3	41	0.41	153
P_2O_5	0.12	0.06	50	0.16	0.07	44	0.04	34
H_2O	1.0	0.3	30	1.86	0.56	29	0.87	87
CO_2	0.14	0.08	57	0.14	0.05	36	0.00	0.7
Cr*	100	75	75	120	60	48	10.76	21
Ni	175	58	33	125	38	32	-49.21	-28
Co	78	11	14	73	9.0	12	-4.54	-6.0
Sc	18.0	6.0	33	28	15	50	10.18	57
V	122	48	40	220	125	57	99.39	82
Zn	95	20	21	100	31	31	5.63	6.0
S	730	280	38	875	550	63	8.75	1.2
Cu	65	22	34	95	55	58	31.61	49
Se	0.11	0.03	27	0.12	0.05	42	-0.02	-16
As	1.75	1.4	80	1.9	1.0	53	-0.04	-2.2
Sb	0.09	0.04	44	0.15	0.05	33	0.05	51
Au (ppb)	0.24	0.12	50	0.37	0.25	68	0.10	39
Rb	21	9.0	43	53	24	45	32.34	154
Cs	0.80	0.30	37	1.0	1.1	110	0.21	26
Ba	110	25	23	186	59	31	77.18	70
Sr	272	60	23	282	102	36	24.82	9.0
Nb	4.0	3.8	95	5.5	3.5	64	1.54	38
Hf	1.2	0.9	75	0.8	0.5	63	-0.40	-33
Zr	88	22	25	103	22	21	15.65	18
Y	38	14	37	46	16	35	8.29	22
Th	0.3	0.2	67	0.25	0.17	68	-0.05	-16
U	0.16	0.07	44	0.18	0.12	67	0.02	13
La	3.6	1.25	35	5.6	1.6	28	2.64	73
Ce	12	4.50	37	14	7.0	50	3.10	26
Sm	2.60	0.40	15	3.8	1.5	39	1.23	45
Eu	0.6	0.2	33	1.4	0.5	36	0.81	135
Tb	0.70	0.35	50	0.65	0.3	46	0.06	8.0
Yb	1.6	0.7	44	1.75	0.7	40	-0.24	-11
Lu	0.16	0.06	37	0.32	0.17	53	0.07	31
F	165	60	36	250	120	48	87	53
Cl	1500	1800	120	3900	1950	57	2425	160
Br	2.0	2.0	100	3.0	3.0	100	0.72	30

x = arithmatic mean σ = standard deviation C. V. = coefficient of variation * elements in ppm

g_A (specific gravity of coronitic gabbros) = 3.16

g_B (specific gravity of amphibolites) = 3

With the assumption that certain elements were immobile during a metamorphic or alteration transformation, the Gresens equation gives an estimate for the volume effect, according to the equation:

$$f_V = (C^A n/C^B n)*(g_A/g_B)$$

For any transformation, volume factor (f_V) may be calculated which corresponds to the isochemical behavior of individual components. Clustering of the f_v's of the components which are empirically known to be relatively immobile, such as Al_2O_3, TiO_2, Zr, would provide a reasonable basis for estimating the volume change of the reactions. Application of this procedure to Laget samples showed a clustering of values around 1.06 ($1\sigma = 0.02$) for SiO_2, Al_2O_3, $Fe_{(total)}$, MnO, Sr, and Co. Independent studies on similar rocks in Bamble and elsewhere have shown that these oxides were the least mobile components in the course of gabbro-amphibolite transition (e.g. Starmer, 1969; Elliot, 1973; Zeck and Willadsen, 1991). For Laget, a 6% increase in volume is compensated by a corresponding decrease (5.06%) in specific gravity. Gresens scores calculated in this manner, and the gain and loss percentages for individual oxides and elements, are shown in Table 4-5.

A graphical solution of Gresens equation, as suggested by Grant (1986), is used to show the relative mobilities of individual elements. The isocon diagram (Figure 4-18) compares the concentration of elements in coronitic gabbros, or original rocks, to the concentration of the same element in amphibolites, or altered rocks.

Gabbro-amphibolite transition at Laget was associated with significant chemical changes, as many elements plot far from the isochemical line (Figure 4-18). However, a primary magmatic origin for the chemical changes can not be ruled out. As proposed by Zeck and Toft (1989), mass balance calculation on the basis of Gresens equation is subject to a basic uncertainty, that is the "sample matching problem". "Original variations within the protolithic rock suite before

alteration, and local variations in the regional metasomatic pattern will put a limit on the precision and validity of the mass balance calculations".

To test for the initial variations within the Laget intrusive, Harker diagrams have been constructed using Niggli Mg# as differentiation index (Figure 4-19 to 4-21). Following, the results of mass balance calculations are discussed. For comparison, a compilation of data from other studies of gabbro-amphibolite transition in Bamble and elsewhere in South-West Scandinavian Domain (SWSD) is shown in the Appendix 4-4.

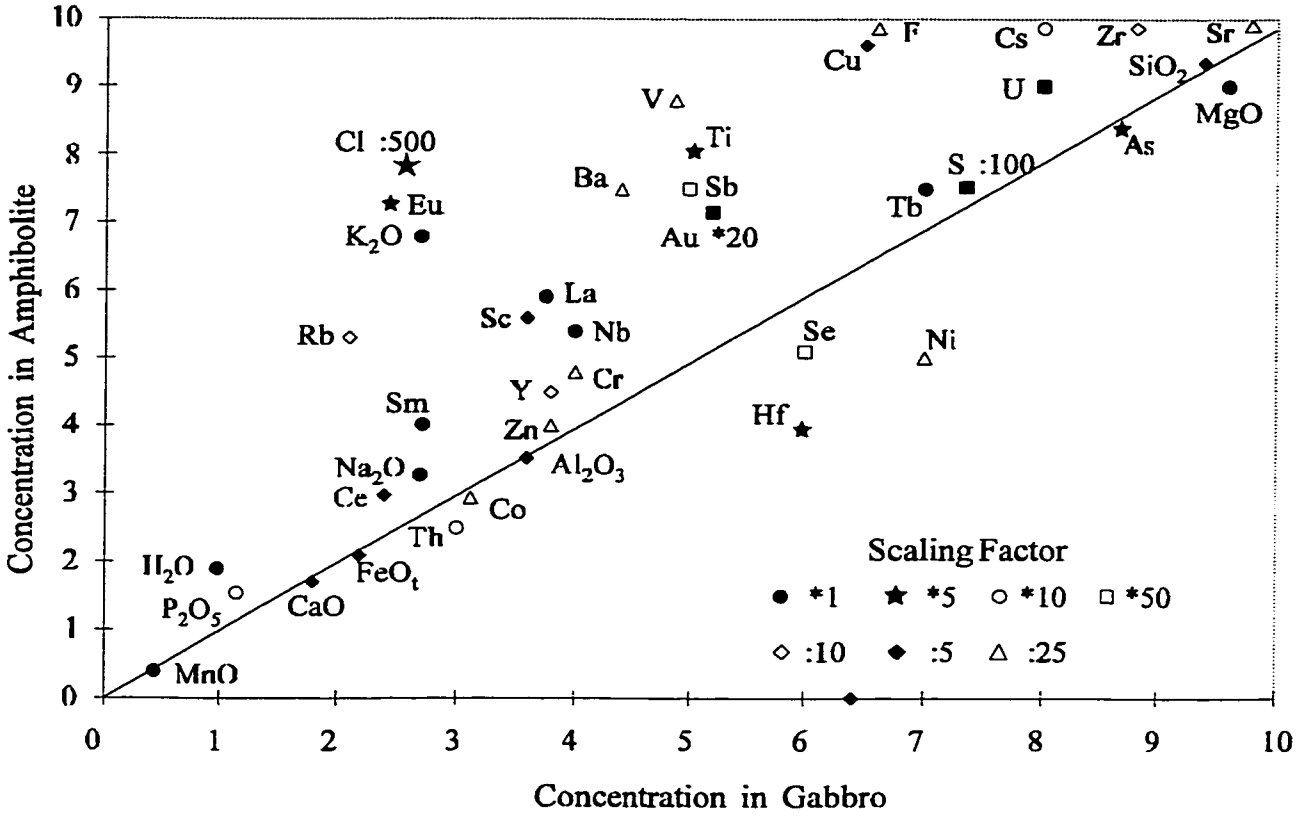

Figure 4-18. Isocon diagram comparing the mean concentration of oxides and elements in Laget coronitic gabbros and amphibolites. SiO_2, Al_2O_3, FeO* (FeO + Fe_2O_3), CaO, and MnO are collinear and define a best fit isocon. The mean values are multiplied by the scaling factors shown to fit in the range 1 to 10. Oxides in %; elements in ppm (Au in ppb).

I. Major Oxides

SiO_2, Al_2O_3, and MnO are similarly distributed in the gabbros and amphibolites. Slight enrichment of CaO in coronitic gabbros may be attributed to magmatic fractionation processes. This is supported by plot of Niggli C against Mg# (Figure 4-19-G). Data from other studies in Bamble and elsewhere in SWSD show that these oxides were of the least mobile components during gabbro-amphibolite transition (e.g. Frodesen, 1968, 1973; Starmer, 1967, 1969; Elliot, 1973; Morthorst et al, 1983; Zeck and Toft, 1989).

$Fe_{(total)}$ has frequently been reported to remain constant during gabbro-amphibolite transition (Appendix 4-4). However, Fe_2O_3 and FeO ratios may change. Amphibolites display a more oxidized assemblage. This is supported by a higher score for $Fe_2O_3/FeO + Fe_2O_3$ (0.18 vs 0.14). Similar observations have been reported from other parts of Bamble (Frodesen, 1968, 1973; Elliot, 1973; Field and Elliot, 1974) and Kongsberg (Waque, 1996). A higher oxidation state in the amphibolites is also supported by the common presence of hematite exsolution lamellae in ilmenite, and replacement of pyrrhotite by pyrite + magnetite.

Contrasting data exist on the behavior of Mg during gabbro-amphibolite transition. Field (1966) reported local occurrences of cordierite-anthophyllite schists within amphibolitized gabbros in Risor area. Similarly, Frodesen (1968, 1973) recorded a considerable enrichment of Mg in the scapolitized and amphibolitized margins of Hiåssen gabbro, Bamble. In contrast, Starmer (1967, 1969) showed that alteration of gabbros at Risor-Sondeled area, Bamble, was associated with strong depletion of Mg. Removal of Mg was also reported from Modum Complex, Kongsberg (Waque, 1996). Alternatively, Elliot (1973) and Morthorst et al. (1983) showed that Mg was immobile and remained constant during gabbro-amphibolite transition.

Variations of MgO in Laget appear to be of primary magmatic origin rather than a metasomatic overprint. This is clearly evident from the variations of the least mobile elements against Niggli Mg# as differentiation index (Figure 4-19-A-F). Titanium, P, Ni, Sc, Y, and Zr are amongst the least mobile elements in metamorphic and alteration processes (e.g. Pearce and Cann, 1973; Floyd and Winchester, 1975, 1983; Winchester and Floyd, 1976; Pearce et

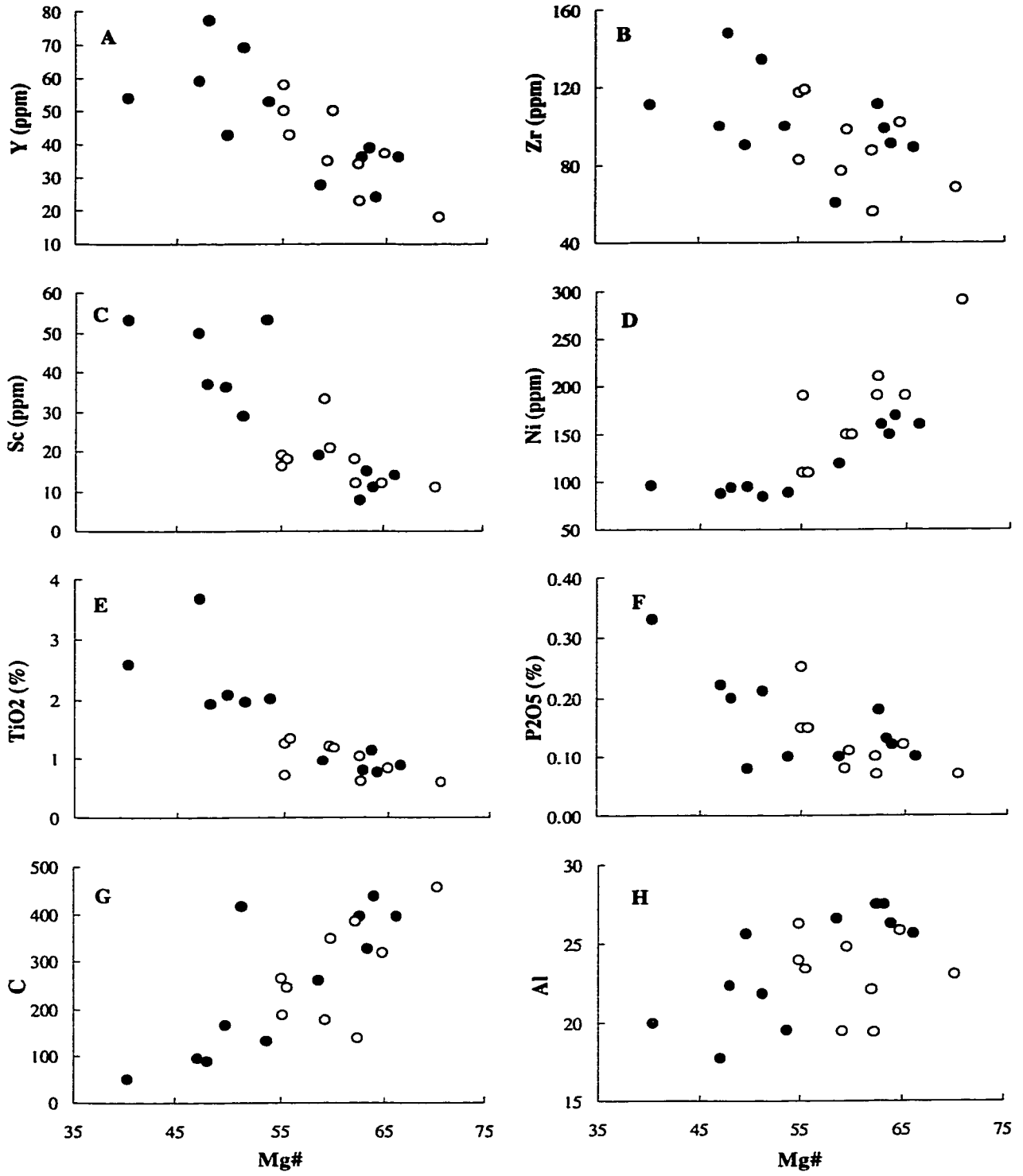

Figure 4-19. Whole rock variation diagrams with Niggli Mg# as differentiation index, Laget Intrusive, Bamble. Open and solid circles represent coronitic gabbros and amphibolites, respectively.

al., 1984). Trends of variations in Figure 4-19 indicate that Laget intrusive is a differentiated mafic body with higher concentrations of incompatible elements towards the margins.

Distribution of Ti in Laget intrusive follows a typical magmatic differentiation trend (Figure 4-19-E), with higher Ti in the marginal, more fractionated rocks (now amphibolites). Titanium has alternatively been reported to be immobile (Field, 1969; Elliot, 1973; Morthorst et al. (1983) or variably mobile (Batey, 1965; Starmer, 1967, 1969; Verdonk et al., 1986) during gabbro-amphibolite transition. Starmer (1967) reported the occurrence of sporadic sphene-rich patches and the development of marginal rutile ore bodies in the peripheral amphibolites in Risor area.

Higher contents of P_2O_5 in Laget amphibolites can be explained by magmatic differentiation processes rather than metasomatism (Figure 4-19-F). Phosphorous behaves incompatibly during crystallization of mafic magmas, concentrating in the late, Fe-rich fractionates (e.g. Bourdreau and McCallum, 1989). Variable enrichment and depletion of P_2O_5 have been reported from Bamble (Griffin et al., 1972; Elliot, 1973; Field and Elliot, 1974) and Kongsberg (Waque, 1996). Morton et al. (1970) and Griffin et al. (1972) reported the occurrence of apatite-phlogopite-enstatite-rutile veins in scapolitized gabbros in Bamble. However, a similar study on Värmland hyperite, Sweden, showed that P_2O_5 was relatively immobile (Zeck and Toft, 1989).

H_2O has invariably been added to the amphibolites. Replacement of anhydrous minerals, olivine and pyroxenes, by hornblende and other hydrous minerals required the introduction of considerable amounts of water.

CO_2 is, in most samples, below the detection limit of 0.1%, and will not be discussed. Data from other areas show that CO_2 has locally been an important constituent of the infiltrating fluids. Munz et al. (1994) and Waque (1996) documented extensive carbonatization associated with amphibolitized hyperites in Modum Complex, Kongsberg.

Na_2O is slightly enriched in the amphibolites. An increase in Na is reflected in the plagioclase composition, as plagioclase in amphibolites is generally more sodic than that in unaltered gabbros (c.f. Starmer, 1967, 1969). Extensive sodium metasomatism and albitization has been reported from Modum Complex, Kongsberg (Munz, 1994; Waque, 1996).

II. Lithophile Transition Metals

No significant changes are recorded for Co and Zn. Co^{2+} replaces both Fe^{2+} and Mg^{2+} sites, and Zn^{2+} prefers Fe^{2+} sites in silicates (e.g. Wedepohl, 1970; Mason and Moore, 1982; Deer et al., 1992). Higher Ni in gabbros corresponds to higher Mg in these rocks, and can easily be explained by magmatic differentiation processes (Figure 4-19-D). Ni^{2+} behaves compatibly during magmatic crystallization replacing Mg^{2+} sites in Mg-bearing silicates, particularly olivine.

Chromium is slightly enriched in the amphibolites. No independent Cr-mineral was found on microscope. A positive correlation exists between the concentration of Cr and the modal abundance of magnetite, implying that Cr is carried as an impurity in magnetite. Magnetite is known as a suitable host to Cr in mafic rocks (Deer, 1992).

Higher contents of Sc and V in Laget amphibolites can best be explained by a magmatic differentiation model. Variations of Sc with Mg# is shown in Figure 4-19-C. Field and Elliot (1974) reported an enrichment of V^{3+} in amphibolitized gabbros from Risor. The enrichment was attributed to higher oxidation state of amphibolites that provided more Fe^{3+} sites for V^{3+}.

III. Large Ion Lithophile Elements

Slight enrichment of Zr and Y in the amphibolites corresponds to a magmatic differentiation trend (4-20-A-B). A similar trend is displayed by Nb. The abundances of U, Th, and Hf are, for most samples, below the detection limits of 0.1, 0.1, and 0.5, respectively.

Potassium, Rb, Cs, and Ba are considerably enriched in the amphibolites. Fields of variations for the elements in the amphibolites plot well above those for the gabbros at similar Mg#

(Figure 4-20-E-H). Distribution of the elements was largely controlled by metasomatism rather than magmatic fractionation processes. This is supported by the common occurrence of secondary biotite laths in the amphibolites.

There seems to be a consensus on the enrichment of alkaline ions during gabbro-amphibolite transition in Bamble and elsewhere in South West Scandinavian Domain (Appendix 4-4). Potassium metasomatism has locally resulted in the production of biotite-schists (Starmer, 1969, de Haas, 1994). Enrichment of Rb and Ba in the amphibolites appears to be related to K-metasomatism and the formation of secondary biotite. Cations with large radii and low electric charge can replace K^+ in K-bearing minerals, in agreement with the regularities of distribution of elements in igneous and metasomatic rocks (c.f. Krauskopf, 1979).

IV. Rare Earth Elements

Rare earth elements (REE) behave incompatibly during crystallization of mafic magmas (e.g. McKay, 1989; Hanson, 1989). Enrichment of REE in the amphibolites can be explained by a magmatic differentiation model. This is evident from variations of La and Sm as representatives of light and heavy REE (Figure 4-20-C-D).

Our data on the immobility of REE supports an earlier study by Smalley and Field (1991) on gabbro-amphibolite transition in Kragero and Risor areas, Bamble. However, Munz et al. (1994) and Waque (1996) showed that REE were variably mobile during amphibolitization and albitization of gabbros and amphibolites in Modum Complex, Kongsberg.

V. Halogens

Chlorine is considerably introduced into the amphibolites (Figure 4-20-A). Chlorine metasomatism has also affected the coronitic gabbros. Amphibolites also appear to be enriched in F. However, the consistent variations of F with Mg# (Figure 4-20-B) suggests that distribution of F was mostly controlled by primary magmatic processes. The concentration of

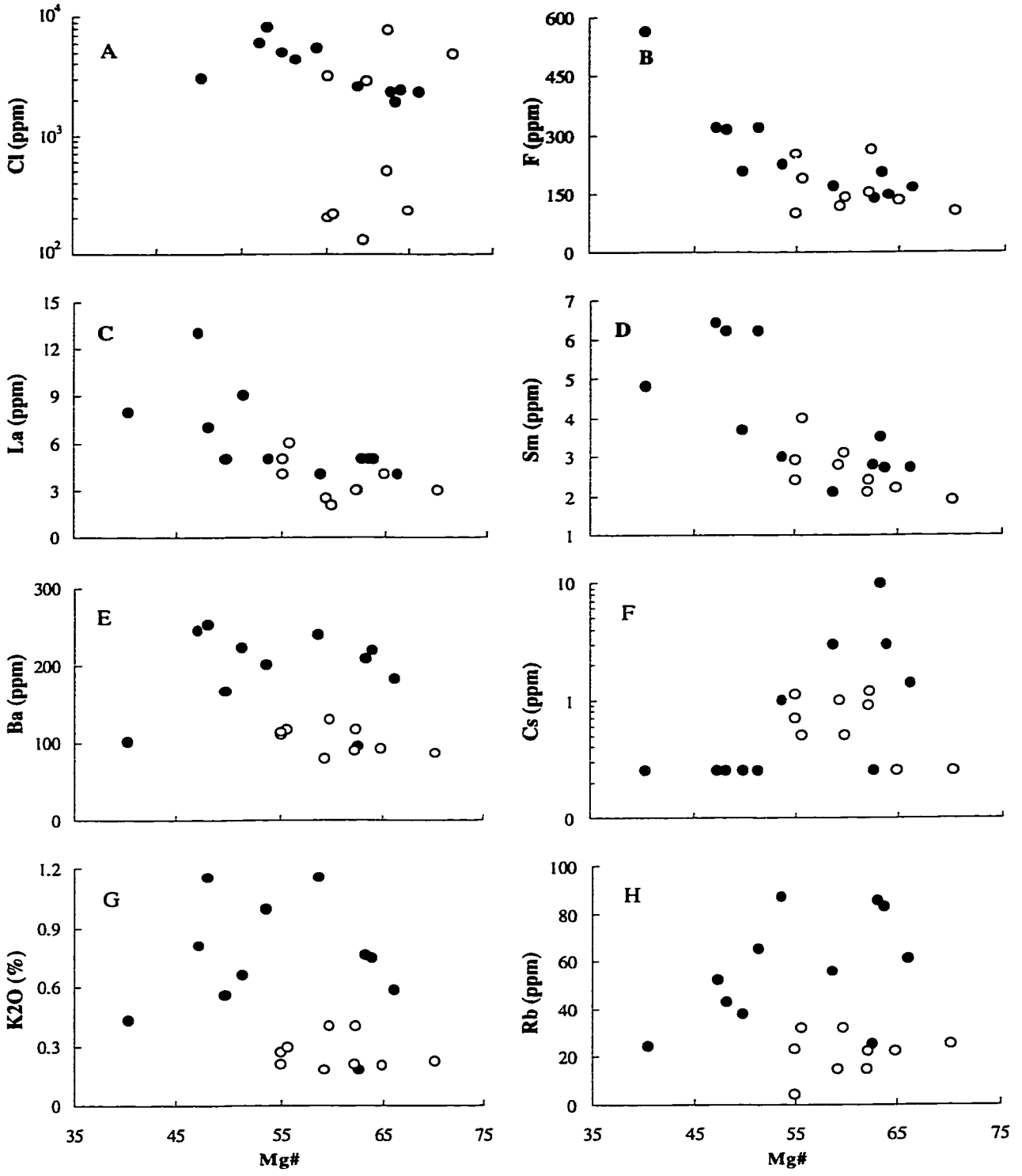

Figure 4-20. Distribution of the large ion lithophile elements (E-H), REE (C-D) and halogens (A-B) with respect to Niggli Mg# as differentiation index, Laget Intrusive, Bamble. Open and solid circles represent coronitic gabbros and amphibolites, respectively.

Br in most gabbros is below the detection limit of 1 ppm. However, half of the amphibolites contain Br well above the detection limit. Two gabbros enriched in Cl also contain detectable Br. Chlorine metasomatism appears to be a common feature in Bamble (Field and Elliot, 1974; Frodesen, 1973; Lieftink et al., 1993) and elsewhere in SWSD (Munz et al., 1994; Zeck and Wiladsen, 1991; Waque, 1996).

Bamble is one of the world's most famous scapolite areas (Lieftink et al., 1993, and references therein). The Bamble scapolites are mainly of Cl-CO_2-rich and CO_2-SO_3-rich varieties, the first type being predominant. Chlorine in amphibolitized hyperites is not only in scapolite, but also in hornblende and apatite. Frodesen (1968) reported concentrations of up to 1.61% Cl in hornblende from Hiåssen gabbro, Bamble. Similar concentrations are discovered in Modum Complex, Kongsberg (Waque, 1996). Griffin et al. (1972) reported an average of 1.60% Cl in apatite from Ødegaarden, Bamble.

4-2-3-D. Distribution of Chalcophile Elements

The elements discussed under this group, S, Cu, Se, As, Sb, and Au, have a great tendency to occur in sulfides and sulfosalts. Gold is also a siderophile element. Arsenic and Sb have some lithophile tendency and may substitute for Si^{+4}, Al^{+3}, Fe^{+3}, and Ti^{+4} in rock-forming minerals (Esson et al., 1965; Bauer and Onishi, 1974; Boyle and Jonasson, 1984).

Chalcophile elements remained relatively constant during gabbro-amphibolite transition. Slightly higher concentrations of S, Cu, and Au in the amphibolites appear to be of magmatic origin (Figure 4-21). Chalcophile elements are known to behave incompatibly during differentiation of mafic magmas (e.g. Hamlyn et al., 1985; Naldrett and Barnes, 1986; Brügman et al., 1987; Noll et al., 1996).

Interstitial pyrrhotite is the dominant sulfide in coronitic gabbros, commonly associated with minor chalcopyrite and pentlandite. In amphibolites, however, pyrrhotite has partially to totally been replaced by pyrite ± magnetite. Amphibolites also contain minor secondary pyrite

as fracture filling and replacement bodies. The similar abundance of chalcophile elements in the two rock types indicates that gabbro-amphibolite transition and sulfide phase change was not associated with significant introduction or removal of chalcophile elements.

Variable depletion and enrichment of chalcophile elements have been reported from Bamble and elsewhere in SWSD. Cameron (1989a, b, 1993) reported a depletion in Au, As, and Sb with amphibolitization of gabbros and hyperites in Bamble. Zeck and Toft (1989) reported up

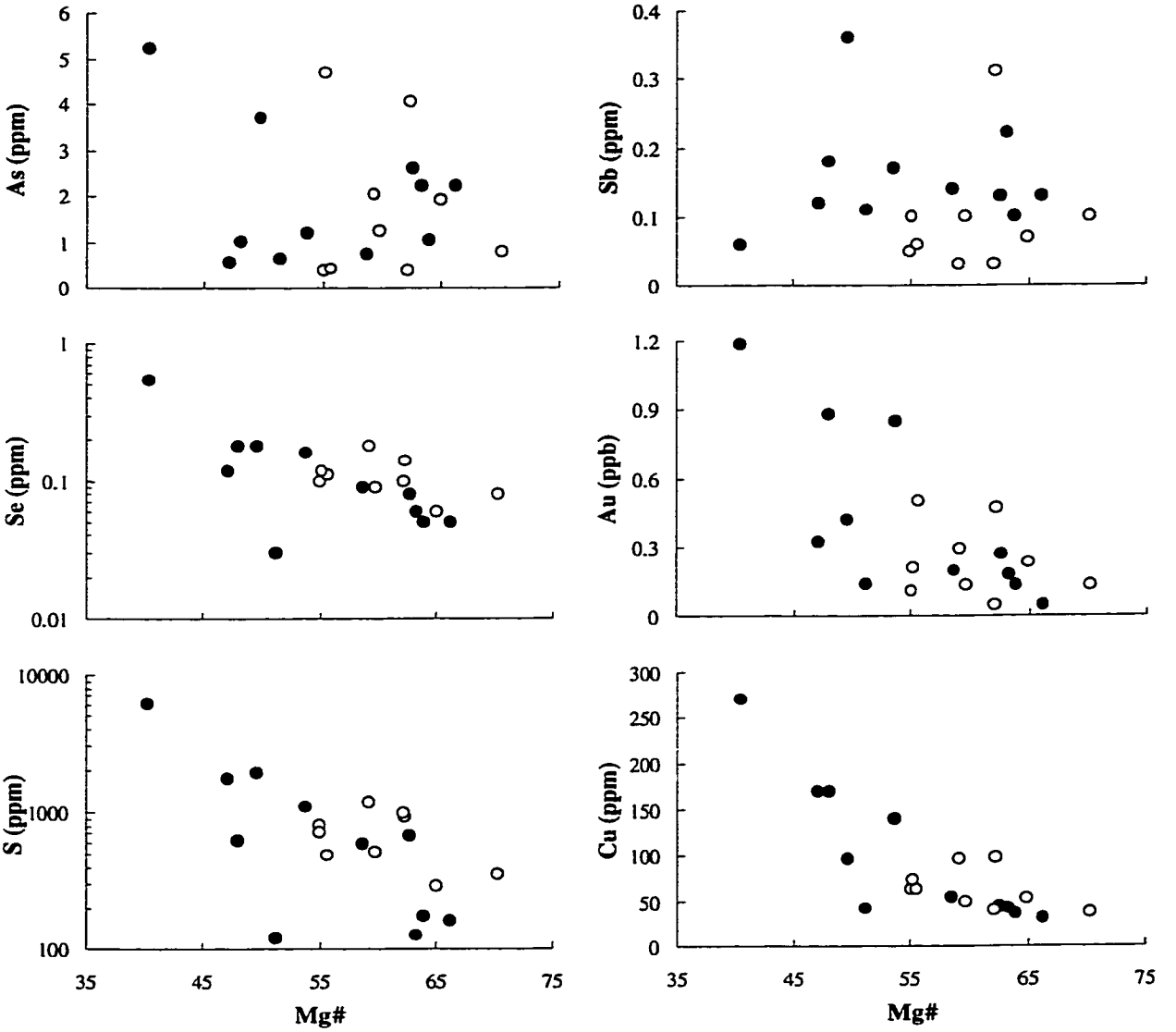

Figure 4-21. Variations of chalcophile elements with Niggli Mg# as differentiation index, Laget Intrusive, Bamble. Open and solid circles represent coronitic gabbros and amphibolites, respectively.

to 60% depletion in S from Värmland hyperite, Sweden. A similar depletion in S was reported from Risor area, Bamble (Field and Elliot, 1974). Alternatively, Waque (1996) showed that amphibolitization of gabbros in Modum Complex, Kongsberg, was accompanied by 50% enrichment in S and Cu. The author further showed that Au remained constant during the alteration. Frodesen (1973) reported a slight enrichment in As with scapolitization of the Hiåssen gabbro, Bamble.

The Laget gabbros and amphibolites are significantly depleted in Au compared to the mean composition of mafic rocks elsewhere (Figure 4-22). They are also depleted in Sb. Sulfur, Cu, Se, and As, however, are in the same range as in the mean mafic rocks.

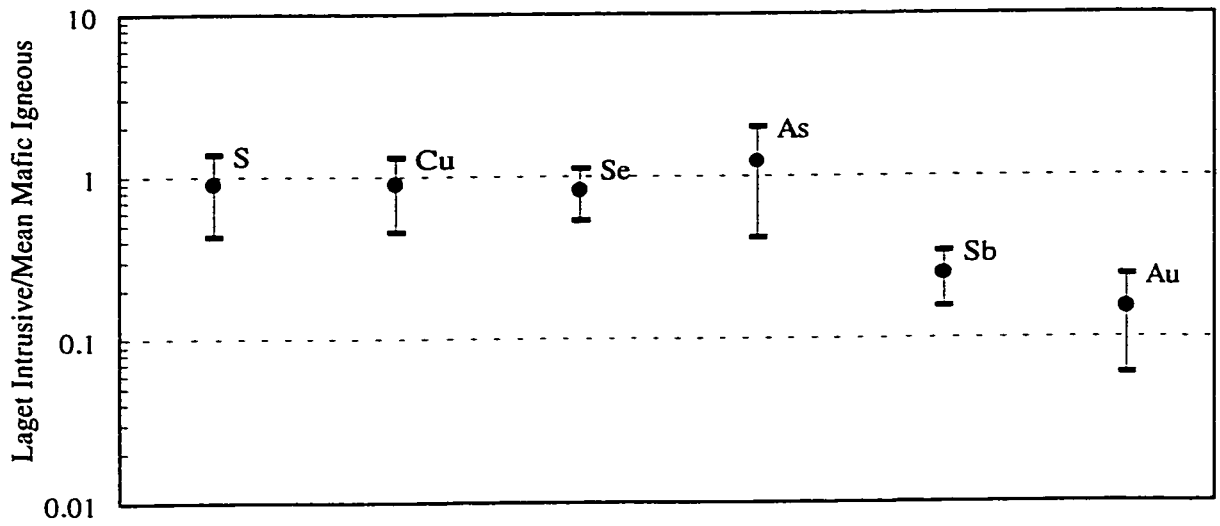

Figure 4-22. The abundance of chalcophile elements in Laget intrusive, normalized to the mean composition of mafic igneous rocks. Spheres represent the mean values and bars display 1σ standard deviation. See Appendix 2-2 for normalization data.

4-2-4. Tromoy Coronitic Gabbro

Metamorphism of gabbros at Bamble was mostly at amphibolite grade. However, gabbro bodies at Tromoy are metamorphosed under hornblende-granulite conditions (Brickwood, 1984; Cameron et al., 1989a). One coronitic gabbro dyke, ~20 m wide, was sampled from

Tromoy (sample series 5201-4). Unlike Laget, no considerable amphibolite margin is developed at Tromoy.

4-2-4-A. Mineralogy and Geochemistry

The mineralogy and modal composition of Tromoy coronitic gabbros is different from that of Laget, the main differences being:

- Unlike Laget, primary olivine is almost totally replaced by corona-forming minerals.
- Garnet corona, a minor constituent in Laget, are well developed in Tromoy.
- Orthopyroxene, a minor mineral in Laget, is common in Tromoy, constituting up to 10% modal composition of the rocks. Orthopyroxene is mainly of bronzite composition (En_{68-89}) (Cameron and Cogulu, unpublished data).
- Magnetite, subordinate to ilmenite in Laget, is common in Tromoy. The magnetite/ilmenite ratio varies from 1/10 to 1/5 in Laget, but 1/3 to 1/1 in Tromoy. Also, minor hematite is present as exsolution lamellae within ilmenite in Tromoy.
- Pyrite, rare in Laget gabbros, forms up to 40% of the total sulfides in Tromoy. Secondary pyrite is rare.
- Tromoy coronitic gabbros represent a relatively more oxidized rock. This is supported by a higher score for $Fe_2O_3/(Fe_2O_3 + FeO)$ (0.22 vs 0.14), a higher "magnetite/ilmenite" ratio, the presence of hematite, and the replacement of pyrrhotite by pyrite + magnetite.

Plagioclase displays the same zonal habit as in Laget, with an inner cloudy zone rich in spinels, and a clean and more sodic marginal zone. Clinopyroxene occurs interstitial to plagioclase and appears to be of primary origin. It generally contains abundant needles of Fe-Ti oxides parallel to cleavage planes. The clinopyroxene is a diallage variety (Cameron and Cogulu, unpublished data). Orthopyroxene is of secondary metamorphic origin. It displays three different habits: 1) replacing olivine at the central portion of the corona structures; 2) rods of corona-forming bronzite about the central pyroxene; and 3) granular aggregates and symplectite of bronzite in marginal zones of plagioclases. Hornblende corona has developed around both primary clinopyroxene and secondary orthopyroxene. Hornblende is also common around Fe-Ti oxides.

The modal composition, and the recalculated mode, of the Tromoy gabbro is shown in Table 4-6. Reconstruction of the initial mineralogy was carried out in the same manner already described for Laget. Considering the classification of Starmer (1969), Tromoy gabbro falls into the olivine-gabbro class (Figure 4-17). Summary statistics for Tromoy gabbro is shown in Table 4-7; the mean composition of Laget gabbro is also shown for comparison.

In spite of the differences in mineralogy and modal composition, the whole rock geochemistry of the Tromoy intrusive is closely similar to that of the Laget. The relatively low scores for coefficients of variations suggest that the Tromoy dyke is a fairly homogenous intrusion.

4-2-4-B. Distribution of Chalcophile Elements

Chalcophile elements are uniformly distributed in all samples, further supporting the homogeneous nature of the Tromoy dyke. The primary pyrrhotite, or pyrrhotite monosulfide solid solution (Po-mss), is variably replaced by pyrite ± magnetite. Both pyrite and pyrrhotite are equally associated with lamellae and patches of chalcopyrite and pentlandite. As in Laget, the Tromoy gabbro is strongly depleted in Au and Sb relative to the general abundance of these elements in mafic rocks elsewhere (Figure 4-23). The Tromoy gabbro is further depleted in As.

Table 4-6. Modal composition of the Tromoy coronitic gabbro

	Coronitic Gabbro (n = 4)	Recalculated Mode
Plagioclase	48	50
Olivine	2	8
Orthopyroxene	5	
Clinopyroxene	25	40
Hornblende (spinel)	10	
Garnet	8	
Biotite	trace*	
Fe-Ti oxides	2	2
Sulfides	trace	trace
Apatite	trace	trace

* less than 1%

Table 4-7. Summary statistics for Tromoy coronitic gabbro. Mean composition of the Laget gabbro shown for comparison.

	X	1 σ	C. V.	Laget Gabbro
SiO_2	48.2	0.8	2.0	46.65
TiO_2	1.4	0.4	28	1.3
Al_2O_3	16.0	0.9	6.0	17.7
Fe_2O_3	2.6	0.33	13	1.75
FeO	9.2	0.23	3.0	9.15
$Fe_2O_3/(FeO+Fe_2O_3)$	0.22	0.03	14	0.14
MnO	0.2	0.01	5.0	0.2
MgO	7.9	1.2	15	8.7
CaO	10.4	0.8	8.0	8.8
Na_2O	2.8	0.2	7.0	2.95
K_2O	0.25	0.07	28	0.27
P_2O_5	0.12	0.03	25	0.14
H_2O	0.5	0.05	11	1.0
CO_2	0.05	0.06	120	0.14
Cr*	198	60	30	110
Ni	120	45	38	150
Co	75	10	13	76
Sc	40	12	30	23
V	238	75	32	170
Zn	106	15	14	97
S	1070	218	20	800
Cu	86	17	20	80
Se	0.17	0.02	12	0.11
As	0.145	0.04	28	1.82
Sb	0.023	0.01	44	0.12
Au (ppb)	0.24	0.05	21	0.3
Rb	23	8.0	31	21
Cs	0.6	0.4	67	0.80
Ba	90	11	12	110
Sr	200	14	7.0	275
Nb	3.5	1.5	42	4.0
Hf	1.0	0.5	50	1.0
Zr	105	25	24	95
Y	56	13	23	42
Th	0.3	0.2	80	0.27
U	0.2	0.1	50	0.17
La	4.9	1.4	29	4.6
Ce	12.7	0.4	3.0	13
Sm	3.67	0.7	19	3.2
Eu	0.7	0.25	36	1.0
Tb	1.15	0.4	35	0.67
Yb	2.9	0.75	26	1.7
Lu	0.35	0.13	37	0.24
F	200	50	25	53
Cl	50	57	114	160
Br	0.9	0.2	22	2.0

X = arithmetic mean σ= standard deviation C. V. = coefficient of variation * elements in ppm

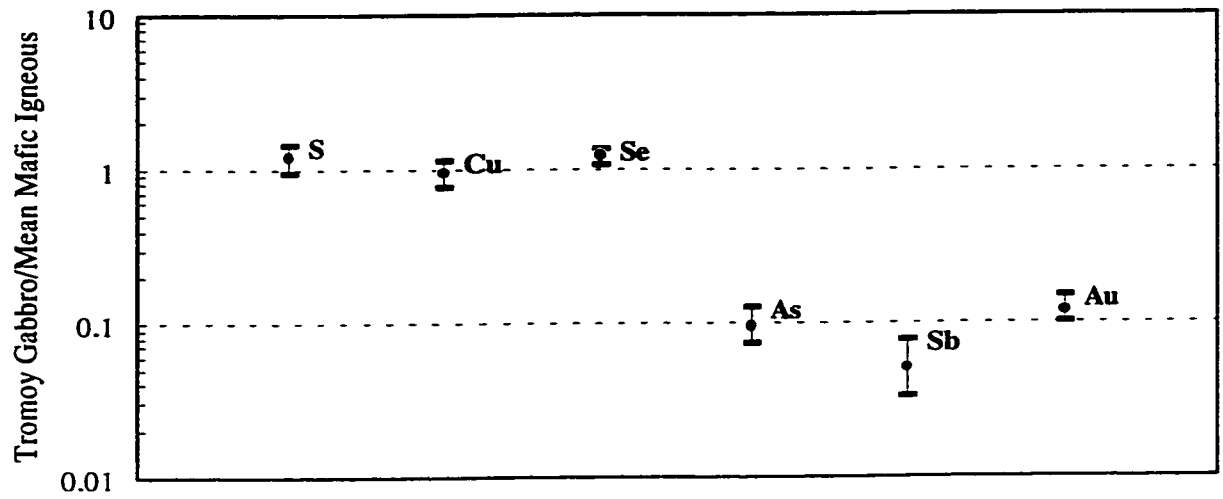

Figure 4-23. Distribution of chalcophile elements in Tromoy coronitic gabbro, normalized to the mean composition of mafic rocks. See Appendix 2-2 for normalization data.

4-2-5. Tvedestrand Hyperite and Amphibolite

The term "hyperite" here is applied to orthopyroxene-gabbros. The primary olivine is totally replaced by pyroxene ± hornblende, and magmatic textures are obscured by metamorphic recrystallization. One hyperite dyke with an exposed width of 22 meter was sampled from Tvedestrand in the transition zone B (sample series 4001-9).

4-2-5-A. Mineralogy

The central, least altered, part of the dyke is granoblastic to weakly foliated with orthopyroxene, clinopyroxene, plagioclase and hornblende as the main minerals. Accessory minerals include Fe-Ti oxides, sulfides, and apatite. Orthopyroxene occurs as relicts within clinopyroxene, as xenoblastic to sub-idioblastic grains, and as granular and triple-jointed crystals interstitial to plagioclase. The composition of the orthopyroxene has been determined to be of En_{34-36} (Cameron and Cogulu, unpublished data). Clinopyroxene occurs as large xenoblasts of igneous diallage, and as patches replacing orthopyroxene. Plagioclases are zoned, with spinel-rich cores and inclusion-free margins. A relict corona texture is shown by spinel symplectite.

The marginal rocks are strongly amphibolitized and foliated, with essential hornblende and andesine (An_{35-48}) in subequal proportions. Quartz, biotite, Fe-Ti oxides, apatite, and sulfides occur as accessory phases. Hornblende commonly occurs in aggregates of green to green-brown crystals. Little remnant pyroxene exists in a state of partial alteration within hornblende aggregates. Quartz occurs as interstitial, xenoblastic and irregular crystals, and as blebs within hornblende. Red-brown biotite occurs as laths or xenoblastic crystals, occasionally forming patches in hornblende. Chlorite and sericite may occur locally as secondary alteration products after hornblende and plagioclase. A visual estimate of the modal composition of the Tvedestrand hyperites and amphibolites is shown in Table 4-8.

Ilmenite is the dominant oxide in both hyperites and amphibolites, being accompanied by subordinate magnetite and hematite. Ilmenite and magnetite occur as discrete grains as well as exsolution lamellae and patches of one in the other. Hematite is common as exsolution lamellae within ilmenite in the amphibolites; it is not common in the hyperites.

Pyrrhotite, the dominant sulfide in the hyperites, is replaced by pyrite ± magnetite in the amphibolites. Both pyrite and pyrrhotite are equally associated with minor chalcopyrite and pentlandite. The replacement of pyrrhotite by pyrite ± magnetite occurred in response to oxidation of the enclosing rocks. A higher oxidation state for amphibolites is supported by higher ratio of $Fe^{+3}/Fe^{+3} + Fe^{+2}$ (0.32 vs. 0.26) and the common occurrence of hematite in ilmenite. Summary statistics for Tvedestrand hyperite-amphibolite dyke is shown in Table 4-9.

Table 4-8. Modal composition of Tvedestrand hyperite and amphibolite

	Hyperite (n = 5)	Amphibolite (n = 4)
Plagioclase	42	42
Orthopyroxene	15	1
Clinopyroxene	5	trace
Hornblende	35	50
Quartz	trace *	3
Biotite	trace	1
Apatite	trace	trace
Fe-Ti oxides	2	2
Sulfides	trace	trace

* less than 1%

Table 4-9. Summary statistics for Tvedestrand hyperites and amphibolites

	Hyperite (n = 5)			Amphibolite (n = 4)			Gresens	Gain and
	X	1 σ	C. V.	X	1 σ	C. V.	Xn Scores	Loss %
SiO_2	46.7	0.3	1.0	46.4	0.54	1.0	-0.31	-1.0
TiO_2	3.1	0.29	9.0	2.8	0.12	4.0	-0.30	-10
Al_2O_3	14	0.49	3.0	14.1	0.08	1.0	0.10	1.0
Fe_2O_3	4.2	0.7	17	5.2	0.56	11	1.00	24
FeO	12	0.31	3.0	10.9	0.34	3.0	-1.10	-9.0
$Fe_2O_3/(FeO+Fe_2O_3)$	0.26	0.03	0.1	0.32	0.03	1.0	0.06	24
MnO	0.26	0.02	8.0	0.25	0.01	5.0	-0.01	-4.0
MgO	5.7	0.23	4.0	5.9	0.16	3.0	0.40	7.0
CaO	9.0	0.14	2.0	9.3	0.23	2.0	0.30	3.0
Na_2O	2.9	0.08	3.0	2.8	0.2	7.0	-0.10	-4.0
K_2O	0.65	0.07	11	0.63	0.09	14	-0.02	-3.0
P_2O_5	0.36	0.02	6.0	0.33	0.05	15	-0.03	-8.0
H_2O	0.8	0.13	16	1.2	0.12	10	0.40	50
CO_2	0.12	0.05	40	0.12	0.1	77	0.00	0.0
Cr*	46	6.0	13	54	4.65	9.0	7.99	17
Ni	67	8.0	12	75	4.11	5.0	7.98	12
Co	54	2.0	4.0	54	1.0	2.0	-0.01	0.0
Sc	46	5.0	11	46	1.0	1.0	-0.01	0.0
V	305	30	10	302	10.0	3.0	-3.07	-1.0
Zn	175	31	18	168	10.0	6.0	-7.04	-4.0
Rb	11	3.0	28	14	9.27	66	3.00	27
Cs	0.8	0.12	15	0.9	0.22	25	0.10	13
Ba	194	13	7.0	202	39	19	7.95	4.0
Sr	143	12	9.0	140	6.0	4.0	-3.03	-2.0
Hf	6.0	0.5	9.0	6.0	0.8	14	0.00	0.0
Zr	195	13	7.0	175	26	15	-20	-10
Y	48	5.0	11	44	1.5	3.0	-4.01	-8.0
Th	1.1	0.18	16	0.9	0.18	20	-0.20	-18
U	0.4	0.05	13	0.4	0.1	23	0.00	0.0
Be	1.3	0.08	6.0	1.2	0.08	7.0	-0.10	-8.0
S	1095	220	24	1120	190	17	25	2.0
Cu	155	29	18	142	33	23	-13.04	-8.0
Se	0.19	0.06	31	0.19	0.06	30	0.00	0.0
As	1.7	0.6	35	1.53	0.62	40	-0.17	-10
Au (ppb)	0.58	0.21	36	0.36	0.08	21	-0.22	-38
Sb	0.28	0.15	53	0.31	0.14	44	0.03	11
La	13	2.5	19	12	0.5	4.0	-1.00	-8.0
Ce	27	1.4	5.0	26	3.0	12	-1.01	-4.0
Sm	6.4	0.84	13	6.1	0.14	2.0	-0.30	-5.0
Eu	2.25	0.5	22	1.75	0.5	29	-0.50	-22
Tb	2.1	0.22	11	1.8	0.14	8.0	-0.30	-14
Yb	5.0	0.96	18	5.0	0.0	0.0	0.00	0.0
Lu	0.8	0.08	10	0.8	0.08	10	0.00	0.0
F	392	34	9.0	477	88	18	85	22
Cl	2430	1050	43	3114	720	23	683	28
Br	15	9.0	62	12	4.0	37	-3.00	-20

X = arithmatic mean σ = standard deviation C.V. = coefficient of variation * elements in ppm (Au in ppb)

4-2-5-B. Mass Balance in Hyperite-Amphibolite Transition

The geochemistry of central (least altered) and marginal (most altered) parts of the Tvedestrand hyperite dyke are compared using the equation of Gresens (1967). The data are treated in the same manner already described for Laget. Intense amphibolitization and recrystallization has affected the whole body of the dyke, and even the least altered rocks contain considerable amounts of hornblende. Therefore, the comparison is between the least and the most altered fractions.

From modal compositions, specific gravities were calculated to be 3.056 and 3.024 for hyperites and amphibolites, respectively, corresponding to 1% decrease in mass unit. Alternatively, f_v (volume factor) was calculated to be 1.015, suggesting 1.5% increase in volume. Volume factor was estimated from the average of f_v's for Al_2O_3, SiO_2, CaO, MnO, and lithophile transition metals that tightly cluster around 1.015 ($1\sigma = 0.005$).

Results from mass balance calculations (Table 4-9) show no significant differences between the central and marginal rocks. Slight differences recorded for some elements (e.g. Ti, Cr, Ni, Au, Zr), may be attributed to initial magmatic variations, rather than a metasomatic overprint.

4-2-5-C. Magmatic or Metasomatic Nature of Chemical Variations

The Tvedestrand dyke is strongly hydrated and recrystallized. Whether the primary magmatic patterns survived the alteration is not clear. As an approach to the problem, the distribution of the elements commonly known as immobile in alteration and metamorphic processes are compared against Niggli Mg# as an index of fractionation (Figures 4-24-A-F).

Variations of elements in Figure 4-24 are mostly consistent with magmatic differentiation trends implying that the primary magmatic patterns are still preserved, at least for the less mobile elements. They further show that the Tvedestrand dyke, although small in size, is a differentiated body with higher concentration of incompatible elements in the center.

Tvedestrand intrusive crystallized from a highly fractionated magma. It is depleted in MgO, but enriched in $FeO_{(total)}$, compared to Laget and Tromoy gabbros. A comparison to the mean composition of the Laget coronitic gabbro (Figure 4-25) indicates that Tvedestrand dyke is depleted in compatible elements (Ni, Cr, Co), but enriched in incompatible elements (LILE, REE, and chalcophile elements). This can best be explained by a magmatic differentiation model. Most elements are equally distributed in the hyperites and amphibolites.

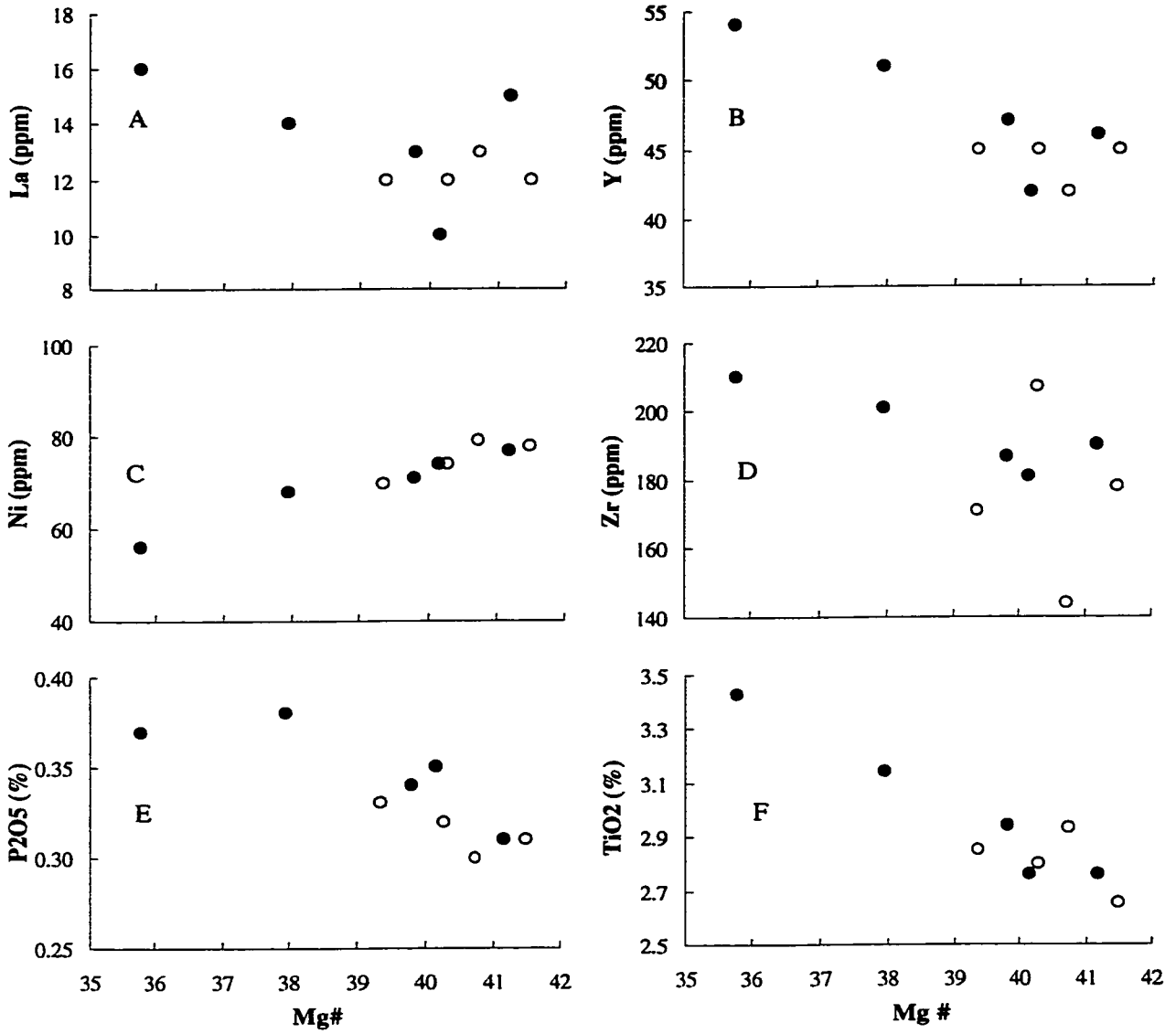

Figure 4-24. Distribution of elements with Mg# as differentiation index in Tvedestrand hyperites (solid circles) and amphibolites (open circles).

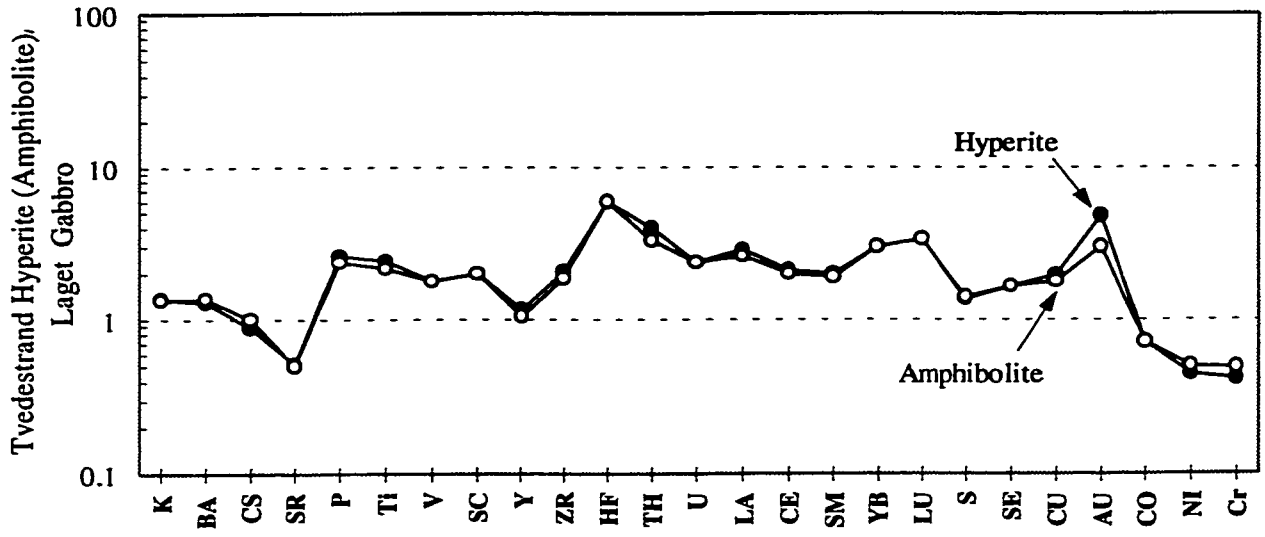

Figure 4-25. Distribution of elements in Tvedestrand hyperites and amphibolites, normalized to the mean composition of Laget intrusive.

In the absence of fresh, unaltered rocks, it is not known whether any alkaline metasomatism occurred. Potassium, Ba, Rb, and Cs are similarly distributed in the two rock types. However, the possibility that both rock types were equally effected by LILE metasomatism, can not be ruled out.

Chlorine and F are slightly enriched in the amphibolites (Table 4-9); Br is equally distributed in both rock types. Considering the significantly lower concentration of Cl in Laget and Tromoy coronitic gabbros, Tvedestrand dyke is probably influenced by Cl metasomatism.

4-2-5-D. Distribution of Chalcophile Elements

No significant enrichment or depletion in chalcophile elements occurred with hydration and recrystallization of the hyperites (Table 4-9). Slightly higher values in the hyperites can be attributed to magmatic differentiation processes. Oxidation and replacement of the primary magmatic pyrrhotite by pyrite + magnetite did not influence the initial abundance of Au.

Although containing considerably higher Au than Laget and Tromoy gabbros, the Tvedestrand dyke is still strongly depleted in this element compared to the mean mafic rocks; it is also depleted in Sb (Figure 4-26). Copper and Se are enriched.

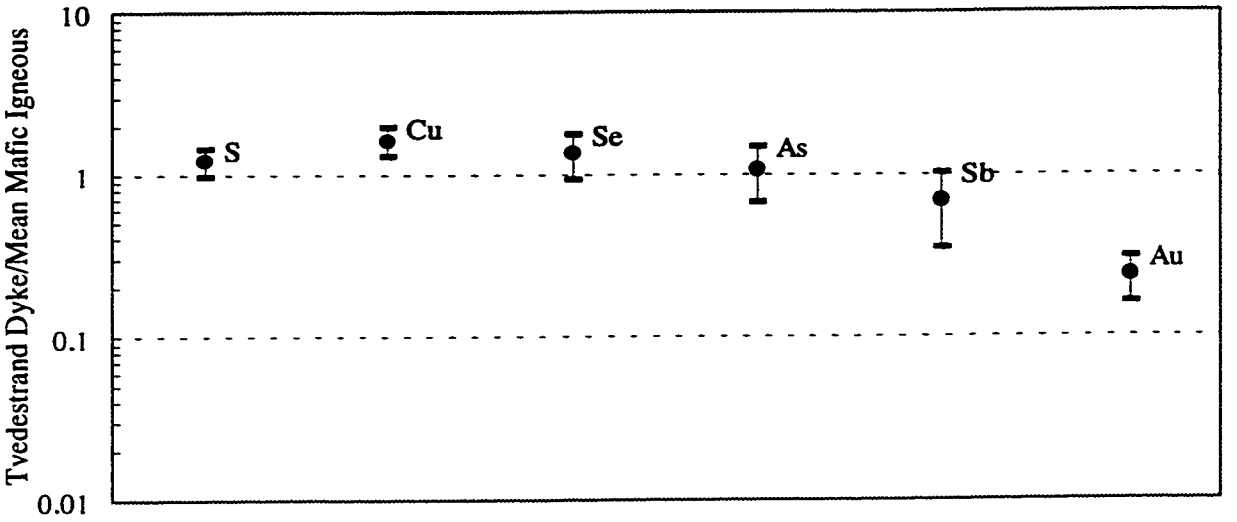

Figure 4-26. Distribution of chalcophile elements in Tvedestrand dyke, normalized to the mean composition of mafic rocks. Spheres represent the mean values and bars display 1σ standard deviation. See Appendix 2-2 for normalization data.

4-2-6. Tromoy Hyperite and Amphibolite Dyke-1

Two hyperite dykes, metamorphosed under hornblende-granulite facies, were sampled from Tromoy, sample series 5001-9 from dyke-1, and sample series 5101-4 from dyke-2. Amphibolitization has severely affected the whole body of the dykes; even the central, least altered parts contain considerable amounts of hornblende. The Tromoy dyke-1 is a relatively small body, with an exposed width of ~ 40 m.

4-2-6-A. Mineralogy

Considering the silicate mineralogy, two rock types are identified, one containing ortho-pyroxene (Opx) from the center (hyperite), and the other, Opx-free from the margin (amphibolite). Hyperites include plagioclase, hornblende, Opx, Cpx, and minor garnet and Fe-

Ti oxides. Amphibolites are essentially made of hornblende and plagioclase, with minor quartz, Cpx, and biotite; they lack sulfides and oxides. The absence of the metallic minerals does not seem to be a characteristic of the amphibolitized samples, as two Opx-bearing hyperites are also free of sulfides and oxides.

Pyrrhotite and pyrite are the dominant sulfide minerals commonly containing lamellae and patches of chalcopyrite and pentlandite. Pyrite may be accompanied by some magnetite. As in Laget and Tvedestrand, pyrite appears to be after pyrrhotite. Secondary, fracture filling pyrite is rare. Little marcasite occurs associated with pyrite, apparently replacing this mineral. A visual estimate of the modal composition of the two rock types is given in Table 4-10.

4-2-6-B. Geochemistry

Based on the whole rock geochemistry, four rock types can be distinguished: low Mg-hyperite, low-Fe hyperite, high-Mg amphibolite, and high-Al amphibolite (Table 4-11). The occurrence of the different facies in the same body may be attributed to:

1) Differentiation from a single parent magma;

2) Involvement of more than one magma pulse;

3) Variable post-solidus alteration.

Table 4-10. Modal composition of Tromoy hyperite and amphibolite Dyke-1

	Hyperite (n = 5)	Amphibolite (n = 4)
Plagioclase	45	45
Orthopyroxene	10	1
Clinopyroxene	2	trace
Hornblende	40	50
Garnet	2	o **
Quartz	trace *	3
Biotite	trace	1
Apatite	trace	trace
Fe-Ti oxides	1	trace
Sulfides	trace	o
Chlorite	trace	trace
Sericite	trace	trace

* less than 1% ** not found

Table 4-11. Summary statistics for Tromoy hyperite and amphibolite Dyke-1

	Low-Mg Hyperite(3)*		Low-Fe Hyperite(3)		High-Mg Amphibolite(2)		High-Al Amphibolite(1)
	X	1 σ	X	1 σ	X	1 σ	X
SiO_2	46.2	0.17	49.7	0.4	47.1	0.8	42.6
TiO_2	2.19	0.1	0.17	0.02	0.3	0.0	0.19
Al_2O_3	15.8	0.35	17.1	0.66	11.4	1.4	20.5
Fe_2O_3	3.2	0.06	1.5	0.35	2.8	0.3	2.0
FeO	11	0.17	5.7	0.15	7.8	0.4	6.6
MnO	0.22	0.01	0.17	0.01	0.2	0.0	0.22
MgO	7.0	0.18	9.9	0.33	15.2	0.1	10.46
CaO	9.0	0.14	11.9	0.18	10.6	0.5	9.45
Na_2O	3.1	0.1	2.2	0.06	1.4	0.1	1.3
K_2O	0.31	0.03	0.29	0.11	0.5	0.0	2.40
P_2O_5	0.23	0.01	0.01	0.0	0.015	0.0	0.02
H_2O	1.2	0.1	1.33	0.2	2.3	0.0	3.5
CO_2	0.10	0.0	0.07	0.06	0.0	0.0	0.00
Cr**	72	5.0	316	185	740	510	210
Ni	103	6.0	120	26	220	42.4	120
Co	76	2.0	51	2.0	73	1.4	55
Sc	36.0	5.0	35.0	2.0	35.5	10.6	27
V	236	15.0	120	17	150	14.1	110
Zn	133	6.0	86	9.0	125	7.1	110
S	1484	183	25	0.0	44	26	88
Cu	116	20	16	7.0	9.0	2.0	23
As	0.35	0.07	0.4	0.4	0.8	0.7	0.2
Se	0.19	0.03	0.027	0.01	0.02	0.0	0.02
Sb	0.08	0.02	0.027	0.01	0.045	0.01	0.05
Au (ppb)	1.18	0.57	1.50	1.7	0.215	0.01	0.14
Rb	23	0.6	31	13	43	2.8	116
Cs	0.25	0.0	0.25	0.0	0.3	0.0	3.0
Ba	123	23	83	16	60	22	130
Sr	198	5.0	248	25	69	0.0	133
Nb	3.0	2.6	<1	0.5	2.5	3.5	<1
Hf	1.0	0.0	0.5	0.0	0.5	0.0	0.5
Zr	176	8.0	33	1.0	32	0.7	31
Y	47	21	11	7.0	50	2.1	19
Th	0.4	0.12	0.1	0.0	0.5	0.3	0.3
U	0.3	0.1	0.1	0.0	0.3	0.0	0.1
La	7.6	0.6	2.0	1.7	4.0	0.0	1.0
Ce	12	1.5	2.0	0.0	5.0	1.0	2.0
Sm	5.50	0.36	0.90	0.34	3.5	0.2	0.60
Eu	2.0	1.0	0.5	0.0	0.5	0.0	0.5
Tb	1.70	0.12	0.25	0.0	0.8	0.1	0.25
Yb	3.3	0.6	1.0	0.0	1.5	0.7	1.0
Lu	0.5	0.06	0.1	0.0	0.3	0.1	0.1
F	312	11	124	50	341	49.5	653
Cl	263	50	406	520	1210	338	1288

X: arithmetic mean σ: standard deviation * number of samples ** elements in ppm; Au in ppb

4-2-6-C. Magmatic or Metasomatic Nature of Chemical Variations

As an approach to the problem of the origin of the variations, Harker diagrams have been constructed using Niggli Mg# as index of differentiation (Figure 4-27-A-J). Plots of data points reveal big compositional gaps among various rock facies. No consistent trends of variations can be inferred; while distribution of some elements is consistent with a magmatic differentiation trend, such a relation is rejected by other elements. This is clearly evident from variations of Ni and Co, as representatives of compatible elements, and Ce and Y, as representatives of incompatible elements (Figure 4-27-C-F).

Variations of Ce and Y follow a magmatic differentiation trend for low-Mg and low-Fe hyperites. However, variations of Ni and Co do not follow this trend. The high-Mg hyperites and high-Al amphibolite form separate groups and can not be matched with any other facies. The Tromoy Dyke-1 appears to be a composite dyke with multiple reopening and injections. Similar composite intrusions have been reported from Nelaug area, Bamble (de Haas, 1992).

Large ion lithophile elements, particularly K and Rb, seem to have been variably introduced into the amphibolites (Figure 4-27-A-B). The high-Al amphibolite is significantly enriched in K and Rb. This is supported by the common presence of secondary biotite occurring as laths cutting across other minerals. An enrichment in K and Rb is also displayed by high-Mg amphibolites. Amphibolites are also enriched in Cl.

4-2-6-D. Distribution of Chalcophile Elements

Distribution of chalcophile elements in various rock types can best be explained by a magmatic differentiation model (Figure 4-28-A-F). The low-Mg hyperites are enriched in all chalcophile elements compared to other facies. They are also considerably enriched in S, Cu, Se, and Au compared to other intrusions in the study area. This is corresponding to the relatively high Fe

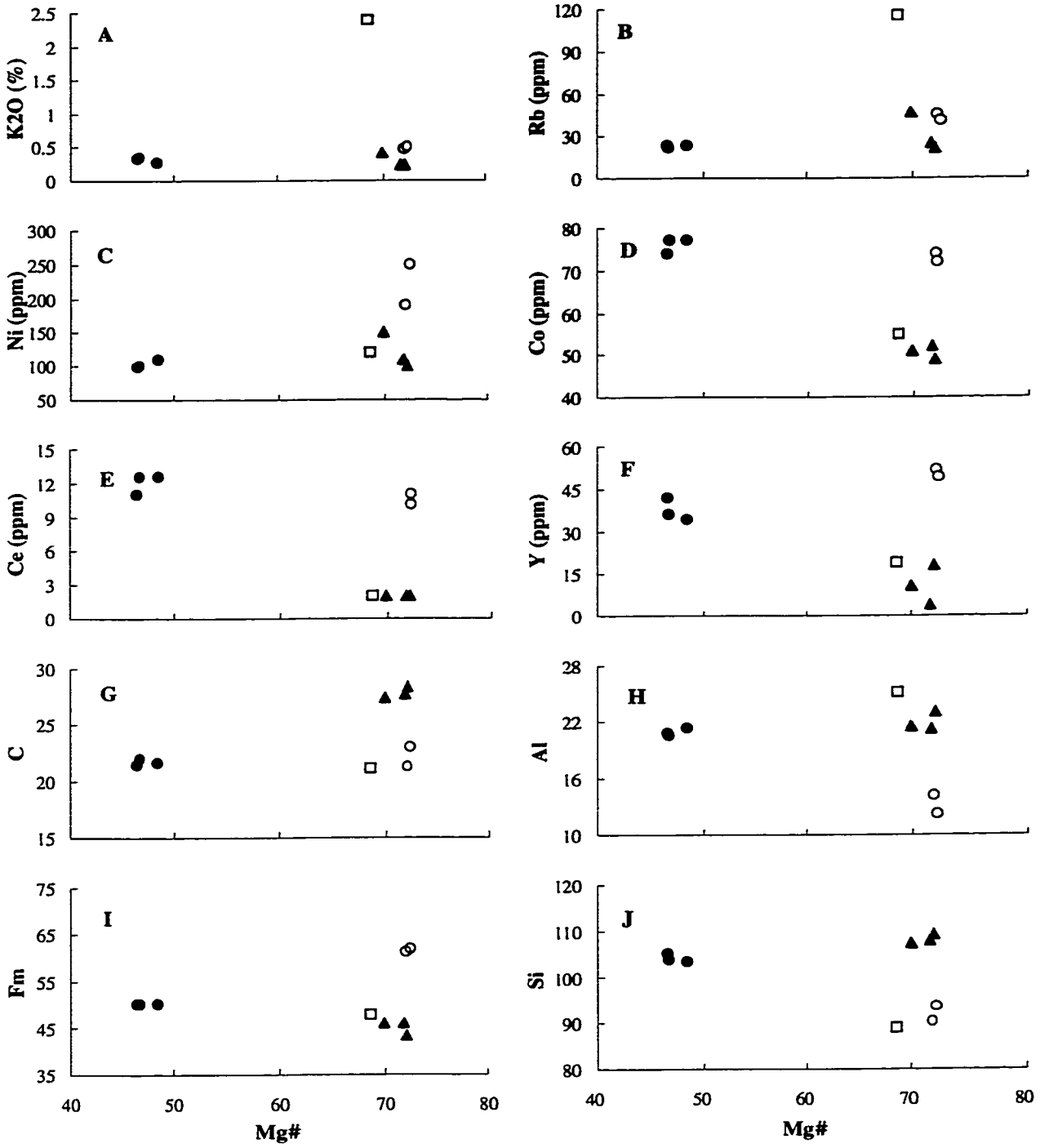

Figure 4-27. Plot of Niggli Fm, Si, C, and Al (G-H) and selected elements (A-F) with Mg# as differentiation index; Tromoy Dyke-1. Symbols represent:

● Low Mg hyperite ○ High Mg amphibolite ▲ Low Fe hyperite □ High Al amphibolite

in these rocks. Solubility of S is known to be strongly dependent on the FeO_t content of silicate melts (Haughton et al., 1974, Wendlandt, 1982). Copper, Se, and Au strongly partition into sulfides during magmatic crystallization.

Various facies are depleted in As, Sb, and Au compared to the mean composition of mafic rocks elsewhere (Figure 4-29). Only in the low-Mg hyperites, does Au come close to the general abundance of this element in mafic rocks. The low-Mg hyperites contain the highest of Fe, Ti, and S, and carry considerable amounts of Fe-Ti oxides and Fe-sulfides. Other rock types lack these minerals.

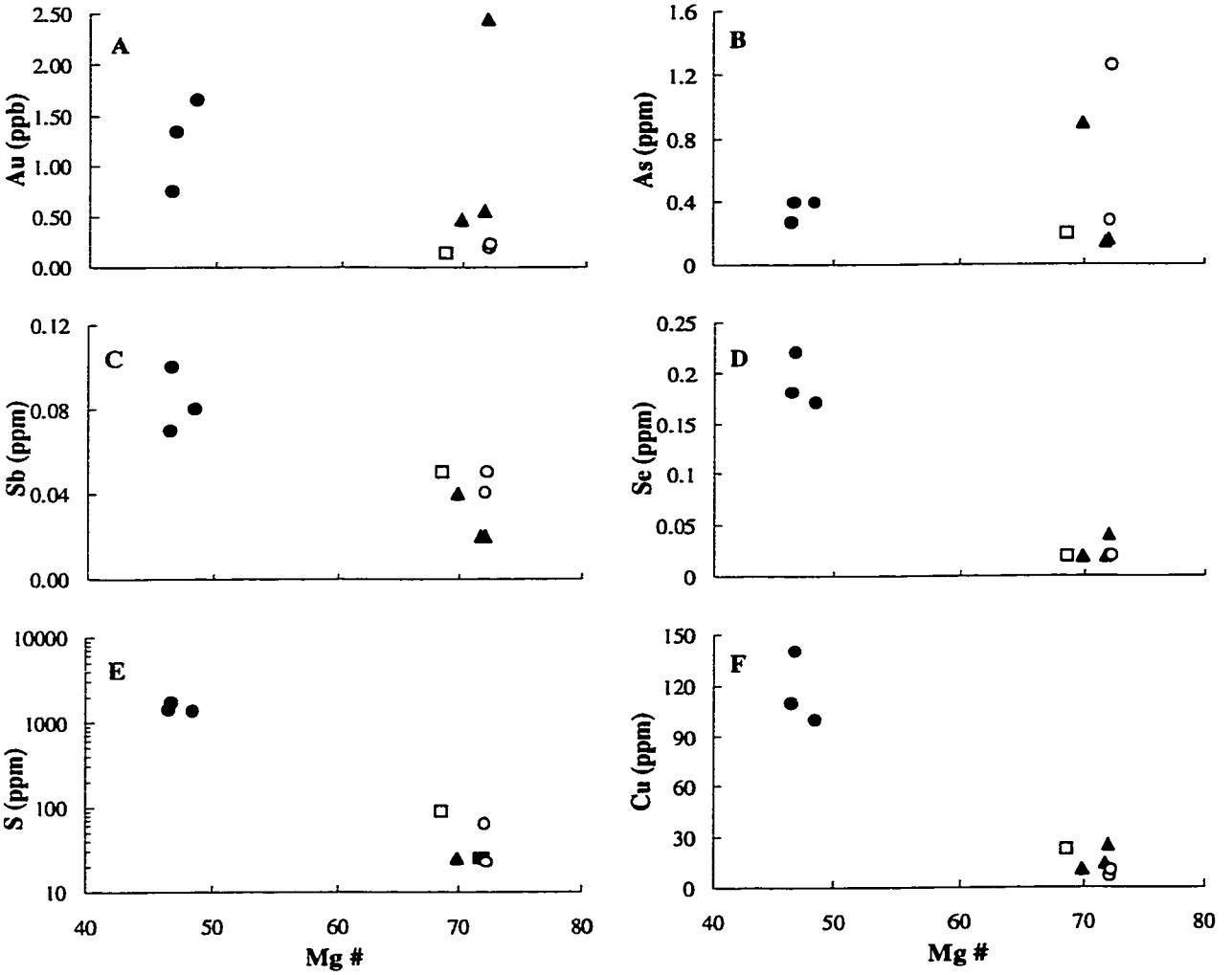

Figure 4-28. Variations of chalcophile elements with Niggli Mg# as differentiation index; Tromoy Dyke-1. Symbols as in Figure 3-4-16.

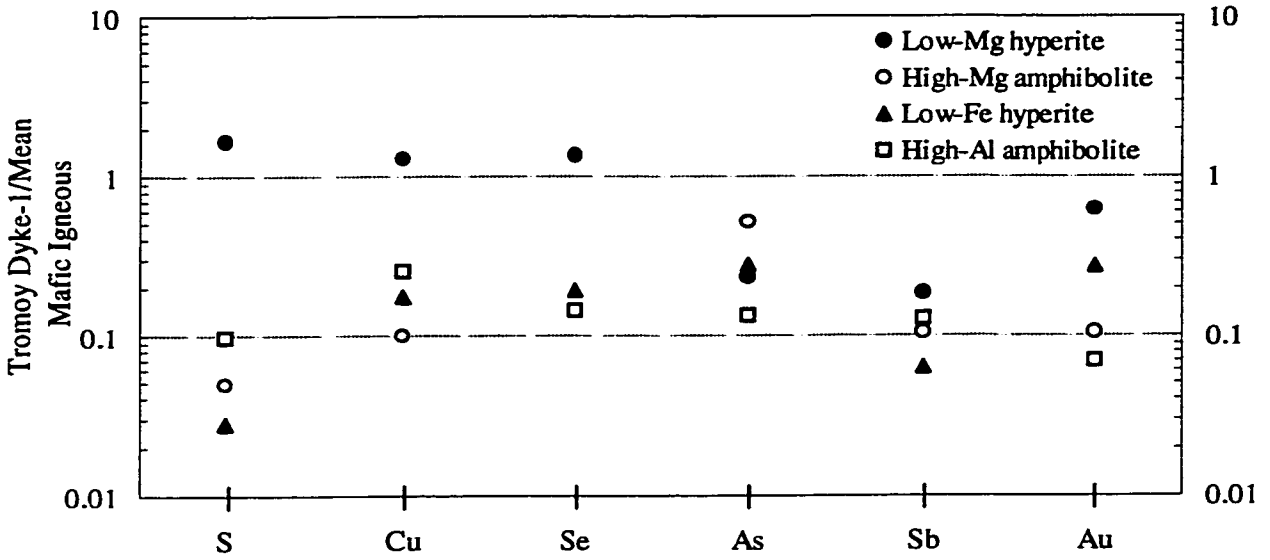

Figure 4-29. Distribution of chalcophile elements in Tromoy hyperite and amphibolite Dyke-1, normalized to the mean composition of mafic igneous rocks. See Appendix 2-2 for normalization data.

4-2-7. Tromoy Hyperite and Amphibolite Dyke-2

From a second dyke in Tromoy, with an exposed width of 15 m, four samples were collected, one from the central, least altered part (5104), and three from the amphibolitized margin (5101-1- 3). As in the Dyke-1, extensive hydration and recrystallization has obscured the primary mineralogy and texture.

4-2-7-A. Mineralogy

The least altered rock (hyperite) is characterized by the presence of pyroxenes and garnet. The altered rocks (amphibolites) are essentially composed of hornblende and plagioclase. They are further distinguished by the occurrence of secondary biotite as laths cutting across other minerals, particularly hornblende. Oxides include ilmenite and magnetite. Minor hematite occurs as exsolution lamellae within ilmenite in the amphibolites. A visual estimate of the modal composition of the Tromoy hyperite dyke-2 is shown in Table 4-12.

Trace sulfides (< 0.5% by mode) occur in both hyperite and amphibolites. As in other mafic bodies, sulfide paragenesis includes pyrrhotite, pyrite, chalcopyrite and pentlandite. Pyrrhotite,

the dominant sulfide in the hyperite, is replaced by pyrite ± magnetite in the amphibolites. Both pyrrhotite and pyrite are commonly accompanied by lamellae and patches of chalcopyrite and pentlandite. Summary statistics for Tromoy dyke-2 is shown in Table 4-13.

4-2-7-B. Mass Balance

Considering the small number of samples, and the fact that the single sample from the central part of the dyke is also strongly amphibolitized, gain or loss of elements during hydration and recrystallization is difficult to assess. In the absence of the primary unaltered rocks, a comparison is made to the mean composition of Tromoy gabbro (Table 4-13, Figure 4-30).

The whole rock geochemistry of the Tromoy Dyke-2 is comparable to that of the Tromoy gabbro, a notable difference being enrichment of LILE, particularly in Cs, U, and Th, in the latter. Introduction of LILE is strongly supported by the marked enrichment of the elements in the amphibolites relative to the hyperite (Figure 4-30). This is consistent with the common occurrence of secondary biotite in the amphibolites. The amphibolites are also considerably enriched in Cl (Table 4-13) implying that the LILE were transported in halide complexes.

Table 4-12. Modal composition of Tromoy hyperite and amphibolite Dyke-2

	Hyperite (n=1)	Amphibolite (n=3)
Plagioclcase	40	40
Orthopyroxene	8	0
Clinopyroxene	7	0
Hornblende	40	55
Garnet	4	o
Quartz	o *	o
Biotite	trace **	3
Apatite	trace	trace
Fe-Ti oxides	1	1
Sulfides	trace	trace

* not found ** less than 1%

Table 4-13. Summary statistics for Tromoy Dyke-2. Mean Tromoy gabbro shown for comparison

	Hyperite (n=1)	Amphibolite (n = 3)			Tromoy Gabbro
	X	X	1 σ	C. V.	X
SiO_2	46.5	47.0	0.7	1.0	48.2
TiO_2	1.63	1.5	0.1	7.0	1.4
Al_2O_3	16.7	16.0	0.2	1.0	16.0
Fe_2O_3	2.9	3.2	0.3	9.0	2.6
FeO	10.1	9.2	0.2	2.0	9.2
$Fe_2O_3/(FeO+Fe_2O_3)$	0.22	0.26	0.02	8.0	0.22
MnO	0.18	0.22	0.01	5.0	0.2
MgO	7.76	7.82	0.24	3.0	7.9
CaO	9.87	8.20	0.45	5.0	10.4
Na_2O	3.0	3.0	0.2	7.0	2.8
K_2O	0.31	1.05	0.09	9.0	0.25
P_2O_5	0.17	0.15	0.01	7.0	0.12
H_2O	1.3	1.9	0.0	0.0	0.5
CO_2	0.40	0.17	0.11	65	0.05
Cr*	110	113	15	13	198
Ni	120	140	10	7.0	120
Co	72	69	3.0	4.0	75
Sc	29.5	30.0	1.6	5.0	40
V	210	220	10	5.0	238
Zn	78	140	17	12	106
S	700	760	260	34	1070
Cu	74	77	15	19	86
As	nd	2.9	0.25	9.0	0.145
Se	nd	0.14	0.03	21	0.17
Sb	nd	0.17	0.02	12	0.023
Au (ppb)	nd	0.38	0.09	24	0.24
Rb	19	48	0.0	0.0	26
Cs	1.10	1.32	1.30	98	0.6
Ba	84	130	35	27	90
Sr	207	245	35	14	200
Nb	11	11	4.0	36	1.0
Hf	2.0	1.3	0.7	58	0.9
Zr	103	123	4.0	3.0	105
Y	34	76	4.0	5.0	56
Th	0.4	1.1	0.5	45	0.3
U	0.4	0.7	0.5	71	0.2
La	5.0	7.0	0.6	9	4.9
Ce	12.50	14.2	2	67	7.7
Sm	4.10	4.8	0.9	19	3.7
Eu	1.0	1.2	0.8	67	0.7
Tb	1.40	1.1	0.3	30	1.2
Yb	4.0	3.3	0.5	15	2.1
Lu	0.3	0.5	0.1	20	0.4
F	nd	294	28	10	200
Cl	nd	810	140	17	50
Be	0.7	1.0	0.2	20	0.5

x: arithmetic mean σ: standard deviation CV: coefficient of variation nd: not determined *: elements in ppm

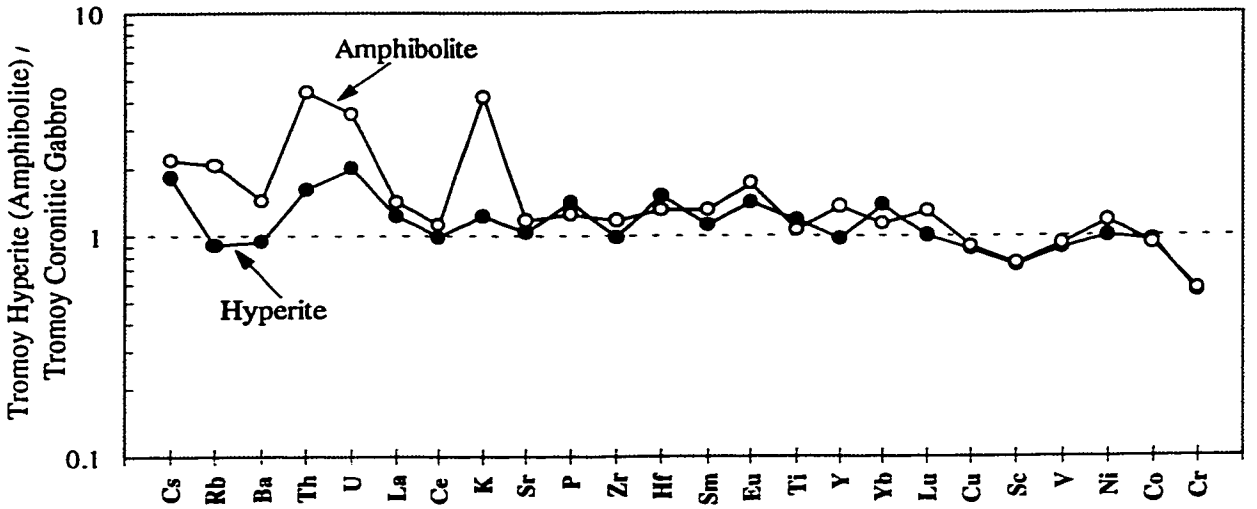

Figure 4-30. Distribution of elements in Tromoy Dyke-2 hyperite and amphibolite, normalized to the mean composition of Tromoy coronitic gabbro.

Considering the mineralogy and modal composition of the hyperite and amphibolites, the two rock types are comparable in specific gravity and volume, requiring no significant correction for mass or volume effect. Accordingly, mass balance calculation would yield the same results as shown in Figure 4-30: considerable enrichment of LILE in the amphibolites.

Addition of K_2O into the amphibolites (1.05 vs 0.31 wt%) is probably balanced by a decrease in CaO (8.25 vs 9.85 wt%). The amphibolites further display a more oxidized mineral assemblage. This is reflected by a higher score for $Fe_2O_3/FeO + Fe_2O_3$ (0.26 vs. 0.22), occurrence of hematite lamellae in ilmenite, and replacement of pyrrhotite by pyrite.

4-2-7-3. Distribution of Chalcophile Elements

Sulfur and Cu are equally distributed in both hyperite and amphibolites. No data is available for other elements in the single hyperite sample. Compared to the mean composition of Tromoy gabbro, the amphibolites are enriched in As and Sb, and marginally enriched in Au (Table 4-13). Sulfur, Cu, and Se are in the same range as in the Tromoy gabbro. In the absence of data on the single hyperite sample, it is not known whether the higher contents of

As and Sb are of primary magmatic, or of metasomatic origin. Analysis of pyrite and pyrrhotite concentrates from hyperite and amphibolites disclosed no significant differences in the abundances of the chalcophile elements. This is discussed in Section 4-4.

The Tromoy amphibolites are considerably depleted in Au compared to the mean composition of mafic rocks (Figure 4-31). They are also depleted in Sb. Sulfur, Cu, and Se are in the same range as in the mean mafic rocks. Arsenic is enriched.

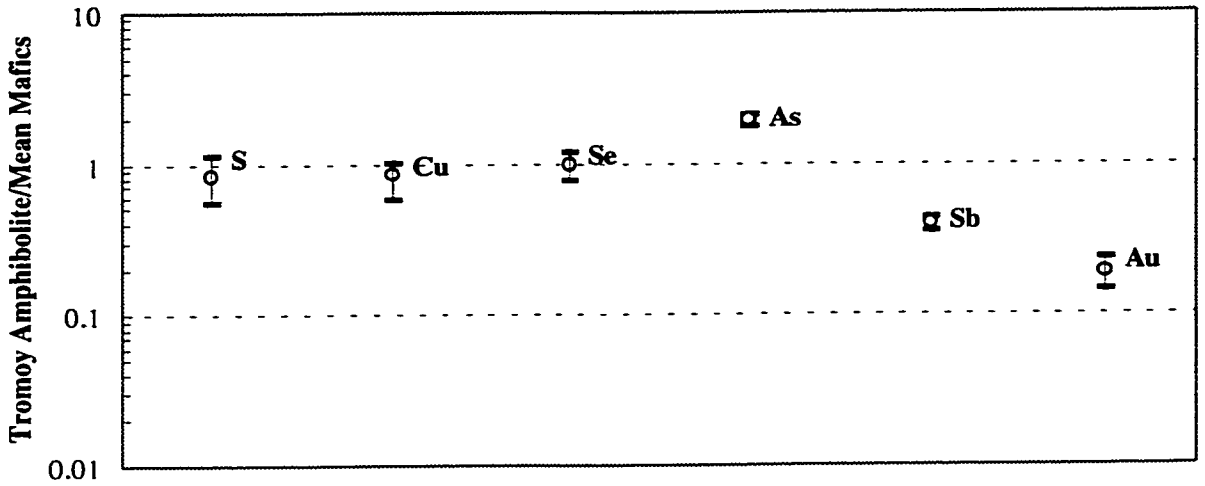

Figure 4-31. Distribution of chalcophile elements in Tromoy Dyke-2 hyperite and amphibolite, normalized to the mean composition of mafic rocks. The circles represent the mean values and the bars show 1σ standard deviation. See Appendix 2-2 for normalization data.

4-2-8. Tectonic Setting

On Jensen oxide diagram (Jensen, 1976), most samples plot in the tholeiitic field (Figure 4-32). This is in agreement with earlier studies on Sveconorwegian mafic magmatism in Bamble (c.f. Touret, 1969; Starmer, 1985, Smalley and Field, 1991; de Haas, 1992) and elsewhere in SWSD (Atkin and Brewer, 1990; Zeck and Wiladsen, 1990; Munz et al., 1994; Waque, 1996). The samples range in composition from high-Fe tholeiitic basalt (HFTB) to high-Mg tholeiitic basalt (HMTB).

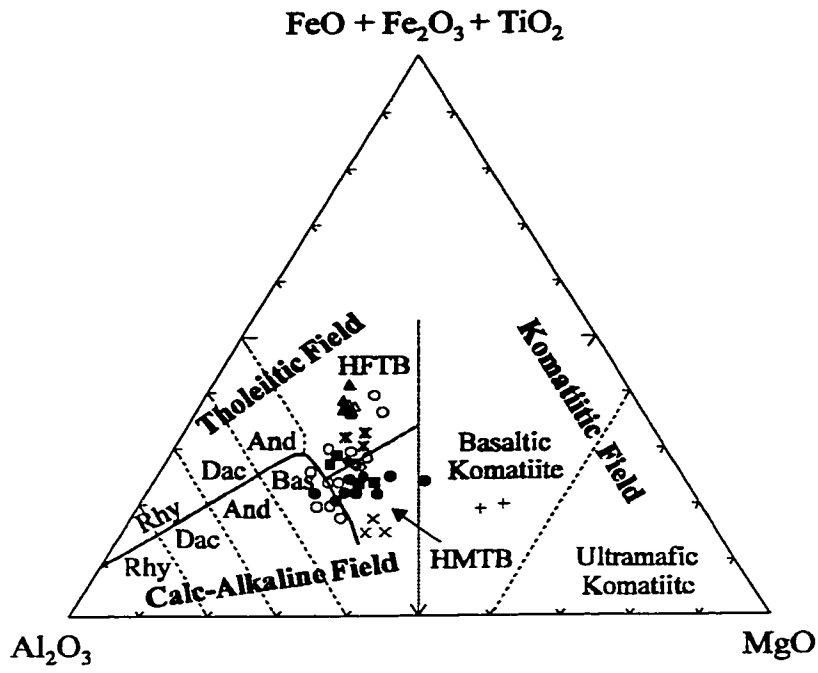

Figure 4-32. Plot of gabbros (hyperites) and amphibolites on Jensen oxide plot. HFTB: High-Fe Tholeiitic Basalt; HMTB: High-Fe Tholeiitic Basalt. Symbols represent:

Tvedestrand:	▲ Hyperite	△ Amphibolite	
Tromoy Gabbro	■		
Tromoy Dyke-1:	✱ Low-Mg Hyperite	+ High-Mg Amphibolite	× Low-Fe Hyperite
Tromoy Dyke-2:	◆ Hyperite	◇ Amphibolite	
Laget:	● Coronitic gabbro	○ Amphibolite	

MORB-normalized plots for elements in the mafic rocks provide further information on the nature of the magmatism (Figure 4-33). The main features of the Bamble gabbros (hyperites) are:

- Large ion lithophile elements (LILE) and light rare earth elements (LREE) are variably enriched relative to MORB. Enrichment in LREE is a common feature among continental tholeiites (Norrey and Fitton, 1982; Pearce, 1982, 1983; Dupuy and Dostal, 1984). A continental setting for Sveconorwegian mafic magmatism in southern Norway has been proposed by several authors (e.g. Starmer, 1985, 1990; Atkin and Brewer, 1990; Zeck and Willadsen, 1990; Smalley and Field, 1991).
- LILE are considerably enriched compared to HFSE and REE.
- Most mafic bodies show low Th abundance relative to other LILE, and distinct Nb troughs.

The above features are characteristic of tholeiitic basalts produced in continental arc settings at destructive plate margins (c.f. Wood et al., 1979, 1981; Pearce, 1982; Kay, 1984, Holm, 1985; McCulloch and Gamble, 1991). A subduction-related origin is further supported by Ba/Nb ratios, as most samples have Ba/Nb ratios in excess of 25 (c.f. Hawksworth et al., 1983). A destructive margin setting for the mafic bodies has also been proposed by Smalley and Field (1991), and de Haas (1992). The Bamble gabbros (hyperites) are broadly contemporaneous with alkaline mafic magmatism in southern Norway, central Scandinavia, southern Greenland, and North America. Earlier they were interpreted as expression of anorogenic or tensional tectonic regimes (Patcehtt et al., 1978; Milne and Starmer, 1982; Starmer, 1985).

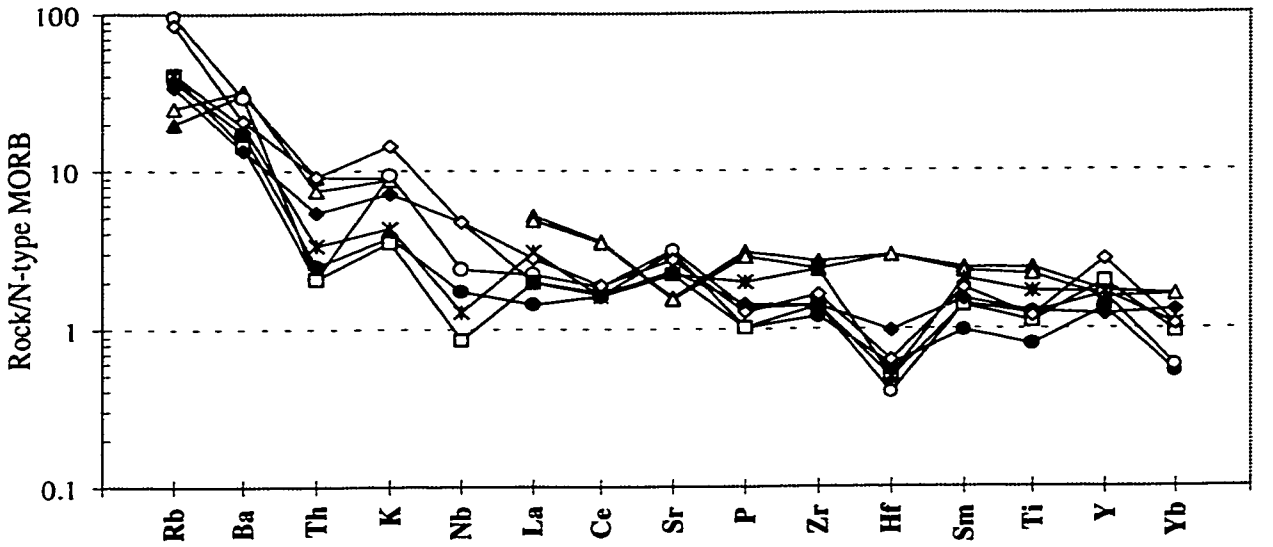

Figure 4-33. MORB-normalized spidergram for elements in gabbros and hyperites, and their amphibolitized equivalents. Normalization data after Sun and McDonough (1989). Symbols as in Figure 4-32.

4-2-9. Source of the Fluids in Gabbro-Amphibolite Transition

The transformation of the marginal parts of the mafic intrusives into amphibolites and garnet-amphibolites required the introduction of considerable amounts of aqueous fluids. Mass balance calculations indicate that halogens, particularly Cl, and LILE, notably K, Rb, and Ba,

were introduced into the amphibolites. The hydration and metasomatism was balanced by removal of ions and increase in volume. There is evidence for removal of Ca from amphibolites.

Infiltration of aqueous fluids into deep ductile shear zones, and retrograde reactions, have been documented from many metamorphic terrains. Examples include: Lewisian Complex, Scotland (Drury, 1974; Holland and Lambert, 1975); Pyrenees, France (McCaig, 1984); Mount Helene, Wyoming (Hulsebosch and Frost, 1989); Storø and Stromfjord, East Greenland (Glassley and Bridgewater, 1985); and southern Norway (Starmer, 1969; Verdonk et al., 1986; Brickwood and Craig, 1987; Cameron, 1989a, b; de Haas, 1992; Munz, 1990).

Different sources have been proposed for the fluids. Drury (1974) envisages a dehydrating source region (a contemporaneous area of high grade metamorphism) for the fluids involved in the retrograde reactions in the Lewisian Complex, Scotland. Holland and Lambert (1975) showed that the source of H_2O and CO_2 in the reactions was a fluid in equilibrium with granulite. According to the authors, the release of stored stresses during uplift would free the H_2O-CO_2 fluids leading to retrograde reactions in shear zones. Similarly, Bridgwater (1979) proposed that the source of the fluids and solutes introduced into the Storø and Stromfjord ductile shear zones, East Greenland, were the underlying granulite facies terrains which liberated fluids during dehydration. Source of the fluids in retrograde reactions in Pyrenees was related to the underthrusting of materials beneath the shear zone (McCaig, 1984).

Starmer (1969) proposed that the fluids responsible for gabbro-amphibolite transition in Bamble originated from granitic pegmatites that presumably migrated along the same structures already employed by the mafic intrusives. Verdonk et al. (1986) proposed an underlying magma source for the fluids. A pegmatitic source has been criticized by Field and Elliot (1974) based on the field observations and the timing of amphibolitization and granitic intrusions in Bamble.

Country rocks have been considered as possible sources of fluids and solutes in retrograde reactions, particularly when igneous intrusion is involved (Brickwood and Craig, 1987; Verdonk et al., 1986; Munz, 1990; de Haas, 1992). According to the authors, the injection of large volumes of magmas generates high heat flows around the margins of the intrusions, promoting influx of brines from the surrounding rocks into the cooling rocks.

Munz (1990) reported extensive fluid circulation around gabbros in Modum Complex, Kongsberg, with the production of bimodal orthoamphibole-cordierite rocks and talc-kyanite schists (white-schists) in contact zones between gabbros and supracrustal rocks. The contact zones are also characterized by extensive vein and dyke network of albite, scapolite, and calcite. Strontium and Nd isotopic signatures of albite and calcite from the altered gabbros and metasediments in Modum Complex suggest a crustal source for the fluids (Munz et al., 1994).

One mole of H_2O is required to produce one mole of hornblende. Accordingly, hydration of a gabbro to amphibolite with 50% hornblende would require a volume of H_2O that, at 650°C and 5 kbar, is approximately 2 times the rock volume (Hulsebosch and Frost, 1989). The authors showed that fluid volumes on the order of 2 times rock volume infiltrated the Mt. Helene shear zone and were nearly in chemical equilibrium with country rocks.

Unlike at Mt Helene shear zone and Lewisian Complex, the retrogressive re-equilibration at Bamble occurred under limited and only locally high p_{H2O}. Hydration and recrystallization at Bamble is restricted to the marginal parts of the mafic intrusives. Variable enrichment and depletion of elements from one place to the other suggests that the mafic rocks did not all equilibrate with a single pervasive fluid. The composition of the fluids and their dissolved ions were controlled principally by local host rocks. A country rock source is supported by the fact that hydration is less extensive in gabbros intruded into the dry, granulite grade hostrocks. The Cl-rich nature of the fluids suggests that K, Rb, and Ba were most likely carried in halide complexes (c.f. Henley, 1984).

4-2-10. Discussion

Mafic intrusive bodies, traditionally known as hyperites, are widespread in Bamble and elsewhere in South West Scandinavian Domain (SWSD). The intrusive series varies from subordinate ultramafic rocks, through troctolitic gabbro, olivine ferrogabbro, and olivine-free gabbros and norites. The intrusion age has been determined by different methods to be in the range 1150 ± 100 Ma, corresponding to Sveconorwegian Orogeny. The mafic intrusives are tholeiitic in nature and bear features characteristic of continental basalts emplaced at destructive plate margins.

After differentiation and emplacement, some of the mafic bodies underwent post-solidus alteration under a prolonged high pressure and temperature. Corona growth around ferromagnesian minerals and metamorphism converted the rocks into coronitic gabbro and amphibolite. Hydration and recrystallization is most profound at the margins, but locally also in the cores. It is more extensive in the intrusions emplaced into the amphibolite-facies country rocks. Considered in three dimensions, most bodies have a dominantly coronitic core which passes outwards into an amphibolitized margin.

Amphibolitization of gabbros was associated with introduction, removal, and local remobilization and reprecipitation of elements. While LILE, notably K, Ba, and Rb, and halogens, particularly Cl, were introduced into the altered rocks, CaO was removed. Chlorine metasomatism locally led to the scapolitization of both gabbros and amphibolites. Chalcophile elements remained constant or were locally remobilized and reprecipitated. No net removal or addition of chacophile elements occurred.

Fluids and solutes involved in the gabbro-amphibolite transition originated from the country rocks. The injection of large volumes of mafic magmas into the metasedimentary and granitic gneisses generated high heat flows around the margins of the intrusions and promoted influx of brines from the surrounding rocks into the cooling crystallisates (c.f. Brickwood, 1984, 1986; Brickwood and Craig, 1987; Verdonk et al., 1986; Munz, 1990; de Haas, 1992).

Plots of the elements commonly known as the least mobile in alteration and metamorphism against Niggli Mg# as differentiation index follow typical magmatic differentiation trends, both within individual bodies and in a regional scale (Figure 4-34). Phosphorous, Ti, Ni, Ce, Zr, and V are considered amongst the least mobile elements in metamorphic and alteration processes (e.g. Pearce and Cann, 1973; Floyd and Winchester, 1975; Pearce et al., 1984). Trends of variations in Figure 4-34 further suggest that the mafic intrusives belong to a regional fractionation trend and possibly originated from the same source.

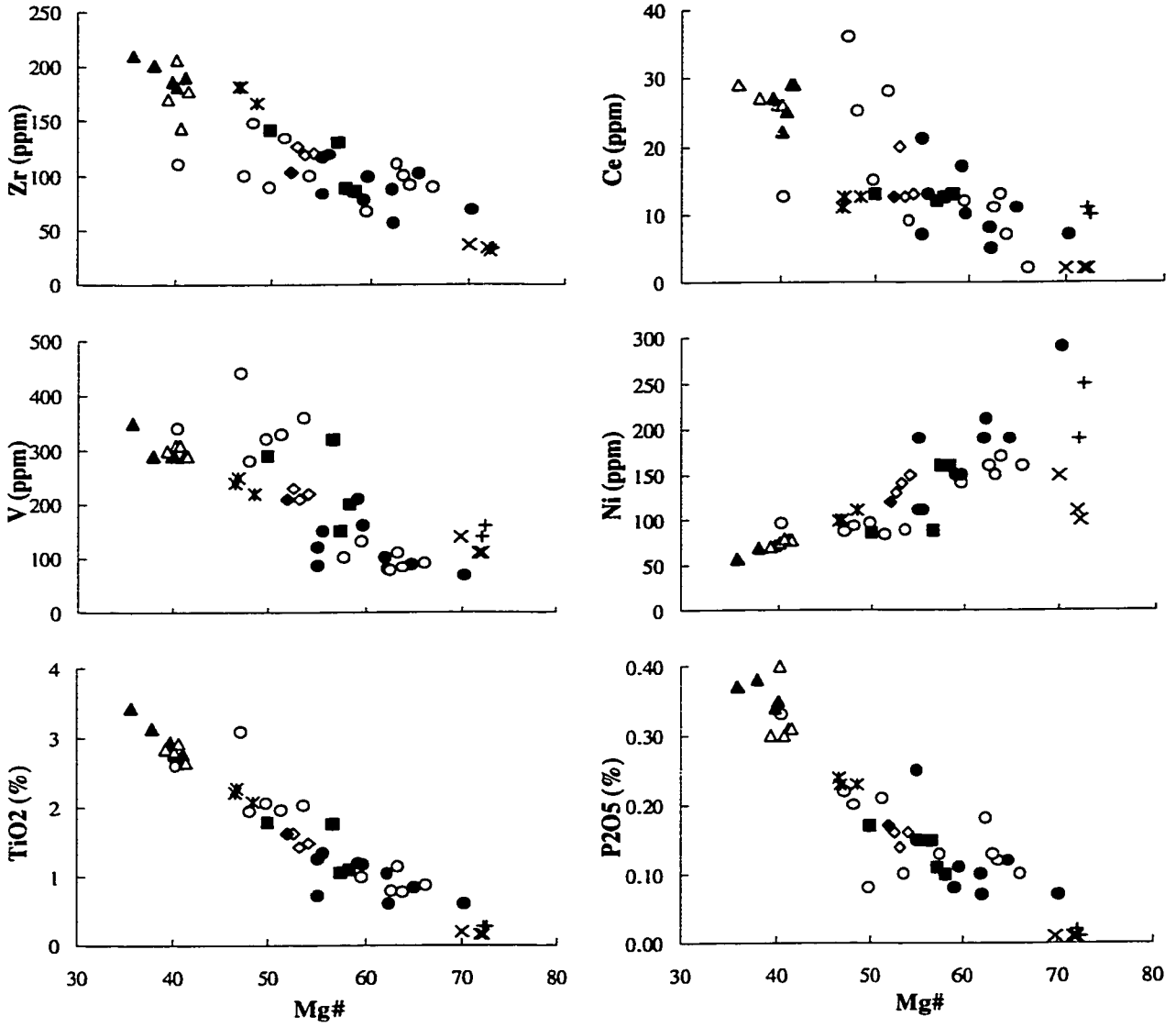

Figure 4-34. Distribution of elements (oxides) against Niggli Mg# as differentiation index; Bamble gabbros (hyperites) and amphibolites. Symbols as in Figure 4-32.

For large ion lithophile elements (LILE), the primary magmatic patterns are variably disturbed (Figure 4-35). Potassium, Rb, Cs, and Ba exhibit large scatters, all considerably enriched in the amphibolites (Figure 4-35-C-F). Uranium and Th show no significant enrichment or depletion (Figure 4-35-A-B). The relatively large scatter of plots for U and Th might be attributed to analytical error at low concentrations, as U and Th in many samples are at or below the detection limit of 0.1 ppm.

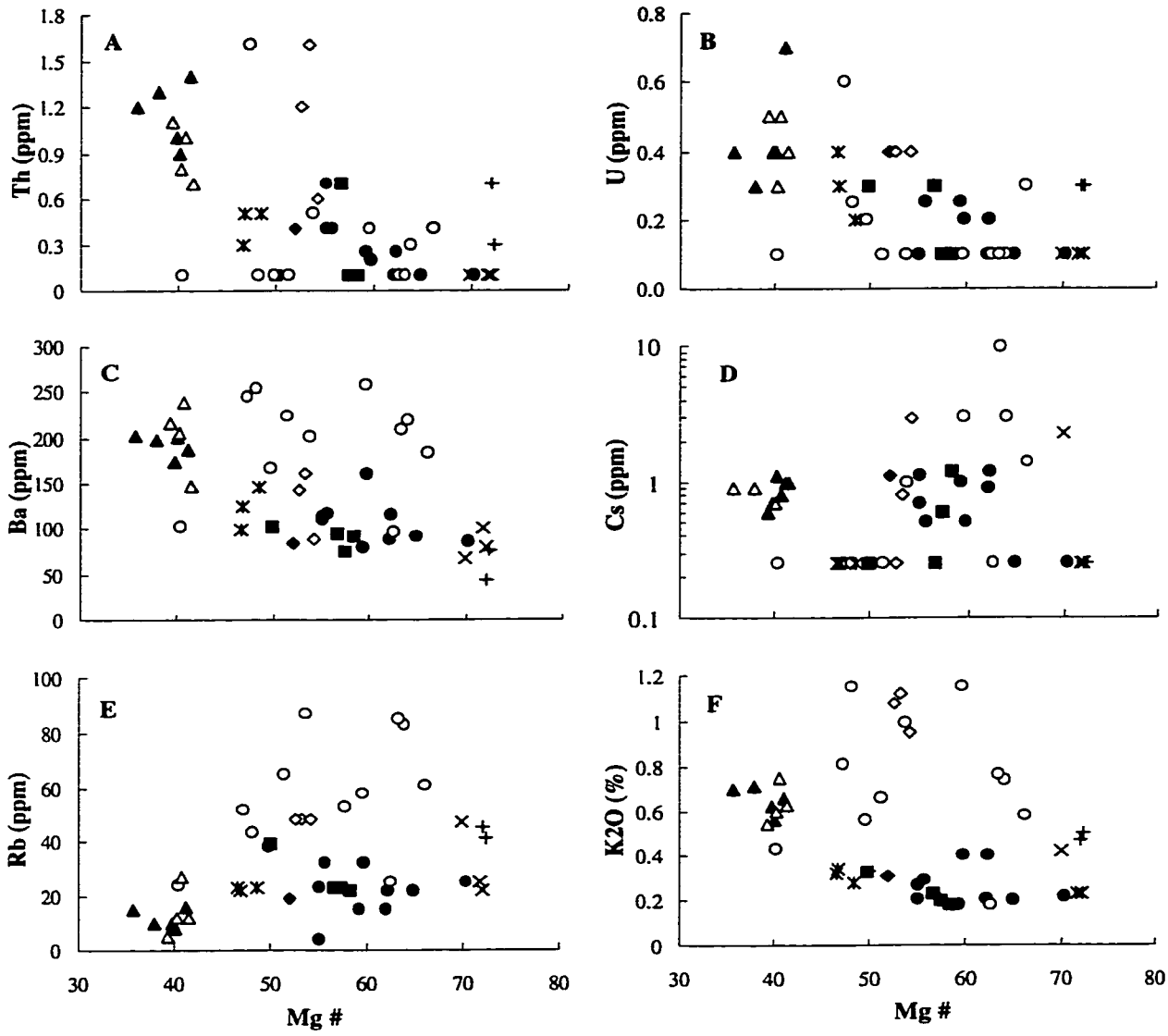

Figure 4-35. Plot of LILE against Niggli Mg# as differentiation index; Bamble gabbros (hyperites) and amphibolites. Symbols as in Figure 4-32.

Halogens behave incompatibly during crystallization of mafic magmas. Distribution of F follows a typical magmatic fractionation trend (Figure 4-36-A). Chlorine, however, is clearly enriched in the amphibolites (Figure 4-36-B). Bromine is slightly enriched in the Laget amphibolites.

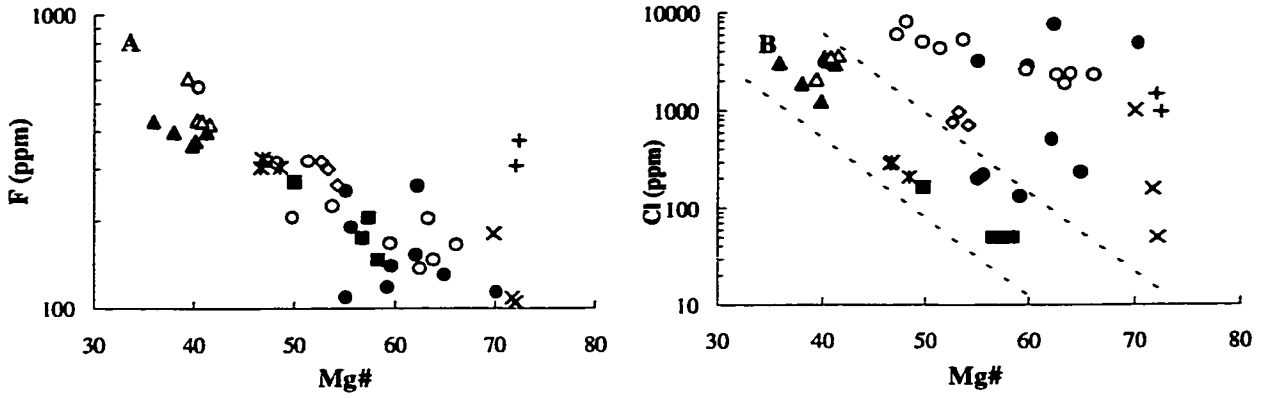

Figure 4-36. Distribution of halogens, fluor (A) and chlorine (B) against Niggli Mg# as differentiation index; Bamble gabbros (hyperites) and amphibolites. Parallel broken lines in B show the inferred range of Cl^- in the least altered rocks. Symbols as in Figure 4-32.

Variations of chalcophile elements follow typical magmatic fractionation trends implying that initial magmatic patterns survived alteration and metamorphism (Figure 4-37-A-F). Chalcophile elements behave incompatibly during differentiation of mafic magmas, being increasingly concentrated in the late fractionates (e.g. Hamlyn et al., 1985; Naldrett and Barnes, 1986; Brügman et al., 1987; Noll et al., 1996). The relatively large scatters displayed by As and Sb might be of primary origin. Both As and Sb also have a lithophile tendency and substitute for Si^{+4}, Al^{+3}, Fe^{+3}, and Ti^{+4} in rock-forming minerals (Esson et al., 1965; Bauer and Onishi, 1974; Boyle and Jonasson, 1985). Alternatively, it might be attributed to variable mobilization and reprecipitation of the elements during hydration and recrystallization of gabbros (hyperites).

The abundances of S, Cu, Se, and As are in the same common range as in mafic igneous rocks elsewhere; Au and Sb, however, are depleted (Figure 4-38). Only in Tvedestrand, the most fractionated of all intrusives, do Au and Sb come close to the mean mafic rocks.

Coronitic gabbros and hyperites are characterized by the presence of primary pyrrhotite as the main sulfide phase. The amphibolitized rocks, however, show varying degrees of replacement of pyrrhotite by pyrite ± magnetite, proportional to the magnitude of hydration and recrystallization. This suggests an external buffering for the sulfide phase change, probably by the same fluids involved in the amphibolitization (c.f. Cameron, 1989b).

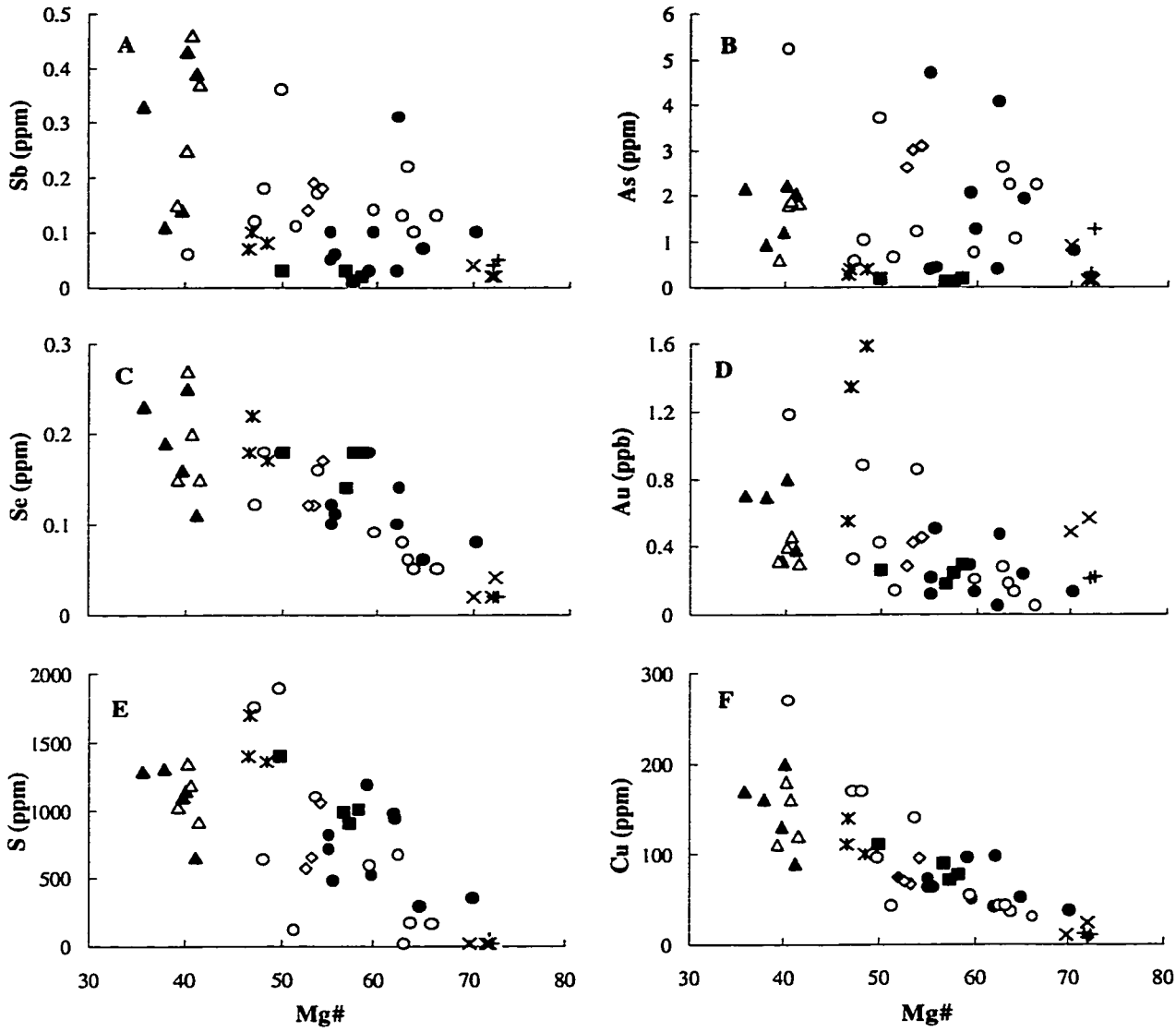

Figure 4-37. Variations of chalcophile elements with respect to Mg# as index of differentiation; Bamble gabbros (hyperites) and amphibolites. Symbols as in Figure 4-32.

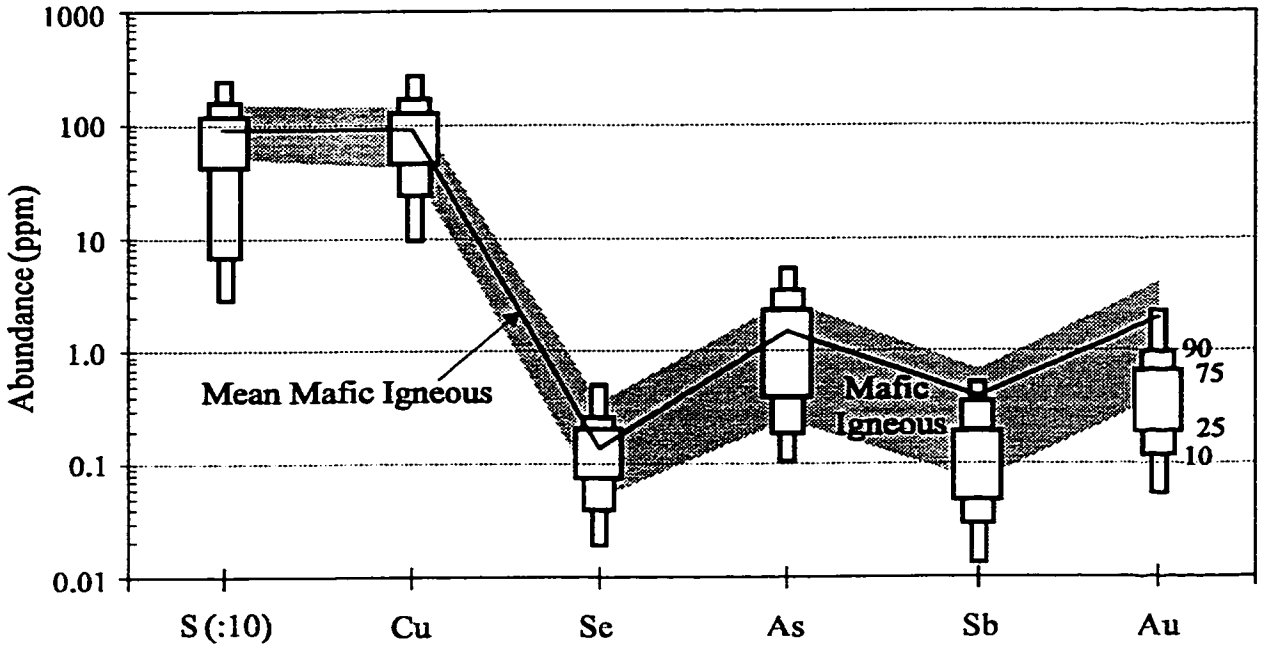

Figure 4-38. Abundance of chalcophile elements in the Bamble gabbros (hyperites) and amphibolites, with cumulative frequencies indicated for 10, 25, 75, and 90%. The common range (shaded area) and the mean abundance (solid line) of chalcophile elements in mafic igneous rocks are shown for comparison. See Appendix 2-2 for the composition of mafic rocks.

Sulfides are known to be the main host to Au in mafic rocks (e.g. Gottfried et al., 1972; Keays et al., 1981; Korobeynikov, 1989; Peach et al., 1990; Crocket et al., 1991, 1997). Considering the normal abundance of S in the Bamble mafic rocks, depletion of Au requires a strong fractionation of this element from S.

The ratio $Fe_2O_3/FeO + Fe_2O_3$ may be used as a rough index of oxidation. To evaluate the effect of oxidation on the fractionation of Au, variations of Au/S are shown against Fe_2O_3/Fe_t (Figure 4-39). Amphibolites are commonly distinguished by higher ratios of Fe_2O_3/Fe_t relative to their less altered equivalents, gabbros and hyperites. However, no consistent trends of variations can be inferred from the plots in Figure 4-39. This implies that the abundance of chalcophile elements was not solely controlled by the oxidation state of enclosing rocks.

Replacement of pyrrhotite to pyrite and magnetite may occur without removal of S and chalcophile elements, but simply an oxidation reaction:

$$6FeS + 2O_2 \leftrightarrow 3FeS_2 + Fe_3O_4$$

However, mantling of pyrite by magnetite suggests that S was mobile. Cameron et al (1993) proposed the following reaction:

$$3FeS + 2H_2O + 2O_2 \leftrightarrow 2H_2S + SO_2 + Fe_3O_4$$

Mass balance calculations indicated that no net removal or addition of chalcophile elements occurred during gabbro-amphibolite transition. The restricted oxidizing capacity of the infiltrating fluids was buffered by Fe^{+3}/Fe^{+2} ratios in the Fe-bearing minerals, protecting sulfides from decomposition. Sulfur and chalcophile elements released during incipient oxidation of pyrite were reprecipitated in very short distances. This is supported by the presence of minor secondary pyrite in microfractures and cleavage planes in the amphibolites. The mobile S was principally in its reduced form. A significant removal of chalcophile elements could occur only with continued oxidation and liberation of S in oxidized form.

No distinction can be made among various metamorphic zones with respect to the variations of chalcophile elements. The abundance of chalcophile elements was principally controlled by the geochemistry of the parent magmas and the degree of fractionation, rather than the depth of intrusion and ambient P-T, or post-solidus alteration.

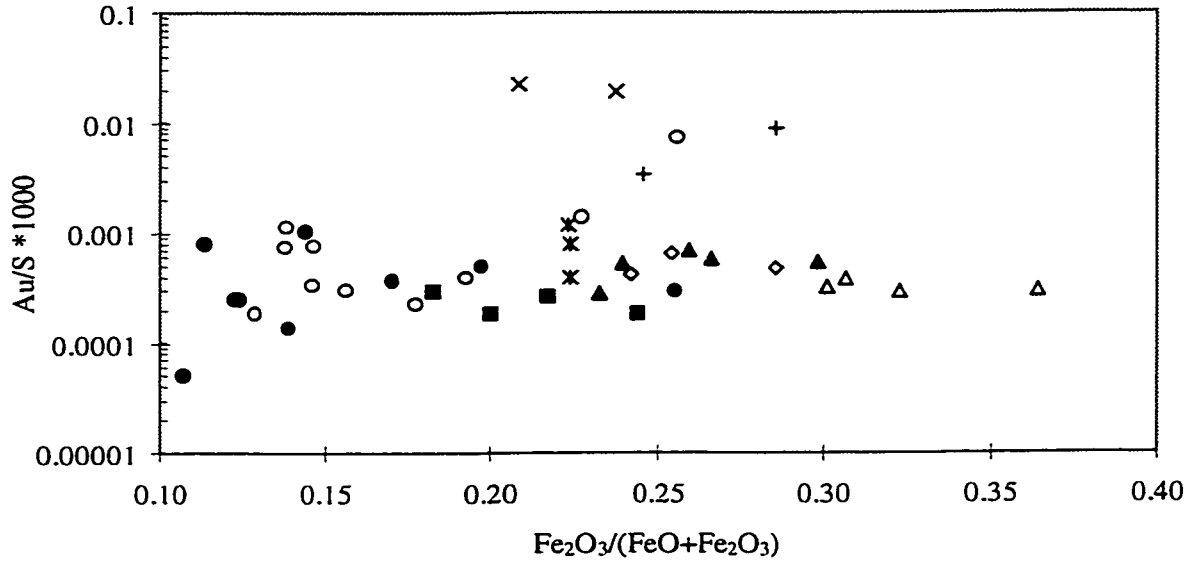

Figure 4-39. Variation of Au/S with $Fe_2O_3/(FeO + Fe_2O_3)$ as index of oxidation in hyperites (gabbros) and amphibolites; Bamble. Symbols as in Figure 4-32.

4-3. Fe-Ni-Cu Sulfide ores

Fe-Cu-Ni sulfide deposits are locally associated with hyperites in Bamble (e.g. Morton et al., 1970; Brickwood, 1984). The deposits, sporadically worked between 1859 and 1945, are comparatively small, having yielded some 10,000 tones of Ni in total (Bugge, 1978). They are commonly situated in the marginal parts of the host intrusions (Brickwood, 1984, 1986). Similar deposits have been reported from Kongsberg Sector (Dibb, 1981; Brickwood, 1984; Waque, 1996). Some 15 ore specimens from several deposits in Tvedestrand and Arendal areas were studied for mineral paragenesis and variations of chalcophile elements.

4-3-1. Mineral Paragenesis

Considering the mineral paragenesis and textures, three stages of ore formation can be identified (c.f. Brickwood, 1984, 1986): 1) primary orthomagmatic crystallization; 2) metamorphic recrystallization; and 3) supergene alteration.

4-3-1-A. Primary Orthomagmatic Crystallization

The primary ore occurs as disseminations and networks, as well as massive, in the marginal parts of the host intrusions. In the disseminated ore, sulfides occur in the cumulus and intercumulus sites otherwise occupied by primary pyroxene, and may sub-poikilitically enclose olivine and pyroxene crystals (Plate 4-4-A). In the network ore, sulfides occur as matrix enclosing euhedral to subhedral olivine and pyroxene. The massive sulfides occur as irregular lenses of different sizes and may contain xenoliths of the host intrusion. Brickwood (1984) reported the presence of xenoliths of the country rock gneisses in the massive ores from several deposits in the Bamble area.

Pyrrhotite, pentlandite, and chalcopyrite are the main sulfides in the primary ores. Ilmenite and magnetite are present as accessory phases. Pyrrhotite is the dominant mineral occurring commonly as coarse, interlocking anhedra, up to 20 mm in diameter. Chalcopyrite occurs both as fine to coarse grained anhedra interstitial to pyrrhotite, and as exsolution lamellae

within coarser pyrrhotite anhedra. Pentlandite forms typical blocky veinlets, as well as fine flame-like exsolution intergrowths, within pyrrhotite. Pyrite sporadically forms fine to coarse grained euhedra or subhedra, commonly enclosed within, or marginal to pyrrhotite crystals (Plate 4-4-B).

4-3-1-B. Metamorphic Recrystallization

As in the mafic host rocks, the sulfide ores experienced recrystallization and retrograde reactions during Sveconorwegian metamorphism or regeneration. The marginal parts of the mafic intrusions were amphibolitized, and the primary pyrrhotite-rich assemblages partially recrystallized to secondary pyrite-rich assemblages (Plate 4-4-C-D). Both primary and recrystallized ores form polycrystalline schlieren and stringers concordant with the dominant foliation. In the less altered ores, annealed textures have developed from the original intercumulus sulfide textures, with the retention of the primary sulfide assemblage (c.f. Brickwood, 1984).

In the more altered ores, the sulfide-silicate contacts are distorted, with sulfides occurring as granular aggregates as well as scattered xenoblasts and veinlets replacing silicates along fractures and cleavage planes (Plate 4-4-E). The sulfide assemblages in the recrystallized ores consist of polycrystalline pyrite associated with subordinate chalcopyrite and pentlandite. Millerite and cobaltite may occur as accessory phases.

Overgrowths of secondary sulfides on metamorphic amphibole and plagioclase are common (Plate 4-4-F), implying that sulfide recrystallization and redistribution continued at low temperatures following primary silicate recrystallization (c.f. Brickwood, 1984, 1986). Reaction rims of secondary materials are commonly developed along sulfide-silicate interfaces (Plate 4-4-D). Electron probe analysis of the reaction rims indicated the presence of Fe-rich chlorite as the main mineral. Other phases include quartz and carbonates.

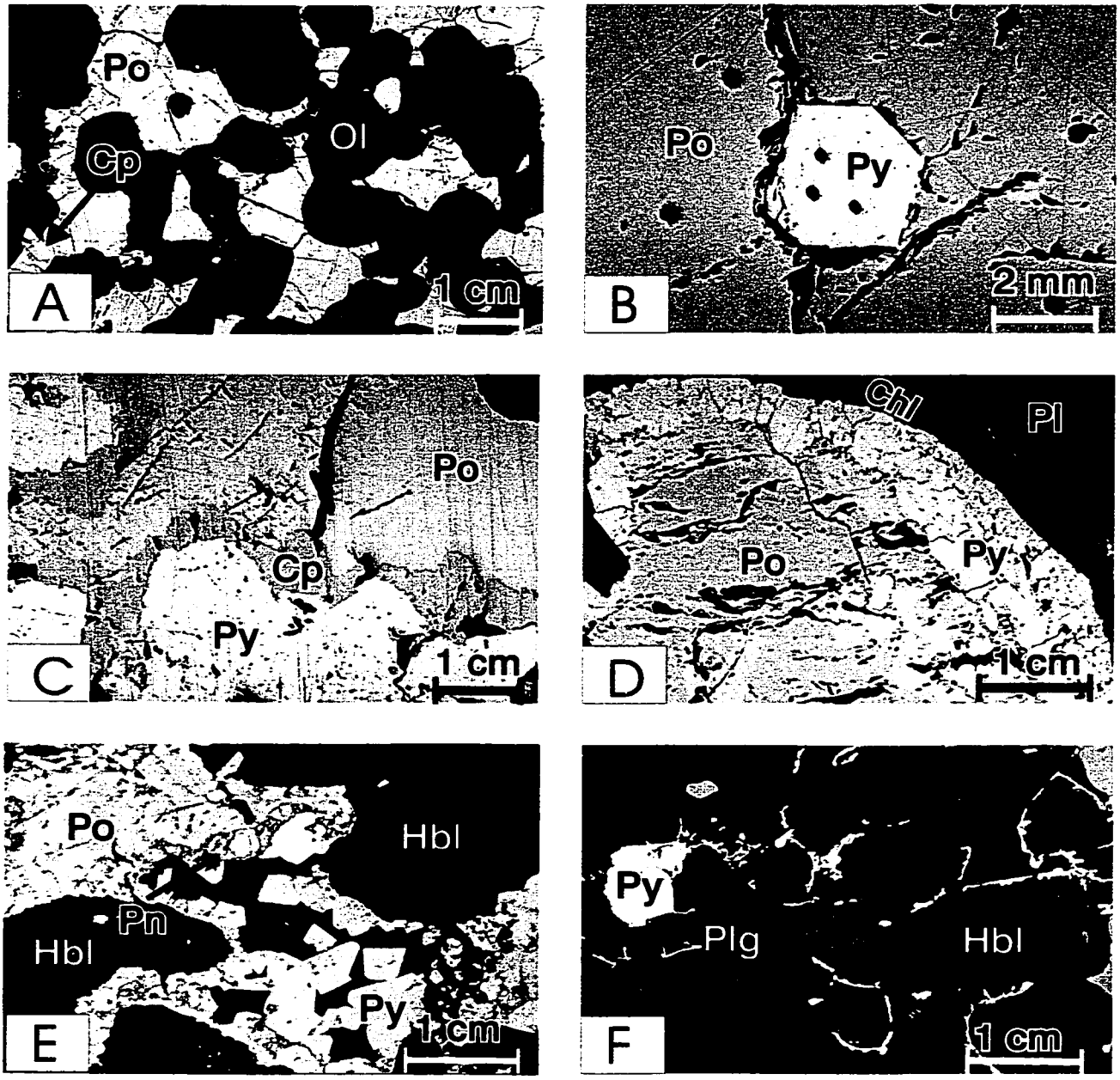

Plate 4-4. Ore textures from Bamble Fe-Ni-Cu deposits: (A) Disseminated ore, with sulfides in intercumulus sites. (B) Euhedral pyrite enclosed in pyrrhotite in disseminated ore. (C-D) Recrystallized ore; granoblastic, polycrystalline aggregates of pyrite replacing pyrrhotite, with chalcopyrite at pyrite-pyrrhotite boundary. (D) Reaction rim of Fe-rich chlorite developed along sulfide-silicate interface (E) Recrystallized ore; Pyrite occurring as granular aggregates and veinlets replacing silicates. (F) Secondary pyrite (PYs) occurring as overgrowth on metamorphic minerals. Symbls after Kretz (1983).

4-3-1-C. Supergene Alteration

Minor violarite occurs as pseudomorphs after pentlandite in both magmatic and metamorphic ores. The porous and fractured nature of the violarite suggests a supergene origin, in accord with that in most Fe-Ni-Cu sulfide deposits worldwide (e.g. Keele, 1974; Nickel et al., 1974).

4-3-2. Mineral Chemistry

4-3-2-A. Analytical Techniques

Some 300 electron microprobe analyses of sulfides and oxides from the Fe-Ni-Cu ores were performed at the Geological Survey of Canada using a Cameca SX50 microprobe. Analytical conditions employed a 20 kv accelerating potential, a counting time of 100 seconds and a spot diameter of about 3 microns. Various generations of sulfides were probed for a range of elements including As, Sb, Se, Bi, Cu, Ni and Co. Nickel and Co were well above the detection limit of 50 ppm in most runs. Copper was found to be above the detection limit of 50 ppm, and Se below the detection limit of 30 ppm, in most runs. Only in a few samples, As and Sb were present above the detection limit of 100 ppm. Bismuth was below the detection limit 50 ppm in all runs. A list of the analyses is shown in the Appendix 4-5.

4-3-2-B. Fe-Ti oxides

Ilmenite and magnetite occur as minor constituents (<2% by mode) in most ore samples. Both ilmenite and magnetite show little variation in composition. Magnetite is a Ti-rich variety containing up to 5% TiO_2. Both magnetite and ilmenite are rich in V containing up to 4% V_2O_5 in solid solution.

4-3-2-C. Chalcopyrite

Chalcopyrite displays little variation in composition in both primary and recrystallized ores (Appendix 4-5). This is in accordance with the near-perfect stoichiometry displayed by this mineral in the magmatic Fe-Ni-Cu ores worldwide (c.f. Naldrett, 1989).

4-3-2-D. Pentlandite

Pentlandite from primary and recrystallized ores shows no significant variation in composition. The Ni/Fe ratio falls in the range 0.75 to 0.8, in agreement with Ni/Fe ratios from other deposits in the Bamble (c.f. Brickwood, 1984) and elsewhere in Canada and Western Australia (c.f. Graterol and Naldrett, 1971; Harris and Nickel, 1972). The metal/S ratio of the pentlandite ranges between 1.12 to 1.15 that is slightly higher than stoichiometric proportions, in accordance with most pentlandite composition from magmatic Fe-Ni-Cu deposits (c.f. Graterol and Naldrett, 1971; Harris and Nickel, 1972).

The variable concentrations of Co in pentlandite (Figure 4-40) may be attributed to the presence or absence of pyrite and its paragenetic order with respect to pentlandite (c.f. Brickwood, 1984). Pentlandites from the primary, pyrite-free ores contain more than 1% Co, while those from the recrystallized, pyrite-rich ores are poor in this element, carrying commonly < 0.05% Co. The considerably higher Co in pentlandite from primary ores may be attributed to a higher temperature of formation (c.f. Misra and Fleet, 1974), or absence of pyrite which is a suitable host to Co.

4-3-2-E. Pyrrhotite

The composition of pyrrhotite from the primary and recrystallized ores shows no considerable stoichiometric deviations. The metal/sulfur ratios (100 [Fe + Ni + Co + Cu]/[Fe + Ni + Co + Cu + S]) suggest the presence of two types of pyrrhotites, in agreement with the variations described by Arnold (1966) for hexagonal (>47.2%) and monoclinic (<47.2%) polymorphs. This supports an earlier work by Brickwood (1984) who used ammonium dichromate-HCl staining method to distinguish between the two polymorphs of pyrrhotite.

Pyrrhotite from the primary, less altered, ores was found to be almost exclusively of hexagonal (Fe_9S_{10}) and that from the recrystallized ores of monoclinic (Fe_7S_8) type. In the recrystallized ores, minor hexagonal pyrrhotite is present as subordinate relics within the monoclinic pyrrhotite.

The hexagonal pyrrhotite contains lower Ni, but higher Co than the monoclinic polymorph (Figure 4-40). The low Ni and high Co concentration is not necessarily a characteristic of the hexagonal pyrrhotite (c.f. Misra and Fleet, 1973; Brickwood, 1984, 1986). Brickwood (1984) found similarly high Ni in coexisting hexagonal and monoclinic pyrrhotite from Østerå deposit in Tvedestrand area, Bamble. Distribution of Ni and Co in hexagonal and monoclinic pyrrhotite is shown in Figure 4-40.

4-3-2-F. Pyrite

Pyrites of various textural types show little deviation from stoichiometric composition, although considerable variations occur in the concentration of minor elements (Appendix 4-5). Various textural types of pyrite are distinguished by different contents of Ni and Co (Figure 4-40):

1. Fine grained, sporadic, euhedral pyrite enclosed in pyrrhotite (Plate 4-4-B). This pyrite is enriched in Ni and Co relative to the associated pyrrhotite; it is referred to as $PY_{Ni\text{-}Co}$.

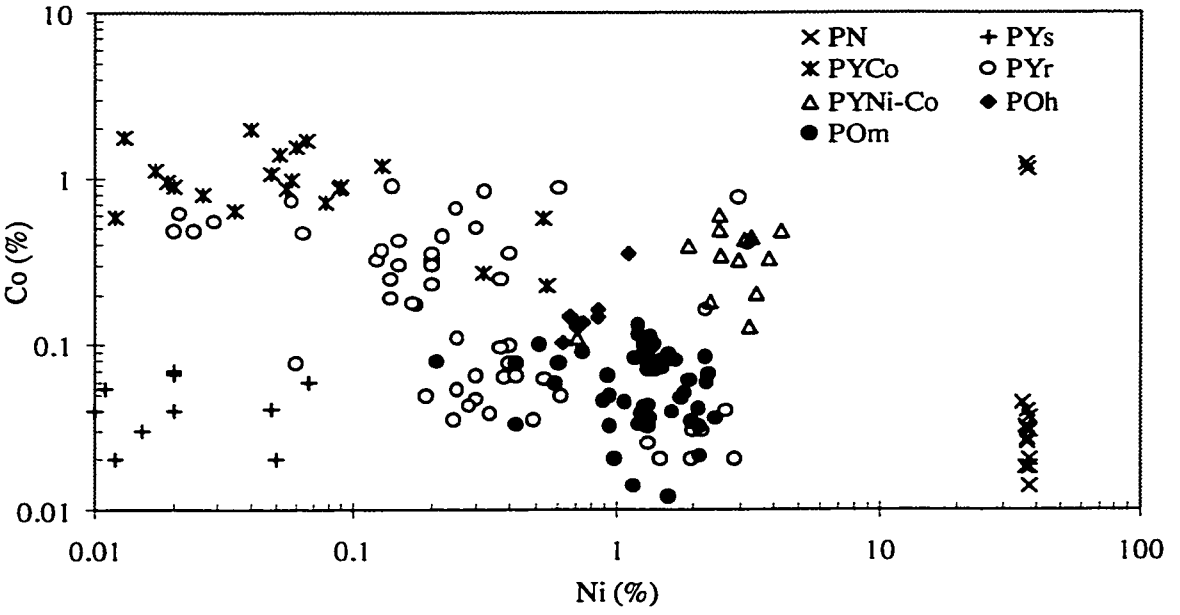

Figure 4-40. Distribution of Co and Ni in different types of pyrrhotite, pyrite and pentlandite in Bamble Fe-Ni-Cu ores. Abbreviations represent: POm (monoclinic pyrrhotite), POh (hexagonal pyrrhotite), $PY_{Ni\text{-}Co}$ (Ni-Co rich pyrite), PY_{Co} (Co-rich pyrite), PYr (pyrite replacing pyrrhotite), PYs (secondary pyrite), PN (pentlandite).

2. Granoblastic, polycrystalline aggregates of pyrite. This type appears to have replaced primary pyrrhotite along grain boundaries inward. In cases of incomplete replacement, rims and patches of chalcopyrite and pentlandite occur at the pyrite-pyrrhotite boundary (Plate 4-4-C-D). In the advanced stages of replacement, pyrite occurs as poikiloblasts enclosing patches of chalcopyrite and pentlandite. This pyrite is referred to as PYr.

3. Coarse grained, euhedral to subhedral pyrite, marginal to the grains of pyrrhotite (Plate 4-4-F). This type is considerably enriched in Co, but depleted in Ni, relative to the associated pyrrhotite; it is referred to as PYCo. Pyrite types 1 and 2 are minor constituents of ores, rarely exceeding 3% by mode.

4. Polycrystalline aggregates of pyrite commonly exhibiting a spongy texture. Minor chalcopyrite may accompany this pyrite; pyrrhotite is rare. The spongy pyrite occurs as overgrowths on amphibole and plagioclase or replacing these minerals along grain boundaries (Plate 4-4-F). It is characterized by low Ni and low Co. Overgrowths of secondary sulfides on metamorphic minerals indicates that sulfide recrystallization and redistribution continued at low temperature following hydration and recrystallization of the primary silicates.

5. Fracture filling in silicate minerals. This pyrite is also characterized by low Ni and low Co. The pyrite types 4 and 5 are collectively referred to as secondary pyrite (PYs) as they are clearly late in paragenesis.

4-3-3. Discussion

Ni-Cu sulfide ores associated with hyperites in Bamble display textures and mineral paragenesis typical of the Ni-Cu deposits of magmatic segregation origin elsewhere (c.f. Naldrett and Kullerud, 1967; Mathison and Marshall, 1981; Naldrett, 1989). The Bamble ores contain 5 to 15% pentlandite and chalcopyrite; minor ilmenite and magnetite (<2% by mode) accompany the sulfide minerals. Using the available data from experiments as well as data

from studies on natural assemblages, a tentative paragenesis for the crystallization of the minerals in Bamble ores is shown in Figure 4-41.

4-3-3-A. Primary Pyrrhotite, Chalcopyrite, and Pentlandite

Phase relations related to the genesis of magmatic Fe-Ni-Cu ores have been experimentally studied by several authors (e.g. Kullerud, 1963, 1967; Kullerud et al., 1969; Craig and Kullerud, 1969; Graterol and Naldrett, 1971; Cabri, 1973; Craig, 1976). Application of the experimental data to natural Fe-Ni-Cu ores (e.g. Craig, 1966; Naldrett and Kullerud, 1967; Naldrett, 1969; Brickwood, 1984) shows that crystallization of a pyrrhotite monosulfide solid solution (Po-mss) from an immiscible sulfide melt would begin at approximately 1125°C. The Po-mss would be joined by magnetite and ilmenite at ~1055°C and crystallization would be complete by 1000°C. With decreasing temperature, exsolution from the high temperature Po-mss occurs.

Solubility of Cu in Po-mss is approximately 5 wt% at 900°C, decreasing to 1 wt% at 500°C (Kullerud et al, 1969). Phase relations in the Fe-Cu-S system (Kullerud et al. 1969; Graterol and Naldrett, 1971; Cabri, 1973) show that chalcopyrite starts to exsolve below about 575°C. Craig (1966) showed an exsolution temperature of 400°C for chalcopyrite from Strathcona ore, Sudbury. Craig and Kullerud (1969) indicated that 4-5 % Ni in solid solution in pyrrhotite does not significantly affect the solubility of Cu. Solubility of Ni in Po-mss is up to 10 wt% at 600-400°C (Naldrett and Kullerud, 1966). Under equilibrium conditions, exsolution of pentlandite occurs below 350°C. Craig (1966) found that the presence of up to 4-5% Cu in Po-mss does not measurably influence the temperature of pentlandite exsolution.

4-3-3-B. Ni-Co rich Pyrite

The origin of the common Fe-sulfides, pyrrhotite and pyrite, and their behavior during geochemical processes can best be explained by the simplified redox reaction (Hall, 1986):

$$2FeS \leftrightarrow FeS_2 + 2e- \quad (1)$$

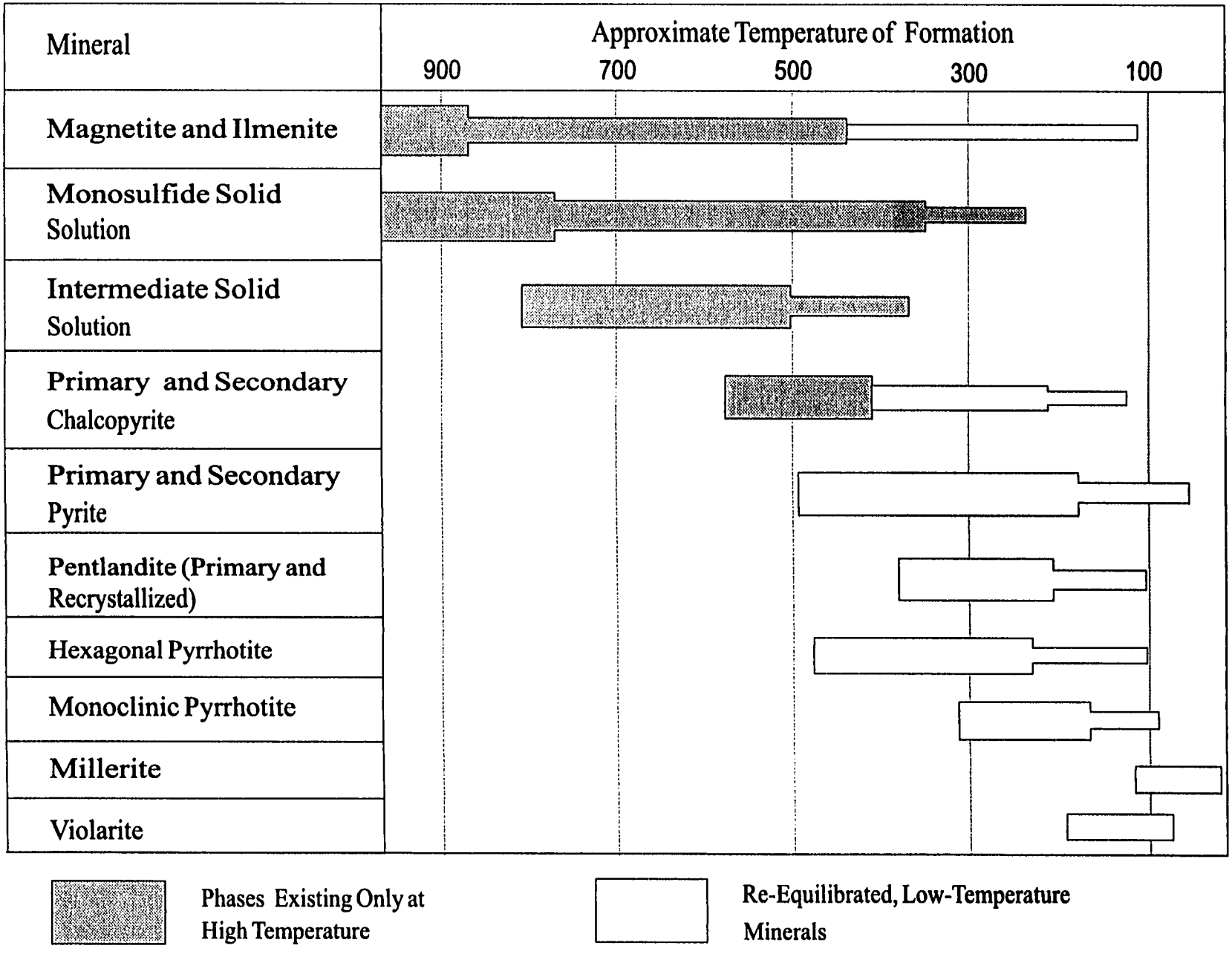

Figure 4-41. Paragenetic sequence for crystallization of minerals in the Bamble Fe-Ni-Cu ores

Pyrrhotite is more reduced than pyrite and their relative stabilities in nature depend on oxidation reactions, or, electron transfer reactions, which may or may not involve oxygen (Hall, 1986). Pyrrhotite is considered to be indicative of lower, and pyrite indicative of higher oxygen and sulfur fugacities which are generally interdependent and positively correlated in natural systems (e.g. Kullerud and Yoder, 1959, 1967; Ferry, 1981; Hall, 1986).

Exsolution of pyrite from pyrrhotite is a well known phenomenon; it has been documented by both studies on natural assemblages (Naldrett and Kullerud, 1967; Graterol and Naldrett, 1971; Misra and Fleet, 1973; Scott et al., 1977; Garuti et al., 1986) as well as laboratory experiments (e.g. Kullerud, 1967; Yund and Hall, 1969; Graterol and Naldrett, 1971; Mohr and Newton, 1983).

The composition of natural pyrrhotites ranges from 54 atom% S at 700°C to 52.42 atom% S at 300°C (e.g. Toulmin and Barton, 1964; Kissin and Scott, 1982). Under equilibrium conditions, cooling of hexagonal, high temperature, pyrrhotite saturated with S (S/Fe > 8/7) will result in the exsolution of pyrite and the formation of a progressively less Fe-deficient pyrrhotite of hexagonal low temperature type (Arnold, 1962; Kullerud, 1967). The hexagonal low temperature pyrrhotite under equilibrium conditions will react about 310°C with the previously exsolved pyrite to produce monoclinic pyrrhotite (Kullerud, 1967, Kissin and Scott (1982). Depending on the S/metal ratio of the original pyrrhotite, the final assemblage at or slightly above 100°C will be either hexagonal low temperature pyrrhotite and monoclinic pyrrhotite or monoclinic pyrrhotite and pyrite.

Yund and Hall (1969) indicated that exsolution of pyrite at 325°C occurs by heterogeneous nucleation and subsequent growth by volume diffusion of Fe away from the nuclei into the pyrrhotite matrix. Sulfur atoms are required to move only short distances to form S-S bonds. The authors also showed that nucleation rate increases with the degree of supersaturation, and that impurities such as, Sb, or Bi retard the exsolution rate by 2 or more orders of magnitude at 325°C. The impurities reduce the diffusivity of Fe in pyrrhotite thus reducing the nucleation rate. The exsolved pyrite grains tend to be equidimensional and located at grain margins.

Naldrett and Kullerud (1967) consider the 5 to 6% pyrite associated with pyrrhotite and pentlandite in Strathcona ores, Sudbury, as having exsolved from 70-80% pyrrhotite in the ore upon cooling. This pyrite occurs as small euhedra evenly distributed around pyrrhotite grain boundaries. A similar occurrence of pyrite, consistently associated with monoclinic pyrrhotite, was reported from Ivrea-Verbano igneous Complex, Italy (Garuti et al., 1986). The occurrence of minor (< 1% by mode) euhedral pyrite within, or marginal to, the grains of pyrrhotite in Bamble ores may be attributed to the exsolution processes.

4-3-3-C. Granoblastic Polycrystalline Pyrite

The pyrite type 3, the most common of all pyrites, occurs as granoblastic, polycrystalline aggregates replacing primary pyrrhotite. Replacement of pyrrhotite by pyrite is also common in the host hyperites. Although possessing a stoichiometric composition, the pyrite displays a large variation in Co and Ni (Figure 4-40) with Co/Ni ratios varying from 0.1 to 20. In the pyrite and pyrrhotite formula, Co and Ni invariably substitute for Fe. Nickel is known to prefer pyrrhotite with Ni-arsenide structure; cobalt prefers pyrite (e.g. Graterol and Naldrett, 1971; Cambel and Jarkovsky, 1969). The wide variation in Co and Ni may be attributed to initial variations of the metals in the primary pyrrhotite, the order of pyrite with respect to pentlandite in the paragenetic sequence, or variable involvement of the surrounding silicates.

With respect to the phase equilibria in Fe-O-S system at high temperature (e.g. Kullerud and Yoder, 1959; Arnold, 1971), pyrite could form as a primary phase on the liquidus only in magmas of almost pure S. For normal magmas (less S-rich), pyrite may appear at lower temperatures by the reaction of pyrrhotite with gas.

Phase relations in Fe-O-S system (e.g. Kullerud, 1967; Toulmin and Barton, 1964) show that below ~700°C the addition of oxygen to a pyrrhotite saturated with S would lead to the oxidation of Fe in the pyrrhotite to magnetite and the formation of pyrite:

$$6FeS + 2O_2 \leftrightarrow 3FeS_2 + Fe_3O_4 \qquad (2)$$

This mechanism for the conversion of pyrrhotite to pyrite is favored because:

- Pyrite is usually associated with magnetite.
- Interstitial pyrite ± magnetite closely mimics pyrrhotite in texture.
- It does not require the dissolution or remobilization of the constituents by an aqueous fluid; so it is more likely that pseudomorphs would form.

A similar reaction was proposed by Gitlin (1985) to explain the common replacement of pyrrhotite by pyrite + magnetite in mid-Atlantic basalts. Similarly, the common occurrences of pyrite ± magnetite in gabbros from Deer Lake Complex, Minnesota, and Dore Lake Complex, Manitoba, have been attributed to an increase in f_{O2} and breakdown of the initial magmatic pyrrhotite (Ripley, 1983; Kline, 1984). Glassley (1983) reported an extensive oxidation and replacement of pyrrhotite and pyrite by magnetite in granulite facies rocks from Nordre Stromford shear zone, west Greenland.

Oxidation of pyrrhotite according to the reaction 2 may occur in a system closed to removal of S and chalcophile elements. Cameron et al. (1993) indicated that oxidation of pyrrhotite in the granulite grade rocks from Bamble was the consequence of internal buffering by an oxidized mineral assemblage, without introduction of a fluid-borne oxidant. However, the confinement of the recrystallized, pyrite-rich ores to amphibolitized host rocks, suggests an external buffering for the sulfide phase change, probably by the same fluids involved in the amphibolitization. Cameron (1989b) suggested the following reaction to account for mantling of pyrite by magnetite in the amphibolized hyperites.

$$3FeS + 2H_2O + 2O_2 \leftrightarrow 2H_2S + SO_2 + Fe_3O_4 \quad (3)$$

Replacement of pyrrhotite by pyrite according to the reactions 2 and 3 requires the removal of considerable amounts of Fe. Brickwood (1984) reported the occurrence of abundant secondary magnetite in the pyrite-rich ores from Meikjær and Nystein deposits in Gjerstad area. However, magnetite is a minor constituent of the pyrite-rich ores in the studied specimens; the magnetite/sulfide ratio rarely exceeds 5%. The excess Fe is possibly involved in the silicate reactions. Reaction rims are common at the sulfide-silicate interface (Plate 4-4-D).

Fe-rich chlorite is the most common mineral. The composition of the chlorite is shown in Table 4-14.

Alternatively, the replacement of pyrrhotite by pyrite may be attributed to an increase in sulfur activity:

$$FeS + \frac{1}{2}S \leftrightarrow FeS_2 \quad (4)$$

The above reaction requires post-solidus introduction of S. This is not supported by the existing evidence. The textures and paragenesis of sulfides can best be explained by cooling and oxidation of an initial magmatic monosulfide solid solution. This is supported by S isotope data. The $\delta^{34}S$ values for the recrystallized, pyrite-rich ore are in the same range as in the primary pyrrhotite-rich ore. Where coexisting, pyrite and pyrrhotite are in isotopic equilibrium. Isotopic composition of sulfide is discussed in Chapter 5.

Table 4-14. Composition of chlorite from reaction rims at sulfide-silicate interface

SiO_2	27.01	25.35	25.39	25.64	28.44	26.49	25.88	27.3
Al_2O_3	18.9	19.96	18.82	17.03	16.55	17.84	15.96	16.82
TiO_2	0	0	0.1	0	0.25	0	0	0.1
FeO*	31.16	31.22	35.78	36.39	30	33.16	31.18	29.28
MnO	0.21	0.24	0.17	0.15	0.15	0.13	0.13	0.25
MgO	12.24	12.01	7.81	8.17	13.59	9.98	12.93	13.44
K_2O	0.05	0	0.2	0.15	0	0.09	0.12	0
CaO	0	0.08	0	0.09	0.11	0.08	0.17	0.11
Total	89.57	88.86	88.27	87.62	89.09	87.77	86.37	87.3

4-3-3-D. Metamorphic Chalcopyrite and Pentlandite

The common occurrence of chalcopyrite and pentlandite at the boundary between pyrrhotite and pyrite in the recrystallized ores suggest that formation of pyrite predated the exsolution of chalcopyrite and pentlandite. Where both minerals are present, the former usually forms the outer, and the latter the inner, rims, implying that pentlandite postdated chalcopyrite. This is in agreement with the experimental data on the exsolution of these minerals from Po-mss (e.g. Craig and Kullerud, 1969; Kullerud et al., 1969). With progressive replacement of Po-mss by

pyrite, supersaturation of Cu and Ni arrives, and they exsolve as chalcopyrite and pentlandite at the replacement front. This process might lead to the formation of the minerals above their common temperature of exsolution (c.f. Craig et al., 1967).

4-3-3-E. Overgrowth and Fracture Filling Pyrite

The pyrite types 4 and 5 are depleted in both Ni and Co. They are clearly late in the paragenesis, and appear to be the result of local dissolution and remobilization of other generations of sulfides. The close association of the pyrites with Fe-bearing silicates suggest that Fe is provided by the host silicates. The secondary pyrite might be rich in As. Electron probe analysis indicated the presence of up to 2000 ppm As in the pyrites.

4-4. Geochemistry of Sulfides

4-4-1. Introduction

Both Kongsbergian and Sveconorwegian mafic rocks and their associated Fe-Ni-Cu ores at Bamble are considerably depleted in Au, compared to the mean composition of mafic rocks. The Bamble mafic rocks and ores are characterized by extensive oxidation and partial to complete replacement of primary magmatic pyrrhotite by pyrite ± magnetite. Ion microprobe analysis of composite pyrrhotite-pyrite grains showed that pyrite was significantly depleted in Au compared to the coexisting pyrrhotite (Cameron, 1993a) (Figure 4-42). Cameron suggests the serial replacement of pyrrhotite by pyrite and magnetite as a possible explanation for Au depletion in the Bamble mafic rocks.

To investigate the variations of chalcophile elements during oxidation of primary sulfides, concentrates of sulfides from metabasites, hyperites, and Fe-Ni-Cu ores associated with hyperites, were analyzed by a combination of instrumental neutron activation (INA) and hydride inductively coupled plasma mass spectrometry (ICPMS) methods. An initial in-situ analysis of the sulfides by proton induced x-ray emission (PIXE) technique failed to yield satisfactory results, as concentrations of the elements were below, or close to, the detection limits of PIXE.

4-4-1-A. Sample Preparation and Analytical Procedures

An initial test of mechanical separation failed to yield enough materials of high purity from hyperites and metabasites, because of the low contents of sulfides (<0.5% by mode) and the small sizes of the sulfide grains (commonly <400 μm). Accordingly, sulfide concentrates were prepared using an HF-digestion method following Neuerburg (1975). To recover 0.2-0.5 grams of sulfide concentrates required for analysis, 50 to 100 grams of rock slabs were treated by HF-digestion. The method has proven to be very efficient in removing most common silicates and oxides, and providing clean and physically unharmed sulfide grains.

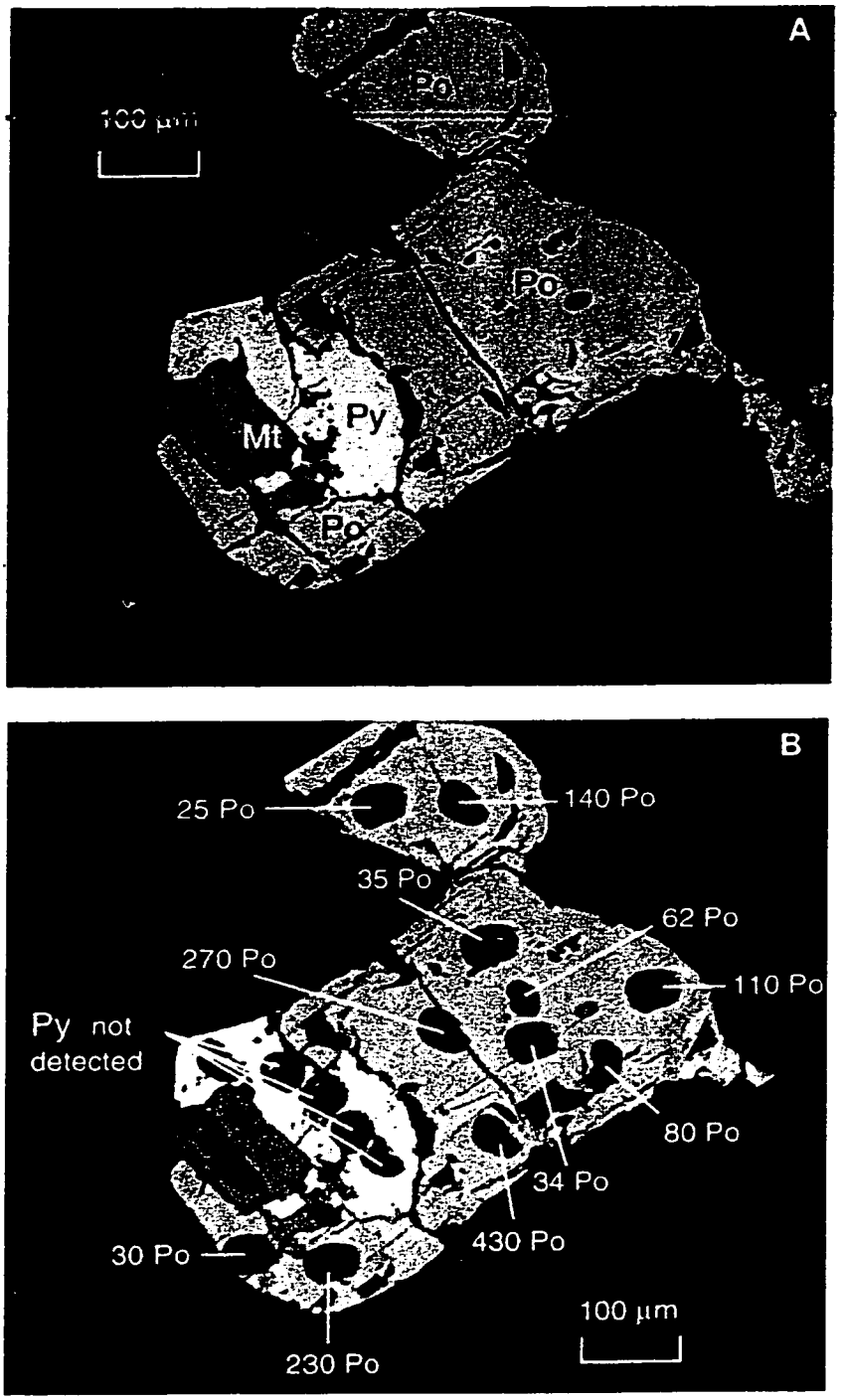

Figure 4-42. (A) A grain of interstitial pyrrhotite (Po) partially transformed to pyrite (Py) and magnetite (Mt); sample 4008 from the interior part of a hyperite dyke in Tvedestrand. (B) The same grain as in A after spot analysis by ion microprobe. Results of analyses are shown in ppb Au. After Cameron (1993a).

Four different parageneses of sulfides can be identified in both hyperites and metabasites:

1. Interstitial pyrrhotite ± chalcopyrite ± pentlandite, representing primary orthomagmatic sulfide assemblages.
2. Interstitial pyrrhotite + pyrite ± magnetite ± chalcopyrite ± pentlandite, representing partially oxidized sulfide assemblages, with pyrrhotite variably replaced by pyrite ± magnetite.
3. Interstitial pyrite ± magnetite ± chalcopyrite ± pentlandite, representing oxidized sulfide assemblages, with extensive replacement of pyrrhotite by pyrite ± magnetite.
4. Secondary pyrite occurring as overgrowth and fracture filling.

Individual samples may contain one or more of the above parageneses. To prepare concentrates of primary (pyrrhotite-dominant) and oxidized (pyrite-dominant) sulfide assemblages, care was taken to avoid contamination by secondary overgrowth and fracture filling pyrite. To ensure this, two to three closely spaced polished sections from each hand specimen were studied on reflected light microscope. Magnetite, a minor constituent in most mafic rocks, is relatively resistant to HF solution. Accordingly, in preparing pyrrhotite concentrates, samples with no or negligible magnetite component were selected. To check for the composition of the secondary sulfides, concentrates were also prepared from samples containing secondary fracture filling and replacement pyrite.

To ensure a high purity of >98%, and to identify the potential impurities, polished grain mounts of average materials were studied using reflected light microscopy at the resolution of X200. Chalcopyrite and pentlandite are equally associated with pyrrhotite and pyrite, and impurities, if any, include magnetite, ilmenite, or fluoride salts. A high purity was further supported by data from the analyses.

Sulfide ores display the same paragenesis as in the disseminated sulfides in their mafic hostrocks. Some 10 samples of orthomagmatic (pyrrhotite-rich) and recrystallized (pyrite-rich) ores were selected for analysis. Twenty to 50 grams of the samples were reduced to 5-2 mm in a steel-faced jaw crusher and then were screened at 2 mm; fines were discarded. After washing in an ultrasonic bath, the samples were ground to ~50-100 mesh in a ceramic plate

crusher and then were screened between 100 to 80 mesh. The ground materials were further washed by acetone. To prepare sulfide concentrates, the silicate impurities were removed by floating on methylene iodide. The residual sulfides were then treated by mechanical separation.

Pyrrhotite from the recrystallized pyrite-rich ore is principally of magnetic monoclinic type; it was easily recovered by means of a hand magnet. Pyrrhotite from the primary orthomagmatic ore consists mainly of hexagonal type with subordinate monoclinic polymorph. Pyrite, chalcopyrite, pentlandite, and hexagonal pyrrhotite were separated by means of a Franz magnetic separator. Pyrite was separated at 1 to 1.2 amperes, chalcopyrite at 0.6 to 0.8, pentlandite between 0.2 to 0.6, and hexagonal pyrrhotite below 0.2 amperes. A forward slope of 15 to 20° and a side slope of 5 to 15° was applied to all tests. To ensure a high purity of >95%, polished grain mounts of average materials were studied using reflected light microscopy at the resolution of X200. In cases where the required purity was not achieved by magnetic separator, the visible impurities were removed by use of a binocular at magnifications of X100 to X200.

The final products from both mafic rocks and sulfide ores were analyzed by a combination of INAA and hydride ICPMS techniques by Actlabs (Activation Laboratories Limited), Ancaster, Ontario. Gold, Ir, As, Sb, and Se were analyzed by INAA at detection limits of 2 ppb, 5 ppb, 0.5 ppm, 0.1 ppm, and 3 ppm, respectively. Nickel and Co were also measured by this method at detection limit of 20 ppm. Bismuth, Ag, Cu, Zn, and Pb were analyzed by ICPMS at the detection limits of 5, 0.5, 1, 1, and 5 ppm, respectively.

4-4-1-B. Precision and Accuracy

Precision and accuracy were evaluated using standard materials. To cover all elements of interest in this study, particularly Au, Bi, Se, As, and Sb, in a wide range of concentrations, five reference samples kindly supplied by Canada Center for Mineral and Energy Technology (CANMET) were analyzed in replicate along with the sulfide concentrates. The reference materials include:

RTS-2. Low-pyrrhotite material from Sudbury

PTC-1a. Noble metals-bearing sulfide concentrate from Sudbury

CCU-1b. Copper flotation concentrate from Ruttan Mine, Manitoba

WMS-1. Massive sulfide PGE materials from Wellgreen Complex, Yukon Territory

CH-3. Gold bearing sulfide ore from Chibougamau, Quebec

Results from the replicate analyses are in good agreement with the values recommended by CANMET (Appendix 4-6). Precision, or coefficient of variation, and accuracy were evaluated according to the equations:

Precision = (standard deviation/mean concentration)*100

Accuracy = (analyzed – certified/certified)*100

Precision and accuracy are calculated for individual elements (Table 4-15). Analytical accuracy is better than ± 10% in most cases. Precision is also better than 10%. A general tendency for refinement in precision and accuracy is clear with increasing concentrations.

To test for lack of reaction of sulfides to HF solution, concentrates of pyrite and pyrrhotite from a recrystallized ore were prepared by both mechanical (magnetic separation) and chemical (HF-digestion) methods. Polished grain mounts from the two sets of concentrates indicated a high purity of >98%, the impurities being chalcopyrite, pentlandite and silicates. Analysis of the mineral concentrates indicated similar abundances of chalcophile elements in the two fractions (Figure 4-43-A-B). Slight differences might be attributed to initial variations of the elements between the two sets of concentrates, or to analytical error, or, both. Following, the results are discussed for individual units.

Table 4-15. Evaluation of precision and accuracy of the experiments by replicate analyses of reference materials.

	Runs	Mean (Analyzed)	Std. Dev. (1σ)	Mean (Certified)	Precision	Accuracy
Au						
PTC-1a	3	1217	105	1310	8	-7
CCU-1b	2	6345	280	5890	4	8
CH-3	2	1260	65	1400	5	-10
WMS-1	2	315	18	279	6	13
RTS-2	2	40	5	*38**	12	5
Ir						
PTC-1a	3	97	10	110	10	12
WMS-1	2	215	5	235	2	8
As						
PTC-1a	3	100	10	*120*	10	-16
CCU-1b	2	65	4	58	6	12
CH-3	2	140	10	143	7	2
Ag						
PTC-1a	3	52	5	56	10	-7
CCU-1b	2	178	6	178	3	0
CH-3	2	3	0.2	2.6	7	15
Se						
CCU-1b	2	157	7	*139*	4	12
RTS-2	2	66	3	*57*	5	15
Co						
PTC-1a	3	3033	115	*3000*	4	1
CCU-1b	2	22	3	*26*	13	-15
RTS-2	2	74	4	72	5	3
Ni						
RTS-2	2	2591	40	2430	2	7
WMS-1		38660	25	*37000*	0.1	5
Cu					1	
CH-3		8300	100	8300	2	0
WMS-1		12150	250	*13000*	4	-7
RTS-2		750	28	670	4	12
Zn						
CH-3		170	2	164	1	4
RTS-2		114	6	117	5	-3

* Figures in italics represent provisional values

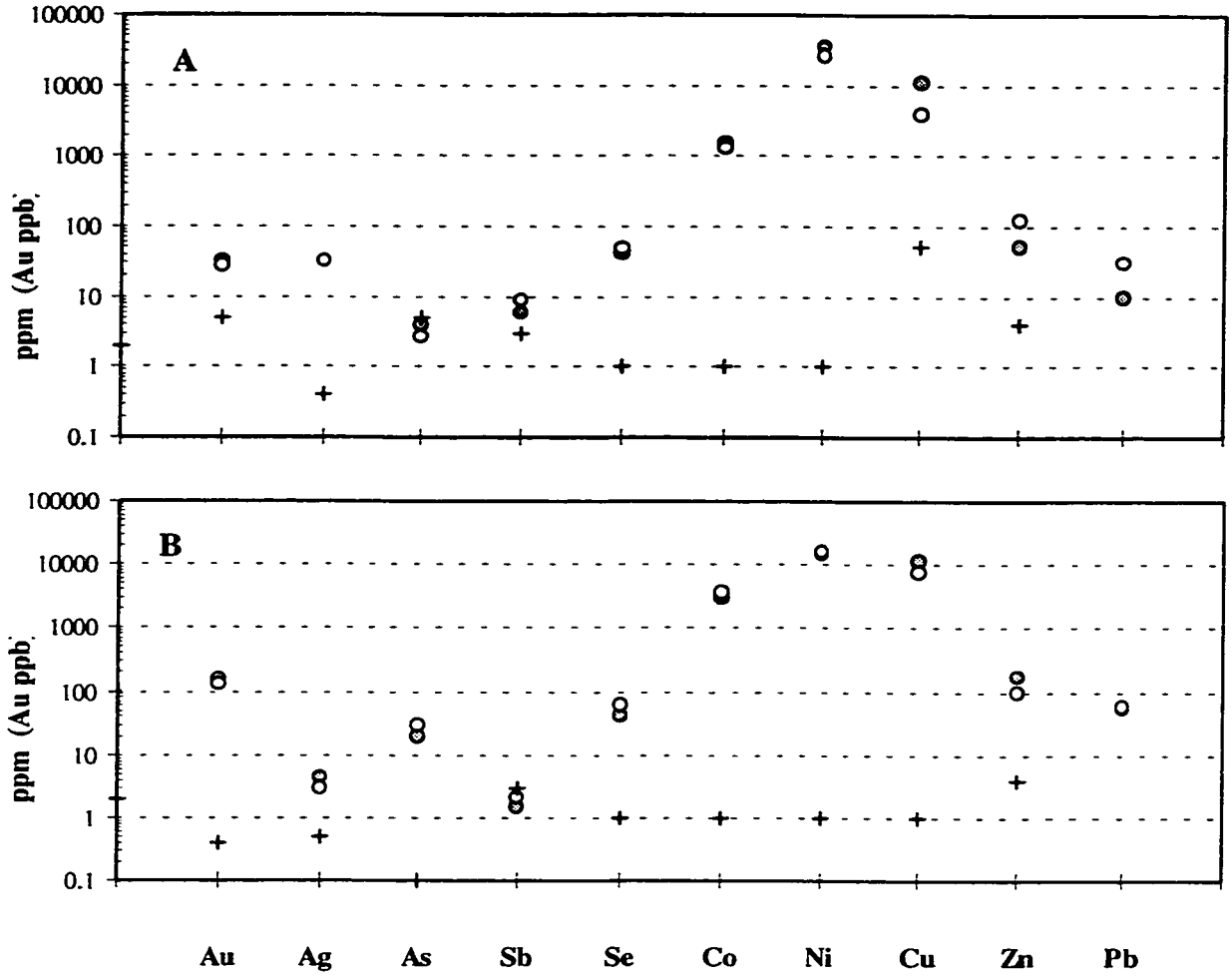

Figure 4-43. Distribution of elements in pyrrhotite (A) and pyrite (B) concentrates prepared by mechanical (shaded circles) and chemical (open circles) methods from a recrystallized ore. Crosses represent the detection limits.

4-4-2. Hyperites (Gabbros) and Amphibolites

Hyperites (gabbros) occur in a metamorphic gradient from upper amphibolite to granulite facies conditions. Intrusions emplaced into the amphibolite facies country rocks are extensively amphibolitized, while those emplaced into the relatively dry granulite facies country rocks generally bear only thin marginal sheet of amphibolite. Pyrrhotite, the main sulfide in the central, least altered, parts of the mafic bodies, is increasingly replaced by pyrite + magnetite towards the margins. Sulfide concentrates from several samples of hyperites, coronitic gabbros, and amphibolites were analyzed. The samples include:

- Three samples (4006, 4007, 4009) from the central, least altered portion, and one sample (4001) from the amphibolitized margin, of a hyperite dyke from the transition zone B in Tvedestrand.
- Three samples (5001, 5002, and 5003) from the central, least altered, portion of a hyperite dyke from the granulite grade zone at Tromoy.
- One sample (5202) from a coronitic gabbro dyke from the granulite grade zone at Tromoy.
- Two samples, one from the central (5104) and the other (5102) from the marginal, portions of a hyperite body from granulite grade zone at Tromoy.

Both coronitic gabbro and hyperite dykes are partially amphibolitized and even the least altered rocks contain considerable amounts of hornblende. Primary pyrrhotite has variably been replaced by pyrite ± magnetite, allowing the analysis of pyrrhotite and pyrite from the same sample. Pyrrhotite is rarely preserved in the marginal amphibolites. Analytical results are presented in Table 4-16.

4-4-2-A. Mass Balance

To investigate the distribution and behavior of chalcophile elements with changes in sulfide phases, and to evaluate the partitioning of the elements between sulfide and silicate phases, data from pyrite and pyrrhotite concentrates are compared to each other, and to those from whole rocks.

The mineral concentrates are of two distinct parageneses, one pyrrhotite-dominant consisting of pyrrhotite + chalcopyrite + pentlandite, and the other pyrite-dominant, consisting of pyrite + chalcopyrite + pentlandite. Mass balance calculation is based on 100% pyrrhotite, or 100% pyrite for pyrrhotite-dominant and pyrite-dominant assemblages, respectively. Chalcopyrite and pentlandite are minor phases (<10%) almost equally distributed in the two parageneses.

Table 4-16. Analysis of sulfide concentrates from hyperites, gabbros, and amphibolites.

Element		Au	Ag	As	Ir	Sb	Bi	Se	Co	Ni	Cu	Zn	Mo	Pb
Unit		ppb	ppm	ppm	ppb	ppm	ppm	ppm	ppm	ppm	ppm	ppm	ppm	ppm
Detection Limit		2.0	0.4	0.5	5.0	0.1	5.0	3.0	20	20	1.0	1.0	2.0	4.0
Tvedestrand hyperite (4006-9) and amphibolite (4001)														
4001	Py	83	7.4	22	<5	9.7	11	75	3400	5249	23641	1223	20	119
4006	Po	90	12.4	22	<5	5.0	25	54	1800	5716	33006	313	16	15
	Py	143	16.1	79	<5	18	26	72	3600	8177	35266	389	24	31
4007	Po	105	15	38	<5	1.0	14	55	2300	7426	45958	382	21	18
	Py	146	20	93	<5	5.5	28	68	4400	7292	40950	630	24	15
4009	Po	146	17.7	24	<5	2.5	57	84	1800	7500	56200	490	11	29
	Py	153	29.6	65	<5	17	69	100	2900	8700	52500	614	20	36
Tromoy hyperite dyke-1														
5001	Po	290	5.3	26	<5	0.5	18	74	2100	9930	24128	895	16	19
	Py	373	7.0	51	<5	5.8	22	100	5200	9897	19820	619	15	33
5002	Po	321	6.1	13	<5	1.0	28	48	2500	7763	26464	451	16	40
	Py	708	9.1	41	<5	8.0	24	65	4800	8108	24649	458	14	80
5003	Po	112	2.6	34	<5	0.6	8.0	75	1300	7932	26196	943	15	26
	Py	175	6.0	72	<5	3.5	5.0	110	4600	8431	25300	648	17	16
Tromoy hyperite (5104) and amphibolite (5102) dyke-2														
5102	Py	113	8.2	59	<5	7.0	24	80	5300	6300	12200	293	38	110
5104	Po	97	2.9	14	<5	1.0	19	78	2000	11156	10622	214	15	34
	Py	166	4.9	42	<5	12	21	98	4500	14769	16266	236	9.0	29
Tromoy coronitic gabbro														
5202	Po	32	8.5	18	<5	0.3	35	55	3000	13200	17500	222	7.0	69
	Py	45	14.2	61	<5	3.7	39	75	5100	12100	14800	252	8.0	36

Considering the concentration of S in the whole rocks, and the pyrrhotite/pyrite ratios, the sulfide wt% is calculated according to the equation:

$$\text{Sulfide wt\%} = S_w + Fe_{Po} + Fe_{Py}$$

where

$$Fe_{Po} = ((S_w \,.\, a) \,.\, Po_X)/100$$

$$Fe_{Py} = ((S_w \,.\, b) \,.\, Py_X)/100$$

S_w = S in whole rock (wt%)

Po_X = wt% pyrrhotite in sulfide concentrate

Py_X = wt% pyrite in sulfide concentrate

Fe_{Po} = wt% Fe in pyrrhotite fraction

Fe_{Py} = wt% Fe in pyrite fraction

a = mass constant for pyrrhotite (Fe/S = 1.56)

b = mass constant for pyrite (Fe/S = 0.88)

The contribution of sulfides to the whole rock budget of chalcophile elements, and the concentrations of elements in the silicate fractions were calculated from the abundances of elements in sulfides and whole rocks, and the "sulfide/whole rock" mass ratios.

To further evaluate the role of metamorphism and oxidation on the initial distribution of chalcophile elements, the partitioning of elements between sulfide and silicate phases are investigated. The partitioning of elements between two phases in equilibrium is usually considered in terms of Nernst distribution coefficient:

$$D = \frac{wt\%\ of\ element\ in\ phase\ A}{wt\%\ of\ element\ in\ phase\ B}$$

Following, the results are discussed for individual elements.

I. Gold

Gold is enriched in the pyrite concentrates by a factor of 1.3 to 1.6 relative to the pyrrhotite concentrates (Table 4-16). Mass balance calculations indicate that minor sulfides account for 45 to 85% of the total Au in their enclosing rocks. The distribution coefficient (D) of Au between sulfide and silicate phases varies from 350 to 1500, with an average of 700 ± 300 (Figure 4-44). Variations of D_{Au} values are large between various bodies; however, small within individual bodies.

During magmatic crystallization, Au strongly partitions into the sulfide fraction (e.g. Gottfried et al., 1972; Tilling et al., 1973; Bornhorst and Rose, 1986; Keays et al., 1981; Saager et al.,

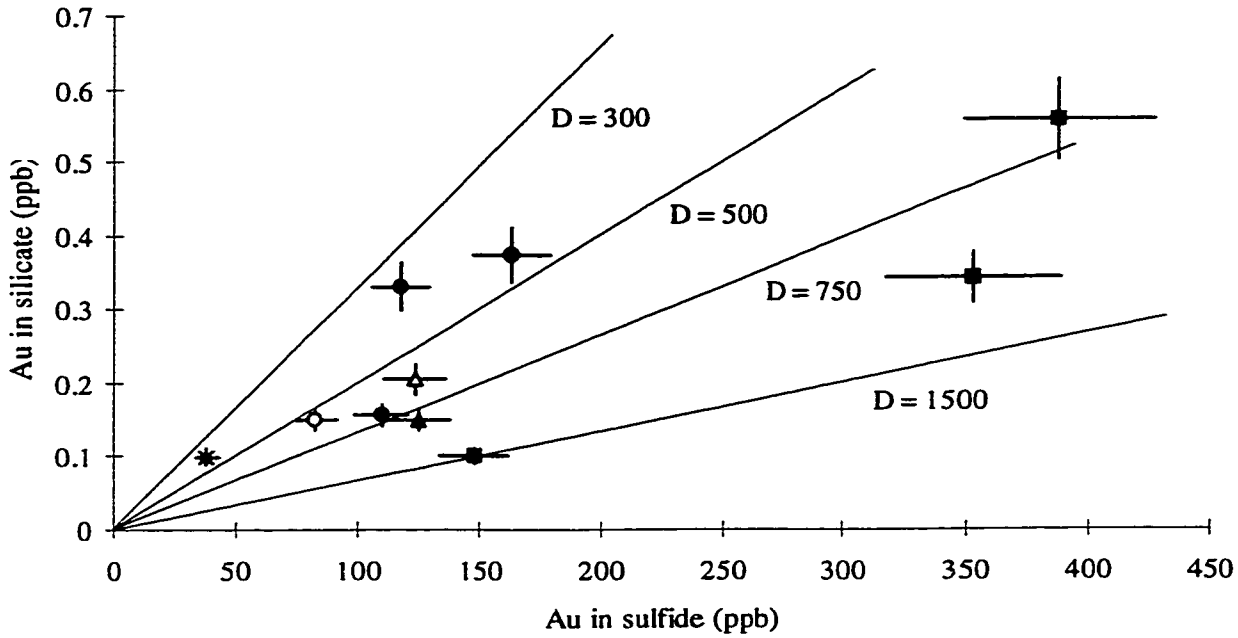

Figure 4-44. Partitioning of Au between sulfide and silicate phases in Bamble hyperites. Bars represent 10% error. Symbols show:
● Tvedestrand hyperite; o Tvedestrand amphibolite; * Tromoy coronitic gabbro;
■ Tromoy dyke-1 hyperite; ▲ Tromoy dyke-2 hyperite; Δ Tromoy dyke-2 amphibolite

1982; Korobeynikov, 1989). The partitioning of Au between sulfide liquids and silicate liquids has experimentally been determined to be in the range 1000 to 10000 (e.g. Stone et al., 1990; Crocket et al., 1991; Fleet et al., 1996, 1999; Crocket et al., 1997).

Variable D_{Au} values have been reported from natural assemblages. Mathez and Peach (1987) and Peach et al. (1990) reported values in excess of 10000 for basalts from mid-Atlantic Ridge. Korobeynikov (1986) estimated D_{Au} values in the range 1000-2000 for Quaternary calc-alkaline volcanic rocks from Guatemala. In contrast, Klöck and Palme (1988) determined a distribution coefficient of ~154 between immiscible sulfides and basaltic glasses from Disco Island basalts. Data from layered mafic intrusions indicate D_{Au} values in the range 250-850 (e.g. Keays and Campbell, 1981; Sharpe, 1982; Perendergast and Keays, 1989). The mean D_{Au} value for Bamble hyperites and amphibolites (700 ± 300), although lower than those estimated from laboratory experiments and those from mid-ocean ridge basalts, is in agreement with data from non-metamorphosed mafic intrusions.

II. Selenium

Selenium is a strongly chalcophile element. Sulfur and Se are very closely related in ionic size (1.84Å and 1.98Å, respectively) and commonly Se^{-2} substitutes for S^{-2} in sulfide minerals (Fischer and Leutwein, 1974).

Mass balance calculations indicate that sufides account for more than 90% of the Se in whole rocks. The distribution coefficient of Se between sulfide and silicate phases falls in the range 7000 to 18000 (Figure 4-45). This is in agreement with an earlier study by Peach and Mathez (1987) who estimated a distribution coefficient of 1 x 10^4 to 2 x 10^4 between immiscible sulfide globules and basaltic glasses from mid-Atlantic ridge basalts.

In-situ analysis of coexisting pyrrhotite-pyrite, by PIXE technique, showed that Se was almost equally distributed between the two minerals (Table 4-17). This is also supported by data from ore samples, where no preferential enrichment in Se was found in any of the coexisting pyrrhotite, pyrite, chalcopyrite, and pentlandite. Consistent partitioning of Se between coexisting sulfides has been reported from Sudbury and Bushveld (Paktunc et al., 1990) and Norilsk (Czamanske et al., 1992).

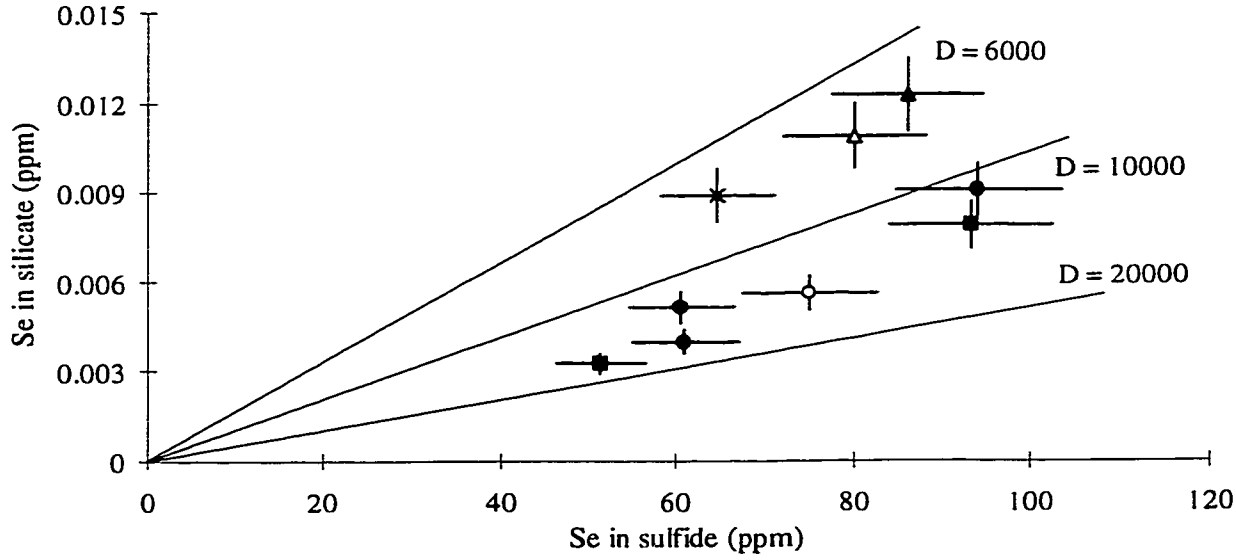

Figure 4-45. Partitioning of Se between sulfide and silicate phases in Bamble hyperites. Bars represent 10% error. Symbols as in Figure 4-44.

Table 4-17. Variations of Se (ppm) in coexisting pyrrhotite and pyrite in Tvedestrand hyperites

Sample No.	n*	pyrrhotite	pyrite
4004	4	71	76
4007	3	67	62
4009	4	74	81

* Number of analysis

III. Copper

Copper is almost equally distributed in both pyrite- and pyrrhotite-dominant concentrates (Table 4-16). Copper is known to partition strongly into the sulfide phase during magmatic crystallization (e.g. Naldrett, 1987). Minor sulfides in the Bamble hyperites account for 35-60% of the total Cu in their enclosing rocks. Distribution coefficient of Cu between sulfide and silicate phases varies from ~200 to ~1000 with a mean of 650 ± 250 (Figure 4-46)

Partitioning of Cu between sulfide and silicate phases is controlled by the initial abundances of Cu and S in the parent magma. Saturation of S early in the crystallization history of a magma would lead to scouring of Cu principally by sufides. The two dykes with the lowest D values are relatively depleted in S and Cu. The average D_{Cu} value (650 ± 250) for Bamble hyperites is

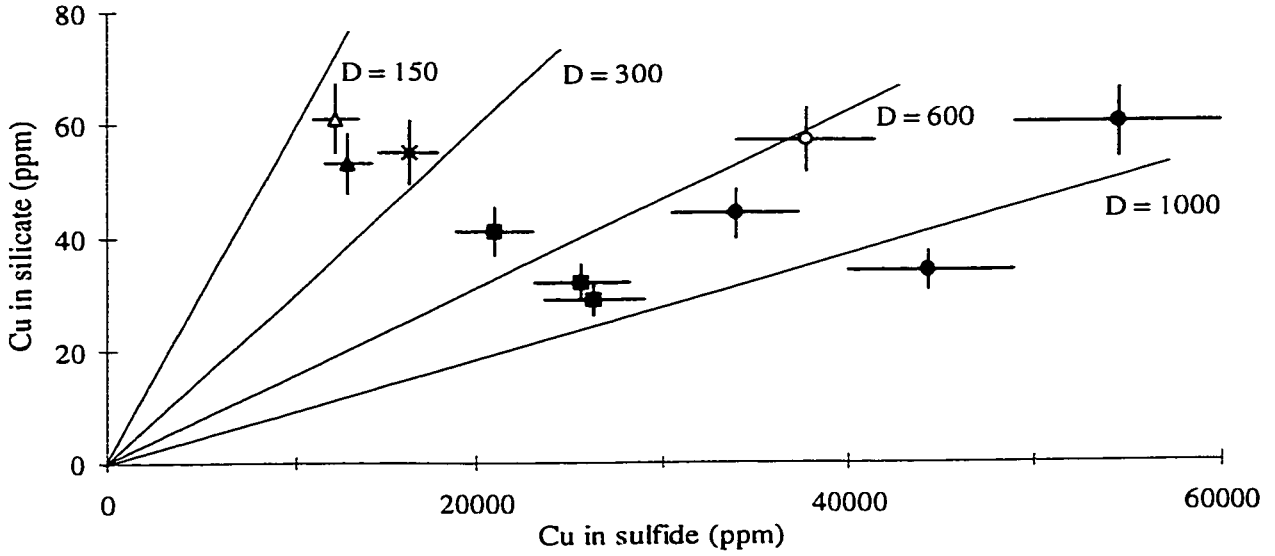

Figure 4-46. Partitioning of Cu between sulfide and silicate phases in Bamble hyperites. Bars represent 10% error. Symbols as in Figure 4-44.

in agreement with data from other studies on natural assemblages (c.f. Sharpe, 1982; Klöck and Palme, 1988). Partitioning of Cu between sulfide and silicate in synthetic basaltic melts has been determined to be around 250 (Rajamani and Naldrett, 1978).

IV. Bismuth

Bismuth is a strongly chalcophile element. Bismuth in igneous rocks is mainly carried by minor sulfides (Greenland et al., 1973; Kupčik et al., 1974). Concentration of Bi in the whole rocks is not known. Assuming that all Bi is carried by sulfides, mass balance calculations suggest an average Bi concentration of 0.065 ± 0.03 ppm in Bamble hyperites. Bismuth is slightly enriched in the pyrite-dominant concentrates (Table 4-16).

Concentration of Bi in mafic rocks varies in a wide range from 0.02 ppm to 0.2 ppm (Kupčik et al., 1974). Krauskopf (1979) estimated a mean Bi concentration of 0.1 ppm for basalts. Greenland et al. (1973) reported a mean Bi content of 0.033 ppm from Great Lake dolerites, Tasmania, and of 0.035 ppm from gabbros in Southern California Batholith. Zientek et al. (1990) determined Bi concentrations in the range 0.01 to 0.13 ppm in mafic rocks from J-M Reef, Stillwater Complex, Montana. Crustal abundance of Bi falls in the range 0.05-0.08 ppm (Greenland et al., 1973; Marowsky and Wedepohl, 1971; Wedepohl, 1995). Considering that some Bi might be present in other phases than sulfides, Bamble hyperites, containing at least 0.065 ± 0.03 ppm Bi, seem to be carrying normal abundance of this element.

V. Arsenic and Antimony

Sulfide concentrates are poor in As and Sb (mean = 40 ppm and 5 ppm, respectively). Mass balance calculations indicate that As and Sb in sulfides account for only a small fraction (commonly <5%) of these elements in the whole rocks. Arsenic (ionic radii As^{+3} = 0.58Å and As^{+5} = 0.46Å) substitutes for Si^{+4}, Al^{+3}, Fe^{+3}, and Ti^{+4}, and Sb (ionic radii Sb^{+3} = 0.76Å and Sb^{+5} = 0.62Å) substitutes for Fe^{+2} and Fe^{+3} in rock-forming minerals (Esson et al., 1965; Bauer and Onishi, 1974; Boyle and Jonasson, 1985). Arsenic and Sb in sulfides do not appreciably contribute to the whole rock budgets of As and Sb (c.f. Esson et al., 1965; Bauer and Onishi, 1974).

Both As and Sb are enriched in the pyrite concentrates (Table 4-16). No independent As or Sb minerals were found by microscope. The elements are carried as solid solution in sulfides. Enrichment of As and Sb in pyrite might be related to local remobilization and reprecipitation of the elements during silicate phase changes. Pyrite is known to be a suitable host for As and Sb in many types of rocks and mineral deposits (Bauer and Onishi, 1974; Boyle and Jonasson, 1973, 1985).

VI. Nickel and Cobalt

Nickel is equally distributed in both pyrrhotite and pyrite concentrates. Cobalt, however, is enriched in pyrite-dominant assemblages by a factor of 2 to 3.5. Nickel is carried mainly by pentlandite that occurs as lamellae and patches in both pyrrhotite and pyrite; it also occurs as an impurity in the two minerals.

Electron probe analysis of coexisting pyrite and pyrrhotite indicated that the former was invariably enriched in Co relative to the latter. Pyrite is known as a suitable host to Co (Hawley and Nichol, 1961; Graterol and Naldrett, 1971; Campbell and Jarkovsky, 1974; Vaughan, 1976).

The distribution coefficient of Ni falls in a narrow range from 100 to 150, excluding Tromoy coronitic gabbro (Figure 4-47-A). Nickel contents of magmas are largely controlled by the amount of normative olivine, and to a lesser extent, of pyroxene (e.g. Rajamani and Naldrett, 1978; Boctor and Yoder, 1983). Partitioning of Ni between sulfide and silicate phases in synthetic basaltic melts have been determined to vary from 25 to 250, increasing with decreasing initial MgO (MacLean and Shimazaki, 1976; Rajamani and Naldrett, 1978; Boctor and Yoder, 1983). Rajamani and Naldrett (1978) determined D_{Ni} values in the range 25-50 for basalts containing 20-10% MgO. The relatively high D_{Ni} values for Bamble hyperites corresponds to their low MgO contents (generally $< 8\%$).

The distribution coefficient of Co varies from 15 to 60 (Figure 4-47-B). As for Ni, the Co contents of magmas, and the partitioning of Co between sulfide and silicate phases, are controlled by normative olivine and pyroxene (Rajamani and Naldrett, 1978; Naldrett, 1979).

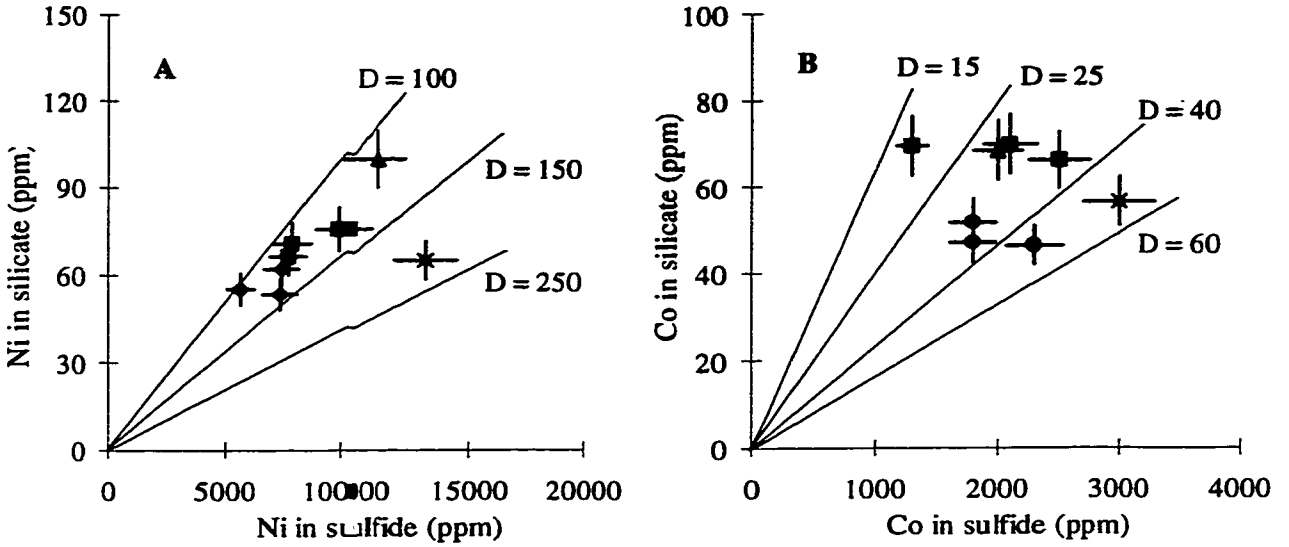

Figure 4-47. Partitioning of Ni (A) and Co (B) between sulfide and silicate phases in Bamble hyperites. Bars represent 10% error. Symbols as in Figure 4-44.

VII. Zinc, Molybdenum, Silver, and Lead

Zinc, Mo, and Ag are slightly enriched in the pyrite-dominant concentrates (Table 4-16). These elements are mainly carried by minor chalcopyrite. This is supported by data from ore sample, where chalcopyrite is enriched in Zn, Ag, and Mo by more than one order of magnitude relative to pyrite and pyrrhotite. The ionic radii of Ag^{+2} is very close to that of Cu^{+2}, permitting a limited replacement of Cu by Ag (Harris et al., 1984). Enrichment of the elements in the pyrite-dominant concentrates might be attributed to the presence of discrete chalcopyrite grains in the original rock that were recovered in the pyrite concentrates.

4-4-3. Metabasites

Basic rocks metamorphosed under amphibolite and granulite grades are widespread in Bamble. The basic rocks, known as metabasites, form sub-concordant to concordant minor dykes and sheets, parallel to the northeast-southwest regional foliation. The metabasites intruded older supracrustal rocks during the early stages of the Kongsbergian (Gothian) Orogeny (Smalley and Field, 1985; Starmer, 1991, 1993).

Unlike in the hyperites, the initial magmatic sulfide assemblage is rarely preserved in the metabasites. Primary pyrrhotite has extensively been replaced by pyrite ± magnetite. Sulfide concentrates, prepared from various metamorphic zones, are mostly of pyrite-dominant type consisting of pyrite-chalcopyrite-pentlandite. Two samples from the amphibolite zone are of pyrrhotite-dominant type, consisting of pyrrhotite-chalcopyrite-pentlandite; and one sample from the granulite zone contains both pyrite and pyrrhotite. Secondary sulfides as fracture filling and replacement bodies are common in the metabasites. Sulfide concentrates from three samples rich in secondary pyrite are also analyzed. Results are shown in Table 4-18.

4-4-3-A. Mass Balance

To investigate the role of metamorphism and sulfide phase changes on the variations of chalcophile elements, the geochemistry of sulfides from various metamorphic zones are compared to each other and to that of the whole rocks. Following, data for individual elements are discussed.

I. Gold

Minor sulfides in metabasites account for 50-75% of the total Au in the whole rocks. The distribution coefficient (D) of Au between sulfide and silicate phases varies from ~350 to ~1200, with most values falling in the range 600-1000 (Figure 4-48). Metabasites from various metamorphic zones display fairly similar D_{Au} values. However, data for the granulite

zone is based on only one sample, preventing a solid conclusion to be made. The average D_{Au} for metabasites (700 ± 250) is similar to that in the hyperites (700 ± 300).

Sample 4402 from transition zone B displays a relatively low partition coefficient. Microscopic studies indicated that most sulfide grains in this sample were partially replaced by secondary silicates, particularly chlorite, and magnetite. The chlorite was found, by electron microprobe, to be of Fe-rich type. Mobilization of S was possibly associated with a considerable removal of Au.

Table 4-18. Analysis of sulfide concentrates from Bamble metabasites

Element		Au	Ag	As	Sb	Bi	Se	Co	Ni	Cu	Zn	Mo	Pb
Units		ppb	ppm	ppm	ppm	ppm	ppm	ppm	ppm	ppm	ppm	ppm	ppm
Detection Limit		2.0	0.10	0.50	0.10	5.0	3.0	20	20	1.0	1.0	2.0	4.0
Zone A													
6801	Po	30	3.2	15	1.5	51	82	3500	15400	16300	378	9	60
7501	Po	74	4.7	28	11	35	88	2900	20900	26100	458	7.0	108
Zone B													
3902	Py	37	1.8	11	1.8	27	70	3600	13600	18000	201	7.0	66
3907	Py	39	1.1	11	1.3	7.8	56	3930	6766	18070	240	7.0	28
4101	Py	40	6.0	4.5	1.0	25	82	1300	2200	23700	817	5.0	114
4103	Py	53	6.9	37	0.3	41	70	3600	14800	18700	578	22	139
4401	Py	13	5.4	12	1.8	49	54	3700	5200	18400	243	10	95
4402	Py	8.0	3.1	12	1.4	22	95	4000	8200	20700	320	9.0	82
Zone C													
5405	Py	74	3.2	8	0.2	24	54	3800	6400	15100	104	14	73
5410	Py	57	3.7	16	4.7	22	69	4500	10400	16600	372	4.0	123
5414	Py	45	3.5	24	8.8	15	87	3900	11700	18800	418	7.0	146
5420	Py	38	8.9	14	1.2	28	80	3700	26500	38300	439	22	157
5422	Py	69	7.9	35	0.4	35	110	4700	1000	7500	1220	7.0	58
Zone D													
3805-1	Po	76	3.8	73	1.9	13	61	3000	16600	13200	547	9.0	86
3805-2	Py	120	18	140	8.0	44	78	5200	23400	11400	643	15	472
Secondary Pyrite													
6401	Py	348	6.5	39000	140	62	56	23000	18200	17500	276	12	349
6403	Py	832	6.7	2000	160	42	75	3500	7500	22900	207	57	387
6408	Py	185	4.9	1500	54	28	100	2700	3000	6100	310	5.0	292

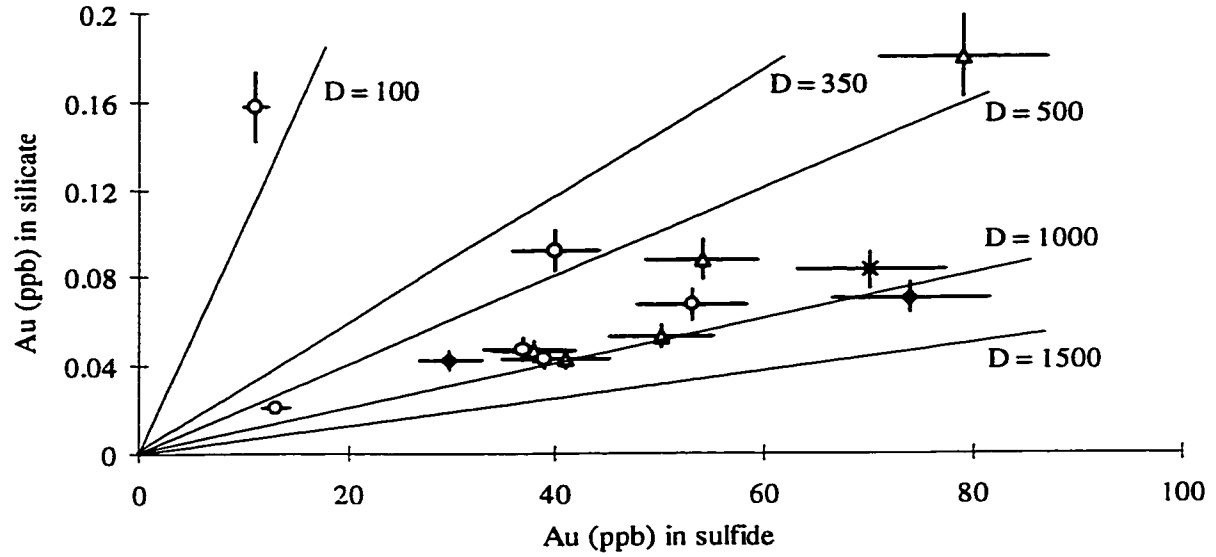

Figure 4-48. Partitioning of Au between sulfide and silicate phases in Bamble metabasites. Bars represent 10% error. Symbols represent:
♦: Zone A ○: Zone B ▲: zone C ✳: Zone D

II. Selenium

As in the hyperites, almost all Se is carried by minor sulfides. Distribution coefficient of Se between sulfide and silicate phases varies from 5000 to 20000 (Figure 4-49). No distinction can be made between various metamorphic zones with respect to the concentration of Se.

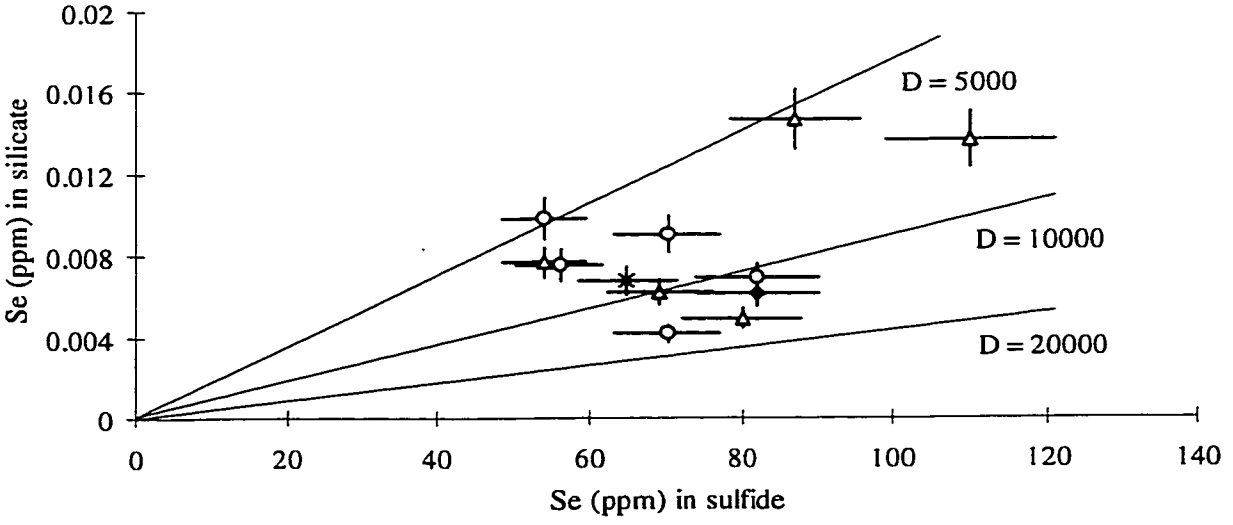

Figure 4-49. Partitioning of Se between sulfide and silicate phases in Bamble metabasites. Bars represent 10% error. Symbols as in Figure 4-48.

III. Bismuth

The Bi budget of disseminated sulfides in metabasites (28 ± 10 ppm) is similar to that in hyperites (24 ± 9 ppm). Provided that all Bi is carried by sulfides, the concentration of Bi in whole rocks would be in the range 0.04 to 0.1 ppm. As in hyperites, the metabasites also carry normal abundance of Bi compared to the mean composition of mafic rocks.

IV. Copper

Minor sulfides account for 45-70% of Cu in the whole rocks (Table 4-18) reflecting the strong chalcophile tendency of this element. Distribution coefficient of Cu in the metabasites (485 ± 120) is close to that in the hyperites (640 ± 250). The lower D_{Cu} values for metabasites might be attributed to the initially lower concentrations of Cu in the parent magmas. The mean contents of Cu in the hyperites and metabasites are 90 ppm and 60 ppm, respectively.

V. Nickel and Cobalt

Distribution coefficient of Ni in metabasites is in the same range as in the hyperites (D_{Ni} = 135 and 127, respectively). Cobalt, however, displays a higher value of partitioning in metabasites relative to hyperites (D_{Co} = 65 and 36, respectively).

VI. Arsenic and Antimony

Concentrations of As and Sb in metabasites are similar to those in hyperites. Exceptions are secondary sulfides that are considerably enriched in As and Sb (Table 4-18). Secondary sulfides are also enriched in Au.

4-4--3-B. Secondary sulfides

Secondary sulfides occurring as overgrowth and fracture filling are common in the metabasites, and in some samples dominate interstitial sulfides. Pyrite is the principal mineral; marcasite and chalcopyrite may accompany pyrite, or occur as discrete grains. Analysis of sulfide concentrates from three samples with abundant secondary pyrite indicated a significant enrichment in As, Sb, and Au (Table 4-18).

4-4-4. Fe-Ni-Cu ores

Fe-Ni-Cu ores are locally associated with the hyperites. During hydration and recrystallization of the hyperites, the primary, pyrrhotite-rich ores were variably recrystallized to secondary, pyrite-rich products. Concentrates of coexisting sulfide minerals from the primary and recrystallized ores were analyzed for distribution of chalcophile elements. Concentration of elements in bulk ores are estimated from the relative abundances of individual minerals. The results are shown in Table 4-19.

4-4-4-A. Primary Orthomagmatic Ore

Pyrrhotite coexisting with chalcopyrite carries relatively lower contents of chalcophile elements (Table 4-19). Gold is enriched in chalcopyrite by more than one order of magnitude (Figure 4-50). A preferential concentration of Au in chalcopyrite has been reported from several magmatic Ni-Cu ores (e.g. Keays and Davidson, 1976; Naldrett, 1987; Jonasson et al., 1987; Czamanske et al., 1992). Replacement of Ag^{+2} for Cu^{+2} was indicated by Harris et al. (1984).

Selenium is similarly distributed between pyrrhotite and chalcopyrite. Equal partitioning of Se between coexisting sulfides has been reported from magmatic Ni-Cu deposits in Sudbury and Bushveld (Paktunc et al., 1990) and Norilsk (Czamanske et al., 1992).

4-4-4-B. Recrystallized Ore

Recrystallized ores are characterized by variable replacement of pyrrhotite by pyrite. Analysis of coexisting pyrrhotite-pyrite-chalcopyrite-pentlandite indicates that pyrrhotite is invariably depleted in Au, As, and Sb relative to other minerals. Distribution of Au in coexisting sulfides from recrystallized ores is shown in Figure 4-50. Selenium is similarly distributed among the coexisting minerals (Table 4-19). Silver is enriched in the order chalcopyrite >Pyrite = pyrrhotite = pentlandite. Bismuth in most primary and recrystallized ores occurs at or below the detection limit of 5 ppm. In two samples with Bi levels above the detection limit of 5 ppm, this element is similarly distributed between coexisting minerals.

Table 4-19. Concentration of elements in coexisting sulfides from Bamble Ni-Cu ores

Element		Au	Ag	Ir	As	Sb	Bi	Se	Cu	Zn	Pb	Co	Ni
Units		ppb	ppm	ppb	ppm	ppm	ppm	ppm	ppm	ppm	ppm	ppm	ppm
Detection Limit		2.0	0.4	5.0	0.5	0.1	5.0	3.0	1.0	1.0	5.0	20	20
A. Primary, pyrrhotite-rich ore													
91001	Po	14	4.7	<5	2.7	0.2	<5	83	4630	14	26	940	26039
	Ccp	150	51.6	<5	39	3.7	<5	73	>10%	597	44	800	5108
	Bulk ore*	23.5	8.0	<5	5.5	0.45	<5	82		55	27	930	24570
91010	Po	25	1.3	10	1.6	0.1	23	42	3026	45	21	340	12537
	Ccp	370	36.3	<5	8.6	0.9	33	59	>10%	680	84	58	513
	Bulk ore	59.5	4.8	<5	2.3	0.18	24	48		108	27	312	11340
91024	Po	2.0	4.0	<5	0.5	0.1	n.d.	37	n.d.	50	n.d.	1800	12000
	Ccp	24	33	10	12	0.9	n.d.	44	n.d.	530	n.d.	830	4100
	Bulk ore	5.3	5.45	<5	1.1	0.14	n.d.	39	n.d.	74		1650	10600
91027	Po	5.0	3.3	<5	0.5	0.1	<5	22	9419	12	n.d.	2100	8102
	Ccp	27	18	<5	17	0.1	<5	34	>10%	600	n.d.	610	1600
	Bulk ore	8.3	5.5	<5	3.0	0.1	<5	24		100		1875	7125
91028	Bulk ore	12	1.2	<5	4.1	0.1	<5	21	2400	88	32	1700	14900
B. Recrystallized, pyrite-rich ore													
91003	Po	50	n.d.	<5	11	0.7	n.d.	21	n.d.	n.d.	n.d.	1000	29000
	Py	103	n.d.	<5	5.5	0.8	n.d.	22	n.d.	n.d.	n.d.	2500	15000
	Ccp	333	n.d.	<5	1.0	0.2	n.d.	15	n.d.	n.d.	n.d.	1600	800
	Bulk ore	92	n.d.	<5	8.5	0.75	<5	20	n.d.	n.d.	n.d.	1746	22598
91004	Po	13	2.7	32	0.5	0.1	19	48	3896	44	30	1300	26186
	Py	97	3.0	43	29	2.1	24	71	7710	97	57	3700	16203
	Bulk ore	34	2.8	35	8.0	0.6	20	54	4850	57	37	1900	23690
91006	Po	25	2.0	21	2.4	0.4	<5	25	3268	2.0	18	300	21168
	Py	109	1.7	<5	5.6	1.7	7.0	15.0	7441	23	22	4100	14963
	Pentl.	53	2.0	22	0.5	1.3	<5	25	n.d.	n.d.	n.d.	1500	250000
	Bulk ore	51	1.9	20	3.2	0.84	<5	22	4355	8.0	18	1500	30750
91007	Po	33	3.9	32	0.5	0.1	6.0	41	11043	11	10	1500	13524
	Py	165	4.4	5	20	1.5	5.0	41	11327	176	56	3100	5484
	Bulk ore	66	4.0	25	5.4	0.45	6.0	41	11115	52	21	1900	10755
91011	Po	34	9.6	<5	3.1	0.1	<5	70	10203	6.0	50	1300	26879
	Py	124	0.8	<5	75	0.1	12	63	3454	4.0	5.0	9600	401
	Ccp	35	51	<5	6.3	0.8	<5	78	>10%	631	12	150	2334
	Pentl	148	18	<5	9.2	0.3	<5	54	36143	34	86	12000	250000
	Bulk ore	45	11	<5	17	0.14	<5	65	9530	38	44	2285	26500

* Data for bulk ores are calculated from the mass ratios of the coexisting sulfides.

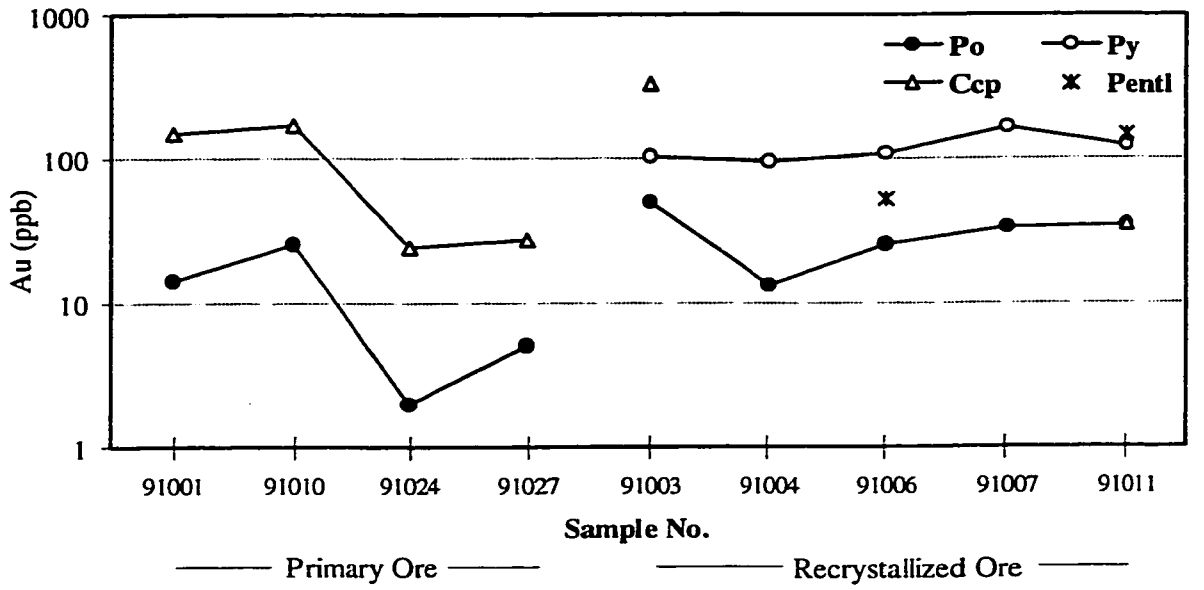

Figure 4-50. Variations of Au among coexisting minerals from primary and recrystallized Fe-Ni-Cu ores; Bamble.

The mean concentration of Au in the Ni-Cu ores is considerably lower than that in the disseminated sulfides in hyperites (40 and 155 ppb, respectively). The Ni-Cu ores are also depleted in other chalcophile elements (Figure 4-51).

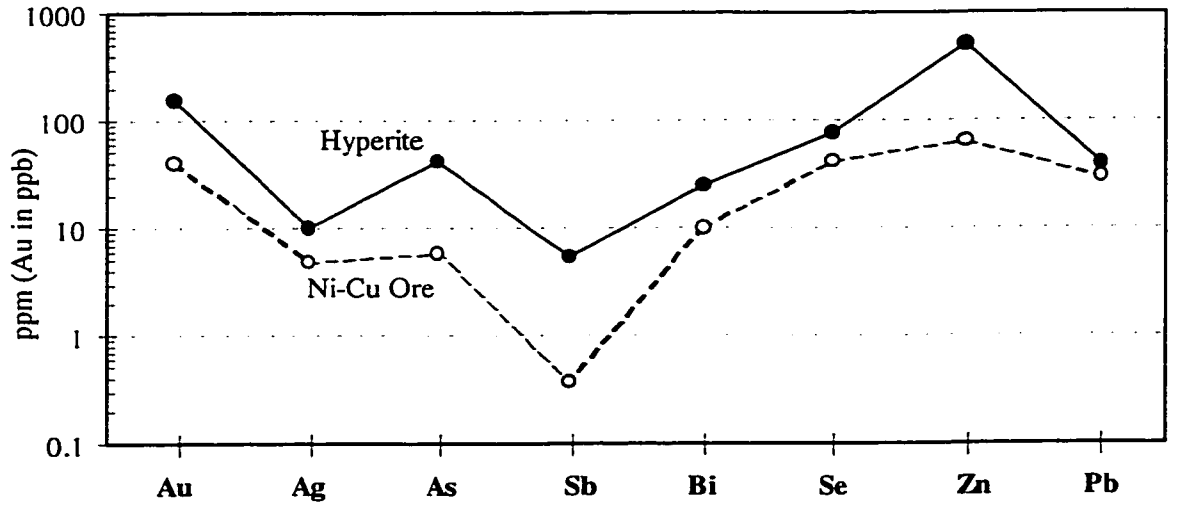

Figure 4-51. Concentration of chalcophile elements in disseminated sulfides in hyperites and their associated Ni-Cu ores.

The Bamble Ni-Cu ores are depleted in Au by one order of magnitude compared to similar deposits elsewhere (c.f. Hoffman et al., 1979; Naldrett, 1987; Barnes et al., 1987; Boyd et al., 1987; Czamanske et al., 1992). They are also strongly depleted in Ir. The abundance of Ir in most Ni-Cu ores and in all sulfide concentrates from the host hyperites was found to be below the detection limit of 5 ppb. Concentration of Ir in Ni-Cu ores associated with mafic rocks has been reported to be in the range 20-100 ppb (Hoffman et al., 1979; Naldrett, 1987; Barnes et. al., 1987; Barnes and Naldrett, 1985).

4-4-5. Discussion

Analysis of pyrite and pyrrhotite concentrates from hyperites indicates an enrichment of the chalcophile elements, Au, Se, Bi, and Ag, in pyrite by a factor of 1.2 to 1.5. Copper and Ni are similarly distributed in the two fractions. Cobalt, As, and Sb are variably enriched in pyrite. Enrichment of trace elements in the pyrite concentrates might be attributed to:

1- Uneven distribution of the elements in the initial pyrrhotite, or pyrrhotite monosulfide solid solution (Po_{mss}), with preferential replacement of Po_{mss} grains rich in chalcophile elements. Microscopic studies indicated no textural differences between the pyrite- and pyrrhotite-dominant assemblages. The accessory minerals, chalcopyrite and pentlandite, are equally associated with both pyrite and pyrrhotite.

2- The presence of secondary pyrite rich in the trace elements. In preparing the mineral concentrates, ultimate care was taken to select samples free of secondary sulfides. However, the presence of sub-microscopic sulfides of secondary origin can not be ruled out. Analysis of secondary overgrowth and fracture filling pyrite in metabasites indicated a considerable enrichment of As and Au relative to the primary interstitial sulfides.

3- Involvement of surrounding minerals (silicates and oxides) in the reactions. Considerably higher concentrations of Co in the pyrite-dominant assemblages can not be explained by a closed system process. Cobalt in both pyrite and pyrrhotite is carried in solid solution; no

independent cobalt mineral was found. Excess Co in the pyrite-dominant assemblages might have been provided by surrounding mafic silicates during alteration of olivine and pyroxenes. The higher contents of As and Sb in the pyrite-dominant assemblages might also be attributed to this process.

4- Increase in concentration due to mass reduction. Earlier in Section 4-3 it was discussed that pyrrhotite was replaced by pyrite according to the reaction:

$$6FeS + 2O_2 \rightarrow 3FeS_2 + Fe_3O_4$$

This reaction requires a considerable removal of Fe to produce one mole pyrite at the expense of two moles pyrrhotite. This could have led to an increase in the concentration of trace elements in the newly formed pyrite relative to the initial pyrrhotite. The liberated Fe was, at least partly, consumed at the reaction site to form magnetite. Mass balance calculations suggest that the pyrrhotite-pyrite phase change was simply an oxidation reaction, without significant addition or removal of chalcophile elements.

For granulite grade metabasites, Cameron (1993a, 1993b) suggested that oxidation of pyrrhotite to pyrite was controlled by internal buffering of the rocks with no need to introduction of a fluid borne oxidant. According to Cameron, the oxygen required for the oxidation was provided by reduction of hematite to magnetite upon cooling below 600°C:

$$6FeS + 12Fe_2O_3 \rightarrow 3FeS_2 + 9Fe_3O_4$$

Cameron (1989a, 1993a) showed that hematite-rich ilmenite (hemoilmenite) was the stable oxide phase at peak metamorphic temperature, around 800°C. During cooling from peak metamorphism, the ilmenite-hematite solvus was intersected at approximately 740°C leading to exsolution of ilmenite and hematite. Further cooling down to below 600°C, was associated with the formation of magnetite lamellae in ilmenite grains by reduction of hematite.

Coronitic gabbros and hyperites are characterized by the presence of pyrrhotite as the main sulfide phase. The amphibolitized rocks, however, display varying degrees of replacement of pyrrhotite by pyrite, proportional to the extent of amphibolitization. This suggests an external

buffering for the sulfide phase change, apparently by the same fluids involved in hydration and amphibolitization of gabbros (c.f. Cameron, 1989b, 1993a, b). The similar abundances of S and chalcophile elements in the gabbros (hyperites) and their amphibolitized equivalents indicate that oxidizing capacity of the fluids was buffered by mafic silicates, and no significant desulfidation occurred.

Mass balance calculations indicate that minor sulfides in hyperites and metabasites account for up to 85% of the total Au in these rocks. The mean D_{Au} values for Bamble hyperites (700 ± 300) and metabasites (700 ± 250), although lower than those estimated from laboratory experiments, are in agreement with data from other mafic intrusions (c.f. Keays and Campbell, 1981; Sharpe, 1982; Perendergast and Keays, 1989). The large variation in D_{Au} values reported in the literature suggests that partitioning of Au between sulfide and silicate phases in magmatic systems is not a simple and invariable process.

High D_{Au} values, as reported from mid-ocean ridge basalts, have been interpreted to be the result of equilibration of sulfides with large reservoirs of magmas (Campbell, 1983; Mathez and Peach, 1989). Distribution of Au between sulfide and silicate phases is also controlled by the initial abundance of Au in the parent magma. Crocket et al. (1997) reported a marked increase in D_{Au} value, from ~1.21 x 10^3 to 13.6 x 10^3, with an increase in the initial Au from ppb to ppm levels. The relatively low D_{Au} values in Bamble hyperites and metabasites compared to data from experiments might be attributed to the low Au contents of the parent magmas.

The initial abundance of Au is dictated by the composition of the source region and the magnitude of partial melting and magmatic crystallization. Korobeynikov and Pertsev (1995) reported a wide range in the abundance of Au in various basaltic rocks worldwide. The authors showed that in all geological settings, there are basalts with low levels of Au (<0.5-2.2 ppb) and also elevated ones (2.8-4.8 ppb).

Alternatively, the low D_{Au} values may be attributed to the mobility of Au in late-magmatic or post-solidus processes. Keays and Kirkland (1972) reported a post-cumulus transport and redistribution of precious metals, by Cl-rich fluids, from Thomson River Copper Mine, Australia. A similar remobilization of precious metals was documented by Boudreau et al. (1986) from Stillwater and Bushveld Complexes. Post-solidus re-equilibration of sulfides with silicate-oxide assemblages might also result in the breakdown of sulfides and loss of S and precious metals (von Gruenwaldth et al., 1986; Naldrett and Lehmann, 1988; Cameron, 1989b, 1993).

Partitioning of Au is extremely sensitive to intensive variables such as f_{O2} and f_{S2} which may differ from one system to the other (Peach et al., 1990; Crocket et al., 1992). Crocket et al. (1992) showed that partitioning of Au between Fe-Ni sulfide liquid and basaltic melt decreased from 3030 ± 980 at iron-silica-fayalite (IQF) buffer to 1400 at iron-wustite (IW) buffer. The low D_{Au} value recorded for Disco Island basalts may be attributed to the reduced nature of the magmas.

Textures and mineral paragenesis indicate that the interstitial pyrrhotite-chalcopyrite-pentlandite assemblages in the hyperites are of primary magmatic origin unaffected by metamorphism. Primary sulfide paragenesis is rarely preserved in the metabasites; pyrrhotite has been replaced by pyrite ± magnetite. However, similar concentrations and distribution coefficients of chalcophile elements in hyperites and metabasites suggest that metamorphism and sulfide phase changes did not significantly alter the initial distribution of the chalcophile elements.

The consistency of D_{Au} values for Bamble hyperites and metabasites with the common range of the D_{Au} values in mafic rocks suggests that no post-solidus removal of Au occurred. Both hyperites and metabasites carry normal concentrations of S relative to the mean composition of mafic rocks elsewhere. Any post-solidus removal of Au would be expected to lead to dramatic reduction of the initial D_{Au} values. The relatively low D_{Au} value in one metabasite sample is attributable to such process. This sample is characterized by partial replacement of

sulfides by Fe-rich chlorite and magnetite. Mobilization of S was associated with a considerable removal of Au.

The mobilized S was reprecipitated as secondary fracture filling and replacement pyrite. The secondary pyrite is also enriched in As and Au, implying a genetic relation between the two elements. Arsenic is a common associate of Au in lode gold deposits (e.g. Boyle, 1979; Roberts, 1987; Kerrich, 1989; Groves et al., 1992, 1998). Au-As minerals are not known in nature. Arsenic is usually involved in the mobilization and transport of Au as a result of formation of transient, thermodynamically unstable and readily reduced Au-As compounds (Plant et al., 1989). Reintroduction of Au was also indicated by Cameron (1993b) who reported the presence of sulfides and retrogressive biotite and epidote on joint surfaces in Tromoy metabasites.

Distribution coefficients of Se and Cu in both hyperites and metabasites fall in the same range as in the non-metamorphosed mafic rocks, indicating that the immiscible sulfide globules formed in equilibrium with silicate liquid, and that no significant post-solidus modifications occurred. Relatively high D_{Ni} values for both hyperites and metabasites can be attributed to the low-Mg nature of the parent magmas.

The Ni-Cu ores associated with the hyperites are significantly depleted in most chalcophile elements relative to the disseminated sulfides in their host rocks. The lower concentration of the elements in the ores may be attributed to assimilation of sulfidic rocks poor in chalcophile elements, rapid crystallization and precipitation of sulfides, or both.

Assimilation of sulfide-rich country rocks has been proposed to be of critical significance in the formation of magmatic Ni-Cu deposits (e.g. Groves et al., 1979; Green and Naldrett, 1981; Naldrett, 1981; Lesher et al., 1984). Assimilation of country rocks in Bamble is supported by sulfur isotope data and by S/Se ratios. This is discussed in Chapter 5. Assimilation of sulfidic rocks may lead to local oversaturation of magma in S and rapid crystallization and precipitation of sulfides. This would prevent the immiscible sulfides from

efficiently removing the chalcophile elements of the silicate liquid. Earlier in Chapter 2 it was shown that Bamble supracrustal rocks are considerably depleted in Au relative to the mean composition of the continental crust. Assimilation of the Au-depleted rocks could lead to a further drop in the concentration of Au in the magma.

The data presented on the distribution of Au in pyrite and pyrrhotite conflicts with an earlier study by ion probe technique (Figure 4-42), where Cameron (1993a) reported a considerable depletion of Au in pyrite coexisting with pyrrhotite in Tvedestrand hyperite. Gold was detected to be well above the detection limit of 10 ppb in pyrrhotite, but below that in pyrite. The mean concentration of Au in pyrrhotite (110 ppb, excluding one spot with 430 ppb Au) is comparable to that from neutron activation analysis (105 ppb), both on samples from the same dyke.

The relatively lower concentrations of Au in pyrite, as detected by ion probe, might be attributed to:

1) variable partitioning of Au among coexisting phases;
2) concentration of Au at grain boundaries during pyrite growth;
3) a combination of the above processes.

Chalcopyrite is usually present as an accessory phase in the composite pyrite-pyrrhotite grains. Data from ion probe analysis of composite sulfide grains in mafic rocks from Lewisian Complex, Scotland, and Bamble, Norway, show a strong partitioning of Au into chalcopyrite, by up to one order of magnitude, relative to pyrrhotite and pyrite (Cameron, 1993a). In a study of Au partitioning among pyrrhotite, pyrite, chalcopyrite, and magnetite in Au-saturated chloride solutions at high temperatures, Cygan and Candella (1995) demonstrated an enrichment of Au in pyrrhotite, by a factor of 1.5-3, relative to pyrite. The same study showed a very strong partitioning of Au, by up to 2.5 orders of magnitude, into chalcopyrite relative to the coexisting pyrite and pyrrhotite. All tests were carried out under pyrrhotite-pyrite-magnetite buffer conditions. Preferential partitioning of Au into chalcopyrite has frequently been reported from magmatic Ni-Cu ores (e.g. Rowe, 1969; Keays and Davidson,

1976; Naldrett, 1987; Jonasson et al., 1987; Czamanske et al., 1992; present study). Chalcopyrite from Bamble Ni-Cu ores is enriched in Au by more than one order of magnitude, relative to the pyrrhotite.

Using a radioactive tracer method, Mironov and Galetiy (1979) showed that in pyrite crystals, Au occurs on crystal faces as microinclusions, or is dispersed in the near surface part of the grains. In pyrrhotite and chalcopyrite, however, most Au was found to be irregularly distributed within mineral grains. Pyrite and pyrrhotite have different crystal lattices. In pyrite crystals with close packing lattices, Au is generally not incorporated into the crystal lattice and is displaced during crystal growth towards the edges, whereas in pyrrhotite with Ni-As type lattice, it is trapped by lattice defects and forms structures of the injected solid solution type (Mironov and Galetiy, 1979). The authors further showed that in chalcopyrite with close packing lattice, Au is present as substitutional isomorphism. Concentration of Au at mineral surfaces and mineral grain boundaries has is also reported by Parry (1984) and Cygan and Candella (1995).

5. Sulfur Isotope Geochemistry

5-1. Introduction

Sulfur isotope ratios have been widely used to investigate the conditions of formation of ores and rocks. Sulfur isotope analysis has traditionally been carried out by combustion of mineral powders, 10 to 30 mg in weight, to extract SO_2 for mass spectrometry. Modern mass spectrometers, of increased sensitivity, have helped to reduce the quantities of the material combusted to below 1 mg. However, conventional combustion methods provide the average isotopic composition of the bulk materials. Fine-scale variations in isotopic ratios, that might be of critical importance, are not revealed.

Determinations of isotopic composition of sulfides when they occur as fine disseminated grains, as in normal sedimentary, igneous, or metamorphic rocks, are subject to two more uncertainties. Extraction of SO_2 from bulk rocks by leaching of sulfides, as in the Kiba method, or preparation of sulfide concentrates, are tedious and give, at best, the average isotopic composition of all sulfide phases present. Sulfides are susceptible to remobilization and reprecipitation, and it is common to find more than one generation of sulfides occurring even at a hand specimen scale. With bulk analysis, no distinction can be made between various sulfide generations and different sulfide minerals.

Techniques of in-situ analysis with high spatial resolution allow selective analysis of sulfide grains and detection of subtle changes in isotope ratios. Application of ion microprobe technique to the study of sulfur isotopes in the late 80's showed that considerable variations in $\delta^{34}S$, up to 30‰, might exist in a 0.5 mm interval (Eldridge et al., 1988; McKibben and Eldridge, 1989).

Two techniques are currently being used for the high spatial resolution analysis of sulfur isotope ratios in geological materials: Secondary Ion Mass Spectrometry (SIMS) and Laser Vaporization Mass Spectrometry (LVMS) or laser microprobe. SIMS utilizes an ion beam to

produce positively charged secondary ions from a mineral surface, which are analyzed by mass spectrometers for sulfur isotope ratios. The spatial resolution (spot sizes 20 to 60 μm in diameter and 2-5 μm in depth) well exceeds that of the LVMS. However, large mineral-specific fractionations during analysis, up to 65‰, and relatively poor precision, $1\sigma = 0.5\text{-}2‰$ (Eldridge et al., 1987; Chaussidon and Lorand, 1990; Beaudoin and Taylor, 1994) restrict the application of the technique.

5-2. Laser Microprobe

Laser microprobe provides the measurement of stable isotope ratios with high spatial resolution and high precision. The spatial resolution is limited by the sample size required by the mass spectrometer. Modern mass spectrometers permit a spatial resolution down to 30 microns. Precision or reproducibility are demonstrated to be in the same range as in the conventional methods at $1\sigma = 0.2‰$ (Crowe et al., 1990, Kelley and Fallick, 1990, Crowe and Vaughan, 1996; present study).

The technique includes a laser system that is used to melt or vaporize small areas of a sample to release gases that can be analyzed in the mass spectrometer. Laser microprobes in isotopic analysis were first used to extract noble gases from meteoric samples (Megrue, 1967). Jones et al. (1986) and Franchi et al. (1986) reported success extracting isotopes of S, O, and C with a Nd-YAG laser. During the past decade, techniques of laser microprobe analysis have been developed and successfully applied to geological materials by several workers and research groups (e.g. Franchi et al., 1989; Smalley et al., 1989, 1992; Crow et al., 1990; Sharp, 1990; Kelley and Fallick, 1990; Fallick et al., 1992; Crowe and Vaughan, 1996).

5-2-1. General Considerations

The word "laser" is an acronym for the most significant feature of laser action: *light amplification by stimulated emission of radiation*. There are many different kinds of lasers, but they all share a crucial element; each contains material capable of amplifying radiation. This material is called the gain medium, because radiation gains energy passing through it. The

physical principle responsible for this amplification is called stimulated emission. The principles of lasers and their functions have been explained in numerous textbooks (e.g. Milonni and Eberly, 1988; Svelto, 1989).

Fundamental laser properties such as the wavelength and threshold conditions are determined by the active species, or gain mediums, such as Nd^{+3} in Nd-YAG (Nd-doped Yttrium-Aluminum Garnet) lasers. Lasers can be operated in either "normal mode (fixed Q)" or "Q-switched mode". The "Q" or "quality factor" refers to the efficiency of energy storage in the laser. In the normal mode of operation, laser output consists of a series of microsecond spikes which continue until the pump light can no longer supply enough energy for lasing. Continuous wave (CW) operation is achieved by high-power pumping rates on high gain materials with good thermal properties, such as Nd-YAG. "Q-switching" is a technique used to generate shorter duration (nanosecond) laser pulses and higher peak powers. Various groups have reported success using "CW" lasers (e.g. Kelley and Fallick, 1990; Crowe et al., 1990; Crowe and Valley, 1992; Crowe and Vaughan, 1996).

The size of the reacted volume is a function of the irradiance (wavelength and incident energy per unit time per unit surface area), the mineral matrix absorbing the radiation, and the chemical reaction produced by ignition of the mineral in an oxidizing atmosphere. Too low an irradiance will merely lead to heating, and too high an irradiance will generate shock waves and ejection of the target materials. Optimum irradiance for melting and vaporization to occur is in the range 10^9-10^{12} Wm^{-2} (Ready, 1971).

Lasers commonly used in stable isotope geochemistry are CO_2, Nd-YAG or Nd-glass, and Ar. The characteristics of each laser are different so that no laser may be ideal in all respects. Nd-YAG lasers with operating wavelength of 1.064 μm are suitable for metallic and opaque minerals. For optically clear materials, such as silicates and carbonates, high transmissivity at 1 μm makes Nd-YAG systems less appropriate. For these materials, CO_2 lasers are more suitable, as radiation at 10 μm is absorbed by all oxygen bearing compounds.

Two different analytical techniques have been developed for sulfur isotope analysis using laser microprobe: laser-SF_6 and laser-SO_2. The laser-SF_6 technique uses F_2 to oxidize sulfur and to produce SF_6 for mass spectrometry (Rumble et al., 1993; Beaudoin and Taylor, 1994). Reproducibility of runs, or analytical precision, has been shown to be comparable to those of the conventional methods.

The laser-SO_2 technique uses O_2 to oxidize sulfur and to produce SO_2 for mass spectrometry. The technique has an associated instrumental sulfur isotope fractionation (up to 6‰) which is mineral-specific, and varies with the chemical composition of the matrix and laser operating conditions (Crowe et al., 1990; Fallick and Kelley, 1990). The laser-SO_2 technique yields a mineral-dependent precision ranging from 0.1‰ to 0.5‰ (Crowe et al., 1990; Fallick and Kelley, 1990). Experimental considerations related to the analysis of sulfur isotopes with laser-SO_2 technique have been discussed by Kelley and Fallick (1990), Crowe et al. (1990), and Fallick et al. (1992).

5-2-2. University of Ottawa Laser Microprobe System

The main components of the laser microprobe system include a Nd-YAG laser and a microscope connected to a gas-source isotope-ratio mass spectrometer via a cryogenic extraction and separation line (Figure 5-1). The laser is a Spectron 130 Nd-YAG capable of operating in continuous wave (CW) as well as pulsed (Q-switched) mode at 1064 nm, and has an average power output of 11 W. The microscope allows to locate the desired spots for analysis; the image under microscope can be viewed also on a video monitor that permits safe viewing of the sample during laser combustion. The mass spectrometer is a VG SIRA-12 triple collector with microinlet.

The sample chamber, consisting of a stainless steel holder 1.5″ across and 2″ deep and a removable quartz window, is mounted on the microscope stage and can be adjusted in all directions. The diameter of laser beam is adjustable and can be set from ~50 to ~500 μm. The laser beam is reflected onto the sample chamber by a high reflectivity mirror.

The sample chamber is connected to a stainless steel cryogenic trap of triple loop design through a flexible stainless steel tube, 1/8" ID, that permits articulation of the sample chamber for replacing samples and for focusing. Gas is moved directly from the cryogenic trap to the small volume (0.2 ml) inlet system of a VG SIRA-12 triple collector mass spectrometer for analysis.

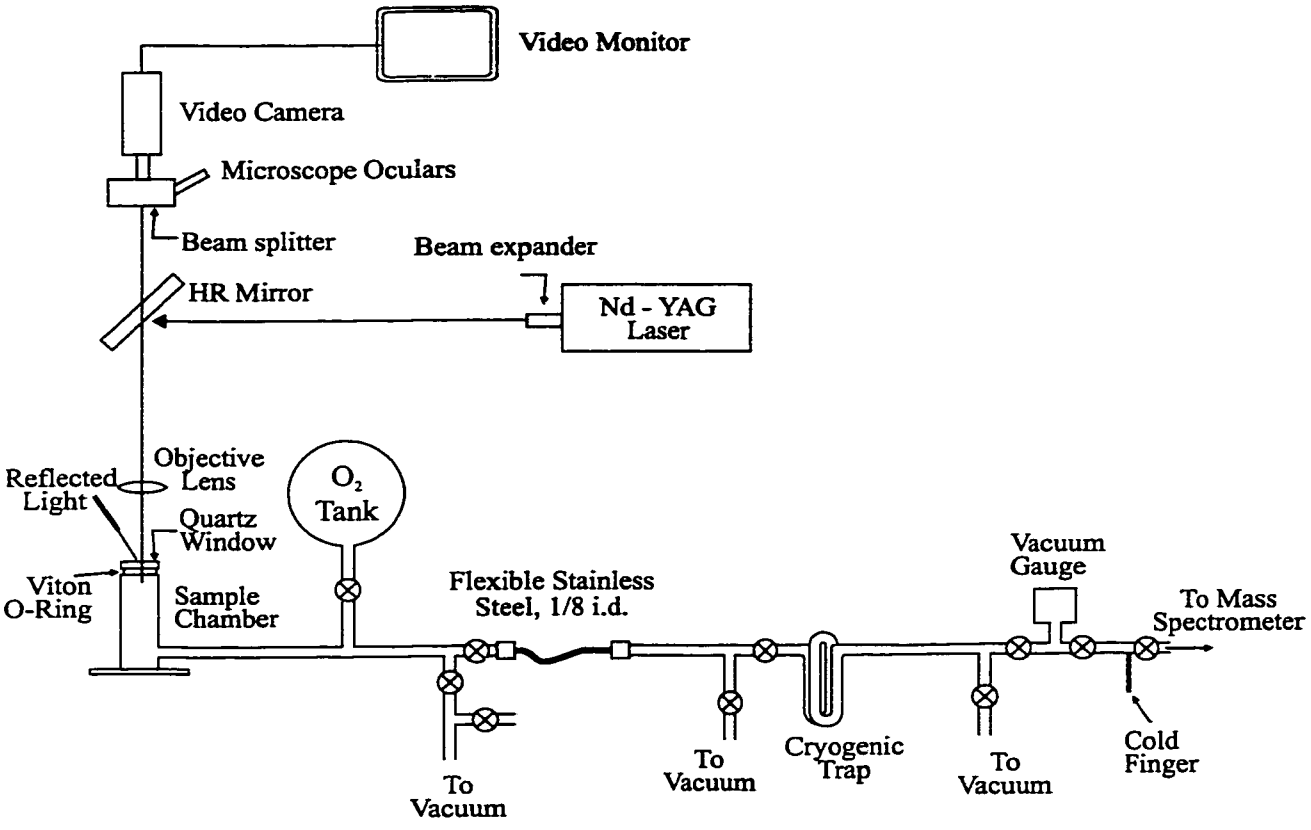

Figure 5-1. Schematic diagram of the University of Ottawa laser microprobe and mass spectrometer system.

5-2-3. Analytical Procedure

5-2-3-A. Sample Preparation

Small slabs (<1.5″ across) suitable for insertion into the sample chamber were cut from hand specimens. The slabs were polished to enable microscopic identification of the sulfide grains. The polished slabs were ultrasonically cleaned in deionized H_2O and were heated in a vacuum vessel at 250°C until outgassing stopped.

The samples so prepared were placed into the sample chamber of the laser probe system, and the chamber was evacuated. Oxygen was directed to the chamber from the O_2 tank with P_{O_2} varying from 50 to 100 torr, while the chamber was closed to the cryogenic N_2 trap. In their preliminary experiments, Crowe et al. (1990) heated the mass spectrometer inlet system and source to 80°C to facilitate the flow of SO_2 gas and overcome the memory effect. However, as Kelley and Fallick (1990) indicated, memory effect is negligible, and there is no need to keep the spectrometer and inlet system heated during the runs.

To avoid excessive heating of the materials around the pit that causes solid-state diffusion of sulfur and poorer precision, combustion times were minimized (c.f. Crow et al., 1990). Burning duration of 0.3 to 0.5 seconds were found to be sufficient to burn pyrite, pyrrhotite, and chalcopyrite and produce enough SO_2 for analysis. The experiments were conducted under Q-switched mode at modulation frequency of 5 Khz, flashlamp current of 14-17 A and output power of 8.3 W. At power levels below ~12 A, little or no combustion occurred.

After laser combustion, the sample chamber was opened to the cryogenic N_2 trap to collect condensable gases produced during combustion. Excess O_2, as well as non-condensable gases produced during combustion, were slowly pumped through the cryogenic N_2 trap. After pumping the non-condensable phases away, the N_2 trap was replaced by ethanol bath, already cooled down to -80°C, to separate H_2O, if any, and SO_2. The sample gas was frozen into the

VG SIRA-12 microinlet using liquid N_2. The purified gas was then let into the mass spectrometer to measure mass ratio 66/64. $\delta^{34}S_{CDT}$ was calculated using standard techniques.

5-2-3-B. Spatial Resolution

Spatial resolution is dictated by the amount of gas the mass spectrometer requires for analysis of isotope ratios. The VG SIRA-12 mass spectrometer used in our experiments requires a minimum of ~1 μmole SO_2, corresponding to a pit approximately 10^{-2} mm^3, or ~200 μm in diameter and depth where pyrite is the target mineral; for minerals with lower SO_2 yield, broader beams were applied. Modern mass spectrometers are capable of measuring gas samples on the order of 10-100 nm (nanomoles), greatly enhancing the spatial resolution.

5-2-3-C. Pit Morphology and Composition of Ejecta

Laser combustion creates pits that vary in shape according to mineralogy and the power and duration of the laser combustion. The intensity profile of the laser beams are Gaussian in shape producing funnel-shaped pits. The combusted pits are typically encircled by a raised rim of ejected melt and an oxide halo (Figure 5-2-A). The oxide halo forms only a thin (<2 μm) layer at the surface and is typically colored according to the composition of the metal oxide: red-orange (pyrite, pyrrhotite), black and red-orange (chalcopyrite), and white (sphalerite).

Reducing beam diameter increases the power density of the beam and the depth of the pit that is burned into the sample. Deep penetration of the laser beams may lead to contamination due to the combustion of the underlying materials. A deep pit can be avoided by reducing the duration of the laser burn for smaller beam diameters. Combustion duration of 0.3 to 0.5 seconds were found to produce shallow pits (200-300 μm) at beam diameters of ~200 μm. Narrower beam diameters produce deeper pits that may extend into the underlying minerals, and thus undesirable. Crowe et al. (1990) showed that deep penetration of the laser beams results in a more sporadic combustion of the sample, probably due to insufficient O_2 at the bottom of the pit and production of undesirable SO^+.

5-2-4. Analytical Fractionation

The $^{34}S/^{32}S$ ratios of SO_2 gas produced by laser combustion are different from those produced by conventional combustion technique. However, the high precision of laser microprobe analysis indicates that analytical fractionations are reproducible and that the fractionations can be corrected if uniform optimized conditions are maintained during analysis.

Kelley and Fallick (1990) showed that SO_2 yield from laser extraction depends upon the bond strength. The authors further showed that variation of the resultant $\delta^{34}S_{SO2}$ is related to the percent yield by a Rayleigh fractionation process and that there is a strong relationship between the Gibbs free energy of formation (ΔG^0_{298}) and $\delta^{34}S_{SO2}$. The ΔG^0_{298} of sulfides is related to the metal/sulfur bond strength and thus fractionation is greatest in minerals with low bond strength. The main causes of fractionation include sulfur diffusion from the heated halo and oxygen pressure and oxygen isotope variations.

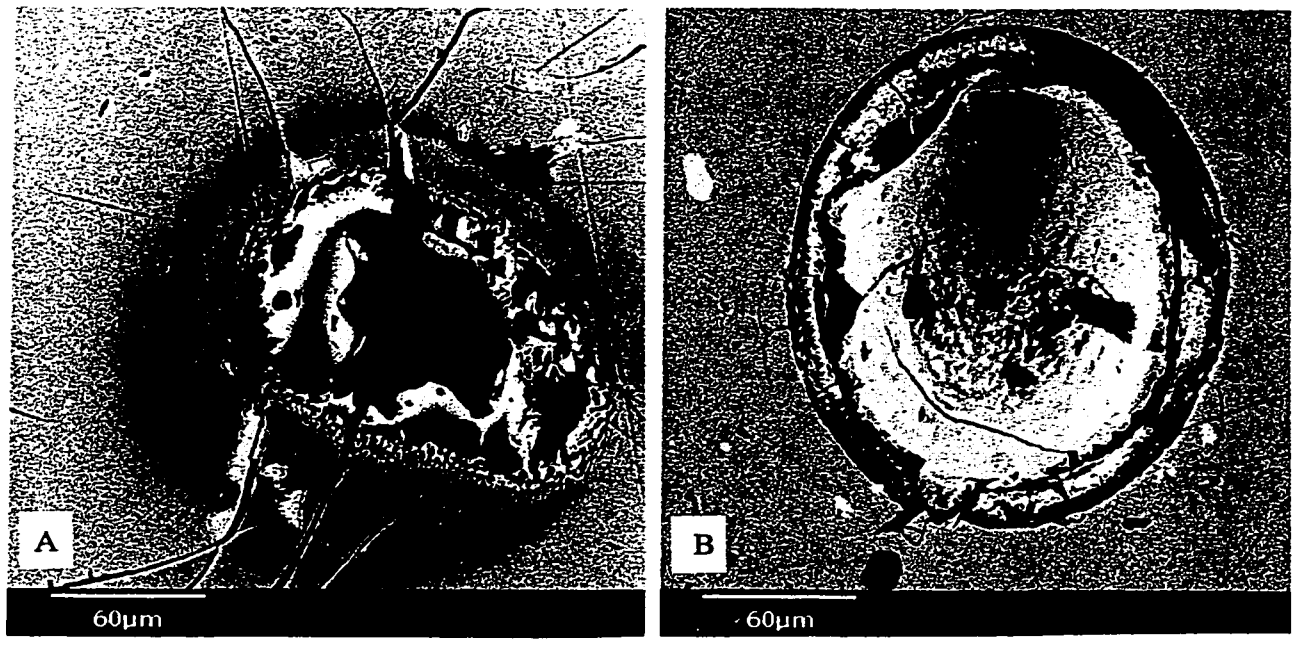

Figure 5-2. (A) Image of a laser-combusted pit with ejected rim and oxide halo. (B) Image of a combusted pit after leveling the surface. Note the actual thickness of the heated halo. Both pits in pyrrhotite from Bamble Fe-Ni-Cu ore.

5-2-4-A. Sulfur Diffusion from the Heated Halo

The thermally affected materials around the combusted pits are commonly depleted in S. The dimensions of the S-depleted halos vary with the laser mode and duration of combustion. Using CW mode, Crowe et al. (1990) observed a complex zone of S-deficient materials ~200 μm out from the edge of a laser pit ~200 μm in diameter in a chalcopyrite. However, in our experiments with Q-switched mode, due to the nature of the beams, the thickness of the effected halo is < 1/4 of the diameter of the pit (Figure 5-1-B).

The magnitude of the solid state sulfur loss depends on the mineral structure and is probably the main mechanism controlling the mineral-specific fractionation (e.g. Crowe et al., 1990; Kelley and Fallick, 1990; Crowe and Vaughan, 1996). Crowe et al. (1990) showed that the S-depleted halo around a combusted pit in a chalcopyrite was enriched in $\delta^{34}S$ by 2‰ relative to unaltered materials. Vaporization and removal of S from the materials adjacent to the laser pits impose further restrictions to spatial resolution.

5-2-4-B. Oxygen Pressure and Oxygen Isotope Variations

Sulfur isotope fractionation is not considerably affected by varying O_2 pressure. Kelley and Fallick (1990) showed that variation in $\delta^{34}S$ was less than 0.5‰ for P_{O2} from 3 to 250 torr (SO_2/O_2 = 0.01-1). Too low or too high P_{O2} in the sample chamber might lead to the production of SO^+ or SO^{+3} causing fractionation. However, as shown by Crowe et al. (1990), SO_3 is negligible, and the ratio of SO^+ and SO_2 peaks are the same for gases produced by conventional combustion methods, laser combustion methods, and for reagent tank SO_2, implying that no SO^+ is produced by laser. Crowe et al. (1990) showed that varying P_{O2} from 40 to 70 torr did not affect the sample combustion or the reproducibility of the their experiments. Our experiments were all carried out under P_{O2} between 50 to 100 torr.

Different sources of oxygen in laser probe and conventional methods require a correction to be made for the oxygen isotope effect. In laser-extraction method, oxygen is supplied by a tank of pure O_2 while in conventional method, CuO is the source of oxygen. This leads to an

additional oxygen-related term in calculating $\delta^{34}S$ from the raw 66/(64 + 65) ratio measured by the mass spectrometer. The oxygen isotope effect can be canceled out by using a consistent and homogenous source of oxygen in laser probe experiments.

An additional factor resulting from the oxygen isotope effect is the possible fractionation of the oxygen isotopes during formation of SO_2 by the laser. This effect is small during conventional combustion, since the sample and CuO are held at over 1000°C for at least 15 minutes, leading to equilibrium fractionation which is very small at high temperatures. Experiments by Kelley and Fallick (1990) to relate the variations of $\delta^{34}S$ with SO_2/initial O_2 indicated that no fractionation occurred as a result of oxygen depletion.

Most carbonates and silicates dissipate the Nd-YAG laser energy. Mafic silicates, however, absorb much of the incident beams and may provide a potential source of contamination. To avoid melting of surrounding silicates where sulfide grains were too small (< 250 μm), lower powers were applied. However, involvement of mafic silicates were inevitable, particularly from the underlying materials. Controlled experiments with wide beam diameters (~500 μm) to cover both sulfides and mafic silicates with different proportions indicated no significant variations in $\delta^{34}S$ values.

5-2-4-C. Laser Power and SO_2 Yield

The effects of varying power and SO_2 yield on the fractionation of sulfur isotopes was evaluated by replicate analysis of pyrrhotite from a granulite facies sulfidic metasediment from Bamble. (Initial conventional analysis of powders microdrilled from the sample indicated a fairly homogenous isotopic composition at millimeter scale.) To avoid deep penetration of laser beams, a combustion duration of 0.5 seconds was applied to all runs. Results from the experiments (Table 5-1) show no considerable variation in $\delta^{66}S_{SO2}$ values over a wide range of power and SO_2 yield. This is in agreement with an earlier work by Kelley and Fallick (1990) who used an Argon-Ion continuous wave laser to extract SO_2 from mineral powders.

Table 5-1. Variations of S isotope ratios with varying power and SO_2 yield

Flashlamp Current (A)	SO_2 (μmole)	$\delta^{66}SO_2$
12.5	1.5	-0.9
14	3.5	-0.8
15	5	-1.0
16	6	-0.7
17	8	-0.6
18	11	-1.1

5-2-5. Calibration

Sulfur isotope ratios of SO_2 gas produced by laser combustion are different from those produced by conventional combustion technique, due to the fractionations inherent to the laser combustion technique. However, the high precision of the laser-probe analyses indicates that the fractionation processes are reproducible and that they can be corrected if uniform optimized conditions are maintained during the experiments.

To convert the raw mass spectrometric data ($\delta^{66}S_{raw}$) obtained by conventional combustion techniques to $\delta^{34}S_{CDT}$, it is assumed that:

$$\delta^{34}S_{mineral} = \delta^{34}S_{SO2} \qquad (1)$$

where $\delta^{34}S_{mineral}$ is the isotopic composition of the sample relative to CDT (Cañon Diablo Troilite) and $\delta^{34}S_{SO2}$ is the isotopic composition of the SO_2 generated by conventional combustion of the sample or standards. Any shifts in the above equation are reproducible and would be cancelled by the use of a working curve (c.f. Crowe et al., 1990, Crowe and Vaughan, 1996).

By analyzing the SO_2 by mass spectrometer, $\delta^{34}S_{SO2}$ of the mineral can be calculated from the equation:

$$\delta^{34}S_{SO2} = K_1 \cdot \delta^{66}S_{raw} + K_2 \qquad (2)$$

where $\delta^{66}S_{raw}$ is the raw value for the mass ratio (66/64) in SO_2, and K_1 and K_2 are the slope and the *y*-intercept, respectively, of the working curve.

For SO_2 generated by laser, the equation (1) would not hold true due to the laser-induced fractionation inherent in the laser microprobe system. This fractionation is mineral-specific. Thus

$$\delta^{34}S'_{SO2} = K_3 \cdot \delta^{66}S_{raw} + K_4 \quad (3)$$

where $\delta^{34}S'_{SO2}$ is the isotopic composition of the SO_2 generated by laser, and K_3 and K_4 are, respectively, the slope and the *y*-intercept of the laser calibration curve. Crowe et al. (1990) introduced an additional term, K_5, to correct for the mineral-specific effects:

$$\delta^{34}S_{mineral} = \delta^{34}S'_{SO2} + K_5 \quad (4)$$

The K_5 factor for common sulfide minerals has been measured to be in the range -0.1‰ (sphalerite) to +1.4‰ (pyrrhotite) (Crowe et al., 1990). The mineral-specific effects require separate calibration curves to be constructed for individual minerals. Use of a calibration curve also corrects for any systematic fractionation related to laser combustion or gas purification such as boundary effects around laser pits, volatile speciation, SO_2 loss during cryogenic separation of SO_2 and O_2, and S sublimation due to sample heating (Crowe et al., 1990; Crowe and Vaughan, 1996).

Isotopically homogeneous materials are required to standardize the $\delta^{66}S_{raw}$ data of the SO_2 gas obtained by laser combustion. Initial analyses of powders microdrilled from several specimens of sulfidic rocks from the study area indicated that four samples were homogeneous at centimeter scale. Replicate analyses of the samples by laser combustion method under similar conditions indicated that two samples were isotopically homogenous at sub-millimeter scale. The samples include:

- Pyrrhotite from a sulfidic metasediment metamorphosed under granulite facies conditions. The pyrrhotite occurs as discrete subhedral to anhedral crystals, 1-5 mm in size, interstitial to silicates; minor pyrite and chalcopyrite may accompany the pyrrhotite. The scattered grains locally coalesce to form lenses up to 2 cm thick and 5 cm long. The pyrrhotite is exclusively of monoclinic Fe_7S_8 composition, with trace Ni and Co impurities (Table 5-2).

- Pyrite from a sulfidic metasediment metamorphosed under amphibolite facies conditions. Pyrite and minor pyrrhotite and chalcopyrite occur as discrete euhedral to subhedral grains 1-6 mm in diameter, as well as discontinuous bands and patches 0.5 to 2 centimeters thick, enclosed within silicates. Electron probe analysis of the pyrite indicated a stoichiometric FeS_2 composition with minor Ni and Co impurities (Table 5-2).

Additional samples, proven to be isotopically homogeneous (Crowe and Vaughan, 1996), were kindly donated by Dr. Crowe from the University of Georgia. The samples include:

- Pyrite from Ruttan massive sulfide deposit, Leaf Rapid, Manitoba. This includes a mixture of anhedral pyrite porphyroblasts in a matrix of pyrrhotite and chalcopyrite.
- Pyrrhotite from Anderson mine, Snow Lake, Manitoba. This is a relatively pure pyrrhotite with small (<1 mm) scattered patches of biotite. Both Ruttan pyrite and Anderson pyrrhotite have stoichiometric compositions and are poor in minor elements, Ni, Co, Cu, Zn, Se, and As (Crowe and Vaughan, 1996).
- Chalcopyrite from Trout Lake massive sulfide, Flin Flon, Manitoba.
- Chalcopyrite from Norilsk.
- Sphalerite from Balmat Deposit, Adirondack Mountains, New York.

Table 5-2. Electron microprobe analysis of reference materials.

Fe (%)	Co (%)	Ni (%)	S (%)	Total
A. Bamble Pyrrhotite				
60.86	0.02	0.03	38.82	99.74
61.36	0.03	0.06	38.94	100.39
61.15	0.03	0.07	39.08	100.33
61.24	0.04	0.05	39.13	100.46
61.05	0.04	0.07	38.96	100.12
60.97	0.03	0.05	38.75	99.8
B. Bamble Pyrite				
47.21	0.28	n.d.	52.45	99.94
47.22	0.2	n.d.	52.79	100.21
47.16	0.51	0.02	52.82	100.5
47.19	0.14	n.d.	52.77	100.1
46.16	0.45	n.d.	52.57	99.18
47.02	0.3	0.02	52.79	100.13

Ruttan pyrite, Anderson pyrrhotite, and Balmat sphalerite are metamorphosed under mid- to upper-amphibolite facies. Trout Lake chalcopyrite is metamorphosed under greenschist facies. High grade metamorphism has resulted in coarsening of grain sizes and homogenization of sulfur isotopes (Crowe and Vaughan, 1996).

All reference materials were analyzed in replicates by laser combustion technique. To enhance the reproducibility or precision of the data, experiments were carried out under similar working conditions. Plots of replicate $\delta^{66}SO_{2(raw)}$ values for pyrite and pyrrhotite are shown in Figure 5-3. Data for chalcopyrite and sphalerite will be discussed elsewhere.

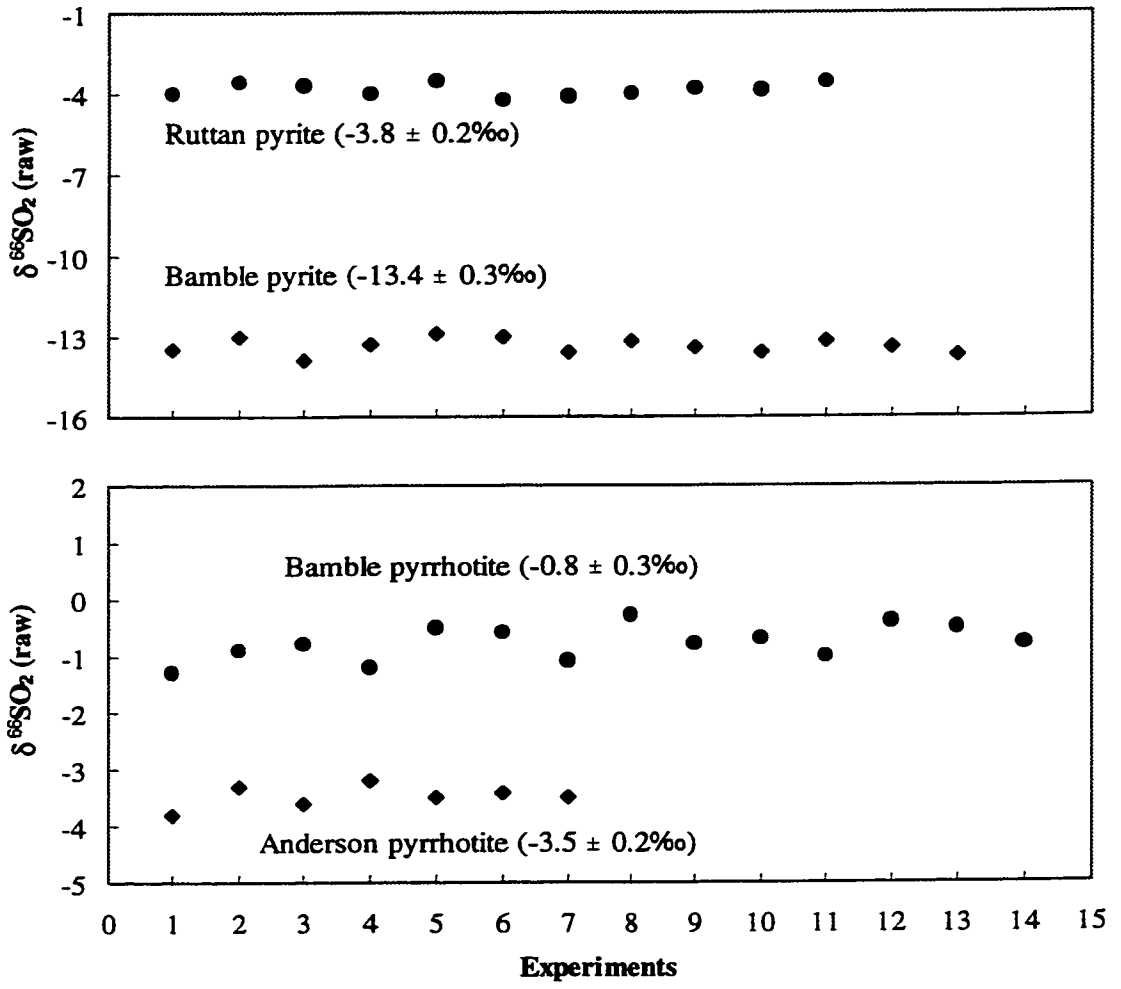

Figure 5-3. Plot of replicate analyses of reference materials by laser combustion technique.

Powders microdrilled from the same reference materials were subjected to SO_2 extraction by conventional combustion technique following Robinson and Kusakabe (1975). The powder samples, combined with Cu_2O, were combusted under vacuum at 1000 to 1100°C for 15 minutes to produce SO_2 gas for isotopic analysis. Plots of replicate $\delta^{34}S_{CDT}$ analyses are shown in Figure 5-4.

The $\delta^{66}SO_{2\,(raw)}$ values obtained from laser extraction are compared against $\delta^{34}S_{CDT}$ values of the same materials determined by conventional combustion technique to construct calibration curves (Figure 5-5). The equations of the lines for pyrite and pyrrhotite are:

$$\delta^{34}S_{CDT} = (0.98 \times \delta^{66}SO_2\,(raw)) + 4.82 \qquad \text{pyrite}$$

$$\delta^{34}S_{CDT} = (1.07 \times \delta^{66}SO_2\,(raw)) + 5.06 \qquad \text{pyrrhotite}$$

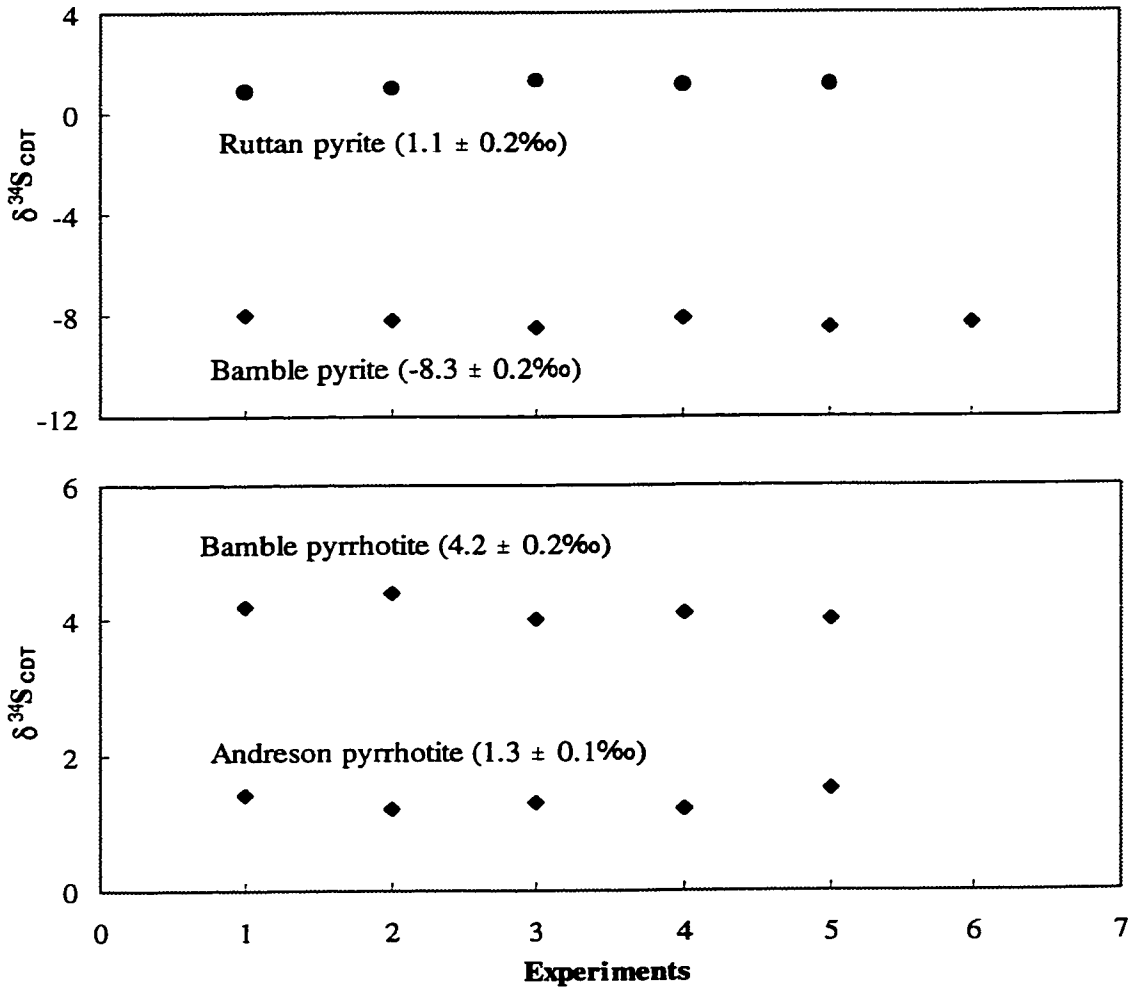

Figure 5-4. Plot of replicate analyses of reference materials by conventional combustion technique.

Reproducibility, or precision, of $\delta^{66}SO_{2\ (raw)}$ values from laser probe technique (1σ = 0.2-0.3‰) is comparable to that from conventional combustion techniques (1σ = 0.1-0.2‰).

Variations of sulfur isotope ratios in replicate analysis of reference materials might be attributed to either sample heterogeneity or analytical uncertainty. In the absence of other techniques to provide independent verification of the results from laser probe method, it can not be ascertained whether the isotopic variations are due to the initial isotopic heterogeneities within the samples, or due to instrumental errors, generated either during laser combustion and gas extraction, or during mass spectrometry.

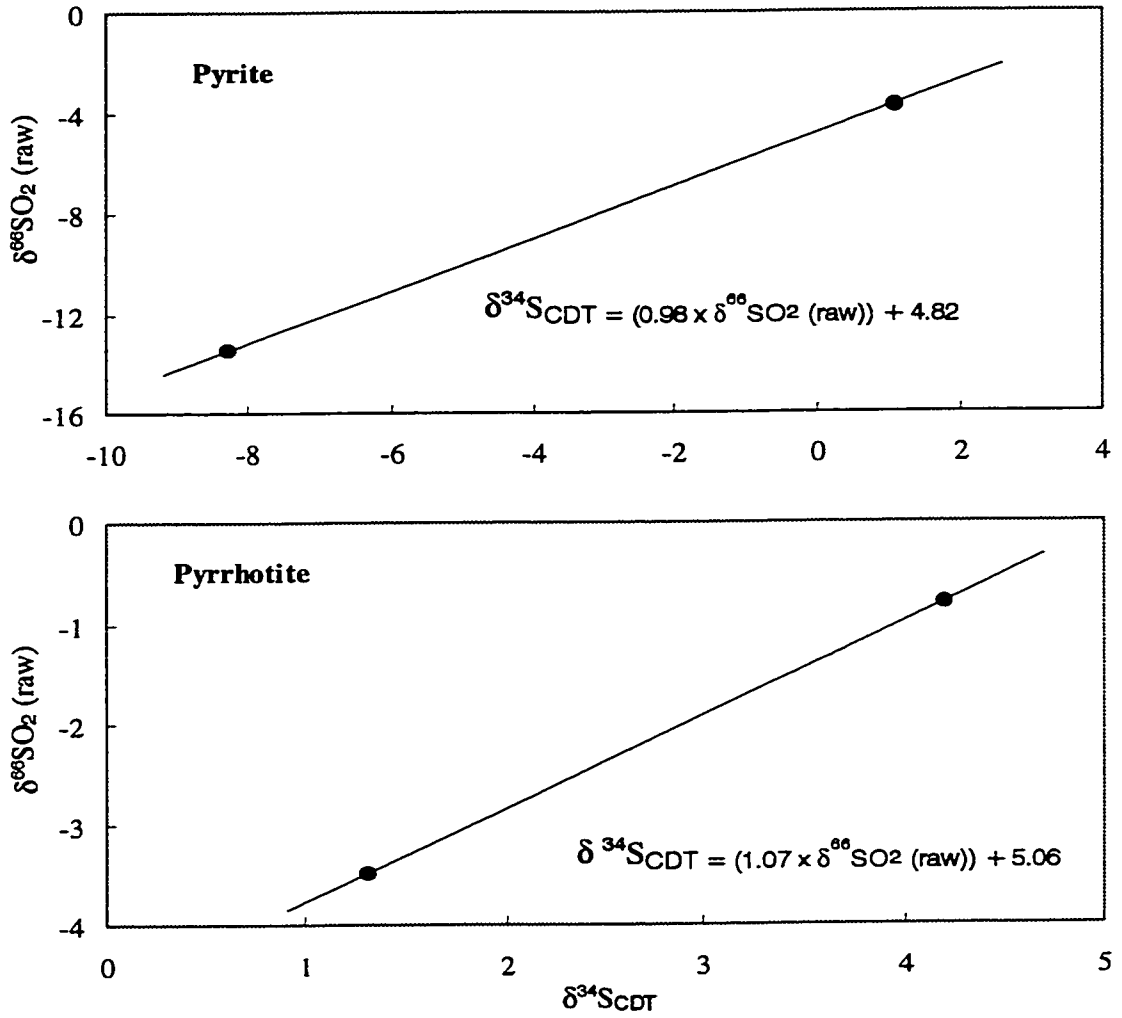

Figure 5-5. Calibration curves for pyrite and pyrrhotite. Equations of the lines regressed through the plots are indicated.

5-3. Applications

Sulfur isotope ratios have been determined for selected samples from various lithologic units in Bamble. To check for possible variations at the hand specimen scale, and to reduce the analytical error, three sulfide grains were analyzed for each sample, and the results averaged. A summary of instrumentation and working conditions is shown in Table 5-3. Using equation of the lines for pyrite and pyrrhotite, the $\delta^{66}SO_{2(raw)}$ data were transformed into $\delta^{34}S_{CDT}$ values. All sulfur isotope data are reported in the δ notation where δ is defined by

$$\delta^{34}S = 1000 \left(R_{sample} / R_{standard} \right) - 1$$

and R is the isotope abundance ratio of the rarer (^{34}S) to the more common (^{32}S) isotope.

Table 5-3. Working conditions for the laser SO_2 extraction experiments

Laser Mode	Modulation Frequency	Flashlamp Current (A)	Output Power (W)	O_2 Pressure (Torr)	Beam Diameter (μm)	Burn Duration (S)	SO_2 Yield (μmole)
Q-Switched	5 khz	12-15	170-190	50-100	200-300	0.3-0.5	1.5-3

5-3-1. Supracrustal rocks

Supracrustal rocks consist of sedimentary, as well as intercalations of volcanic and metasomatic, materials. Sedimentary units include quartzite, variable gneisses and schists, and minor calc-silicates and marbles. Volcanic component includes a variety of mafic to felsic materials. The original sediments are from early- to mid-Proterozoic times (Knudsen et al., 1997). Some 53 samples of supracrustal rocks from amphibolite, transition, and granulite zones were analyzed. A complete list of sulfur isotope data is shown in the Appendix 5-1.

Sulfides are minor constituents of the supracrustal rocks, rarely exceeding 1% by mode. Pyrite and pyrrhotite are the main sulfide minerals, occurring commonly as fine (<0.5 mm in diameter), subhedral to anhedral grains interstitial to silicates. Chalcopyrite may occur associated with pyrite and/or pyrrhotite in composite grains, or less commonly, as discrete

grains. Pyrite also occurs as fracture filling and replacement bodies. Other phases are rare; trace pentlandite, sphalerite, arsenopyrite, and marcasite were observed in few samples. Most analyses were carried out on the interstitial sulfides. A frequency distribution of $\delta^{34}S_{CDT}$ values for various supracrustal rocks is shown in Figure 5-6.

5-3-1-A. Source of Sulfur

Bamble supracrustal rocks are of early- to mid-Proterozoic age, the time when bacterial reduction of sulfates had already been established in the sedimentary basins. It is well known that major fractionation of sulfur isotopes started at about 2.7 to 2.5 Ga (Goodwin et al., 1976; Schidlovsky, 1979; Cameron, 1982, 1983a, b; Skyring and Donnelly, 1982; Cameron and Hattori, 1987a; Bottomley et al., 1992).

Post-Archean sedimentary rocks display a very wide range of $\delta^{34}S$ values, mainly because of the kinetic isotope effects during bacterial sulfate reduction. Bacterial reduction of seawater sulfate can take place in environments that are both open and closed to SO_4^{-2} (Ohmoto and Rye, 1979; Hoefs, 1987). The combination of these two processes with the $\delta^{34}S$ variations of

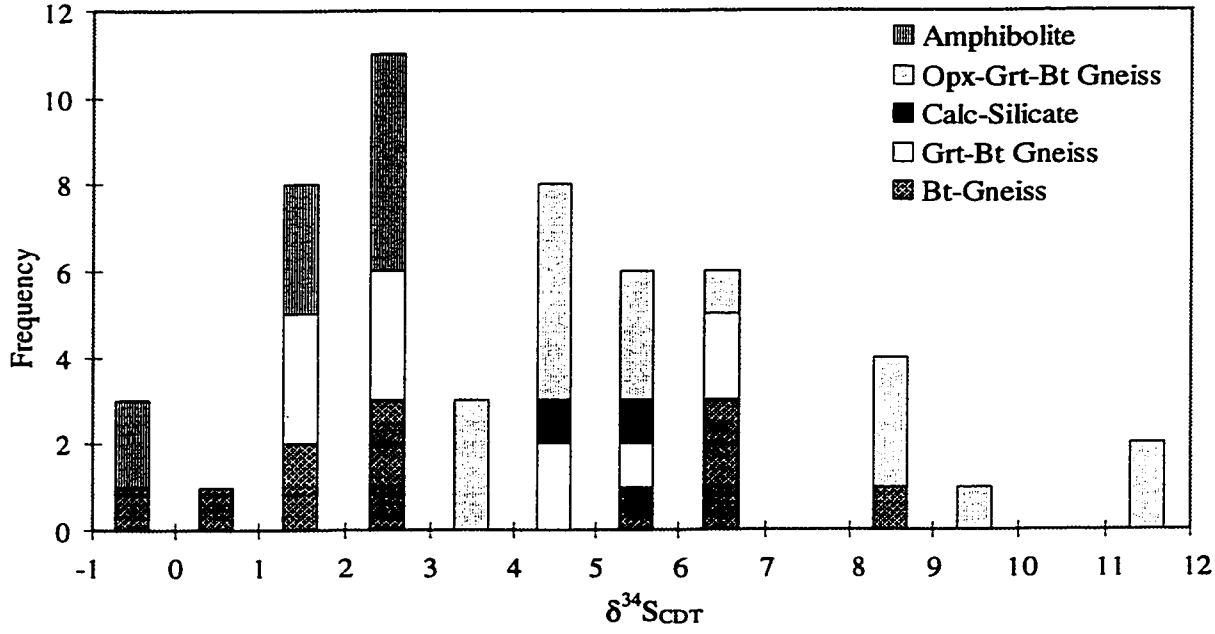

Figure 5-6. Variations of $\delta^{34}S_{CDT}$ for various supracrustal rocks, Bamble.

seawater sulfate during the geological time resulted in a large variation of $\delta^{34}S$ values, in the range -60 to +50‰, in sedimentary rocks (e.g. Ohmoto and Rye, 1979; Ohmoto, 1986; Hoefs, 1987; Strauss, 1997).

The Bamble metasedimentary units are characterized by enrichment of ^{34}S and a fairly large variation in $\delta^{34}S$ (-1‰ to 12‰), consistent with data from sedimentary rocks of early- to mid- Proterozoic ages (c.f. Cameron and Garrels, 1980; Veizer et al., 1980; Cameron, 1983a, b; Norman et al., 1990; Bottomley et al., 1992; Strauss, 1997). Cameron and Garrels (1980) determined a large variation in $\delta^{34}S$, in the range 2.4 to 16.5‰, for Proterozoic sediments of the Canadian shield. Similarly, Bottomley et al. (1992) reported a large spread (-2 to +14.2‰) for sulfides in platform sediments of Proterozoic age worldwide. Other examples include sedimentary sulfides from McArthur and Mount Isa Groups, Australia, with mean $\delta^{34}S = 8 \pm 8.5$‰ and 14.2 ± 4.6‰, respectively (Solomon, 1965; Smith and Croxford, 1973; Smith et al., 1978; Rye and Willimas, 1981).

Proterozoic units with negative $\delta^{34}S$ values are rare in the geologic record. Examples include sulfides from Newland Formation, Belt Supergroup, Montana ($\delta^{34}S = -1 \pm 9$‰; Strauss and Schieber, 1990) and Sullivan ore body, British Columbia ($\delta^{34}S = -3 \pm 7$‰, Campbell et al., 1978). The predominantly negative sulfur isotopic signature for Newland has been interpreted as an open marine sulfur isotope signal (Strauss and Schieber, 1990).

The sulfur isotope composition of the late Proterozoic marine sulfate has been determined to be in the range +15 to +18‰ (Thode and Monster, 1965; Claypool et al., 1980; Strauss and Schieber, 1990). Scattered data from older sedimentary rocks suggest that the early- to mid-Proterozoic seas were more enriched in ^{34}S. The $\delta^{34}S$ values of marine sulfates from McArthur Group, Australia (1700 Ma) and Coronation Supergroup, Northwest Territories (1900 Ma) have been determined to vary from +22‰ to +31‰ (Bottomley et al., 1997).

Considering the deposition age of the Bamble metasedimentary units (1900-1500 Ma; Knudsen et al., 1997), the isotopic signature of sulfides can be explained by bacteriogenic reduction of seawater sulfate with an initial $\delta^{34}S$ value of 20-30‰. An isotopic fractionation of 10-30‰, reasonable for bacteriogenic reduction of sulfate under closed conditions, could have led to the formation of sulfides with $\delta^{34}S$ values of -1 to +12‰ in Bamble.

Concordant amphibolites display a narrow spread in $\delta^{34}S$ values (-1‰ to +3‰). Earlier in Chapter 2, it was shown that concordant amphibolites formed from submarine basic volcanic materials. Slight enrichment in ^{34}S compared to unaltered mafic rocks of mantle origin ($\delta^{34}S$ = 0.5 ± 1‰; Schneider, 1970; Sakai et al., 1982, 1984) might be attributed to the involvement of seawater sulfate. Experiments have shown that seawater sulfate would be reduced to H_2S at high temperature of 250°C by reaction with basaltic rocks (Mottle et al., 1979). Basalts from Pacific spreading centers have yielded $\delta^{34}S$ values between +1‰ to +4‰ (Arnold and Sheppard, 1981; Keridge et al., 1983).

5-3-1-B. Pyrite-Pyrrhotite Phase Relations

Fe-sulfides, pyrite and pyrrhotite, are the main sulfide phases in Bamble supracrustal rocks. Pyrrhotite occurs mainly in metasediments from transition and granulite zones. The formation of pyrite during diagenesis via the reaction of detrital iron minerals with H_2S is a well known phenomenon (e.g. Raiswell, 1982; Berner, 1984). Pyrrhotite, however, is not common as a sedimentary-diagenetic mineral; it usually forms as a result of the reduction or breakdown of the diagenetic pyrite during progressive metamorphism (e.g. Carpenter, 1974; Ferry, 1981, Hall, 1982).

Pyrrhotite is slightly enriched in ^{34}S (Figure 5-7); however, the difference in $\delta^{34}S$ values is not statistically important. Several mechanisms have been proposed for the formation of pyrrhotite in metamorphic rocks.

1. Thermal decomposition of pyrite.
2. Reduction and decomposition of pyrite.

3. Hydration of pyrite at constant whole-rock iron.

4. Reduction of pyrite associated with uptake of Fe^{+2} from surrounding Fe-bearing minerals.

Consideration of the phase relations in Fe-S system (e.g. Kullerud and Yoder, 1959, Kullerud, 1967; Yund and Hall, 1969) suggests the following reaction with increasing temperature:

$$FeS_2 \leftrightarrow Fe_{1-x}S + S^{-2}$$

Experimental results of Kajiwara et al. (1981) show that a large kinetic isotope effect can occur during this reaction: an early fraction of the liberated sulfur vapor is depleted in ^{34}S by almost 12‰ relative to the source pyrite. Toward the end of the reaction, the produced pyrrhotite has an isotopic ratio up to 4.5‰ higher than the initial pyrite. This reaction is expected to lead to a strong enrichment of ^{34}S in pyrrhotite. The similar spread in $\delta^{34}S$ values for pyrite and pyrrhotite in Bamble metasediments argues against the above reaction.

A reaction that converts pyrite to pyrrhotite by hydration at constant whole-rock iron content was proposed by Ferry (1981):

$$2FeS_2 + 2H_2O + C \leftrightarrow 2FeS + 2H_2S + CO_2$$

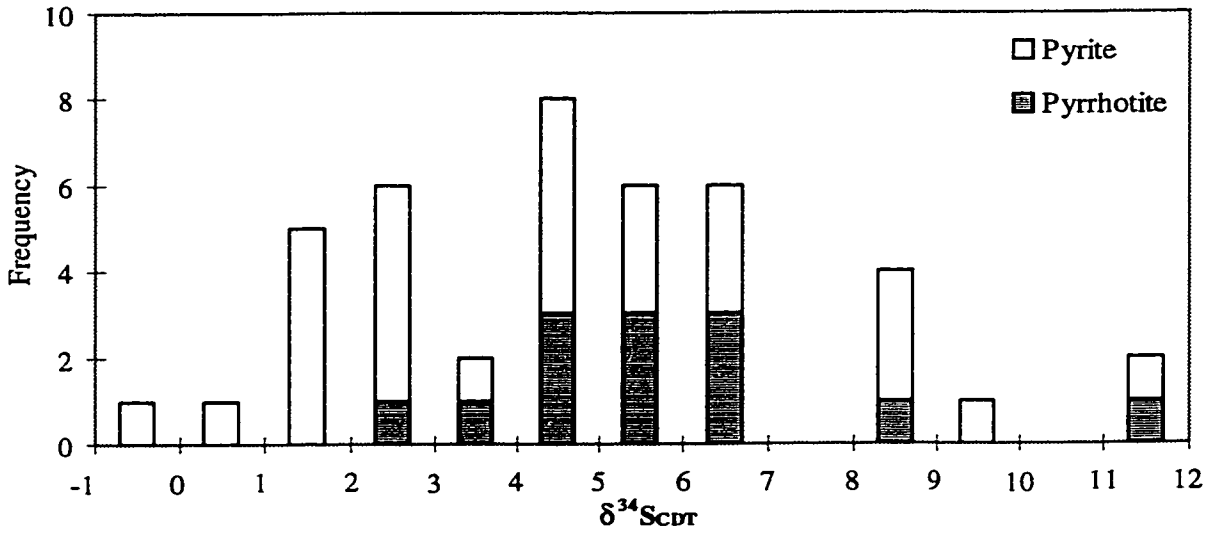

Figure 5-7. Frequency distribution of $\delta^{34}S$ values for pyrite and pyrrhotite from various metasedimentary units, Bamble.

As reactions go faster with the lighter isotopes, it might be presumed that H_2S is enriched in ^{32}S, and consequently ^{34}S increases relatively in the remnant sulfides. However, the thermodynamic fractionation between various sulfur species is quite small at metamorphic temperatures (e.g. Ohmoto and Rye, 1979; Rumble, 1982; Ohmoto, 1986). Similar reactions were studied by Grinenko and Grinenko (1967) who observed that H_2S was enriched in ^{34}S from 1 to 3‰ relative to the initial pyrite at temperatures of 350-550°C. This process may lead to a slight depletion of ^{34}S in the remnant pyrrhotite. The liberated H_2S would react with Fe^{+2} bearing minerals to form pyrrhotite or pyrite.

Ferry (1981) suggested the following reaction to emphasize the soluble nature of FeS_2:

$$2FeS_2 + CH_4 \rightarrow 2Fe^{2+} + 4HS^- + C$$

The generated HS^- can not travel far, as it would easily react with any Fe^{+2}-bearing mineral to form pyrrhotite. Accordingly, this reaction is expected to lead to homogenization of sulfur isotopes, at least at a local scale. The fairly large variation in $\delta^{34}S_{pyrrhotite}$ values argues against the occurrence of the above reaction as a mechanism of pyrrhotite formation.

Carbon is the most effective reducing substance in metasedimentary rocks (Frost, 1988). According to the author, pyrite will persist in metasedimentary rocks which do not attain a low enough oxidation state for the formation of pyrrhotite (i.e. in graphite-free rock units). Preservation of pyrite in high grade metamorphic rocks has been reported from Lake Superior Iron Formation (James, 1969) and from contact metamorphic rocks in Mount Morgan, Australia (Lawrence, 1972). The occurrence of pyrite in the granulite facies metasediments in Bamble might be explicable in terms of a high f_{O2} for these rocks. Cameron (1989b) reported a high f_{O2}, ~2.7 log unit above the QFM buffer, for granulite facies rocks in Bamble.

The formation of pyrrhotite from pyrite also depends on the available Fe ions for reaction. Tracy and Robinson (1988) showed that in the sulfidic-graphitic schists of Partridge Formation, Central Massachusette, very magnesian assemblages were formed through conversion of pyrite to pyrrhotite. In rocks with very high S/Fe ratios, where removal of Fe

from the silicate-oxide assemblage could occur before all pyrite was converted, this mineral is still preserved. The author further showed that metamorphism proceeded under isochemical conditions with only minor loss of C and S.

Replacement of pyrite by pyrrhotite in the Bamble metasediments was associated with an uptake of Fe from surrounding Fe-Mg silicates, rather than a desulfidation process. This is supported by the presence of Fe-poor pyroxene and biotite ($FeO_t < 10\%$) in pyrrhotite-rich samples from transition and granulite zones (7302 and 121, respectively). A possible reaction would be (c.f. Thompson, 1972; Mohr and Newton, 1981):

$$\text{pyrite} + \text{Fe-silicate} + C \rightarrow \text{pyrrhotite} + \text{Fe-poorer silicate} + CO_2$$

This reaction occurs in a system closed to addition or removal of S, and the resultant pyrrhotite is expected to inherit the isotopic signatures of the initial pyrite. The similarity in $\delta^{34}S$ values of pyrite and pyrrhotite might be taken as a further evidence for the occurrence of the above reaction.

5-3-2. Charnockites

The highest grade portion of the Bamble Shear Belt (zone D) contains a dark green, poorly foliated, charnockitic gneiss. The charnockites intruded the older supracrustal rocks and were metamorphosed during Kongsbergian orogeny. They are of tonalite-trondhjemite composition.

Sulfides occur as accessory minerals in the charnockites, rarely exceeding 0.05% by mode. Pyrite is the main sulfide, followed by pyrrhotite and chalcopyrite. All three minerals occur both as discrete and composite grains, 20-250μ in diameter, located interstitially to silicates. In few samples, pyrite was also found as fracture filling and replacement bodies.

Interstitial pyrite is commonly associated with magnetite in composite pyrite + magnetite ± chalcopyrite grains, and appears to be pseudomorphous after pyrrhotite, or pyrrhotite monosulfide solid solution, Po_{mss} (c.f. Cameron, 1989b, 1993a). Similar textures have been

reported from Shevaroy Hills charnockites, India (Harlov et al., 1997). Considering that pyrite is not stable above ~740 °C (Kullerud and Yoder, 1959), pyrrhotite was the stable phase at peak metamorphism, at ~ 800 °C. Upon cooling and oxidation, however, the magmatic pyrrhotite was replaced by pyrite ± magnetite. It has been indicated that Bamble charnockites equilibrated, at peak metamorphism, under a high f_{O2}, ~2.5 log unit above the QFM buffer (Cameron, 1989b; Harlov, 1992).

5-3-2-A. Sample Preparation

Due to the small sizes of the sulfide grains (commonly <200 μm), an initial laser combustion analysis failed to yield enough SO_2 for mass spectrometry. To assure proper analysis of sulfide sulfur, sulfide concentrates were prepared using HF-digestion method following Neuerburg (1975). The method has proven to be very efficient in providing clean and physically unharmed sulfide grains.

Some 17 samples with interstitial sulfides, were selected for HF-digestion. Ten to 20 grams of samples were treated by this method to prepare ~5 milligram sulfide concentrates for extraction by elemental analyzer EA 1110. The extracted SO_2 was analyzed by a VG SIRA-12 triple collector mass spectrometer. The reproducibility or precision of the experiments is in the same range as in the conventional combustion technique at ~ 0.2‰. All experiments were carried out at the Department of Earth Sciences, University of Ottawa. A list of the results is shown in the Appendix 5-2.

5-3-2-B. Variation of Sulfur Isotopes

Bamble charnockites display a large variation in $\delta^{34}S$ (Figure 5-8). Unlike mafic rocks with $\delta^{34}S$ values commonly clustering around 0‰, felsic igneous rocks have frequently been shown to show a wide scatter in $\delta^{34}S$ (e.g. Siewers, 1974; Sasaki and Ishihara, 1979; Poulson et al., 1991).

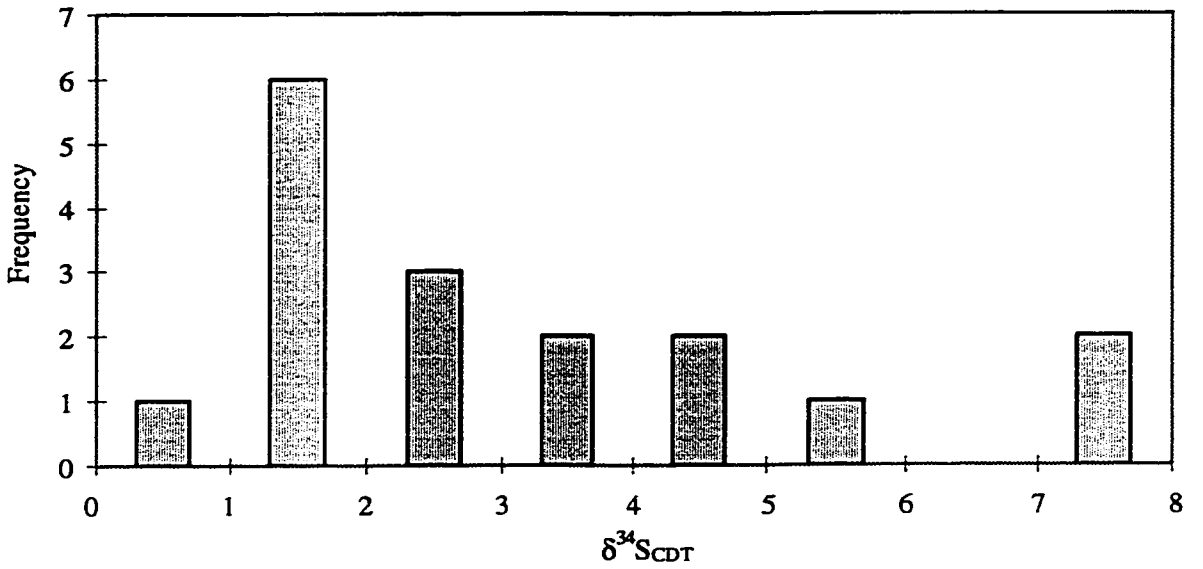

Figure 5-8. Variations of $\delta^{34}S$ values in the Bamble tonalitic-trondhjemitic charnockites.

5-3-2-C. Source of Sulfur

The isotopic composition of sulfur in granitoids is a function of the isotopic composition of source rocks and oxidation state of the parent magma (Coleman, 1979; Sasaki and Ishihara, 1979; Ishihara and Sasaki, 1989; Poulson et al., 1991). Reduced rocks generally have negative $\delta^{34}S$ values, while oxidized rocks have positive values. Coleman (1979) found $\delta^{34}S$ values in the range -3.6 to +4.2‰ for I-type granitoids and -10.5 to -5.7‰ for the relatively reduced S-type granitoids from New England batholith, Eastern Australia.

Similarly, Ishihara and Sasaki (1989) determined $\delta^{34}S$ values of 1.6 to 4‰ for the relatively oxidized magnetite-series granites and -3.7 to -5.3‰ for ilmenite-series granites from Sierra Nevada batholith. According to the authors, the ilmenite-series formed from reduction of the magnetite series by carbonaceous sedimentary wallrocks.

Bamble charnockites are enriched in ^{34}S and in this respect are comparable to oxidized granitoids. The oxidized character of the charnockites is supported by the dominance of magnetite over ilmenite, and by the common presence of hematite lamellae in ilmenite.

Cameron (1989b) and Harlov (1992) showed that Bamble charnockites equilibrated under relatively oxidized conditions, ~2.5 log units above QFM buffer, at peak metamorphism. However, the relatively high oxidation state is thought to be the consequence of granulite metamorphism rather than a feature inherited from the parent magma. A comparison of the isotopic composition of Bamble charnockites and various types of granitoids worldwide is shown in Figure 5-9.

Sulfur in igneous rocks is carried mainly by minor sulfides (Poulson et al., 1991). However, some S is usually present as SH^- replacing OH^- in silicate phases such as biotite and hornblende, or as SO_4^{-2} in sulfates or replacing PO_4^{-3} in apatite (Banks, 1982; Poulson et al., 1991; Nijland et al., 1993). Silicate-S might be an important source of S, accounting for up to 50% of the total S in the enclosing rocks (Banks, 1982; Poulson et al., 1991). Poulson et al. (1991) showed that sulfide-S was isotopically heavier than bulk-S in the South Mountain Batholith, Nova Scotia. The authors estimated a total range of $\Delta^{34}S_{(\text{sulfide-S} - \text{silicate-S})} = 0$ to 3‰ with most values falling between 0.5 to 1‰. This is in agreement with experimental data by Ohmoto and Rye (1979) who estimated a value of 0.8‰ at 700°C for $\Delta^{34}S_{(\text{pyrrhotite} - HS^-)}$.

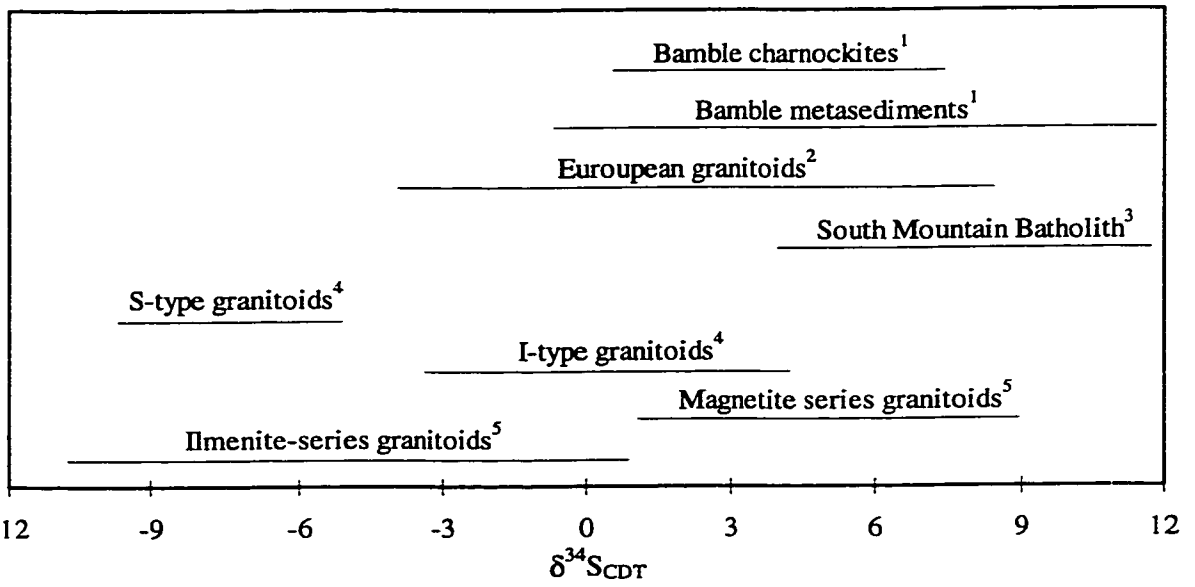

Figure 5-9. Variations of $\delta^{34}S$ values in the Bamble charnockites and various granitoids worldwide. The isotopic range of the Bamble metasediments shown for comparison.
1. Present study; 2. Siewers (1974); 3. Poulson et al. (1991); 4. Coleman (1979); 5. Sasaki and Ishihara (1979).

All sulfur isotope data are on the sulfide-S. The absence of sulfates and the scarcity of apatite as the main sources of oxidized S implies that S is present mostly in its reduced state. Hornblende and biotite, potential sources of HS^-, are accessory phases in the charnockites, rarely exceeding 10% by mode. Accordingly, the $\delta^{34}S$ values obtained for sulfide concentrates can confidently be considered as representative of the bulk rock S.

The wide range of the $\delta^{34}S$ values in the charnockites may be attributed to incorporation of fractionated S from external sources. The metasedimentary host rocks show a large variation in $\delta^{34}S$ values in the range -1 to +12‰, and could be a potential source of S. Cooper and Field (1977) reported the presence of intercalations of metasedimentary rocks in the Bamble charnockites.

Metasedimentary rocks have been proposed as possible sources of S in granitoids (e.g. Shima et al., 1963; Coleman, 1979; Sasaki and Ishihara, 1979; Poulson et al., 1991). At the high temperature of crustal anatexis, little or no isotopic fractionation occurs. Poulson et al. (1991) showed that sulfur isotopic ratios for South Mountain batholith, Nova Scotia, are similar to those from the enclosing Maguma Group metasediments, both enriched in ^{34}S. South Mountain batholith is known as a typical S-type granitoid (Poulson and Ohmoto, 1990; Poulson et al., 1991).

5-3-3. Metabasites

Mafic bodies, known as metabasites, occur in various metamorphic zones in Bamble. They form subconcordant to concordant minor dykes and sheets, parallel to the northeast-southwest regional foliation. The metabasites intruded older supracrustal rocks during the Kongsbergian orogeny at ~1600-1500 Ma (Smalley and Field, 1985; Starmer, 1991, 1993). The metabasites have totally metamorphic textures and mineral assemblages, implying that they have equilibrated to the conditions of metamorphism. Hornblende, the principal ferro-magnesian silicate in the amphibolite zone, is increasingly replaced by pyroxenes towards the granulite zone.

Sulfides are minor constituents of the Bamble metabasites, rarely exceeding 0.5% by mode. They include pyrite, pyrrhotite, chalcopyrite, pentlandite, and marcasite. Pyrite is the principal sulfide in all zones, followed by pyrrhotite. Chalcopyrite and pentlandite usually occur as minor phases associated with both pyrite and pyrrhotite in composite grains; chalcopyrite also occurs as discrete grains. Pyrrhotite, or pyrrhotite monosulfide solid solution (Po_{mss}) was the stable sulfide phase during magmatic crystallization (c.f. Vaughan et al., 1971; Naldrett, 1989). However, metamorphic recrystallization of the metabasites was associated with extensive replacement of the pyrrhotite by pyrite.

Sulfides commonly occur as fine, subhedral to anhedral grains, <500 μm in diameter, interstitial to silicates and oxides. Pyrite also occurs as fracture filling and replacement bodies. Some 38 samples of metabasites from various metamorphic zones were studied for sulfur isotope variations. Most analyses were carried out on interstitial sulfide grains. A list of the analytical data is given in the Appendix 5-3.

5-3-3-A. Variation of Sulfur Isotopes

Frequency distribution of $\delta^{34}S$ values (Figure 5-10) indicates a clustering of data around 0‰, consistent with a mantle origin for sulfur (c.f. Schneider, 1970; Sakai et al., 1982; Ohmoto, 1986; Kyser, 1990). Secondary pyrite, however, is relatively enriched in ^{34}S. The frequency distribution diagram further indicates that metabasites from various metamorphic zones are comparable in their sulfur isotope composition, and that metamorphic recrystallization did not alter the initial magmatic patterns.

Interstitial pyrite is the dominant sulfide in metabasites; accordingly, most experiments were carried out on this mineral. However, few samples with pyrrhotite as the main sulfide were also analyzed. A comparison of data on pyrite and pyrrhotite (Figure 5-11) indicates a similar isotopic composition for the two minerals, implying that replacement of pyrrhotite by pyrite had no effect on the initial isotopic composition of sulfur.

Pyrite also occurs as fracture filling as well as overgrowth and replacement bodies of secondary origin. Few isotopic data on the secondary pyrite indicate a relative enrichment in ^{34}S compared to the interstitial sulfides (Figure 5-10). The ^{34}S-rich S in secondary sulfides might have originated from internal sources (remobilization and reprecipitation of S within metabasites) or from external sources, such as metasedimentary country rocks.

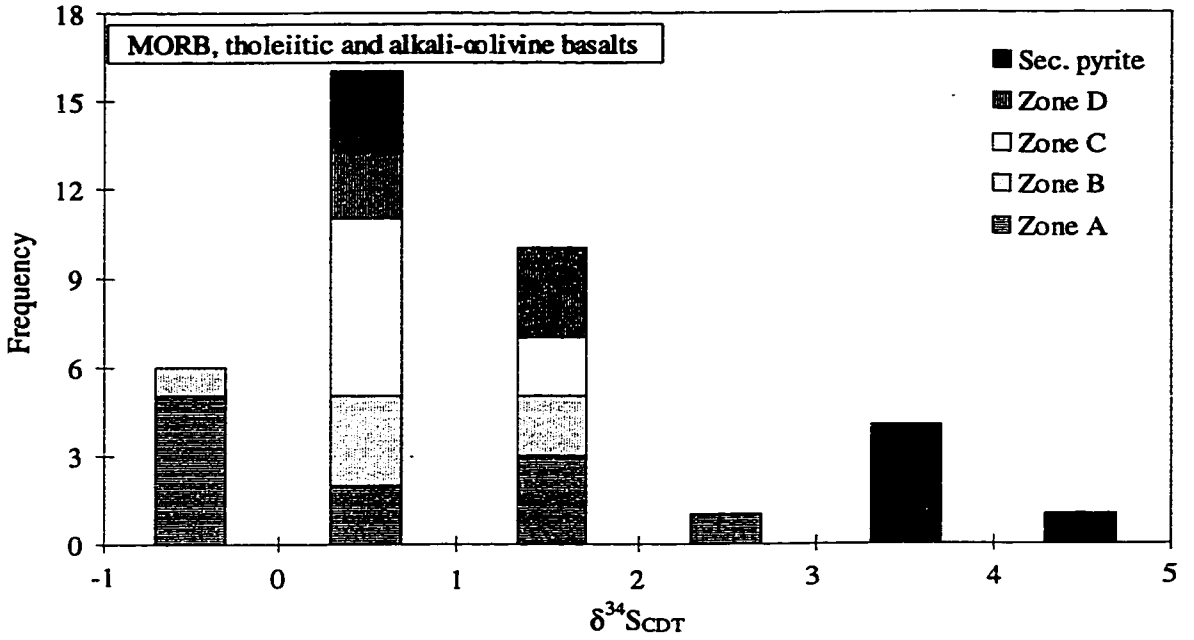

Figure 5-10. Variations of $\delta^{34}S$ in metabasites from various metamorphic zones. Secondary pyrite belongs to the amphibolite zone A. Field of MORB, tholeiitic and alkali-olivine basalt from Schneider (1970), and Sakai et al. (1982, 1984).

Pyrite is the main sulfide mineral in both metabasites and metasedimentary country rocks. Reactions have been proposed for breakdown of pyrite at high temperature (Ohmoto and Rye, 1979; Ohmoto, 1986):

$$6FeS_2 + 11H_2O = 3Fe_2O_3 + 11H_2S + SO_2$$

$$3FeS_2 + 2H_2O + 6H^+ = 3Fe^{2+} + 5H_2S + SO_2$$

Desulfidation may lead to a considerable fractionation only if it occurs in an open system and S is released in oxidized form. Reduced S would immediately react with Fe^{2+} bearing minerals to form Fe-sulfide (c.f. Kullerud and Moh, 1972; Mallio and Gheith, 1972). Reactions similar

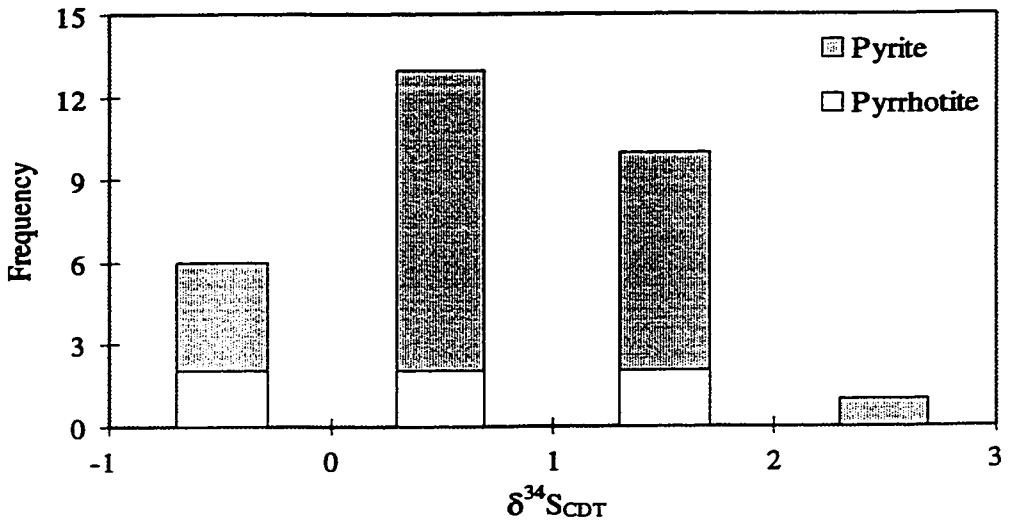

Figure 5-11. Variations of $\delta^{34}S$ in interstitial pyrite and pyrrhotite in metabasites from various metamorphic zones; Bamble.

to the above reactions were investigated by Grinenko and Grinenko (1967, 1975) who showed that H_2S liberated from breakdown of pyrite at temperatures of 350-550°C is enriched in ^{34}S between 1 to 3‰ relative to the initial pyrite.

An internal source of S for secondary pyrite requires that the net isotopic composition of the metabasites remain unchanged, provided that all reactions occurred in a closed system. The normal abundance of S in metabasites rules out a significant metamorphic desulfidation. Enrichment of ^{34}S in the secondary sulfides should be balanced by a corresponding depletion in the interstitial sulfides. No ^{34}S-depleted interstitial sulfide was detected. The ^{34}S-rich S in secondary pyrite probably originated from surrounding metasedimenatry rocks. The Bamble metasedimentary rocks display positive $\delta^{34}S$ values in the range 0-12‰. Migration of ^{34}S-rich S most likely took place from metasedimentary rocks with low content of Fe^{2+} towards the mafic rocks rich in Fe-Mg silicates and Fe-Ti oxides.

5-3-4. Hyperites

Numerous mafic intrusions as small stocks, lopolithic and dyke-like bodies, traditionally termed "hyperites" intruded older supracrustal and igneous rocks at the initial stages of the Sveconorwegian orogenic event (e.g. Touret et al., 1968; Starmer, 1969, 1985; Brickwood and Craig, 1987). The intrusion age of the hyperites has been determined to be ~1250-1100 Ma (e.g. Jacobsen and Heier, 1978; Dahlgren et al., 1990; de Haas, 1992).

After differentiation and intrusion, some of the mafic bodies underwent deuteric and metamorphic alteration. Corona growth around ferromagnesian minerals and metamor-phism converted the rocks into coronitic gabbro and amphibolite. Hydration and recrystallization is more extensive in the hyperite bodies intruded into the amphibolite facies country rocks.

"Hyperite" has variously been applied to all kinds of gabbroic rocks and their amphiboitized equivalents. In this study, the term "hyperite" has been limited to hypersthene-gabbros. Olivine-gabbro, where displaying coronitic texture, is referred to as "coronitic gabbro". Amphibolitized gabbros and hyperites are referred to as "amphibolite".

Sulfides are minor constituents of the Bamble hyperites (gabbros), rarely exceeding 0.5% by mode. Pyrrhotite, the main sulfide in coronitic gabbros and hyperites, is partially to totally replaced by pyrite ± magnetite in the marginal amphibolites. Both pyrrhotite and pyrite may contain lamellae and patches of chalcopyrite and pentlandite. Sulfides commonly occur as fine subhedral to anhedral grains (<500μ in diameter) interstitial to silicates and oxides. Pyrite may also occur as fracture filling and replacement bodies in the amphibolites.

Some 20 samples of hyperites, coronitic gabbros, and amphibolites from several bodies in Laget (amphibolite zone), Tvedestrand (transition zone), and Tromoy (granulite zone) were studied for sulfur isotope ratios. A summary of the analytical results is given in the Appendix 5-4.

5-3-4-A. Variations of Sulfur Isotopes

As in metabasites, all $\delta^{34}S$ values for interstitial sulfides fall in a narrow range around 0‰ (Figure 5-12), consistent with a mantle origin for sulfur. Secondary sulfides are relatively enriched in ^{34}S. No distinction can be made between various metamorphic zones with respect to the $\delta^{34}S$ values.

Hyperite dykes from Tromoy and Tvedestrand are partially amphibolitized and provide examples of transition from primary pyrrhotite to pyrite ± magnetite. To investigate the effects of the oxidation and sulfide phase changes on the variations of sulfur isotopes, individual grains of pyrrhotite and pyrite from the same samples were analyzed. The results show similar isotopic compositions for the two minerals (Figure 5-13). Variations are very small (0.1-0.3‰) and fall in the error range of the laser combustion technique.

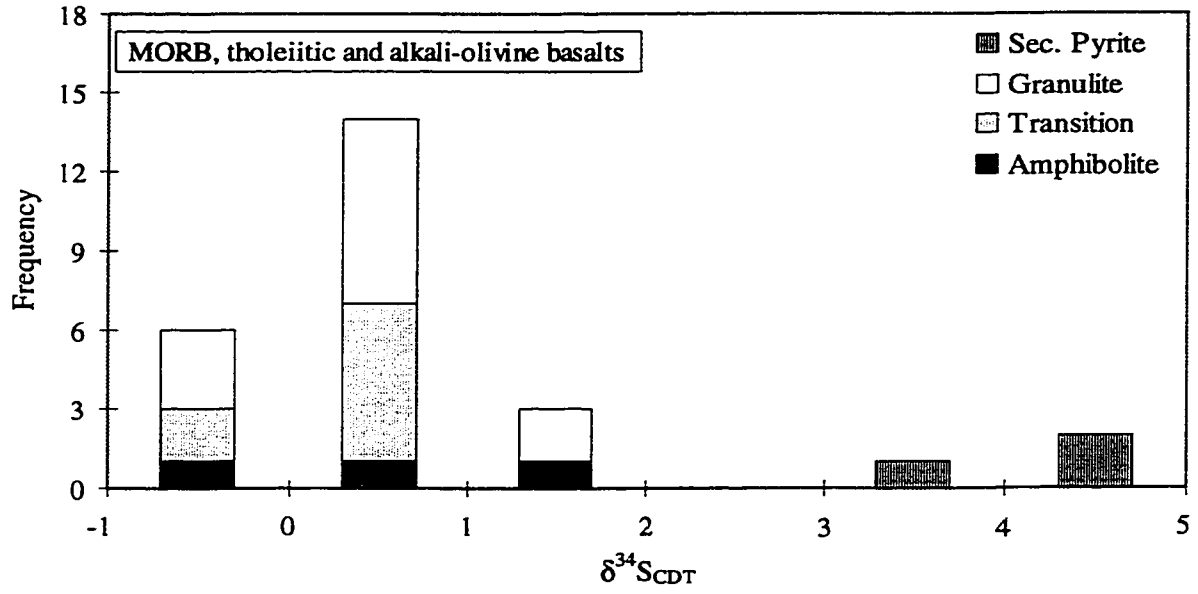

Figure 5-12. Variations of $\delta^{34}S$ in gabbros (hyperites) and their amphibolitized margins from various metamorphic zones, Bamble. Field of MORB, tholeiitic and alkali-olivine basalts from Schneider (1970) and Sakai et al. (1982, 1984). Secondary pyrite belongs to the amphibolite zone.

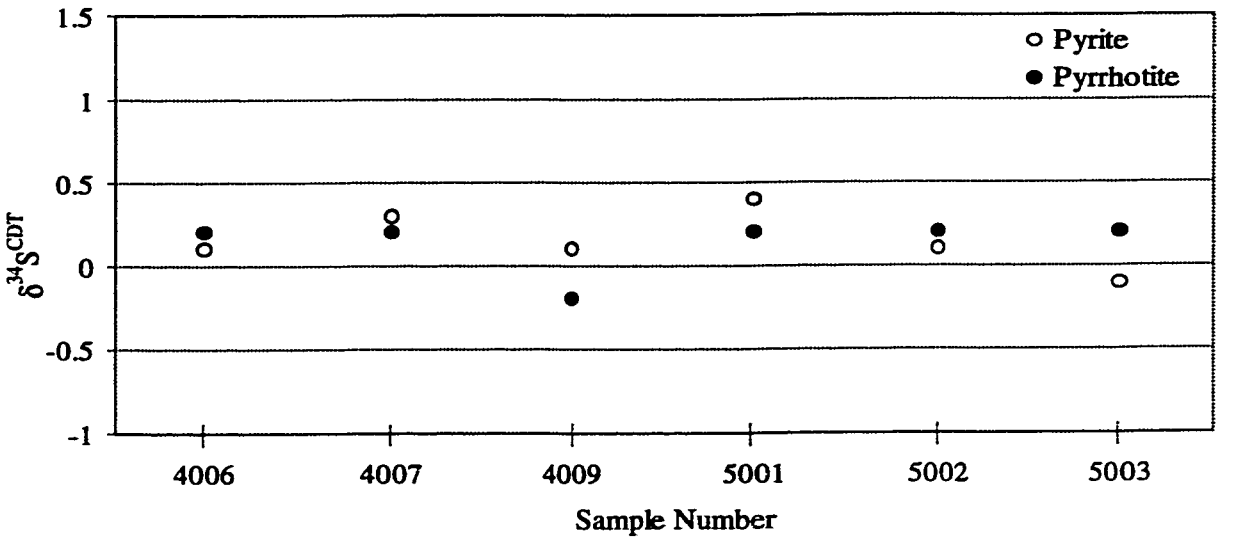

Figure 5-13. Variations of $\delta^{34}S$ values in disseminated pyrrhotite and pyrite from hyperite dykes in Tvedestrand (transition zone, 4006-4009) and Tromoy (granulite zone, 5001-5003).

5-3-5. Fe-Ni-Cu Ores

Fe-Cu-Ni sulfide deposits are locally associated with the hyperites. The deposits, generally situated in the marginal parts of the host intrusions, are comparatively small having yielded some 10,000 tones of Ni in total (Bugge, 1978). Considering the mineral parageneses and textures, three stages of ore formation can be identified (c.f. Brickwood, 1984, 1986):

1) Primary orthomagmatic crystallization;

2) Metamorphic recrystallization; and

3) Supergene alteration.

The primary ore occurs as network and disseminated, as well as massive, in the marginal parts of the host intrusions. Pyrrhotite, pentlandite, and chalcopyrite are the main sulfides in the primary ore. Brickwood (1984) reported the presence of xenoliths of the country rock gneisses in the massive ores from several deposits in the Bamble area.

As in their mafic host rocks, the sulfide ores also experienced retrograde reactions, with partial to complete replacement of pyrrhotite by pyrite. The sulfide-silicate contacts are

distorted, with sulfides occurring as scattered discrete xenoblasts and granular aggregates, as well as overgrowths and veinlets replacing silicates along grain boundaries and cleavage planes.

To investigate the source of sulfur and variations of sulfur isotopes with recrystallization of the primary orthomagmatic ores, some 15 samples of ores from small deposits in Arendal and Tvedestrand areas were analyzed. The ore samples represent various paragenetic and textural types, including:

- Primary orthomagmatic ore, or pyrrhotitic ore, with pyrrhotite as the main sulfide mineral.
- Moderately recrystallized ore, or composite ore, with partial replacement of pyrrhotite by pyrite.
- Strongly recrystallized ore, or pyritic ore, with complete replacement of pyrrhotite by pyrite and local remobilization and reprecipitation of sulfides as overgrowth and fracture filling.

Pyrrhotite is the dominant sulfide in the orthomagmatic ore, constituting up to 98% of the total sulfides. Accordingly, isotopic composition of pyrrhotite can safely be considered as representative of the bulk ore; as is the case for pyrite in the strongly recrystallized ore. Minor chalcopyrite and pentlandite (commonly <10% by mode) are associated with both types of ores. For the moderately recrystallized ore, or composite ore, experiments have been carried out on coexisting pyrrhotite and pyrite. A complete list of the analytical data is included in the Appendix 5-5.

5-3-5-A. Variations of Sulfur Isotopes

A frequency distribution of $\delta^{34}S$ values is shown in Figure 5-14. No distinction can be made between various types of ores with regard to the sulfur isotope composition. The average $\delta^{34}S$ values for recrystallized and composite ores are similar and in the same range as in the primary orthomagmatic ore, implying that no significant fractionation of S isotopes occurred during replacement of pyrrhotite by pyrite. Slight enrichment of ^{34}S in pyrite relative to the coexisting pyrrhotite in composite ore is consistent with equilibrium isotope exchange between the two

minerals (c.f. Bachinski, 1969; Kajiwara and Krouse, 1971). The Ni-Cu ores are intimately associated with hyperites; however, they are enriched in ^{34}S by up to 4‰. Secondary overgrowth and fracture filling pyrite is relatively depleted in ^{34}S.

5-3-5-B. Source of Sulfur in the Primary and Recrystallized Ores

The relative enrichment of ^{34}S in the sulfide ores, compared to their host hyperites, can not be easily explained by a magmatic crystallization model, as fractionation of S isotopes between crystallizing sulfides and silicate melts is very small, < 1‰ (c.f. Ohmoto and Rye, 1979, Ohmoto, 1986). Sulfur occurs in a melt predominantly as HS^- that behaves isotopically in a similar manner to aqueous HS^- (Ohmoto and Rye, 1979). The early fraction of sulfides crystallizing from a magma tends to be enriched in ^{34}S with respect to HS^-. However, due to the small value of $\Delta_{(sulfide - HS^-)}$ at high magmatic temperatures (<1‰), depletion of ^{34}S in the residual melt is negligible, even after the removal of a considerable amount of S in the initial magma assuming a Rayleigh distillation process (Ohmoto and Rye, 1979).

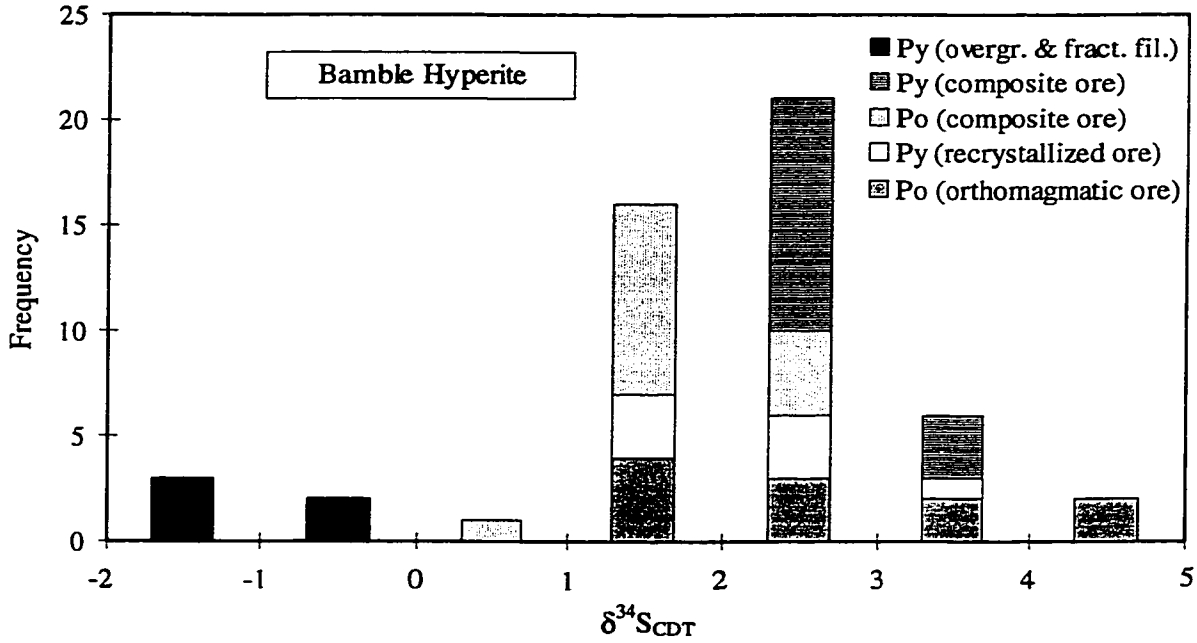

Figure 5-14. Variations of $\delta^{34}S$ for pyrite and pyrrhotite from various types of ores, Bamble. Box representing the isotopic composition of hyperites is shown for comparison.

5-3-5-C. Crustal Contamination

I. Evidence from Sulfur Isotope Ratios

Local assimilation of sulfidic metasedimenatry rocks could be a possible explanation for the marked shift in the isotopic composition of the ores (c.f. Sasaki, 1969; Ripley, 1981, 1983; Mainwaring and Naldrett, 1977; Garuti et al., 1986). This is supported by the localization of mineralized zones at the boundary between the mafic intrusions and the metasedimentary country rocks, and the presence of xenoliths of metasediments in the massive ores.

Assimilation of country rocks and incorporation of S from sulfide-rich sedimentary and metamorphic rocks is a key factor in the formation of many Ni-Cu deposits associated with mafic and ultramafic intrusions (e.g. Groves et al., 1979; Green and Naldrett, 1981; Naldrett, 1981; Lesher et al., 1984; Ripley et al., 1999). This process would lead to local supersaturation of S in the magma, and subsequent exsolution and precipitation of sulfides (c.f. Hopwood, 1981; Naldrett, 1989). Pyritic sediments are major units in the host stratigraphy adjacent to some magmatic Ni-sulfide deposits from Western Australia (Prider, 1970; Ross and Hopkins, 1975; Hopwood, 1981) and Canada (Naldrett, 1969; Naldrett and Gasparrini, 1971; Paktunc, 1989). Assimilation of silicic country rocks would contribute to the formation of sulfide deposits by lowering the solubility of S within mafic magmas.

II. Evidence from S/Se Ratios

The Fe-Ni-Cu ores are also considerably depleted in Se (mean Se = 30 ppm) compared to the interstitial sulfides in the host gabbros (mean Se = 75 ppm). S/Se ratios for various types of ores fall in a wide range from 4000-24000 (mean 9000), while those for the host hyperites range from 3000 to 6000 (mean 4800). A compilation of data on S/Se ratios and $\delta^{34}S$ values in sulfide ores and various rock units from Bamble is shown in Figure 5-15.

Sedimentary sulfides are relatively depleted in Se, and sedimentary rocks are commonly characterized by S/Se>10000 (Hawley and Nicol, 1959; Stanton, 1972; Naldrett, 1981; Eckstrand and Hulbert, 1987). Magmatic sulfides, on the other hand, are enriched in Se. S/Se

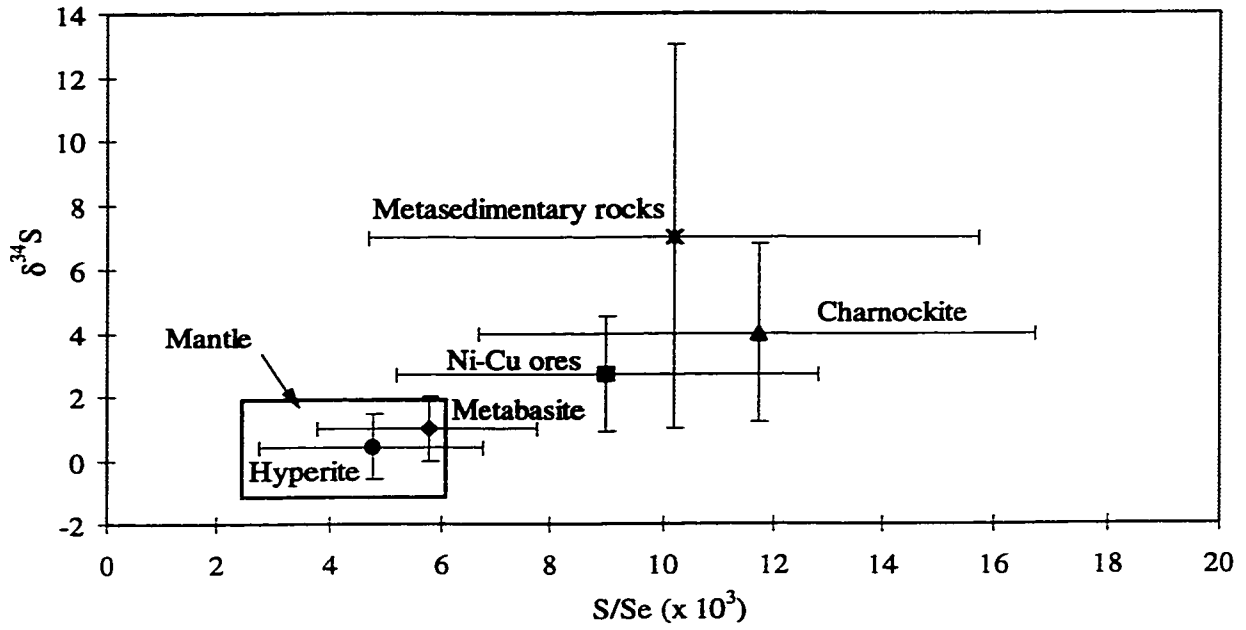

Figure 5-15. Variations of $\delta^{34}S$ values with S/Se ratios for various rock units in Bamble. Mantle range is shown for reference: S/Se ratio after Eckstrand et al. (1989) and $\delta^{34}S$ after Kyser et al. (1990). Bars represent 1σ standard deviation.

ratios in various magmatic sulfide ores have been determined to be in the range 3 x 10^3 to 6 x 10^3 (Hawley and Nicol, 1959; Green and Naldrett, 1981; Paktunc, 1989, 1990; Eckstrand et al., 1989; Brügman et al., 1990). Relatively high S/Se ratios (>10^6) in mafic rocks and magmatic sulfide ores have frequently been attributed to assimilation of sedimentary sulfides (e.g. Groves et al., 1979; Green and Naldrett, 1981; Lesher et al., 1984; Eckstrand et al., 1989; Paktunc, 1989, 1990). Depletion of Se in sulfide ores might also be explained by rapid crystallization and precipitation of sulfides before complete equilibration with the silicate melt.

5-3-5-D. Overgrowth and Fracture Filling Pyrite

The overgrowth and fracture filling pyrite is relatively depleted in ^{34}S. The occurrence of the pyrite on metamorphic amphibole and plagioclase indicates that sulfide redistribution continued at low temperatures following primary metamorphic recrystallization. Common association of the pyrite with mafic silicates suggests that Fe was most likely supplied by the host minerals.

Depletion of ^{34}S in the overgrowth and fracture filling pyrite might be attributed to deposition from alkaline solutions. Experiments by Grinenko and Grinenko (1975) have shown that isotope fractionation in acid solutions is determined by equilibrium between sulfide and H_2S, the latter being enriched in ^{34}S by 1 to 3‰ at temperatures of 350-550°C. In alkaline solutions, however, the bulk of the sulfide S occurs in ionic form and isotope equilibrium between sulfide and solution leads to enrichment of S in solution in ^{32}S.

Alternatively, the depletion in ^{34}S may be explained by deposition from a solution containing both oxidized and reduced sulfur compounds. Sulfides deposited from a solution containing oxidized sulfur are depleted in ^{34}S compared to the decomposed sulfides. The magnitude of the depletion depends on temperature and the ratio of the oxidized to reduced sulfur in solution.

5-3-5-E. Variations of Sulfur Isotopes in Coexisting Sulfides

Pyrrhotite, the main sulfide in the primary orthomagmatic ores, has variably been replaced by pyrite in the recrystallized ores. To further identify the nature of the oxidation and recrystallization of primary ores, experiments have been carried out on coexisting pyrrhotite and pyrite. The results are shown in the Appendix 5-5.

In almost all samples, pyrite was found to be enriched in ^{34}S relative to the coexisting pyrrhotite, in agreement with theoretical and experimental data on the isotopic equilibrium fractionation between coexisting pyrite and pyrrhotite (c.f. Bachinski, 1969; Kajiwara and Krouse, 1971). The $\Delta\delta^{34}S_{Py\text{-}Po}$ values for Bamble sulfide ores fall in the range 0.5-1.2‰.

Variable enrichment of ^{34}S in pyrite coexisting with pyrrhotite have been reported from metamorphosed rocks and ores (Speelman and Schwarcz, 1966; Lusk and Crocket, 1969; Mauger, 1972, Gehrisch and Maucher, 1975). Speelman and Schwarcz (1966) determined a $\Delta\delta^{34}S_{Py\text{-}Po}$ = 0.1‰ to 1.4‰ for coexisting pyrite and pyrrhotite in metamorphic rocks from Haliburton-Madoc area, Ontario. The authors noted that the range of fractionation decreases

with increasing metamorphic grade. Lusk and Crocket (1969) reported an average $\Delta\delta^{34}S_{Py\text{-}Po}$ = 0.50 ± 0.14‰ from Heath Steel B-1 Orebody, New Brunswick. Similarly, Mauger (1972) showed that pyrite was enriched in ^{34}S between 0.3-1.6‰ relative to the associated pyrrhotite in the massive sulfide lenses at Ducktown, Tennessee. Gehrisch and Maucher (1975) documented a $\Delta\delta^{34}S_{Py\text{-}Po}$ between 0.5 to 1‰ in Sulitjelma massive sulfide ore bodies, northern Norway.

Theoretical and experimental studies of sulfur isotope exchange between common sulfide minerals have indicated that variations in $^{32}S/^{34}S$ ratios among coexisting sulfides are systematic and consistent with the relative strengths of metal/sulfur bonds (Sakai, 1968; Bachinski, 1969; Kajiwara and Krouse, 1971; Nielsen, 1979). The studies have further shown that the extent of isotope exchange between coexisting sulfides is temperature-dependent.

Sulfur isotope fractionation curves have been developed that relate the extent of isotope exchange to temperature of equilibration (Kajiwara and Krouse, 1971; Bachinski, 1969; Nielsen, 1979). Plots of the $\Delta\delta^{34}S_{Py\text{-}Po}$ values on the fractionation curve of Kajiwara and Krouse shows a wide range of temperature from 200 to 650°C (Figure 5-16). However, most

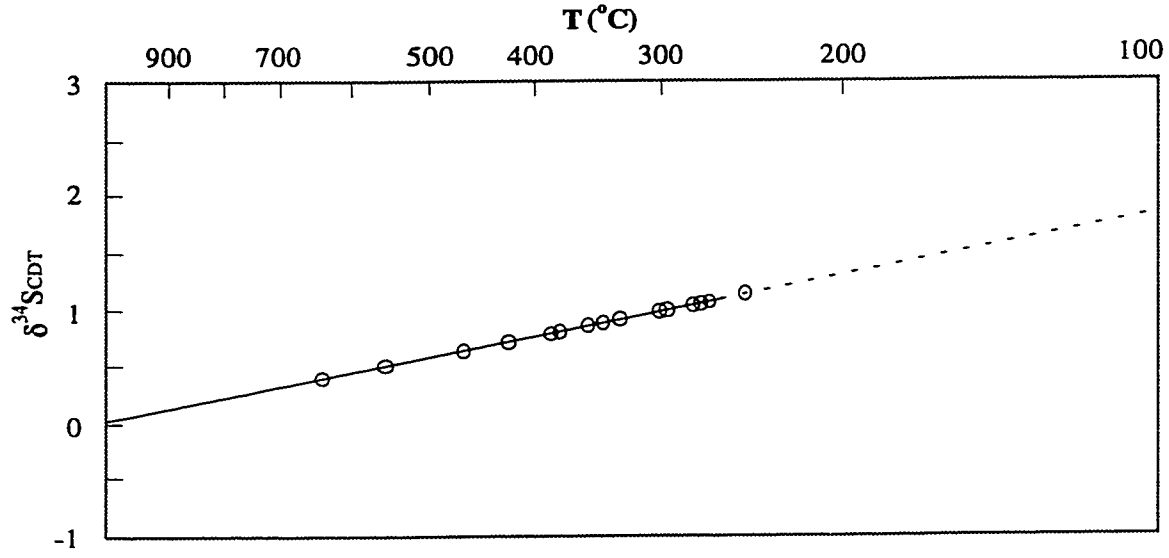

Figure 5-16. Variations of $\Delta\delta^{34}S_{Py\text{-}Po}$ in coexisting pyrite-pyrrhotite pairs in Bamble Fe-Ni-Cu ores. Fractionation line after Kajiwara and Krouse (1971).

values fall in the range 0.7 to 1‰, implying a temperature of 280 to 400°C. This is consistent with the temperature of formation of pyrite and subsequent equilibration with pyrrhotite with decreasing temperature (c.f. Kullerud and Yoder, 1959, Arnold, 1971; Naldrett and Kullerud, 1967; Scott et al., 1977). This further supports an earlier study by Brickwood (1984) who determined a low temperature of equilibration (< 500°C) for coexisting magnetite-ilmenite pairs from several sulfide deposits in Bamble.

5-4. Discussion

The Bamble metasedimentary rocks display a large variation in $\delta^{34}S$ in the range -1‰ to +12‰ consistent with data from sedimentary rocks of early- to mid-Proterozoic age. Metasedimentary rocks from various metamorphic zones display similar spreads in $\delta^{34}S$ values. However, granulite grade rocks are slightly enriched in ^{34}S. Our data on the variations of $\delta^{34}S$ do not support an earlier study by Andreae (1974) who reported a smaller spread in $\delta^{34}S$ for granulite grade rocks, and attributed it to homogenization of sulfur isotopes during high grade metamorphism.

The granulite facies gneisses, containing on average 3200 ppm S, are considerably enriched in S relative to metasedimentary rocks from amphibolite and transition zones, both containing <1000 ppm S. An enrichment of S in the granulite grade rocks was also recognized by Andreae (1974). There is evidence that replacement of pyrite by pyrrhotite in sedimentary rocks from transition and granulite zones was associated with uptake of Fe from surrounding Fe-Mg silicates, rather than a desulfidation process.

Plot of $\delta^{34}S$ values against S contents for various rock units (Figure 5-17) indicates a general tendency for enrichment in ^{34}S with increasing S and increasing metamorphic grade. Enrichment of S in the granulite facies gneisses is explicable in terms of the low solubility of S in the products of anatexis (c.f. Banks, 1982; Kubilius, 1983; Poulson et al., 1991). However, in the absence of evidence for significant partial melting in Bamble (Knudsen et al., 1997;

present study), the relatively high concentration of S in the granulite facies rocks might be a feature inherited from their protoliths.

Sulfur and S-isotopes behave variably during metamorphism. Grinenko and Grinenko (1975) reported a decrease in S but an increase in $\delta^{34}S$ with progressive replacement of pyrite by pyrrhotite in a metamorphosed pyritic vein. In contrast, Siewers (1974) indicated a depletion in ^{34}S, but an enrichment in S with increasing metamorphic grade in Cevennen metamorphic Complex, France, and in Keuper metamorphic series, Switzerland. A depletion in ^{34}S with increasing metamorphic grade was also reported by Ronov et al. (1977) from Ladoga Formation, Russia; however, the authors showed that concentration of S also decreased in the same direction.

Yamamoto et al. (1984) showed that metamorphic pyrrhotitization in Besshi massive sulfide deposits, Central Shikoku, Japan, did not significantly alter the $\delta^{34}S$ values of the remaining pyrite and chalcopyrite. Poulson et al. (1991) reported a decrease in S, but no consistent trends of variation in $\delta^{34}S$, with increasing metamorphic grade from greenschist to amphibolite in Maguma Group metasediments, Nova Scotia. The contrasting behavior of S and S-isotopes indicates that metamorphism proceeds under variable conditions from one place to the other.

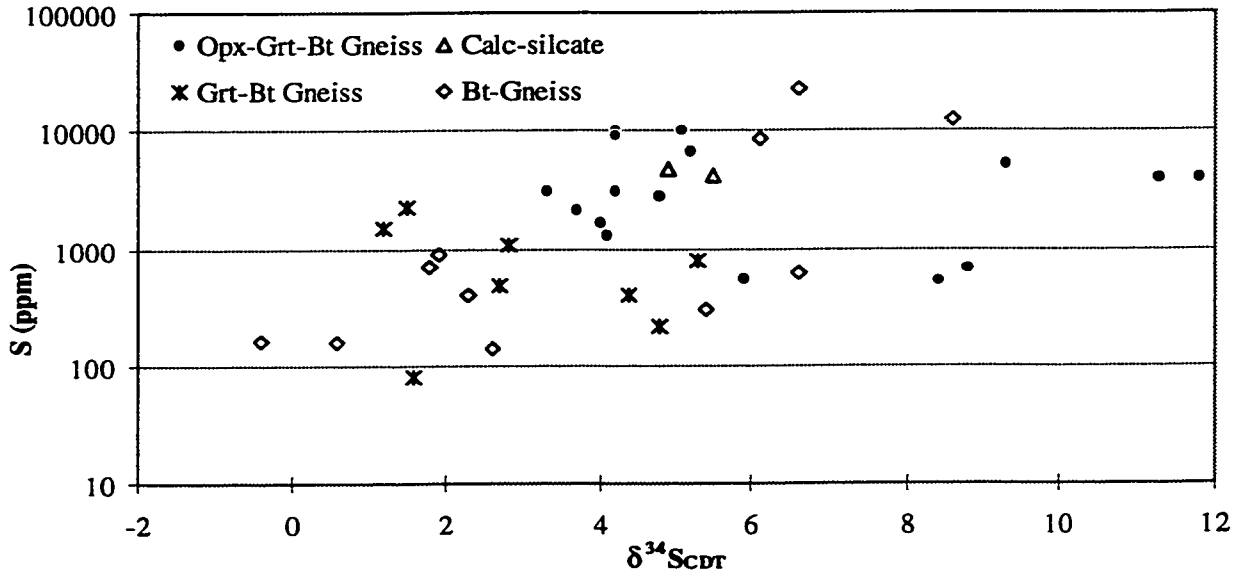

Figure 5-17. Variations of $\delta^{34}S$ with S for various metasedimentary units, Bamble.

Mafic rocks from various metamorphic zones display a clustering of $\delta^{34}S$ values around 0‰ suggesting a mantle origin for S. Pyrrhotite, the main sulfide in gabbros and hyperites, is replaced by pyrite ± magnetite in the marginal amphibolites. The similar isotopic composition of pyrrhotite and pyrite suggests that oxidation and breakdown of pyrrhotite occurred in a system closed to significant fractionation of S isotopes. This is supported by the similar S contents in hyperites and gabbros and their amphibolitized margins.

There is strong evidence that ^{34}S-rich S from metasedimentary country rocks was involved in the formation of Fe-Ni-Cu ores. This is supported by both S isotope and S/Se ratios. The mean $\delta^{34}S$ values and S/Se ratios from the ores (3‰ and 9000, respectively) are considerably higher than those from the host hyperites (0.5‰ and 4700, respectively).

Similarly, tonalitic-trondhjemitic charnockites show a wide spread in $\delta^{34}S$ values, in the same range as in the granulite facies metasedimentary rocks. They also exhibit a high S/Se ratio, well above the normal range for mantle-derived tonalite-trondhjemite series (c.f. Kerrich, 1989). These features cast doubt on the general belief that Bamble charnockites are of juvenile magmatic origin. If they are of magmatic origin, the parent magma must have been strongly contaminated with crustal materials.

Most data in the literature on the metamorphic isotopic equilibrium in sulfides come from sulfidic ore bodies where sulfides occur in direct grain-to-grain contact. Studies of the metamorphosed sulfide deposits have demonstrated localized small-scale re-equilibration of S isotopes between sulfide minerals, but little evidence of homogenization on the deposit scale (e.g. Lusk and Crocket, 1969; Von Gehlen et al., 1983; Willan and Coleman, 1983; Seccombe et al, 1985; Skauli et al, 1992; Crowe, 1994).

Von Gehlen et al. (1983) showed that the original isotopic patterns in the Precambrian polymetallic sulfide deposits at Aggeneys-Gamsberg, South Africa, were not obliterated in spite of upper amphibolite to granulite grade metamorphism. Preservation of the primary sedimentary isotopic features have also been reported from metamorphosed sulfide deposits in

Broken Hill, Australia (Stanton and Rafter, 1967; Spry, 1987), Adirondacks, New York (Buddington et al., 1969), Rosebery, Tasmania (Green et al., 981), Kanmantoo, Southern Australia (Seccombe et al., 1985), Ducktown, Tennessee (Bachinski, 1969; Mauger, 1972), Norwegian Caledonides (Skauli et al., 1992, Cook and Hoefs, 1997) and Aberfeldy, Scotland (Willan and Coleman, 1983).

Metamorphism may lead to a reduction in the original isotopic variations. However, as proposed by Rye and Ohmoto (1974), the weighted average $\delta^{34}S$ value of the metamorphosed sulfides is consistent with that of the primary materials. A change in the average isotope ratio can only be achieved if the whole rock complex acts as an open system for sulfur, and large amounts of isotopically fractionated sulfur can leave or enter the system (e.g. Rye and Ohmoto, 1974; Grinenko and Grinenko, 1975). This is only possible if sulfur occurs in an oxidized species; reduced sulfur will immediately react with the available Fe^{2+} to form iron sulfide (c.f. Kullerud and Moh, 1972; Mallio and Gheith, 1972). Grinenko and Grinenko (1975) suggested that isotope equilibrium is not established unless the minerals undergo complete dissolution and redeposition.

In normal metamorphic rocks, where sulfides commonly occur as accessory disseminated grains with no direct isotopic communication, there is a greater chance for original isotopic patterns to be preserved. A compilation of data on isotopic composition of sulfides from high-grade metamorphic terrains worldwide (Zheng, 1990) indicates large variations, up to 20‰, within individual areas. Crow (1994) showed that disseminated monomineralic sulfide grains in metamorphosed VMS stockwork feeder zones preserved their original isotopic compositions, in spite of greenschist to upper amphibolite facies metamorphism.

A large scale isotopic equilibrium may occur only in the presence of a pervasive infiltrating fluid of uniform isotopic and chemical composition, given a sufficient quantity over a long enough period of time (Valley, 1986). In the absence of fluid flow, isotopic exchange may occur over much more limited distances by solid state diffusion, or diffusion through a static fluid (Rumble, 1982; Valley and O'Neil, 1984; Valley, 1986; Broekmans et al. 1994).

6. Depletion of Gold

6-1. Supracrustal Rocks

The Bamble supracrustal rocks are considerably depleted in Au, As, Sb, and Se relative to the mean composition of the continental crust (Figure 6-1). The mean abundance of Au in the Bamble rocks (0.30 ppb) is only 20% of the crustal abundance of this element. A comparison to shales and greywackes as the most likely protoliths for Bamble metasediments would imply a stronger depletion in the chalcophile elements. Calc-silicates are slightly enriched in Au; however, these rocks are considerably enriched in other chalcophile elements. Sulfur and Cu display large variations, with marked enrichment in the granulite-grade gneisses and calc-silicates. The relatively low concentration of Au in the Bamble supracrustal rocks might be of primary sedimentary, or secondary metamorphic, origin, or both.

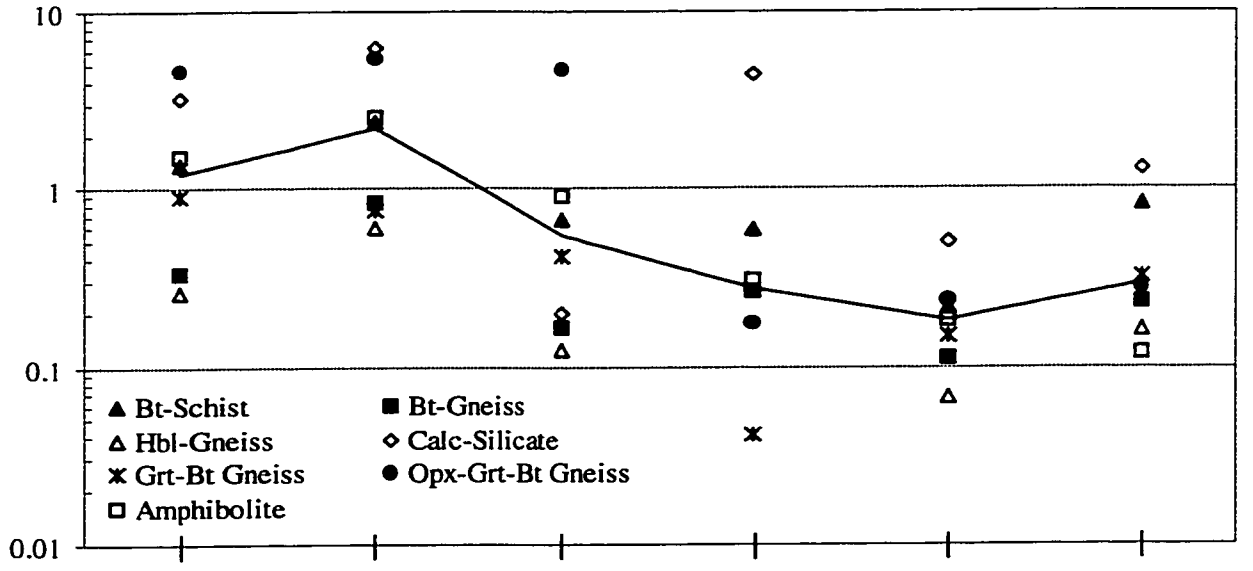

Figure 6-1. Distribution of chalcophile elements in the Bamble supracrustal units, normalized to the mean continental crust. Solid line joins the mean of the mean values. See Appendix 2-2 for normalization data.

6-1-1. Source Rock Influence

Geochemical characteristics of the Bamble metasediments (i.e. relatively low Sr, P, and transition metals, and high Y and HREE) suggest that they derived mostly from granitic rocks (c.f. Collins et al., 1982; Taylor, 1986; Kerr et al., 1993; Whalen et al., 1987, 1996). Such origin is further supported by strongly negative Eu anomalies. The mean Eu/Eu* values for various supracrustal rocks in Bamble are considerably lower than those for the average post-Archean sedimentary rocks (c.f. Taylor and McLennan, 1985). Derivation from felsic igneous or metamorphic rocks is also reflected in the common occurrence of quartzites and impure quartzites in Bamble. Felsic rocks are commonly depleted in chalcophile elements compared to other rock types (Appendix 2-2).

A comparison of the abundance of Au in the Bamble supracrustal rocks with that in shales and greywackes as the most likely protoliths indicates an extreme depletion of Au in the Bamble rocks (Figure 6-2). This is difficult to be attributed solely to the initial, pre-metamorphic materials.

Concordant amphibolites are of igneous origin and display features characteristic of calc-alkaline basalts emplaced at destructive plate margins. Hornblende-gneisses also appear to be of igneous origin. Both amphibolites and hornblende-gneisses are strongly depleted in Au, As, and Sb, compared to equivalent rocks elsewhere. That all supracrustal units in Bamble, of varied origin, composition, and age, are depleted in certain elements, suggest that factors other than source rocks or depositional environments were involved.

6-1-2. Metamorphic Effect

Although strongly depleted in Au, the Bamble supracrustal rocks carry relatively high contents of S (Figure 6-1). Sulfides are the main host to Au in sedimentary and metasedimentary rocks (e.g. Lagedza, 1969; Glasson and Keays, 1978; Keays et al., 1981; Korobeynikov, 1995). Depletion of Au requires a strong fractionation of this element from S during metamorphism.

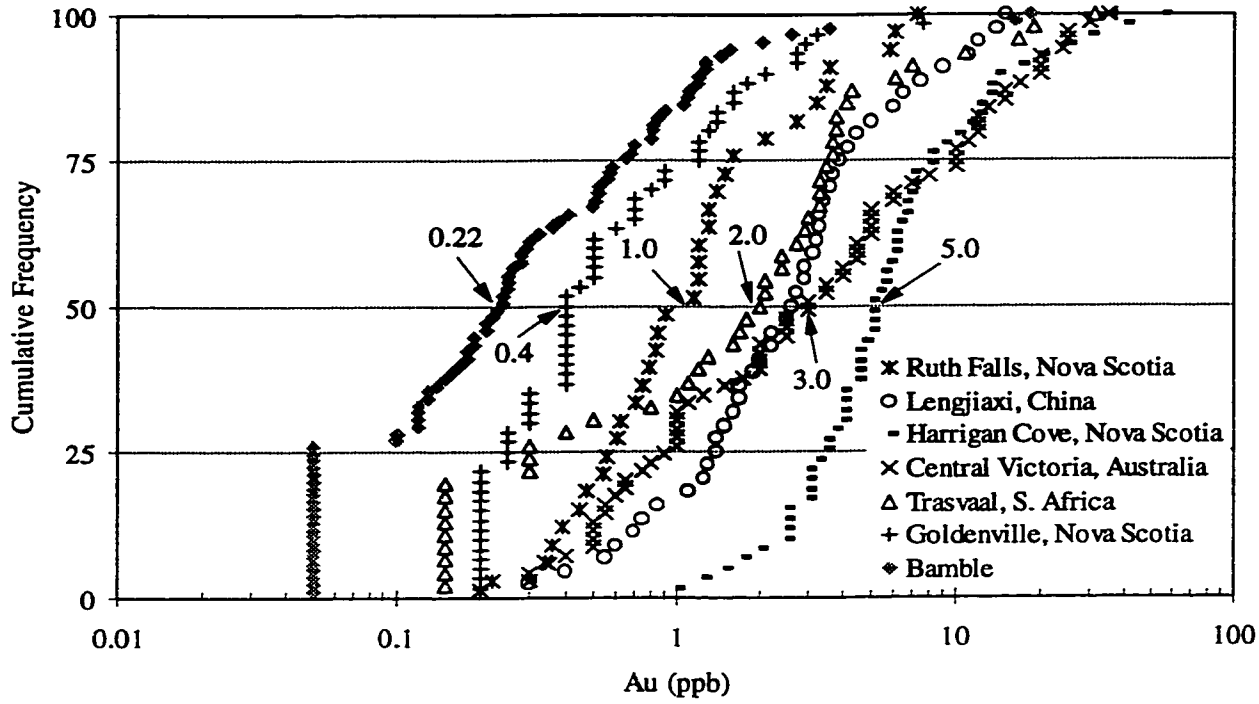

Figure 6-2. Cumulative frequency of Au in the Bamble supracrustal rocks. The abundance of Au in the greenschist facies shales and greywackes elsewhere shown for comparison. Arrows indicate the median values. Data for the greenschist facies rocks from: Transvaal (Minnitt et al., 1973); Goldenville (Thorpe and Thomas, 1976); Central Victoria (Glasson and Keays, 1978); Ruth Falls (Crocket et al., 1983); Harrigan Cove (Crocket et al., 1986); Lengjiaxi (Yingjun et al., 1992).

Arsenic and Sb have both chalcophile and lithophile affinities. Relative abundance of chalcophile elements with respect to S may be used as a rough index of differentiation of the elements during progressive metamorphism (Figure 6-3).

The ratios of Au/S, Sb/S, and As/S for all rock units fall well below unity, compared to the mean continental crust, implying a significant fractionation of Au, As, and Sb from S in the Bamble rocks. Moreover, a decrease in the elemental ratios is evident towards granulite zone, indicating extreme fractionation of the elements under granulite metamorphism. The ratios of Cu/S and Se/S are close to unity, suggesting that Cu and Se were not significantly fractionated during metamorphism. Copper has rarely been reported to be enriched in lode gold deposits; Se may or may not be enriched (e.g. Boyle, 1979; Colvine et al., 1988; Roberts, 1987; Kerrich, 1989 a, 1990; Groves et al., 1992, 1998).

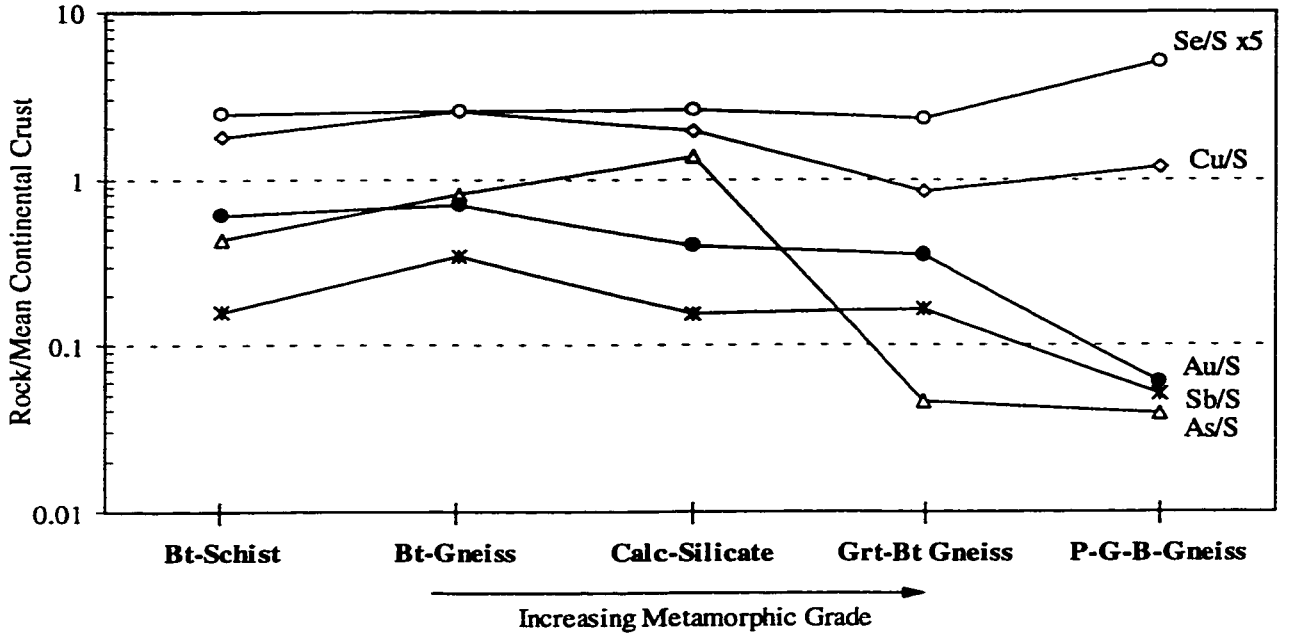

Figure 6-3. Relative abundance of chalcophile elements with respect to S for various metasedimentary units, normalized to the mean continental crust. Bt-schist and Bt-gneiss are from amphibolite zone, Calc-silicate and Grt-Bt gneiss from transition zone, and Px-Grt-Bt gneiss from granulite zone. See Appendix 2-2 for normalization data.

Arsenic has frequently been reported to be depleted in high grade metamorphic rocks (e.g. Rösler and Beuge, 1983; Taylor and McLennan, 1985; Sims et al., 1990; Wedepohl, 1995). Rösler and Beuge (1983) demonstrated a strong depletion in As, by up to 70%, with progressive metamorphism of sedimentary rocks. The authors also documented a marked depletion in Sb. However, estimations by Taylor and McLennan (1985) and Wedepohl (1995) show no significant depletion in Sb in the lower crustal rocks.

Sulfur behaves variably during metamorphism. While some authors have shown a decrease in S (e.g. Ronov et al., 1977; Rösler and Beuge, 1983; Poulson et al., 1991), others have indicated that mass transfer of S does not normally occur during progressive metamorphism (e.g. Thompson, 1972; Robinson and Tracy, 1976). Yet, another group have documented an increase in S with increasing metamorphic grade (Siewers, 1974; Andreae, 1974).

The preservation of the initial, pre-metamorphic $\delta^{34}S$ patterns, and the large spread in $\delta^{34}S$ values, for various rock units in Bamble indicates that no significant fractionation or exchange of S isotopes occurred during metamorphism. There is evidence that replacement of pyrite by pyrrhotite in metasedimentary rocks from transition and granulite zones was associated with uptake of Fe from surrounding silicates rather than a desulfidation process. The above features argue against a significant metamorphic remobilization of S in Bamble.

Enrichment of S, Cu and Se in the granulite grade rocks might be attributed to partial melting processes. Due to the low solubility of S in SiO_2-rich melts (Haughton et al., 1974; Wendladth, 1982; Banks, 1982; Poulson et al., 1991) this element would be enriched in the residue of anatexis. However, in the absence of evidence for significant partial melting in Bamble (Knudsen, 1996; Knudsen et al., 1997; present study), the relatively high S, Cu, and Se contents in the granulite facies rocks is probably of initial sedimentary origin. Copper and Se are strongly chalcophile and follow S in behavior. They are known to be variably enriched in the lower crustal rocks (Taylor and McLennan, 1985; Wedepohl, 1995).

Behavior of Au during progressive metamorphism is controversial. According to one view, regional metamorphism does not cause any loss of Au from the rocks but may redistribute it (e.g. Petrov et al., 1972; Sighinolfi and Santos, 1976; Li and Shokhina, 1974; Gavrilenko et al., 1974; Rösler and Beuge, 1983; Dolazhenko, 1994). According to another view, Au is highly mobile, particularly under high grade metamorphism, and high grade rocks are considerably depleted in this element compared to their lower grade equivalents (e.g. Buryak, 1970, 1978; Stephenson and Ehmann, 1971; Weber and Stephenson, 1973). Yet, another group believe that there are differences in behavior in given metamorphic processes in different regions (e.g. Cameron, 1989a, b, 1993a, b; Korobeynikov, 1991).

Gold in sedimentary and metamorphic rocks occurs as both atomic and molecular forms (Rowe, 1969; Boyle, 1979; Mironov and Galetiy, 1979), as well as in a particulate form in sulfides (Lagedza, 1969; Bakken et al., 1989; Korobeynikov, 1991), at grain boundaries (Parry, 1984), in microcracks and dislocation structures (Davletov et al., 1974), adsorbed on

crystals, and in the interlayer position in minerals (Bakken et al., 1989; Korobeynikov, 1991) and in interstitial fluids (Korobeynikov, 1991).

Gold occurring in the particulate form is more mobile and may be extensively extracted and redistributed by metamorphogenic solutions, even under moderate metamorphic conditions (Davletov, 1974; Glasson and Keays, 1978; Romberger, 1988; Korobeynikov, 1991; Huston et al., 1993). Glasson and Keays (1978) reported a significant depletion of Au during cleavage development in Paleozoic slates and phyllites from Central Victoria, Australia. The loss of Au was attributed to dissolution of pyrite. Experiments on the recrystallization of Au-bearing pyrite by chloride solutions at 400-500°C have shown a significant loss of Au, by 40-80%, from pyrite to the fluids (Korobeynikov, 1991).

Huston et al. (1993) proposed that Au and As are present as nonstoichiometric lattice substitution in sulfides; Sb, Bi, and Cu are present in inclusions. Studying metamorphosed massive sulfide deposits, the authors concluded that metamorphic recrystallization cleans pyrite of inclusions or nonstoichiometric lattice substitution. Gold is depleted by one order of magnitude in the amphibolite grade deposits relative to the sub-greenschist equivalents. A similar depletion is displayed by As, Sb, and Bi. It has been indicated that solubility of As in pyrite significantly decreases with increasing temperature (Clark, 1960; Huston et al., 1993). Removal of Au during recrystallization of sulfides might be attributed to the extremely rapid rate of equilibration of sulfides at moderate to high grade metamorphic temperature (c.f. Barton, 1970; Barton and Skinner, 1979).

Simple minerals (e.g. quartz and sulfides) congruently dissolve, leaving no solid phase behind, whereas most silicates dissolve incongruently, with the formation of a new, less reactive phase (Fyfe et al., 1987). Base and precious metals are therefore potentially more prone to dissolution from sulfides than from silicates. The preferential early dissolution of sulfide-hosted metals is supported by experimental works (Bischoff and Dickson, 1975; Mottle et al, 1979; Potter and Dickson, 1980; Seyfried, 1981).

Supracrustal rocks of varied type and origin in Bamble all contain Au at abundance levels well below equivalent rock types elsewhere and below the general crustal abundance of this element. Other chalcophile elements are also low, but not so consistently as Au. This consistently low abundance of Au through rock types of different origin suggests that a common process caused its scarcity. It is difficult to model a series of independent processes that can account for the scarcity of this element in all individual rock types.

Cameron et al. (1989b) and Harlov (1992) showed that granulite grade rocks at Bamble equilibrated under a relatively high f_{O2} at peak metamorphic conditions, well above magnetite-fayalite-quartz (FMQ) fence. Metasediments from the granulite zone represent a relatively more oxidized mineral assemblage. This is supported by the dominance of magnetite over ilmenite, the occurrence of hematite, higher values of $Fe_2O_3/Fe_2O_3 + FeO$, general absence of graphite, and partial replacement of pyrrhotite by pyrite + magnetite. Cameron (1991a) argued that the uniformity in f_{O2} within the granulite grade rocks in Bamble is consistent with their equilibration in the presence of a high fluid flux.

Gold, Sb, and As were possibly depleted during progressive metamorphism from the initial protoliths. Under typical metamorphic conditions, H_2O, CO_2, CH_4 and H_2S are the principal fluid species with H_2S favored by higher temperature, lower pressure and lower f_{O2} conditions (Poulson and Ohmoto, 1989). Extraction of Au from sulfides by chloride solutions and gaseous chlorine is also an effective way of dissolution and transportation of Au at high temperatures (Li and Shokhina, 1974; Korobeynikov, 1991; Nekrasov, 1996). Mikucki (1998) showed that transportation of Au in ore fluids responsible for some high temperature Au deposits in the amphibolite facies host rocks was probably in the form of $AuCl^-$.

Neither special Au-enriched rock units, nor unreasonably large volumes of source rocks are required to produce a gold deposit (c.f. Phillips et al., 1987; Cameron, 1989a, b). To create a giant gold deposit with an Au reserve of ~1000 t, a source area of 10 x 10 km and 5 km thick would be required to undergo a depletion of Au by only 50%, assuming a crustal average of 1.5 ppb.

6-2. Mafic Rocks and Associated Sulfide Ores

Both metabasites and hyperites*, and Ni-Cu sulfide ores associated with the hyperites, are strongly depleted in Au, compared to the general abundance of this element in mafic rocks and magmatic sulfide ores elsewhere. They are also depleted in Sb. However, they carry normal concentrations of S, Cu, Se, As, and Cu (Figure 6-4). All chalcophile elements, but Au, are almost equally distributed in the two mafic series. A comparison of the abundance of Au in metabasites and hyperites implies a significant difference between the two rock types (Figure 6-5). In 20% of the metabasites, Au was below the detection limit of 0.1 ppb. The abundance of gold in these samples is arbitrarily taken as half the detection limit.

In all geochemical respects, the Sveconorwegian hyperites are closely similar to the Kongsbergian metabasites. Both mafic series are of Fe-rich tholeiitic type and bear features typical of destructive continental margin settings. The hyperites postdate the ~1.45-1.25 Ga

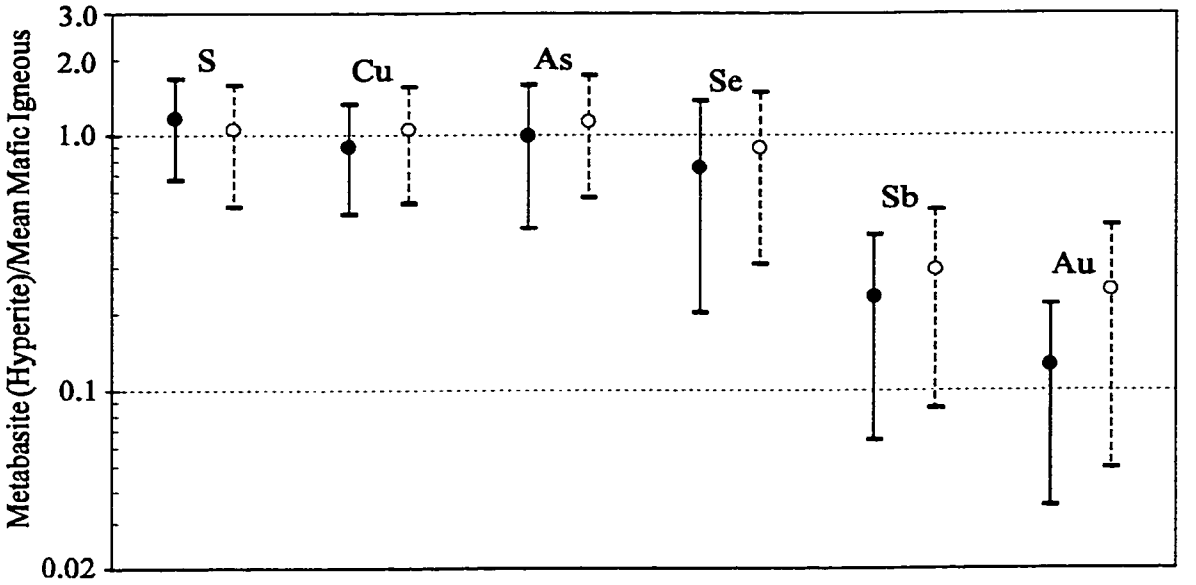

Figure 6-4. Distribution of chalcophile elements in the Bamble Metabasites (solid lines) and Hyperites (broken lines), normalized to the mean mafic rocks. Circles show the mean values and bars represent 1σ standard deviation. See Appendix 2-2 for normalization data.

** For the sake of simplicity, hyperite refers, collectively, to Sveconorwegian olivine gabbros, coronitic gabbros, hypersthene gabbros (hyperites) and their amphibolitized equivalents.*

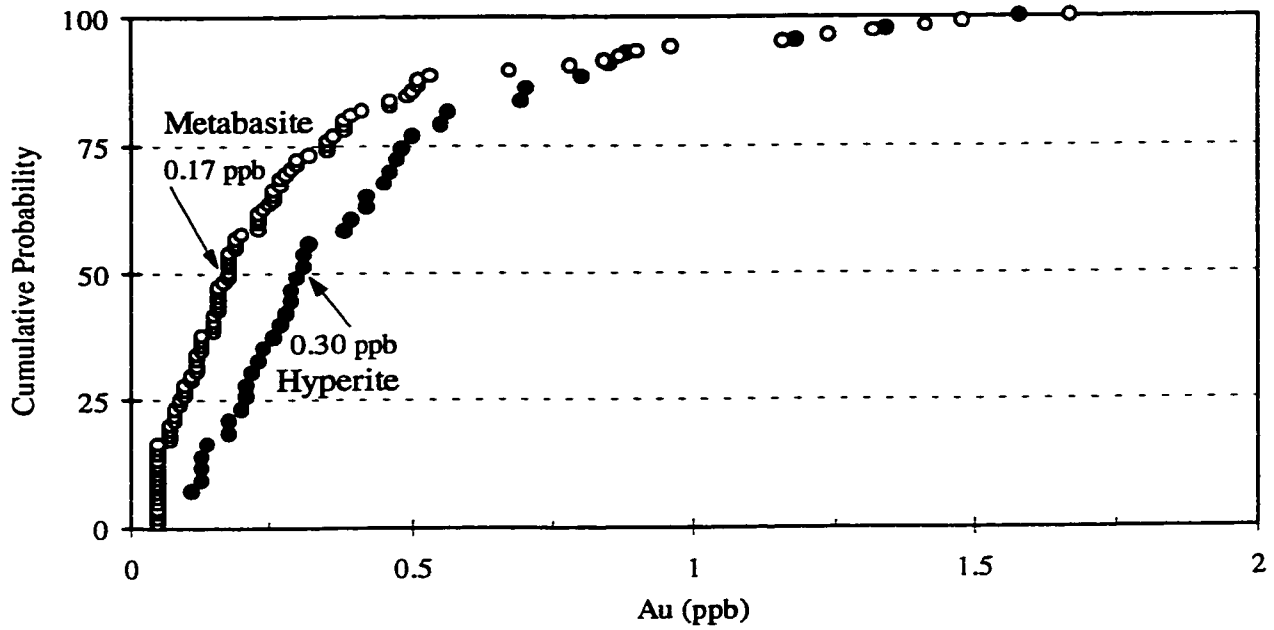

Figure 6-5. Cumulative probability distribution of Au in the Bamble metabasites and hyperites. Arrows indicate the median values.

anorogenic period in southern Norway and represent the prelude to a new phase of subduction event, involving "Sveconorwegian" metamorphism and hydrothermal activity (c.f. Smalley, 1983; Smalley and Field, 1991; de Haas, 1992).

The composition of olivine in Bamble hyperites falls in the range Fo_{75-36} (Starmer, 1969; Brickwood and Craig, 1987; de Haas, 1992), that is more fayalitic than that in the typical tholeiitic mafic plutons (Fo_{60-80}, Wilson, 1989; Deer et al., 1982). Primary magmatic olivine is not preserved in the metabasites; however, Niggli Mg# for metabasites is in the same range as in the hyperites (32-67 and 35-72, respectively), suggesting a similar composition for the primary olivines.

Primary magmas in equilibrium with typical upper mantle mineral assemblages (olivine + orthopyroxene ± clinopyroxene ± garnet ± spinel) are enriched in MgO (>15%), Ni (>400 ppm) and Cr (>1000 ppm) (Wilson, 1989). The Bamble hyperites and metabasites are of low-Mg type (MgO commonly < 10%) and considerably depleted in Ni and Cr. The absence of

more magnesian rocks in Bamble might be attributed to melting conditions at the source region in upper mantle, or separation of an olivine-rich fraction elsewhere.

The absence of Mg-rich cumulates, such as peridotites, simultaneous to the metabasites and hyperites, argues against the removal of an olivine-rich fraction. However, separation of an Mg-rich fraction early in the evolution and ascent of magma at crust-mantle boundary can not be ruled out (c.f. de Haas, 1992).

On MORB-normalized plots, both hyperites and metabasites exhibit marked enrichments in LILE and LREE relative to HREE and HFSE. Enrichment of LILE and LREE in tholeiitic basalts have alternatively been attributed to:

- Crustal contamination (Watson, 1982; Dupuy and Dostal, 1984; Thompson et al., 986; Brickwood, 1984, 1986).
- Derivation of the parent magmas from a variably enriched mantle source (Weaver and Tarney, 1983; Pearce, 1983; Menzies et al., 1983; de Haas, 1992).
- Introduction of LILE from subducted oceanic crust (Kay, 1980, 1984; Pearce, 1983).
- A low degree of partial melting (Smalley et al., 1983; Morgan, 1986; Klein and Langmuir, 1987).
- A combination of the above processes.

Brickwood (1984, 1986) proposed that magmatic stoping was the main mechanism of emplacement of gabbros at Bamble, and that it may have resulted in crustal contamination of the intruded melts. Crustal contamination is rejected by the consistency of the variations of REE with typical magmatic fractionation trends, both within individual plutons, and in a regional scale. Enrichment of LILE, particularly K and Rb, in the amphibolitized gabbros, and in some metabasites, is of secondary origin. A crustal contamination is further renounced by S isotope and S/Se ratios. $\delta^{34}S$ values for disseminated sulfides in both hyperites and metabasites tightly cluster around 0‰, consistent with a mantle source for S. S/Se ratios fall in the range 3×10^3 to 6×10^3 in agreement with S/Se ratios in mantle-derived mafic rocks (c.f. Eckstrand et al., 1989; Paktunc, 1989, 1990).

LILE and LREE are sensitive indicators of partial melt removal. Lanthanum, for example, may be considerably depleted by a few percent loss of a partial melt (Morgan, 1986). Spinel lherzolites that have not been modified by metasomatism generally have REE patterns that are notably depleted in LREE (Basaltic Volcanic Study Project, 1981).

Primary magmas of the ocean ridge basalts with 10-15 wt% MgO are the result of ~8-20% partial melting of the average upper mantle composition (Klein and Langmuir, 1987). Enrichment of LILE and LREE in the Bamble hyperites and metabasites might be the consequence of a low degree of partial melting. This is supported by the Mg-poor nature of the rocks (MgO <10%). However, derivation of the parent magmas from a variably enriched mantle source (de Haas, 1992), or introduction of the elements from the subducted oceanic crust can not be ruled out.

The origin of Au depletion in the Bamble hyperites and metabasites may alternatively be attributed to:

1. Depleted mantle source.
2. Segregation of sulfides from the parent magmas on ascent or during emplacement.
3. Partial melting processes and sulfur saturation at the source region.
4. Transportation of Au in complex ions by magmatic volatiles.
5. Massive addition of S from an external source.
6. Post-solidus (deuteric and metamorphic) alteration, and loss of Au to infiltrating fluids
7. A combination of two or more of the above processes

6-2-1. Depleted Mantle Source.

It is well known that upper mantle is vertically and horizontally heterogeneous with respect to its chalcophile and siderophile elements (e.g. Ivanov et al., 1977; Jagoutz et al., 1979; Mitchell and Keays, 1981; Garuti et al., 1984; Sims et al., 1992). Ivanov et al. (1977) reported highly variable concentrations of Au, Ag, and Cu in spinel and garnet-lherzolites from different

kimberlite diatremes, Au being in the range 0.6 to 8.1 ppb. Similarly, Garuti et al. (1984) determined variable concentrations of chalcophile and siderophile elements in mantle peridotites and lherzolites. Gold was found to be in the range 1.3-8 ppb and Pt in the range 1.1-11.7 ppb. Garuti et al (1984) showed that even a primitive and rather undepleted mantle could chemically be heterogeneous.

Alternatively, Sharpe (1982) showed that the marginal rocks of the Bushveld Complex contained on average 21 ppb Au that is one order of magnitude greater than that in MORB. According to the author, the Bushveld Complex was derived from an enriched source, or the magmas were evolved prior to emplacement. Similarly, Bobin and Sazanov (1989) reported an average Au content of 16.8 ppb in mafic rocks from Southern Yenisey Ridge, Siberia. Extraction of melts may accentuate the small-scale and large-scale heterogeneities in the mantle source region.

6-2-2. Segregation of Sulfides During Ascent or Emplacement of the Parent Magmas

Immiscible sulfides control the absolute chalcophile metal contents of magmas (e.g. Keays, 1987; Barnes, 1987; Paktunc, 1989; 1990). An early saturation of S in mafic magmas leads to early formation and removal of immiscible sulfides which deplete the magmas from ore-forming elements (e.g. Boyd and Mathiesen, 1979; Lesher et al., 1981; Crocket, 1981; Barnes et al., 1985, 1988; Paktunc, 1989, 1990).

The low contents of PGEs in MORB magmas have been attributed to the fractionation of sulfides during evolution of the primary melts prior to eruption (Crocket, 1981; Barnes et al., 1985). Similarly, segregation of olivine-sulfide cumulates has been considered as a possible mechanism responsible for depletion of Au and PGEs in several tholeiitic mafic-ultramafic intrusions in the Appalachian Orogen (Paktunc, 1989, 1990), in Bruvann Ni-Cu deposit, Northern Norway (Boyd and Mathiesen, 1979), and in the Komatiite-related Agnew Ni deposit, Western Austarlia (Barnes et al. 1988).

Ni contents of magmas are largely controlled by the amount of normative olivine, and, to a lesser extent, of pyroxene (Gunn, 1971; Thompson et al., 1984). Distribution coefficient of Ni (D_{Ni}) between sulfide and silicate phases has been determined to be in the range 25-50 for basalts containing 20-10% MgO (Rajamani and Naldrett, 1978). Naldrett (1979) reported a considerable increase in D_{Ni} from high-Mg komatiitic magmas to basaltic magmas. The relatively high D_{Ni} values for Bamble hyperites and metabasites (100-150) corresponds to the low MgO contents (generally < 8%).

Nickel is partitioned from magma into olivine by a factor of 5 to 18 (Hakli and Wright, 1967; Gunn, 1971; Thompson et al., 1984), whereas Cu enters the olivine lattice in only trace amounts (MacLean and Shimazaki, 1976). Olivine fractionation is expected to deplete magmas and sulfide liquids in Ni and enrich them in Cu, leading to a significant decrease in the Ni/Cu ratios (c.f. MacLean and Shimazaki, 1976).

The Ni/Cu ratios in the Bamble hyperites (1.75 ± 1.25) and metabasites (2.1 ± 1.4) are in the same range as in the average tholeiitic basalts (2 ± 1; various sources in Wedepohl, 1974). This, and the relatively high values for partitioning of Ni between sulfide and silicate phases in both hyperites and metabasites (D_{Ni} = 100-150) suggest that parent magmas were not depleted in Ni due to an early fractionation of olivine. No major olivine-sulfide cumulate has yet been reported from Bamble. The Fe-Ni-Cu ores associated with the hyperites are small and of local nature. The mean concentration of Au in the ores is considerably lower than that in the disseminated sulfides in the hyperites (40 and 155 ppb, respectively). Sulfur isotope ratios suggest that sulfur from external sources was involved in the formation of the deposits.

Selenium and Bi are strongly chalcophile. Partitioning of Se between sulfide and silicate phases in the hyperites and metabasites falls in the range 6000-20000. Minor sulfides account for more than 90% of the total Se in these rocks. No data is available on the abundance of Bi in the whole rocks. However, assuming that all Bi is carried by sulfides, mass balance calculations suggest an average Bi concentration of 0.065 ± 0.03 ppm in the Bamble mafic rocks. This is in the same common range of Bi in mafic igneous rocks elsewhere (c.f. Kupčik

et al., 1974; Krauskoph, 1979; Greenland et al., 1973; Zientek et al., 1990; Yoon (1991). The normal abundances of Se and Bi argue against fractionation of sulfides as a possible mechanism of Au depletion, as this would be expected to lead to a similar depletion in other highly chalcophile elements, such as Se and Bi.

6-2-3. Partial Melting Processes and Sulfur Saturation in the Source Region

The abundance of chalcophile elements in igneous rocks is principally controlled by the nature of source region (Hamlyn et al., 1985; Mathez and Peach, 1989; Peach and Mathez, 1990). Magmas generated by low to moderate degrees of partial melting in a mildly depleted to undepleted source region (e.g. MORB) are S-saturated and become rapidly depleted in precious metals during the early stages of silicate fractionation, due to the coprecipitation of an immiscible sulfide component (Naldrett and Duke, 1980; Hamlyn et al., 1985; Keays, 1987; Mathez and Peach, 1989; Peach et al., 1990).

The extraction of an immiscible sulfide component in the source region is supported by the ubiquitous presence of sulfides in mantle xenoliths (Jagoutz et al., 1979; Keays, 1981; Morgan and Baedecker, 1983; Dromgoole and Pasteris, 1987). The process may result in the concentration of the elements having high $D^{S/L}$ values (i.e. PGE and Au) in the residual mantle sulfide fraction and the removal of the elements having low $D^{S/L}$ values (i.e. base metals) by the melts (c.f. Naldrett and Duke, 1980; Hamlyn et al., 1985; Peach et al., 1990). Subsequent remelting of this refractory source produces S-deficient, precious metal-enriched magmas, such as boninites (Hamlyn et al., 1985).

Prior to melting, S and chalcophile elements principally reside in a sulfide phase (e.g. Schneider, 1978; Mitchell and Keays, 1981; Morgan and Baedecker, 1983; Garuti et al., 1984; Peach et al., 1990). From analysis of sulfides in spinel-lherzolite xenoliths, Morgan and Baedecker (1983) estimated that ~80% of the Au and Cu in the whole rocks resided in the sulfide phase. Mitchell and Keays (1981) attributed a similar fraction of Au to an interstitial sulfide phase in spinel-lherzolite xenoliths. Garuti et al (1984) showed that trace sulfide

component is the principal carrier of most Pt-group elements (PGEs) and Au in mantle peridotites and lherzolites. During partial melting, the sulfides dissolve and release the accompanying Au which may enter the melt.

Residual sulfides in the source region will influence the abundance of the chalcophile elements in a magma by acting as a sink for these elements and preventing their enrichment in the silicate partial melt (e.g. Wendlandt, 1982; Morgan, 1986; Peach et al., 1990). It has been indicated that chalcophile and siderophile elements (i.e. Au and PGE) behave incompatibly during mantle partial melting, particularly when a sulfide component is involved (e.g. Dupuy and Dostal, 1981; Oshin and Crocket, 1982; Garuti et al., 1984). Fe-Ni-Cu sulfide, or pyrrhotite monosulfide solid solution (Po_{mss}), melts at temperatures that are easily achieved during partial melting; however, the sulfide liquid need not necessarily dissolve in the silicate magma. If a sulfide liquid is present but does not dissolve, it will have the same effect as a restite phase (Barnes et al., 1985).

Assuming an equilibrium batch partial melting in which an immiscible sulfide liquid in the mantle dissolves in proportion to the degree of melting, Peach et al. (1990) showed that small degrees of partial melting result in significant fractionation of the noble metals (PGE and Au) from the moderately chalcophile elements (i.e. Cu, Se). The authors showed that only at relatively high degrees of partial melting, do noble metals enter partial melts to an appreciable degree. The model shows that a partial melting of ~10% would lead to a significant depletion of Cu and Se, in the residual phase, while Au is enriched, relative to the average upper mantle composition.

The relatively low concentration of Au in the Bamble mafic rocks may be attributed to a low degree of partial melting in the source region. The Bamble mafic rocks are characterized by high FeO_t, low MgO, and marked enrichment in LILE and LREE. A low degree of partial melting is also supported by the strong depletion of Ir. Analysis of sulfide concentrates from hyperites, metabasites, and sulfide ores, by INAA technique, indicated that Ir was below the detection limit of 5 ppb. No data is available on the whole rocks. Concentration of Ir in Fe-Ni-

Cu sulfides associated with mafic rocks has been reported to be in the range 20-100 ppb (Hoffman et al., 1979; Keays and Davison, 1976; Naldrett and Duke, 1980, Naldrett, 1987; Barnes and Naldrett, 1985; Barnes et. al., 1987). Peach et al. (1990) reported the occurrence of 300-650 ppb Ir in sulfide globules from mid-oceanic ridge basalts.

It has been indicated that Ir in upper mantle is mainly carried by olivine that is the most refractory phase (Crocket, 1979; Naldrett and Duke, 1980; Brügmann et al., 1987). The low concentration of Ir in the Bamble mafic rocks might be a consequence of the compatible behavior of this element during partial melting processes, or removal of Ir along with Au in a sulfide fraction early in the evolution of the partial melts.

6-2-4. Transportation of Au in Complex Ions by Magmatic Volatiles

According to this model, Au was transported in complex ions by magmatic volatiles, and was involved in the formation of the lode gold deposits at higher levels (now eroded). However, the normal abundances of S, As, Se, Bi, and LILE, the elements commonly associated with Au in lode gold deposits, argue against this assumption.

Data on the ability of fluids to transport precious metals in the environment of a crystallizing magma are rare in the literature. Wood (1987) showed that solubility of precious metals in fluids is strongly dependent on oxygen fugacity (f_{O2}) and temperature, with solubilities generally decreasing with decreasing f_{O2} and increasing temperature. The author further showed that halogens enhance PGE solubilities only marginally.

Cameron (1989b) and Harlov (1992) showed that charnockites and metabasites from the granulite zone equilibrated under a relatively oxidizing condition ($f_{O2} \cong 2.5$ log units above the QFM buffer) during peak metamorphism. The relatively high f_{O2} was alternatively attributed to the pervasive infiltration of oxidizing fluids during granulite metamorphism, or crystallization from an originally oxidized magma. Hyperites equilibrated near the QFM buffer and represent a less oxidized mineral assemblage (Cameron et al., 1989b, 1993).

Depletion of Au in the granulite grade metabasites might be attributed to the removal of this element by oxidizing magmatic volatiles. However, that the less oxidized metabasites from amphibolite and transition zones, and the hyperites, are similarly depleted in Au, argues against this supposition as a viable mechanism of Au depletion in Bamble.

Transportation of precious metals by magmatic volatiles has been considered as a possible process in alkaline basalts, but not in the tholeiitic magmas (Carmichael, 1991). Alkaline basalts record very high primary oxidation states, implicating a fundamental role for the volatile oxidants H_2O, CO_2, and SO_2 in the origin, in contrast to the drier, more reduced, tholeiitic basalts.

6-2-5. Massive Addition of Sulfur from an External Source

According to this model, the parent magmas were initially depleted in S and Au. Assimilation of sulfidic, Au-poor countryrocks by the mafic magmas led to a significant increase in S and in the initial S/Au ratios. There is strong evidence for the involvement of S from sulfidic metasedimentary hostrocks in the formation of Ni-Cu ores associated with the hyperites. This is supported by a marked enrichment of ^{34}S, but considerably lower S/Se ratios, in the ores relative to the hyperites.

However, the Ni-Cu ores are of local nature, sporadically occurring in small bodies at the boundary between hyperite and gneissic host rocks. The hyperites do not seem to have been significantly affected by the local assimilation of the countryrocks. This is supported by the whole rock geochemical data, sulfur isotopes, and S/Se ratios.

6-2-6. Post-Solidus (Alteration and Metamorphic) Alteration, and Loss of Au to Infiltrating Fluids.

Metabasites have totally metamorphic textures and mineral assemblages, implying that they equilibrated to the conditions of metamorphism. The initial magmatic pyrrhotite is commonly replaced by pyrite ± magnetite. Hyperites are partially amphibolized, particularly at their

margins. The initial magmatic textures are preserved in the less altered rocks. Pyrrhotite, the dominant sulfide in the hyperites, is partially to totally replaced by pyrite ± magnetite in the marginal amphibolites.

Metabasites represent a more oxidized mineral assemblage compared to the hyperites. Cameron (1989b, 1993a) showed that metabasites from the granulite and transition zones equilibrated under a relatively high f_{O2}, well above the QFM buffer (Figure 6-6). This is consistent with the stability field of pyrite-magnetite-pyrrhotite. The high f_{O2} was attributed to the pervasive infiltration of oxidizing fluids during high-grade metamorphism.

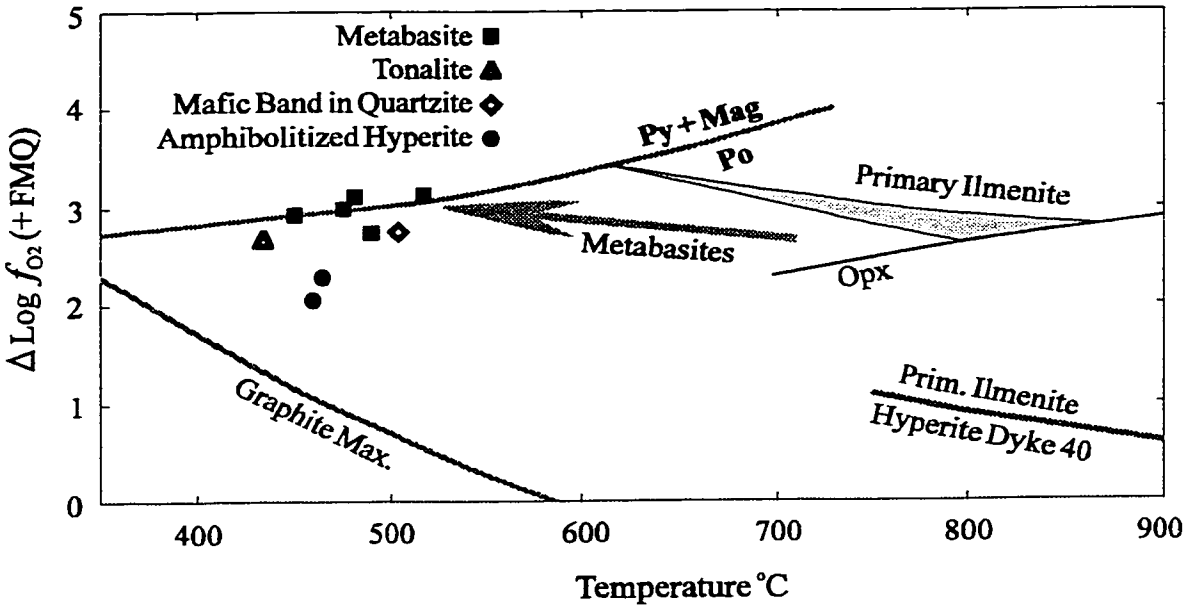

Figure 6-6. Location of Bamble metabasites and hyperites in f_{O2} -T space at peak metamorphism and the path of subsequent cooling (Cameron, 1993a). The location at peak metamorphism is derived from the intersection of an isopleth band for ilmenite with an orthopyroxene isopleth. The termination of the cooling curve is obtained from the composition of lamellae of magnetite and ilmenite in ilmenite-hematite-magnetite (IHM) type ilmenite grains. The points cluster along the pyrrhotite-pyrite-magnetite buffer. The primary ilmenite isopleth for a hyperite dyke from Tvedestrand (hyperite dyke 40) represents a much less oxidized mineral assemblage relative to the metabasites. However, the position defined by IHM-type ilmenite grains from the amphibolite margin of this dyke indicates an increase in Δf_{O2} during amphibolitization. Additional points are shown for a sample of tonalite and a mafic band in quartzite, both at granulite grade. Δf_{O2} is relative to QFM buffer.

Hyperites equilibrated near the QFM buffer, in the field of stability of pyrrhotite. The amphibolitized hyperites, however, represent a relatively more oxidized mineral assemblage (Figure 6-6). This is supported by higher ratios of $Fe^{+3}/(Fe^{+2} + Fe^{+3})$, occurrence of hematite lamellae in ilmenite, and replacement of the initial pyrrhotite by pyrite + magnetite.

Depletion of Au in metabasites and hyperites might be attributed to oxidation and breakdown of the primary magmatic sulfides under oxidative metamorphism (c.f. Cameron, 1989b, 1993a, 1994). The ratio of $Fe_2O_3/(FeO + Fe_2O_3)$ may be used as a rough index of oxidation. Plots of Au against $Fe_2O_3/(FeO + Fe_2O_3)$ (Figure 6-7) shows no consistent trend of variations, implying that the distribution of Au was not controlled solely by oxidation state of the rocks.

For hyperites, data from mass balance calculations, analysis of sulfide concentrates from the least and the most altered rocks, and sulfur isotope ratios suggest that no significant removal of chalcophile elements occurred during gabbro-amphibolite transition. The relatively low concentration of Au and Sb in the hyperites is of primary magmatic origin, rather than a metamorphic overprint.

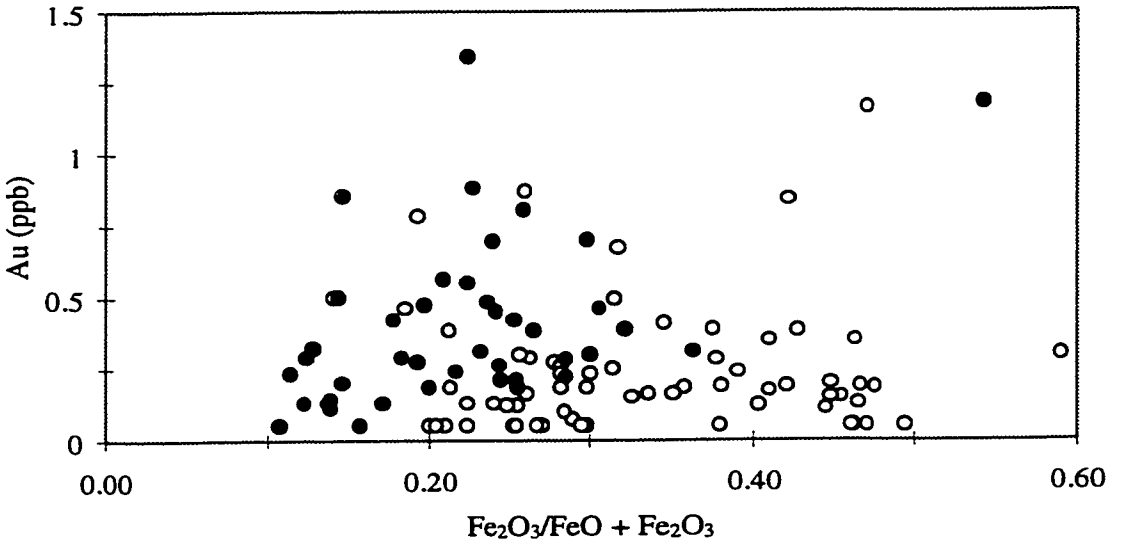

Figure 6-7. Variation of Au vs $Fe_2O_3/FeO + Fe_2O_3$ for metabasites (open circles) and hyperites (solid circles), Bamble.

Metabasites have undergone extensive recrystallization; the primary magmatic textures and mineral assemblages are not preserved. The abundance of chalcophile elements in metabasites from amphibolite and transition zones closely follow that in the hyperites (Figure 6-3), the only exception being Au that is depleted in the metabasites by ~40%. The granulite grade metabasites are relatively depleted in S, Cu, Se, but not in As or Au. Considering the close geochemical similarities between hyperites and metabasites, the lower contents of Au in the metabasites might, at least partly, be attributed to metamorphic processes.

Arsenic and Sb behave incompatibly during crystallization of mafic magmas. It has been indicated that both As and Sb can be correlated with the light rare earth element, Ce, and that the As/Ce and Sb/Ce ratios are independent of the magmatic evolution (Newsom et al., 1986; Sims et al., 1990; Noll et al., 1996). The ratios As/Ce and Sb/Ce may be used to monitor the depletion or enrichment of chalcophile elements relative to contents of other highly incompatible and relatively immobile trace elements, such as REE (c.f. Noll et al., 1996). There is strong evidence that Ce remained immobile during metamorphism and rehydration at Bamble (Clough and Field, 1983; Smalley et al., 1983, 1985; Smalley and Field, 1991; present study).

Noll et al. (1996) reported a wide range in the ratios of As/Ce (0.01-1) and Sb/Se (0.001-0.1) in volcanic rocks from magmatic arcs worldwide. The authors proposed that the As/Ce and Sb/Ce ratios decrease from the volcanic front towards the back-arc basin, reflecting the declining role of fluids with distance and depth. The mean As/Ce and Sb/Ce ratios for Bamble metabasites (0.08 and 0.008, respectively) are similar to those in volcanic rocks from magmatic arcs (c.f. Noll et al., 1996), or the average continental crustal values (As/Ce = 0.08 $\pm$ 0.03 and Sb/Ce = 0.007 $\pm$ 0.002; Sims et al., 1990).

Variations of As/Ce and Sb/Ce in hyperites and metabasites from various metamorphic zones display similar patterns (Figure 6-8) implying that no significant fractionation of As and Sb from Ce occurred. The normal ratios of As/Ce and Sb/Ce argue against a post-solidus origin for depletion of As and Sb; such process would be expected to lead to a significant drop in the

As/Ce and Sb/Ce ratios. This may be interpreted as an evidence that the low concentrations of Sb in the Bamble mafic rocks is of primary magmatic origin unaffected by metamorphism. Variations of Au closely follow those of Sb in the mafic rocks.

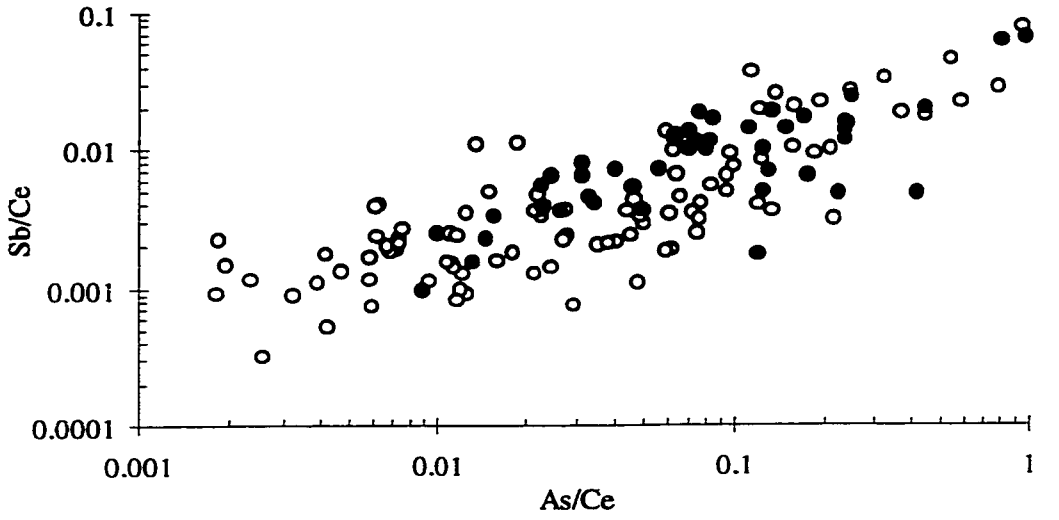

Figure 6-8. Variations of As/Ce vs Sb/Ce in the Bamble metabasites (open circles) and hyperites (solid circles).

6-3. Felsic Rocks (Tonalite-Trondhjemite Gneisses and Post-Orogenic Granites)

Both Kongsbergian tonalite-trondhjemite gneisses and Sveconorwegian post-orogenic granites are strongly depleted in Au relative to the general abundance of this element in felsic igneous rocks elsewhere. They are also depleted in As, Sb, and Se. The granites are further depleted in S and Cu. Containing on average 0.22 ppb Au, the Bamble tonalite-trondhjemite gneisses are one of the most depleted felsic rocks reported in the literature (c.f. Gottfried et al., 1972; Saager and Meyer, 1983; Korobeynikov, 1986; Grabezhev et al., 1986; Yoon, 1991; Feng et al., 1993). The mean value of Au in the granites is only 0.18 ppb.

Depletion of Au along with As, Sb, and Se in the gneisses might be attributed to pervasive oxidation of the rocks. This is supported by the relatively high f_{O2} recorded for the gneisses (Figure 6-6). Pyrrhotite, the stable Fe-sulfide at peak metamorphic conditions, is replaced by

pyrite; mantling of pyrite by magnetite is common. Gold might have been transported as sulfide complexes.

The Bamble granites are characterized by low Fe_t, compared to similar granites elsewhere (c.f. Collins et al., 1982; Whalen et al., 1987; Whalen et al., 1997). Experimental studies have indicated that solubility of S in magmas depends strongly on FeO content (e.g. Haughton et al., 1974; Wendladth, 1982). The relatively low contents of Au and other chalcophile elements in the Bamble granites is, at least partly, explicable in terms of the low initial Fe_t content.

Alternatively, the depletion of chalcophile elements might be attributed to the source rocks. Given a crustal source for alkali granites (c.f. Longstaffe et al., 1980; Chappell et al., 1987; Kerr et al., 1993; Whalen et al., 1997), partial melts derived from the Au-depleted supracrustal rocks of the Bamble would be similarly deficient in Au.

7. Conclusions

Gold ores associated with quartz-carbonate veins in metamorphic rocks have been a major source of gold. The deposits, also known as "mesothermal gold" or "lode gold" typically occur along shear zones. They occur over a wide range of temperature and pressure, with the majority of the deposits hosted by greenschist to lower-amphibolite facies rocks. The deposits share many features, such as structural hosting, ore fluid chemistry, carbonate alteration, alkali metasomatism, and metal inventory (e.g. Kerrich and Fryer, 1981; Colvine et al., 1988; Roberts, 1987; Kerrich, 1989b, 1993; Groves et al., 1992, 1998; Witt and Vanderhor, 1998). Considering the unique temporal and spatial association with orogeny, the term "orogenic gold deposits" has recently been proposed for this class of gold deposits (Groves et al., 1998; Goldfarb et al., 1998; Witt and Vanderhor, 1998).

The origin of gold and fluids is controversial. The hypothesized sources include: felsic magmas, alkaline, mantle-derived magmas, structurally focused metamorphic outgassing, lateral secretion, submarine volcanic exhalations, meteoric water circulation, and granulitization-mantle degassing.

Direct magmatic links have been rejected based on the inconsistent geochronological, as well as stable and radiogenic isotope, data (Wyman and Kerrich, 1989; Kerrich, 1988, 1989 b, 1990, Hattori, 1993; Witt and Vanderhor, 1998). Neither felsic nor alkaline magmas are particularly Au-enriched (Wymann and Kerrich, 1989; Barron, 1990; Rowins et al., 1993).

The occurrence of lode gold deposits under amphibolite and granulite facies conditions cogenetic with the common greenschist facies mineralization argue against the models based on the high level sources such as exsolution of fluids from high level felsic magmas, meteoric water circulation, or greenschist-amphibolite devolatilisation of greenstones. The occurrence of the deposits in major shear zones and under a variety of crustal regimes suggests that gold was derived from the deep and wider portions of the shears (Cameron, 1988, 1989b, 1993;

Wymann and Kerrich, 1989 b; Witt and Vanderhor, 1998).

As a test of the "deep source model" Bamble Shear Belt of southern Norway was studied. Earlier data from Bamble showed that the lower crustal rocks in this terrain are strongly depleted in Au and the elements commonly associated with Au in lode gold deposits, i.e. As and Sb (Cameron, 1988, 1989a, b; 1993a, b, 1994). Cameron (1989a) showed that granulite facies rocks at Bamble equilibrated under a relatively high f_{O2} at peak metamorphic conditions. The f_{O2} calculated for charnockites and metabasites was found to be ~2.7 log units above QFM buffer. The author further suggested the "oxidative metamorphism of deep ductile shear zones" as a possible mechanism for dissolution of sulfides and mobilization of chalcophile elements, including Au, from deep crustal rocks (Cameron, 1988, 1989a, b, 1993a, 1994).

The present work was undertaken to further characterize the origin of Au depletion in Bamble. Some 400 samples from various rock units across the shear zone were analyzed for a wide range of elements. The results, combined with petrographic studies and data from elemental and isotopic composition of sulfides, are interpreted with emphasis on the processes that have affected the distribution of gold.

7-1. Bamble Shear Belt

The Bamble Shear Belt is part of the South-West Scandinavian Domain (SWSD) of the Baltic Shield. It comprises an area 20-30 km wide and about 150 km long of variably deformed high-grade metamorphic rocks along the east coast of southern Norway. The area is polymetamorphic with maximum metamorphism under upper amphibolite and granulite conditions.

Variations in mineralogy and chemical composition allow the coastal area of the Bamble to be divided into amphibolite, transition, and granulite zones (c.f. Field et al., 1980; Smalley et al., 1983). The amphibolite zone is separated from the transition zone by Opx-in isograd. The granulite zone is characterized by the common presence of Opx and the scarcity of hydrous minerals.

The geology of Bamble is the result of two separate, high-grade, metamorphic events. The first took place during Kongsbergian Orogeny (1600-1450 Ma) under upper amphibolite and granulite grades (O'Nions and Baadsgard, 1971; Starmer, 1977, 1990, 1991; Starmer and Milne, 1982; Field et al., 1985). The second occurred during Sveconorwegian Orogeny (1250-950 Ma) under amphibolite and locally granulite grade conditions (O'Nions and Baadsgard, 1971; Jacobsen and Heier, 1978; Munz and Morvick, 1991; Kullerud and Dahlgren, 1993; Knudsen and Anderson, 1999). The pressure and temperature at peak metamorphic conditions have been estimated to be in the range 7.3 ± 0.5 kbar and 800 ± 60°C, respectively (Lamb et al., 1986; Cameron, 1989b; Harlov, 1992; Visser, 1993; Neijland and Maijer, 1993).

7-2. Whole Rock Geochemistry

The oldest exposed rocks in Bamble include a suite of supracrustal units consisting of quartzites, variable gneisses, graphitic and sulfidic schists, calc-silicates, and minor volcanic components. They are of early- to mid-Proterozoic age (Knudsen, 1997). All supracrustal rocks were metamorphosed and intruded by felsic and mafic magmas during Kongsbergian and Sveconorwegian orogenic episodes.

The supracrustal rocks include a variety of protoliths and depositional environments, from shallow littoral sandstones to deeper greywackes and pelites, with local euxinic conditions to produce graphitic and sulfidic sediments. Intercalations of volcanic materials are common, implying that sedimentation occurred in a mobile basin. Amphibolite bands are of igneous origin and bear features typical of calc-alkaline basalts produced at destructive plate margins. Hornblende gneisses are highly modified felsic-alkaline volcanic material. There is evidence that biotite schists are, at least partly, the product of alkaline metasomatism of basaltic materials. Metasediments from granulite zone are considerably depleted in LILE, REE, and HFSE, relative to those from amphibolite and transition zones.

The highest grade portion of Bamble, Island of Tromoy, contains outcrops of poorly foliated charnockites. On a ternary albite-anorthite-orthoclase diagram, the charnockites fall in the composition range tonalite-trondhjemite. They intruded the older supracrustal rocks and were subsequently metamorphosed during the Kongsbergian orogeny (Field and Råheim, 1979, Field et al, 1980, 1985; Machado, 1991).

Considering the geochemical classification of tonalite-trondhjemite series (Barker et al., 1976; Barker, 1979; Condie, 1981), the Tromoy charnockites, containing 14.2% Al_2O_3 at 67% SiO_2, fall in the low-Al series. They are characterized by relatively low Sr (commonly <200 ppm) but enriched Y and HREE contents, flat or mildly fractionated chondrite-normalized REE patterns, and marked negative Eu anomalies. The charnockites are strongly depleted in LILE and LREE relative to their equivalent rocks from amphibolite zone.

The low Al and Sr contents, and negative Eu anomalies, suggest that feldspar fractionation, either in the source region (residual phase), or during fractional crystallization (cumulate phase), had a significant influence (c.f. Barker et al., 1976; Hanson, 1978; Mc Kay, 1989). Fractionation of feldspar would also deplete the magma in LREE. The relatively low La_N/Yb_N ratios and flat chondrite-normalized REE patterns suggest that garnet was not residual.

The absence of basic and intermediate rocks temporally and genetically associated with the charnockites favors an origin of the rocks by partial melting rather than fractional crystallization. The Bamble tonalite-trondhjemite series define a calc-alkaline trend, and bear features typical of continental arc setting (c.f. Barker, 1979; Smalley and Field, 1985; Grabezhev et al., 1986; Smith et al., 1997).

Two major mafic igneous series occur in Bamble: 1) Entirely metamorphosed, concordant to discordant plutons known as metabasite, emplaced during Kongsbergian Orogeny; and 2) Composite bodies with cores of coronitic gabbro and amphibolitized margins, known as hyperite, emplaced during early phases of Sveconorwegian orogeny.

A syn-metamorphic origin has been proposed for the metabasites based on the evidences such as the absence of fine grained chilled margins, lack of signs of progressive replacement of hornblende by pyroxene, and the emplacement of the basic bodies along the same single regional foliation as their gneissic host rocks (Field and Clough, 1976; Clough and Field, 1980).

Metabasites occur in various metamorphic zones. Those from amphibolite and transition zones are comparable in their major and minor element geochemistry and belong to a regional differentiation trend. The granulite facies rocks, however, are strongly depleted in of LILE, REE, HFSE. They are further distinguished by higher contents of Na_2O and SiO_2. Metabasites from various metamorphic zones bear features characteristic of tholeiitic basalts emplaced at active continental margins.

The lower concentration of the incompatible lithophile elements in metabasites from the granulite zone might partly be attributed to the absence of more Fe-rich fractionates in this zone. However, that fields of variations for these elements fall below those of the other zones at equal Mg# values, imply that processes other than magmatic fractionation were involved.

Our data on the distribution of REE in the granulite grade metabasites do not support an earlier study by Smalley et al. (1983) who, based on a small number of samples, reported higher contents of REE in these rocks. The authors further proposed that the granulite zone contains the most fractionated of all metabasites.

After the Kongsbergian orogeny, there was a period of extension under upper amphibolite and locally granulite facies conditions (Starmer, 1990b). Numerous alkaline complexes associated with voluminous granite bodies intruded the older rocks during 1240-1450 Ma (Smalley et al., 1988; Starmer, 1990b; Nijland and Senior, 1991).

The post-Kongsbergian anorogenic period was followed by Sveconorwegian Orogeny. Numerous mafic dykes and stocks, known as hyperites, intruded older rocks in Bamble and

elsewhere in SWSD at 1150 ± 100 Ma (Jacobsen and Heier, 1978; Dahlgren et al., 1990; Munz and Morvik, 1991; de Haas, 1992). The intrusive series varies from minor ultramafic rocks through troctolitic gabbro, olivine ferrogabbro, and olivine-free gabbros and norites. They are tholeiitic in nature and bear features characteristic of continental tholeiites emplaced at destructive plate margins. Fe-Cu-Ni sulfide deposits are locally associated with the hyperites.

Hyperites occur in a metamorphic gradient from amphibolite to granulite facies conditions. After emplacement, some of the mafic bodies underwent post-solidus alteration under prolonged high P-T conditions. Corona growth around ferromagnesian minerals and metamorphism converted the rocks into coronitic gabbro and amphibolite. Considered in three dimensions, most bodies have a dominantly coronitic core which passes outwards into an amphibolitized margin. Hydration and recrystallization is more extensive in hyperites intruded into the amphibolite facies country rocks. Hyperites from various metamorphic zones belong to a regional differentiation trend.

Amphibolitization of hyperites was associated with introduction, removal, or local remobilization and reprecipitation of certain elements. Mass balance calculations indicate that LILE, particularly K and Rb, and halogens, particularly Cl, were introduced into the altered rocks, while CaO was removed. Chlorine metasomatism has locally led to the scapolitization of both coronitic gabbros and amphibolites. Chalcophile elements remained constant, or were only locally remobilized and reprecipitated. No net removal or addition of chalcophile elements occurred.

Fluids and solutes involved in the amphibolitization of the hyperites originated, at least partly, from the country rock gneisses. The injection of large volumes of mafic magmas into the metasedimentary and granitic gneisses generated high heat flows around the margins of the intrusions and promoted influx of brines from the surrounding rocks into the cooling rocks (c.f. Brickwood, 1984, Brickwood and Craig, 1987; Munz, 1990; de Haas, 1992). A crustal

source for the fluids is supported by radiogenic isotope data (Munz et al., 1994).

In all geochemical respects, the Sveconorwegian hyperites are closely similar to the Kongsbergian metabasites. Both mafic series are of low-Mg tholeiitic nature (MgO <10%), and bear features characteristic of destructive continental margin settings. It has been proposed that the hyperites represent the prelude to a new phase of subduction-related event after the post-Kongsbergian anorogenic period (Smalley, 1983; Smalley and Field, 1991).

The composition of olivine in the hyperites falls in the range Fo_{36-75}, that is more fayalitic than that in the typical tholeiitic mafic plutons (Fo_{60-80}, Deer et al., 1982; Wilson, 1989). Primary magmatic olivine is not preserved in the metabasites; however, Niggli Mg# for metabasites is in the same range as in the hyperites (32-67 and 35-72, respectively), suggesting a similar composition for the primary olivines.

The absence of more magnesian rocks might be attributed to a low degree of partial melting, or fractional crystallization processes. The lack of Mg-rich cumulates, such as peridotites, consanguineous with the metabasites and hyperites, argues against fractional crystallization. However, separation of an Mg-rich fraction early in the evolution and ascent of magma can not be ruled out (c.f. de Haas, 1992).

On MORB-normalized plots, both hyperites and metabasites exhibit marked enrichments in LILE and LREE relative to HREE and HFSE. Enrichment of LILE and LREE in the Bamble mafic rocks may be attributed to crustal contamination, derivation of the parent magmas from a variably enriched mantle source, introduction of LILE from subducted oceanic crust, a low degree of partial melting, or a combination of these.

Crustal contamination is rejected by the consistency of the variations of LILE and REE with typical magmatic fractionation trends, both within individual plutons, and in a regional scale. Crustal contamination is further negated by S isotope and S/Se ratios. Clustering of $\delta^{34}S$ values tightly around 0‰, and S/Se ratios in the range 3×10^3 to 7×10^3, support a pristine

mantle origin for the parent magmas (c.f. Schneider, 1970; Green and Naldrett, 1981; Sakai et al., 1982, 1984; Eckstrand et al., 1989; Kyser et al., 1990; Brügman et al., 1990).

A model consistent with all geochemical data favors a low degree of partial melting as the most likely mechanism for enrichment of LILE and LREE (c.f. Smalley et al., 1983; Morgan, 1986; Klein and Langmuir, 1987). This is supported by the Mg-poor nature of the rocks (MgO <10%), and the absence of Mg-rich cumulates, such as peridotites. However, derivation of the parent magmas from a variably enriched mantle source (de Haas, 1992), or introduction of elements from the subducted oceanic crust can not be ruled out.

The Sveconorwegian magmatic activity in Bamble culminated with the emplacement of post-tectonic granitic batholiths and stocks, dated at 0.96 ± 0.06 Ga (Brueckner, 1972; Kullerud and Machado, 1991). The intrusive bodies bear the distinctive geochemical features of A-type granites, such as enrichment in K, REE (except Eu), Zr, and Y, and depletion of Sr, Ba, and transition metals (c.f. Loiselle and Wones, 1979; White and Chappel, 1983; Whalen et al., 1987; 1996).

The spatial, temporal, and geochemical features of the various rock units (supracrustal rocks with calc-alkaline basalt intercalations, calc-alkaline tonalite-trondhjemite series, tholeiitic mafic rocks, and alkaline complexes) suggest that Bamble evolved from a primitive arc setting to an evolved arc and finally to an anorogenic environment, corresponding to an Andean (Cordilleran) type magmatic arc setting (c.f. Thorske, 1977; Smalley, 1983; Smalley and Field, 1991; de Haas, 1992).

7-3. Depletion of Incompatible Lithophile Elements

The highest grade portion of the Bamble (Zone D) makes up the islands of Tromoy and Hissoy. All rocks in this zone, also known as Tromoy Complex, are strongly depleted in LILE and LREE, and most HFSE relative to their lower grade equivalents. Depletion of LILE during granulite metamorphism is well established (e.g. Heier, 1973; Rollinson and Windley, 1980; Newton et al., 1980; Weaver and Tarney, 1981; Condie and Allen, 1984; Lamb and

Valley, 1985; Newton, 1990). However, REE and HFSE have frequently been reported as being inert during metamorphism (e.g. Drury, 1978; Weaver and Tarney, 1980, 1981; Pride and Muecke, 1982; Jahn and Zhang, 1984; Condie and Allen, 1984).

Depletion of elements during granulite metamorphism has alternatively been attributed to:
1) Partial melting with partitioning of the incompatible lithophile elements into the melts (e.g. Fyfe, 1973; Pride and Muecke, 1980; Nesbitt, 1980).
2) Crystallization from a depleted parent magma (e.g. Holland and Lambert, 1973; Tarney et al., 1979).
3) Intrusion of water-undersaturated magma in dry crust during, or subsequent to, granulite-facies metamorphism (e.g. Holland and Lambert, 1975; Drury 1978; Martignole, 1979; Field et al., 1980; Tarney and Weaver, 1987; Frost et al., 1989).
4) Metasomatic fluid processes, involving either dehydration with increasing pressure and temperature (c. f. Heier 1973, Thompson, 1984, Newton, 1992) or CO_2 streaming (e.g. Tarney 1976; Newton, 1980, 1992; Stahle et al., 1985; Frost et al., 1989).

The Tromoy Complex as a whole is SiO_2-rich. Metabasites from Tromoy contain higher contents of SiO_2 relative to those from transition and amphibolite zones. The Tromoy Complex is one of the most silicic Precambrian granulite terrains reported in the literature (c.f. Glikson, 1979; Clough and Field, 1980; Weaver and Tarney, 1980; Rao and Rao, 1980; Jahn and Zhang, 1984; Martin, 1987).

Both metabasites and charnockites are enriched in Na_2O. They are further characterized by lower Sr contents, and more pronounced negative Eu anomalies, relative to the equivalent rocks from amphibolite and transition zones. The above features argue against a significant partial melting in Tromoy, as this process is expected to lead to a decrease in SiO_2, and an increase in modal plagioclase. This supports earlier works by Knudsen (1996) and Knudsen et al. (1997) who showed that granulite grade metasediments at Bamble experienced only local anatexis.

The lower contents of LILE and REE in the Tromoy Complex can not be explained by magmatic fractionation processes. A cumulate origin, as proposed by Field et al. (1980, 1985), is based on the finding of positive Eu anomaly in the charnockites and negative Eu anomaly in the equivalent rocks from transition and amphibolite zones. However, our data based on a larger number of samples indicates a marked negative Eu anomaly for charnockites. A cumulate origin is further rejected by the lower concentration of Sr in the granulite facies rocks.

Intrusion under lower P-T conditions with subsequent dehydration and recrystallization to granulite facies rocks is not supported by the whole rock geochemical data. A metasomatic model of this type would be able to account for depletion of LILE (c.f. Heier 1973a, b; Thompson, 1984). The lower concentrations of REE and HFSE can not be easily explained by this model.

Depletion of incompatible elements in deep-seated intrusive rocks might be a feature inherited from the parent magma, and not necessarily a metamorphic overprint. Tarney et al. (1979) argued that if the source material was the subducting oceanic crust, incompatible elements may have been removed by hydrothermal activities during subduction. This model can not be applied to Bamble, as depletion of incompatible elements is restricted to granulite zone; equivalent rocks from transition and amphibolite zones carry normal concentrations of incompatible elements.

The LILE-deficiency in Tromoy charnockites and metabasites may be attributed to a sufficient supply of CO_2 to suppress the formation of hydrous phases during magmatic crystallization (c.f. Wyllie, 1977; Weaver and Tarney, 1981; Lamb et al., 1986). This is supported by the presence of abundant carbonic fluid inclusions in Tromoy gneisses (e.g. Touret, 1971, Hoefs and Touret, 1975; Van Den Kerkhof et al., 1994).

Alternatively, depletion of certain elements in Tromoy Complex might be a feature related to granulite metamorphism. Fluids during granulite metamorphism are known to be CO_2-rich

(e.g. Touret, 1974; Newton et al., 1980), and could be the agent responsible for complexing and removal of LILE (Weaver and Tarney, 1981; Newton et al., 1980; 1985; Janardhan, 1982; Condie et al., 1982; Condie and Allen, 1984; Hanson et al., 1984; Stahle et al., 1987).

There is compelling evidence that transition from amphibolite to granulite at Bamble occurred in response to progressive change in fluid composition from H_2O-rich to CO_2-rich, rather than increasing pressure and temperature (Touret, 1971, 1974; Hoefs and Touret, 1975; Touret and Dietworst, 1983; Van den Kerkhof et al., 1994; Knudsen and Lidwin, 1996). This is supported by studies on mineral assemblages (Lamb et al., 1986; Visser and Senior, 1985, Cameron, 1989b; Harlov, 1992; Visser, 1993) and fluid inclusions (Touret and Dietworst, 1983). A mantle source is proposed for the CO_2 (Hoefs and Touret, 1975; Newton et al., 1980; Anderson et al., 1984; Lamb et al., 1986).

Rare earth elements form stable carbonate complexes and strongly partition into CO_2-rich fluids over a wide range of temperatures (Kosterin, 1959; Wendlandt and Harrison, 1979; Cantrell and Byrne, 1987). Carbonate complexes are also extremely important for transport of uranium (e.g. Langmuir, 1978; Taylor and McLennan, 1988). Depletion of REE was possibly associated with dissolution of REE-bearing minerals, zircon, apatite, and monazite (c.f. Stahle et al., 1987). This would also explain the low concentrations of HFSE, Y, Zr, Hf, and Nb, in Tromoy Complex. Partitioning of REE into carbonic fluids is supported by the presence of REE-rich carbonate veins in metamorphic terrains (c.f. Lausch et al., 1974; Bogoch et al., 1986; Dahlgren et al., 1993).

The marked negative Eu anomaly in Tromoy rocks is explicable in terms of the presence of an oxidizing fluid during magmatic crystallization, or metamorphic recrystallization. Partitioning of Eu is strongly dependent on oxygen fugacity (Darke, 1975; Darke and Weill, 1975; Mysen et al., 1978). Europium occurs in two oxidation states, Eu^{+2} and Eu^{+3}. Eu^{+2} preferentially occurs in feldspars, for which rather low oxygen fugacity is required (Puchelt and Emmermann, 1976). Apatite structure favors Eu^{+3} with a lower ionic radii. A high f_{O2}, as indicated for Tromoy complex (Cameron, 1991a; Harlov, 1992), could prevent Eu from

incorporation into the feldspars during magmatic crystallization (c.f. O'Nions and Pankhurst, 1974), or lead to the extraction of Eu into solutions during metamorphic recrystallization.

Under oxidizing conditions, Eu, occurring mainly in its trivalent state, is taken up by apatite. A positive Eu anomaly in apatite suggests a high f_{O2} (Puchelt and Emmermann, 1976). Analysis of apatite would probably show whether the parent magmas crystallized under oxidizing conditions, or the high oxidation state recorded for charnockites and metabasites, is a secondary metamorphic overprint.

Whether depletion in certain elements occurred during crystallization under granulite facies conditions, or due to a subsequent discrete metamorphic event, can not be resolved from the chemical data alone. In either case, CO_2 appears to have played a critical role, either by suppressing the formation of hydrous phases during magmatic crystallization, or by complexing and removal of LILE and REE during granulite metamorphism.

7-4. Geochemistry and Phase Relations of Sulfides

Pyrite and pyrrhotite are the principal sulfide minerals in metasediments, commonly occurring as interstitial grains. Subordinate chalcopyrite may accompany pyrite or pyrrhotite in composite grains, or less commonly, as discrete grains. Trace sphalerite, pentlandite, and marcasite were observed in few samples. Pyrite is the main sulfide in the amphibolite zone, but subordinate to pyrrhotite in the transition and granulite zones. Replacement of pyrite by pyrrhotite with increasing metamorphic grade was associated with uptake of Fe from surrounding Fe-Mg silicates, rather than a desulfidation process. This is supported by the presence of Fe-poor silicates in pyrrhotite-rich metasediments, and the similar isotopic composition of pyrite and pyrrhotite.

The granulite grade gneisses, containing on average 3200 ppm S, are considerably enriched in S relative to metasedimentary rocks from amphibolite and transition zones, both containing <1000 ppm S. Enrichment of S in high-grade metamorphic rocks is explicable in terms of the low solubility of S in the products of anatexis. However, in the absence of evidence for a

significant partial melting at Bamble, the relatively high contents of S in the granulite grade metasediments could be of primary origin.

Interstitial pyrite and pyrrhotite are the main sulfide phases in the charnockites. Subordinate chalcopyrite may accompany both pyrite and pyrrhotite in composite grains. Mantling of pyrite by magnetite is common. Pyrrhotite was the stable Fe-sulfide phase at peak metamorphism, at ~ 800 °C, given that pyrite is not stable above ~740 °C (Kullerud and Yoder, 1959).

The least altered hyperites are distinguished by the presence of disseminated, interstitial pyrrhotite as the main sulfide. The pyrrhotite is commonly associated with lamellas and patches of chalcopyrite and pentlandite. The amphibolitized rocks, however, display varying degrees of replacement of pyrrhotite by pyrite ± magnetite, proportional to the extent of amphibolitization. Metabasites are characterized by the dominance of pyrite; initial pyrrhotite is rarely preserved.

Pyrrhotite is considered to be indicative of lower, and pyrite indicative of higher oxygen and sulfur fugacities which appear to be generally interdependent and positively correlated in natural systems (c.f. Kullerud and Yoder, 1959, 1967; Ferry, 1981; Hall, 1986).

It has been indicated that charnockites and metabasites from the granulite zone equilibrated under a relatively oxidizing condition, ~2.5 log unit above the QFM buffer, in the stability field of pyrite + magnetite (Cameron et al., 1989b). Hyperites equilibrated near the QFM buffer, in the stability field of pyrrhotite-magnetite. The amphibolitized hyperites, however, represent a relatively more oxidized mineral assemblage. This is supported by higher ratios of $Fe^{+3}/(Fe^{+2} + Fe^{+3})$, and replacement of the initial pyrrhotite by pyrite ± magnetite.

Oxidation of pyrrhotite to pyrite in the charnockites and granulite grade metabasites was possibly controlled by internal buffering of the rocks with no need to introduction of a fluid-

borne oxidant (Cameron, 1993a, b). The oxygen required for the oxidation was provided by reduction of hematite to magnetite upon cooling below 600°C (Cameron, 1993a):

$$6FeS + 12Fe_2O_3 \rightarrow 3FeS_2 + 9Fe_3O_4$$

However, replacement of pyrrhotite by pyrite and magnetite in the amphibolitized hyperite suggests an external buffering, apparently by the same fluids involved in the hydration and recrystallization of the hyperites (c.f. Cameron, 1989b, 1993a, b).

$$6FeS + 4H_2O = 3FeS_2 + Fe_3O_4 + 4H_2$$

Analysis of the sulfide concentrates from hyperites (pyrrhotite-dominant) and amphibolites (pyrite-dominant), by a combination of INA and hydride-ICP methods, indicated that chalcophile elements were equally distributed in the two assemblages. Replacement of pyrrhotite to pyrite and magnetite was simply an oxidation reaction, without significant addition or removal of elements. Analysis of sulfide concentrates from metabasites revealed the same abundances of chalcophile elements as in the least altered hyperites and amphibolites.

Mass balance calculations indicate that minor sulfides in hyperites and metabasites accounts for up to 85% of the total Au in these rocks. The disseminated sulfide also account for a considerable amount of Se, Bi, and Cu in their enclosing rocks. The partitioning of the elements between sulfide and silicate liquids ($D_{\text{sulfide liquid/silicate liquid}}$) were calculated to be: Au (700 ± 250), Se (12000 ± 5000), and Cu (650 ± 250). These values are in the same common range as in the non-metamorphosed mafic rocks, indicating that the immiscible sulfide globules evolved and crystallized in equilibrium with the silicate liquid, and that metamorphism and sulfide phase changes did not alter the initial magmatic patterns.

Fe-Ni-Cu ores are locally associated with hyperites. The primary orthomagmatic sulfide paragenesis includes pyrrhotite-pentlandite-chalcopyrite. As in their host hyperites, the sulfide ores underwent extensive hydration and recrystallization, leading to the replacement of the primary, pyrrhotite-rich ore by a secondary, pyrite-rich assemblage. Analysis of sulfide concentrates from primary and recrystallized ores revealed no significant differences in the

abundance of Au. The sulfide ores carry lower contents of Au relative to the disseminated sulfides in the host hyperites.

7-5. Sulfur Isotope Ratios

The Bamble metasedimentary rocks exhibit a large variation in $\delta^{34}S$ in the range -1‰ to +12‰ consistent with data from sedimentary rocks of early- to mid-Proterozoic age (c.f. Veizer et al., 1980; Cameron, 1983a, b; Bottomley et al., 1992; Strauss, 1997). The isotopic signature of the metasediments can be explained by bacteriogenic reduction of seawater sulfate with an initial $\delta^{34}S$ value of 20-30‰, a range proposed for early- to mid-Proterozoic seawater sulfate (c.f. Thode and Monster, 1965; Strauss and Schieber, 1990; Bottomley et al., 1997).

Metasedimentary rocks from various metamorphic zones display similar spreads in $\delta^{34}S$ values. However, the granulite grade rocks are slightly enriched in ^{34}S. Our data on the variations of $\delta^{34}S$ do not support an earlier study by Andreae (1974) who reported a smaller spread in $\delta^{34}S$ for granulite grade rocks, and attributed it to homogenization of sulfur isotopes during high grade metamorphism.

Charnockites show a wide spread in $\delta^{34}S$ values, almost in the same range as in the granulite facies metasedimentary rocks. They further display S/Se ratios well above the common range for mantle-derived magmas. These features cast doubt on the general belief that Bamble charnockites are of juvenile magmatic origin. In case of a magmatic origin, the parent magma should have been strongly contaminated with crustal materials.

Mafic rocks from various metamorphic zones display a clustering of $\delta^{34}S$ values around 0‰ indicating a mantle source for sulfur. Pyrrhotite and pyrite exhibit similar isotopic composition implying that no fractionation of S isotopes occurred upon oxidation and breakdown of pyrrhotite to pyrite. This is consistent with data from mass balance calculations that no net addition or removal of S occurred during gabbro-amphibolite transition.

There is evidence that ^{34}S-rich sulfur from metasedimentary country rocks was involved in the formation of Ni-Cu sulfide ores. This is supported by both S isotope and S/Se ratios. The mean $\delta^{34}S$ values and S/Se ratios in the ores (3‰ and 9000, respectively) are considerably higher than those in the host hyperites (0.5‰ and 4700, respectively). Involvement of S from sulfide-rich country rocks is known to be a key factor in the formation of many magmatic Ni-Cu deposits (e.g. Groves et al., 1979; Naldrett, 1981; Lesher et al., 1984, Ripley et al., 1999). The lower concentration of Au in the Ni-Cu ores relative to the host hyperites might be attributed to the assimilation of Au-depleted country rocks, or alternatively, to rapid crystallization of the ores before equilibration with the silicate magma.

The preservation of the initial, pre-metamorphic $\delta^{34}S$ patterns in all rock units indicates that no significant isotopic fractionation occurred during metamorphism. A change in the sulfur isotope ratios may occur if the whole rock complex acts as an open system for S, and large amounts of S can leave or enter the system (e.g. Rye and Ohmoto, 1974; Grinenko and Grinenko, 1975). This is only possible if S occurs in an oxidized species; reduced S will immediately react with available Fe^{2+} to form iron sulfide (c.f. Kullerud and Moh, 1972; Mallio and Gheith, 1972).

7-6. Implications for Granulite Facies Metamorphism

Geochemical, stable isotope, and fluid inclusion studies in Bamble alternatively provide evidence for a high and a low fluid/rock ratio during granulite metamorphism. A significant depletion of REE and HFSE, as displayed by the Tromoy Complex, requires pervasive infiltration of fluids under a high fluid/rock ratio (c.f. Sun and Nesbitt, 1978; Collerson and Fryer, 1978; Weaver and Tarney, 1981; Vocke et al., 1987; Stahle et al., 1987). Such a process would be expected to lead to isotopic homogenization.

Observation of abundant CO_2 inclusions in the Bamble granulite-facies rocks, and the correspondence of the isotopic signatures of the CO_2 to magmatic carbonic fluids, has long been considered as an evidence for pervasive infiltration of lower crustal rocks by fluids of

mantle origin (Touret, 1971, 1974; Hoefs and Touret, 1975; Van Den Kerkhof et al., 1994).

It has been indicated that Bamble charnockites and metabasites equilibrated, at peak metamorphic conditions, under a high f_{O2}, ~2.7 log units above the QFM buffer (Cameron, 1989b, Harlov, 1992). This is supported by scarcity of evidence for the presence of CH_4 in fluid inclusions (Touret, 1985), and by Fe^{+3}/Fe_{total} ratios of whole rocks (Field, 1969; Beeson, 1972; present study) and individual minerals (Nijland, 1993). Cameron (1991a) argued that the uniformity in f_{O2} within the metabasites and charnockites is consistent with their equilibration in the presence of a high fluid flux.

Further evidence for infiltration of homogeneous fluids in Bamble is provided by the common occurrence of coarse grained dolomite veins with uniform chemical and stable isotope compositions (Bugge, 1965; Touret, 1968; Dahlgren et al., 1993). Considering the uniform isotopic composition of the dolomite ($\delta^{18}O$ = +9.6 to +10.7‰ and $\delta^{13}C$ = -8.5 to -6.2‰), Dahlgren et al. (1993) proposed that the hydrothermal fluids were supplied from a very large, homogeneous reservoir. According to the author, the vein fluids were exsolved from crystallizing charnockitic intrusions and subsequently interacted with the crust.

Pineau et al. (1981) identified two populations of $\delta^{13}C$ values in carbonic fluid inclusions in the Tromoy Complex, suggesting two sources of carbon: an organic source of supracrustal origin for the early fluids, and, partial outgassing of the mantle-derived CO_2 for the later fluids.

Besides CO_2 rich fluid inclusions, the Tromoy granulites carry ubiquitous, minute carbonate crystals generally situated on microfractures and on grain boundaries (Pineau et al., 1981; Touret, 1985). The carbonates have a Fe-dolomitic to ankeritic composition very similar to the dolomite veins (c.f. Touret, 1985). The large spread in the isotopic composition of carbon and oxygen ($\delta^{13}C$ = -11.4 to -4.3‰; $\delta^{18}O$ = 10.6 to 24‰) in the disseminated carbonates from Arendal granulites was explained by mixing of carbon from different sources (Pineau et al., 1981; Javoy et al., 1986).

Alternatively, the preservation of the initial, pre-metamorphic $\delta^{34}S$ patterns, and the large spread in $\delta^{34}S$ values for various metasedimentary units argue against pervasive infiltration of oxidizing fluids in Bamble. There is no evidence for a significant desulfidation and removal of S during high grade metamorphism at Bamble. A change in the sulfur isotope ratios may occur if large amounts of isotopically fractionated S, particularly in an oxidized form, can leave or enter the system; reduced S will immediately react with available Fe^{2+} to form iron sulfide (c.f. Kullerud and Moh, 1972; Rye and Ohmoto, 1974; Grinenko and Grinenko, 1975). There is evidence for local (millimeter to centimeter scale) remobilization and reprecipitation of sulfides, implying that mobile S was principally present in its reduced form.

That metamorphism at Bamble proceeded under a low fluid/rock ratio is further supported by data from oxygen and carbon isotope ratios (c.f. Andreae, 1974; Pineau et al., 1981; Javoy et al., 1986; Broekmans et al., 1994), as well as chemical and textural studies (Nijland et al., 1993; Kihle and Bucher-Nurminen , 1992).

Large variations in $\delta^{13}C$ and $\delta^{18}O$ values, up to 20‰, have been reported from primary and secondary carbonates, graphite, and quartz segregations from the granulite zone at Bamble (Andreae, 1974; Pineau et al., 1981; Javoy et al., 1986; Broekmans et al., 1994). The isotopic composition of carbonates and graphite from granulite zone corresponds to those from the non-metamorphosed mid-Proterozoic rocks (Andreae, 1974; Broekmans et al., 1994). A low fluid/rock ratio is also supported by the presence of small scale variations in the abundances of halogens in high grade metamorphic minerals (Nijland et al., 1993). Kihle and Bucher-Nurminen (1992) reported common occurrences of disequilibrium textures in granulite grade metasediments from Grimstad, Bamble.

The role of CO_2 in granulite facies metamorphism may have been overestimated in earlier studies. It has been indicated that the low wetting ability of high pressure CO_2 on the grain boundaries of silicate minerals greatly favors its capture and retention as fluid inclusions (Harlov et al., 1997).

7-7. Depletion of Gold

The Bamble supracrustal rocks of varied types and origins are strongly depleted in Au, as well as As, Sb, and Se, compared to the equivalent lower grade rocks elsewhere, or to the mean composition of the continental crust. The supracrustal rocks contain, on average, 0.30 ppb Au, which is 25% of the crustal abundance of this element. Similarly, the mean abundance of Au in the tonalite-trondhjemite gneisses is 0.2 ppb, that is only 20% of the general abundance of Au in felsic igneous rocks. The gneisses are also depleted in As, Sb, and Se. The consistently low abundance of Au through rock types of different origin suggests that a common process caused its scarcity. It is difficult to model a series of independent processes that can account for the scarcity of this element in all individual rock units.

Gold occurs as both atomic and molecular, as well as in a particulate form in sulfides, at grain boundaries, in microcracks and dislocation structures, in interlayer position in minerals, and in the interstitial fluids (e.g. Rowe, 1969; Davletov, 1974; Boyle, 1979; Mironov and Galetiy, 1979; Parry, 1984; Bakken et al., 1989; Korobeynikov, 1991; Huston et al., 1993).

Gold occurring in the particulate form is more mobile and may be extensively extracted and redistributed by metamorphogenic solutions, even under moderate metamorphic conditions (Korobeynikov, 1991; Huston et al., 1993). In the shear zone environment, Au can be transported in complex forms involving Cl^-, HS^-, S^{-2}, $(AsS_2)^-$, and $(SbS_2)^-$ (Weissberg, 1970; Henley, 1973; Barnes, 1979; Seward, 1984, Mikucki, 1998), or carbonyl ions (Kerrich and Fyfe, 1981). Mikucki (1998) emphasized the role of chloride complexes for transportation of Au in lower crust. Experiments on the recrystallization of Au-bearing pyrite by chloride solutions at 400-500°C have shown a significant loss of Au, by 40-80%, from the pyrite to the fluids (Korobeynikov, 1991).

The Bamble post-orogenic granites carry, on average, 0.18 ppb Au that is less than 20% of the general abundance of this element in granitic rocks elsewhere. They are also depleted in S, As and Sb. The relatively low contents of the elements in the Bamble granites may partly be explicable in terms of the low initial Fe_t content. However, given a crustal source for the

granites (c.f. Longstaffe et al., 1980; Chappell et al., 1987; Kerr et al., 1993; Whalen et al., 1997), partial melts derived from the Au-depleted rocks of the Bamble would be similarly deficient in Au.

The mean abundance of Au in the metabasites and hyperites (0.25 and 0.45 ppb, respectively) is considerably lower than that in most tholeiitic mafic suites reported in the literature (c.f. Crocket and Truta, 1977; Gottfried and Greenland, 1972; Kwong and Crocket, 1978; Davies and Tredoux, 1985; Zentilli et al., 1985; Korobeynikov and Pertsev, 1995). Gold in mafic rocks is principally carried by minor sulfides. Mass balance calculations indicated that minor disseminated sulfides in the Bamble metabasites and hyperites account for 50 to 85% of the total Au in their enclosing rocks.

Metabasites have totally metamorphic textures and mineral assemblages, implying that they equilibrated to the conditions of metamorphism. The initial pyrrhotite is commonly replaced by pyrite and magnetite in the metabasites. Hyperites are partially amphibolitized, particularly at their margins. The initial magmatic textures are preserved in the less altered rocks. During hydration and recrystallization, primary magmatic pyrrhotite was oxidized to pyrite and magnetite.

Metabasites represent a more oxidized mineral assemblage compared to the hyperites. Those from granulite and transition zones equilibrated under a relatively high f_{O2} ($\log f_{O2} \cong -11.8$), well above the QFM buffer, at peak metamorphism (Cameron, 1989b, 1993a). This is consistent with the stability field of pyrite-magnetite-pyrrhotite. Hyperites equilibrated near the QFM buffer, in the field of stability of pyrrhotite. The amphibolitized hyperites, however, represent a relatively more oxidized mineral assemblage. For hyperites, there is strong evidence that amphibolitization and sulfide phase changes did not influence the initial variations of the chalcophile elements. This is supported by data from mass balance calculations, analysis of sulfides from the least and the most altered rocks, and sulfur isotope ratios.

The origin of Au depletion in the Bamble metabasites and hyperites could be attributed to:

1. Depleted mantle source.
2. Segregation of sulfides from the parent magmas during ascent or emplacement.
3. Partial melting processes and sulfur saturation at the source region.
4. Transportation of Au in complex ions by magmatic volatiles.
5. Massive addition of S from an external source (crustal contamination).
6. Post-solidus (deuteric and metamorphic) alteration, and loss of Au to infiltrating fluids.
7. A combination of two or more of the above processes.

A model consistent with all geochemical data supports the "partial melting processes and sulfur saturation at the source region", as the most likely mechanism of Au depletion in the mafic rocks. Both metabasites and hyperites are characterized by high FeO_t, low MgO, and marked enrichment in LILE and LREE, consistent with a low degree of partial melting.

Magmas generated by low to moderate degrees of partial melting of a normal source region in the upper mantle are S-saturated and become rapidly depleted in precious metals during the early stages of silicate fractionation, due to the coprecipitation of an immiscible sulfide component (Naldrett and Duke, 1980; Hamlyn et al., 1985; Keays, 1987; Mathez and Peach, 1987; Peach et al., 1990). The process may result in the preferential removal of elements having low $D^{S/L}$ values (i.e. base metals) and concentration of those elements with high $D^{S/L}$ values (i.e. PGE and Au) in the residual mantle sulfide fraction (c.f. Naldrett and Duke, 1980; Hamlyn et al., 1985; Peach et al., 1990).

It has been indicated that small degrees of partial melting result in significant fractionation of the noble metals, PGE and Au, from the moderately chalcophile elements, Cu, Se (Peach et al., 1990). Only at relatively high degrees of partial melting, do noble metals enter partial melts to an appreciable degree. A partial melting of ~10% would lead to a significant depletion in Cu and Se, while Au is enriched, relative to the average upper mantle composition (Peach et al., 1990).

A low degree of partial melting for Bamble mafic rocks is also supported by the strong depletion of Ir. The low concentration of Ir in the Bamble mafic rocks might be a consequence of the compatible behavior of this element during partial melting processes (c.f. Naldrett and Duke, 1980; Brügmann et al., 1987), or removal of Ir along with Au in a sulfide fraction early in the evolution of the partial melts.

While low concentration of Au in mafic rocks (metabasites and hyperites) and post-orogenic granites can be ascribed to processes in the source region, depletion of Au in the supracrustal rocks and charnockites appears to be of metamorphic origin. Gold could have been remobilized at different stages during evolution of Bamble:

1) During progressive metamorphism. Depletion of Au in supracrustal rocks of varied type and origin from both amphibolite and granulite zones indicates that loss of Au, together with As and Sb, may have occurred during prograde devolatilization of these rocks and any magmatic rocks that had been intruded by that time. Oxidation of the rocks throughout the belt during metamorphism is well established as a result of the works of Cameron (1989b) and Harlov (1992). Loss of Au, As and Sb could have occurred during the pervasive flow of fluid that produced this oxidation.

2) Oxidation of sulfides during isobaric cooling, hydration and recrystallization. This is evident from replacement of pyrrhotite by pyrite, and mantling of the latter by magnetite, in metabasites, amphibolitized hyperites, and charnockites. For an efficient remobilization of chalcophile elements to occur, the f_{O2} should be above the pyrrhotite-pyrite-magnetite buffer. The boundary was hardly crossed at Bamble; oxidation of sulfides occurred commonly in systems closed to significant removal of chalcophile elements.

3) Replacement of sulfides by alteration minerals (Fe-rich chlorite, quartz, and carbonates). This is a low temperature retrograde reaction, occurring during uplift. The silicate and carbonate alteration is generally of local nature, rarely affecting more than 10% of the total sulfides. When pervasive, however, the enclosing rock is strongly depleted in chalcophile

elements. The remobilized elements were, at least partly, reprecipitated as secondary sulfides. Secondary pyrite occurring as overgrowth and fracture filling in metabasites was found to be considerably enriched in Au, As, and Sb, relative to the interstitial sulfides.

A felsic magmatic model for the origin of gold and ore fluids, as proposed by some workers (e.g. Emmons, 1937; Mason and Melnik, 1986; Burrows and Spooner, 1987; Mueller et al., 1991, Hattori, 1987; Cameron and Hattori, 1987) is not supported by data from Bamble Shear Belt. There is strong evidence that no significant partial melting occurred during the Gothian (Sveconorwegian) high grade metamorphism. Gold was not extracted by a granitic partial melt.

7-8. Depletion of Elements in Lower Crust and Formation of Lode Gold

A comparison of depletion of certain elements in the lower crustal rocks in Bamble and enrichment of elements in lode gold deposits provide evidence for a genetic relation between granulite metamorphism and formation of lode gold. Gold, As, Sb, and Se are strongly depleted in the Bamble lower crustal rocks. Arsenic and Sb are amongst the elements most commonly associated with Au in lode gold deposits (e.g. Boyle, 1979; Kerrich, 1984, Colvine et al., 1988; Witt and Vanderhor, 1998).

The formation of lode gold is commonly associated with alkaline metasomatism (e.g. Boyle, 1979; Colvine et al., 1988; Kerrich and Fyfe, 1981; Kerrich, 1988, 1989 a; Groves et al., 1992, 1998; Witt and Vanderhor, 1998). Enrichment of LILE in lode gold deposits could be complementary to the depletion of the same elements in granulites. Such genetic relation has been challenged based on the ground that the enhanced K/Rb, K/Cs, and Rb/Cs ratios, characteristic of many granulites, are not reflected in the lode gold deposits, where the ratios are commonly in the same range as in the average crustal values (Kerrich, 1989 b). This disparity may be explained in terms of the modification of the initial ratios during ascent and interaction of the fluids with country rocks.

Data on the distribution of REE in lode gold deposits are rare in the literature. The existing evidence indicate an enrichment of REE in the hydrothermal and alteration minerals associated with lode gold (e.g. King and Kerrich, 1986, 1988; Ghaderi et al., 1999; Kontak and Jackson, 1999). King and Kerrich (1988) reported an enrichment in REE from hydrothermal tourmaline in gold bearing veins in Superior Province, Canada. Similarly, Ghaderi et al. (1999) documented an enrichment in REE, particularly LREE, in hydrothermal scheelite associated with lode gold deposits in Western Australia. The authors showed that the scheelite, variably enriched in Eu, formed from both oxidized and reduced fluids.

Kontak and Jackson (1999) demonstrated a considerable enrichment of Sr and REE in hydrothermal carbonates from auriferous quartz veins in Meguma lode gold deposits, Nova Scotia. The similar chondrite-normalized REE patterns displayed by carbonates from various deposits was interpreted as an evidence for derivation of REE from a common source reservoir, or a regional scale homogenization of the ore fluids (Kontak and Jackson, 1999). Studying the REE patterns of various source rocks, the authors suggested the deep crustal mafic and felsic gneisses, represented by granulite-facies xenoliths within lamprophyric dykes, as a possible source reservoir.

The Bamble granulite grade rocks are also depleted in HFSE. Data on the abundances of HFSE in lode gold deposits are rare in the literature. Dahlgren (1993) reported an enrichment of Y in Sveconorwegian hydrothermal dolomite veins from Kragero, Bamble. With respect to carbon and oxygen isotopic composition, the Kragero dolomites are similar to carbonates in lode gold deposits in shear zones. The mineralogy of the veins (carbonates, quartz and sulfides) are also similar to that in lode gold deposits.

The source of CO_2 involved in the dehydration and granulitization of the lower crustal rocks is controversial. A mantle origin for the CO_2, as proposed by several authors (e.g. Newton, 1980, 1992; Touret, 1985; Santosh et al., 1995) is based on the isotopic composition of carbon. However, the average $\delta^{13}C$ values of ~-4‰ for lode gold deposits are not uniquely diagnostic of a mantle source for carbon (Kyser, 1986, Mathews et al., 1987). The average

igneous, metamorphic and sedimentary carbon reservoirs all possess $\delta^{13}C$ values in this range (Ohmoto and Rye, 1979). A crustal source for carbon has been indicated for some granulite terrains (e.g. Glassley, 1983; Lamb et al., 1987; Vry et al., 1988).

The Bamble granulite grade rocks are unique in that they are strongly depleted, not only in LILE, but also in REE and HFSE. Depletion of LILE during granulite metamorphism is well established. Depletions of REE and HFSE are not common. It might be a characteristic feature of oxidized granulites. However, whereas depletion of the incompatible lithophile elements is restricted to the granulite zone, all zones are similarly depleted in Au.

Depletion of Au in rocks of varied type and origin in Bamble suggest a heterogeneous source rock for Au. This is consistent with data from stable and radiogenic isotope studies on lode gold deposits (c.f. Kerrich, 1987; Powell et al., 1991; Hattori, 1993; McNaughton et al., 1993; Groves et al., 1995; Qui and McNaughton, 1999). Even in a single deposit, Au might have been derived from different sources (Kerrich, 1989b; Qui and McNaughton, 1999).

Neither special Au-enriched rock units, nor unreasonably large volumes of source rocks are required to produce a giant gold deposit (c.f. Phillips et al., 1987; Cameron, 1989a, b). To create a giant gold deposit with an Au reserve of ~1000 t, a source area of 10 x 10 km and 5 km thick would be required to undergo a depletion of Au by only 50%, assuming a crustal average of 1.5 ppb for Au. Shear zones serve as major source areas and principal conduits for extraction and transportation of metals and fluids. Many types of deposits, including "lode gold", are spatially associated with these structures.

References

Alberti A. A. and Comin-Chiaramonti (1976) The metamorphic evolution of Tromoy (Arendal Area, south Norway). Tschermarks Min. Petr. Mitt., 23, 205-220.

Allemann R. and Crocket J. H. (1974) Gold. In: Wedepohl (ed) Handbook of Geochemistry. Springer Verlag, 79A-79O.

Andersen T. and Sundvoll B. (1995) Neodymium isotope systematics of the mantle beneath the Baltic Shield: Evidence for depleted mantle evolution since the Archean. Lithos, 35, 235-243.

Anderson J. K. and Cullers R. L. (1978) Geochemistry and evolution of the Wolf River Batholith, a late Precambrian Rapakivi Massif in North Wisconsin, U.S.A.. Precambrian Research, 7, 287-324.

Anderson J. L. and Cullers R. L. (1987) Crust-enriched, mantle-derived tonalites in the early Proterozoic Penokean Orogen of Wisconsin. The Journal of Geology, 95, 139-154.

Andreae M. O. (1974) Chemical and stable isotope composition of the high-grade metamorphic rocks from the Arendal Area, Southern Norway. Contrib. Mineral. Petrol, 47, 299-316.

Anoshin G. N and Kepezhinskas V. V. (1972) Petrochemical features related to gold distribution for the Cenozoic volcanic rocks of the Kuril-Kamchatka Province. Geochemistry International, 9, 618-628.

Appleyard E. C. (1980) Mass Balance Computations in Metasomatism: metagabbro/nepheline syenite pegmatite interaction in northern Norway. Contrib. Mineral. Petrol., 73, 131-144.

Arnold R. G. (1962) Equilibrium relations between pyrrhotite and Pyrite from 325° to 743° C. Economic Geology, 57, 72-90.

Arnold R. G. (1966) Range in composition and structure of 82 natural terrestrial pyrrhotites. The Canadian Mineralogist, 31-50.

Arth J. G (1976) Behavior of trace elements in during magmatic processes – a summary of theoretical models and their applications. J. Res. U. S. Geol. Surv. 4, 41-47.

Arth J. G. (1979) Some Trace elements in trondhjemites – their implications to magma genesis and paleotectonic setting. In: Barker F. (ed.) Trondhjemites, dacites, and related rocks. Developments in Petrology, 6, pp. 123-132. Elsevier.

Arth J. G., Barker F., and Peterman Z. E., and Friedman I. (1978) Geochemistry of the gabbro-diorite-tonalite-trondhjemite suite of southwest Finland and its implications for the origin of tonalitic and trondhjemitic magmas. Journal of Petrology, 19, 289-316.

Arth J. G. and Hanson G. N. (1975) Geochemistry and origin of early Precambrian crust of northeastern Minnesota. Geochimica et Cosmochimica Acta, 39, 325-362.

Ashworth J. R. (1986) The role of magmatic reaction, differentiation and annealing in the evolution of coronitic microstructure in troctolitic gabbro from RisØr, Norway: a discussion. Mineral. Mag., 50, 469-473.

Atkin B. P., and Brewer T. S. (1990) The tectonic setting of basaltic magmatism in the Kongsberg, Bamble, and Telemark Sectors, Southern Norway. In: Gower C. F., Rivers T., and Ryan B. (eds) Mid-Proterozoic Laurentian-Baltica: Geological Association of Canada, special paper 38.

Bachinski D. J. (1969) Bond strength and sulfur isotopic fractionation in coexisting sulfides. Economic Geology, 64, 56-65.

Bakken B. M, Hochella A. F., Marshall A. F., and Turner A. M. (1989) High resolution microscopy of gold in unoxidized ore from the Carline Mine, Nevada. Economic Geology, 84, 171-179.

Banks N. G. (1982) Sulfur and copper in magma and rocks. In: Titley S. R. (ed) Advances in geology of the porphyry copper deposits in southwestern North America. pp. 227-258.

Barker F. (1979) Trondhjemite: Definition, Environment and Hypotheses of Origin. In Barker F. (ed.) Trondhjemites, dacites, and related rocks. Development in Petrology, 6, pp. 1-12, Elsevier.

Barker F., Arth J. G., Peterman Z. E., and Friedman I. (1976) The 1.7 to 1.8 b.y. old trondhjemites of southwestern Colorado and northern New Mexico: Geochemistry and depths of genesis. Geological Society of America Bulletin, 87, 189-198.

Barker F., Arth J. G. (1976) Generation of trondhjemitic-tonalitic liquids and Archean bimodal trondhjemite-basalt suites. Geology, 4, 596-600.

Barnes S. J., Naldrett A. J., and Gorton M. P. (1985) The origin of the fractionation of platinum-group elements in the terrestrial magmas. Chemical Geology, 53, 303-323.

Barnes S. J. (1987) Unusual nickel and copper to noble metal ratios from the Rana layered intrusion, northern Norway. Norske Geologisk Tidsskrift, 67, 215-231.

Barnes S. J. (1993) Partitioning of the platinum group element and gold between silicate and sulfide magmas in the Munni Munni Complex, Western Australia. Geochimica et Cosmochimica Acta, 57, 1277-1290.

Barnes S. J., and Naldrett A. J. (1985) Geochemistry of the J-M (Howland) Reef of the Stillwater Complex, Minneapolis Adit area. I. Sulfide chemistry and sulfide-olivine equilibrium. Economic Geology, 80, 627-645.

Barnes S. J., Gole M. J., and Hill R. E. (1988) The Agnew nickel deposit, Western Australia: Part II. Sulfide geochemistry, with emphasis on the platinum-group elements. Economic Geology, 83, 537-550.

Barnicoat A. C., Fare R., Groves D., and McNaughton N. J. (1991) Synmetamorphic lode-gold deposits in high-grade Archean settings. Geology, 19, 921-924.

Barron K. M. (1991) Relationship of Archean gold to alkaline magmatism, Superior Province, Canada. In: Ladeira (ed.) Brazil Gold' 91, Balkema, Roterdam, pp. 101-107.

Barth T. F. W. (1925) On contact minerals from Precambrian limestones in southern Norway. Nor. Geol. Tidsskr, 8, 93-114.

Barton P. B. and Skinner B. J. (1979) Sulfide mineral stabilities. In: Barnes (ed) Geochemistry of hydro-thermal ore deposits, 2nd edition, chapter 7, pp. 278-403. Wiley Interscience.

Basaltic Volcanism Study Project (1981) Basaltic volcanism on the terrestrial planets. New York: Pergamon Press, 1286 p.

Baur W. H., and Onishi H. (1974) Arsenic. In: Wedepohl (ed) Handbook of Geochemistry. Springer Verlag; 33A-33-O.

Beaudoin G., and Taylor B. E. (1994) High precision and spatial resolution sulfur isotope analysis using MILES laser microprobe. Geochimica et Cosmochimica Acta, 58, 5055-5063.

Beudreau A. E. and McCallum I. S. (1989) Investigation of the Stillwater Complex: Part V. Apatites as indicators of evolving fluid composition. Contr. Min. Petr., 102, 138-158.

Beeson R. (1975) Metasedimentary gneisses from the area between Songe and Ubergsmoen, Aust-Agder, south Norway. Norges Geol. Unders, 321, 87-102.

Berner R. A. (1984) Sedimentary pyrite formation. An update. Geochimica et Cosmochimica Acta, 48, 605-615.

Bischoff J. L. and Dickson F. W. (1975) Seawater-basalt interaction at 200oC and 500 bars: Implications for the origins of heavy metal deposits and regulations of seawater chemistry. Earth Planet. Sci. Lett. 25, 385-397.

Boctor N. Z. and Yoder H. S. (1983) Partitioning of nickel between silicate and iron sulfide melts. Carnegie Inst. of Washington Year Book, 81, 366-369.

Bogoch R., Magaritz M., and Michard A. (1986) Dolomite of possible mantle origin, southeast Sinai. Chemical Geology, 56, 281-288.

Bohlke J. K. (1989) Comparison of metasomatic reactions between a common CO2-rich vein fluid and diverse wall rocks: Intensive variables, mass transfer, and Au mineralization at Alleghany, California. Economic Geology, 84, 291-327.

Bornhorst T. J. and Rose W. I. (1986) Partitioning of gold in young calc-alkaline volcanic rocks from Guatemala. Journal of Geology, 94, 412-418.

Borodin L. S., Nazarenko I. I., and Kislova I. V. (1972) New data on the selenium content of igneous rocks. Geochemistry International, pp. 203-205.

Bottomley D., Viezer J., Nielsen H., Moczydlowska M. (1992) Isotopic composition of disseminated sulfur in Precambrian sedimentary rocks. Geochimica et Cosmochimica Acta, 56, 3311-3322.

Boulter C. A., Fotios M. G., and Phillips G. N. (1987) The golden mile, Kalgoorlie: A giant gold deposit localized in ductile shear zones by structurally induced infiltration of an auriferous metamorphic fluid. Economic Geology, 82, 1661-1678.

Boyd R. and Mathiesen C. O. (1979) The nickel mineralization of the Rana mafic intrusion, Nordland, Norway. Canadian Mineralogist, 17, 287-298.

Boyd R. McDade J. M. Millard H. T and Page N. J. (1987) Platinum metal geochemistry of the Baruvann nickel-copper deposits, Råna, North Norway. Norske Geologiske Tidsskrift, 67, 205-213

Boyle R. (1979) The Geochemistry of gold and its deposits. Geol. Surv. Of Canada, Bulletin 280, 584 p.

Boyle R. W., and Jonasson I. R. (1973)) The geochemistry of antimony and its use as an indicator element in geochemical prospecting: Journal of Geochemical Exploration, 2, 251-296.

Boyle R. W., and Jonasson I. R. (1984) The geochemistry of antimony and its use as an indicator element in geochemical prospecting: Journal of Geochemical Exploration, 20, 75-95.

Brickwood J. D. and Craig J. W. (1987) Primary and re-equilibrated mineral assemblages from the Sveco-norwegian mafic intrusions of the Kongsberg and Bamble areas, Norway. Nor. Geol. Unders. Bull, 410, 1-23.

Brickwood J. D.(1986) The geology and mineralogy of some Fe-Cu-Ni sulfide deposits in the Bamble area, Norway. Norsk Geologisk Tidsskrift, 66, 189-208.

Brickwood J. D.(1984) Basic intrusions and related iron-copper-nickel sulfide deposits in the Kongsberg and Bamble sectors of South Norway. Unpubl. Ph.D. thesis, University of London.

Bridgewater D. and Collerson K. D. (1976) The major petrological and geochemical characters of the 3600 m.y. Uivak gneisses from Labrador. Contrib. Mineral. Petrol. 54, 43-59.

Brøgger W. C. (1934) On several Archean rocks from the south coast of Norway. Vid.-Selsk. Skr. I. No. 1.

Broekmans M. A. T. M., Nijland T. G., and Jansen J. B. H. (1994) Are stable isotopic trends in amphibolite to granulite facies transitions metamorphic or diagenetic? an answer for the Arendal area (Bamble Sector, southeastern Norway) from Mid-Proterozoic carbon bearing rocks. American Journal of Science, 294, 1135-1165.

Brueckner H. K. (1972) Interpretation of Rb-Sr ages from the Precambrian and Paleozoic rocks from southern Norway. Am. J. Sci., 272, 334-358.

Brügmann G. E., Arndt N. T., Hofmann A. W. and Tobschall H. J. (1987) Noble metal abundances in Komatiite suites from Alexo, Ontario, and Gorgona Island, Colombia. Geochimica et Cosmochimica Acta, 51, 2159-2169.

Buddington A. F. and Lindsley D. H. (1964) Iron-Titanium oxide minerals and synthetic equivalents. Journal of Petrology, 5, 310-357.

Buddington A. F., Fahey J., and Vlisides A. (1963) Degree of oxidation of Adirondack iron oxide and iron-titanium oxide minerals in relation to petrogeny. Journal of Petrology, 4, 138-169.

Bugge J. (1939) Geological and petrographical investigations in the Arendal District. Norsk Geol. Tidsskr., 20, 71-112.

Bugge J. A. W. (1943) Geological and petrographical investigations in the Kongsberg-Bamble Formation. Nor. Geol. Unders., 160, 150 p.

Bugge J. A. W. (1978) Norway. In: Bowie S. H. U., Kavalheim A., and Haslam H. W. (eds) Mineral Deposits of Europe. pp. 199-249.

Burrows D. S. and Spooner E. T. C. (1988) Generation of a Magmatic H_2O-CO_2 fluid enriched in Mo, Au, and W within an Archean sodic granodiorite stock, Mink Lake, northwestern Ontario. Economic Geology, 82, 1931-1957.

Buryak V. A. (1978) Gold content of sedimentary strata and behavior of gold in them during metamorphism and granitization. Soviet Geology and Geophysics, 19; 6, 115-118.

Cabri L. J. (1973) New data on phase relations in the Cu-Fe-S system. Economic Geology, 68, 443-454.

Cambel B. and Jarkovsky J. (1969) Geochemistry of pyrrhotite of various genetic types. Bratislava, 227 p.

Cameron E. M (1974) Sulfur in Archean volcanic rocks of the Canadian Shield. Geol. Surv. Can., Pap. 74-18, 9 pp.

Cameron E. M. and Garrels. (1980) Geochemical compositions of some Precambrian shales from the Canadian shield. Chemical Geology, 28, 181-197.

Cameron E. M. (1983) Genesis of Proterozoic Iron-formation: Sulfur isotope evidence. Geochimica et Cosmochimica Acta, 47, 1069-1074.

Cameron E. M. (1988) Archean gold: Relation to granulite formation and redox zoning in the crust. Geology. 16, 109-112.

Cameron E. M. (1989a) Derivation of gold by oxidative metamorphism of a deep ductile shear zone: Part 1. Conceptual model. Journal of Geochemical Exploration, 31, 135-147.

Cameron E. M. (1989b) Derivation of gold by oxidative metamorphism of a deep ductile shear zone: Part 2. Evidence from the Bamble Belt, south Norway. Journal of Geochemical Exploration, 31, 149-169.

Cameron E. M. (1990) Alkaline magmatism at Kirkland Lake, Ontario: Product of strike-slip orogenesis. Geol. Surv. Can. Pap. 90-1C, 261-269.

Cameron E. M. (1993a) Precambrian Gold: Perspectives from the top and bottom of shear zones. The Canadian Mineralogist, 31, 917-944.

Cameron E. M. (1993b) Reintroduction of gold, other chalcophile elements and LILE during retrogression of depleted granulite, Tromøy, Norway. Lithos, 29, 303-309.

Cameron E. M. (1994) Depletion of gold and LILE in the lower crust: Lewisian Complex, Scotland. Journal of the Geological Society, London, 151, 747-754.

Cameron E. M. and Hattori K. (1987a) Archean Sulfur Cycle: Evidence from sulphate minerals and isotopically fractionated sulfides in Superior Province, Canada. Chemical Geology, 65, 341-358.

Cameron E. M. and Hattori K. (1987b) Archean gold mineralization and oxidized hydrothermal fluids: Economic Geology, 82, 1177-1191.

Cameron E. M., Cogulu E. H. and Stirling J. (1993) Mobilization of gold in the deep crust: evidence from Mafic intrusion in the Bamble belt, Norway. Lithos, 30, 151-166.

Cantrell K. G. and Byrne R. L. (1987) Rare earth element complexation by carbonate and oxalate ions. Geochim. et Cosmochim. Acta, 51, 597-605.

Carpenter R. H. (1974) Pyrrhotite isograd in southeastern Tennessee and southwestern Carolina. Geological Society of American Bulletin, 85, 451-456.

White A. J. R. and Chappel B. W. (1997) Ultrametamorphism and granitoid genesis. Tectonophysics 43, 7-22.

Chaussidon M. and Lorand J. P. (1990) Sulfur isotope composition of orogenic spinel lherzolite massifs from Ariege (North-Eastern Pyrenees, France): An ion microprobe study. Geochimica et Cosmochimica Acta, 54, 2835-2846.

Clark L. A. (1960) The Fe-As-S system: Phase relations and applications. Economic Geology, 34, 777-789.

Claypool G. E., Holser W. T., Kaplan I. R., Sakai H. and Zak I. (1980) The Age curves of sulfur and oxygen isotopes in marine sulfate and their mutual interpretation. Chemical Geology. 28, 199-260.

Clough P. W. L. and Field D. (1980) Chemical variation in metabasites from a Proterozoic amphibolite-granulite transition zone, South Norway. Contrib. Mineral. Petrol., 73, 277-286.

Coleman M. L. (1979) Isotopic analysis of trace sulfur from some S- and I-type granitoids: Heredity or environment? In: Atherton M. P. and Tarney J. (Eds) Origin of granite batholiths. Geochemcial evidence, pp. 129-133.

Collerson K. D. and Fryer B. (1979) The role of fluids in the formation and subsequent development of early continental crust. Contib. Mineral. Petrol., 67, 151-167.

Collins W. J., Beams S. D., White A. J. R., and Chappell B. W. (1982) Nature and origin of A-type granites with particular reference to Southeastern Australia. Contrib. Mineral. Petrol, 80, 189-200.

Colvine A. C., Fyon, J. A., Heather K. B., Marmont S., Smith P. M., and Troop D. G. (1988) Archean lode gold deposits in Ontario. Ontario Geological Survey, Miscellaneous Paper, 139, 210 p.

Colvine A. C., Andrews a. J., Cherry M. E., Durocher M. E. et al. (1984) An integrated model for the origin of Archean lode gold deposits. Ontario Geological Survey, Open File Report 5524, 98 p.

Compton P. (1978) Rare earth element evidence for the origin of the Nuk Gneisses, Buksefjorden region, southern Norway. Contrib. Mineral. Petrol., 66, 283-293.

Condie K. C. (1978) Geochemistry of Proterozoic Granitic Plutons from New Mexico, U.S.A. Chemical Geology, 21, 131-149.

Condie K. C. and Allen P. (1984) Origin of Archean Charnockites from Southern India. In: Kröner et al (eds) Archean Geochemistry, Springer Verlag. pp. 182-203.

Condie K. C., Allen P., and Narayana B. L. (1982) Geochemistry of the Archean Low-to High-grade Transition Zone, Southern India. Contrib. Mineral. Petrol., 81, 157-167.
Contrib. Mineral. Petrol., 87, 205-219.

Cook N. J. and Hoefs J. (1997) Sulfur isotope characteristics of metamorphosed Cu-Zn volcanogenic massive sulfide deposits in the Norwegian Caledonides. Chemical Geology, 135, 307-324.

Cooper D. C. and Field D. (1977) The chemistry and origins of Proterozoic low-potash, high iron, charnockitic gneisses from Tromoy, South Norway. Earth and Planetary Science Letters, 35, 105-115

Correia Neves J. M, Lopez Nunes J. E., and Sahama T. G. (1974) High hafnium members of the zircon-hafnon series from the granite pegmatites of Zambeszia, Mozambique. Cont. Min. Petr., 48, 73-80.

Craig J. R. and Scott (1974) Sulfide phase equilibria. In: Ribbe P. H. (ed) Sulfide mineralogy; Reviews in mineralogy, Vol. 1. Mineralogical Society of America; pp. CS1-CS110.

Craig J. R. and Kullerud G. (1969) Phase relations in the Cu-Fe-Ni-S system and their applications to magmatic ore deposits. Economic Geology, Mon. 4, 344-358.

Crocket J. H., MacDougall J. D., and Harris R. C. (1973) Gold, palladium, and iridium in marine sediments. Geochimica et Cosmochimica Acta, 37, 2547-2555.

Crocket J. H., Fueten F., Clifford P. M., and Kabir A. (1983) Distribution and localization of gold in Meguma Group rocks, Nova Scotia, Part 2: Implications of background geochemistry and cleavage development - A preliminary report. Current Research, Part B, Geological Survey of Canada, Paper 83-1B, pp. 285-290.

Crocket J. H., Fueten F., Clifford P. M., and Kabir A. (1986) Distribution of gold and arsenic in turbidites at Harrigan Cove, Nova Scotia: Implications on gold mineralization. In: Keppie J. D., Boyle R. W., and Haynes S. J. (eds) Turbidite-hosted gold deposits. pp. 149-159.

Crocket J. H., Fleet M. E., and Stone W. E. (1991) Experimental studies of the partitioning of PGE between sulfide liquid and basaltic melt. Sixth International Platinum Symposium, Perth, W. A., Prog. Abstr. p. 16.

Crocket J. H., Fleet M. E., and Stone W. E. (1997) Implication of composition for experimental partitioning of platinum-group elements and gold between sulfide liquid and basalt melt: The significance of nickel content. Geochimica et Cosmochimica Acta, 61, 4139-4149.

Crowe D. E. (1994) Preservation of original hydrothermal $\delta^{34}S$ values in greenschist to upper amphibolite volcanogenic massive sulfide deposits. Geology, 22, 873-876.

Crowe D. E., and Vaughan R. G. (1996) Characterization and use of isotopically homogeneous standards for in situ laser microprobe analysis of $^{34}S/^{32}S$ ratios. American Mineralogist, 81, 187-193.

Crowe D. E., Valley J. W. (1992) Laser microprobe study of sulfur isotope variation in a sea-floor hydrothermal spire, Axial Seamount, Juan de Fuca Ridge, eastern Pacific. Chemical Geology (Isotope Science Section), 101, 63-70.

Desborough G. A. and Carpenter R. H. (1965) Phase relations of Pyrrhotite. Economic Geology. 60, 1431-1450.

Crow D. E., Valley J. W., and Baker, K. L. (1990) Micro-analysis of sulfur isotope ratios and zonation by laser microprobe. Geochimica et Cosmochimica Acta, 54, 2075-2092.

Czamanske G., Kunilov V. E., Zientek M. L., Cabri L. J., Likhachev A. P., Calk L. C., and Oscarson R. L. (1992) A proton-microprobe study of magmatic sulfide ores from the Noril'sk-Talnakh district, Siberia. Canadian Mineralogist, 30, 249-287.

Cygan G. L. and Candella Philip A. (1995) Preliminary study of gold partitioning among pyrrhotite, pyrite, magnetite and chalcopyrite in gold-saturated chloride solutions at 600 to 700°C, 140 MPa (1400 bars). In: Thompson J. F. H. (ed) Magmas, Fluids, and Ore Deposits. Mineralogical Association of Canada Short Course Series, Vol. 23, pp. 129-137.

Dahlgren S., Bogoch R., Magaritz M., and Michard A. (1993) Hydrothermal dolomite marbles associated with charnockitic magmatism in the Proterozoic Bamble Shear Belt, South Norway. Cont. Mineral. Petrol. 113, 349-409.

Darke and Weill (1975) Partition of Sr, Ba, Ca, Y, Eu2+, Eu3+, and other REE between plagioclase feldspar and magmatic liquid: an experimental study. Geochimica et Cosmochimica Acta. Vol. 39, pp. 689-712.

Darke M. J. (1975) The oxidation state of europium as an indicator of oxygen fugacity. Geochim. et Cosmochim. Acta, 39, 55-64.

Davletov I. K., Shchelkov, E. E., and Solovena V. V. (1974) Results of an experimental study of the form of gold find in intrusive rocks. Chemical Abstracts, V. 80, p. 174.

de Haas G.-J. L. M. (1992) Source, evolution, and age of coronitic gabbros from the Arendal-Nelaug area, Bamble, southeast Norway. Geologica Ultraiectina. Mededelingen van de Faculteit Aardwetenschappen der Rijksuniversiteit te Utrecht, No 85, 129 p.

de Haas G.-J. L. M., Verschure R. H., and Maijer C. (1993) Isotopic constraints on the timing of crustal accretion of the Bamble Sector, Norway, as evidenced by coronitic gabbros. Precambrian Research, 64, 403-417.

De Ronde C. E. J., Spooner E. T. C., De Wit M. J., and Bray C. J. (1992) Shear zone-related, Au-quartz Vein deposits in the Barberton Greenstone Belt, south Africa: Field and petrographic characteristics, fluid properties, and light stable isotope geochemistry. Economic Geology, 87, 366-402.

Deer W. A., Howie R. A., and Zussman J. (1992) The Rock-forming Minerals. 2nd edition. Longman, England. 696 p.

Dibb T. E. (1981) The effects of metamorphism, tectonics, and host rocks on the location of sulfide ores in the Kongsberg Series, South Norway. Unpub. Ph.D. thesis, Univ. of London.

Dipple G. M. and Ferry J. M. (1992) Metasomatism and fluid flow in ductile fault zones. Contrib. Mineral. Petrol. 112, 149-164.

Dromgoole E. L. and Pasteris J. D. (1987) Interpretation of the sulfide assemblages in a suite of xenoliths from Kilbourne Hole,, New Mexico. In: Morris E. M. and Pasteris J. D. (eds) Mantle Metasomatism and alkaline magmatism. Geol. Soc. Amer. Spec. Pap. 215, pp. 25-46.

Drummond M. S. and Defant M. J. (1990) A model for Trondhjemite–Tonalite-Dacite Genesis and Crustal Growth via Slab melting: Archean to modern comparisons. Journal of Geophysical research., 95, No. B13, 503-521.

Drury S. A. (1978) REE distributions in a High-grade Archaean Gneiss complex in Scotland: Implications for the Genesis of ancient sialic crust. Precambrian Research, 7, 237-257.

Dupuy C. and Dostal J. (1984) Trace element geochemistry of some continental tholeiites. Earth and Planetary Science Letters, 67, 61-69.

Eckstrand O. R., Grinenko L. N., Krouse H. R., Paktunc A. D., Schwann P. L., and Scoates R. F. J. (1989) Preliminary data on sulfur isotope and Se/S ratios, and the source of sulfur in magmatic sulfides from the Fox River Sill, Molson Dykes and Thompson nickel deposits, northern Manitoba. In: Current research, part C, Geological Survey of Canada, paper 89-1C, pp. 235-242.

Eckstrand O. R. and Hulbert L. J. (1987) Selenium and the source of magmatic nickel and platinum deposits: Geol. Assoc. Canada/Mineral. Assoc. Can., Joint annual meeting, Abstracts with Programs, 12, p. 40.

Eldridge A. S., Compston W., Williams I. S., Walshe J. L., and Both R. A. (1987) In situ microanalysis for $^{34}S/^{32}S$ ratios using the ion microprobe SHRIMP: Intern. Jour. Mass Spectrometry, Ion Processes, 76, 65-83.

Eldridge C. S., Compston W., Willimas I. S., and Walshe J. L. (1989) Sulfur isotope analysis on the SHRIMP ion microprobe. In: New frontiers in stable isotope research: Laser probes and small sample analysis. U.S. Geological Survey, Bulletin 1890, pp. 163-174.

Eldridge C. S., Compston W., Willimas I. S., Both R. A., Walshe J. L., and Ohmoto J. L. (1988) Sulfur isotope variability in sediment-hosted massive sulfide deposits as determined using the ion microprobe SHRIMP: I. An example from the Rammelsberg orebody. Economic Geology, 83, 443-449.

Elliot R. B. (1973) The chemistry of gabbro-amphibolite transition in South Norway. Cont. Mineral. Petrol., 47, 63-76.

Emmons W. H. (1937) Gold deposits of the world. McGraw-Hill, New York, 562 p.

Esson J., Stevens R. H., and Vincent E. V. (1965) Aspects of the geochemistry of arsenic and antimony, exemplified by the Skaergaard intrusion. Mineralogical Magazine, 35, 88-105.

Ewart A. (1982) The mineralogy and petrology of Tertiary-Recent orogenic volcanic rocks: With special reference to the andesitic-basaltic compositional range. In: Thorpe (ed) Andesites. John Wiley and Sons, pp. 25-95.

Falkum T. (1985) Geotectonic evolution of Southern Scandinavia in light of a late Proterozoic plate collision. In: Tobi A. C. and Touret J. L. R. (eds) The deep Proterozoic crust in the North Atlantic Provinces, Nato Advanced Science Institute Series, series C, 158, pp. 309-322.

Falkum T. and Petersen A. (1980) The Sveconorwegian Orogenic Belt, a case of late Proterozoic plate collision. Sonderduck aus der geologischen Rundschau, Band 69, 622-647

Fallick A. E., McConville P., Boyce A. J., Burgess R., and Kelley S. P. (1992) Laser microprobe stable isotope measurements on geological materials: Some experimental considerations (with special reference to $\delta^{34}S$ in sulfides). Chemical Geology (Isotope Science Section), 101, 53-61.

Feng R., Fan J. and Kerrich R. (1993) Noble metal abundances and characteristics of six granitic magma series, Archean Abitibi belt, Pontiac Subprovince: Relationships to metallogeny and overprinting of mesothermal gold deposits. Economic Geology, 88, 1376-1401.

Ferry J. M. (1981) Petrology of graphitic sulfide-rich schists from south-central Maine: An example of desulfidation during prograde regional metamorphism. American Mineralogist, 66, 908-930.

Field D. and R(heim (1979) Rb-Sr total rock isotope studies on Precambrian charnockitic gneisses from south Norway: Evidence for isochron resetting during a low grade metamorphic deformational event. Earth Planet. Sci. Lett., 45, 32-44.

Field D. (1969) The geology of the country around Tvedestrand, South Norway. Unpublished Ph.D. thesis, Univ. of Nottingham.

Field D. and Råheim (1981) Age relationships in the Proterozoic high grade gneiss regions of Southern Norway. Precambrian Research, 14, 261-275.

Field D. and Elliot R. B. (1974) The chemistry of gabbro/amphibolite transitions in South Norway; II. trace elements. Cont. Mineral. Petrol., 47, 63-67

Field D., Drury S. A., and Cooper D. C. (1980) Rare-earth and LIL element fractionation in high-grade charnockitic gneisses, South Norway. Lithos, 13, 281-289.

Field D. and Clough P.W.L. (1976) K/Rb ratios and metasomatism in metabasites from a Precambrian amphibolite-granulite transition zone. J. Geol. Soc. London, 132, 277-288.

Field D., Smalley P. C., Lamb R. C., and Raheim A. (1985) Geochemical evolution of the 1.6 -1.5 Ga old amphibolite-granulite facies terrain, Bamble Sector, Norway: Dispelling the myth of Grenvillian high- grade reworking. In: Tobi A. C. and Touret J. L. R. (eds) The deep Proterozoic crust in the North Atlantic Provinces, Nato Advanced Science Institute Series, Series C, 158, pp. 567-578.

Finn G. C. (1991) Major, trace, and rare earth element geochemistry of the Archean Maggo Gneiss, southern Nain Province, Labrador. Can. J. Earth Sci., 28, 44-57.

Fischer R. and Lutwein F. (1974) Selenium. In: Wedepohl (ed) Handbook of Geochemistry. Springer Verlag; 34A-34-O.

Fleet M. E., Crocket J. H., Liu M. and Stone W. E. (1999) Laboratory partitioning of platinum-group elements (PGE) and gold with application to magmatic sulfide-PGE deposits. Lithos, 47, 127-142.

Fleet M. E., Crocket J. H., Liu M. and Stone W. E. (1996) Partitioning of platinum-group elements (Os, Ir, Ru, Pt, Pd) and gold between sulfide liquid and basalt melt. Geochim. Cosmochim. Acta, 60, 2397-2412.

Floyd P. A. and Winchester J. A. (1975) Magma type and tectonic setting discrimination using immobile elements. Earth and Planetary Science Letters, 27, 211-218.

Floyd P. A. and Winchester J. A. (1983) Element mobility associated with meta-shear zones within the Ben Hope amphibolite suite, Scotland. Chemical Geology, 39, 1-15.

Franchi I. A., Wright I. P., Gibson E. K., and Pillinger C. T. (1986) The laser microprobe: A technique for extracting carbon, nitrogen, and oxygen from solid materials for isotopic measurement: Journal of Geophysical Research Supplement, 16, 514-524.

Franchi I. A., Boyd S. R., Wright I. P., and Pillinger C. T. (1989) Application of lasers in small-sample stable isotopic analysis. In: New frontiers in stable isotope research: Laser probes and small sample analysis. US Geological Survey, Bulletin 1890, pp. 51-59.

Fripp R. E. P. (1976) Stratabound gold deposits in Archean Banded Iron Formation, Rhodesia. Economic Geology, 71, 58-75.

Frodesen S. (1968) Coronas around olivine in a small gabbro intrusion, Bamble area, South Norway. Norsk Geologisk Tidsskrift, 48, 201-206.

Frodesen S. (1973) Trace elements in a Precambrian gabbro intrusion, Hiåsen, Bamble Area, South Norway. Norsk Geologisk Tidsskrift, 53, 1-10.

Frost B. R. (1988) A review of graphite-sulfide-oxide-silicate equilibria in metamorphic rocks. Rendiconti Della Societta Italiana Di Mineralogia E Petrologia, 43, 25-40.

Frost R. B., Frost C. D. and Touret J. L. R. (1989) Magmas as a source of heat and fluids in granulite metamorphism. In: Bridgwater (ed) Fluid movements - element transport and the composition of the deep crust. Kluwer Acad. Publ., Holland, pp. 1-18.

Fyfe W. S (1973) The granulite facies, partial melting and Archean crust. Phil. Trans. R. Soc. Lond. A. 273, 457-461.

Fyon A., McDonald A. J., Marmont S., and Troop G. (1988) Shield wide introduction of gold into Archean crust: Coupling between mantle initiated magmatism and lower crustal maturation. Bicentennial Gold 88, Melbourne, pp. 313-318.

Gaal G. and Gorbatschev R. (1987) An outline of the Precambrian evolution of the Baltic Shield. Precambrian Research, 35, 15-52.

Gammon J. B. (1966) Fahlbands in the Precambrian of southern Norway. Economic Geology, 61, 174-188.

Garuti G., Fiandri P. and Rossi A. (1986) Sulfide composition and phase relations in the Fe-Ni-Cu ore deposits of the Ivrea-Verbano basic complex (Western Alps, Italy) Mineral. Deposita. 22, 22-34.

Garuti G., Gorgani C., and Sighinolfi G. P. (1984) Sulfide mineralogy and chalcophile and siderophile element abundances in the Ivera-Verbano mantle peridotites (Western Italian Alps) Earth and Planetary Science Letters, 70, 69-87.

Gavrilenko B. V., Belolipetski A. P., Blotov v. I., and Vorobets A. A. (1974) Geochemistry of gold in the metamorphic complex of Kolmozero-Voronye (Kola Peninsula). Geokhim, V. 1974, No. 1, 132-138,

Gebre-Maryam M., Groves D. I., McNaughton N. J., Mikucki E. J., and Vearncombe J R. (1993) Archean Au-Ag mineralization at Racetrack, near Kalgoorlie, Western Australia: A high crustal-level expression of the Archean composite lode-gold system. Mineralium Deposita, 28, 375-387.

Gehrisch W. and Maucher A. (1975) Sulfur isotope and trace element analysis from Sulitjelma ore bodies, Northern Norway. Mineral. Deposita, 10, 57-69.

Ghaderi M., Michael P. J., Campbell I. H. and Sylvester P. J. (1999) Rare earth element systematics in scheelite from hydrothermal gold deposits in the Kalgoorlie-Norseman region, Western Australia. Economic Geology, 94, 423-438.

Gibson H. L., Watkinson, D. H., and Comba C. D. A. (1983) Hydrothermal alteration in an Archean geothermal system within the Amulet Rhyolite Formation, Noranda, Quebec. Economic Geology, 78, 954-971.

Gitlin E. (1985) Sulfide remobilization during low temperature alteration of seafloor basalt. Geochimica et Cosmochimica Acta. 49, 1567-1579.

Glassley W. E. (1983) The role of CO2 in the chemical modification of deep continental crust. Geochimica et Cosmochimica Acta. 47, 597-616.

Glasson M. J. and Keays R. R. (1978) Gold mobilization during cleavage development in sedimentary rocks from the auriferous slate belt of Central Victoria, Australia: Some important boundary conditions. Economic Geology, 73, 496-511.

Glikson A. Y. (1979) Early Precambrian tonalite-trondhjemite sialic nuclei. Earth Science Reviews, 15, 1-73.

Goldfarb R. J., Newberry R. J. Pickthorn W., and Gent C. A. (1991) Oxygen, hydrogen, and sulfur isotope studies in the Juneau Gold Belt, Southeastern Alaska: Constraints on the origin of the hydrothermal fluids. Economic Geology, 86, 66-80.

Goldfarb R. J., Phillips G. N. and Nokleberg W. J. (1998) Tectonic setting of synorogenic gold deposits of the Pacific Rim. Ore Geology Reviews. 13, 185-218.

Goodwin A. M. Monster J., and Thode H. G. (1976) Carbon and sulfur isotope abundances in Archean Iron Formations and early Precambrian life. Economic Geology, 870-891.

Gottfried D. and Greenland L. P. (1972) Variation of Iridium and gold in Oceanic and Continental basalts. Proc. 24 th Inter. Geol. Congr. 10, pp. 135-144.

Gottfried D., Rowe J, J., and Tilling R. I. (1972) Distribution of gold in igneous rocks. Geological Survey of America, Professional Paper, 727.

Gower C. F., Rivers T., and Ryan B. (1990) Mid-Proterozoic evolution of Laurentia-Baltica: an overview of its geological evolution and a summary of the contributions made by this volume. In: Gower C. F., Rivers T., and Ryan B. (eds) Mid-Proterozoic Laurentia-Baltica. Geological Association of Canada, Special Paper 38, 1-20.

Grabezhev A. I., Levitan G. M., Chashchukhina V. A., Neykur T. A. and Yershova N. A. (1986) Gold in orogenic granitoids of the Ural eugeosyncline. International Geology Reviews, pp. 449-460.

Grant J. A. (1986) The isocon diagram – a simple solution to Gresens' equation for metasomatic alteration. Economic Geology, 81, 1976-1982.

Graterol M. and Naldrett A. J. (1971) Mineralogy of the Marbridge No. 3 and No. 4 Nickel-Iron Sulfide deposits. Economic Geology, 66, 886-900.

Grauch R. I. (1989) Rare earth elements in metamorphic rocks. In: Lipin B. R. and McKay G. A. (eds) - Geochemistry and mineralogy of rare earth elements. Reviews in Mineralogy, 21, pp. 147-167.

Green A. H. and Naldrett A. J. (1981) The Langmuir volcanic peridotite-associated nickel deposits: Canadian equivalents of Western Australian occurrences. Economic Geology, 76, 1503-1523.

Green G. R., Solomon M., and Walshe J. L. (1981) The formation of the volcanic-hosted massive sulfide ore deposit at Rosebery, Tasmania. Economic Geology, 76, 304-338.

Greenland L. P., Gottfried D., and Campbell E. Y. (1973) Aspects of the magmatic geochemistry of bismuth. Geochim. et Cosmochim. Acta, 37, 283-295.

Gresens R. L. (1967) Composition–volume relationships of metasomatism. Chemical Geology, 2, 47-65.

Griffin W. L., Amli R., Heier K. S. (1972) Whitlockite and apatite from lunar rock 14310 and from Ödegården, Norway. Earth Planet. Sci. Letters, 15, 53-58.

Grinenko V. A. and Grinenko L. N (1975) Behavior of sulfur isotopes in the process of metamorphism. In: Tugarinov (ed) Recent contributions to geochemistry and analytical chemistry. John Wiley, New York, pp. 415-423.

Grinenko V. A. and Grinenko L. N. (1967) Fractionation of sulfur isotopes in high temperature decomposition of sulfides by water vapor. Geochemistry International, 4, 843-845.

Gromet P. L., Dymek R. F., Haskin L. A., and Korotev R. L. (1984) The North American shale composite. Its compilation, major and trace element characteristics. Geochimica et Cosmochimica Acta, 48, 2469-2482.

Grootenboer J. and Schwarcz H. P. (1969) Experimentally determined sulfur isotope fractionations between sulfide minerals. Earth and Planetary Science Letters, 7, 162-166.

Grootenboer J. and Schwarcs H. P. (1969) Experimentally determined sulfur isotope fractionation between sulfide minerals. Earth and Planetary Science Letters, 7, 162-166.

Grootenboer J. and Schwarcz H. P. (1969) Experimentally determined sulfur isotope fractionations between sulfide minerals. Earth and Planetary Science Letters, 7, 162-166.

Groves D. I. (1993) The crustal continuum model for late Archean lode gold deposits of the Yilgarn Block, Western Australia. Mineralium Deposita, 28, 366-374.

Groves D. I. and Hudson D. R. (1981) The nature and origin of Archean stratabound volcanic-associated Fe-Ni-Cu sulfide deposits. In: Wolf K. H. (ed) Handbook of strata-bound and stratiform ore deposits. pp. 305-403.

Groves D. I. and Phillips G. N. (1987) The genesis and tectonic control on Archaean gold deposits of the Western Australian Shield; a metamorphic replacement model. Ore Geology Reviews, 2, 287-322.

Groves D. I., Barrett F. M. and McQueen K. G. (1979) The relative roles of magmatic segregation, volcanic exhalation and regional metamorphism in the generation of volcanic-associated Nickel ores of Western Australia. Canadian Mineralogist, 17, 319-336.

Groves D. I., Goldfarb R. J., Gebre-Mariam M., Hagemann S. G. and Robert F. (1998) Orogenic gold deposits: A proposed classification in the context of their crustal distribution and relationship to other gold deposit types. Ore Geology Reviews, 13, 7-27.

Groves D. I., Ridley J. R., Bloem E. M. J., Gebre-Mariam M., Hagemann S. G., Hronsky J. M. A.., Knight J. T., McNaughton N. J., Ojala J., Vielreicher R. M., McCuaig T. C., and Holyland P. W. (1995) Lode-gold deposits of the Yilgarn Block: products of late Archaean crustal-scale overpressured hydrothermal systems. Geological Society, Special Publication, 95, 155-172.

Groves D. I., Barley M. E., Barnicoat A. C., et al. (1992) Sub-greenschist to granulite-hosted Archean lode-gold deposits of the Yilgarn Craton: A depositional continuum from deep sourced hydrothermal fluids in crustal-scale plumbing systems. Geology Department (Key Center) and University Extension, Univ. of W. Australia Publ. 22, pp. 325-337.

Hagemann S. G., Gebre-mariam M., and Groves D. I. (1994) Surface water influx in shallow level Archean lode gold deposits in Western Australia. Geology, 22, 1067-1070.

Haggerty S. E. (1991) Oxide Textures (A Mini-Atlas. In: Lindsley D. H. (ed) Oxide minerals: Petrologic and Magnetic Significance. Review in Mineralogy, 25, pp. 129-213.

Hajash A. Jr. (1984) Rare earth element abundances and distribution patterns in hydrothermally altered basalts. Experimental results. Contrib. Mineral. Petrol., 85, 409-412.

Hall A. J. (1986) Pyrite-Pyrrhotine redox reactions in nature. Mineralogical Magazine, 50, 223-9.

Hamlyn P. R., Keays R. R., Cameron W. E., Crawford A. J. and Waldron H. M. (1985) Precious metals in magnesian Low-Ti Lavas: Implications for metallogenesis and sulfur saturation in primary magmas. Geochimica et Cosmochimica Acta, 49, 1797-1811.

Hanson G. N (1978) The application of trace elements in the petrogenesis of igneous rocks of granitic composition. Earth Planet. Sci. Lett., 38, 26-43.

Hansen E. C. and Newton R. C. (1984) Fluid inclusions in rocks from the amphibolite-facies gneiss to charnockite progression in southern Karanata, India: Direct evidence concerning the fluids of granulite metamorphism. J. Metamorphic Geology, 2, 249-264.

Harlov D. E. (1992) Comparative oxygen barometry in granulites, Bamble Sector, S.E. Norway. Journal of Geology, 100, 447-464.

Harlov D. E., Newton R. C., Hansen E. C. and Janardhan A. S. (1997) Oxide and sulfide minerals in highly oxidized, Rb-depleted, Archaean granulites of the Shevaroy Hills Massif, South India: Oxidation states and role of metamorphic fluids. Metamorphic Geology, 707-717.

Harris D. G., and Nickel E. H. (1972) Pentlandite compositions and associations in some mineral deposits. Canadian Mineralogist, 11, 861-878.

Harris D. C., Cabri L. J., and Nobiling R. (1984) Silver-bearing chalcopyrite, a principal source of silver in the Izok Lale massive sulfide deposit: confirmation by electron- and proton-microprobe analysis. Canadian Mineralogist, 22, 493-498.

Hattori K. (1987) Magnetic felsic intrusions associated with Canadian Archean gold deposits. Geology, 15, 1107-1111.

Hattori K. (1993) Diverse metal sources of Archean gold deposits: Evidence from in situ lead-isotope analysis of individual grains of galena and altaite in the Ross and Kirkland Lake deposits, Abitibi Greenstone Belt, Canada. Contribution to Mineralogy and Petrology, 113, 185-195.

Haughton D. R., Roeder P. L. and Skinner B. J. (1974) Solubility of sulfur in mafic magmas. Economic Geology. Vol. 69. No 4. 451-467.

Hawley J. E. and Nichol I. (1959) Selenium in some Canadian sulfides. Economic Geology, 54, 608-628.

Hawley J. E. and Nichol I. (1961) Trace elements in pyrite, pyrrhotite and chalcopyrite of different ores. Economic Geology, 56, 467-487.

Hayashi K. I., Fujisawa H., Holland H. D., and Ohmoto H. (1997) Geochemistry of ~1.9 Ga sedimentary rocks from northern Labrador, Canada. Geochim. Cosmoch. Acta, 61, 4115-4137.

Heier K. S. (1973) Geochemistry of the granulite facies rocks and problems of their origins. Philosophical Transactions of the Royal Society of London, 273, 429-442.

Henley R. W. (1973) Solubility of gold in hydrothermal chloride solutions. Chemical Geology, 11, 73-87.

Hermes O. d. and Zartman R. E. (1985) Late Proterozoic and Devonian plutonic terrains within the Avalone Zone of the Rhode Island. Geol. Soc. Am. Bull. 96, 272-282.

Hertogen J., Janssens M.-J., and Palme H. (1980) Trace elements in ocean ridge basalt glasses: Implications for fractionation during mantle evolution and petrogenesis. Geochimica et Cosmochimica Acta. 44, 2125-2143.

Hill T. P., Werner M. A., and Horton M. J. (1967) Chemical composition of sedimentary rocks in Colorado, Kansas, Montana, Nebraska, North Dakota, South Dakota, and Wyoming. U.S. Geol. Sur. Prof. Paper 561.

Hodgson C. H., Hamilton J. V., and Hanes J. A. (1989) The late emplacement of gold in the Archean Abitibi greenstone belt: a consequence of thermal equilibration following collisional orogeny. Geol. Assoc. Canada; Mineral. Assoc. Can. Progr. Abstr., 14: A45.

Hoefs J. (1987) Stable isotope geochemistry. Springer, Berlin, 241 p.

Hoefs J. and Touret J. (1975) Fluid inclusion and Carbon isotope study from Bamble granulites (South Norway). Contrib. Mineral. Petrol., 52, 165-174.

Hoffman E. L., Naldrett a. J. Alcock R. A. and Hancock R. G. V. (1979) The noble metal content of ore in the Levac West and little Stobie Mines, Ontario. Canadian Mineralogist, 17, 437-451.

Holland J. G. and Lambert R. J. (1975) The chemistry and origin of the Lewisian gneisses of the Scottish Mainland: The Scourie and Inver assemblages and sub-crustal accretion. Precambrian Research, 2, 161-188.

Hopwood T. (1981) The significance of pyritic black shales in the genesis of Archean Nickel sulfide deposits. In: Wolf K. H. (ed) Handbook of stratabound and stratiform ore deposits, pp. 411-467.

Howard J. H. (1977) Geochemistry of Selenium: formation of ferroselite and selenium behavior in the vicinity of oxidized sulfide and uranium deposits. Geochim. Cosmoch. Acta, 41, 1665-1678.

Hulsebosch T. P. and Frost B. R. (1989) Mineral changes, element mobility, and fluids associated with deep shearing in the Mount Helen Structural Belt, Wyoming, USA. In: Bridgwater (ed) Fluid movements – Element transport and the composition of the deep crust, Kluver Academic Publishers, pp. 139-150.

Huston D. L., Sie S. H., Suter G. F. and Ryan C. G. (1993) The Composition of pyrite in volcanogenic massive sulfide deposits as determined with the proton microprobe. Nuclear Instruments and Methods in Physics Research B75, 531-534.

Hutchinson R. W. and Burlington J. L. (1984) Some broad characteristics of greenstone belt lode gold. In: Foster R. P. (ed) Gold' 82, Rotterdam, Balkema Publ. pp. 339-372.

Ishihara S., Kimura K., Takahashi H., Saito Y., and Hirao Y. (1986) Gold abundance of Japanese plutonic rocks: A preliminary result. Mining Geology, 36 (6), 407-410.

Ishihara S. (1989) Sulfur isotope composition of the magnetite-series and ilmenite-series granitoids of the Sierra Nevada batholith – a reconnaissance study. Geology, 17, 788-791.

Jackson N. J., Walsh J. N. and Pegram E. (1984) Geology , geochemistry and petrogenesis of late Precambrian granitoids in the Central Hijaz Region of the Arabian Shield. Contrib. Mineral. Petrol., 87, 205-219.

Jackson S. B. and Heier K. S. (1978) Rb-Sr isotope systematics in metamorphic rocks. Kongsberg Sector, south Norway. Lithos, 11, 257-276.

Jagoutz E., Palme H., Buddenhausen H. et al. (1979) The abundance of major, minor, and trace elements in the earth's mantle as derived from primitive ultramafic nodules. Proc. Lunar Planet. Sci. Conf. 10th, 2031-2050.

Jahn B-m. and Zhang Z-q. (1984) Archean granulite gneisses from eastern Hebei Province, China: Rare earth geochemistry and tectonic implications. Contrib. Mineral. Petrol., 85, 224-243.

Janardhan A. S., Newton R. C., Hansen E. C. (1982) The transformation of amphibolite facies gneiss to charnockite in Southern Karanatka and Northern Tamil Nadu, India. Contr. Mineral. Petrol., 79, 130-149.

Javoy M., Pineau F., and Delorme H. (1986) Carbon and nitrogen isotopes in the mantle. Chemical Geology, 57, 41-62.

Jensen L. S. (1976) A new cation plot for classifying subalkalic volcanic rocks. Ontario Division of Mines; Ministry of Natural Resources; Miscellaneous Paper 66. 22 p.

Jensen M. L. (1969) Sulfur isotopes of the Narine pyrite deposit, South Australia. Mineral. Deposita, 4, 241-247.

Joesten R. (1986) The role of magmatic reaction, diffusion and annealing in the evolution of coronitic microstructure in troctolitic gabbro from Risör, Norway. Mineralogical Magazine, 50, 441-467.

Jonasson I. R., Eckstrand O. R., and Watkinson D. H. (1987) Preliminary investigation of the abundance of platinum, palladium and gold in some samples of Canadian copper-nickel ores. In: Current Research, Part A, Geological Survey of Canada, Paper 87-1A, pp. 835-846.

Jones L. M., Taylor A. R., Winter D. L., Hurst S. D., and Keen G. W. (2986) The use of laser microprobe for sample preparation in stable isotope mass spectrometry. Terra Gonita, 6, 263.

Kajiwara K. and Krouse H. R. (1971) Sulfur isotope partitioning in metallic sulfide systems. Canadian Journal of Earth Sciences, 8, 1397-1408.

Kajiwara Y., Krouse H. R., and Sasaki A. (1969) Experimental study of sulfur isotope fractionation between coexistent sulfide minerals. Earth and Planetary Science Letters, 7, 271-277.

Kajiwara Y., Sasaki A., and Matsubaya O. (1981) Kinetic sulfur isotope effects in the thermal decomposition of pyrite. Geochemical Journal, 15, 193-197.

Karelin V. V., Maksimov Y. P., Nikitin V. N., and Uyutov V. I. (1974) Gold in the Mesozoic igneous rocks in the eastern part of the Aldan Shield. Geochemistry International, xxxxx, 399-405.

Kay R. W. (1980) Volcanic arc magmas: Implications of a mantle-mixing model for element recycling in the crust-upper mantle system. Journal of Geology, 88, 497-522.

Kay R. W. (1984) Elemental abundances relevant to identification of magma sources. Phil. Trans. R. Soc. London. A 310, 535-547.

Keays R. R. and Davison R. M. (1976) Palladium, iridium, and gold in the ores and host rocks of nickel sulfide deposits in Western Australia. Economic Geology, 71, 1214-1228.

Keays R. R. and Scott R. B. (1976) Precious metals in Ocean-Ridge basalts: Implications for basalts as source rocks for gold mineralization. Economic Geology. Vol. 77. No. 4. 705-718.

Keays R. R., and Campbell I. H. (1981) Precious metals in the Jimberlana intrusion, Western Australia: Implications for the genesis of platiniferous ores in layered intrusions. Economic Geology, 76, 1118-1141.

Keays R. R., Ross J. R., and Wooldrich P. (1981) Precious metals in volcanic peridotite-associated nickel sulfide deposits in Western Australia. II. Distribution within the ores and host rocks at Kambalda. Econ. Geol. 76, xxxxxxx

Keays R. R., and Crocket H. C. (1970) A study of precious metals in the Sudbury Nickel Irruptive Ores. Economic Geology, 65, 438-450.

Kelley S. P. and Fallick A. E. (1990) High precision spatially resolved analysis of $\delta^{34}S$ in sulfides using a laser extraction technique. Geochimica et Cosmochimica Acta, 54, 883-888.

Kerr A., Dickson W. L., Hayes J. P. and Fryer B. J. (1993) Devonian post-orogenic granites on the Southeastern Margin of the Newfoundland Appalachians: A review of geology, geochemistry, petrogenesis and mineral potential. In: Current Research, Newfoundland Department of Mines and Energy. Geological Survey Branch, Report 93-1, pp. 239-278.

Kerrich R. (1983) Geochemistry of gold deposits in the Abitibi greenstone belt. CIM Special Volume 27, pp. 48-71.

Kerrich R. (1984) Geochemistry of gold in the Abitibi Greenstone Belt. The Canadian Institute of Mining and Metallurgy, Special Volume 27. pp. 1-75

Kerrich R. (1988) Source processes for Archean Au-Ag vein deposits: Evidence from lithophile-element systematics of the Hollinger-McIntyre and Buffalo ankerite deposits, Timmins. Ca. J. of Earth Sci. 26, 755-781.

Kerrich R. (1989a) Source processes for Archean Au-Ag vein deposits: evidence from lithophile-element systematics of the Hollinger-McIntyre and Buffalo Ankerite Deposits, Timmins. Canadian Journal of Earth Sciences, 26, 755-781.

Kerrich R. (1989b) Geochemical evidence on the sources of fluids and solutes for shear zone hosted mesothermal Au deposits. In: Bursnall (ed) Mineralization and Shear Zones. Geological Association of Canada Short Course Notes, pp. 129-197.

Kerrich R. (1990) Carbon-isotope systematics of Archean Au-Ag vein deposits in the superior province. Can. J. Earth Sci. 27, 40-56.

Kerrich R. (1990) Mesothermal gold deposits. A critique of genetic hypothesis. In: Robert F., Sheahan P. A., and Green S. B. (eds) Greenstone gold and crustal evolution; Nuna Conference Volume. GAC-MAC, pp. 13-31.

Kerrich R. (1993) Perspectives on genetic models for lode gold deposits. Mineralium Deposita, 28, 362-365.

Kerrich R. and Wyman (1990) The geodynamic setting of the mesothermal gold deposits: An association with the accretionary tectonic regimes. Geology, 18, 882-885.

Kerrich R., La Tour T. E. and Willmore L. (1984) Fluid participation in deep fault zones: evidence from geological, geochemical, and 18O/16O relations. J. of Geoph. Res., Vol. 89, No. B6, 4331-4343.

Kerrich R. and Cassidy K. F. (1994) Temporal relationships of lode gold mineralization to accretion, magmatism, metamorphism and deformation (Archean to present): A review. Ore Geology Reviews, 9, 263-310.

Kerrich R. and Fryer B. J. (1979) Archean Precious metal hydrothermal systems, Dome Mine, Abitibi greenstone belt. II: REE and oxygen isotope relations. Can. J. Earth Sci., 16, 1653-1660.

Kerrich R. Fyfe W. S. (1981) The gold-carbonate association: Source of CO2 fixation reactions in Archean lode deposits. Chemical Geology, 33, 265-294.

Kerrich R., Allison I., Barnett R. L., Moss S., and Starkey J. (1980) Microstructural and chemical transformation accompanying deformation of granite in a shear zone at Mieville, Switzerland; with implications for stress corrosion cracking and superplastic flow. Contrib. Mineral. Petrol., 73, 221-242.

Kihle J. and Bucher-Norminen K. (1992) Orthopyroxene-sillimanite-sapphirine granulites from the Bamble granulite terrain, Southern Norway. J. Metam. Geol., 10, 671-683.

King R. W., Kerrich R. (1988) Fluorapatite fenitization and gold enrichment in sheeted trondhjemites within the Destor-Porcupine fault zone, Taylor Township, Ontario. Can. J. Earth Sci, 24, 479-502.

King R. W., Kerrich R., and Daddar R. (1988) REE distributions in tourmaline: An INAA technique involving pretreatment by devolatilization. American Mineralogist, 73, 424-431.

Kissin S. A. and Scott S. D. (1982) Phase relations involving pyrrhotite below 350° C. Economic Geology, 77, 1739-1754.

Klöck W. and Palme H. (1988) Partitioning of siderophile and chalcophile elements between olivine, sulfide and glass in a naturally reduced basalt from Disco Island, Greenland. Proc. Lunar Planet. Sci. Conf. 18th, 471, 483.

Klein E. M. and Langmuir C. H. (1987) Global correlations of ocean ridge basalt chemistry with axial depth and crustal thickness. J. Geophys. Res. 92 (B8) 8089-8115.

Kline S. W. (1984) Metamorphic mineral chemistry, Petrology, and sulfide mineralogy of the Dore Lake Complex, Chibugamau, Quebec. Unpublished Ph.D. thesis, Georgia State Univ.

Kontak D. J. and Jackson S. J. (1999) Documentation of variable trace- and rare earth element abundances in carbonates from auriferous quartz veins in Meguma lode-gold deposits, Nova Scotia. Canadian Mineralogist, 37, 469-488.

Kretz R. (1994) Metamorphic crystallization. John Wiley and Sons, 507 p.

Knudsen T. L. and Andersen T. (1999) Petrology and geochemistry of the Tromoy gneiss complex, South Norway, an alleged example of Proterozoic depleted lower continental crust. Journal of Petrology. Vol. 40, No 6. 909-933.

Knudsen T. L. (1996) Petrology and geothermobarometry of granulite facies metapelites from the Hisoy-Torungen area, South Norway: new data on the Sveconorwegian P-T-t path of the Bamble Sector. J. Metam. Geol., 14, 267-287.

Knudsen T. L., Andersen T., Maijer C. and Verschure R. H. (1997) Trace-element characteristics and Pb isotopic evolution of metasediments and associated Proterozoic rocks from the amphibolite- to granulite-facies Bamble sector, Southern Norway. Chemical Geology, 143, 145-169.

Koons P. O. and Craw D. (1991) Gold Mineralization as a consequence of continental collision: an example from the Southern Alps, New Zealand. Earth and Planetary Science Letters, 103, 1-9.

Korobeynikov A. F. (1986) The gold distribution in differentiation products of basic and acid magmas of various ages. Geochemistry International, xxx, 101-109.

Korobeynikov A. F. (1989) Behavior of gold in magmatic and metasomatic processes. International Geology Review, xxxx, 171-179.

Korobeynikov A. F. (1990) Background gold content of the ore field in the carboniferous blackschist series of Northeastern Kazakhstan. Geologiya Geofizika, 31, 58-65.

Korobeynikov A. F. (1991) The behavior of gold during the metamorphism of sedimentary-volcanogenic rocks. Geochemistry International, xxxxxx, 31-40.

Korobeynikov A. F. and Pertsev N. N (1995) Gold and palladium in basaltoids of the Costa Rica Rift Zone (Pacific Ocean) and gold levels in Cenozoic basalts. Geochemistry International, 32, 68, 79.

Korobeynikov A. F. (1995) Comparison of gold levels in black shales from crustal structures of various ages. Geochemistry International, 32 (9), 19-37.

Kosterine A. V. (1959) The possible modes of transport of the rare earths by hydrothermal solutions. Geochemistry, 381-387.

Krauskoph K. B. (1979) Introduction to Geochemistry. McGraw Hill, 617 p.

Kretz R. (1983) Symbols for rock-forming minerals. American Mineralogist, 68, 277-279.

Kullerud G. (1967) Sulfide Studies. In: Researches in Geochemistry, 2, New York, John Wiley and Sons.

Kullerud G. and Yoder H. S. (1959) Pyrite stability relations in the Fe-S system. Economic Geology, 54, 534-572.

Kullerud G., Yund R. A., and Moh G. (1969) Phase relations in the Fe-Ni-S, Cu-Fe-S, and Cu-Ni-S systems. Economic Geology, Monograph 4, pp. 323-343.

Kullerud L. and Machado N. (1991) End of a controversy: U-Pb geochronological evidence for significant Grenvillian activity in the Bamble area, Norway. Terra Abstr., 3, 504

Kupčick V., Ahrens L. H., Erlank A. J. and Wedepohl K. H. (1974) Bismuth. In: Wedepohl K. H. (ed) Handbook of Geochemistry. Springer Verlag.

Kwong Y. T. J. and Crocket J. H. (1978) Background and anomalous gold in rocks of an Archean greenstone assemblage, Kagaki Lake area, northwestern Ontario. Economic Geology, 73, 50-63.

Kyser K. T. (1990) Stable isotope in the continental lithospheric mantle. In: Menzies M. (ed) Continental Mantle. Oxford Scientific Publications. pp. 127-156.

Kyser T. K. (1986) Stable isotope variations in the mantle. In: Valley J. W., Taylor H. P., and O'Neil J. R. (eds) Stable isotopes in high temperature geological processes. Reviews in Mineralogy, Vol. 16, 141-166.

Lagedza V. Y. (1969) Mode of concentration of finely divided gold in sedimentary rocks. Doklady Akad. Nauk SSSR, 185, 162-164.

Lamb R. C., Smalley P. C. and Field D. (1986) P-T conditions for the Arendal granulites, Southern Norway: Implications for the role of P, T, CO_2 in the deep crustal LILE-depletion. J. Metam. Geol., 4, 143-160.

Lamb W. M., and Valley J. W. (1985) C-O-H fluid calculation and granulite genesis. In: Tobi A. C. and Touret J. L. R. (eds) The deep Proterozoic crust in the North Atlantic Provinces. Nato Advanced Science Institute Series, series C, 158, pp. 119-131.

Lamb W. M., Valley J. W., and Brown P. E. (1987) Post-metamorphic CO_2-rich fluid inclusions in granulites. Contrib. Mineral. Petrol. 96, 485-495.

Lambert R. St. J. and Holland J. G (1975) Amitsoq gneiss geochemistry: Preliminary observations. In: Windley B. F. (ed) The early history of the earth. pp. 191-201. John Wiley and Sons.

Legedza V. Y. (1968) Mode of concentration of finely divided gold in sedimentary rocks. Doklady Akad. Nauk, USSR. 185, 162-164.

Lesher C. M., Arndt N. T., and Groves D. I. (1984) Genesis of komatiite-associated nickel sulfide deposits at Kambalda, Western Australia; A distal volcanic model. In: Buchanan D. L. and Jones M. J. (eds) Sulfide deposits in mafic and ultramafic rocks. London: Insti. of Min. and Metall. pp. 70-80.

Li L. V. and Shokhina O. I. (1974) Behavior of gold in progressive regional metamorphism of Precambrian rocks of the Yenisey Range. Geochemistry International, xxxx, 314-320.

Lieftink D. J.., Nijland T. G., and Maijer F. C. (1993) Cl-rich scapolite from (degardens Verk, Bamble, Norway. Norsk Geologisk Tidsskrift, 73, 55-57.

Lindsley D. H. (1991) Experimental studies of oxide minerals. In: Lindsley D. H. (ed) Oxide Minerals: Petrologic and magnetic significance. Review in Mineralogy, 25, 69-106.

Loiselle M. C. and Wones D. R. (1979) Characteristics and origin of anorogenic granites. Geol. Soc. Am., Abst. Prog. 11, 468.

Lopez-Escobar L. Frey F. A. and Oyarzun J. (1979) Geochemical characteristics of Central Chile (33o-34o) granitoids. Contrib. Mineral. Petrol., 70, 439-450.

Lopez-Escobar L., Frey F. A., and Vergara M. (1977) Andesites and High-Alumina basalts from the Central-South Chile High Andes: geochemical evidence bearing on their petrogenesis. Contrib. Mineral. Petrol., 63, 199-228.

Lusk J. and Crocket J. H. (1969) Sulfur isotope fractionation in coexisting sulfides from the Heath Steel B-1 Orebody, New Brunswick, Canada. Economic Geology, 64, 147-155.

MacKeag S. A. and Craw D. (1989) Contrasting fluids in gold-bearing quartz vein systems formed progressively in a rising metamorphic belt: Otago Schist, New Zealand. Economic Geology, 84, 22-33.

MacLean W. H. and Shimazaki H. (1976) The Partition of Co, Ni, Cu, and Zn between Sulfide and Silicate Liquids. Economic Geology. 71, 1049-1057.

MacLean W. H. and Shimazaki H. (1976) The partitioning of Co, Ni, Cu, and Zn between sulfide and silicate liquids. Economic Geology, 71, 1049-1057.

Mainwaring P. R. and Naldrett A. J. (1977) Country-rock assimilation and the genesis of Cu-Ni sulfides in the Waterhen Intrusion, Duluth Complex, Minnesota. Economic Geology, 72, 1269-1284.

Mallio W. J. and Gheith M. A. (1972) Textural and chemical evidence bearing on sulfide-silicate reactions in metasediments. Mineral. Deposita, 7, 13-17.

Maniar P. D. and Piccoli P. M. (1989) Tectonic discrimination of granitoids. Geological Society of America Bulletin, 10, 635-643.

Marowsky G. and Wedepohl K. H. (1971) General trends in the behavior of Cd, Hg, Tl, and Bi in some major rock forming minerals. Geochim. et Cosmochim Acta, 35, 1255-1267.

Martignole J. (1979) Charnockite Genesis and the Proterozoic Crust (1979) Metam. Geol., 8, pp. 231-246.

Martin H. (1987) Petrogenesis of Archean trondhjemites, tonalites, and granodiorites from Eastern Finland: Major and trace element geochemistry. Journal of Petrology, 28, 921-953.

Martin R. F., Whitley J. E. and Woolley A. R. (1978) An Investigation of rare-earth mobility: Fenitized quartzites, Borralan complex, N.W. Scotland. Contrib. Mineral. Petrol. 66, 69-73.

Mason R. and Melnik N. (1986) The anatomy of an Archean gold system: The McIntyre-Hollinger Complex at Timmins, Ontario, Canada. In: Macdonald A. J. (ed) Gold' 86, pp. 40-55.

Mathez E. A. and Peach C. L. (1989) The Geochemistry of the Platinum-group elements in mafic and ultramafic rocks. In: Whitney J. and Naldrett A. J. (eds) Ores associated with mafic magmas. Review in Economic Geology, 4, pp. 33-43.

Mathez E. A. (1976) Sulfur solubility and magmatic sulfides in submarine basalt glass. J. Geophys. Res., 81, 4269-4275.

Matthews A., Fouillac C., Hill R.., O'Nions R. K., and Oxburgh E. R. (1987) Mantle-derived volatiles in continental crust: The Massif Central of France. Earth and Planetary Science Letters, 85, 117-128.

Mauger R. (1972) A sulfur isotope study of the Ducktown, Tennessee District, U. S. A. Economic Geology, 67, 497-510.

McCaig A. M. (1984) Fluid-rock interaction in some shear zones from the Pyrenees. J. Metamorphic Geol. 2, 129-141.

McCuaig T. C., Kerrich R., Groves, D. I., and Archer, N. (1993) The nature and dimensions of regional and local gold-related hydrothermal alteration in tholeiitic metabasalts in the Norsman gold fields: the missing link in a crustal continuum of gold deposits? Mineralium Deposita, 28, 420-435.

McDonough W. F. and Sun S.-s. (1995) The composition of the Earth. Chemical Geology, 120, 223-253.

McKay G. A. (1989) Partitioning of rare earth elements between major silicate minerals and basaltic melts. In: Lipin B. R. and McKay G. A (eds) Geochemistry and mineralogy of rare earth elements. Reviews in mineralogy, Vol. 21, pp. 45-78.

McKibben M. A. and Eldridge A. S. (1989) Sulfur isotopic variations among minerals and aqueous species in the Salton Sea geothermal system: A SHRIMP ion microprobe and conventional study of active ore genesis in a sediment-hosted environment. Am. Jour. Sci., 289, 661-707.

McLennan S. M. Fryer S. M., and Young G. M. (1979) Rare earth elements in Huronian (lower Proterozoic) sedimentary rocks: composition and evolution of post-Kenoran upper crust. Geochimica et Cosmochimica Acta, 43, 375-388.

McLennan S. M., and Taylor S. R., and McGregor V. R. (1984) Geochemistry of Archean metasedimentary rocks from West Greenland. Geochimica et Cosmochimica Acta, 48, 1-13.

McLennan S. M., Nance W. B. and Taylor S. R. (1980) Rare earth element-thorium correlations in sedimentary rocks, and the composition of the continental crust. Geochimica et Cosmochimica Acta, 44, 1833-1839.

McNeil A. M. and Kerrich R. (1986) Archean lamprophyre dykes and gold mineralization, Matheson, Ontario: The conjunction of LILE-enriched mafic magmas, deep crustal structures, and Au concentration. Can. J. Earth Sci., 23, 324-343.

McNaughton N. J., Groves D. I., and Witt W. K. (1993) The Source of lead in Archaean lode gold deposits of the Menzies-Kalgoorlie-Kambalda region, Yilgarn block, Western Australia. Mineral. Deposita, 28, 495-502.

Megrue G. J. (1967) Isotopic analysis of rare gases with a laser microprobe. Science, 157, 1555-1556.

Menzies M. A., Leeman W. R., and Hawkesworth C. J. (1983) Isotope geochemistry of Cenozoic volcanic rocks reveals mantle heterogeneity below western U.S.A. Nature, 303, 205-209.

Meyer M. and Saager R. (1985) The gold content of some Archaean rocks and their possible relationship to epigenetic gold-quartz vein deposits. Mineralium Deposita, 20, 284-289.

Mikucki E. J. (1998) Hydrothermal transport and depositional processes in Archean lode-gold systems: A review. Ore Geology Reviews, 13, 307-321.

Milonni P. W. and Eberly J. H. (1988) Lasers. 731 p. Wiley, New York.

Minnitt R. C. A., Button A., and Kable E. J. D. (1973) The gold content of the Pre-Malmani argillaceous sediments in the Transvaal Supergroup, Northeastern Transvaal. Economic Geology Research Unit, Univ. of Witwatersrand, Johannesburg. Information Circular, 82, 11 pp.

Mironov A. G., and Galetiy V. F. (1979) Experimental study of gold distribution in sulfides. Doklady Akad. Nauk SSSR, 247, 194-187.

Misra K. C. and Fleet M. E. (1973) The chemical compositions of synthetic and natural pentlandite assemblages. Economic Geology, 68, 518-539.

Mitcehll R. H. and Keays R. R.(1981) Abundance and distribution of gold, palladium and iridium in some spinel and garnet lherzolites: Implications for the nature and origin of precious metal rich intergranular components in upper mantle. Geochim. Cosmochim. Acta, 45, 2425-2442.

Mohr D. W. and Newton R. C. (1983) Kyanite-staurolite metamorphism in sulfidic schists of the Anakeesta Formation, Great Smoky Mountains, North Carolina. American Journal of Science, 283, 97-134.

Morgan J. W. (1986) Ultramafic xenoliths: Clues to earth's late accretionary history. Journal of Geophysical Research, Vol. 91, No. B12, pp. 12375-12387.

Morgan J. W., Wandless G. A., Petrie R. K., and Irwing A. J. (1981) Composition of earth upper mantle – I. Siderophile trace elements in ultramafic nodules. Tectonophysics, 75, 47-67.

Morgan J. W. and Baedecker P. A. (1983) Elemental composition of sulfide particles from an ultramafic xenolith and the siderophile element content of the upper mantle. Lunar Planet. Sci. XIV, 513-514.

Morthorst J. R., Zeck H. P., and Lundegardh P. H. (1983) The Proterozoic hyperites in southern V(rmland, western Sweden. Sveriges Geol. Unders, Ba 30, 104 p.

Morton R. D. (1971) Metasediments and meta-pyroclastics within the Precambrian metamorphic suite of the S. Norwegian Skaergaard. Nor. Geolog. Tidsskr. 51, 63-83.

Morton R. D. Batey R. and O'Nions R. K. (1970) Geological investigations in the Bamble Sector of the Fennoscandian South Norway. 1. The Geology of Eastern Bamble. Norges Geologiske Unders(kelse, Nr. 263, pp. 1-72.

Mottle M. J., Holland H. D., and Corr R. F. (1979) Chemical exchange during hydrothermal alteration of basalt by seawater. II. Experimental results for Fe, Mn, and sulfur species. Geochimica et Cosmochimica Acta. 43, 869-884.

Muecke G. K., Pride C., and Sarkar P. (1979) Rare-earth element geochemistry of regional metamorphic rocks. In: Ahrens (ed) Origin and distribution of the elements, pp. 449-464. Pergamon.

Mueller A. G. de Laater J. R., and Groves D. I. (1991) Strontium isotope systematics of hydrothermal minerals from epigenetic Archean gold deposits in the Yilgarn Block, Western Australia. Economic Geology, 86,

Munz I. A., Wayne D., and Austrheim H. (1994) Retrograde fluid infiltration in the high- grade Modum Complex, South Norway: Evidence for age, source, and REE mobility. Contrib. Mineral. Petrol. 116, 32-46.

Munz I. A. (1990) White-schists and orthoamphibolite-cordierite rocks and the P-T-t path of the Modum Complex, South Norway. Lithos, 24, 181-200

Munz I. A. and Morvik R. (1991) Metagabbros in the Modum Complex, southern Norway: an important heat source for Sveconorwegian metamorphism. Precambrian Research, 52, 97-113.

Naldrett A. J. (1989) Magmatic sulfide deposits. Clarendon Press. 177 p.

Naldrett A. J. and Gasparrini E. L. (1971) Archean nickel sulfide deposits in Canada: Their classification, geological setting and genesis with some suggestions as to exploration. Geol. Soc. Australia, Publ. No. 3, pp. 201-226.

Naldrett A. J., Innes D. G., Sowa J., and Gorton M. P. (1982) Composition of variations within and between five Sudbury ore deposits. Economic Geology, 77, 1519-1534.

Naldrett A. J. (1969) A portion of the system Fe-S-O between 900 and 1080 °C and its application to sulfide ore magmas. Journal of Petrology, 10, 171-201.

Naldrett A. J. (1979) Partitioning of Fe, Co, Ni, and Cu between sulfide liquid and basaltic melts and the composition of Ni-Cu sulfide deposits – A reply and further discussion. Economic Geology, 74, 1520-1528.

Naldrett A. J. and Barnes S. J. (1986) The behavior of platinum group elements during fractional crystallization and partial melting with special reference to the composition of magmatic sulfide ores. Fortschritte der Mineralogie, 64, 113-133.

Naldrett A. J. and Duke J. M. (1980) Platinum metals in magmatic sulfide ores. Science, 208, 1417-1424.

Naldrett A. J. (1981) Nickel sulfide deposits: Classification, composition, and genesis. Economic Geology 75th Anniv. Volume, 628-685.

Naldrett A. J. Kullerud G. (1967) A Study of the Strathcona Mine and its bearing on the origin of the Nickel-Copper ores of the Sudbury District , Ontario. Journal of Petrology. Vol. 8. Part 3. 453-531.

Nance W. B. and Taylor S. R. (1976) Rare earth element patterns and crustal evolution - I. Australian post-Archean sedimentary rocks. Geochim. et Cosmoch. Acta. 40, 1539- 1551.

Nekrasov I. Y. (1996) Geochemistry, mineralogy, and genesis of gold deposits. Oxford and IBH Publ. 329 p.

Nesbitt B. E. (1988) Gold deposit continuum: A genetic model for lode Au mineralization in the continental crust. Geology. 16, 1044-1048.

Nesbitt B. E. and Muehlenbachs K. (1988) Mesothermal Au (Ag deposits of the Canadian Cordillera: evidence for meteoric water involvement in the genesis of mesothermal Au deposits. Bicentennial Gold 88, Melbourne, pp. 344-346.

Nesbitt B. E., Murowchick J. B., and Muehlenbachs K. (1986) Dual origin of lode gold deposits in the Canadian Cordillera. Geology, 14, 506-509.

Nesbitt H. W. (1980) Genesis of the New Quebec and Adirondack Granulites: Evidence for their Production by Partial Melting. Contrib. Mineral. Petrol., 72, 303-310.

Neumayr P., Cabri L. J., Groves D. I., and Mikucki E. J. and Jackman J. A. (1993) The mineralogical distribution of gold and relative timing of gold mineralization in two Archean settings of high metamorphic grade in Australia. The Canadian Mineralogist, 31, 711-725.

Neurberg G. J. (1975) A procedure, using hydrofluoride acid, for quantitative mineral separations from silicate rocks. Jour. Research U.S. Geol. Survey, Vol. 3, No. 3, pp. 377-378.

Newton R. C. (1986) Fluids of granulite facies metamorphism. In: Walther J. V. and Wood B. J. (eds) Fluid-rock interaction during metamorphism, Springer, pp. 36-59.

Newton R. C. (1990) Fluids and shear zones in the deep crust. Tectonophysics, 182, 21-37.

Newton R. C., Smith J. V., and Windley B. F. (1980) Carbonic metamorphism, granulites and crustal growth. Nature, 288, 45-50.

Nielsen H. (1979) Sulfur isotopes. In: Jager E. and Hunziker J. C. (eds) Lectures in isotope geology, pp. 283-313, Springer Verlag.

Nijland H. (1989) The geology of the Nelaug area, Bamble Sector, South Norway, Unpubl. M.Sc. thesis, University of Utrecht, 85p.

Nijland T. G. and Maijer C. (1993) The Regional amphibolite to granulite facies transition at Arendal, Norway: evidence for a thermal dome. N. Jb. Miner. Abh., 165, 191-221.

Nijland T. G. and Senior A. (1991) Sveconorwegian granulite facies metamorphism of polyphase migmatites and basic dikes, Southern Norway. Journal of Geology, 99, 515-525

Nijland T. G., Jansen J. Ben H. and Maijer C. (1993) Halogen geochemistry of fluid during amphibolite-granulite metamorphism as indicated by apatite and hydrous silicates in basic rocks from the Bamble Sector, South Norway. Lithos, 30, 167-189

Noll P. D., Newsom H. E., Leeman W. P., and Ryan J. G. (1996) The role of hydrothermal fluids in the production of subduction zone magmas: Evidence from siderophile and chalcophile trace elements and boron. Geochimica et Cosmochimica Acta, 60, 587-611.

Norrey M. J. and Fitton J. G. (1983) Compositional differences between oceanic and continental basic lavas and their significance. In: Hawksworth C. J. and Norrey M. J. (ed) Continental basalts and mantle xenoliths. pp. 5-19. Shiva.

Oftedhal C. (1980) The geology of Norway. Nor. Geol. Unders, 319, 3-114.

O'Neil J. R. (1979) Stable isotope geochemistry of rocks and minerals. In Jäger E. and Hunziker J. C. (eds) Isotope Geology, pp. 235-282.

O'Neil J. R. and Ghent E. D. (1975) Stable isotope study of coexisting metamorphic minerals from the Esplanade Range, British Columbia. Geological Society of American Bulletin, 97, 1708-1712.

O'Nions R K. And Baadsgaard H. (1971) A radiometric study of polymetamorphism in the Bamble Region, Norway. Contr. Mineral. Petrol., 34, 1-21.

O'Nions R. K. and Pankhurst R. J. (1974) Rare Earth element distribution in Archaean Gneisses and Anorthosites, Godthab area, west Greenland. Earth and Planetary Science Letters, 22, 328-338.

O'Nions R. K. and Pankhurst R. J. (1978) Early Archean rocks and geochemical evolution of the earth's crust. Earth and Planetary Science Letters, 38, 211-236.

Ohmoto H. (1972) Systematics of Sulfur and Carbon Isotope in Hydrothermal Ore Deposits. Economic Geology, 67, 551-578.

Ohmoto H. (1986) Stable isotope geochemistry of ore deposits. In: Valley J. W., Taylor H. P., and O'Neil J. R. (eds) Stable isotopes in high temperature geological processes. Reviews in Mineralogy, Vol. 16, 491-559.

Ohmoto H. and Rye R. O. (1979) Isotopes of sulfur and carbon. In: Barnes (ed) Geochemistry of hydrothermal ore deposits, 2 nd edition. John Willey and Sons, pp. 509-567.

Oshin I. O., and Crocket J. H. (1982) Noble metals in Tethford Mines ophiolite, Quebec, Canada. Part I: Distribution of Au, Ir, Pt, and Pd in the ultramafic and gabbroic rocks. Economic Geology, 77, 1556-1570.

Padget P. (1990) Tectonic and lithostratigraphic relationships in the Bamble Sector, south Norway: an interpretative view. In Gower, C. F. Rivers T., and Ryan B. (eds) Mid-Proterozoic Laurentian-Baltica: Geological association of Canada, special paper 38, pp. 307-316.

Paktunc D. A., Hulbert L. J. and Harris D. C. (1990) Partitioning of the Platinum-group and other trace elements in sulfides and Canadian occurrences of Nickel-Copper sulfides. Canadian Mineralogist. 28, 475-488.

Paktunc D. A. (1989) Petrology of the St. Stephen Intrusion and the Genesis of Related Nickel-Copper Sulfide Deposits . Economic Geology, 84, 817-840.

Paktunc A. D. (1990) Comparative geochemistry of platinum-group elements of Ni-Cu sulfide occurrence associated with mafic-ultramafic intrusions in the Appalachian Orogen. Journal. of geochemical exploration, 37, 101-111.

Pan Y. and Fleet M. E. (1995) The late Archean Hemlo gold deposit, Ontario, Canada: a review and synthesis. Ore Geology Reviews, 9, 455-488.

Patchett P. J., Bylund G., and Upton B. J. (1978) Paleomagnetism and the Grenvillian Orogeny: New Rb-Sr ages from dolerites in Canada and Greenland. Earth Planet. Sci. Lett., vol. 40, pp_ 349-364

Peach C. L. and Mathez E. A. (1987) Gold and Iridium in sulfides from submarine basalt glasses. In: Prichard H. M., Potts P. J., Bowls J. F. W., and Cribb S. J. (eds) Geoplatinum 87; Elsevier _Appl. Sci.

Peach C. L., Mathez E. A. and Keays R. R. (1990) Sulfide melt-silicate melt distribution coefficients for noble metals and other chalcophile elements as deduced from MORB: Implications for partial melting. Geochimica et Cosmochimica Acta. 54, 3379-3389.

Pearce J. A. (1982) Trace element characteristics of lavas from destructive plate boundaries. In: Thorpe R. S. (ed) Andesites. pp. 525-548.

Pearce J. A. (1983) Role of the sub-continental lithosphere in magma genesis at active continental margins. In: Hawksworth C. J. and Norrey M. J. (eds) Continental basalts and mantle xenoliths. pp. 230-249; Nantwich, Shiva.

Pearce J. A. and Cann J. R. (1973) Tectonic setting of basic volcanic rocks determined using trace element analysis. Earth Planet. Sci. Lett. 19, 290-300.

Prendergast M. D. and Keays R. R. (1989) Controls of platinum group element mineralization and the origin of PGE-rich Main Sulfide Zone in the Wedza Subchamber of the Great dyke, Zimbabwe: Implications for the genesis of, and exploration for, stratiform PGE mineralization in layered intrusions. In: Prendergast M. D and Jones M. J. (eds) Magmatic sulfides - The Zimbabwe Volume, pp. 43-69, Inst. Min. Metall., London.

Peterson D. E. (1988) Application of geothermometry, geobarometry, and oxygen barometry to the LILE/REE depleted granulite facies terrain in Bamble, southeast Norway. Unpubl. M.Sc. thesis. Univ. of Wisconsin, Madison.

Petrov B. V., Krendelev F. P., Bobrov V. A. and Tsimbalist V. G. (1972) Behavior of Radioelements and gold during metamorphism of sedimentary rocks in the Patom uplands. Trans. From Geokhimiya . No. 8, 947-956.

Pettijohn F. J. (1963) Chemical composition of sandstone, excluding carbonates and volcanic sands. In: Fleischer, M. (ed) Data of geochemistry (6th ed.) U.S. Geol. Survey, Professional Papers 440-S.

Phillips G. N. and Powell A. R. (1993) Link between gold provinces. Economic Geology, 88, 1084-1098.

Phillips G. N., Groves D. I., and Brown I. J. (1987) Source requirements for the Golden mile, Kalgoorlie: significance to the metamorphic replacement model for Archean gold deposits. Can. J. Earth Sci., 24, 1643-1651.

Phillips G. N., Groves D. I., and Brown I. J. (1987) Source requirements for the Golden Mile, Kalgoorlie: Significance to the metamorphic model for Archean gold deposits. Can. J. Earth Sci. 24, 1643-1651.

Pineau F., Javoy M., Behar F., and Tourte J. (1981) La géochimie isotopique du faciès granulite du Bamble (Norwège) et l'origine des fluids carbonés dans la croûte profone: Bulletin du Minéralogie, 104, 630-640.

Plant J. A., Breward N., Forrest M. D., and Smith R. T. (1989) The gold pathfinder elements, As, Sb, and Bi – their distribution and significance in the southwest Highlands of Scotland. The Institution of Mining and Metallurgy, 98, B91-B101.

Poulson S. R. and Ohmoto H. (1990) An evaluation of the solubility of sulfide sulfur in silicate melts from experimental data and natural samples. Chem. Geol. 84, 57-75.

Poulson S. R. and Ohmoto H. (1989) Devolatilization equilibria in graphite-pyrite-pyrrhotite bearing pelites with application to magma-pelite interaction. Contrib. Mineral. Petrol. 101, 418-425.

Poulson S. R., Kubilius W. P., and Ohmoto H. (1991) Geochemical behavior of sulfur in granitoids during intrusion of the South Mountain Batholith, Nova Scotia, Canada. Geochimica et Cosmochimica Acta, 55, 3809-3830.

Powell R., Will T. M., and Phillips G. N. (1991) Metamorphism in Archaean greenstone belts: calculated fluid compositions and implications for gold mineralization. J. of Metamorphic Geol., 9, 141-150.

Pride C. and Muecke G. K. (1980) Rare earth element geochemistry of the Scourian Complex, N. W. Scotland: Evidence for the granite-granulite link; Cont. Min. Pet., 73, 403-412.

Prider R. T. (1970) Nickel in Western Austarlia. Nature, 226, 691-693.

Puchelt H. and Emmermann R. (1976) Bearing of rare earth patterns of apatites from igneous and metamorphic rocks. Earth and Planetary Science Letters, 31, 279-286.

Puffer J. H., and Volkert R. A. (1991) Generation of trondhjemite from partial melting of dacite under granulite facies conditions: an example from the New Jersey Highlands, USA. Precambrian Research, 51, 115-125.

Qui Y. and McNaughton N. J. (1999) Source of Pb in orogenic lode-gold mineralization: Pb isotope constraints from deep crustal rocks from the southwestern Archean Yilgarn Craton, Australia. Mineralium Deposita, 34, 366-381.

Raiswell R. (1982) Pyrite texture, isotope composition, and the availability of iron. American Journal of Science, 282, 1244-1263.

Rajamani V. and Naldrett A.. J. (1978) Partitioning of Fe, Co, Ni, and Cu between sulfide liquid and basaltic melts and the composition of Ni-Cu sulfide deposits. Economic Geology, 73, 82-93.

Rao M. V. S. and Rao V. D. (1988) Chemical constraints on the origin of the Charnockites in the Eastern Ghat Mobile belt, India. Chemical Geology, 69, 37-48.

Ready J. F. (1971) Effects of high power laser radiation. Academic Press.

Renmin H., Kerong C., and Lianze Z. (1994) Gold-depleted zone and its metallogenic significance, Yinshan Ore Field, Jiagxi Province, China. Chinese Journal of Geochemistry, 13 (3), 246-253.

Reynolds R. C. and Fredrickson A. F. (1962) Corona development in Norwegian hyperites and its bearing on the metamorphic facies concept. Geol. Soc. Amer. Bull., 73, pp. 59-72.

Ridler R. H. (1976) Stratigraphic keys to the gold metallogeny of the Abitibi Belt. Can. Min. J, V. 97, No. 6, pp. 81-87.

Ripley E. M (1981) Sulfur isotopic studies of the Dunka Road Cu-Ni deposits, Duluth Complex, Minnesota. Economic Geology, 76, 610-620.

Ripley E. M. (1983) Sulfide mineralogy and sulfur isotope geochemistry of layered sills in the Deer Lake Complex, Minnesota. Mineralium Deposita, 18, 3-15.

Ripley E. M. and Al-Jassar T. J. (1987) Sulfur and oxygen isotope studies of melt-country rock interaction, Babbit Cu-Ni Deposits, Duluth Complex, Minnesota. Economic Geology, 82, 87-107.

Ripley E. M., Park Y. R., Li C. and Naldrett A. J. (1999) Sulfur and Oxygen isotopic evidence of country rock contamination in the Voisey's Bay Ni-Cu-Co deposit, Labrador, Canada. Lithos. 47, 53-68.

Roberts R. G. (1986) Archean lode gold deposits. In: Roberts R. G. and Sheahan P. A. (eds) Ore deposit models. Geoscience Canada; Reprint Series 3, pp. 1-19.

Rock N. M. S., Groves D. I., and Perring C. S. (1988) Gold, lamrophyres and porphyries: a new genetic model. In: Bicentennial Gold 88, Melbourne.

Rollinson H. R. and Windley B. F. (1980) Selective Elemental Depletion during Metamorphism of Archaean Granulites , Scourie , NW Scotland. Contrib. Mineral. Petrol., 72, 257-263.

Ronov A. B., Migdisov A. A., and Lobach-Zhuchenko S. B. (1977) Regional metamorphism and sediment composition evolution. Geoch. Intern., 14, 90-112.

Romberger S. (1989) Geochemistry of gold in hydrothermal deposits. In: U.S. geological Survey Bulletin 1857, pp. A9-A25.

Ross J. R. and Keays R. R. (1979) Precious metals in volcanic-type nickel sulfide deposits in Western Australia. Part 1: Relationship with the composition of the ores and their host rocks. Can. Mineral., 17, 417-436.

Ross J. R. and Hopkins G. M. F. (1975) The nickel-sulfide deposits of Kambalda, Western Australia. In: Knight C. (ed) Economic Geology of Papua-New Guinea. Aust. Inst. Min. Metall., Monograph 5, pp. 100-121.

Rösler H. J. and Beuge P. (1983) Geochemistry of trace elements during regional metamorphism. In: Augustithis S. S. (ed) The significance of trace elements in solving petrogenetic problems and controversies. pp. 407-429.

Rowins S. M., Cameron E. M., Lalonde A. and Ernst R. E. (1993) Petrogenesis of the Late Archean Syenitic Murdock Creek Pluton, Kirkland Lake, Ontario: Evidence for An Extensional Tectonic Setting. Canadian Mineralogist, 31, 219-244.

Rudnick R. L. and Taylor S. R. (1986) Geochemical constraints on the origin of Archaean tonalitic – trondhjemitic rocks and implications for lower crustal composition. The nature of the lower continental crust, Geological Society Special Publications, 24, 179-191.

Rudnick R. L., McLennan S. M., and Taylor S. R. (1985) Large ion lithophile elements in rocks from high pressure granulite facies terrains. Geochim. Cosmoch. Acta. 49, 1645-1655.

Rumble D. (1982) Stable isotope fractionation during metamorphic devolatilization reactions. In: Ferrey J. M. (ed) Reviews in Mineralogy, 10, 327-353.

Rumble D., Hoering T. C., and Palin J. M. (1993) Preparation of SF_6 for sulfur isotope analysis by laser heating sulfide minerals in the presence of F_2 gas. Geochimica et Cosmochimica Acta, 57, 4499-4512.

Rye R. O. and Ohmoto H. (1974) Sulfur and carbon isotopes and ore genesis: A review. Economic Geology, 69, 826-842.

Rye D. M. and Williams N. (1981) Studies of the base metal deposits at Mc Arthur River, Northern Territory. III. The stable isotope geochemistry of the H.Y.C. Ridge and Cooley deposits. Economic Geology, 76, 1-26.

Saager R. and Meyer M. (1983) Gold distribution in Archaean granitoids and supracrustal, rocks from Southern Africa: A comparison. In: Foster R. P. (ed) Gold' 82, Rotterdam, Balkema Publ., pp. 53-70.

Saager R., Meyer M. and Muff R. (1982) Gold distribution in supracrustal rocks from Archean Greenstone belts of Southern Africa and from Paleozoic ultramafic complexes of the European Alps: Metallogenic and geochemical implications. Economic Geology, 77, 11-24.

Sakai H. (1968) Isotopic properties of sulfur compounds in hydrothermal processes. Geochem. Journal, 2, 29-49.

Sakai H., De Marais D., Ueda D. J., and Moore J. G. (1984) Concentration of isotope ratios of carbon, nitrogen, and sulfur in ocean-floor basalts. Geochim. et Cosmochim. Acta, 48, 2433-2441.

Santosh M., Nadeau S., and Javoy M. (1995) Stable isotopic evidence for the involvement of mantle-derived fluids in Wynad Gold Mineralization, South India. The Journal of Geology, 103, 718-728.

Sasaki A. (1969) Sulfur isotope study of the Muskox Intrusion. District of Mackenzie. Geological Survey of Canada, Paper 68.

Sasaki A. and Ishihara S. (1979) Sulfur isotope composition of the magnetite-series and ilmenite-series granitoids in Japan. Contrib. Mineral. Petrol., 68, 101-115.

Schneider A. (1970) The sulfur isotope composition of basaltic rocks. Contr. Mineral. and Petrol., 25, 95-124.

Sazanov A. M. and Kremenetskiy A. A. (1995) Gold geochemistry of the North Ladoga Metamorphic Complex. Geochemistry International, 32 (6), 19-33.

Schidlowsky M. (1979) Antiquity and evolutionary status of bacterial sulfate reduction: Sulfur isotope evidence. Origin of life, 9, pp. 299-311.

Schneider A. (1970) The sulfur isotope composition of basaltic rocks. Contrib. Mineral. Petrol. 25, 307-313.

Schneider A. (1978) Sulfur: Abundance in rock-forming minerals, phase equilibria, sulfur minerals. In Wedepohl K. H. (ed) Handbook of Geochemistry, 16 D. Springer-Verlag, Berlin.

Schwarcz H. P. and Burnie S. W. (1973) Influence of sedimentary environments on sulfur isotope ratios in clastic rocks: a review. Mineralium Deposita, 8, 264-277.

Scott S. D., Both R. A. and Kissin S. A. (1977) Sulfide Petrology of the Broken Hill Region, New South Wales. Economic Geology, 72, 1410-1425.

Seccombe P. K., Spry P. G., Both R. A., Jones M. T., and Schiller J. C. (1985) Base metal mineralization in the Kanmantoo Group, South Australia: A regional sulfur isotope study. Economic Geology, 84, 1824-1841.

Seward T. M (1984) Transport and deposition of gold in hydrothermal systems. In: Foster R. P. (ed) Gold' 82, Rotterdam, Balkema Publ, pp. 165-181.

Seyfried W. E. and Bischoff J. L. (1981) Experimental seawater-basalt interaction at 300oC, 500 bars, chemical exchange, secondary mineral formation and implications for transport of heavy metals. Geochimica et Cosmochimica Acta, 45, 135-147.

Sharp Z. D. (1990) A laser-based microanalytical method for the in situ determination of oxygen isotope ratios of silicates and oxides. Geochimica et Cosmochimica Acta. 54, 1353-1357.

Sharpe M. R. (1982) Noble Metals in the Marginal Rocks of the Bushveld Complex. Economic Geology, 77, 1286-1295.

Shaw D. M. (1968) A review of K-Rb fractionation trends by covariance analysis. Geochimica et Cosmochimica Acta, 32, 573-602.

Shaw R. P., Morton R. D., Grey J., and Krouse H. R. (1991) Origins of metamorphic lode gold deposits: Implications of stable isotope data from the Central Rocky Mountains, Canada. Mineralogy and Petrology, 43, 193-209.

Shelton K. L., So, C.-S., and Chang J.-S. (1988) Gold-rich mesothermal deposits of the Republic of Korea: Geochemical studies of the Jungwon Gold Area. Economic Geology, 83, 1221-1237.

Shengfei G., Yumin Q., and Zhongshen Z. (1992) On the potential significance of gold mineralization in Archean high grade terrains: Evidence from North China Craton . In: 29th International Geological Congress; Abstracts. Volume 1, p. 180.

Sheraton J. W. and Black L. D. (1983) Geochemistry of Precambrian Gneisses: Relevance for the evolution of East Antarctic Shield. Lithos, 16, 273-296.

Sheraton J. W., Skinner A. C., and Tarney (1973) The geochemistry of the Scourian gneisses of the Assynt District. In: Park R. G. and Tarney J. (eds) The early Precambrian rocks of Scotland and related rocks of Greenland, Univ. of Keele, pp. 13-30,

Shima M., Ross W. H., and Thode H. G. (1963) Sulfur isotope abundances in basic sills, differentiated granites, and meteorites. Journal of Geophysical Research, 68, No. 9, 2835-2847.

Siewers U. (1974) Beitrag zur Häufigkeit und isotopenzusammensetzung des Schwefels in Magmatischen und Metamorphen Gesteinen. Diss. z. Eralangung d. Doctorgrades d. Mathemat.-Naturwiss. Fakult. Geog-August Univ. Göttingen, 62 pp.

Sighinolfi G. P. (1971) Investigation into the deep crustal level fractionating effects and geochemical trends related to high grade metamorphism. Geochim. Cosmoch. Acta. 35, 1005-1021.

Sighinolfi G. P. and Santos A. M (1976) Geochemistry of gold in Archean granulite fancies terrains. Chemical Geology, 17, 113-123.

Sims K. W., Newsom H. E. and Gladney E. S. (1990) Chemical fractionation during formation of the earth's core and continental crust: clues form As, Sb, W, and Mo. In: Newsom H. E., and Jones J. H. (eds) Origin of the Earth. Oxford University Press, pp. 291-317.

Skauli H., Boyce A. J., Fallick A. E. (1992) A sulfur isotope study of the Bleikvassli Zn-Pb-Cu deposit, Nordland, Northern Norway. Mineralium Deposita, 27, 284-292.

Skyring G. W. and Donnelly T. H. (1982) Precambrian sulfur isotopes and possible role for sulfite in the evolution of biological sulfate reduction. Precambrian Research, 17, 41-61.

Smalley P. C., Maile C. N., Coleman M. L., and Rouse J. E. (1992) LASSIE (Laser ablation sampler for stable isotope extraction) applied to carbonate minerals. Chemical Geology (Isotope Geoscience Section), 101, 43-52.

Smalley P. C., Stifjhoorn D. E., Råheim A., Jonassen H., and Dickson J. A. D. (1989) The laser microprobe and its application to the study of C and O isotopes in calcite and aragonite. Sediment. Geol., 65, 211-221.

Smalley P. C. and Field D. (1985) Geochemical constraints on the evolution of the Proterozoic continental crust in Southern Norway (Telemark Sector) In: Tobi A. C. and Touret J. L. R. (eds) The deep Proterozoic crust in the North Atlantic Provinces. Nato Advanced Science Institute Series. Series C, 158, pp. 551-566

Smalley P. C. and Field D. (1991) REE, Th, Hf, Ta in Bamble gabbros (Southern Norway) and their amphibolitized equivalents: implications for gabbro tectonic setting. Precambrian Research, 53, 233-242.

Smalley P. C., Field D., Lamb R. C., and Clough P. W. L. (1983) Rare earth, Th-Hf-Ta, and large ion lithophile element variations in metabasites from the Proterozoic amphibolite-granulite transition zone at Arendal, South Norway. Earth and Planetary Science Letters, 63, 446-458

Smith J. W. and Coxford N. J. W. (1973) Sulfur isotope ratios in the McArthur lead-zinc-silver deposits: Nature Phys. Sci., 245, 10-12.

Solomon P. J. (1965) Investigation into sulfide mineralization at Mt. Isa, Queensland: Econ. Geol., 60,737-765.

Speelman E. L., and Schwarcz H. P. (1966) Metamorphic sulfur isotope studies in the Haliburton-Madoc area, Grenville Subprovince, Canada. Geological Society of America, Special Paper, No. 101, pp. 209.

Spooner E. T. C. (1991) The magmatic model for the origin of Archean Au-quartz vein ore systems: An assessment of the evidence. In: Ladeira (ed.) Brazil Gold' 91, Roterdam, Balkema Publ., pp. 313-318.

Spry P. G. (1987) A Sulfur isotope study of the Broken Hill deposit, New South Wales, Australia. Mineral. Deposita, 22, 109-115.

Stahle H. J, Raith M., Hoernes S., and Delfs A. (1987) Element mobility during incipient granulite formation at Kabbaldurga , Southern India. Journal of Petrology, 28, 803-834

Stanton R. L. and Rafter T. A. (1967) Sulfur isotope ratios in co-existing Galena and Sphalerite from Broken Hill, New South Wales. Economic Geology, 62, 1088-1091.

Stanton R. L. (1972) Ore Petrology. McGraw Hill, 713 p.

Starmer I. C. (1969) Basic plutonic intrusions of the Risor-Sondeled area, South Norway: The original lithologies and their metamorphism. Norsk Geol. Tidsskrift, 49, 403-431.

Starmer I. C. (1972) The Sveconorwegian Regeneration and earlier events in the Bamble Series, South Norway. Nor. Geol. Unders, 227, 37-52.

Starmer I. C. (1976) The early structure and petrology of rocks in the Bamble series, Sondeled-Sandnesfjord, Aust-Agder. Norges geol. Unders, 327, 77-97.

Starmer I. C. (1985a) The Geology of the Kongsberg Sector, South Norway. Nor. Geol. Unders. Bull. 401, 35-58.

Starmer I. C. (1985b) The evolution of the South Norwegian Proterozoic as revealed by the major and mega-tectonics of the Kongsberg and Bamble Sectors. In: Tobi A. C. and Touret J. L. R. (eds) The deep Proterozoic crust in the North Atlantic Provinces. Nato Advanced Science Institute Series. Series C, 158, 259-290.

Starmer I. C. (1985c) Geological map of the Bamble Sector, South Norway (1/100000); 3 sheets: Nato Advanced Study Institute. 1984, Excursion Guide, In: Maijer C. and Padget P. (eds) The Geology of southernmost Norway. An excursion guide: Norske Geologiske Undersøkelse, Special Publication 1, 109 p.

Starmer I. C. (1991) The Proterozoic evolution of the Bamble Sector, Southern Norway: Correlation across southern Scandinavian, and the Grenvillian controversy. Precambrian Research, 49, 107-139.

Starmer I. C. (1993) The Sveconorwegian orogeny in southern Norway, relative to deep crustal structures and events in the North Atlantic Proterozoic Supercontinent. Norsk Geologisk Tidsskrift, 73, 109-132.

Stephenson J. F. and Ehmann W. D. (1971) Neutron activation analysis of gold in Archean igneous and metamorphic rocks of the Rice Lake-Beresford Lake area, Southeastern Manitoba. Economic Geology, 66, 933-939.

Stone W. E., Crocket J. H., and Fleet M. E. (1990) Partitioning of palladium, iridium, platinum and gold between sulfide liquid and basalt melt at 1200°C. Geochimica Cosmochimica Acta, 54, 2341-2344.

Strauss H. (1986) Carbon and sulfur isotopes in Precambrian sediments from the Canadian Shield. Geochimica Cosmochimica Acta, 50, 2653-2662.

Strauss H. (1997) The isotopic composition of sedimentary sulfur through time. Palaeogeography, Palaeo-climatology, Palaeoecology, 132, 97-118.

Strauss H. and Schieber J. (1990) A sulfur isotope study of pyrite genesis: The mid-Proterozoic Newland Formation, Belt Supergroup, Montana. Geochimica Cosmochimica Acta, 54, 197-204.

Svelto O. (1989) Principles of lasers; translated from Italian and edited by David C. Hanna. Plenum Press, New York; 3rd ed. 604 p.

Taner M. F. (1993) Gold abundance and an aluminosilicate-rich alteration zone in the Val D'Or mining district, Abitibi, Quebec: Examples of the fossil geothermal fields. Ore Geology Reviews, 8, 451-475.

Tarney J. (1976) Geochemistry of high-grade gneisses with implications as to the origin and evolution of Precambrian crust. In: Windley B. F. (ed) The early history of the earth, pp. 405-417.

Tarney J., Weaver B. and Drury A. (1979) Geochemistry of Archean trondhjemitic and tonalitic gneisses from Scotland and East Greenland. In: Barker F. (ed) Trondhjemites, Dacites, and related rocks. Developments in Petrology, 6. Elsevier.

Tarney J. and Weaver B. L. (1987) Geochemistry of the Scourian Complex: Petrogenesis and tectonic models. In: Park R. G. and Tarney J. (eds) Evolution of Lewisian and Comparable high-grade terrains. Geological Society of London. Special Publications, 27, pp. 45-56.

Tarney J. and Windley B. F. (1977) Chemistry, thermal gradients, and evolution of the lower continental crust. Journal of the Geological Society, London, 134, pp. 45-56.

Taylor S. R. and McLennan S. M. (1985) The continental crust: Its composition and evolution. Blackwell, 311p.

Taylor S. R. and McLennan S. M. (1986) The chemical composition of the Archean crust. Geological Society Special Publication, 24, 173-178.

Taylor S. R. and McLennan S. M. (1988) The significance of rare earth in geochemistry and cosmochemistry. In: Schneider K. A. and Eyring L. (eds) Handbook on the physics and chemistry of rare earths. Elsevier Sci. Pubs. North Holland Physics Pub. Div., Amsterdam, Vol. 11, pp. 485-580.

Taylor S. R., Rudnick R. L., McLennan S. M. and Eriksson K. A. (1986) Rare earth element patterns in Archean high-grade metasediments and their tectonic significance. Geochimica et Cosmochimica Acta. 50, 2267-2279.

Thode H. G. and Monster J. (1965) The sulfur isotope abundances in evaporites and in the ancient oceans. Chemical geology, 630-641.

Thomas R. J. (1989) The petrogenesis of the Mzumge Gneiss Suite, a tonalite–trondhjemite orthogneiss suite from the southern part of the Natal Structural and Metamorphic Province. South African Journal of Geology, 92, 322-338.

Thompson J. B. (1979) Oxides and sulfides in regional metamorphism of pelitic schists: Intern. Geol. Cong., 24th, Montreal, Sec. 10, pp. 27-35.

Thompson A. B.(1982) Dehydration melting of pelitic rocks and generation of H_2O-undersaturated granitic liquids. American Journal of Science, 282, 1567-1597.

Thompson J. F. H., and Barnes S. J. and Duke J. M. (1984) The distribution of nickel and iron between olivine and magmatic sulfides in some natural assemblages. Canadian Mineralogist, 22, 55-65.

Thompson R. N., Morrison A. P., Dickin I. L., Gibson I. L., and Harmon R. S. (1986) Two contrasting styles of interaction between basic magmas and continental crust in the British Tertiary Volcanic Province. J. Geophys. Res. 91, 5985-5997.

Thorpe R. I. and Thomas G. M. (1976) Gold content of greywacke and slate of the Goldenville Formation, Nova Scotia, as determined by Neutron Activation Analysis. Geol. Surv. Can., Paper 76-1A, pp. 319-326.

Tilling R. I., Gottfried D. and Rowe J. J. (1973) Gold abundance in Igneous rocks: Bearing on gold mineralization. Economic Geology, 68, 168-186.

Torske T. (1977) The South Norway Precambrian Region – A Proterozoic Cordilleran-type Orogenic Segment. Norske Geologisk Tidsskrift, 57, 97-120.

Toulmin P. and Barton P. B. (1964) A thermodynamic study of pyrite and pyrrhotite. Geochimica et Cosmochimica Acta, 28, 641-672.

Touret J. (1971) Le faciès granulite en Norvège mèridionale. II. Les inclusion fluids. Lithos, 4, 423-436.

Touret J. (1986) Fluid inclusions in rocks from the lower continental crust. In: Dawson J. B., Hall D. A. and Wedepohl K. H. (eds) The Nature of the lower continental crust. Geological Society Special Publication. No. 24, 161-172.

Touret J. L. R. (1968) The Precambrian metamorphic rocks around the Lake Vegår, Aust-Agder, southern Norway: Norske Geolgiske Undersøkelse, 257, 1-45.

Touret J. and Dietworst P. (1983) Fluid inclusions in high grade anatectic metamorphites. J. Geol. Soc. London, 140, 635-649.

Tracy R. J. and Robinson P. (1988) Silicate-sulfide-oxide-fluid reactions in granulite-grade pelitic rocks, Central Massachusetts. American Journal of Science, 288-A, 45-74.

Troop D. G. (1986) Multiple orebody and vein morphologies, Ross Mine, District of Cochrane. In: Thurston P. B., White O. L., Barlow M. E., Cherry A. C., and Colvine A. C. (eds) Summary of field works and other activities. Ontario Geological Survey; Miscellaneous Paper 132, pp. 413-420.

Turekian K. K. and Wedepohl K. H. (1961) Distribution of the elements in some major units of the earth's crust. Bull. Geol. Soc. Am., 72, 175-192.

Uvarov V. V. D'yachkov, Burmistrov V. R., Stepanov V. M., and Madiyanov T. (1972) Geochemistry of gold in the magmatic complexes of the Kalba-Naryamsk region (Eastern Kazakhstan). Geochemistry International, xx, 774-776.

Valley J. W. and O'Neil J. R. (1984) Fluid heterogeneity during granulite facies metamorphism in the Adirondacks: Stable isotope evidence. Contrib. Mineral. Petrol., 85, 158-173.

Valley J. W. (1986) Stable isotope geochemistry of metamorphic rocks. In: Valley J. W., Taylor H. P., and O'Neil J. R. (eds) Stable isotopes in high temperature geological processes. Reviews in Mineralogy, Vol. 16, pp. 445-490.

Van De Kemp P. C. (1969) Origin of amphibolites in the Beartooth Mountains, Wyoming and Montana: New data and interpretation. Geological Society of American Bulletin, 80, 1127-1136.

Van Den Kerkhof A. M., Touret J. L. R. and Kreulen R. (1994) Juvenile CO_2 in enderbites of Tromoy near Arendal, South Norway: A fluid inclusion and stable isotope study. Metamorphic Geol. 12, 301-310.

Van Reenen D. D., Pretorius A. I. and Roering C. (1994) Characterization of fluids associated with gold mineralization and with regional high temperature retrogression of granulites in the Limpopo belt, South Africa. Geochimica et Cosmochimica Acta. Vol. 58. No 3. 1147-1159.

Vaughan D. J., Schwarz E. J. and Owens D. R. (1971) Pyrrhotites from the Strathcona mine, Sudbury, Canada: A thermomagnetic and mineralogical study, Economic Geology, 66, 1131-1144.

Viezer J., Holser W. T., and Wilgus C. K. (1980) Correlation of $^{13}C/^{12}C$ and $^{34}S/^{32}S$ secular variations. Geochimica et Cosmochimica Acta, 44, 579-587.

Verdonk E. M. et al (1986) Coronitic gabbro (hyperite) intruding the lower Proterozoic crust of Bamble, Southern Norway. EOS, 67, No, 44, p 1252.

Verschure R. H. (1985) Geochronological framework for the late Proterozoic evolution of the Baltic Shield in South Scandinavia. In Tobi A. C. and Touret J. L. R. (eds) The deep Proterozoic crust in the North Atlantic Provinces. Nato Advanced Science Institute Series, series C, 158, pp. 381-410.

Vinogradov A. P., and Ronov A. B. (1956) Composition of sedimentary rocks of the Russian Platform in connection with the history of its tectonic movements. Geochemistry (USSR), 6, 3-24.

Visser D., and Senior A. (1990) Aluminous reaction textures in orthoamphibolite-bearing rocks: the pressure-temperature evolution of the high grade Proterozoic of the Bamble Sector, South Norway. J. of Metamorphic Geology, 8, 231-246.

Vocke R. D., Jr., Hanson G. N. and Grüenfelder M. (1987) Rare earth element mobility in the Roffna Gneiss, Switzerland. Contrib. Mineral. Petrol., 95, 145-154.

Von Gehlen. K. Nielsen H., Chunnett I. and Rozendaal A. (1983) Sulfur isotopes in metamorphosed Precambrian Fe-Pb-Zn-Cu sulfides and baryte at Aggeneys and Gamsberg, South Africa. Mineralogical Magazine, 47, 481-486.

Von Gruenwaldth G., Hutton G., Merkle R. K. W., and Gain S. B. (1986) Platinum-group element-chromitite associations in the Bushveld Complex. Economic Geology, 81, 1067-1079.

Voskrewsenskaya and Zvereva (1968) Geochemistry of gold and its distribution in the magmatic complexes of northern Kazakhstan. Geochemistry International, 5, 373-381.

Vry J., Brown P. E., Valley J. W., and Morrison J. (1988) Constraints on granulite genesis from carbon isotope compositions of cordierite and graphite, Nature, 332, xxx

Waque P. (1996) Element mobility during Sveconorwegian metamorphism in the Modum Complex, South Norway. M.Sc. thesis, Univ. of Ottawa, Ottawa, Canada, 241 p.

Watson E. B. (1982) Basalt contamination by continental crust: Some experiments and results. Contrib. Mineral. Petrol. 80, 73-87.

Weaver B. L. (1980) Rare Earth Element Geochemistry of Madras Granulites. Contrib. Mineral. Petrol., 71, 271-279.

Weaver B. L., and Tarney J. (1980) Rare Earth Geochemistry of Lewisian Granulite-Facies Gneisses, Northwest Scotland: Implications for the Petrogenesis of the Archaean Lower continental crust. Earth and Planetary Science Letters, 51, 279-296.

Weaver B. L., and Tarney J. (1981) Lewisian gneiss geochemistry and Archaean crustal development models. Earth and Planetary Science Letters, 55, 171-180.

Weber W. and Stephenson J. F. 91973) The content of mercury and gold in some Archean rocks of the Rice Lake area. Economic Geology, 68, 401-407.

Wedepohl K. H. (1967-1978) Handbook of Geochemistry. Springer.

Wedepohl K. H. (1995) The composition of the continental crust. Geochimica et Cosmochimica Acta, 59, 1217-1232.

Weir R. H. and Kerrick D. M. (1987) Mineralogic, fluid inclusion and stable isotope studies of several gold mines in the Mother Lode, Tuolumne and Mariposa Counties, California: Economic Geology, 82, 328-344.

Weissberg B. G. (1970) Solubility of gold in hydrothermal alkaline sulfide solutions. Economic Geology, 65, 551-556.

Wendlandt R. F. and Harrison W. (1979) Rare earth partitioning between Immiscible Carbonate and Silicate liquids and CO2 Vapor: Results and implications for the formation of light rare earth-enriched rocks. Contrib. Mineral. Petrol. 69, 409-419.

Wendlandt R. F. (1982) Sulfide saturation of basalt and andesite melts at high pressures and temperatures. American Mineralogist, 67, 877-885.

Whalen J. B., Currie K. L. and Chappell B. W. (1987) A-Type Granites: Geochemical characteristics, discrimination and petrogenesis. Contrib. Mineral. Petrol., 95, 407-419.

Whalen J. B., Jenner G. A., Longstaffe F. J., Robert F., and Gariepy C. (1996) Geochemical and isotopic (O, Nd, Pb and Sr) constraints on A-type granite petrogenesis based on the Topsoils igneous suite, Newfoundland Appalachians. Journal of Petrology, 37, 1463-1489.

Willan R. C. R. and Coleman M. L. (1983) Sulfur isotope study of the Aberfeldy barite, zinc, lead deposits and minor sulfide mineralization in the Dalradian metamorphic terrain, Scotland. Economic Geology, 78, 1619-1656.

Wilson M. (1989) Igneous Petrogenesis. A Global Tectonic Approach. Unwin Hyman, London. 466 p.

Winchester J. A. (1974) The control of the whole rock content of CaO and Al_2O_3 on the occurrence of the aluminum silicate polymorphs in amphibolite facies pelites. Geological Magazine, 11.

Witt (1991) Regional metamorphic controls on alteration associated with gold mineralization in the Eastern Goldfields Province, Western Australia: Implications for the timing and origin of Archean lode gold deposits. Geology, 19, 982-985.

Witt W. K. and Vanderhor F. (1998) Diversity within a unified model for Archaean gold mineralization in the Yilgarn Carton of Western Australia: An overview of the late-orogenic, structurally –controlled gold deposits. Ore Geology Reviews, 13, 29-64.

Wolde B., Gore-Gambella Geotraverse Team (1996) Tonalite-trondhjemite-granite genesis by partial melting of newly underplated basaltic crust: an example from the Neoproterozoic Birbir magmatic arc, Western Ethiopia. Precambrian Research, 76, 3-14.

Wood D. A., Joron J. L. and Treuil M. (1979) A re-appraisal of the use of trace elements to classify and discriminate between magma series erupted in different tectonic settings. Earth and Planetary Science Letters, 45, 326-336.

Wood S. A. (1987) Thermodynmic calculations of the volatility of the platinum group elements (PGE): The PGE content of fluids at magmatic temperatures. Geochim. Cosmochim. Acta, 51, 3041, 3050.

Wyllie P. G. (1977) Effects of H_2O and CO_2 on magma generation in the crust and mantle; Journal of the Geological Society of London, 134, 215-234.

Wymann D. and Kerrich R. (1988) Alkaline magmatism, major structures, and gold deposits; implications for greenstone belt gold metallogeny. Economic Geology, 83, 454-461.

Yamamoto M. (1976) Relationship between Se/S and Sulfur isotope ratios of Hydrothermal Sulfide Minerals. Mineral. Deposita. 11, 197-209.

Yingjun L., Junfeng J., Weidong C., and Chengyuan S. (1992) Distribution characteristics of gold and other trace elements in the Proterozoic Lengjiaxi Group, Northeastern Hunan Province. Chinese Journal of Geochemistry, 11 (1), 13-22.

Yoon C. H. (1991) Gold content of Jurassic and Cretaceous granitic rocks in Korea. Mining Geology, 41 (3) 151-158.

Yund R. A. and Hall H. T. (1970) Kinetics and mechanism of pyrite exsolution from pyrrhotite. Journal of Petrology. Vol. 11, Part 2, 381-404.

Zeck H. P. and Kalsbeek F. (1981) Geochemistry of amphibolite facies metamorphism of a suite of basic dykes, Precambrian basement, Greenland. Chem. Erde., 40, 1-22.

Zeck H. P. and Toft J. (1989) Mass balance of a gabbroic rock-amphibolite transition. In: Bridgewater (ed) Fluid movement, element transport and the composition of the deep crust; pp. 203-212. Kluver Academic Publisher.

Zeck H. P. and Willadsen K. (1991) The ca. 1500 Ma Varmland hyperites suite, Southwest Sweden-petrography, magma chemistry and metasomatic changes of a series of partly recrystallized gabbroic intrusions. In: Gower, C. F., Rivers T., and Ryan B. (eds) Mid-Proterozoic Laurentian-Baltica: Geological Association of Canada, Special Paper, 38, 461-470.

Zeck H. P., Lou S. and Ellgaard L. (1983) Statistical evaluation of metasomatic effects in meta-igneous rock series. Chemical Geology, 40, 51-63.

Zeck H. P., Morthorst J. R., and Kalsbeek F. (1983) Metasomatic control of K/Rb ratios in amphibolites. Chemical Geology, 40, 313-321.

Zentilli M., Brooks R. R., Helgason J., Ryan D. E., and Zhang H. (1985) The distribution of gold in volcanic rocks of Eastern Iceland. Chemical Geology, 48, 17-28.

Zheng Y. F. (1990) Sulfur isotope in metamorphic rocks. Neus Jahrbuch Miner. Abh., 161, 303-325.

Zientek M. L., Fries T. L., and Vian R. W. (1990) As, Bi, Hg, S, Sb, Sn, and Te geochemistry of the J-M Reef, Stillwater Complex, Montana: constraints on the origin of PGE-enriched sulfides in layered intrusions. Journal of Geochemical Exploration, 37, 51-73.

Zvereva N. F. and Gavrilenko B. V. (1971) Gold in the rock-forming minerals of the Krykkuduk intrusive complex (northern Kazakhstan); Geokhim., No. 1, 114-118.

Zweng P. L., Mortensen J. K., and Dalaymple G. B. (1993) Thermochronology of the Camflo gold deposit, Malartic, Quebec: Implications for magmatic underplating and formation of gold-bearing quartz veins. Economic Geology, 88, 1700-1721.

Appendix 2-1. Analysis of supracrustal rocks, Bamble (Oxides in %; elements in ppm)

Samp. No.	SiO_2	TiO_2	Al_2O_3	Fe_2O_3	FeO	MnO	MgO	CaO	Na_2O	K_2O	P_2O_5	H_2O	CO_2	Cr
Biotite Schist														
2012	47.3	2.14	17.6	2.9	12.5	0.31	5.07	6.47	1.5	2.62	0.28	1.4	0.20	100
2221	46.7	2.13	13.3	3.4	13.5	0.26	6.52	5.65	1.5	3.89	0.37	2.3	0.40	120
2412	54.8	1.53	14.9	5.0	7.3	0.17	4.08	3.56	4.7	1.97	0.18	1.4	0.10	27
3221	46.9	3.38	12.4	3.0	13.4	0.24	3.97	6.86	1.7	2.39	0.70	3.8	0.00	36
3222	56.7	1.75	14.3	1.6	7.9	0.13	3.48	3.68	3.6	3.26	0.2	2.6	0.10	54
3621	51.3	1.85	15.2	4.9	7.5	0.25	5.33	6.11	3.1	2.97	0.15	1.7	0.00	38
5514	49.9	1.15	15.6	4.3	7.8	0.23	8.08	1.58	3.3	5.69	0.09	1.5	0.20	140
Biotite Gneiss														
1911	70.9	0.68	13.7	0.7	4.6	0.09	1.65	3.33	2.6	1.53	0.12	0.6	0.00	45
2611	72.5	0.31	14.1	0.6	2.2	0.05	0.94	3.33	3.7	1.80	0.05	0.5	0.00	12
2612	72.8	0.35	13.7	0.6	2.0	0.05	1.14	3.24	3.9	1.20	0.05	0.7	0.00	18
2711	70.3	0.39	13.8	1.1	2.8	0.07	1.10	3.19	4.0	2.17	0.05	0.8	0.10	24
3421	62.2	0.83	15.1	1.5	6.1	0.13	2.45	6.09	3.1	1.44	0.15	1.1	0.00	33
3422	74.2	0.57	12.3	0.4	2.4	0.05	0.60	1.77	2.3	4.81	0.06	0.6	0.00	19
3512	69.9	0.48	14.2	1.3	2.8	0.06	1.18	3.54	4.0	1.37	0.08	1.0	0.00	15
3521	65.1	0.61	16.3	1.1	3.8	0.09	2.06	2.51	5.3	2.10	0.09	0.9	0.00	17
3522	67.3	0.48	15.6	0.7	3.1	0.08	1.68	1.98	5.6	1.93	0.07	0.8	0.00	15
3611	72.2	0.41	13.5	1.1	2.5	0.05	1.06	2.28	4.5	1.50	0.04	0.6	0.10	11
3622	60.8	0.85	16.5	2.5	4.4	0.12	3.02	3.53	4.0	2.88	0.13	1.4	0.00	21
5407	68.7	0.65	13.5	1.0	4.1	0.03	2.90	0.66	5.1	2.61	0.09	0.9	0.10	15
7302	63.72	0.76	15.95	2.2	4	0.021	0.99	3.69	4.11	1.689	0.199	0.75	0.2	67
Impure Quartzite														
10208	87.1	0.85	5.7	1.0	1.8	0.01	0.56	0.12	0.5	1.66	0.05	0.5	0.10	35
2222	84.4	0.43	7.1	0.2	2.0	0.02	0.74	0.85	1.1	2.43	0.10	0.8	0.10	24
Hornblende Gneiss														
2811	65.2	0.71	15.1	0.7	3.0	0.02	4.24	7.40	0.5	1.38	0.13	1.3	0.00	30
2812	63.5	0.63	14.2	1.1	3.8	0.02	5.84	6.82	0.5	1.96	0.14	1.6	0.00	27
2821	62.9	0.87	15.5	2.2	3.1	0.02	3.40	10.08	0.4	0.34	0.21	0.9	0.00	43
2822	59.9	1.03	14.9	3.5	3.1	0.02	4.65	10.41	0.5	0.35	0.25	1.1	0.10	54
2911	62.6	1.52	12.4	0.6	5.4	0.03	7.89	4.88	1.1	0.90	0.10	2.6	0.10	74
2912	55.4	1.46	16.6	0.9	6.4	0.03	12.09	2.70	1.0	0.40	0.08	3.4	0.30	82
2921	62.1	0.77	15.0	3.1	2.2	0.01	4.48	9.58	0.5	0.37	0.16	1.0	0.00	33
2922	57.5	1.12	15.8	4.6	2.4	0.02	5.18	10.49	0.7	0.37	0.34	1.1	0.00	110
3011	68.1	0.51	11.3	1.0	4.2	0.04	8.38	5.15	0.1	0.06	0.14	0.7	0.00	62
3012	54.4	1.40	15.8	3.4	3.5	0.03	7.04	12.15	0.4	0.12	0.47	0.8	0.00	120
3021	51.2	2.15	16.7	3.2	3.3	0.02	7.86	11.76	0.3	0.49	0.77	1.5	0.20	51
3022	56.2	1.22	15.8	4.7	2.6	0.02	6.25	8.27	0.4	0.25	0.47	3.0	0.10	140
Concordant Amphibolite														
1921	54.6	1.92	15.4	2.1	10.6	0.19	3.67	3.93	2.0	2.74	0.25	2.0	0.10	61
2211	50.6	2.78	14.0	4.9	11.8	0.31	3.37	7.77	1.7	0.80	0.71	1.7	0.00	12
2212	50.4	2.66	14.0	5.6	11.0	0.27	3.42	7.58	2.5	0.88	0.59	1.6	0.10	23
2411	53.6	1.42	14.0	5.3	7.8	0.20	4.92	6.36	4.4	0.61	0.14	1.1	0.00	43
2421	48.8	1.67	15.3	2.1	10.1	0.21	7.13	8.86	1.5	2.07	0.15	1.7	0.00	180
2422	47.6	2.32	14.6	2.8	12.0	0.22	6.45	9.33	1.8	1.33	0.20	1.8	0.00	160
2511	53.6	0.56	18.7	2.0	5.4	0.13	4.86	8.92	4.2	0.68	0.12	1.1	0.00	89

	Ni	Co	Sc	V	Zn	Mo	Be	S	Cu	Se	As	Sb	Au (ppb)	Rb	Cs
	Biotite Schist														
2012	41	44	42.7	320	200	2.0	2.0	1350	44	0.09	1.11	0.07	1.27	147	4.7
2221	50	47	62.7	320	300	2.0	1.5	610	17	0.03	0.94	0.06	0.12	133	2.4
2412	23	36	31.5	210	340	0.5	2.3	155	41	0.005	0.23	0.02	0.14	172	14
3221	21	48	41.0	200	200	2	3.3	3498	60	0.15	1.39	0.08	0.81	93	3
3222	47	35	16	150	140	0.5	2.5	2065	52	0.08	0.88	0.09	0.52	149	2.1
3621	55	50	33.6	260	160	1.0	1.3	360	55	0.16	2.56	0.21	16.15	92	6.5
5514	83	47	30.8	200	260	1.0	5.2	693	230		0.25	0.02	3.53	364	3.7
	Biotite Gneiss														
1911	17	18	17.0	78	64	1.0	1.4	96	9	0.01	0.19	0.01	0.16	124	0.60
2611	11	23	5.5	32	24	3.0	0.7	141	15	0.01	0.05	0.01	0.05	73	5.90
2612	17	27	3.9	30	24	2.0	1.3	126	21	0.01	0.07	0.05	0.05	106	8.10
2711	11	23	6.5	37	69	2.0	1.6	300	25	0.03	0.11	0.02	0.05	61	1.50
3421	19	30	22.2	130	97	1.0	1.2	90	21	0.03	1.22	0.05	1.20	42	1.10
3422	7.0	22	6.8	36	42	1.0	1.0	402	45	0.04	0.29	0.03	0.19	104	2.90
3512	9.0	21	12.0	51	34	4.0	2.3	163	27	0.01	0.6	0.04	0.05	65	3.30
3521	9.0	21	14.0	46	48	2.0	1.4	693	85	0.14	0.42	0.05	0.18	57	2.50
3522	10	19	11.0	40	43	0.5	1.2	51	9.0	0.005	0.49	0.05	0.05	52	2.20
3611	10	18	8.1	32	35	2.0	1.4	77	60	0.03	0.25	0.03	0.51	72	5.70
3622	20	38	18.0	130	100	1.0	3.0	25	29	0.03	2.98		1.09	119	7.00
5407	7.0	27	12.0	46	29	2.0	0.4	610	22	0.02	0.17	0.02	0.05	82	0.25
7302	43	11	9.5	56	75	2.0	3.0	22400			0.75	0.05	1.10	45	1.20
	Impure Quartzite														
10208	8.0	70	6.5	53	1.0									51	0.70
2222	1.0	9	7.1	43	54		0.2	235	11	1.58	0.03	0.11	0.49	117	0.60
	Hornblende Gneiss														
2811	37	20	8	68	18	0.5	2.2	542	14	0.01	0.13	0.01	0.23	69	26
2812	58	23	9.4	81	30	2	4.1	1290	25	0.02	0.18	0.02	0.65	114	40
2821	40	29	11	90	5.0	0.5	4.2	231	11	0.005	0.33	0.04	0.15	18	2.3
2822	46	21	13	100	5.0	0.5	1.4	25	10	0.005	0.44	0.02	0.05	20	2.9
2911	44	41	52.7	300	10	2.0	0.9	54	9.0	0.02	0.11	0.01	0.80	30	3.4
2912	53	16	47.1	260	14	5.0	1.2	25	8.0	0.01	0.11	0.02	0.05	16	1.10
2921	96	23	8.7	85	5.0	0.5	0.6	316	42	0.11	0.17	0.02	0.26	16	2.3
2922	57	23	16	130	16	0.5	1.3	45	13	0.02	0.33	0.02	0.05	25	3.6
3011	97	23	10	70	15	1.0	1.8	97	18	0.01	0.4	0.02	0.13	12	0.25
3012	110	20	29.4	180	9.0	2.0	1.6	25	8.0	0.005	0.9	0.02	0.05	5.0	0.25
3021	67	17	29.0	260	8.0	0.5	0.9	25	10	0.005	1.12	0.01	0.05	11	0.25
3022	110	19	36.8	190	8.0	0.5	0.9	74	8.0	0.005	0.47	0.01	0.05	14	1.3
	Concordant Amphibolite														
1921	46	46	40.1	230	160	2.0	1.5	3747	93	0.31	0.59	0.04	0.36	54	0.90
2211	21	41	44.2	170	180	2.0	1.9	3206	61	0.19	1.95	0.73	0.32	17	0.25
2212	20	37	47.3	220	160	2.0	2.1	994	72	0.24	1.2	0.13	0.24	22	0.25
2411	19	40	40.0	240	100	2.0	0.8	796	86	0.08	0.14	0.04	0.21	19	3.90
2421	110	54	34.3	200	110	1.0	1.3	25	25	0.005	0.14	0.04	0.05	75	12.00
2422	45	55	42.5	240	130	3.0	1.5	1275	78	0.11	0.2	0.05	0.05	32	6.20
2511	128	40	21.2	130	76	1.0	1.3	507	59	0.04	0.28	0.02	0.05	14	1.70

	Ba	Sr	Hf	Zr	Y	Th	U	La	Ce	Sm	Eu	Tb	Yb	Lu	F	Cl
2012	462	132	7.0	217	61	2.9	1.7	20	40	6.8	1.0	2.00	6.0	0.9	1507	900
2221	620	64	6.0	130	40	1.6	0.8	37	73	10	2.0	3.00	8.0	1.2	1531	9517
2412	281	101	6.0	144	36	2.6	1.2	14	25	4.7	1.0	1.40	3.0	0.5	648	130
3221	521	84	14	445	108	4.6	6.0	43	93	15	4.0	3.90	12	2.0	2053	217
3222	473	161	6.0	178	52	23.5	7.8	48	82	7.2	2	1.8	5.0	1.1	1026	198
3621	439	128	6.0	138	31	1.4	0.8	16	31	4.9	2.0	1.30	2.0	0.4	767	168
5514	353	63	2.0	77	62	0.9	1.4	18	49	6.6	0.5	1.80	6.0	0.8	6972	768
	Biotite Gneiss															
1911	465	111	10.0	224	38	19.0	2.1	57	92	7.2	2.0	1.60	5.0	0.9	459	50
2611	893	299	5.0	128	6.0	0.4	0.7	20	34	2.4	1.0	0.50	2.0	0.2	140	50
2612	360	273	5.0	136	7.0	2.1	1.2	21	24	2.3	0.5	0.35	1.0	0.3	546	50
2711	544	221	9.0	187	40	1.4	1.6	37	55	6.5	2.0	1.40	4.0	0.7	402	132
3421	457	283	5.0	106	24	3.2	1.2	20	33	4.3	2.0	0.90	3.0	0.4	608	142
3422	1172	252	10.0	281	27	16.0	1.5	35	72	5.3	1.0	1.10	4.0	0.6	195	112
3512	471	306	8.0	169	30	9.2	2.0	34	65	5.8	0.5	1.30	3.0	0.5	318	50
3521	685	268	10.0	261	27	7.0	2.0	20	41	4.2	0.5	0.90	3.0	0.5	496	111
3522	628	222	8.0	214	23	5.6	2.1	24	44	4.6	1.0	1.10	3.0	0.5	460	116
3611	352	249	8.0	221	21	11.0	2.6	27	46	3.8	0.5	0.90	3.0	0.4	344	100
3622	460	211	6.0	142	17	3.8	2.9	18	38	3.3	0.5	0.80	1.0	0.4	832	186
5407	309	40	18.0	573	105	31.0	7.5	65	80	14	1.0	3.20	7.0	1.5	371	50
7302	284	413	5.0	193	15	5.0	4.1	28	74	5.0	2.0	0.70	1.0	0.1		
	Impure Quartzite															
10208	348	62	30.0	1113	38	35.8	6.2	72	140	11.50	2.0	1.50	3.0	0.1		
2222	1166	125	14.0	237	16	10.0	0.9	38	71	6.20	1.0	1.20	1.0	0.4	245	340
	Hornblende Gneiss															
2811	99	573	12	343	42	17.0	5.0	86	142	10	2.0	1.8	4.0	0.7	1870	113
2812	95	444	12	340	57	17.0	4.1	100	172	11	2.0	2	6.0	1.0	2705	105
2821	58	601	12	348	47	13.0	5.1	88	144	10	3.0	1.8	5.0	0.8	1151	50
2822	49	573	12	398	48	13.0	7.9	96	152	11	3.0	2.1	5.0	0.9	849	50
2911	100	364	5.0	123	46	10.0	2.8	45	55	3.8	2.0	1.7	5.0	0.7	500	50
2912	95	270	3.0	72	28	4.0	2.7	29	37	2.50	0.5	1.00	4.0	0.6	565	50
2921	69	743	13	384	46	14.0	3.3	97	162	13	2.0	2	4.0	0.7	612	50
2922	72	690	13	354	54	11.0	2.6	99	154	12	3.0	2.2	5.0	0.8	1059	50
3011	45	404	7.0	174	11	4.7	1.4	52	82	2.7	1.0	0.7	2.0	0.2	837	50
3012	61	968	9.0	260	37	5.0	1.9	98	164	13.00	4.0	2.20	4.0	0.6	1388	50
3021	85	951	10.0	293	59	6.5	3.7	211	309	22.60	3.0	3.40	5.0	0.8	1404	120
3022	90	734	13	377	44	10.0	3.2	160	240	18	5.0	2.5	4.0	0.6	1145	50
	Concordant Amphibolite															
1921	773	146	6.0	276	68	3.1	0.6	21	45	5.5	2.0	1.50	5.0	0.8	1036	428
2211	224	142	11	372	71	2.3	0.9	30	51	9.3	3.0	2.90	8.0	1.2	749	313
2212	268	144	9.0	365	81	0.9	0.5	27	52	9.0	3.0	2.60	6.0	1.0	756	379
2411	241	170	4.0	98	29	1.3	0.5	12	19	3.7	0.5	1.00	3.0	0.5	380	50
2421	348	146	4.0	92	27	0.4	0.3	12	19	4.0	2.0	1.10	3.0	0.5	1068	195
2422	202	148	7.0	176	50	0.3	0.7	18	38	7.5	2.0	2.60	6.0	0.8	688	205
2511	196	589	3.0	54	12	0.2	0.5	15	26	3.2	0.5	0.25	2.0	0.2	512	185

	SiO_2	TiO_2	Al_2O_3	Fe_2O_3	FeO	MnO	MgO	CaO	Na_2O	K_2O	P_2O_5	H_2O	CO_2	Cr
2521	53.0	1.23	15.8	3.3	7.2	0.19	5.00	8.25	3.5	0.73	0.25	1.5	0.00	79
2522	50.3	0.97	18.1	3.2	7.0	0.18	4.76	9.29	4.0	0.95	0.12	1.2	0.00	57
2621	55.9	1.63	14.1	3.8	8.1	0.21	4.05	6.74	3.2	1.66	0.31	1.2	0.10	40
2712	46.2	0.90	12.3	3.2	10.1	0.23	11.94	8.30	1.5	2.49	0.10	1.9	0.10	480
2722	47.5	1.17	14.4	4.1	11.0	0.30	6.59	11.22	2.3	0.59	0.28	1.3	0.00	45
3221	46.9	3.38	12.4	3.0	13.4	0.24	3.97	6.86	1.7	2.39	0.70	3.8	0.00	16
3311	45.0	2.91	14.8	2.7	13.0	0.22	6.25	7.53	2.7	1.68	0.32	2.7	0.00	130
3321	48.2	2.95	13.8	3.1	11.6	0.25	3.38	6.95	4.0	1.72	0.53	2.5	0.00	14
3411	53.1	1.10	14.8	2.9	7.9	0.15	6.45	7.38	3.0	1.34	0.15	2.0	0.00	140
3412	49.2	1.23	16.2	3.1	8.2	0.12	7.08	9.50	3.5	0.66	0.06	1.6	0.00	88
	Calc-silicates													
5501	37	0.81	7.8	3.6	3.9	0.3	3.77	25.07	0.1	0.82	0.1	1.4	14.5	68
5502	16.4	0.18	3.8	0.6	3.8	0.48	1.68	38.69	0.9	0.16	0.04	1.2	31.7	37
5503	7.2	0.07	1.7	0.1	1.3	0.37	0.62	48.34	0.5	0.19	0.01	0.2	39.1	16
5504	46.1	1.59	12.5	5.2	10	0.25	6.07	7.16	1.9	2.52	0.14	2.9	3.5	130
7202	45.06	0.601	9.69	4.4	5	0.172	7	21.34	0.46	1.141	0.125	0.25	3.2	1218
7204	42.87	0.567	7.73	4.26	5	0.166	7.27	22.78	0.33	1.284	0.107	0.27	5.7	1182
8003	42.17	2.734	13.44	8.5	5.7	0.194	5.84	10.56	2.45	0.49	0.235	0.65	6.7	70
	Garnet-Biotite Gneiss													
1912	61.0	1.73	14.9	1.3	9.7	0.18	3.06	4.14	1.8	1.67	0.10	0.8	0.10	65
1922	64.4	1.33	13.5	1.6	6.8	0.15	2.12	1.82	2.6	3.17	0.17	1.2	0.00	39
2011	68.8	0.39	15.7	0.6	2.8	0.06	1.10	1.65	2.9	5.04	0.05	1.0	0.20	24
2021	69.3	0.61	13.8	0.6	3.9	0.07	1.32	1.33	2.2	5.45	0.05	0.7	0.10	38
2022	72.7	0.70	12.7	1.0	3.3	0.06	1.43	2.16	3.4	1.71	0.08	0.5	0.10	44
2111	63.2	1.23	16.1	1.3	5.8	0.07	3.13	2.85	3.0	2.70	0.06	1.0	0.00	60
2112	72.4	1.26	10.8	1.3	5.4	0.09	2.20	3.15	1.5	1.17	0.17	0.6	0.10	41
2121	70.3	0.60	14.1	0.6	3.3	0.07	1.14	1.78	2.6	4.75	0.07	0.5	0.00	34
2122	69.1	0.58	13.6	1.3	3.9	0.09	1.67	2.34	1.9	3.37	0.13	1.9	0.10	26
7101	74.5	0.435	11.95	1.0	3.03	0.051	1.32	1.03	2.41	3.046	0.061	0.8	0.2	53
7102	71.24	0.6	13.38	1.2	3.10	0.047	1.65	1.26	2.93	3.372	0.07	0.6	0.2	45
7103	67.93	0.75	14.45	2.0	4.1	0.059	1.79	0.83	2.4	4.782	0.07	0.65	0.2	48
	Opx-Grt-Bt Gneiss													
121	67.3	0.49	13.2	3.6	5.0	0.09	2.51	0.91	5.4	0.35	0.09	1.0	0.10	10
122	54.4	0.83	16.8	4.3	6.3	0.21	3.71	3.79	5.0	1.13	0.12	1.8	1.10	32
811	54.3	0.81	16.7	3.1	7.0	0.21	5.33	6.08	5.1	0.59	0.16	0.8	0.20	83
812	67.2	0.76	13.6	1.8	4.1	0.09	2.13	3.51	4.8	0.47	0.19	0.5	0.10	16
1322	55.6	1.16	12.0	3.6	12.0	0.25	5.53	4.56	3.5	0.19	0.15	0.9	0.00	91
4502	55.6	1.27	15.9	3.3	6.7	0.16	5.94	4.56	4.3	0.75	0.06	1.1	0.00	68
9401	67.4	0.70	11.4	3.4	7.6	0.26	2.84	1.94	2.2	0.65	0.11	0.5	1.00	24
9403	67.4	0.80	11.5	4.9	6.0	0.25	2.86	1.89	3.2	0.48	0.03	0.6	0.20	19
9504	73.1	0.34	12.3	0.0	2.4	0.05	1.38	4.26	2.8	1.12	0.05	0.8	1.30	8
9505	53.7	2.64	13.9	4.2	9.7	0.24	4.46	6.73	2.0	0.29	0.73	0.5	0.10	56
9506	69.7	0.60	13.5	0.7	4.0	0.10	2.28	2.13	3.8	1.83	0.09	0.9	0.10	13
9507	73.7	0.60	10.8	1.0	3.7	0.06	2.51	1.49	2.9	1.92	0.03	0.9	0.10	14
9509	67.8	0.76	14.2	1.1	3.7	0.09	3.00	2.51	3.5	1.85	0.09	0.8	0.00	34
9801	66.8	0.60	16.0	1.3	2.7	0.06	2.11	5.45	3.2	1.18	0.26	0.7	0.20	29
9803	63.9	0.71	14.5	2.8	3.8	0.19	3.21	5.52	4.4	0.36	0.13	0.7	0.20	48
9902	82.6	0.55	7.5	1.0	3.0	0.05	1.40	1.59	1.4	0.95	0.11	0.4	0.00	58

	Ni	Co	Sc	V	Zn	Mo	Be	S	Cu	Se	As	Sb	Au (ppb)	Rb	Cs
2521	59	48	31.0	150	100	1.0	1.2	1033	110	0.1	0.32	0.05	0.05	21	1.80
2522	91	41	31.8	170	93	3.0	0.9	1596	140	0.21	0.29	0.09	0.10	34	2.70
2621	42	37	33.2	210	120	6.0	1.4	775	57	0.02	0.2	0.02	0.05	42	4.40
2712	250	69	35.4	230	170	0.5	0.9	67	11	0.005	0.21	0.01	0.05	76	9.50
2722	135	52	49.8	330	120	2.0	0.7	914	97	0.13	0.1	0.05	0.17	15	0.25
3221	21	48	41.0	200	200	6.0	3.3	3498	60	0.15	1.39	0.08	0.81	93	3.00
3311	52	60	26.2	260	170	2.0	1.6	1055	40	0.06	0.52	0.06	0.12	60	3.20
3321	22	38	32.1	170	160	1.0	3.1	1216	44	0.05	0.94	0.1	0.18	60	3.40
3411	43	43	36.8	210	65	0.5	1.2	71	18	0.06	0.48	0.04	0.12	42	2.40
3412	60	60	42.1	220	47	1.8	0.6	628	50	0.08	0.64	0.04	0.05	20	1.30
	Calc-silicates														
5501	25	32	25	190	160	3.0	0.9	1265	40		4.11	0.34	0.68	59	1.3
5502	1.0	8.0	6.5	54	69	0.5	2.3	1642	1400		2.38	0.11	18.43	16	0.25
5503	1.0	3.0	2.5	19	7.0	0.5	1.6	774	81		1.58	0.03	1.56	21	0.25
5504	57	52	58.8	360	200	0.5	0.5	1912	73		3.97	0.16	0.58	66	2.4
7202	356	49	37.9	178	96	2.0	1.0	4800	275	0.3	33.41	0.13	2.04	70	4.6
7204	427	52	36.3	162	88	1.0	3.0	4200	250	0.2	43	0.13	2.61	85	4.3
8003	60	43	47.2	428	105	0.5	0.5	2200	190		0.75	0.1	1.27	14	1.2
	Garnet-Biotite Gneiss														
1912	37	37	20.4	160	140	2.0	2.2	1526	44	0.09	0.24	0.03	0.10	115	2.60
1922	30	26	16.0	140	87	2.0	0.8	2273	37	0.26	0.64	0.04	0.52	105	1.25
2011	4.0	11	10.0	41	64	2.0	1.5	218	10	0.03	0.9	0.08	0.41	137	1.30
2021	5.0	14	18.0	62	69	2.0	0.4	80	7.0	0.03	0.92	0.08	0.28	134	1.00
2022	22	15	15.0	59	66	2.0	0.3	65	13	0.01	0.11	0.02	0.25	63	0.50
2111	28	25	15.0	110	150	2.0	1.9	395	16	0.04	0.12	0.01	0.29	142	2.50
2112	25	23	31.3	130	94	3.0	1.3	1077	30	0.09	0.21	0.05	0.19	54	1.80
2121	9.0	12	17.0	53	85	2.0	0.9	25	4.0	0.02	0.07	0.01	0.56	141	0.90
2122	11	15	12.0	51	76	2.0	1.4	478	13	0.03	0.31	0.08	0.28	133	1.50
7101	9.0	4.0	13.0	50	53	2.0	1.0	800	20	0.03	0.19	0.05	0.38	109	0.90
7102	17	4.0	18.0	65	51	0.5	0.9	250	12	0.02	0.37	0.05	0.70	97	1.00
7103	20	10	20.0	79	65	1.0	0.7	200	10	0.03	0.19	0.05	0.85	133	1.40
	Opx-Grt-Bt Gneiss														
121	8	47	16	48	230	4.0	0.2	10087	70	0.4	1.05	0.11	0.25	7.0	0.25
122	20	33	31.5	180	1600	3.0	0.7	9270	150	0.8	0.92	0.09	0.89	94	5.00
811	44	33	27.7	200	110	2.0	0.7	529	20	0.13	0.68	0.07	0.22	14	0.25
812	11	25	32.1	59	61	4.0	1.3	5192	430	0.6	0.85	0.11	1.44	15	0.25
1322	50	55	30.1	240	130	2.0	0.7	6681	440	0.43	0.45	0.08	1.18	10	0.25
4502	72	47	35	240	160	0.5	0.9	670	330	0.04	0.05	0.02	0.57	19	0.25
9401	16	59	22	120	53	0.50	0.5	554	40	0.08	0.32	0.04	0.05	48	0.25
9403	13	39	26	100	78	3.0	0.7	235	30	0.08	0.46	0.08	0.30	44	0.50
9504	13	40	7.2	13	78	2.0	1.0	1300	44	0.12	2.6	0.17	0.12	33	1.10
9505	37	62	33	270	270	1.0	1.0	3127	120	0.19	0.17	0.03	0.24	16	0.50
9506	10	36	15	43	42	5.0	0.8	2792	120	8.48	0.51	0.05	0.13	48	0.90
9507	15	31	12	44	51	3.0	0.5	2128	100	9.67	0.32	0.04	0.21	52	0.25
9509	21	44	16	92	710	1.0	0.6	4002	120	0.23	0.49	0.05	0.25	49	1.50
9801	34	35	8.4	68	41	1.0	1.5	25	15	0.02	0.18	0.04	0.05	43	0.25
9803	17	44	19	130	200	2.0	1.0	150	47	0.09	0.09	0.02	0.05	19	0.25
9902	27	56	8.9	75	44	2.0	1.0	1654	54	0.35	0.15	0.02	1.05	60	1.50

	Ba	Sr	Hf	Zr	Y	Th	U	La	Ce	Sm	Eu	Tb	Yb	Lu	F	Cl
2521	197	400	5.0	165	30	0.3	0.2	19	34	5.2	2.0	1.20	3.0	0.4	609	147
2522	129	445	3.0	69	23	0.2	0.4	12	21	4.0	1.0	1.20	3.0	0.4	1087	144
2621	381	177	5.0	108	33	1.9	0.7	48	80	6.5	2.0	1.40	4.0	0.6	780	228
2712	470	100	2.0	42	24	0.7	0.1	12	28	3.6	1.0	0.90	3.0	0.5	2502	208
2722	95	76	1.0	27	20	0.1	0.1	7.0	12	2.4	0.5	0.70	2.0	0.3	1012	275
3221	521	54	14	445	108	4.6	6.0	43	93	15	4.0	3.90	12	2.0	2053	217
3311	509	217	7.0	246	52	1.4	2.0	24	41	6.9	2.0	1.80	5.0	0.8	1042	550
3321	413	78	14	505	96	6.7	5.9	48	92	14	4.0	3.30	9.0	1.5	1424	717
3411	294	157	5.0	110	35	3.0	1.4	17	33	4.9	1.0	1.40	4.0	0.5	706	499
3412	114	213	3.0	47	29	0.3	0.5	5.0	10	3.4	0.5	1.20	3.0	0.4	415	1002
	Calc-silicates															
5501	243	151	3.0	109	50	2.2	2.1	10	24	4.5	0.5	0.8	3.0	0.1	323	380
5502	89	194	0.5	37	38	1.2	0.4	6.0	17	2.3	0.5	0.6	1.0	0.1	25	207
5503	109	187	0.5	38	30	0.7	0.1	10	21	2.6	0.5	0.6	1.0	0.1	25	176
5504	531	107	4.0	112	59	0.1	0.1	11	19	5.2	0.5	1.0	3.0	0.3	722	964
7202	284	93	2.0	59	15	3.0	2.4	6.0	14	3.1	0.5	0.6	2.0	0.1		
7204	452	90	2.0	40	11	1.0	0.6	7.0	14	2.5	0.5	0.5	1.0	0.1		
8003	108	380	4.0	109	23	0.6	0.2	11	33	6.0	2.0	1.3	2.0	0.3		
	Garnet-Biotite Gneiss															
1912	263	156	9.0	238	50	12.0	3.0	47	74	7.0	2.0	1.8	4.0	0.8	792	50
1922	698	119	12.0	319	60	13.0	1.8	46	83	8.0	2.0	1.8	7.0	1.1	646	178
2011	1280	179	9.0	231	36	22.8	2.2	61	105	9.1	0.5	1.7	5.0	0.7	369	206
2021	1801	184	14.0	280	33	26.6	2.7	83	143	11	0.5	2.2	7.0	1.3	321	148
2022	488	181	11.0	247	43	23.5	1.8	77	125	10	1.0	2.1	5.0	0.9	438	50
2111	414	147	15.0	389	40	30.0	3.8	98	152	13	1.0	2.5	4.0	0.9	1127	50
2112	386	132	12.0	392	30	9.4	1.8	39	69	8.1	3.0	2.2	6.0	0.9	688	50
2121	830	144	11.0	291	37	21.3	2.1	70	115	9.2	1.0	1.9	7.0	1.1	253	50
2122	960	181	11.0	284	41	13.0	2.4	44	74	6.2	0.5	1.5	4.0	0.8	489	163
7101	583	157	8.0	220	37	13.0	1.6	38	87	6.1	1.0	1.0	4.0	0.4		
7102	607	123	9.0	263	37	16.0	2.4	54	140	8.7	0.5	1.4	5.0	0.5		
7103	732	114	10.0	287	44	17.0	2.5	57	130	10	2	1.7	5.0	0.6		
	Opx-Grt-Bt Gneiss															
121	59	42	10	82	23	2.0	0.4	12	16	2.6	0.5	1.00	3.0	0.5	25	137
122	137	94	2.0	30	18	0.3	0.6	8.0	11	2.8	0.5	0.25	1.0	0.4	519	50
811	134	109	3.0	38	16	0.1	0.1	8.0	12	2.6	1.0	0.70	1.0	0.1	616	167
812	123	99	7.0	116	40	4.4	1.7	31	53	7.4	0.5	2.20	5.0	0.7	341	286
1322	93	75	6.0	121	45	0.1	0.1	5.0	6	2.1	0.5	0.90	3.0	0.6	495	50
4502	320	216	3.0	51	12	0.5	0.5	5.0	8	1.3	0.5	0.50	1.0	0.2	103	50
9401	231	33	2.0	142	45	1.4	0.5	10	20	6.5	1.0	2.00	5.0	1.0	430	127
9403	152	55	5.0	154	92	0.3	0.3	6	19	2.4	2.0	2.00	17	3.0	222	136
9504	151	62	6.0	254	38	3.2	0.6	13	25	6.0	0.5	1.40	1.0	0.1	413	141
9505	164	117	3.0	215	52	4.2	1.4	23	44	12	3.0	2.00	7.0	0.9		
9506	249	71	4.0	228	42	4.3	0.9	15	33	6.5	1.0	1.70	6.0	0.9	391	136
9507	246	50	4.0	229	77	3.7	0.6	12	21	4.2	2.0	0.90	4.0	0.7	427	136
9509	252	76	5.0	236	37	6.7	0.7	20	58	7.8	1.0	1.30	5.0	0.8	690	130
9801	199	122	3.0	174	18	3.6	0.6	33	67	6.4	1.0	0.70	1.0	0.1	521	50
9803	90	340	3.0	177	27	1.1	0.7	11	28	5.1	0.5	1.20	3.0	0.6		
9902	264	68	3.0	201	71	6.1	1.1	24	43	6.1	0.5	1.50	3.0	0.4	1660	422

Appendix 2-2. Normalization Data Used for Chalcophile Elements

The studied area, Bamble Shear Belt of southern Norway, is a high grade metamorphic terrain composed essentially of amphibolite- and granulite-grade rocks. In the absence of equivalent rocks from lower metamorphic grades in Bamble, a comparison may be made to comparable rocks elsewhere. Comparisons such as this are subject to some uncertainties, the most significant of which being the large variations, in both local and regional scales, in the composition of individual rock types.

The comparisons are only significant if they are based on a large number of representative samples. Small differences among sample populations can be attributed to differences in the original (premetamorphic) materials. In this respect, sedimentary rocks are far more complicated. They include a wide range of original materials, from entirely detrital to entirely chemical components, and variable combinations of these two end members. Volcanic activities simultaneous to sedimentation may contribute to the initial materials of the sedimentary rocks both directly (volcanic fragments and ashes) and indirectly (thermal springs). Abundance of S and Au in shales, for example, have been reported to vary in a wide range from <100 to >10000 ppm and <0.1 to >100 ppb, respectively. Such comparisons become more complicated when considering the fact that even low grades of metamorphism may lead to mobilization and depletion of chalcophile elements (c.f. Glasson and Keays, 1978; Crocket et al., 1983; Korobeynikov, 1991; Renmin et al., 1994).

In an attempt to provide a data base for comparison, a literature compilation has been carried out for chalcophile elements of concern in this study, i.e. Au, As, Sb, Se, S, and Cu (Appendixes 2-2-A-E). A summary of the data is given in the Appendix 2-2-F.

Appendix 2-2-A. Abundance of S, Cu, and Se (ppm) in Various Rocks

I. Sulfur	Range	Mean	Reference
Shale (Post-Archean)	300 - >5000	2700	Various Sources in Wedepohl (1974)
Shale (Archean)	500 - >10000	6600	Cameron and Garrels (1980)
Greywacke	200-1200	700	Pettijohn (1963)
Carbonate Rocks		1200	Turekian and Wedepohl (1961)
Carbonate Rocks		500	Hill et al. (1967)
Felsic Igneous	50-550	300	Various Sources in Wedepohl (1974)
Mafic Igneous	300-1500	900	Various Sources in Wedepohl (1974)
			Cameron (1974)
II. Copper			
Shale (Post-Archean)	15-55	35	Various Sources in Wedepohl
Shale (Archean)	25-115	70	Cameron and Garrels (1980)
Black Shale	20-120	70	"
Greywacke	10-50	30	"
Pelagic Sediments	100-500	300	"
Limestone and Dolomite	1-11	6	"
Schists and Gneisses	10-40	22	"
Granitoids	5-25	13	"
Gabbros and Basalts	50-140	90	"
III. Selenium			
Shale		0.33	Rösler and Beuge (1983)
Shale	0.1-1	0.4	Various Sources in Wedepohl (1974)
Black Shale	0.25-5	2.5	"
Arkose		0.2	"
Carbonates	0.4-30		"
Schist and Gneiss		0.2	Rosler and Beuge (1983)
Granitoids*	0.25-2	0.75	Yoon C. H. (1991)
"	0.02-0.08	0.04	Borodin et al. (1972)
"	<0.1-0.2	0.14	Various Sources in Wedepohl (1974)
Gabbro	0.39-0.73	0.6	Yoon C. H. (1991)
Mafic (Intrusive and extrusive)	<0.1-0.2	0.13	Various Sources in Wedepohl (1974)
Basalts	0.05-0.3	0.15	Borodin et al. (1972)

* A general term for intrusive igneous rocks dominated by quartz and feldspar.

Appendix 2-2-B. Abundance of As (ppm) in Various Rocks

I. Sedimentary	Range	X	1σ	GM	Reference
Shale (Archean)	10-75	46			Cameron and Garrles (1980)
Shales and Slates (Various ages)	0.3-30	12			Various Sources in Wedepohl (1974)
Sahle and Argillite (Precambrian)	0.3- >100	14.5	13.8	9.4	Boyle and Jonasson (1973)
Claystone and Shale (Paleozoic)		15			Rösler and Beuge (1983)
Shale (PAAS)[1]	4-10	7			Sims et al. (1990)
Shale (NASC)[2]		28.4			Gromet et al. (1984)
Shale (LPCS)[3]	5-80	23			Cameron and Garrels (1980)
Pelagic Clays		11			Crocket et al. (1973)
Limestone, Dolomite	0.1-20	2.6	3	1.5	Boyle and Jonasson (1973)
Limestone, Dolomite	0.2-8	1.5			Various Sources in Wedepohl (1974)
II. Metasedimentary (Greenschist Facies)					Post-Archean australian Shale
Greywacke		11			Glasson and Keays (1978)
Greywacke	1-3.8	2.3	0.96		Crocket et al. (1983)
Slate	0.75-5.3	2.12	2.5		Crocket et al. (1983)
Greywacke and Slate		17.2	12.3		Yingjun and Junfeng (1992)
Slate and Phyllite	0.5-100	18	16.5	10.7	Boyle and Jonasson (1973)
Shale (NAMSC)[4]		11.4	3.1		Gromet et al. (1984)
Siltstone		39			Glasson and Keays (1978)
Sandstone		17		12	Various Sources in Wedepohl (1974)
III. Igneous (Felsic)					
Granite-Granodiorite	0.25-10	1.7			Yoon C. H. (1991)
Granitoids*	0.18-15	1.29	1.38	0.93	Boyle and Jonasson (1973)
Granitoids		1.5	0.9		Taner (1993)
Granite	0.4-3	1.5			Various Sources in Wedepohl
Granite-Granodiorite	0.2-1	0.5			Esson et al. (1965)
Intermediate		2.1			Various Sources in Wedepohl
IV. Igneous (Mafic)					
Gabbro	0.4-4	1.25			Yoon Chuang Han (1991)
Gabbro, Diabase	0.06-28	1.5	1.6	0.85	Boyle and Jonasson (1973)
Gabbro	0.2-5	1.4			Various Sources in Wedepohl
Basalt	0.5-4	1.5			Various Sources in Wedepohl
Basalt	0.18-100	2.3			Boyle and Jonasson (1973)
Basalt	0.1-6	1			Bartel et al. (1963)

X = Arithmetic Mean σ = Standard Deviation G.M. = Geometric Mean

1. Post-Archean Australian Shale; 2. North American Shale Composite; 3. Lower Proterozoic Canadian Shale; 4. North American Metamorphosed Shale Composite

* A general term for intrusive igneous rocks dominated by quartz and feldspar.

Appendix 2-2-C. Abundance of Sb (ppm) in Various Rocks.

I. Sedimentary	Range	X	1σ	GM	Reference
Shale (Phanerozoic)		1.5			Various sources in Wedepohl (1974)
Shale and Argillite	0.1-100	1.1	1.3	0.6	Boyle and Jonasson (1984)
Black Shale and Pyritic Shale	<1-48	1.7			Boyle and Jonasson (1984)
Claystone and Shale		1.5			Rösler and Beuge (1983)
Shale (PAAS)[1]	0.3-0.8	0.54			Sims et al. (1990)
Shale (NASC)[2]		2.09			Gromet et al. (1984)
Shale (ACSC)[3]	0.1-6	1.2			Cameron and Garrels (1980)
Shale (LPCSC)[4]	0.1-5	1.3			Cameron and Garrels (1980)
Limestone, Dolomite	0.09-1	0.46	0.28	0.39	Boyle and Jonasson (1984)
Recent Sediments	0.05-1000*	<2.5			Boyle and Jonasson (1984)
Lake Sediments	0.20-1.8	0.75			Boyle and Jonasson (1984)
Ocean Sediments	0.1-7.03	1.9	2.28	0.99	Boyle and Jonasson (1984)
Sandstone and Conglomerate	0.22-54	0.59	0.27	0.54	Boyle and Jonasson (1984)
II. Metamorphic (Greenschist Facies)					
Slate and Phyllite	0.3-1.9	0.9	0.6	0.7	Boyle and Jonasson (1984)
Phyllite		1			Rösler and Beuge (1983)
Mica Schist	1-3.1	2.1	1.5	1.8	Boyle and Jonasson (1984)
Shale (NAMSC)[5]		0.79	4.6		Gromet et al. (1984)
Siltstone		1.8			Glasson and Keays (1978)
Greywacke		1.4			Glasson and Keays (1978)
Greywacke and Slate		1.1	0.9		Yingjun et al., (1992)
Quartzite	<1-1.5	0.8	0.6	0.7	Boyle and Jonasson (1984)
III. Igneous (Felsic)					
Granitoids**	0.015-6.2	0.36	0.66	0.24	Boyle and Jonasson (1984)
"		0.5		0.3	Taner (1993)
"	0.05-1.9	0.48			Yoon (1991)
"		0.2			Onishi and Sandell (1955)
"		0.24			Hamaguchi et al. (1961)
Felsic-Interm.	0.1-0.2	0.15	0.05		Esson et al. (1965)
IV. Igneous (Mafic)					
Intrusive	0.014-2	0.54	0.49	0.27	Boyle and Jonasson (1984)
"	0.03-0.25	0.11	0.08		Esson et al. (1965)
"	0.08-0.51	0.14			Yoon (1991)
Extrusive	0.016-10	1.18	2.21	0.29	Boyle and Jonasson (1984)
"		0.15			Onishi and Sandell (1955)
Mafic-Ultramafic	<0.05-0.15			0.05	Zientek et al. (1990)

X = Arithmetic Mean σ = Standard Deviation G.M. = Geometric Mean

* Values higher than 5 ppm Sb are invariably associated with Sb-bearing deposits or pyritic rocks.

** A general term for intrusive igneous rocks dominated by quartz and feldspar.

1. Post-Archean Australian Shale; 2. North American Shale Composite; 3. Archean Canadian Shale Compo
4. Lower Proterozoic Canadian Shale Composite; 5. North American Metamorphosed Shale Composite

Appendix 2-2-D. Abundance of Au (ppb) in Sedimentary and Metamorphic Rocks

I. Sedimentary	Range	X	1σ	Reference
Argillites and Siltstones (Carbonaceous)	1.4-7	3.20	1.5	Korobeynikov (1990)
Claystone and Shale		1.65		Rösler and Beuge (1983)
Argillite and Slate	0.34-10	1		Allmann and Crocket (1972)
Shale	0.66-8.6	2.3		Shcherbakov (1967)
Carbonaceous Shale	0.1-15	4		Korobeynikov (1985)
Argillite, Sandstone, Siltstone	<1 7	2.60		Voskresenskaya and Zvereva (196
Argillite, Siltstone, Tuffwackes	0.14-8.84	1.12	1.95	Kwong and Crocket (1978)
Carbonate Rocks	0.25-22.4	1.5		Allmann and Crocket (1972)
Conglomerate	1.8-6.3	3.60	1.5	Korobeynikov (1990)
Limestone	<1-3.2	1.00		Voskresenskaya and Zvereva (196
Limestone		2.1		Korobeynikov (1985)
II. Metamorphic (Greenschist Facies)				
Greywacke		3.60	2.23	Yingjun et al. (1992)
Silty Slate		3.10	2.83	Yingjun et al. (1992)
Argillaceous Slate		3.80	3.5	Yingjun et al. (1992)
Argillaceus Quartzite and Shale	0.5-5	2.50		Minnitt et al. (1973)
Siltstone	0.6-1.2	0.77		Glasson and Keays (1978)
Greywacke	0.3-1	0.74		Glasson and Keays (1978)
Phyllite and Slate	<0.5- 7	2.50		Renmin et al. (1994)
Phyllite and Micaschist		1.00		Rösler and Beuge (1983)
Greywacke	<0.2-1.5	0.62		Thorpe and Thomas (1976)
Slate	<0.2-3	1.23		Thorpe and Thomas (1976)
Greywacke	0.22-3.5	1.19	1.05	Crocket et al. (1983)
Slate	0.4-14	1.39	2.44	Crocket et al. (1983)
Greywacke		8.70		Crocket et al. (1986)
Slate		8.00		Crocket et al. (1986)
Shale, Silt, and Sandstone		3.3		Buryak (1971)
Metapelite	2.4-8.2	6.2		Sazanov and Kremenetskiy (1995)
Schists	0.35-9	2.2		Allmann and Crocket (1972)
Micaschists	1.5-2	1.7		Voskresenskaya and Zvereva (196
Carbonaceous Schists	2.33-4.4			Korobeynikov (1990)

X = Arithmetic Mean σ = Standard Deviation G.M. = Geometric Mean

Appendix 2-2-E. Abundance of Au (ppb) in Igneous Rocks

I. Felsic Rocks	Range	X	1σ	G. M.	Reference
Granitoids*	0.1-5.5	1.1			Gottfried et al (1972)
"	0.4-2.74	1.05	0.74	0.88	Kwong and Crocket (1978)
"		2.2			Karelin et al. (1976)
"	0.2-4	1.2			Uvarov et al. (1972)
"	0.2-8	2			Korobeynikov (1986)
"	0.2-7	3			Ishihara et al. (1986)
Granite	0.5-7.4	2.8			Yoon (1991)
Granodiorite	0.4-7.9	1.8			Yoon (1991)
Tonalite-Granodiorite	1-7	2.5			Grabezhev et al. (1986)
Granite	1-6	2			Grabezhev et al. (1986)
Leucogranite-Adamellite	1-8	2.7			Grabezhev et al. (1986)
Tonalite-Trondhjemite	0.5-7.5	1.2	1.1	0.9	Saager and Meyer (1983)
Granodiorite, Adamellite, Granite	0.4-5.2	0.9	0.8	0.9	Saager and Meyer (1983)
Syeno-Granite; Granite; Granodior.	0.4-5.5	0.9	0.8	1.3	Saager and Meyer (1983)
Tonal-Trondhj-Granodior.	0.3-2.4	1.5	1.2	1	Saager and Meyer (1983)
Tonal.-Trondhjem.-Granodior.	1.1-2.6	1.5			Feng et al. (1993)
Tonal.- Granod.- Qtz-Monzonite	0.05-0.6	0.4			Feng et al. (1993)
Syenite-Monzonite-Granite		0.05			Feng et al. (1993)
Syenite and Qtz-Syenite	0.2-2	0.7			Feng et al. (1993)
II. Mafic Rocks					
Tholeiitic Basalts (MORB)	0.5-9	3	3		Crocket and Truta (1977)
Basalts (MORB)		2.3	2		Gottfried and Greenland (1972)
Tholeiitic Basalts	0.33-8.14	1.75	1.67	1.28	Kwong and Crocket (1978)
Tholeiite		0.66	0.5		Gottfried and Greenland (1972)
Basalts (Island Arc)		1.73	1.7		Anoshin and Kepezhinskas (1972)
Basalts (MORB)	0.05 - 5.2	2.1	1.6		Korobeynikov and Pertsev (1995)
Basalts (Island Arc)	0.4 - 7	3.1			Korobeynikov and Pertsev (1995)
Basalt (Continental)	0.5 - 5.2	2.8			Korobeynikov and Pertsev (1995)
Basalt (Earth's crust as a whole)	0.05 - 7	2.7			Korobeynikov and Pertsev (1995)
Gabbroids (Magnetite-Series)	0.4-5.3	1.8			Ishihara et al. (1986)
Gabbroids (Ilmenite-Series)	0.2-0.6	0.4			Ishihara et al. (1986)
Gabbro	0.7-5	2.2			Gavrilenko et al. (1974)
Tholeiitic Gabbro	1.55-3.22	2.44	0.55		Davies and Tredoux (1985)
Magnesian Gabbro	1.77-4.38	3.05	0.89		Davies and Tredoux (1985)
Olivine-normative Tholeiite	0.5-5	1.45	0.95		Zentilli et al. (1985)
Qtz-normative Tholeiite	0.4-6.2	2	1.6		Zentilli et al. (1985)
Mafic Dykes	0.9-12	3.04	3.49		Zentilli et al. (1985)
Gabbro-Diabase	0.2-10	2.8			Korobeynikov (1986)
Mafic-Ultamafic (Intrusive)	0.11-3.25	0.78	0.78	0.55	Kwong and Crocket (1978)

X = Arithmetic Mean σ = Standard Deviation G.M. = Geometric Mean

* A general term for intrusive igneous rocks dominated by quartz and feldspar.

Appendix 2-2-F. Mean (Min-Max) abundance of selected chalcophile elements in principal rock types.

Values extracted from Tables 2-2-A-E .

	S (ppm)	Cu (ppm)	Se (ppm)	As (ppm)	Sb (ppm)	Au (ppb)
Shales and Slates*	2700 (500-5000)	35 (15-55)	0.35 (0.15-0.5)	18 (2-30)	1.5 (0.5-3)	2.5 (0.25-4)
Greywacke*	750 (250-1250)	30 (10-50)	0.25 (0.1-0.5)	5 (1-15)	1 (0.2-2.5)	1.5 (0.1-2.5)
Carbonates	500 (100-1000)	6 (2-10)		2 (0.1-5)	0.45 (0.1-1)	1 (0.1-2)
Felsic Igneous	300 (50-500)	13 (3-25)	0.1 (0.03-0.75)	1.3 (0.25-2.75)	0.2 (0.05-0.5)	1 (0.1-2.5)
Mafic Igneous	900 (500-1400)	90 (40-140)	0.14 (0.05-0.3)	1.5 (0.25-3)	0.45 (0.1-0.75)	2 (0.5-4)
Continental Crust**	697	25	0.12	1.7	0.3	2.5 (1.25)***

* The mean values for shales and greywackes represent, mostly, the post-Archan sediments.

* Wedepohl (1995)

** Considering a dominant granitic composition for the continental crust, the mean value of Au is expected to be close to that in the granitoids. A mean value of 2.5 ppb, as proposed by Wedepohl, seems unrealistic. Considering the relative abundance of the principal rock types and their Au contents, a mean Au value of 1.25 ppb is proposed for the continental crust.

Appendix 3-1. Analysis of acid-intermediate gneisses, Bamble.

Sample No.	SiO_2	TiO_2	Al_2O_3	Fe_2O_3	FeO	MnO	MgO	CaO	Na_2O	K_2O	P_2O_5	H_2O	CO_2	Cr
I. Granulite-Facies														
112	71.1	0.65	14.7	0.7	2.2	0.03	0.6	3.16	4.9	0.46	0.13	0.9	0.3	7.0
211	63.6	0.42	16.2	1.1	3.7	0.08	3.47	5.91	4.5	0.31	0.05	0.6	0.0	115
321	61.0	0.81	15.6	4.4	5.9	0.12	1.76	5.75	3.9	0.13	0.06	0.4	0.3	8.0
411	76.7	0.15	11.1	1.9	1.2	0.04	1.51	1.14	5.2	0.29	0.04	0.5	0.5	8.0
412	67.3	0.61	12.9	3.8	3.7	0.03	1.76	2.77	4.6	0.2	0.05	1.8	0.3	7.0
421	77.6	0.18	11.8	0.8	1.5	0.02	0.52	1.27	5.4	0.11	0.01	0.4	0.3	9.0
422	76.4	0.3	11.6	1.7	2.4	0.07	0.9	1.13	4.7	0.16	0.02	0.4	0.1	10
511	77.7	0.23	11.6	0.7	1.5	0.03	0.23	2.74	3.9	0.39	0.03	0.3	0.5	7.0
512	76.6	0.22	12.2	0.8	1.6	0.04	0.31	2.66	4.1	0.63	0.02	0.3	0.2	9.0
521	73.9	0.29	13.2	1.6	1.9	0.05	0.36	3.46	3.9	0.36	0.02	0.4	0.5	9.0
522	74.6	0.24	12.7	1.5	1.8	0.04	0.34	3.38	3.8	0.35	0.02	0.6	0.3	7.0
611	60.9	0.88	14.4	3.0	7.0	0.19	3.6	4.45	4.8	0.15	0.08	0.6	0.1	24
621	58.7	0.96	15.6	2.3	6.2	0.23	3.87	5.51	5.7	0.21	0.11	0.7	0.0	20
622	57.6	0.95	15.8	2.4	4.8	0.15	2.09	5.82	5.4	0.21	0.09	2.0	2.9	23
711	54.6	1.19	16	4.4	9.0	0.28	5.05	4.89	4.2	0.12	0.1	0.4	0.0	10
712	56.4	1.1	15	4.2	8.0	0.34	4.94	5.81	3.5	0.17	0.11	0.6	0.0	9.0
721	64.9	0.69	14.3	1.9	4.6	0.14	2.74	4.71	4.1	1.07	0.07	0.5	0.0	36
722	65.5	0.69	14.3	1.8	4.8	0.17	2.86	4.72	4.2	0.79	0.08	0.5	0.0	38
821	71.1	0.5	13.8	2.9	1.0	0.03	1.11	3.16	4.8	0.57	0.12	0.6	0.1	23
911	62.2	0.76	14.6	2.5	5.2	0.13	3.34	6.49	3.7	0.54	0.13	0.5	0.1	39
912	63.0	0.79	15.2	2.5	4.7	0.15	3.26	6.03	3.9	0.59	0.11	0.6	0.0	65
921	73.8	0.49	11.4	1.6	2.3	0.07	1.39	3.63	3.3	0.59	0.12	0.8	0.1	26
922	68.9	0.7	13.7	1.8	3.4	0.09	1.95	4.04	4.0	0.64	0.13	0.4	0.0	29
1011	73.5	0.38	13.6	1.5	1.7	0.02	0.76	2.63	4.7	0.76	0.06	0.5	0.1	9.0
1012	68.4	0.58	14.7	2.0	2.6	0.06	1.67	3.8	5.4	0.32	0.1	0.6	0.2	11
1021	71.3	0.59	13.4	1.4	2.8	0.08	1.36	2.82	4.8	0.36	0.14	0.4	0.1	10
1022	69.9	0.54	14.4	2.0	2.1	0.03	1.19	2.97	4.7	1.16	0.15	0.8	0.1	7.0
1111	63.9	0.88	15.5	1.5	5.2	0.21	2.68	3.66	4.8	0.87	0.14	0.6	0.1	40
1112	64.1	0.82	13	2.3	5.2	0.12	3.67	4.54	3.3	1.38	0.14	1.3	0.3	34
1121	58.0	0.85	17.6	1.7	6.1	0.08	4.63	1.89	7.2	0.38	0.12	0.8	0.2	16
1122	71.8	0.46	14	1.2	2.9	0.05	1.33	1.37	5.4	0.94	0.04	0.6	0.1	11
1212	66.2	0.69	15	3.1	2.5	0.07	1.35	4.5	4.8	0.36	0.13	0.6	0.9	35
1222	55.7	1.09	15.4	4.3	9.4	0.31	4.37	3.88	4.8	0.23	0.25	0.7	0.1	9.0
1311	75.2	0.32	12.2	2.0	3.3	0.11	0.73	1.71	4.3	0.23	0.03	0.6	0.1	11
1312	66.3	0.4	15.8	0.9	3.3	0.07	2.61	5.71	4.1	0.41	0.08	0.6	0.0	110
1321	58.7	1.06	14.4	4.3	7.6	0.29	3.3	5.31	4.0	0.36	0.25	0.5	0.2	20
1421	74.1	0.25	12.9	1.0	2.2	0.06	0.46	2.51	4.0	0.73	0.06	1.3	0.7	10
1422	72.4	0.3	13.4	1.6	2.6	0.06	0.47	2.74	4.4	0.54	0.04	0.8	0.6	10
1511	64.8	0.49	14.2	2.0	6.8	0.12	2.32	2.29	3.8	0.45	0.05	2.8	0.7	15

Sample No.	Ni	Co	Sc	V	Zn	Mo	Be	S	Cu	Se	As	Sb	Au (ppb)	Rb	Cs	Ba
112	8.0	18	18	22	26	3.0	0.4	1502	92	0.01	3.51	0.09	1.21	12	1.1	62
211	51	33	14	90	63	4.0	0.5	320	41	0.01	0.25	0.02	0.66	2.0	0.25	82
321	10	38	28	120	55	2.0	0.5	459	19	0.02	0.05	0.02	0.17	1.0	0.25	68
411	8.0	22	9.0	8.0	18	3.0	0.3	125	6.0	0.01	0.02	0.02	0.12	2.0	0.25	97
412	6.0	24	23	22	48	3.0	0.4	699	23	0.04	0.78	0.07	0.17	2.0	0.25	85
421	8.0	22	9.0	11	5.0	4.0	0.5	279	15	0.01	0.02	0.02	0.14	0.5	0.25	90
422	4.0	37	11	23	15	3.0	0.1	120	5.0	0.01	0.04	0.01	0.05	1.0	0.25	77
511	8.0	21	5.0	24	15	3.0	0.4	635	46	0.08	0.2	0.04	0.54	4.0	0.25	113
512	8.0	25	8.0	16	19	3.0	0.5	418	30	0.07	0.05	0.02	0.12	9.0	0.25	168
521	9.0	41	10	11	15	2.0	0.5	119	11	0.01	0.24	0.02	0.05	4.0	0.25	118
522	7.0	33	9.0	9.0	14	3.0	0.6	123	9.0	0.01	0.39	0.04	0.13	4.0	0.7	85
611	28	38	27	170	77	3.0	1.1	1586	94	0.07	0.24	0.04	1.11	1.0	0.25	102
621	23	29	31	200	49	3.0	0.9	142	19	0.01	0.15	0.03	0.05	2.0	1.1	85
622	25	24	31	200	70	3.0	1.3	205	18	0.01	0.41	0.05	0.05	6.0	0.8	68
711	24	41	37	270	140	2.0	0.8	293	41	0.01	0.01	0.01	0.05	1.0	0.25	71
712	16	39	33	270	130	2.0	0.8	121	16	0.01	0.01	0.01	0.05	1.0	0.25	82
721	19	37	19	100	100	3.0	0.6	386	50	0.04	0.02	0.01	0.16	18	0.25	377
722	20	46	20	100	110	3.0	0.6	334	49	0.04	0.04	0.02	0.15	7.0	0.25	319
821	17	8.0	11	48	36	4.0	1.1	255	11	0.03	0.03	0.01	0.62	5.0	0.25	95
911	22	23	22	160	81	3.0	0.6	742	61	0.15	0.18	0.01	0.33	3.0	0.25	196
912	23	20	23	150	81	2.0	0.6	60	7.0	0.01	0.12	0.1	0.05	4.0	0.25	144
921	11	11	18	75	65	2.0	0.5	97	19	0.02	0.26	0.03	0.3	8.0	0.25	161
922	14	13	18	98	71	2.0	0.7	122	16	0.02	0.28	0.03	0.35	7.0	0.25	168
1011	5.0	6.0	5.0	34	23	3.0	0.5	25	5.0	0.01	0.04	0.01	0.1	21	0.25	234
1012	9.0	9.0	5.0	93	36	3.0	0.8	142	10	0.01	0.13	0.01	0.17	3.0	0.25	123
1021	16	9.0	12	44	41	4.0	0.6	273	16	0.01	0.14	0.03	0.26	2.0	0.9	193
1022	6.0	8.0	10	43	33	2.0	0.4	51	4.0	0.01	0.08	0.01	0.05	25	0.25	305
1111	14	15	20	110	92	2.0	0.7	195	27	0.04	0.25	0.01	0.15	4.0	0.25	129
1112	22	21	17	120	87	2.0	0.6	119	16	0.02	0.11	0.01	0.54	51	0.25	250
1121	12	19	26	130	50	3.0	0.3	293	14	0.06	0.02	0.01	0.1	3.0	0.25	111
1122	7.0	7.0	11	41	26	2.0	0.4	25	8.0	0.01	0.06	0.01	0.1	6.0	0.25	148
1212	16	13	14	97	49	4.0	0.6	304	15	0.03	0.21	0.01	0.16	3.0	0.25	147
1222	21	28	33	140	94	3.0	0.6	1554	130	0.06	0.16	0.03	0.38	1.0	0.25	105
1311	10	8	10	35	47	4.0	0.3	25	13	0.02	0.55	0.03	0.13	3.0	0.25	67
1312	44	21	11	75	68	3.0	0.6	77	7.0	0.01	0.17	0.01	0.05	3.0	0.25	138
1321	20	29	32	230	110	3.0	0.7	110	18	0.03	0.24	0.03	0.78	3.0	0.7	156
1421	8.0	6.0	9.0	12	40	2.0	0.6	66	8.0	0.01	1.89	0.24	0.44	16	0.25	123
1422	8.0	7.0	10	15	46	2.0	0.5	25	9.0	0.01	2.11	0.12	0.12	4.0	0.25	132
1511	16	17	21	97	100	2.0	0.8	59	14	0.02	6.77	0.1	2.73	8.0	0.25	90

Sample No.	Sr	Hf	Zr	Y	Th	U	La	Ce	Sm	Eu	Tb	Yb	Lu	F	Cl
112	205	7.0	77	17	0.8	0.5	14	28	3.3	0.5	0.8	2.0	0.4	147	136
211	361	6.0	39	10	0.1	0.1	11	9.0	1.6	0.5	0.8	1.0	0.2	356	50
321	128	6.0	58	29	0.1	0.1	6.0	9.0	2.3	1.0	1.2	3.0	0.5	263	50
411	73	12	214	66	2.5	0.7	24	31	5.0	0.5	1.8	7.0	1.1	54	50
412	98	5.0	52	50	2.3	0.3	9.0	20	4.3	0.5	1.5	5.0	0.7	109	50
421	92	12	219	67	2.8	1.2	16	32	5.4	0.5	2.0	7.0	1.2	25	50
422	82	11	141	41	1.1	0.3	10	15	3.0	0.5	1.6	5.0	0.8	25	50
511	114	10	174	36	0.1	0.3	16	9.0	0.78	0.5	0.7	5.0	0.3	25	50
512	105	10	147	40	4.1	0.5	9.0	44	5.5	0.5	1.7	5.0	0.9	105	50
521	119	9.0	143	37	0.1	0.3	12	10	2.1	0.5	1.6	4.0	0.7	64	50
522	125	9.0	104	35	1.2	0.5	10	16	3.0	0.5	1.6	4.0	0.7	91	50
611	75	6.0	95	24	0.5	0.4	11	14	2.6	1.0	1.1	3.0	0.5	217	152
621	114	4.0	56	34	0.1	0.2	7.0	9.0	3.5	0.5	1.1	3.0	0.5	773	50
622	151	3.0	49	19	0.3	0.3	17	11	2.2	1.0	0.8	2.0	0.3	443	155
711	69	4.0	74	22	0.2	0.1	8.0	14	2.8	2.0	0.8	2.0	0.4	157	50
712	86	4.0	59	31	0.1	0.1	7.0	8.0	2.8	0.5	1.1	2.0	0.4	594	50
721	229	7.0	111	26	0.1	0.2	8.0	18	2.9	0.5	1.1	3.0	0.4	625	50
722	222	8.0	154	31	0.1	0.1	10	20	3.5	0.5	1.5	3.0	0.6	381	50
821	188	10	154	22	3.9	0.9	8.0	25	3.3	0.5	0.9	3.0	0.4	209	50
911	171	7.0	111	30	0.1	0.1	16	21	3.3	0.5	1.1	3.0	0.5	577	50
912	158	5.0	75	27	1.2	0.4	11	18	3.2	0.5	1.2	3.0	0.5	487	50
921	157	11	254	24	0.8	0.5	13	18	3.2	0.5	1.1	3.0	0.6	381	126
922	158	8.0	209	37	0.4	0.4	14	23	4.6	0.5	1.4	4.0	0.6	270	105
1011	146	13	174	15	1.5	0.4	8.0	12	2.4	0.5	1.2	1.0	0.4	341	50
1012	167	12	131	30	2.2	0.5	10	17	2.5	0.5	1.3	1.0	0.3	783	50
1021	125	9.0	212	25	1.6	0.7	15	27	4.1	0.5	1.6	4.0	0.5	92	50
1022	155	9.0	171	12	1.0	0.5	19	15	2.0	0.5	0.6	1.0	0.2	552	50
1111	154	10	234	22	1.7	0.6	11	26	4.4	1.0	1.5	4.0	0.7	167	50
1112	126	8.0	198	57	1.0	0.6	19	21	3.7	1.0	1.2	3.0	0.5	848	50
1121	95	6.0	191	22	2.6	1.0	7.0	20	4.4	2.0	1.3	3.0	0.5	414	50
1122	81	8.0	233	38	5.2	0.9	5.0	19	3.2	0.5	1.4	5.0	0.8	587	50
1212	202	10	171	17	2.2	0.6	10	23	3.4	0.5	1.3	3.0	0.5	296	50
1222	116	6.0	62	27	0.1	0.1	7.0	14	3.8	0.5	1.4	3.0	0.6	177	50
1311	63	11	148	47	1.3	0.1	8.0	21	3.7	1.0	2.2	6.0	1.0	55	179
1312	331	6.0	57	14	0.1	0.1	13	16	1.6	0.5	0.8	1.0	0.1	504	50
1321	146	4.0	46	22	0.1	0.1	14	16	3.2	0.5	0.8	3.0	0.4	858	114
1421	150	7.0	113	25	0.1	0.2	7.0	15	2.4	0.5	1.2	3.0	0.6	93	195
1422	144	6.0	128	27	0.1	0.3	13	13	2.5	0.5	1.1	4.0	0.7	62	185
1511	99	5.0	103	30	0.7	0.4	10	15	4.1	0.5	1.7	4.0	0.6	106	485

Sample No.	SiO_2	TiO_2	Al_2O_3	Fe_2O_3	FeO	MnO	MgO	CaO	Na_2O	K_2O	P_2O_5	H_2O	CO_2	Cr
1512	70.7	0.41	14	2.0	3.1	0.08	1.06	3.62	3.7	0.52	0.07	1.2	0.3	11
1521	71.6	0.2	14.6	1.4	1.9	0.08	0.46	3.83	3.6	0.86	0.05	0.9	0.5	11
1522	57.1	1.3	15.3	3.5	5.4	0.12	1.89	9.09	3.1	0.74	0.48	1.6	0.8	96
1612	64.1	0.65	16.7	1.2	3.6	0.1	2.53	3.86	5.3	1.06	0.21	0.6	0.2	42
1621	54.3	1.37	16.1	4.6	6.4	0.19	4.68	6.98	4.7	0.36	0.21	0.7	0.1	58
1622	62.2	0.75	17	1.3	4.1	0.1	2.88	5.14	4.9	0.71	0.26	0.4	0.1	43
1721	60.2	0.83	14.5	4.9	4.2	0.11	2.85	5.18	5.4	0.88	0.19	0.7	0.1	57
1811	75.4	0.15	14.5	0.1	1.1	0.01	0.4	1.46	6.9	0.16	0.05	0.6	0.1	7.0
3803	69.6	0.5	14	2.1	3.2	0.13	1.68	1.47	6.8	0.46	0.14	0.6	0.1	9.0
9803	63.9	0.71	14.5	2.8	3.8	0.19	3.21	5.52	4.4	0.16	0.13	0.7	0.2	48
II. Amphibolite-Facies														
2311	75	0.2	12.4	0.3	2.2	0.02	1.64	2.06	3.7	1.38	0.02	0.9	0.0	21
2312	76.9	0.21	11.4	0.4	2.7	0.03	0.94	0.99	4.6	1.03	0.01	0.6	0.0	9.0
2321	77.5	0.19	11.6	0.8	2.2	0.02	0.37	1.56	4.4	0.85	0.01	0.4	0.0	7.0
2322	75.2	0.2	12.1	1.0	2.7	0.03	0.97	2.4	3.7	1.09	0.02	0.5	0.0	35
2512	57.3	0.88	18.6	2.3	4.6	0.1	2.67	7.67	4.3	0.76	0.1	0.8	0.0	27
2622	64.3	0.59	14.9	1.7	4.7	0.14	2.66	3.93	4.3	1.75	0.04	0.8	0.1	44
3511	57.0	0.79	16.2	2.5	5.4	0.14	3.6	7.4	4.1	1.34	0.1	1.2	0.0	46
3612	64.7	0.87	13.7	3.0	4.7	0.2	2.3	4.22	3.8	1.53	0.09	0.9	0.0	28
3806	63.3	0.66	14.8	2.6	4.8	0.19	3.01	3.4	4.3	1.34	0.07	1.4	0.1	41

Sample No.	Ni	Co	Sc	V	Zn	Mo	Be	S	Cu	Se	As	Sb	Au (ppb)	Rb	Cs	Ba
1512	11	11	19	24	67	3.0	0.6	104	16	0.03	0.81	0.06	0.36	5.0	0.7	178
1521	9.0	8.0	8.0	14	38	3.0	0.6	62	13	0.01	1.43	0.05	0.21	17	0.25	177
1522	41	24	13	82	110	2.0	0.7	501	42	0.05	3.76	0.59	0.75	20	0.9	162
1612	33	21	9	68	99	2.0	0.8	25	7.0	0.01	0.05	0.01	0.05	12	0.7	421
1621	49	40	25	220	93	4.0	0.9	772	140	0.09	0.05	0.01	0.17	1.0	0.25	129
1622	38	22	11	83	77	2.0	0.7	53	9.0	0.01	0.06	0.01	0.05	5.0	0.25	249
1721	30	22	18	130	69	2.0	0.7	25	9.0	0.01	0.25	0.02	0.16	5.0	0.25	142
1811	6.0	4.0	14	16	51	3.0	0.3	25	7.0	0.01	0.56	0.03	0.05	0.5	0.25	53
3803	14	8	15	41	50	0.5	0.7	240	4.0	0.02	0.08	0.02	0.14	4.0	0.25	102
9803	17	44	19	130	200		0.5	150		0.09	0.09	0.02	0.05	19	0.25	90
2311	12	33	3.0	15	23	3.0	8.4	441	43	0.05	0.12	0.03	0.05	96	48	183
2312	9.0	27	7.0	13	52	4.0	3.4	336	23	0.03	0.04	0.03	0.05	39	10	274
2321	6.0	26	5.0	10	15	5.0	2.1	266	20	0.02	0.07	0.03	0.11	28	5.9	172
2322	15	21	8.0	14	22	3.0	12	134	19	0.02	0.05	0.03	0.05	60	16	180
2512	33	38	18	130	66	0.5	1.1	601	64	0.07	0.29	0.03	0.25	25	1.3	200
2622	35	32	14	78	120	1.0	3.2	303	26	0.03	0.1	0.04	0.05	99	18.2	281
3511	29	36	27	190	72	2.0	1.4	931	99	0.16	1.89	0.09	0.17	38	1.3	336
3612	21	27	18	120	78	2.0	1.8	50	14	0.01	1.12	0.16	0.05	56	5.3	319
3806	41	48	17	130	190	1.0	0.5	5795	630	0.91	8.38	0.16	2.99	40	0.7	262

Sample No.	Sr	Hf	Zr	Y	Th	U	La	Ce	Sm	Eu	Tb	Yb	Lu	F	Cl
1512	83	6.0	56	66	1.0	0.3	11	16	6	0.5	2.3	5.0	0.9	103	149
1521	203	5.0	84	32	0.1	0.1	12	12	1.4	2.0	1.1	3.0	0.5	77	232
1522	235	7.0	176	27	2.3	1.0	5.0	41	6.3	0.5	1.1	1.0	0.4	387	618
1612	374	6.0	115	7.0	0.1	0.1	14	26	2.1	0.5	0.25	1.0	0.1	225	106
1621	267	5.0	81	29	0.1	0.1	8.0	16	2.5	0.5	1.0	1.0	0.3	341	50
1622	434	5.0	128	14	0.1	0.1	5.0	25	3.1	0.5	0.8	1.0	0.2	25	50
1721	134	4.0	91	23	0.1	0.1	7.0	21	3.2	2.0	0.9	3.0	0.4	156	132
1811	70	5.0	165	20	2.6	0.3	11	18	2.2	1.0	0.25	3.0	0.3	414	50
3803	59	5.0	105	22	2.7	0.5	11	37	4.4	0.5	1.0	2.0	0.5	72	50
9803	340	3.0	177	27	1.1	0.7	6.0	28	5.1	0.5	1.2	3.0	0.6	944	50
2311	226	18	348	85	7.4	3.1	28	50	18	2.0	5.6	14	2.3	1500	50
2312	96	18	385	96	6.9	2.6	48	87	13	2.0	3.9	10	1.5	475	50
2321	161	18	383	98	6.5	2	43	86	13	3.0	4.0	12	1.9	133	50
2322	256	18	358	102	7.9	2.9	63	123	15	3.0	4.7	14	2.0	462	50
2512	412	4.0	107	27	0.4	0.2	22	40	3.0	2.0	0.6	1.0	0.2	265	241
2622	173	4.0	68	31	1.3	1.1	17	22	1.9	1.0	1.2	4.0	0.6	956	100
3511	396	6.0	112	24	5.4	1.1	25	40	4.6	2.0	1.1	3.0	0.4	472	159
3612	232	7.0	229	39	4.6	2.5	16	27	5.3	2.0	1.3	4.0	0.8	496	153
3806	220	4.0	100	20	1.0	0.3	27	73	2.0	0.5	0.7	1.0	0.3	419	703

Appendix 3-2. Comparison of Archean and Proterozoic High-Al and Low-Al Tonalite-Trondhjemite Suites

Age	Proterozoic	Proterozoic	Archean	Archean	Archean	Proterozoic	Proterozoic
Type	Low-Al	Low-Al	High-Al	High-Al	Low-Al	High-Al	Low-Al
Metam. Facies	Granulite[1]	Amphibolite[1]	Granulite[2]	Amphibolite[3]	Greensch.-Amphib.[4]	Amphibolite[5]	Amphibolite[6]
Cs *	0.25	4.5	0.7	0.55	0.6	0.55	1.2
Rb	6.3	45	10	52	15	50	32
Ba	132	250	590	550	292	575	390
K_2O	0.5	1.22	1.3	1.75	0.63	1.95	0.4
Th	1.1	4.5	1.5	7.0	3.3	4.0	na#
U	0.38	1.7	0.4	2.0	1.2	1.5	na
La	11	30	23.5	25	17.5	18	32
Ce	19	55	41	43	40.4	35	50
Sr	144	240	450	425	131	410	145
P_2O_5	0.11	0.07	0.15	0.16	0.11	0.08	0.04
Zr	126	225	150	160	222	150	150
Hf	7.2	11	3.8	4.0	4.6	4.75	6.5
Sm	3.3	8.0	2.9	3.65	4.2	3.1	5.5
TiO_2	0.62	0.57	0.44	0.349	0.51	0.47	0.18
Y	28	57	7.0	10	55	15	30
Yb	3.06	7.0	0.8	0.95	3.68	1.15	4.85
Lu	0.52	1.1	0.16	0.19	0.58	0.19	0.81
Sc	17	18	9.0	12	10	7.0	na
V	88	82	25	na	83	19	na
Zn	63	60	32	na	41	35	na
Cr	26	33	28	24	21	na	1.0
Co	22	31	21	25	11	na	3.0
Ni	17	24	24	14	17	18	na

1. Present study
2. Weaver and Tarney (1980); Jahn and Zhang (1984); Condie and Allen (1984); Rudnick and Taylor (1986)
3. Martin (1987); Arth et al. (1978)
4. Feng et al. (1993)
5. Anderson and Cullers (1978); Puffer and Volkert (1991)
6. Barker et al. (1978); Condie (1978)

* oxides in %; elements in ppm.

not available

Appendix 3-3. Analysis of Bamble Alkali Granites. (Oxides in %, Elements in ppm)

	SiO_2	TiO_2	Al_2O_3	Fe_2O_3	FeO	MnO	MgO	CaO	Na_2O	K_2O	P_2O_5	H_2O	CO_2	Cr	Ni
5506	75.6	0.16	11.1	1.7	1.1	0.04	0.41	0.78	1.6	7.21	0.02	0.2	0.50	7.0	2.0
5507	76.4	0.19	11.3	1.5	1.3	0.02	0.54	0.23	1.7	7.16	0.02	0.2	0.00	5.0	0.0
5508	77.1	0.20	11.9	0.4	0.8	0.01	0.46	0.55	3.1	4.74	0.01	0.2	0.00	17	0.0
5509	77.2	0.18	12.4	0.5	0.8	0.03	0.29	1.77	3.2	3.98	0.01	0.2	0.20	13	1.0
5510	76.6	0.20	12.3	0.1	1.2	0.01	0.56	0.65	3.6	4.84	0.03	0.8	0.10	4.0	1.0
5513	77.9	0.21	11.6	0.2	0.8	0.02	0.33	0.86	2.9	4.74	0.01	0.2	0.10	42	0.0
5515	75.7	0.22	11.8	0.6	0.6	0.03	0.24	1.10	2.5	5.75	0.01	0.3	0.40	6.0	3.0
10104	75.5	0.19	11.6	0.5	1.0	0.02	0.76	0.50	2.1	7.17	0.02	0.4	0.30	4.0	1.0
10105	75.9	0.19	11.9	0.4	0.8	0.02	0.46	1.06	3.2	5.68	0.02	0.3	0.20	3.0	1.0
10107	77.2	0.19	12.1	0.7	0.5	0.01	0.34	0.78	2.9	5.56	0.03	0.4	0.10	2.0	1.0
10108	79.8	0.21	10.2	0.1	1.2	0.01	0.73	0.42	2.6	4.68	0.03	0.4	0.20	3.0	1.0

	Co	Sc	V	Cu	Zn	Mo	Be	S	As	Sb	Au (ppb)	Rb	Cs	Ba	Sr
5506	27	6.8	11	7.0	8.0	0.5	0.3	149	0.6	0.1	0.39	120	0.25	1053	93
5507	41	6.1	1.0	2.0	10	0.5	0.3	25	0.2	0	0.05	141	0.50	963	35
5508	53	5.1	0.0	14	7.0	0.5	1.7	181	0.2	0.1	0.16	106	0.25	470	79
5509	50	4.9	0.0	9.0	8.0	0.5	4.3	85	0.2	0	0.18	94	0.25	470	63
5510	240	5.7	1.0	3.0	6.0	nd	1.7	nd	nd	nd	nd	96	0.50	413	32
5513	46	6.9	0.0	20	1.0	0.5	2.3	51	0.2	0.1	0.26	113	0.25	525	31
5515	26	6.5	1.0	6.0	55	0.5	2.3	63	0.3	0	0.05	150	0.60	548	66
10104	25	4.4	1.0	nd*	9.0	nd	nd	nd	nd	nd	nd	180	0.25	523	31
10105	30	4.9	1.0	nd	2.0	nd	nd	nd	nd	nd	nd	137	0.25	535	46
10107	45	5.0	1.0	nd	1.0	nd	nd	nd	nd	nd	nd	133	0.25	645	73
10108	52	2.8	2.0	nd	6.0	nd	nd	nd	nd	nd	nd	124	0.90	372	32

	Nb	Hf	Zr	Y	Th	U	La	Ce	Sm	Eu	Tb	Yb	Lu	F	Cl
5506	23	5.0	231	76	4.3	0.9	42	76	7.8	0.5	0.90	4.0	0.3	84	50
5507	30	5.0	226	27	6.7	1.8	27	46	7.0	0.5	1.30	3.0	0.4	188	50
5508	56	6.0	295	77	25.6	4.6	57	130	12.0	2.0	3.30	7.0	0.5	247	50
5509	24	7.0	259	78	30.1	5.0	67	140	14.0	2.0	3.20	8.0	0.6	59	50
5510	50	7.0	239	103	nd	nd	nd	nd	nd	nd	nd	nd	nd	nd	nd
5513	22	8.0	317	118	33.1	3.6	84	190	19.0	3.0	4.20	10	1.1	189	50
5515	25	8.0	298	101	30.3	6.2	79	170	17.0	0.5	3.80	10	0.7	89	50
10104	38	6.0	231	67	23.2	3.7	44	97	11.4	2.0	2.00	5.0	0.2	nd	nd
10105	52	7.0	231	99	26.7	5.0	54	nd	15.6	1.0	2.90	8.0	0.3	nd	nd
10107	67	5.0	264	49	27.3	4.2	33	71	8.5	0.5	1.60	5.0	0.1	nd	nd
10108	35	4.0	239	40	41.4	4.0	57	110	12.9	0.5	1.90	4.0	0.2	nd	nd

* Not determined

Appendix 4-1. Electron probe analysis of chlorite replacing sulfides in metabasites.

Sample No.	SiO_2	Al_2O_3	TiO_2	Cr_2O_3	FeO	MnO	MgO	CaO	K_2O	Cl	Total
3901	28.77	14.22	0.06	o*	34.08	0.19	10.76	0.21	0.01	o	88.3
3901	27.44	15.28	o	0.04	39.01	0.13	6.45	0.19	o	o	88.54
3904	27.84	15.19	o	0.05	38.61	0.19	6.86	0.3	0.1	0.12	89.26
3904	29.18	15.84	o	0.04	32.27	0.3	11.35	0.26	o	0.02	89.26
3904	28.48	15.78	0.01	0.05	32.2	0.39	11.34	0.31	o	o	88.56
4001	30.1	12.95	o	0.02	29.87	0.2	14.87	0.13	0.02	o	88.16
4001	30.5	14.08	0.03	0.03	28.41	0.25	15.48	0.23	o	0.01	89.02
4001	29.95	15.16	0.06	0.06	28.93	0.27	14.55	0.21	o	0.02	89.21
4003	32.08	11.42	o	0.03	30.03	0.52	11.61	0.72	0.08	0.06	86.55
4003	32.44	11.78	0.03	o	30.2	0.57	12.01	0.67	0.01	o	87.71
4003	37.59	8.68	0.01	0.03	21.84	0.46	12.28	1.94	0.27	0.04	83.14
4003	40.61	8.34	0.05	o	23.06	0.54	12.74	2.19	0.43	0.04	88
4403	29.03	14.4	0.11	0.04	33.62	0.42	11.15	0.35	o	0.01	89.13
4403	28.68	14.83	o	0.04	36.29	0.2	10.32	0.09	o	o	90.45
4403	30.27	13.75	o	0.13	32.8	0.18	10.25	0.31	o	0.35	88.04
4403	26.58	14.2	o	0.13	35.96	0.13	9.57	0.26	o	0.23	87.06
4403	26.62	14.83	o	o	35.67	0.23	9.41	o	o	0.16	86.92
4403	26.54	14.29	o	o	35.08	0.5	9.63	0.24	o	0.22	86.5
5405	26.78	15.76	o	o	32.34	0.19	11.76	1.03	o	0.09	87.95
5405	27.97	16.38	o	0.14	30.19	0.14	13.41	0.99	o	0.25	89.47
5408	28.41	13.9	o	0.03	34.56	0.62	10.23	0.25	o	0.01	88.01
5408	29.87	12.39	0.06	0.09	31.61	0.42	11.93	0.45	0.07	o	86.89
5419	33.89	9.85	o	o	18.43	1.35	19.00	0.46	o	0.04	83.02
5419	34.53	10.32	o	0.02	19.7	0.35	17.53	0.86	o	0.03	83.34

* below detection limit

Appendix 4-2. Analysis of Bamble metabasites. (Oxides in %; Elements in ppm)

	SiO_2	TiO_2	Al_2O_3	Fe_2O_3	FeO	FeO_t	MnO	MgO	CaO	Na_2O	K_2O	P_2O_5	H_2O	CO_2	Cr
Zone A															
6401	45.50	2.03	16.5	2.5	10.5	13.0	0.20	7.10	8.54	3.0	1.03	0.24	1.80	0.30	110
6402	45.80	2.00	16.4	2.3	10.1	12.4	0.23	7.36	9.16	3.1	0.78	0.23	1.60	0.10	84
6404	43.60	3.95	13.45	*	19.0	19.0	0.21	5.06	8.7	2.63	1.43	0.38	0.81	0.4	28
6405	43.97	1.66	14.71		17.0	17.0	0.21	10.6	7.48	2.65	0.46	0.22	0.94	0.2	222
6406	41.47	2.03	11.22		22.1	22.1	0.27	13.6	5.03	1.4	1.20	0.18	2.04	0.4	310
6407	44.03	1.98	16.31		15.9	15.9	0.19	8.39	7.44	3.26	0.81	0.21	1.33	0.2	181
6408	44.52	2.97	15.28		16.2	16.2	0.19	5.81	8.62	3.01	1.35	0.19	1.36	0.4	74
6501	42.16	1.59	16.08		12.8	12.8	0.12	7.4	12.2	1.72	1.96	0.14	2.83	0.9	100
6502	46.55	1.57	16.84		12.3	12.3	0.13	6.51	9.18	3.62	1.09	0.13	1.44	0.4	104
6503	44.84	1.55	16.2		12.8	12.8	0.10	7.79	9.61	3.27	0.91	0.15	2.41	0.4	98
6504	45.04	1.70	15.86		14.0	14.0	0.17	7.69	8.78	3.16	1.20	0.15	1.17	0.3	108
6601	44.09	1.98	16.32		15.8	15.8	0.19	8.38	7.43	3.26	0.81	0.21	1.09	0.3	196
6701	51.07	1.90	15.37		12.5	12.5	0.19	4.04	11.2	2.13	0.81	0.12	0.70	0.2	167
6702	45.48	1.92	14.68		16.4	16.4	0.24	6.98	10.2	2.55	0.58	0.14	0.72	0.2	90
6703	49.09	1.27	15.1		12.4	12.4	0.15	7.94	11	2.16	0.29	0.11	0.86	0.1	155
6801	46.42	2.10	17.7		13.5	13.5	0.23	6.11	8.96	2.98	0.77	0.24	0.77	0.5	67
6802	46.84	1.78	17.9		12.0	12.0	0.16	5.97	8.61	3.24	1.56	0.25	1.27	0.2	58
6803	47.34	3.29	11.9		18.6	18.6	0.31	2.79	7.95	3.46	1.93	1.62	0.97	0.4	
6804	37.88	9.32	10.36		25.3	25.3	0.35	3.53	7.85	2.33	1.11	0.60	0.56	0.4	35
6805	42.64	2.64	12.88		19.5	19.5	0.25	8.55	7.92	2.44	0.75	0.16	0.73	0.4	202
6901	46.21	1.65	18.93		8.6	8.6	0.04	4.66	10	5.62	0.44	0.16	2.01	1.1	77
6902	48.04	1.09	10.92		9.7	9.7	0.06	14.1	10.3	3.06	0.60	0.23	1.42	0.2	60
7001	45.86	1.71	15.33		15.7	15.7	0.22	7.86	9.42	2.28	0.29	0.19	1.24	0.3	64
7002	46.31	1.98	15.32		15.5	15.5	0.21	7.01	8.77	2.78	0.94	0.21	1.05	0.3	71
7201	46.99	1.68	17.11		13.6	13.6	0.17	6.46	9.39	3.19	0.53	0.17	0.61	0.6	54
7203	49.35	1.70	18.41		12.7	12.7	0.25	3.92	8.23	3.42	1.34	0.34	0.88	0.2	14
7401	50.99	1.75	13.68		14.2	14.2	0.21	5.47	9.18	2.92	1.01	0.24	0.26	0.2	114
7404	45.36	2.96	15.77		16.3	16.3	0.23	5.81	9.34	2.8	0.50	0.34	0.42	0.2	120
7501	46.34	1.61	16.51		14.0	14.0	0.23	7.55	8.42	2.75	1.13	0.16	1.22	0.4	101
7502	45.98	1.66	16.46		14.4	14.4	0.21	7.66	9.62	2.36	0.58	0.17	1.01	0.4	88
7503	45.64	1.98	14.17		16.2	16.2	0.21	8.01	8.36	2.39	0.94	0.31	2.01	0.6	57
7601	51.11	0.30	14.27		7.2	7.2	0.13	8.12	12.9	2.65	0.72	0.36	1.88	0.7	244
7602	48.92	0.60	11.29		10.5	10.5	0.20	12.2	12.8	1.77	0.67	0.10	1.15	0.2	275
7701	46.38	1.95	15.49		9.4	9.4	0.02	7.24	9.24	5.5	0.32	0.31	3.08	0.4	130
7703	43.67	2.40	15.01		15.3	15.3	0.11	7.97	9.96	3.31	0.62	0.28	1.31	0.2	104
7801	46.61	1.46	16.25		13.0	13.0	0.17	7.47	10.1	2.78	0.93	0.15	1.31	0.2	113
7802	47.39	1.48	16.12		13.3	13.3	0.18	7.71	10.4	2.5	0.60	0.17	0.66	0.1	116
7901	47.18	0.50	19.73		11.6	11.6	0.10	8.63	9.51	1.67	0.46	0.06	1.18	0.2	51
7902	45.29	3.26	14.36		16.0	16.0	0.25	5.26	8.11	2.92	1.72	1.25	0.87	0.3	49
8301	46.58	1.69	19.73	3.8	7.5	11.3	0.14	5.06	9.89	3.26	0.89	0.15	1.41	0.3	71
9901	51.30	1.54	13.3	3.1	9.0	12.1	0.22	6.19	8.38	3.6	1.42	0.16	1.10	0.20	110

* Blanks: not determined

	Ni	Co	Sc	V	Cu	Zn	S	As	Se	Sb	Au (ppb)	Rb	Cs	Ba	Sr
Zone A															
6401	160	86	25.9	220	110	140	990	45	0.12	1.16	0.78	58	2.90	454	380
6402	120	74	31.0	200	91	120	878	1.82	0.12	0.29	0.46	33	0.25	156	274
6404	66	53	59.6	456		120	2700	1.59		0.13	0.51	26	0.80	392	248
6405	222	84	25.4	190		136	1000	4.01		0.27	1.32	13	0.25	171	417
6406	260	100	21.9	280		178	1200	3.86		0.4	0.53	33	4.30	600	102
6407	167	74	24.8	249		130	1100	10.3		0.4	0.51	19	1.00	416	409
6408	86	53	38.7	316		130	1500	10.6		0.4	1.24	35	0.25	353	295
6501	109	53	39.8	223		42	1800	8.8		0.13	0.27	57	1.00	174	103
6502	67	44	37.3	226		55	400	1.87		0.13	0.16	26	0.25	91	244
6503	121	55	38.7	228		36	1600	2.66		0.13	0.36	19	0.25	61	142
6504	113	56	40.5	241		54	900	0.84		0.05	0.07	25	0.25	45	189
6601	169	78	43.3	250		131	200	1.59		0.05	0.18	20	0.25	432	413
6701	86	59	55.0	292		104	8400	0.75		0.05	1.48	21	0.80	178	149
6702	38	39	63.8	393		135	700	2.46		1.08	0.90	11	0.25	121	160
6703	78	44	58.7	295		77	400	0.93		0.05	0.46	12	0.60	76	203
6801	106	54	28.0	230		116	1400	10.7	0.23	0.54	0.15	15	0.90	409	397
6802	100	47	28.0	202		72	1100	1.4		0.13	0.10	48	0.25	358	386
6803	25	35	42.3	52		181	3300	3.06		0.27	0.96	33	0.80	1086	272
6804	26	61	54.7	475		131	4500	4.76		0.27	0.23	22	0.70	188	117
6805	153	72	34.0	342		129	1400	3.56		0.27	0.16	74	0.25	281	227
6901	35	27	35.9	192		19	700	1.5		0.05	0.09	17	1.40	38	170
6902	91	32	22.8	173		25	100	1.59		0.05	0.08	17	1.10	27	44
7001	111	65	47.2	248		117	100	2.86		0.54	0.26	8	0.60	101	185
7002	87	62	47.8	269		116	1200	3.66		0.4	0.32	31	0.25	245	180
7201	74	56	40.6	231		122	1900	1.21		0.05	0.11	14	0.60	156	239
7203	14	27	36.2	246		115	2000	1.03		0.05	0.38	77	3.90	217	304
7401	50	42	59.0	360		104	900	0.47		0.05	1.41	23	0.25	138	164
7404	73	53	40.3	293		147	1100	1.78		0.13	0.12	11	0.25	124	208
7501	100	55	43.7	242		111	400	50.8		0.94	0.26	49	1.80	139	203
7502	116	60	40.7	211		108	1500	3.46		0.4	0.08	23	0.90	115	198
7503	113	58	47.3	170		141	1800	5.22		0.67	0.23	33	0.70	140	173
7601	109	29	46.9	144		59	100	7.53		0.05	0.18	18	0.25	95	350
7602	199	46	77.0	226		89	100	0.75		0.05	0.27	17	0.25	59	173
7701	91	44	49.4	284		17	400	2.16		0.05	0.04	9.0	18.00	27	69
7703	123	56	39.6	252		24	900	0.37		0.05	0.07	10	0.25	73	185
7801	106	52	45.6	283		57	400	0.93		0.05	0.16	32	0.25	216	275
7802	113	53	44.4	285		64	400	0.84		0.05	0.10	14	0.25	182	283
7901	35	45	45.8	128		36	100	3.26		0.27	0.35	15	1.00	213	412
7902	44	42	42.6	219		193	2500	4.53		0.27	0.09	33	1.60	1166	476
8301	47	38	35.3	198		45	400	0.37	0.08	0.05	0.07	28	1.30	136	294
9901	63	61	39.0	360		160	906	2.5	0.21	0.24	0.87	77	0.50	252	167

	Nb	Hf	Zr	Y	Th	U	Be	La	Ce	Sm	Eu	Tb	Yb	Lu	F	Cl
Zone A																
6401	2.0	0.5	153	62	0.8	0.1	1.0	11	21	4.0	2.0	1.[illegible]0	1.0	0.4	327	3763
6402	1.0	0.5	170	62	0.1	0.1	1.1	8.0	15	4.3	2.0	1.[illegible]0	2.0	0.4	394	3014
6404	8.0	6.0	170	32	0.8	0.6		17	36	8.2	2.0	1.[illegible]0	4.0	0.5		
6405	3.0	3.0	81	17	0.5	0.1		9.0	17	4.3	0.5	0.[illegible]0	2.0	0.2		
6406	4.0	2.0	62	12	0.5	0.3		7.0	12	3.0	1.0	0.[illegible]5	1.0	0.1		
6407	4.0	2.0	72	18	0.4	0.1		10	23	4.1	0.5	0.[illegible]0	1.0	0.2		
6408	5.0	3.0	73	20	1.4	0.2		8.0	18	4.3	2.0	0.[illegible]0	1.0	0.3		
6501	4.0	2.0	90	25	0.4	0.3		13	41	7.3	2.0	1.[illegible]0	3.0	0.4		
6502	3.0	4.0	98	27	0.1	0.2		8.0	20	4.7	1.0	1.[illegible]0	3.0	0.4		
6503	4.0	4.0	88	23	0.5	0.7		12	37	5.2	1.0	1.[illegible]0	4.0	0.3		
6504	3.0	3.0	92	26	0.1	0.4		6.0	17	4.9	1.0	1.[illegible]0	3.0	0.4		
6601	5.0	4.0	72	18	0.3	0.5		11	26	5.8	2.0	1.[illegible]0	4.0	0.4		
6701	5.0	2.0	86	23	1.0	0.9		10	24	3.8	1.0	1.[illegible]0	3.0	0.3		
6702	11.0	3.0	95	26	0.3	0.3		5.0	7.5	3.3	1.0	1.[illegible]0	4.0	0.4		
6703	6.0	3.0	70	21	0.4	0.3		7.0	12	3.8	2.0	0.[illegible]0	3.0	0.2		
6801	6.0	3.0	92	22	0.9	0.1		12	29	5.0	2.0	1.[illegible]0	3.0	0.3		
6802	5.0	4.0	93	23	0.8	0.5		13	30	5.4	2.0	0.[illegible]0	3.0	0.2		
6803	16.0	9.0	256	78	2.3	0.8		42	110	19.0	5.0	3.[illegible]0	9.0	1.1		
6804	12.0	7.0	184	48	1.0	2.0		30	79	12.0	3.0	2.[illegible]0	6.0	0.6		
6805	7.0	5.0	79	12	0.5	0.7		15	36	7.2	1.0	1.[illegible]0	3.0	0.4		
6901	4.0	2.0	87	21	0.5	0.1		8.0	20	4.2	0.5	1.[illegible]0	2.0	0.3		
6902	12.0	6.0	176	31	3.5	0.3		9.0	27	6.1	1.0	1.1 0	4.0	0.5		
7001	5.0	3.0	100	27	0.3	0.1		7.0	21	5.4	2.0	1.[illegible]0	4.0	0.6		
7002	5.0	3.0	110	30	0.6	0.1		7.0	15	5.7	2.0	1.1 0	4.0	0.5		
7201	6.0	4.0	94	25	0.2	0.4		7.0	16	4.8	1.0	1.[illegible]0	3.0	0.4		
7203	12.0	4.0	163	46	1.4	1.3		21	58	7.5	1.0	1.[illegible]0	7.0	0.8		
7401	8.0	4.0	113	34	2.5	1.4		16	38	6.2	2.0	1.1 0	5.0	0.4		
7404	10.0	6.0	177	38	0.6	0.3		10	36	9.1	2.0	2.[illegible]0	4.0	0.4		
7501	3.0	3.0	83	24	0.1	0.1		5.0	12	4.7	0.5	1.1 0	3.0	0.3		
7502	5.0	3.0	99	26	0.6	0.2		7.0	18	4.9	2.0	1.[illegible]0	3.0	0.4		
7503	8.0	7.0	169	40	0.8	0.5		13	33	8.5	2.0	1.[illegible]0	6.0	0.6		
7601	1.0	1.0	31	9.0	0.4	0.6		3.0	6.0	1.5	0.5	0.[illegible]5	1.0	0.1		
7602	4.0	0.5	25	16	0.1	0.1		6.0	9.0	2.7	0.5	0.[illegible]0	1.0	0.1		
7701	9.0	5.0	177	40	1.0	0.1		11	45	9.0	0.5	1.[illegible]0	5.0	0.7		
7703	7.0	5.0	139	32	0.7	0.3		14	33	8.1	3.0	1.[illegible]0	4.0	0.5		
7801	7.0	3.0	73	21	0.6	0.2		10	23	4.7	1.0	1.1[illegible]0	3.0	0.3		
7802	5.0	3.0	80	23	0.8	0.1		12	24	4.8	1.0	1.[illegible]0	2.0	0.3		
7901	1.0	0.5	13	8	0.1	0.1		6.0	6	1.2	0.5	0.[illegible]5	1.0	0.1		
7902	27.0	19.0	702	64	2.3	0.9		86	210	21.1	7.0	2.[illegible]0	8.0	0.9		
8301	4.0	3.0	85	29	0.1	0.1		9.0	33	6.2	0.5	1.[illegible]0	4.0	0.4		
9901	2.0	1.0	127	72	0.8	1.1		9.0	26	5.2	0.5	0.5[illegible]0	2.5	0.6		

	SiO_2	TiO_2	Al_2O_3	Fe_2O_3	FeO	FeO_t	MnO	MgO	CaO	Na_2O	K_2O	P_2O_5	H_2O	CO_2	Cr
Zone B															
3901	44.70	2.50	15.6	7.1	8.9	16.0	0.20	7.40	9.14	2.2	0.80	0.19	1.90	0.10	100
3902	47.80	1.36	17.9	4.3	7.7	12.0	0.15	7.42	9.28	2.9	0.55	0.26	1.20	0.00	82
3903	47.90	1.52	16.7	4.5	8.3	12.8	0.17	7.57	8.27	2.6	1.09	0.17	1.40	0.10	54
3904	46.20	1.81	16.2	5.9	8.5	14.4	0.19	7.61	8.79	2.7	0.68	0.18	1.80	0.10	96
3905	46.00	2.09	15.7	5.7	8.9	14.6	0.19	7.70	9.33	2.5	0.38	0.20	1.20	0.00	77
3906	46.50	2.10	16.0	5.8	8.0	13.8	0.17	6.96	9.31	2.8	0.41	0.32	1.20	0.10	150
3907	45.20	2.59	15.3	7.4	8.9	16.3	0.19	7.27	8.88	2.8	0.64	0.24	1.30	0.00	130
4101	46.70	2.93	16.6	4.4	10.2	14.6	0.20	4.20	8.04	3.7	1.20	0.24	1.30	0.00	36
4102	47.70	3.25	14.6	4.2	10.9	15.1	0.19	4.73	8.88	2.9	0.71	0.22	1.20	0.10	25
4103	45.40	1.88	16.0	3.5	10.2	13.7	0.18	7.50	7.86	2.8	1.72	0.13	1.80	0.00	170
4201	45.70	1.68	15.7	4.1	9.6	13.7	0.22	8.69	7.34	2.6	2.14	0.14	1.90	0.00	150
4301	47.00	2.86	13.9	10.2	6.3	16.5	0.26	6.38	7.17	1.9	1.39	0.19	2.20	0.70	59
4302	46.40	3.03	14.5	10.0	6.6	16.6	0.28	6.18	6.72	1.4	2.36	0.19	2.20	0.30	60
4401	45.90	2.38	14.9	6.7	9.0	15.7	0.24	6.21	8.74	2.9	0.66	0.14	1.30	0.10	97
4402	47.10	2.41	15.1	5.9	9.6	15.5	0.23	6.12	8.80	2.8	0.58	0.14	1.20	0.00	74
4403	46.10	2.45	15.4	6.0	9.8	15.8	0.24	6.50	9.05	2.9	0.55	0.12	1.10	0.00	86
Zone C															
5401	48.00	1.52	16.7	2.7	10.2	12.9	0.21	7.49	8.36	2.8	0.47	0.13	0.80	0.00	110
5402	45.10	3.08	12.8	3.9	13.5	17.4	0.26	6.54	9.30	1.8	1.66	0.30	1.20	0.00	140
5403	48.40	2.94	13.6	5.4	11.1	16.5	0.39	6.32	6.82	0.6	2.21	0.35	1.60	0.10	130
5404	51.40	2.34	15.3	3.4	8.6	12.0	0.16	6.71	8.26	0.8	1.05	0.41	1.10	0.00	200
5405	49.20	2.11	15.9	3.0	7.6	10.6	0.15	6.94	8.37	1.7	2.02	0.56	1.90	0.00	220
5406	50.70	2.57	13.6	7.0	7.9	14.9	0.21	4.82	6.37	3.8	0.59	0.33	1.40	0.00	49
5408	46.60	2.60	16.5	4.3	10.1	14.4	0.22	4.87	9.21	2.8	0.83	0.38	0.80	0.10	90
5409	47.00	1.53	17.4	3.2	9.4	12.6	0.17	7.50	9.09	2.7	0.57	0.21	0.80	0.00	250
5410	45.20	1.31	17.1	3.5	9.4	12.9	0.17	9.42	8.04	2.4	1.02	0.18	2.00	0.00	290
5411	45.90	1.29	17.8	3.4	8.1	11.5	0.12	8.40	7.63	2.5	2.15	0.17	2.80	0.00	200
5412	45.70	1.25	17.6	3.1	8.5	11.6	0.16	9.73	8.94	2.3	0.79	0.16	1.70	0.10	171
5413	44.90	1.64	17.1	3.4	9.3	12.7	0.19	8.79	9.26	2.2	0.58	0.22	1.60	0.10	98
5414	45.30	1.78	17.1	3.1	9.3	12.4	0.17	8.22	9.47	2.6	0.60	0.19	1.60	0.00	110
5415	47.00	1.37	18.5	2.6	8.2	10.8	0.16	7.88	9.18	3.0	0.37	0.18	1.50	0.10	75
5416	48.20	1.88	16.9	4.3	7.1	11.4	0.14	6.75	7.46	2.2	1.53	0.28	2.80	0.30	65
5417	49.30	2.73	14.1	5.1	8.5	13.6	0.19	6.21	7.54	0.6	1.76	0.35	2.90	0.10	150
5418	46.20	1.14	17.3	2.6	9.0	11.6	0.19	8.88	10.28	2.50	0.19	0.09	1.40	0.00	72
5419	46.70	0.89	18.6	2.3	8.0	10.3	0.17	9.14	10.09	2.2	0.39	0.09	1.00	0.00	218
5420	45.90	1.11	18.3	2.1	8.4	10.5	0.17	8.82	10.72	2.3	0.21	0.09	1.40	0.10	191
5421	45.10	1.93	16.0	2.9	10.8	13.7	0.22	7.43	9.54	2.6	0.54	0.20	1.50	0.70	100
5422	49.30	1.75	13.3	6.1	7.1	13.2	0.34	6.34	9.04	4.1	0.68	0.25	1.00	0.30	170
5423	51.80	0.69	15.6	4.3	6.2	10.5	0.26	6.68	6.34	4.7	0.77	0.14	1.80	0.90	150

	Ni	Co	Sc	V	Cu	Zn	S	As	Se	Sb	Au (ppb)	Rb	Cs	Ba	Sr
Zone B															
3901	87	57	38.9	230	90	67	1435	0.41	0.1	0.05	0.11	46	0.60	218	186
3902	120	63	23.1	130	130	70	900	0.34	0.21	0.05	0.18	18	0.25	136	238
3903	110	60	23.3	140	28	87	501	0.53	0.04	0.03	0.16	17	0.60	252	203
3904	110	60	26.4	180	75	81	1380	0.36	0.15	0.06	0.17	37	1.00	136	173
3905	110	59	34.9	190	95	71	1442	0.3	0.13	0.05	0.24	9.0	0.25	90	149
3906	83	64	33.1	200	120	63	1778	0.59	0.18	0.05	0.19	6.0	0.25	97	174
3907	76	60	38.3	260	110	62	1733	1.01	0.16	0.23	0.15	14	0.25	97	157
4101	54	50	27.3	260	190	130	1836	0.23	0.29	0.05	0.23	22	0.25	675	330
4102	57	58	39.6	360	170	110	2255	0.4	0.28	0.09	0.27	6.0	0.25	308	287
4103	150	63	20.1	170	75	110	1032	0.42	0.14	0.09	0.12	48	1.60	503	306
4201	160	62	20.0	150	19	120	125	0.11	0.01	0.07	0.05	59	1.10	410	283
4301	79	57	48.7	330	18	130	150	0.19	0.07	0.06	0.30	30	1.10	307	131
4302	69	51	48.7	330	18	130	175	0.34	0.04	0.07	0.05	120	1.80	415	113
4401	76	61	39.4	290	110	130	1184	0.25	0.13	0.07	0.05	4.0	0.25	140	180
4402	79	63	37.0	280	92	120	1546	0.13	0.14	0.05	0.19	11	0.25	222	190
4403	84	66	42.2	320	100	130	1635	0.15	0.14	0.04	0.05	5.0	0.25	175	193
Zone C															
5401	110	78	37.0	290	16	190	198	0.31	0.03	0.25	0.05	24	0.25	96	177
5402	62	79	50.6	540	69	150	1276	0.31	0.21	0.11	0.13	104	5.00	368	119
5403	54	74	49.0	450	19	200	330	0.08	0.03	0.06	0.05	131	6.00	390	50
5404	87	63	33.0	260	66	120	2130	0.1	0.15	0.12	0.26	59	1.00	277	164
5405	110	68	33.4	230	72	100	1599	0.11	0.17	0.03	0.18	86	1.90	251	212
5406	34	67	48.0	390	55	84	189	0.08	0.05	0.03	1.16	20	0.50	277	97
5408	55	71	37.0	310	130	160	2051	0.05	0.24	0.02	0.18	33	0.50	371	250
5409	100	79	20.0	210	29	100	306	0.02	0.05	0.02	0.05	19	0.25	194	256
5410	160	92	20.0	160	59	110	1031	0.07	0.14	0.02	0.05	89	0.25	324	216
5411	140	78	18.0	150	59	110	1161	0.08	0.12	0.01	0.05	66	1.90	858	345
5412	210	86	18.0	140	56	120	962	0.07	0.14	0.02	0.05	76	0.50	318	276
5413	190	88	23.0	210	55	120	613	0.4	0.11	0.04	0.05	35	0.50	166	219
5414	170	92	27.0	250	100	110	1290	1.45		0.1	0.12	25	0.50	168	245
5415	170	83	20.7	170	25	83	25	0.12	0.02	0.03	0.13	19	0.25	88	347
5416	140	69	25.0	210	70	100	1977	1.2	0.15	0.07	0.28	57	1.40	316	228
5417	100	77	33.0	320	65	130	2007	2.11	0.12	0.33	0.39	79	2.00	278	197
5418	160	86	29.0	220	100	99	919	0.07	0.15	0.02	0.13	24	0.25	77	190
5419	200	82	20.0	170	82	100	666	0.11	0.13	0.03	0.05	19	1.20	70	214
5420	180	81	26.0	220	100	95	1031	0.03	0.16	0.01	0.05	14	0.25	68	190
5421	130	80	34.0	250	92	150	1037	2.6	0.18	0.13	0.38	28	0.25	138	189
5422	76	70	41.0	350	170	250	1143	1.73	0.25	0.18	0.35	15	0.25	134	182
5423	72	61	34.0	320	100	320	92	0.91	0.03	0.29	0.35	38	0.25	255	232

	Nb	Hf	Zr	Y	Th	U	Be	La	Ce	Sm	Eu	Tb	Yb	Lu	F	Cl
Zone B																
3901		4.0	102	29	0.5	0.1	0.8	27	44	5.0	2.0	1.40	3.0	0.4	398	437
3902		3.0	114	20	0.6	0.3	0.9	6.0	15	3.0	1.0	0.90	2.0	0.3	332	379
3903		3.0	99	25	0.7	0.3	0.8	6.0	14	3.0	0.5	0.80	3.0	0.4	335	551
3904		4.0	102	26	0.7	0.4	0.8	7.0	16	3.4	1.0	1.20	3.0	0.4	398	571
3905		4.0	105	28	0.7	0.3	0.8	9.0	14	4.1	2.0	1.10	4.0	0.5	314	481
3906		4.0	169	33	0.6	0.2	1.0	9.0	22	5.2	2.0	1.40	4.0	0.6	442	552
3907		4.0	128	32	0.5	0.3	0.8	8.0	17	4.5	2.0	1.20	4.0	0.5	541	597
4101		6.0	177	42	0.8	0.3	1.3	21	37	5.8	2.0	1.70	3.0	0.5	512	2421
4102		6.0	167	43	1.4	0.9	1.4	18	36	6.3	2.0	1.80	3.0	0.6	561	2580
4103		4.0	97	26	1.2	0.8	0.9	12	19	3.6	1.0	1.00	2.0	0.3	770	1239
4201		2.0	85	24	0.9	0.4	0.9	12	18	3.4	1.0	0.80	2.0	0.4	1207	1106
4301		7.0	185	50	1.0	0.5	1.7	12	26	5.9	1.0	1.70	6.0	0.8	1028	116
4302		6.0	196	55	0.9	0.3	1.5	13	29	6.2	2.0	1.80	6.0	0.9	947	178
4401		4.0	138	41	0.5	0.4	1.1	9.0	20	5.0	2.0	1.60	4.0	0.6	866	923
4402		5.0	135	42	0.7	0.3	1.1	9.0	21	4.8	1.0	1.50	3.0	0.6	443	1097
4403		5.0	121	42	0.5	0.3	1.1	9.0	21	4.9	2.0	1.50	4.0	0.6	412	885
Zone C																
5401	0.0	2.0	105	61	0.7	0.9	1.9	6.5	23	5.4	0.5	1.00	3.0	0.5	754	50
5402	10.0	1.0	212	49	1.3	0.4	1.6	16	41	11.0	3.0	1.70	5.0	0.6	876	381
5403	16.0	4.0	222	51	1.9	1.2	2.3	17	41	10.0	3.0	3.30	7.0	0.6	1304	341
5404	35.0	5.0	276	50	2.1	1.2	2.0	21	54	12.0	2.0	2.00	6.0	0.9	497	318
5405	23.0	0.5	223	41	2.8	1.2	1.5	26	34	7.1	2.0	2.10	3.0	0.5	757	422
5406	27.0	7.0	293	61	1.3	0.6	1.7	26	61	12.0	2.0	2.50	6.0	1.0	509	50
5408	7.0	3.0	208	39	1.0	0.3	1.2	22	55	9.4	2.0	2.00	5.0	0.9	466	693
5409	9.0	1.0	131	57	0.1	0.1	0.7	13	28	5.1	1.0	1.10	4.0	0.4	354	563
5410	2.0	2.0	109	57	0.1	0.1	0.6	10	15	4.7	3.0	1.20	1.0	0.4	351	376
5411	0.0	2.0	108	41	0.1	0.1	0.6	10	19	3.8	0.5	0.80	2.0	0.3	693	452
5412	0.0	1.0	109	61	0.1	0.3	0.6	9.0	18	3.9	0.5	0.50	2.5	0.3	281	446
5413	0.0	1.0	141	56	0.3	0.3	0.7	13	25	5.0	0.5	1.50	2.5	0.5	316	479
5414	0.0	1.0	120	53	0.9	0.3	0.7	9.0	22	4.6	0.5	0.50	2.5	0.2	303	291
5415	1.0	0.5	110	46	0.3	0.1	0.9	11	12	3.2	2.0	1.00	2.0	0.3	288	147
5416	16.0	4.0	168	40	2.0	0.6	1.9	20	49	7.7	3.0	1.80	6.0	0.9	559	288
5417	23.0	4.0	237	40	1.9	0.8	1.4	19	34	10.0	3.0	2.10	5.0	0.7	952	198
5418	0.0	0.5	80	40	0.4	0.1	0.6	3.0	12	3.3	1.0	0.25	2.0	0.2	150	50
5419	7.0	0.5	74	39	0.7	0.2	0.6	4.0	16	2.5	0.5	0.25	1.0	0.3	212	50
5420	6.0	1.0	84	51	0.1	0.1	0.6	4.0	2	3.2	2.0	0.80	1.0	0.4	124	50
5421	0.0	3.0	154	37	0.1	0.3	0.9	6.0	14	6.0	1.0	1.00	2.5	0.7	508	1939
5422	0.0	2.0	153	74	0.4	0.4	1.2	10	27	6.1	2.0	1.50	4.0	0.6	653	301
5423	9.0	0.5	72	29	0.7	0.1	0.7	6.0	8	3.4	0.5	0.25	1.0	0.3	666	272

	SiO_2	TiO_2	Al_2O_3	Fe_2O_3	FeO	FeO_t	MnO	MgO	CaO	Na_2O	K_2O	P_2O_5	H_2O	CO_2	Cr
Zone D															
111	53.60	0.97	14.6	3.7	7.0	10.7	0.40	6.59	7.07	4.5	0.54	0.03	1.10	0.10	110
212	47.90	0.92	15.4	3.3	8.3	11.6	0.18	7.8	10.6	3.3	0.38	0.10	1.60	0.6	240
221	49.50	0.55	15.1	2.9	8.5	11.4	0.19	9.87	10.10	2.2	0.22	0.01	0.90	0.00	150
222	52.70	0.52	15.1	2.0	7.8	9.8	0.17	8.50	9.62	2.9	0.38	0.02	0.90	0.10	290
311	47.55	1.42	18.0	5.1	7.9	13.0	0.24	5.7	8.3	4.5	0.22	0.17	1.30	0.1	55.5
312	50.60	0.53	20.5	3.5	5.6	9.1	0.14	4.31	8.50	4.8	0.16	0.12	0.90	0.10	56
322	46.40	0.86	16.2	2.9	8.1	11.0	0.21	6.21	10.93	3.2	0.17	0.12	2.00	2.70	280
612	53.70	2.31	13.1	6.7	7.7	14.4	0.21	3.31	7.17	4.3	0.16	0.20	0.90	0.00	15
822	48.20	1.33	14.8	5.9	7.3	13.2	0.21	7.18	8.98	4.0	0.75	0.13	1.10	0.20	80
1211	49.10	3.04	12.5	9.1	9.3	18.4	0.28	4.34	7.71	3.0	0.30	0.69	1.10	0.20	29
1411	55.20	1.13	16.3	3.7	7.3	11.0	0.18	3.66	8.45	3.5	0.39	0.30	0.70	0.00	14
1412	52.00	0.35	13.9	1.2	7.9	9.1	0.19	9.22	11.57	2.6	0.19	0.02	0.70	0.10	260
1611	53.40	0.34	15.3	1.2	7.3	8.5	0.17	6.78	11.12	3.2	0.26	0.03	0.70	0.10	330
1711	49.00	1.20	16.2	5.5	6.2	11.7	0.13	6.47	8.80	4.5	0.73	0.39	1.00	0.00	96
1712	45.80	1.14	15.4	6.6	7.7	14.3	0.24	8.08	10.08	3.1	0.71	0.26	1.20	0.10	73
1812	52.70	1.56	15.0	3.9	9.9	13.8	0.17	7.34	3.49	5.0	0.13	0.30	0.50	0.10	64
1821	49.70	1.03	14.7	3.8	8.2	12.0	0.38	7.76	8.42	4.2	0.28	0.15	1.00	0.10	270
1822	50.30	1.01	14.8	3.4	7.3	10.7	0.24	7.83	8.56	4.3	0.42	0.09	1.10	0.10	270
3711	47.00	0.76	19.0	2.7	7.8	10.5	0.17	8.19	11.24	2.0	0.15	0.03	1.10	0.00	69
3712	46.60	0.75	18.1	2.3	8.5	10.8	0.18	8.96	10.94	1.8	0.22	0.04	1.20	0.20	74
3805	46.70	1.66	16.9	3.4	9.6	12.8	0.20	7.55	9.96	2.7	0.26	0.17	1.00	0.60	84
4501	48.70	1.09	16.3	5.1	7.0	12.1	0.20	6.97	8.95	3.9	0.77	0.24	1.00	0.00	130
4503	48.00	1.16	16.4	5.3	7.1	12.4	0.18	6.89	8.93	3.6	1.12	0.44	1.10	0.00	130
4504	47.60	1.18	16.5	5.9	6.8	12.7	0.20	7.24	9.18	3.7	0.65	0.24	1.20	0.10	57
4505	47.80	1.23	15.7	5.9	7.3	13.2	0.23	7.48	9.35	3.3	0.68	0.11	1.30	0.00	71
4506	47.10	1.12	16.6	6.4	7.5	13.9	0.27	6.82	9.04	3.4	0.45	0.15	1.10	0.00	69
4507	52.50	1.10	14.5	4.4	6.5	10.9	0.15	7.04	8.62	4.1	0.26	0.03	0.50	0.10	210
9402	49.60	1.18	16.7	8.5	9.4	17.9	0.47	4.81	3.29	4.3	0.34	0.19	0.80	0.60	25
9508	47.60	1.53	15.7	4.1	8.9	13.0	0.34	7.36	9.01	3.0	0.83	0.09	1.20	0.20	83

	Ni	Co	Sc	V	Cu	Zn	S	As	Se	Sb	Au (ppb)	Rb	Cs	Ba	Sr
Zone D															
111	66	44	37.3	210	75	300	360	0.3	0.06	0.18	0.41	2.0	0.25	120	212
212	110	51	36.4	230	8	96	136	0.75	0.01	0.05	0.1	10	0.50	64	185
221	110	62	36.0	190	13	91	25		0.01	0.01	0.05	2.0	0.25	42	70
222	110	55	29.9	150	14	100	25	0.14	0.01	0.01	0.05	3.0	0.25	96	142
311	39	53.0	34.6	300	65	89.5	162	0.1	0.02	0.02		10.5	0.25	62.0	190
312	44	35	26.9	150	15	78	25		0.01	0.02	1.67	1.0	0.25	80	277
322	120	46	33.6	140	34	100	441	0.1	0.07	0.02	0.29	4.0	1.80	67	108
612	23	46	42.8	290	170	130	1476	0.28	0.1	0.03	0.19	1.0	0.25	116	97
822	87	52	33.2	260	53	130	609	0.08	0.09	0.01	0.15	3.0	0.25	67	181
1211	32	40	40.6	270	76	160	1956	0.08	0.19	0.01	0.05	9.0	0.50	116	84
1411	23	35	28.0	270	10	120	25	0.02	0.01	0.01	0.16	0.5	0.25	89	238
1412	68	53	48.2	210	12	100	25	0.3	0.01	0.01		3.0	0.25	89	130
1611	63	42	39.2	150	12	86	25	0.14	0.01	0.02	0.50	1.0	0.25	81	135
1711	42	42	30.7	250	10	71	25	0.24	0.01	0.02	0.05	5.0	0.25	280	352
1712	110	60	33.8	310	11	180	25	0.38	0.01	0.01	0.05	9.0	0.25	126	162
1812	42	44	48.2	300	48	110	881	0.16	0.06	0.02	0.23	2.0	0.60	118	52
1821	76	53	39.3	260	91	420	1774	0.22	0.19	0.03	0.49	2.0	0.25	81	151
1822	89	58	40.9	240	54	190	469	0.75	0.2	0.04	0.67	3.0	0.25	58	189
3711	120	60	31.7	180	61	74	25	0.29	0.01	0.02	0.30	0.5	0.25	72	172
3712	130	65	29.7	170	29	87	25	1.97	0.01	0.07	0.18	4.0	0.25	70	169
3805	120	59	32.3	200	68	110	1046	1.47	0.14	0.04	0.16	1.0	0.25	117	171
4501	56	51	32.4	250	32	160	86	0.04	0.02	0.02	0.84	4.0	0.25	123	297
4503	46	43	39.5	250	10	130	58	0.07	0.01	0.03	0.38	7.0	1.00	158	197
4504	91	47	39.4	260	11	140	25	0.1	0.01	0.03	0.13	5.0	0.25	138	225
4505	96	52	39.0	270	12	160	25	0.14	0.01	0.01	0.20	8.0	0.25	98	220
4506	96	54	37.1	280	12	200	25	0.2	0.01	0.02	0.05	6.0	0.25	109	255
4507	130	54	21.4	160	160	100	936	0.74	0.05	0.05	0.12	5.0	0.25	112	194
9402	20	41	42.0	290	16	130	70	1.13	0.02	0.06	0.18	17	0.50	90	71
9508	110	58	46.0	320	72	210	350	0.14	0.17	0.04	0.25	27	0.50	81	123

	Nb	Hf	Zr	Y	Th	U	Be	La	Ce	Sm	Eu	Tb	Yb	Lu	F	Cl
Zone D																
111	*	4.0	60	29	0.1	0.1	0.7	8.0	16	3.9	0.5	1.30	3.0	0.4	1127	147
212	6.0	2.0	49	38	0.5	0.1	0.6	4.5	4.8	2.3	0.5	0.4	2.0	0.3	2200	285
221		0.5	29	16	0.1	0.1	0.3	1.0	2.5	1.3	0.5	0.60	1.0	0.3	400	50
222		3.0	53	18	0.5	0.5	0.6	5.0	11	1.8	0.5	0.60	1.0	0.3	627	235
311	19	1.8	72	44.5	0.1	0.1	0.7	3.5		2.4	0.5	0.8	2.0	0.3	294	161
312		2.0	11	7	0.3	0.2	0.5	3.0	2.5	0.8	0.5	0.25	1.0	0.1	414	50
322		2.0	49	43	0.1	0.1	0.8	8.0	17	3.8	1.0	1.50	4.0	0.6	774	128
612		7.0	165	49	0.6	0.6	1.2	13	23	5.7	0.5	1.70	5.0	0.7	329	222
822		3.0	65	20	0.3	0.1	0.8	5.0	7.0	2.3	1.0	0.50	1.0	0.3	1957	108
1211		11.0	395	56	1.6	0.9	1.3	16	31	7.5	3.0	2.20	6.0	0.8	1442	50
1411		2.0	50	19	0.1	0.1	0.6	8.0	11	2.7	0.5	0.70	2.0	0.3	649	193
1412		0.5	4	8	0.1	0.1	0.3	2.0	2.5	1.2	0.5	0.25	1.0	0.1	248	126
1611		2.0	34	27	0.1	0.1	0.6	4.0	13	2.2	0.5	0.60	3.0	0.4	298	130
1711		2.0	50	20	0.3	0.1	0.7	11	20	3.1	0.5	0.70	1.0	0.3	854	135
1712		1.0	37	22	0.1	0.1	0.6	5.0	13	2.0	0.5	0.60	2.0	0.3	376	522
1812		4.0	89	31	1.1	0.6	0.9	15	27	5.0	2.0	1.50	5.0	0.7	292	50
1821		1.0	38	22	0.1	0.1	0.7	6.0	8.0	2.4	0.5	0.70	1.0	0.4	622	50
1822		1.0	61	18	0.1	0.1	0.7	4.0	8.0	1.7	1.0	0.60	1.0	0.3	1349	50
3711		0.5	56	16	0.1	0.1	0.4	1.0	6.0	1.4	0.5	0.60	1.0	0.3	52	50
3712		2.0	71	18	0.1	0.1	0.4	1.0	2.5	1.5	0.5	0.25	2.0	0.3	91	50
3805		4.0	85	26	0.1	0.1	0.7	6.0	11	3.4	1.0	1.00	3.0	0.4	862	236
4501		2.0	38	19	0.3	0.1	0.7	10	17	2.8	2.0	0.70	1.0	0.3	468	470
4503		1.0	35	18	0.3	0.1	0.9	11	17	3.6	3.0	0.60	2.0	0.3	500	311
4504		1.0	57	21	0.1	0.1	0.6	7.0	15	2.7	0.5	0.90	3.0	0.4	404	380
4505		2.0	38	25	0.1	0.1	0.5	5.0	12	2.6	1.0	0.80	1.0	0.4	371	402
4506		2.0	40	18	0.1	0.1	0.5	5.0	11	2.1	0.5	0.80	1.0	0.3	280	478
4507		2.0	32	15	0.3	0.1	0.5	4.0	6.0	2.2	0.5	0.70	1.0	0.1	352	115
9402		1.0	84	50	0.3	0.3		7.0	25	5.1	1.0	1.00	7.0	1.0		
9508	8.0	2.0	117	78	0.6	0.7		7.0	19	6.8	2.0	1.40	4.0	0.6		

Appendix 4-3. Analysis of Bamble Hyperites (Gabbros) & Amphibolites (Oxides in %; Elements in ppm)

	SiO_2	TiO_2	Al_2O_3	Fe_2O_3	FeO	FeO_t	MnO	MgO	CaO	Na_2O	K_2O	P_2O_5	H_2O	Cr	Ni
Tromoy Coronitic gabbro															
5201	48.80	1.79	15.4	2.9	9.0	11.9	0.21	6.54	10.60	3.0	0.33	0.17	0.4	210	85
5202	49.00	1.7	15.2	2.6	9.0	11.6	0.2	7.1	11.4	3.0	0.3	0.1	0.5	275	76
5203	47.40	1.09	16.3	2.1	9.4	11.5	0.19	8.95	10.06	2.6	0.18	0.10	0.5	190	160
5204	47.70	1.05	17.2	2.6	9.4	12.0	0.19	8.95	9.49	2.7	0.20	0.11	0.5	120	160
Laget Coronitic Gabbro															
8501	48.30	1.26	19.2	1.4	8.7	10.1	0.16	6.90	9.37	3.3	0.27	0.15	0.8	54	110
8502	45.00	0.61	15.2	2.7	11.0	13.7	0.23	12.55	7.61	2.2	0.40	0.07	1.4	74	210
8503	47.50	1.34	17.6	1.7	10.1	11.8	0.18	8.25	8.63	3.0	0.29	0.15	0.8	180	110
8504	47.40	1.20	15.3	1.5	10.6	12.1	0.19	9.82	9.56	2.6	0.18	0.08	0.8	270	150
8505	45.50	0.60	18.9	1.5	7.3	8.8	0.13	11.53	9.74	2.6	0.22	0.07	1.5	69	290
8506	43.90	0.72	19.1	3.7	10.8	14.5	0.36	9.94	7.63	1.8	0.21	0.25	1.2	52	190
8507	48.00	1.17	18.8	1.2	8.6	9.8	0.16	8.13	9.78	3.0	0.40	0.11	0.8	99	150
8508	47.00	1.03	17.5	1.2	10.0	11.2	0.17	10.27	8.80	2.5	0.21	0.10	0.7	72	190
8411	47.40	0.84	19.8	1.0	7.8	8.8	0.13	9.08	9.27	2.8	0.20	0.12	1.1	44	190
Laget Amphibolite															
8401	44.00	2.58	13.7	10.7	9.0	19.7	0.39	7.18	7.82	1.0	0.43	0.33	1.6	150	96
8402	46.10	1.96	16.2	1.7	10.6	12.3	0.20	7.24	9.79	2.9	0.66	0.21	1.5	160	84
8403	45.50	3.68	12.8	1.9	12.9	14.8	0.24	7.37	9.06	2.0	0.81	0.22	1.7	200	87
8404	45.60	1.94	16.0	3.0	10.2	13.2	0.17	6.74	8.43	3.2	1.15	0.20	1.8	120	93
8405	47.20	2.01	14.3	1.7	9.9	11.6	0.22	7.52	10.32	2.7	0.99	0.10	1.5	370	88
8406	47.80	2.06	17.7	1.9	8.8	10.7	0.17	5.88	8.90	3.5	0.56	0.08	1.6	230	95
8407	46.85	1.0	19.2	1.8	7.9	9.6	0.2	7.6	7.8	3.5	1.2	0.1	2.7	85	118
8408	47.00	0.76	19.8	1.2	7.5	8.7	0.14	8.59	8.83	3.1	0.74	0.12	2.0	40	170
8409	47.90	0.79	20.2	1.6	6.7	8.3	0.16	7.73	9.48	3.2	0.18	0.18	1.4	27	160
8410	47.00	1.14	19.8	2.2	6.4	8.6	0.16	8.19	7.66	3.6	0.76	0.13	2.6	60	150
8412	48.30	0.87	18.5	1.3	7.0	8.3	0.14	9.05	6.82	4.0	0.58	0.10	2.9	59	160
Tvedestrand Hyperite															
4005	46.80	2.76	14.2	4.2	11.6	15.8	0.25	6.08	9.02	3.0	0.66	0.31	1.2	51	77
4006	46.80	2.94	14.4	3.6	11.9	15.5	0.24	5.65	8.93	2.9	0.62	0.34	0.8	45	71
4007	46.60	3.14	14.2	3.9	12.4	16.3	0.24	5.49	8.84	2.9	0.71	0.38	0.7	40	68
4008	46.30	3.43	13.3	5.2	12.2	17.4	0.27	5.31	8.93	2.8	0.70	0.37	0.8	41	56
4009	47.00	2.76	14.2	4.1	11.7	15.8	0.27	5.84	9.16	3.0	0.56	0.35	1.0	54	74
Tvedestrand Amphibolite															
4001	46.70	2.85	14.1	6.0	10.5	16.5	0.27	5.83	9.22	2.5	0.54	0.33	1.1	58	70
4002	46.80	2.80	14.1	5.1	10.7	15.8	0.24	5.82	9.35	2.9	0.60	0.32	1.1	55	74
4003	46.40	2.65	14.2	4.7	10.9	15.6	0.25	6.06	9.72	2.9	0.63	0.31	1.3	47	78
4004	45.60	2.93	14.0	5.0	11.3	16.3	0.25	6.13	9.23	2.9	0.75	0.30	1.3	54	79

	Co	Sc	V	Cu	Zn	Mo	Be	S	Se	As	Sb	Au (ppb)	Rb	Cs	Ba	Sr
	Tromoy Coronitic gabbro															
5201	73	50	290	110	120	0.5	0.6	1392	0.18	0.19	0.03	0.26	39	0.25	102	213
5202	62	50	315	86	85	1.0	0.7	983	0.14	0.12	0.03	0.2	20.0	0.3	90	180
5203	84	31	200	78	110	1.0	0.4	1002	0.18	0.17	0.02	0.29	22	1.20	91	206
5204	82	28	150	71	110	0.5	0.4	906	0.18	0.1	0.02	0.24	23	0.60	75	205
	Laget Coronitic Gabbro															
8501	68	19	120	63	89	0.5	0.7	811	0.39	0.1	0.05	0.11	23	0.70	110	323
8502	100	12	80	97	140	1.0	0.5	931	4.06	0.14	0.31	0.47	22	1.20	116	169
8503	74	18	150	63	97	2.0	0.6	485	0.43	0.11	0.06	0.50	32	0.50	117	269
8504	78	33	210	96	94	1.0	0.4	1184	2.02	0.18	0.03	0.29	15	1.00	79	222
8505	76	11	68	38	85	3.0	0.3	351	0.78	0.08	0.1	0.13	25	0.25	86	338
8506	89	16	84	73	70	3.0	0.2	717	4.68	0.12	0.1	0.21	4	1.10	113	188
8507	64	21	160	50	86	3.0	0.5	518	1.25	0.09	0.1	0.13	32	0.50	131	318
8508	77	18	100	41	95	0.5	0.4	973	0.39	0.1	0.03	0.05	15	0.90	89	282
8411	71	12	88	52	78	0.5	0.6	291	1.92	0.06	0.07	0.23	22	0.25	92	342
	Laget Amphibolite															
8401	95	53	340	270	110	0.5	0.7	6100	5.22	0.54	0.06	1.18	24	0.25	102	69
8402	74	29	330	42	140	0.5	1.1	121	0.64	0.03	0.11	0.14	65	0.25	223	320
8403	85	50	440	170	170	2.0	0.9	1751	0.56	0.12	0.12	0.32	52	0.25	245	167
8404	68	37	280	170	94	3.0	1.0	636	1.01	0.18	0.18	0.88	43	0.25	253	217
8405	69	53	360	140	130	0.5	0.7	1099	1.2	0.16	0.17	0.85	87	1.00	201	233
8406	68	36	320	96	85	1.0	1.0	1890	3.7	0.18	0.36	0.42	38	0.25	167	315
8407	76.5	19	115	54	63	1.0	0.6	593	0.8	0.1	0.1	0.2	55.5	3.0	240	346
8408	71	11	82	36	80	1.0	0.5	175	1.04	0.05	0.1	0.13	83	3.00	219	385
8409	69	8	77	43	84	2.0	0.6	673	2.6	0.08	0.13	0.27	25	0.25	96	405
8410	65	15	110	42	80	0.5	0.6	125	2.21	0.06	0.22	0.18	85	9.70	209	350
8412	62	14	90	31	90	0.5	0.6	163	2.2	0.05	0.13	0.05	61	1.40	183	302
	Tvedestrand Hyperite															
4005	54	50	290	90	160	2.0	1.2	654	0.11	2.04	0.39	0.38	16	1.00	187	138
4006	52	45	290	130	140	2.0	1.3	1093	0.16	1.19	0.14	0.31	10	0.70	174	148
4007	54	50	290	160	160	0.5	1.3	1302	0.19	0.93	0.11	0.69	10	0.90	198	141
4008	53	51	350	170	190	1.0	1.4	1284	0.23	2.15	0.33	0.70	15	0.90	202	127
4009	57	39	290	200	210	2.0	1.2	1144	0.25	2.2	0.43	0.80	8	0.70	201	157
	Tvedestrand Amphibolite															
4001	54	46	300	130	160	2.0	1.3	1024	0.15	0.61	0.15	0.31	5	0.60	216	144
4002	54	47	310	180	160	0.5	1.2	1350	0.27	1.8	0.25	0.39	12	1.10	206	144
4003	54	46	290	120	170	2.0	1.2	919	0.15	1.83	0.37	0.30	12	1.00	147	136
4004	56	47	310	160	180	2.0	1.1	1187	0.2	1.89	0.46	0.46	27	0.80	238	133

	Nb	Hf	Zr	Y	Th	U	La	Ce	Sm	Eu	Tb	Yb	Lu	F	Cl	Br
	Tromoy Coronitic gabbro															
5201	0	0.5	142	75	0.1	0.3	7	13	4.40	0.5	1.70	3	0.5	270	160	1.0
5202	4.0	2.0	102	54.0	0.7	0.3	4.5	12.3	4.5	0.8	0.9	3.5	0.4	170	50	0.6
5203	0	1.0	86	45	0.1	0.1	4	13	3.20	0.5	1.10	3	0.3	150	50	1.0
5204	0	0.5	88	48	0.1	0.1	4	12.5	2.60	1.0	0.90	2	0.2	210	50	1.0
	Laget Coronitic Gabbro															
8501	5	0.5	117	50	0.4	0.1	5	7	2.90	1.0	1.10	1	0.1	250	200	1.0
8502	0	0.5	56	23	0.3	0.2	3	5	2.40	0.5	0.25	1	0.1	260	7580	1.0
8503	8	3.0	119	43	0.4	0.3	6	13	4.00	0.5	1.00	2	0.2	190	210	1.0
8504	0	1.0	77	35	0.3	0.3	2.5	17	2.80	0.5	0.50	2.5	0.3	120	130	1.0
8505	10	2.0	68	18	0.1	0.1	3	17	1.90	0.5	0.25	1	0.1	100	4810	1.0
8506	0	1.0	83	58	0.7	0.1	4	21	2.40	0.5	1.20	5	0.8	100	3120	1.0
8507	4	1.0	98	50	0.2	0.2	2	10	3.10	0.5	0.50	2.5	0.2	140	2850	9.5
8508	5	0.5	87	34	0.1	0.1	3	8	2.10	1.0	0.70	1	0.1	150	500	3.8
8411	5	0.5	102	37	0.1	0.1	4	11	2.20	1.0	0.70	1	0.1	130	230	1.0
	Laget Amphibolite															
8401	4	0.5	111	54	0.1	0.1	8	25	4.80	2.0	1.90	6	1.1	560	3030	1.0
8402	6	1.0	134	69	0.1	0.1	9	28	6.20	1.0	1.00	2	0.4	320	4300	1.0
8403	11	1.0	100	59	1.6	0.6	13	36	6.40	3.0	1.20	3	0.4	320	5890	1.0
8404	0	3.0	148	77	0.1	0.3	7	25	6.20	1.0	0.50	2.5	0.8	310	8110	1.0
8405	9	0.5	100	53	0.5	0.1	5	9	3.00	1.0	0.80	1	0.3	220	5430	4.3
8406	12	0.5	90	43	0.1	0.2	5	15	3.70	1.0	0.90	2	0.3	210	4950	1.0
8407	4.5	0.5	61	27.5	0.4	0.1	4.0	12	2.1	2.0	0.3	1.0	0.1	170	2550	1.0
8408	4	0.5	91	24	0.3	0.1	5	7	2.70	0.5	0.25	1	0.1	150	2400	4.7
8409	3	1.0	111	36	0.1	0.1	5	11	2.80	0.5	0.70	1	0.3	140	2300	8.9
8410	1	2.0	99	39	0.1	0.1	5	13	3.50	2.0	0.60	1	0.2	200	1890	8.4
8412	6	0.5	89	36	0.4	0.3	4	2	2.70	2.0	0.25	1	0.1	165	2300	4.4
	Tvedestrand Hyperite															
4005		7.0	190	46	1.4	0.7	15	29	6.90	2.0	2.10	6	0.8	400	2920	20
4006		6.0	187	47	1.0	0.4	13	26	6.20	3.0	2.00	5	0.8	360	1240	5.6
4007		6.0	201	51	1.3	0.3	14	27	7.00	2.0	2.30	6	0.9	400	1880	8.8
4008		6.0	210	54	1.2	0.4	16	29	7.10	2.0	2.20	6	0.8	440	3070	25
4009		5.0	181	42	0.9	0.4	10	26	5.30	2.0	1.80	4	0.7	375	3530	22
	Tvedestrand Amphibolite															
4001		6.0	171	45	1.1	0.5	12	27	6.00	2.0	1.80	5	0.7	610	2060	5.7
4002		5.0	207	45	0.8	0.3	12	22	6.10	1.0	1.90	5	0.8	440	3300	12
4003		6.0	178	45	0.7	0.4	12	29	6.00	2.0	1.90	5	0.8	420	3630	15
4004		7.0	144	42	1.0	0.5	13	25	6.30	2.0	1.60	5	0.9	430	3470	15

	SiO_2	TiO_2	Al_2O_3	Fe_2O_3	FeO	FeO_t	MnO	MgO	CaO	Na_2O	K_2O	P_2O_5	H_2O	Cr	Ni
Tromoy Dyke-1, Low Mg-Hyperite															
5001	46.10	2.07	16.2	3.1	10.8	13.9	0.21	7.21	9.00	3.0	0.28	0.23	1.2	67	110
5002	46.10	2.27	15.6	3.2	11.1	14.3	0.22	6.93	9.13	3.1	0.34	0.23	1.3	76	100
5003	46.40	2.22	15.6	3.2	11.1	14.3	0.23	6.88	8.85	3.2	0.32	0.24	1.1	74	99
Tromoy Dyke-1, High Mg Amphibolite															
5007	46.50	0.27	12.4	2.6	8.0	10.6	0.22	15.13	10.21	1.5	0.47	0.02	2.3	380	190
5008	47.60	0.27	10.4	3.0	7.5	10.5	0.24	15.21	10.94	1.3	0.50	0.01	2.3	510	250
Tromoy Dyke-1, Low Fe-Hyperite															
5004	49.90	0.15	16.7	1.5	5.7	7.2	0.17	10.20	11.97	2.2	0.23	0.01	1.2	230	110
5005	49.90	0.15	17.9	1.1	5.5	6.6	0.16	9.55	12.10	2.3	0.23	0.01	1.2	190	100
5009	49.20	0.20	16.8	1.8	5.8	7.6	0.18	9.82	11.73	2.2	0.42	0.01	1.6	330	150
Tromoy Dyke-1, High Al-Amphibolite															
5006	42.60	0.19	20.5	2.0	6.6	8.6	0.22	10.46	9.45	1.3	2.40	0.02	3.5	210	120
Tromoy Dyke-2 Amphibolite															
5101	47.80	1.43	15.8	3.1	9.1	12.2	0.21	7.66	7.75	3.2	1.12	0.14	1.9	100	140
5102	46.30	1.50	16.0	3.0	9.4	12.4	0.23	8.10	8.64	2.8	0.95	0.16	1.9	130	150
5103	46.80	1.62	16.1	3.6	9.0	12.6	0.24	7.70	8.22	3.0	1.08	0.16	1.9	110	130
Tromoy Dyke-2 Hyperite															
5104	46.50	1.63	16.7	2.9	10.1	13.0	0.18	7.76	9.87	3.0	0.31	0.17	1.3	110	120

	Co	Sc	V	Cu	Zn	Mo	Be	S	Se	As	Sb	Au (ppb)	Rb	Cs	Ba	Sr
	Tromoy Dyke-1, Low Mg-Hyperite															
5001	77	30	220	100	130	0.5	0.8	1356	0.17	0.39	0.08	1.65	23	0.25	146	202
5002	77	41	250	140	130	0.5	0.9	1694	0.22	0.39	0.1	1.34	22	0.25	125	192
5003	74	37	240	110	140	0.5	0.9	1402	0.18	0.27	0.07	0.75	23	0.25	99	199
	Tromoy Dyke-1, High Mg Amphibolite															
5007	74	28	140	7	120	2.0	0.3	62	0.02	0.28	0.04	0.20	45	0.25	54	69
5008	72	43	160	10	130	2.0	0.4	22	0.02	1.25	0.05	0.23	41	0.25	76	69
	Tromoy Dyke-1, Low Fe-Hyperite															
5004	52	37	110	14	80	1.0	0.2	25	0.02	0.14	0.02	0.56	25	0.25	101	245
5005	49	34	110	25	81	1.0	0.2	25	0.04	0.16	0.02	2.45	22	0.25	79	274
5009	51	33	140	11	97	0.5	0.4	25	0.02	0.89	0.04	0.48	47	2.30	70	225
	Tromoy Dyke-1, High Al-Amphibolite															
5006	55	27	110	23	110	1.0	0.1	88	0.02	0.2	0.05	0.14	116	3.00	130	133
	Tromoy Dyke-2 Amphibolite															
5101	67	30	210	66	130	0.5	0.9	650	0.12	2.98	0.19	0.42	48	0.80	160	286
5102	73	29	220	95	160	1.0	0.9	1058	0.17	3.07	0.18	0.45	48	2.90	88	219
5103	68	32	230	70	130	2.0	1.2	574	0.12	2.6	0.14	0.28	48	0.25	142	230
	Tromoy Dyke-2 Hyperite															
5104	72	30	210	74	78	*	0.7	700					19	1.10	84	207

* Blanks: not determined

	Nb	Hf	Zr	Y	Th	U	La	Ce	Sm	Eu	Tb	Yb	Lu	F	Cl	Br
	Tromoy Dyke-1, Low Mg-Hyperite															
5001	2	1.0	167	34	0.5	0.2	7	12.5	5.20	2.0	1.60	3	0.4	310	210	
5002	1	1.0	182	36	0.5	0.3	8	12.5	5.90	1.0	1.80	4	0.5	325	300	
5003	6	1.0	181	42	0.3	0.4	8	11	5.40	3.0	1.60	3	0.5	305	290	
	Tromoy Dyke-1, High Mg Amphibolite															
5007	0	0.5	32	52	0.7	0.3	4	11	3.30	0.5	0.70	1	0.2	310	1450	
5008	5	0.5	33	49	0.3	0.3	4	10	3.60	0.5	0.80	2	0.4	380	970	
	Tromoy Dyke-1, Low Fe-Hyperite															
5004	1	0.5	34	4	0.1	0.1	1	2	0.70	0.5	0.25	1	0.1	100	160	
5005	0	0.5	32	18	0.1	0.1	1	2	0.70	0.5	0.25	1	0.1	90	50	
5009	0	0.5	34	11	0.1	0.1	4	2	1.30	0.5	0.25	1	0.1	180	1020	
	Tromoy Dyke-1, High Al-Amphibolite															
5006	0	0.5	31	19	0.3	0.1	1	2	0.60	0.5	0.25	1	0.1	650	1290	
	Tromoy Dyke-2 Amphibolite															
5101	6	1.0	120	71	1.6	1.2	7	12.5	3.90	2.0	1.10	3	0.4	300	970	2.0
5102	13	1.0	121	78	0.6	0.4	6	13	4.90	1.0	0.70	3	0.6	260	710	1.0
5103	13	2.0	127	78	1.2	0.4	7	17	5.70	0.5	1.30	4	0.4	320	760	1.0
	Tromoy Dyke-2 Hyperite															
5104	11	2.0	103	54	0.4	0.4	6	12.5	4.10	1.0	1.40	4	0.35			3.9

Appendix 4-4. Chemical Changes in Gabbro-Amphibolite Transition in Bamble and Elsewhere in SWSD

	1	2	3	4	5	6	7	8	9	10	11	12
SiO_2	o	o	o			o			o	o	-	o
TiO_2	o	o	o	+		o			o	+	o	o
Al_2O_3	o	o	o			o			o		o	o
Fe_2O_3	+	+	+			+			+	+		+
FeO	-	-	-			-			-			-
FeOt	o	o	o			o			o		o	o
MnO	o	o	o			o			-	o	o	x
MgO	o	o	o	-	-	o			+	-	o	o
CaO	o	o	-			-			+	-	o	x
Na_2O	+	o	o			o			+	+	o	x
K_2O	+	+	+	+		+			+	o	+	+
P_2O_5	o	o	o			+				+	o	o
H_2O	+	+	+			+			+	+	+	+
CO_2	o	o	o									
Cr	o	o	o						o	+		
Ni	o	o	o				o			-	o	o
Co	o	o	o				o		o	o		
Sc	o	o	o				o			+		
V	o	o	o				+		~	+		
Zn	o	o	o				-		x			x
S	o	o	o				-			+		-
Cu	o	o	o				o		~	+		o
As	o	o	o						x			
Se	o	o	o									
Sb	o	o	o									
Au	o	o	o							?		
Rb	+	+	+				+	+	-	o	+	+
Cs	?	?	+									
Ba	+	o	+				+	+	+		o	o
Sr	o	o	o				o		+	o	-	o
Nb	o	o	o							+		
Hf	o	o	o					o				
Zr	o	o	o				x		~	o	o	o
Y	o	o	o				o		~		o	o
Th	o	o	o					o		+	-	+
U	o	o	o							+	-	
La	o	o	o				o	+	~	+		
Ce	o	o	o				o	o	~	+		
Sm	o	o	o				o	o		+		
Eu	o	o	o					o		+		
Tb	o	o	o					o		+		
Yb	o	o	o					o		+		
Lu	o	o	o					o		+		
F	+	o	o									
Cl	+	+	+				+		+			+

Symbols represent: o: relatively immobile; +: added; ~: slightly added. -: removed; x: variable;

1-3. Laget, Tvedestamd and Tromoy (present study); 4. Arendal (Starmer, 1967); 5. Risor (Field, 1969); 6-8. Kragero, Risor, Laget (6. Elliot, 1973; 7. Field and Elliot, 1974; 8. Smalley and Field, 1991); 9. Hiasen (Frodesen, 1968, 1973); 10. Modum, Kongsberg (Waque, 1996); 11. Zeck and Kalsbeek (1981); 12. Zeck and Wiladsen (1990).

Appendix 4-5. Composition of Sufides from Fe-Ni-Cu Ores Associated with Hyperites; Bamble.

Monoclinic Pyrrhotite (PO_m)

Fe (%)	S (%)	Cu (ppm)	Ni (%)	Co (%)	Total
56.21	40.52	150	1.84	0.051	98.64
55.97	40.18	10	1.804	0.048	98.00
56.12	40.6	0*	1.725	0.081	98.53
55.92	41.1	0	2.111	0.021	99.15
56.04	40.88	30	1.972	0.034	98.93
55.62	41.11	0	1.94	0.061	98.73
55.67	40.91	0	1.605	0.012	98.20
56.68	41.05	0	1.51	0.08	99.32
55.96	41.06	580	1.616	0.088	98.78
55.73	41.12	300	2.103	0.041	99.02
56.58	40.71	270	1.517	0.072	98.91
56.04	40.78	40	1.668	0.039	98.53
59.31	39.92	10	1.36	0.036	100.63
59.27	39.71	0	1.22	0.033	100.23
58.66	39.82	20	1.27	0.038	99.79
58.59	39.53	10	1.34	0.043	99.50
58.77	39.76	20	1.29	0.042	99.86
58.67	40.01	20	1.34	0.032	100.05
58.02	40.11	110	1.231	0.131	99.50
57.81	39.82	0	1.402	0.078	99.11
58.41	39.98	0	1.422	0.071	99.88
57.88	39.03	270	1.4	0.101	98.44
57.76	39.79	0	1.367	0.112	99.03
57.94	39.5	110	1.224	0.115	98.79
59.05	38.92	70	0.997	0.02	98.99
55.75	41.19	10	2.138	0.032	99.11
55.27	40.71	0	2.253	0.059	98.29
58.31	39.94	50	1.166	0.014	99.44
58.47	39.4	0	1.09	0.045	99.01
55.23	40.78	40	2.29	0.067	98.37
58.43	39.48	80	0.929	0.065	98.91
55.49	41.32	470	2.208	0.085	99.15
55.16	40.92	0	2.443	0.036	98.56
58.15	38.98	0	0.893	0.046	98.07
57.97	39.5	0	0.949	0.049	98.47
58.43	39.51	0	0.954	0.032	98.93
58.38	39.76	0	1.339	0.071	99.55
57.71	39.5	310	1.287	0.099	98.63
57.99	39.88	0	1.34	0.079	99.29
57.87	39.71	0	1.186	0.082	98.85
58.38	39.9	0	1.373	0.109	99.76
57.76	39.19	90	1.522	0.074	98.56
58.05	39.31	20	1.322	0.083	98.77
57.89	39.23	0	1.357	0.094	98.57
59.00	39.26	160	0.422	0.078	98.78
58.66	39.85	0	0.747	0.09	99.35
59.10	39.52	0	0.424	0.033	99.08
59.09	39.36	10	0.592	0.058	99.10
59.27	39.53	0	0.612	0.078	99.49
58.47	38.99	0	0.519	0.1	98.08

Hexagonal Pyrrhotite (PO_h)

Fe (%)	S (%)	Cu (ppm)	Ni (%)	Co (%)	Total
60.27	38.67	0	0.853	0.148	99.94
60.55	38.71	20	0.631	0.102	100.00
60.40	38.66	10	0.726	0.13	99.92
60.15	38.76	10	0.85	0.163	99.93
60.21	38.92	10	0.715	0.129	99.97
59.84	38.66	10	1.123	0.351	99.98
60.44	38.72	0	0.672	0.15	99.98
60.42	38.7	10	0.748	0.138	100.01
60.24	38.94	10	0.708	0.134	100.02
60.00	39.12	10	0.665	0.145	99.93

Ni-Co Pyrite (PY_{Ni-Co})

46.11	53.02	220	0.706	0.109	99.97
43.35	53.24	10	3.47	0.204	100.27
43.69	53.64	50	2.53	0.603	100.47
42.08	53.08	10	3.09	0.426	98.68
42.28	54.14	0	3.837	0.328	100.59
44.90	53	140	2.536	0.347	100.80
41.88	53.58	0	4.255	0.476	100.19
44.10	53.66	0	1.922	0.391	100.07
43.29	53.1	0	2.977	0.324	99.69
44.83	52.42	1300	2.334	0.182	99.90
43.02	53.85	0	3.324	0.444	100.64
43.65	53.94	0	2.498	0.495	100.58
43.26	53.89	700	3.249	0.127	100.60

Pyrite Replacing Pyrrhotite (PYr)

45.96	53.55	4670	0.299	0.047	100.32
46.21	54.03	700	0.243	0.035	100.59
46.06	53.6	2230	0.279	0.043	100.21
46.04	53.42	1130	0.339	0.038	99.95
44.20	53.5	0	2.222	0.163	100.09
46.21	53.85	240	0.491	0.035	100.61
43.19	53.42	20	2.97	0.759	100.34
43.13	53.24	0	3.19	0.416	99.98
46.04	53.87	40	0.124	0.326	100.36
46.58	54.02	790	0.06	0.078	100.82
46.39	53.66	110	0.192	0.049	100.30
46.20	53.44	0	0.254	0.111	100.01
45.86	53.7	150	0.141	0.889	100.61
46.31	54.45	0	0.254	0.053	101.07
46.07	53.72	0	0.176	0.174	100.14
46.16	53.39	400	0.38	0.063	100.03
46.78	51.972	30	0.064	0.469	99.28
46.78	52.228	60	0.201	0.23	99.44
46.15	54.14	0	0.021	0.606	100.92
46.43	52.111	20	0.029	0.554	99.12
46.59	52.283	20	0.02	0.479	99.38
46.39	52.123	30	0.024	0.477	99.02
45.74	53.81	1050	0.058	0.736	100.45
46.60	53.95	110	0.401	0.099	101.06

Pyrite Replacing Pyrrhotite (PYr)					
46.84	54.35	250	0.54	0.062	101.82
45.85	53.6	20	0.32	0.834	100.61
44.54	51.68	380	0.608	0.878	97.74
46.39	54.33	350	0.367	0.097	101.22
45.51	53.88	100	0.621	0.049	100.07
46.10	54.02	1880	0.421	0.065	100.79
45.90	53.45	860	0.3	0.065	99.80
44.75	53.15	0*	2	0.03	99.93
44.15	52.68	100	2.87	0.02	99.73
45.87	51.88	200	1.96	0.02	99.75
44.55	52.6	100	2.68	0.04	99.88
44.15	53.38	100	2.17	0.03	99.74
45.88	52.64	100	1.35	0.025	99.91
Co-rich Pyrite (PYCo)					
45.21	53.62	1428	0.53	0.578	100.08
45.52	53.78	90	0.55	0.227	100.09
45.95	53.76	0	0.088	0.861	100.66
45.58	53.25	310	0.089	0.896	99.85
45.99	54.04	0	0.078	0.721	100.83
46.17	53.93	60	0.035	0.641	100.78
44.98	54.04	680	0.013	1.747	100.85
45.84	53.41	0	0.026	0.791	100.07
46.03	54.77	340	0.055	0.866	101.76
45.71	53.56	140	0.017	1.104	100.41
44.61	53.62	260	0.066	1.674	100.00
45.97	53.84	380	0.317	0.274	100.44
44.83	53.84	240	0.04	1.976	100.71
45.79	54.02	300	0.019	0.944	100.80
45.33	53.67	290	0.052	1.393	100.47
45.68	53.97	0	0.048	1.056	100.75
45.77	53.53	0	0.008	1.197	100.51
45.66	53.83	0	0.129	1.178	100.80
45.96	53.36	0	0.02	0.885	100.23
45.45	53.56	0	0.058	0.97	100.04
45.68	54.05	80	0.012	0.588	100.34
Secondary Pyrite (PYs)					
46.63	54.11	300	0.011	0.055	100.84
45.60	52.8	100	0.05	0.02	98.48
45.94	53.18	50	0.012	0.02	99.16
45.62	53.3	200	0.02	0.04	99.00
45.78	53.7	100	0.015	0.03	99.54
45.70	53.85	100	0.01	0.04	99.61
45.90	53.55	100	0.02	0.07	99.55
46.01	53.45	600	0.02	0.066	99.61
46.78	53.66	0	0.048	0.041	100.53
46.70	53.94	0	0.067	0.059	100.77

* not detected

Pentlandite					
26.83	33.29	920	37.682	0.02	97.91
26.73	35.56	80	36.755	0.018	99.07
26.54	34.82	1440	35.589	0.045	97.14
26.76	32.5	740	37.706	0.018	97.06
27.06	32.95	20	37.861	0.037	97.91
27.64	32.77	350	36.956	0.026	97.43
27.11	33.3	930	37.654	0.014	98.17
26.79	33.35	750	37.032	0.04	97.29
26.96	32.99	380	37.396	0.027	97.41
27.14	33.12	360	37.636	0.02	97.95
27.26	32.96	230	37.675	0.03	97.95
27.38	32.56	330	36.858	0.032	96.86
27.21	32.49	550	37.313	0.031	97.10
26.46	33.4	750	37.12	1.139	98.19
26.78	32.77	280	36.345	1.214	97.14
Chalcopyrite		Cu (%)			
30.00	33.87	34.06	0.007	0.023	63.90
29.87	34.15	34.03	0.009	0.036	64.07
29.58	34.17	34.02	0.053	0.035	63.84
29.95	34.88	33.98	0.183	0.004	65.02
29.65	34.4	33.82	0.044	0.058	64.16
30.54	33.708	34.60	0.002	0.003	64.26
30.37	33.891	34.40	0.002	0.003	64.27
30.89	34.716	34.40	0.003	0.003	65.62
29.53	34.65	34.38	0.035	0.034	64.25
29.57	34.66	34.19	0.014	0	64.25
29.88	35.08	34.52	0.057	0.05	65.07
29.64	34.95	34.34	0.018	0.044	64.66
29.60	35.11	34.11	0.053	0.065	64.83
30.11	34.72	34.50	0.001	0.07	64.90
29.76	34.63	34.27	0.045	0	64.44
29.97	35.15	34.19	0.026	0.025	65.17
29.90	34.56	34.04	0.057	0.028	64.55
30.02	34.83	34.08	0.015	0.046	64.91
29.92	35.03	34.35	0.006	0.036	65.00
31.11	34.807	33.86	0.437	0.192	66.54
30.49	34.648	33.53	0.001	0.002	65.14
30.65	34.564	34.18	0.003	0.003	65.23
30.71	34.819	34.24	0.002	0.001	65.54
30.87	34.856	34.47	0.002	0.003	65.73

Appendix 4-6. Replicate Analysis of Reference Materials (INAA and Hydride ICPMS Techniques)

	Reference (X ± 1σ)	1	2	3
	Au (2ppb)*			
PTC-1a	1310 ±110	1120	1200	1330
CCU-1b	5890 ± 100	6150	6560	
CH-3	1400 ± 30	1230	1290	
WMS-1	279 ± 33	294	338	
RTS-2	*38 ± 10***	36	45	
	Ag (0.4 ppm)			
PTC-1a	56 ±1.4	48	51	58
CCU-1b	178 ± 2	172	184	
CH-3	2.63± 0.2	3.2	2.8	
	As (0.5 ppm)			
PTC-1a	*120 ± 9*	98	92	110
CCU-1b	58 ± 7	62	67	
CH-3	143 ± 14	130	150	
	Se (3 ppm)			
CCU-1b	*139 ± 27*	150	164	
RTS-2	*57*	62	70	
	Sb (0.1 ppm)			
CCU-1b	*4 ± 2*	5.5	6.5	
	Ir (5 ppb)			
PTC-1a	*110 ± 30*	83	91	110
WMS-1	235 ± 25	210	220	
	Co (1 ppm)			
PTC-1a	*3000 ± 100*	2900	3100	3100
CCU-1b	*26 ± 10*	19	25	
RTS-2	72 ± 7	70	78	
	Ni (1 ppm)			
RTS-2	2430 ± 100	2550	2632	
WMS-1	*37000*	38650	38670	
	Cu (1 ppm)			
CH-3	8300 ± 200	8200	8400	
WMS-1	*13000*	11900	12400	
RTS-2	670 ± 32	720	778	
	Zn (1 ppm)			
CH-3	164 ± 15	168	171	
RTS-2	117 ± 10	107	120	

* Figures in brackets show the detection limits ** Figures in italics represent provisional values

Appendix 5-1. Sulfur Isotope Composition of Various Supracrustal Rocks; Bamble.

Sample No.	Mineral	$\delta^{34}S_{CDT}$ (‰)
I. Bt-Gneiss (Amphibolite Zone)		
2612	Py	0.6
2811	Py	2.6
2812	Py	6.6
3222	Py	5.4
3322	Py	1.9
3422	Py	2.3
3521	Py	-0.4
3521	Py	1.8
7301	Po	6.6
7302	Po	8.6
7303	Po	6.1
2012	Py	2.7
II. Concordant Amphibolite (Amphibolite Zone)		
2211	Py	1.3
2212	Py	2.3
2522	Py	2.5
2522	Py	3.0
2621	Py	-0.1
3221	Py	1.6
3311	Py	-0.3
3321	Py	2.6
3412	Py	1.6
2521	Py	2.6
III. Grt-Bt Gneiss (Transition Zone)		
1912	Py	1.2
1922	Py	1.5
2011	Py	4.8
2021	Py	1.6
2111	Py	4.4
Grt-Bt Gneiss; contin.		
2112	Py	2.8
2122	Py	2.7
7101	Po	5.3
7101	Py	6.2
7102	Po	6.1
7305	Po	2.4
IV. Calc-Silicate (Transition Zone)		
7202	Po	4.9
7204	Po	5.5
V. Opx-Grt-Bt Gneiss (Granulite Zone)		
121-1	Po	4.2
121-2	Py	5.1
122	Po	4.2
811	Py	8.4
812	Py	9.3
1322	Po	5.2
4502	Py	8.8
9401	Py	5.9
9403	Py	8.9
9502	Py	6.1
9504	Py	4.1
9505-1	Po	3.3
9505-2	Py	4.2
9506	Py	4.8
9507	Py	3.7
9509-1	Po	11.3
9509-2	Py	11.8
9902	Po	4.0

Appendix 5-2. Sulfur Isotope Composition of Charnockites; Bamble

Sample No.	Mineral	$\delta^{34}S_{CDT}$
412	Py*	7.1
421	Py	0.4
511	Py	5.3
512	Py	1.1
611	Po*	1.7
612	Po	1.5
722	Py	4.8
911	Py	2.7
1011	Py	3.0
1111	Py	4.5
1112	Py	1.7
1212	Py	3.3
1221	Py	7.4
1222	Po	1.1
1522	Py	1.5
1621	Py	3.0
1621	Py	3.3

* Both pyrite and pyrrhotite are accompanied by minor chalcopyrite

Appendix 5-3. Sulfur Isotope Composition of Metabasites from Various Metamorphic Zones; Bamble.

Zone A	Mineral	$\delta^{34}S_{CDT}$
6401	Py	-0.2
6406	Py	2.1
6407	Py	-0.7
6504	Py	1.4
6801	Po	-0.6
6803	Po	0.0
6804	Py	0.5
6804	Po	0.6
7401	Py	1.9
7502	Po	1.9
7702	Py	0.0
Zone B		
3902	Py	1.9
3905	Py	0.2
3906	Py	1.8
3907	Py	0.4
4101	Py	-0.3
4103	Py	0.4
4402	Py	0.9
Zone C		
5405	Py	0.9
5408	Py	0.8
5410	Py	1.4
5412	Py	0.3
5414	Py	0.7
5416	Py	0.2
5421	Py	0.6
5512	Py	1.6
Zone D		
1211	Py	1.2
1812	Py	1.5
3805-1	Po	0.9
3805-2	Py	1.1
4507	Py	0.5
Secondary Sulfide (Overgrowth and Fracture Filling)		
5519	Py	3.4
6401	Py	3.1
6403	Py	0.8
6408	Py	1.0
6804	Py	3.6
5422	Py	4.6
6501	Py	4.0

Appendix 5-4. Sulfur Isotope Composition of Hyperites (Gabbros) and Amphibolites.

Sample No.	Mineral	$\delta^{34}S$
4002	Py*	-0.1
4003	Py	0.3
4006-1	Po**	0.2
4006-2	Py	0.1
4007-1	Po	0.2
4007-2	Py	0.3
4009-1	Po	-0.2
4009-2	Py	0.1
5001-1	Po	0.5
5001-2	Py	0.2
5002-1	Po	0.2
5002-2	Py	0.1
5003-1	Py	0.2
5003-2	Py	-0.1
5102	Py	0.8
5102	Py	1.0
5201-1	Po	1.2
5201-2	Py	1.4
5202-1	Po	-0.1
5202-2	Py	0.0
8403	Po	1.4
8406	Py	0.1
8407	Py	0.0
8401	PYs***	4.4
8407	PYs	4.9
8512	PYs	3.7

* Pyrite ** Pyrrhotite *** Secondary Pyrite

Appendix 5-5. Sulfur Isotope Composition of Magmatic Sulfide Ores, Bamble.

Sample No.	Mineral	$\delta^{34}S_{CDT}$	$\Delta\delta^{34}S_{Py\text{-}Po}$
A. Orthomagmatic, Pyrrhotite-rich Ore			
91001	Po	1.9	
91002	Po	1.9	
91004	Po	2.1	
91006	Po	2.5	
91007	Po	2.2	
91010	Po	1.9	
91011	Po	1.7	
91026	Po	5	
91027	Po	3.2	
91028	Po	4.7	
91028	Ccp	3.8	
B. Composite Ore (Pyrrhotite Coexisting with Pyrite)			
91004	Py	2.3	0.9
	Po	1.4	
91004	Py	2.2	1.3
	Po	0.9	
91005	Py	2.1	0.9
	Po	1.2	
91006	Py	2.1	0.6
	Po	1.5	
91006	Py	2.4	0.8
	Po	1.2	
91006	Py	1.7	-0.4
	Po	2.1	
91006	Py	2.8	0.4
	Po	2.4	
91006	Py	3.2	0.3
	Po	2.9	
91006	Py	2.5	1
	Po	1.5	
91006	Py	2.4	0.8
	Po	1.6	
91007	Py	2.5	1.1
	Po	1.4	
91007	Py	2.5	1
	Po	1.5	
91011	Py	3.2	0.7
	Po	2.5	
91011	Py	3	1
	Po	2	
C. Strongly Recrystallized, Pyrite-rich Ore			
91001	Py	2.1	
91002	Py	2	
91003	Py	3.4	
91004	Py	1.8	
91006	Py	2.5	
91007	Py	2.1	
91011	Py	1.6	
D. Overgrowth and Fracture Filling Pyrite			
91002	Py	-2.5	
91006	Py	-1.1	
91007	Py	-1.1	
91007	Py	-0.1	
91011	Py	-2.2	